01 Aug 1986

Design of automotive structural components using high strength sheet steels: web crippling of cold-formed steel beams

Chiravut Santaputra

Wei-Wen Yu
Missouri University of Science and Technology, wwy4@mst.edu

Civil Engineering Study 86-1
Structural Series

Eighth Progress Report

DESIGN OF AUTOMOTIVE STRUCTURAL COMPONENTS USING HIGH STRENGTH SHEET STEELS

WEB CRIPPLING OF COLD-FORMED STEEL BEAMS

by

Chiravut Santaputra
Research Assistant

Wei-Wen Yu
Project Director

A Research Project Sponsored by American Iron and Steel Institute

August 1986

Department of Civil Engineering

University of Missouri-Rolla

Rolla, Missouri

PREFACE

This report is based on the dissertation presented to the Faculty of the Graduate School of the University of Missouri-Rolla (UMR) in partial fulfillment of the requirements for the degree of Doctor of Philosophy in Civil Engineering.

The financial assistance granted by the American Iron and Steel Institute (AISI) and the technical guidance provided by members of the AISI Task Force on Structural Design and Research of the Transportation Department and the AISI staff are gratefully acknowledged. These members are: Messrs. S. J. Errera, D. M. Bench, A. E. Cornford, Jim Davidson, Charles Haddad, Emil Hanburg, Al Houchens, L. J. Howell, A. L. Johnson, R. G. Lang, B. S. Levy, Kuang-Huei Lin, Hickmat Mahmood, Don Malen, D. J. Meuleman, M. S. Rashid, Joe Rice, W. J. Riffe, Robin Stevenson, Brian Taylor, R. J. Traficanti, T. L. Treece, M. J. Vecchio, and David Whittaker.

All materials used in the experimental study were donated by Bethlehem Steel Corporation, Inland Steel Company, and National Steel Corporation.

Appreciation is also expressed to Messrs. K. Haas, R. Haselhorst, and J. Tucker, staff of the Department of Civil Engineering, for their support. The valuable assistance provided by Mr. M. B. Parks in the preparation and performance of the tests is greatly appreciated.

ABSTRACT

The structural behavior of high strength cold-formed steel beams subjected primarily to web crippling was investigated analytically and experimentally. In this study hat sections and I-beams, formed from five different types of high strength sheet steels commonly used in the automobile industry, were investigated under various loading conditions. The yield strengths of these sheet steels vary from 58 to 165 ksi.

In addition to the test data gathered in this phase of study, the experimental results obtained from the beam tests conducted at Inland Steel Company and Ford Motor Company were carefully evaluated. The evaluation indicated that the present available design criteria are not suitable for high strength materials with yield strengths exceeding 80 ksi.

Following the analytical and experimental studies, new design formulas were derived for different types of loading conditions on the basis of available test data with material yield strengths ranging from 30 to 165 ksi. These empirical equations distinguish between web crippling failure caused by overstressing (bearing failure) and web buckling. Interaction formulas were derived for sections with single unreinforced webs and I-beams under combined web crippling and bending moment.

Additional tests were also performed for the transition ranges between the basic loading conditions. These test data were used to verify the newly proposed design equations which can eliminate the problem of discontinuity between different basic loading conditions.

TABLE OF CONTENTS

TABLE OF CONTENTS (cont'd)

TABLE OF CONTENTS (cont'd)

TABLE OF CONTENTS (cont'd)

TABLE OF CONTENTS (cont'd)

TABLE OF CONTENTS (cont'd)

LIST OF ILLUSTRATIONS

LIST OF ILLUSTRATIONS (Cont'd)

LIST OF ILLUSTRATIONS (Cont'd)

LIST OF ILLUSTRATIONS (Cont'd)

LIST OF ILLUSTRATIONS (Cont'd)

LIST OF ILLUSTRATIONS (Cont'd)

LIST OF ILLUSTRATIONS (Cont'd)

LIST OF TABLES

LIST OF TABLES (Cont'd)

LIST OF TABLES (Cont'd)

LIST OF TABLES (Cont'd)

LIST OF TABLES (Cont'd)

LIST OF TABLES (Cont'd)

LIST OF TABLES (Cont'd)

LIST OF TABLES (Cont'd)

I. INTRODUCTION

A. GENERAL

In recent years, automotive engineers have altered the design philosophy for safer and more fuel economy vehicles. High strength steels have been widely used in automotive structural components to achieve weight reduction while complying with federal safety standards. The substitution of relatively new high strength steels for traditional materials of low to moderate strengths can provide substantial weight savings at competitive costs.[1,2] However, there is only a limited amount of information to assist the designers for the design and use of such high strength sheet steels.

The current design recommendation, "Guide for Preliminary Design of Automotive Structural Components"[3] was issued by the American Iron and Steel Institute (AISI) in February, 1981. It was recommended for an application to materials with yield strength up to 80 ksi. These design expressions are based primarily on the 1968 Edition of the AISI "Specification for the Design of Cold-Formed Steel Structural Members"[4] which was written for the design of buildings.

The AISI Specification was revised in 1980[5] and in 1986.[6] Some of the design criteria were revised and others were added in keeping with technical developments and the results of continued research programs sponsored by the American Iron and Steel Institute. Furthermore, in view of the fact that many types of high strength steels with yield strengths from 80 to 190 ksi[7-13] are now used for automotive structural components, a comprehensive design guide is highly desirable.

Since early 1982, a research project entitled "Design of Automotive Structural Components Using High Strength Sheet Steels" has been conducted at the University of Missouri-Rolla under the sponsorship of the American Iron and Steel Institute. The main purpose of the overall project has been to determine the characteristics of high strength automotive sheet steels and to develop additional design criteria for the use of a broader range of high strength steels in automotive structures.[14] Web crippling and a combination of web crippling and bending moment are two areas that have been studied as a part of this research project.[15-17]

B. PURPOSE OF INVESTIGATION

The main purpose of this portion of the investigation was to study the structural behavior of high strength cold-formed steel beams subjected primarily to web crippling and a combination of web crippling and bending moment. It was intended to use the research findings for a possible development of new and/or modified design criteria and to extend the use of materials having yield strengths exceeding the limitations presently included in the AISI Guide[3] and Specification.[6]

This study was also extended to develop the transition equations between the four basic loading conditions for web crippling.

C. SCOPE OF INVESTIGATION

This study consisted primarily of experimental investigations of the structural behavior of high strength cold-formed steel beam webs subjected to web crippling and a combination of web crippling and bending moment. The beam webs considered in this investigation are unreinforced

elements without any transverse stiffeners. Test specimens included hat sections with single webs and I-beams having high degree of restraint against rotation of the webs. It was assumed that the information obtained from the tests of hat sections can also be used for channels, Z-sections, rectangular tubes and similar shapes.

As the first step of investigation, the available research reports and technical publications relative to the behavior of web elements subjected to edge loading have been studied in detail. Section II contains a summary of such literature survey.

The experimental study of beam webs subjected primarily to web crippling and a combination of web crippling and bending moment is discussed in Section III. Details of test specimens, test procedures, and test results are given in this section.

In Section IV, the results of tests conducted in this phase of investigation are evaluated by comparing the tested failure loads to the predicted ultimate web crippling loads calculated on the basis of the present AISI design procedures. Evaluations of test data obtained from Inland Steel Company and Ford Motor Company are also included.

Section V presents the analytical investigation of web crippling of cold-formed steel beams. The ultimate web crippling loads of sections with single unreinforced webs are predicted by using an available finite element computer program.

The development of empirical expressions to predict the ultimate web crippling loads for various cases is discussed in Section VI. The interaction equations for combined bending and web crippling for sections with single webs and I-beams are derived. Also included in this section is an introduction of a new concept for the prediction of

ultimate web crippling loads and combined bending and web crippling in the form of design recommendations. Finally, the research findings are summarized in Section VII.

II. REVIEW OF LITERATURE

A. GENERAL

In the initial phase of this investigation, numerous publications and research reports have been carefully studied. They are related to previous analytical and experimental studies of the strength of web plates subjected primarily to web crippling and a combination of web crippling and bending moment. In addition, the present available design criteria being used in different specifications for preventing web crippling were also reviewed in detail.

B. ANALYTICAL STUDY

The theoretical background for the problem of web crippling has been carefully studied. Even though web and flange of the section are interactive, it is useful to consider the behavior of idealized separate rectangular flat plates subjected to locally distributed in-plane edge forces. This subject has been studied by numerous investigators and is summarized as follows:

1. Two Opposite Uniformly Distributed Loads:

The critical buckling stress of a simply supported plate subjected to two opposite uniformly distributed loads as shown in Fig. 2.1a can be determined by solving Bryan's differential equation based on small deflection theory as follows:

$$\frac{\partial^4 \omega}{\partial x^4} + 2\frac{\partial^4 \omega}{\partial x^2 \partial y^2} + \frac{\partial^4 \omega}{\partial y^4} + \frac{P\partial^2 \omega}{DL\partial x^2} = 0 \qquad (2.1)$$

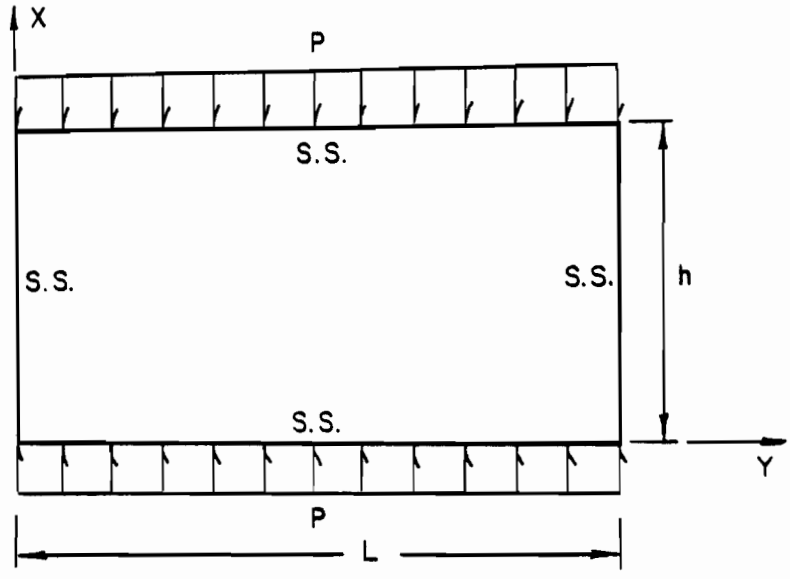

(a) Plate Loading

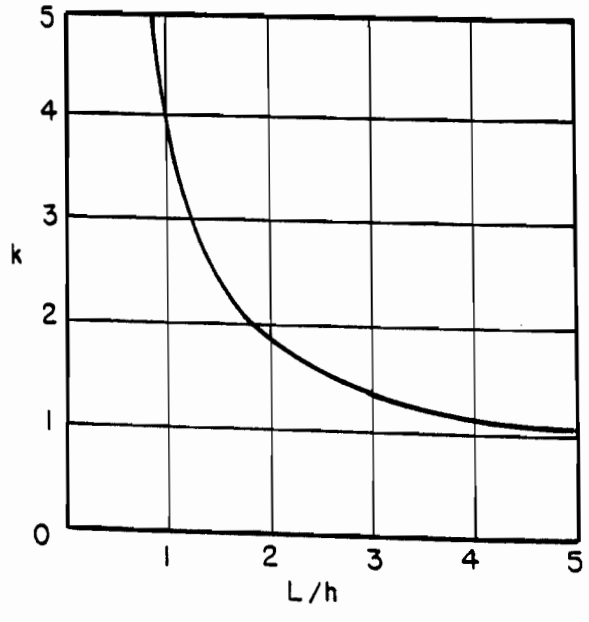

(b) Plate Buckling Coefficient, k

Fig. 2.1 Simply Supported Plate Subjected to Uniformly Distributed Load[18]

where $D = Et^3/(12(1-\mu^2))$

E = modulus of elasticity

μ = Poisson's ratio

t = thickness of plate

ω = deflection of plate perpendicular to surface

P = total uniform load

By considering the deflected shape of the plate to be half sine waves in both directions, the deflection of the plate perpendicular to the surface may be determined from

$$\omega = A_0 \sin(\pi x/h)\sin(\pi y/L). \tag{2.2}$$

Solving Eq. (2.1) by using Eq. (2.2), one can obtain an equation for critical buckling load as follows:[18]

$$P_{cr} = k\pi^2 DL/h^2 \tag{2.3}$$

where P_{cr} = elastic buckling load

$k = ((L^2+h^2)/L^2)^2$

The values of buckling coefficient, k, is shown in Fig. 2.1b for different L/h ratios. It should be noted that for the case of square plate (L/h = 1), the value of k equals 4.

2. Two Opposite Concentrated Loads:

According to Timoshenko and other researchers,[19,20] the elastic critical load of a simply supported rectangular plate subjected to two equal and opposite concentrated loads, as shown in Fig. 2.2a, can be determined by Eq. (2.4) below

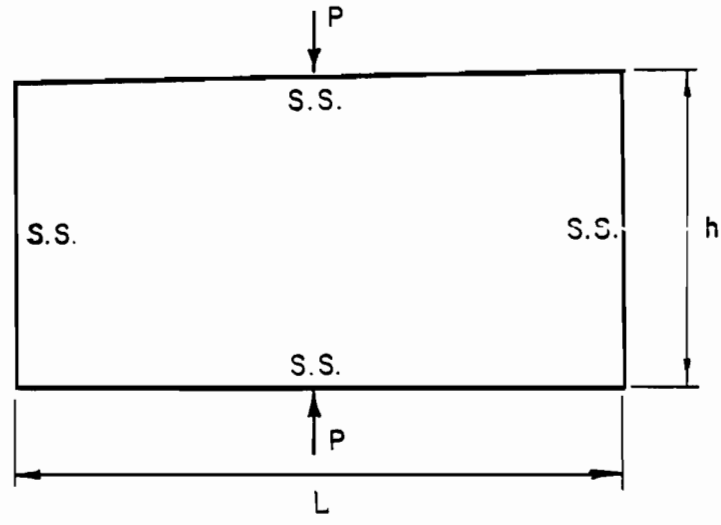

(a) Plate Loading

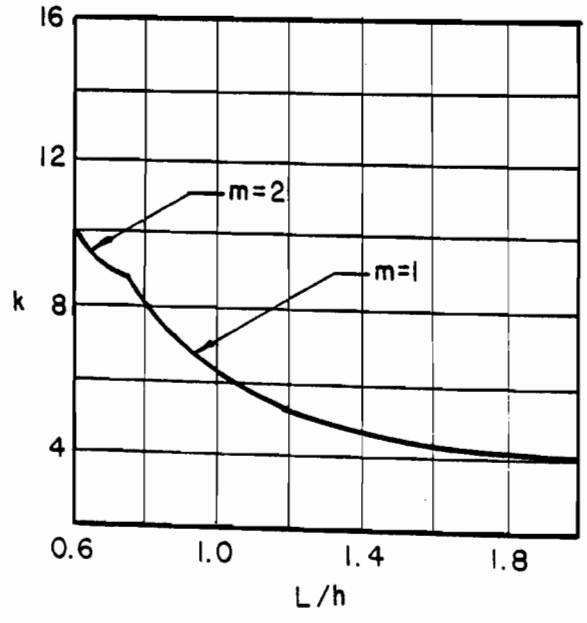

(b) Plate Buckling Coefficient, k

Fig. 2.2 Simply Supported Plate Subjected to Two Opposite Concentrated Load[20]

$$P_{cr} = k\pi D/h \tag{2.4}$$

where P_{cr} = elastic buckling load

k = buckling coefficient.

The above equation was developed by using the strain energy approach. Because the buckling coefficient, k, varies with the aspect ratio, L/h, Yamaki[20] studied the variation of k with L/h and summarized the results as shown in Fig. 2.2b. In this figure, m represents the number of half sine waves in the longitudinal direction along the beam length.

3. Two Opposite Partially Distributed Loads:

The problem of a simply supported plate subjected to two opposite partially distributed loads as shown in Fig. 2.3a was analyzed in 1972 by Khan and Walker.[21,22] By using a simple expression to describe the buckled shape together with an assumed solution of the stress distribution, the critical buckling load can be determined from

$$P_{cr} = k\pi^2 D/h \tag{2.5}$$

where P_{cr} = elastic critical buckling load

k = buckling coefficient depending on the ratios L/h and N/h

N = bearing length of the applied load.

Figure 2.3b gives the value of buckling coefficient, k, as the function of L/h ratio for two different ratios of N/h.

4. Partial Load on One Edge:

In 1936, Girkmann[23] was the first to study the problem of buckling of a simply supported plate subjected to a single edge load but the results of his finding were not readily usable by engineers.

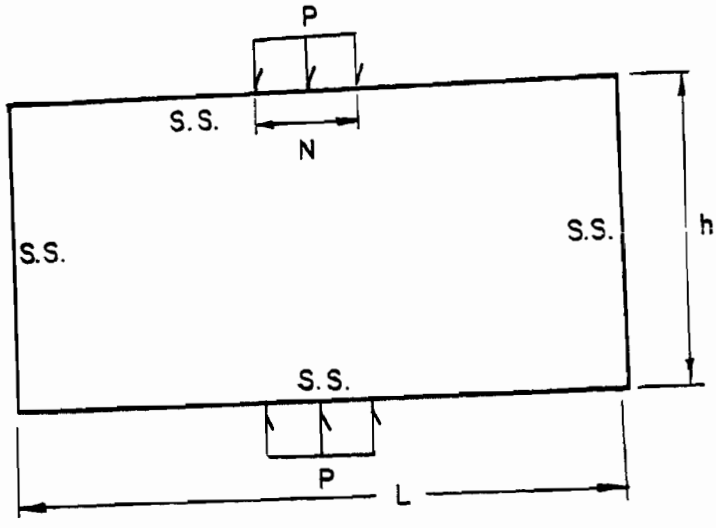

(a) Plate Loading

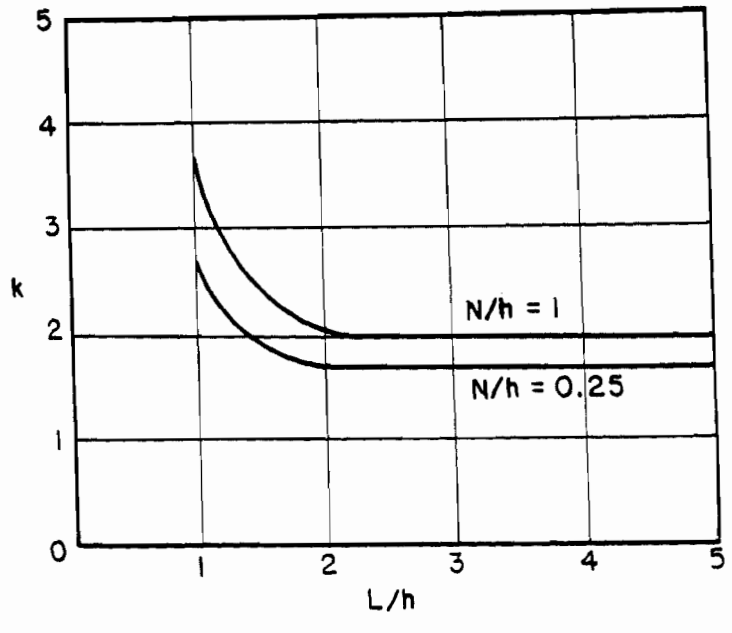

(b) Plate Buckling Coefficient, k

Fig. 2.3 Simply Supported Plate Subjected to Two Opposite Partially Distributed Load[21,22]

In 1955, Zetlin[24] studied further on this subject. He assumed that the rectangular plate was simply supported along all four edges and the applied load was distributed symmetrically about the mid-span section along one of the longitudinal edges as shown in Fig. 2.4a. One exception to Fig. 2.4a was that the plate was supported at both ends by shear stresses which were parabolically distributed along the tranverse edges of the plate instead of the reaction shown. He used Raleigh-Ritz energy method to show that

$$P_{cr} = k\pi^2 D/L \tag{2.6}$$

where P_{cr} = elastic buckling load

k = buckling coefficient depending on the ratios h/L and N/L.

Zetlin gave the values of buckling coefficient, k, in graphical form as shown in Fig. 2.4b. This solution does not deal with the plate supported at its corners. However, if the plate is sufficiently long he claimed that his results could be used.

In 1962, White and Cottingham[25] used the finite difference method to examine the buckling of a web-plate with partial loading and end reactions that support a substantial length of the plate. For each loading case, they provided curves giving the relationship between the buckling coefficient and aspect ratio. It should be noted that the plates studied by these two investigators are relatively short with L/h ratio from 1/3 to 3.

In 1972, Khan and Walker[21,22] also studied the buckling problem of plates with the same configuration assumed by Zetlin as shown in Fig. 2.4a. By formulating only a statically determinate stress distribution

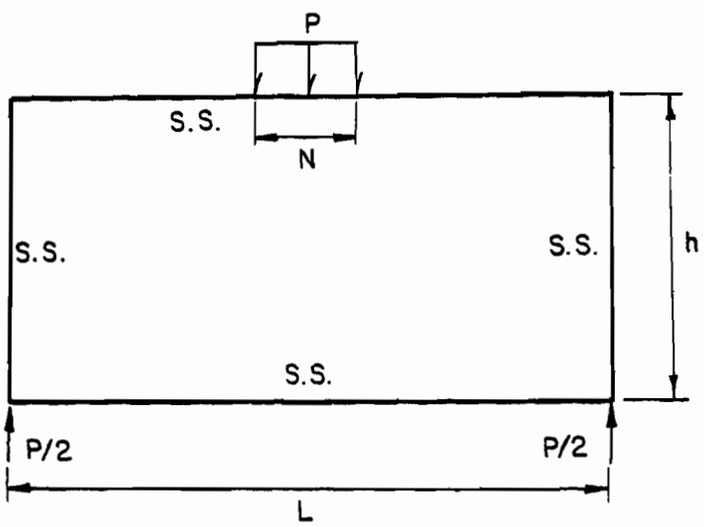

(a) Plate Loading

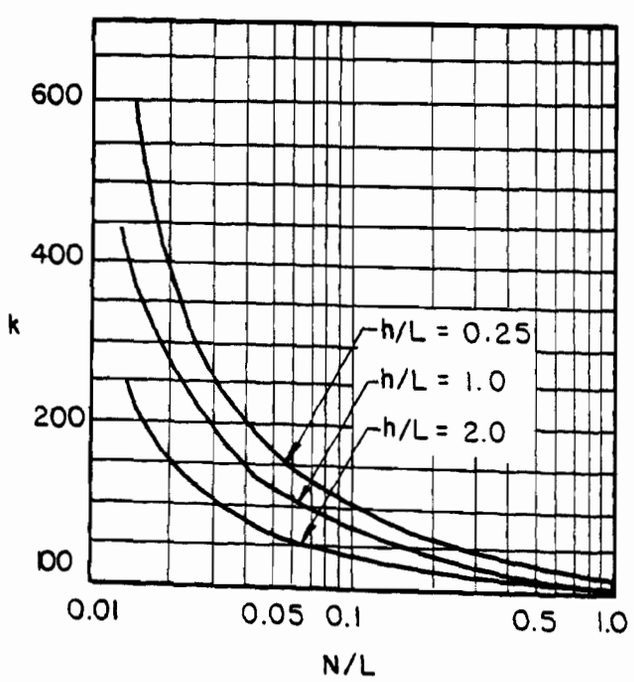

(b) Plate Buckling Coefficient, k

Fig. 2.4 Simply Supported Plate Subjected to Partial Edge Loading[24]

with an approximate deflected shape of the plate, they showed that the buckling load can be determined from

$$P_{cr} = k\pi^2 D/h \tag{2.7}$$

where P_{cr} = elastic buckling load

k = buckling coefficient depending on the ratios of N/h and L/h.

Figure 2.5a gives the values of buckling coefficient, k, as a function of L/h for different N/h ratios.

During the period from 1975 to 1977, Khan, Johns and Hayman[26] performed the parametric study concerning the buckling of partially loaded plates (Fig. 2.4a) by reducing some degree of mathematical complexity. They used a method suggested by Alfutov and Balabukn,[27] in which the stress distribution needs to be satisfied only for the equilibrium condition. Thus, the stress field does not need to correspond to the strains that satisfy compatibility. The purpose of the study was to determine the prebuckling stress distribution throughout the plate and to use it in the buckling calculation. Graphical results of buckling coefficient, k, were presented for Eq. (2.7) as shown in Fig. 2.5b.

For beams having webs connected to flanges, the theoretical analysis of web crippling is extremely complicated because it involves the following factors:[28]

1) nonuniform stress distribution under the applied load;
2) elastic and inelastic instability of the web element;
3) local yielding in the immediate region of load application;
4) bending produced by eccentric load when it is applied on the

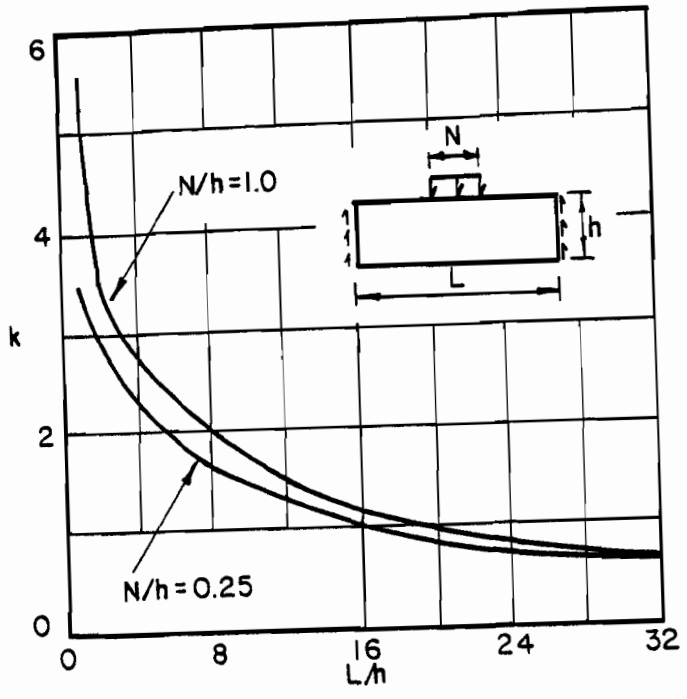

(a)

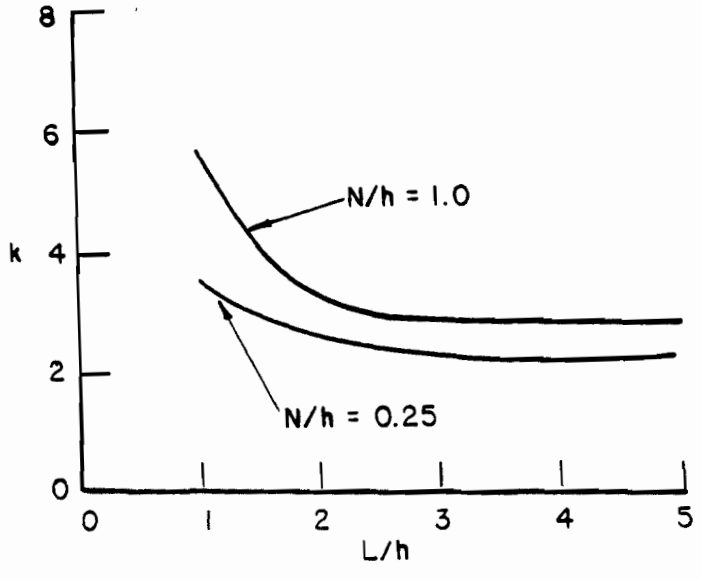

(b)

Fig. 2.5 Buckling Coefficient for Simply Supported Plate Subjected to Partial Edge Loading[21,22,26]

bearing flange at a distance beyond the curved transition of the web;

5) initial out-of-plane imperfection of plate elements;

6) various edge restraints provided by beam flanges and interaction between flange and web elements.

Mathematical difficulties arising from the nature of complex stress field associated with this problem prohibit an exact solution. Many researchers have attempted to use the numerical approximation methods such as finite element and finite strip to predict the ultimate web crippling load. During 1968 to 1972, the buckling problem of plate girder webs subjected to partial edge loading was studied by Rockey, Bagchi and El-gaaly.[29-32]

In 1968, Rockey and Bagchi[29] used the finite element technique to find the elastic buckling load of plate girder webs with transverse stiffeners subjected to partial edge loading. The flange was modeled by beam-elements having flexural and torsional properties while plate-elements were used for the web plate. The critical load was determined by using the concept that the second partial derivative of the total energy expression with respect to the nodal displacements is zero at the point of instability.

Later in 1972, Rockey, El-gaaly and Bagchi combined the problem of shear loading and in-plane bending moment to the problem of buckling of web plate under patch loading supported at both ends by shear forces. They found that the presence of either the additional in-plane moment or shear would reduce the critical buckling load.

The finite strip method is an alternative to the finite element method. The latter is relatively expensive especially for the localized

problem as web crippling which requires large numbers of small elements. However, the finite strip method is restricted only to simple loading cases due to its nature of formulation. In 1978, Graves Smith and Sridharan[33] developed a finite strip computer program to predict the elastic buckling load of plate structures under arbitrary edge loading. They gave the examples of a web plate under partial edge loading and a box girder under partial web loading (Fig. 2.6). The results show that the elstic buckling load of the latter case is about 50% higher than the case of simulated square plate with all four sides simply supported. This indicates the stiffening effect of the flanges.

The geometric nonlinear analysis of prismatic thin-walled members using the finite strip method was presented by Gierlinski and Graves Smith[34] in 1984. The theory was based on the moderately large displacement assumption and can be applied in particular to problems containing load maxima.

Recently, Lee, Harris, and Hsu[35] developed a nonlinear finite element computer program to analyze thin-walled structural members. The program has the capability of handling both geometric and material nonlinearities so that the post buckling behavior and ultimate strength of members can be predicted. In this study, Marguerre's shallow shell theory was adopted for the strain-displacement relationships. A bending-membrane element with six degrees of freedom at each node forms the type of element used in this program. They suggested that the finite element program of this type may be able to handle the problem of web crippling of cold-formed steel beams.

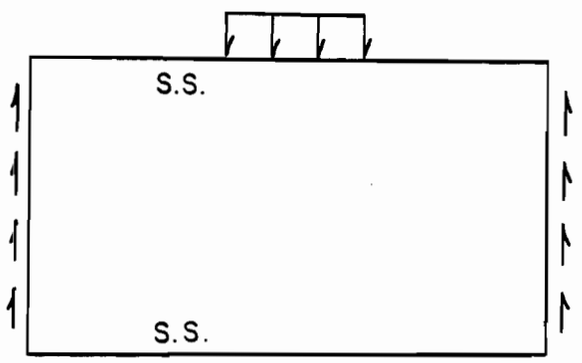

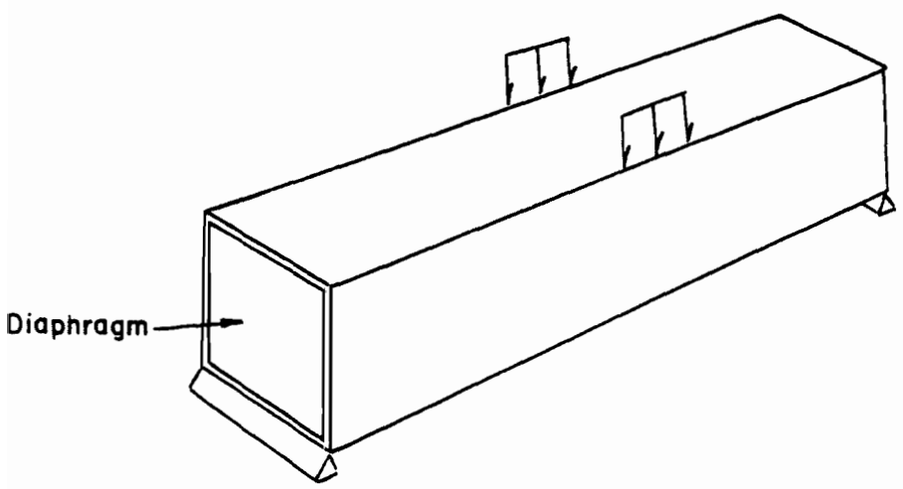

Fig. 2.6 Web Plate under Partial Edge Loading and Box Girder under Web Loading[33]

C. EXPERIMENTAL STUDY

Due to the mathematical difficulties encountered in a solution for web crippling load, the current design criteria are based on the experimental study of various shapes of cold-formed steel members.

In 1935, Lyse and Godfrey[36] performed the experimental study on web crippling strength of hot-rolled I-beams. They reported that the maximum bearing stress in the web under the concentrated load can be computed by:

$$f_p = R/(t(N + 2k)) \tag{2.8}$$

where f_p = Bearing stress

R = Applied load

k = Distance from outer face of the flange to web toe of fillet of the rolled section

Equation (2.8) is now being used by AISC in the specification for the design of hot-rolled beams and welded plate girders.[37]

During the 1940s and 1950s, experimental work on web crippling of cold-formed steel beams was investigated at Cornell University by Winter, Pian and Zetlin.[24,38-40] In the first phase of that study, I-beams, which provide a high degree of restraint against rotation, were tested under various loading conditions. The test results showed that the ultimate web crippling loads of I-beams depend primarily on the ratio N/t and the yield strength of material, F_y.

In the second phase of their investigation, cold-formed steel beams having single unreinforced webs (such as hat sections, channels, Z-sections and rectangular tubes) were studied. It was found that the ratios N/t, R/t, h/t and the yield strength, F_y, are the main parameters that control the ultimate web crippling loads for these types of sections.

Empirical expressions were derived on the basis of the Cornell research findings for predicting the ultimate web crippling loads for each type of sections. These formulas were used as a basis for the design criteria in early editions of the AISI Specification[4] and the 1981 Guide.[3]

The provisions of the 1980 and 1986 Editions of the AISI Specification[5,6] for the design of cold-formed steel beam webs subjected to web crippling were modified from the 1968 Edition. The modifications were based on the original Cornell study and the additional research work conducted by Hetrakul and Yu[41] at the University of Missouri-Rolla. The classification of loading conditions is based on the values of Z and e (Fig. 2.7), where Z is the distance between the edge of the bearing plate of a reaction or a concentrated load and the free end of the beam, and e is the distance between the edges of the adjacent opposite bearing plates of concentrated loads or reactions.

The following four loading conditions are classified in the 1980 and 1986 Editions of the AISI Specification:[42,43]

1. Interior one-flange loading (IOF): $Z \geq 1.5h$ and $e \geq 1.5h$
2. End one-flange loading (EOF): $Z < 1.5h$ and $e \geq 1.5h$
3. Interior two-flange loading (ITF): $Z \geq 1.5h$ and $e < 1.5h$
4. End two-flange loading (ETF): $Z < 1.5h$ and $e < 1.5h$

The classification of these four loading conditions is illustrated in Fig. 2.7. According to the above four loading conditions, there is a discontinuity between different equations when the value of Z/h or e/h is 1.5. In 1984, Lin[44] conducted an experimental investigation to study this problem by disregarding the clearance limit of 1.5h. It was found that the ratios of Z/h and e/h are not the only factors that control the

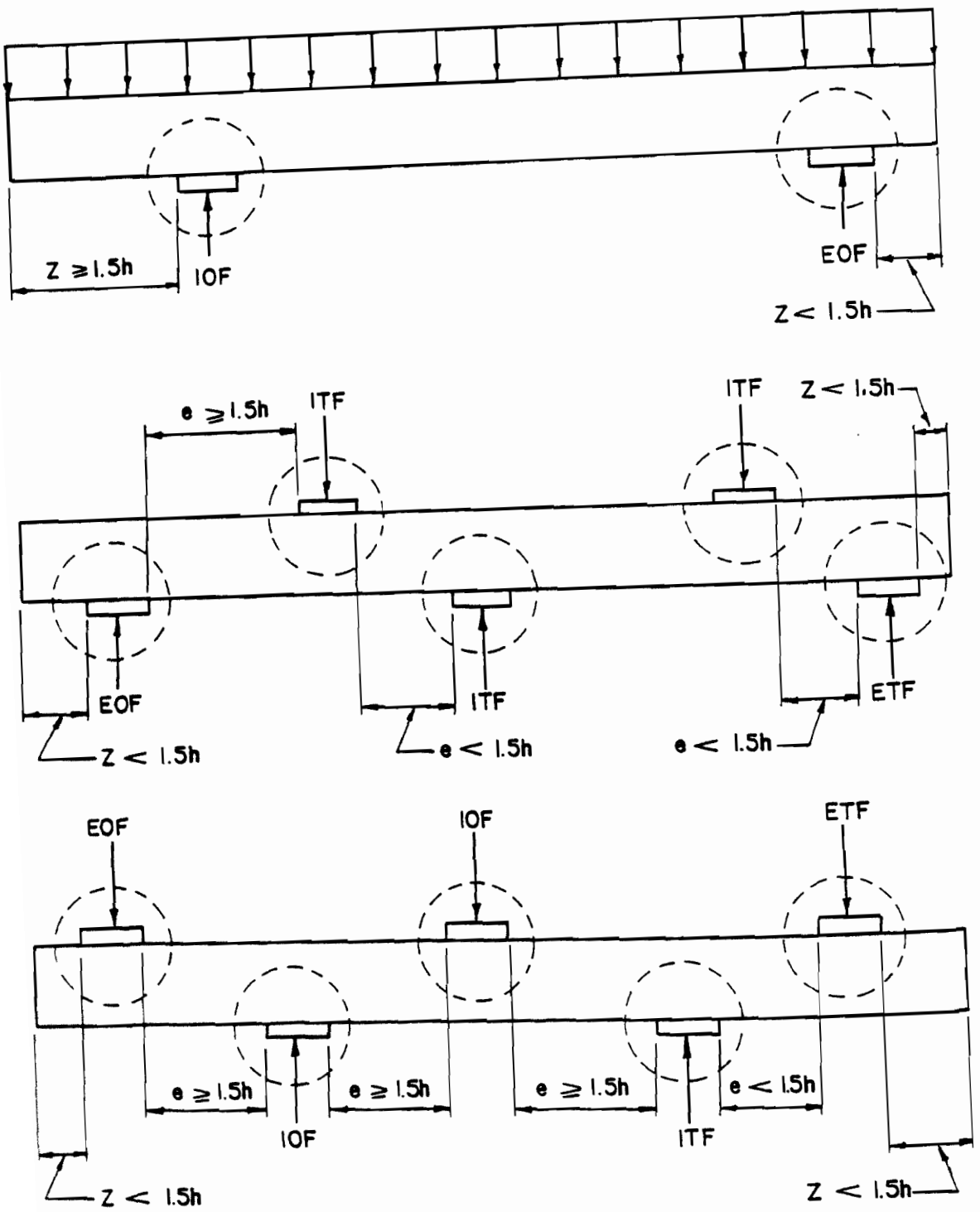

Fig. 2.7 Classification of Loading Conditions for Web Crippling in the 1980 and 1986 Editions of the AISI Specifications

type of web crippling failure. He noted that some of the specimens failed by buckling in the webs and developed the equations to predict the ultimate loads for this type of failure.

In 1969, Rockey, El-gaaly and Bagchi[31] conducted a series of tests to obtain an empirical relationship between the ultimate load capacity of a panel and its buckling load. The post-buckling strength represented by the ratio of P_u/P_{cr} was evaluated. The relationship between P_u/P_{cr}, N/L and h/t was found to be:

$$P_u/P_{cr} = (4.5 + 6.4(N/L))(h/t)x10^{-3} \tag{2.9}$$

In the above equation, P_{cr} is the theoretical elastic buckling load and P_u is the tested ultimate load.

In Sweden, Baehre[45] has performed some experiments on hat sections with trapezoidal profiled sheets. He concluded that for the reaction of interior support or concentrated load located anywhere on the span provided that the reaction or load is at least a distance of 1.5h from the end of the member, the ultimate load can be computed by

$$P_{ult} = 1.8F_y t^2(2.8-(F_y/50))(1-0.1\sqrt{R/t})(1+0.01(N/t))(2.4+(\theta/90))^2 \tag{2.10}$$

In Eq. (2.10), θ is the angle between the plane of web and the plane of bearing surface, in degrees. It was noticed by Baehre that the depth to thickness ratio, h/t, has little or no effect on the ultimate web crippling load for this group of specimens. He also found that when the ratio of the applied moment to the ultimate moment capacity of the section was less than 0.3, the bending moment had little or no effect on the ultimate web crippling load.

Equation (2.10) was modified to make it applicable to aluminum sections, as recommended by the 1978 Swedish Code:[46]

$$P_{ult} = 1.8t^2\sqrt{EF_y}(1-0.1\sqrt{R/t})(1+0.01(N/t))(2.4+(\theta/90))^2. \quad (2.11)$$

In the current European Recommendations (ECCS-1983)[47], the N/t function in Eq. (2.12) was modified and the new eqution becomes

$$P_{ult} = 0.15t^2\sqrt{EF_y}(1-0.1\sqrt{R/t})(0.5+\sqrt{0.002(N/t)})(2.4+(\theta/90))^2 \quad (2.12)$$

In 1981, Wing and Schuster[48] performed an experimental investigation on the problem of web crippling of cold-formed steel decks having multi-webs. They derived some empirical equations based on their research findings by using the similar form of equations as used in the 1980 AISI Specification but the constants are slightly different.

All of the previously mentioned experimental studies were conducted on sections using yield strengths in the range from 30 to 55 ksi. In 1982, Levy[10] performed a series of flexural tests of hat sections with material yield strengths up to 190 ksi. The results of tests were evaluated by Errera[9]. It was found that the design criteria for web crippling included in the AISI Guide and the 1980 Edition of the Specification are not applicable to those sections formed from very high strength materials.

D. CURRENT DESIGN CRITERIA

As discussed earlier, the theoretical analysis of web crippling is extremely complicated. The equations presently used in various

specifications to predict the web crippling loads of cold-formed steel beams are empirical expressions. The existing design standards used in the United States and some other countries are reviewed as follows:

1. United States:

As stated in Section I, the 1981 Guide is based primarily on the 1968 Edition of the AISI Specification. The 1980 and 1986 Editions of the AISI Specification include the same requirements for preventing web crippling. The following reviews of the AISI 1981 Guide and the 1980 and 1986 Specification are based on the ultimate web crippling strengths without applying any factor of safety:

a. AISI 1981 Guide for Preliminary Design of Sheet Steel Automotive Structural Components:[3] According to Section 3.4.7 of the 1981 Guide, the ultimate strength of unreinforced beam webs subjected to concentrated loads or reactions can be estimated as follows:

(1) Beams Having Single Unreinforced Webs: The following design equations apply to sections with inside corner radii up to 4t:

For end reactions or for concentrated loads on outer ends of cantilevers:

$$P_u = t^2(2.13-0.28(R/t))(98+4.20(N/t)-0.022(N/t)(h/t)-0.011(h/t))(1.33-0.33(F_y/33))(F_y/33) \quad (2.13)$$

For reactions of interior supports or for concentrated loads located on the span:

$$P_u = t^2(1.96-0.11(R/t))(305+2.30(N/t)-0.009(N/t)(h/t)-0.5(h/t))(1.22-0.22(F_y/33))(F_y/33) \quad (2.14)$$

(2) I-Beams: For I-beams or sections which provide a high degree of restraint against rotation of the webs:

For end reactions or for concentrated loads on outer ends of cantilevers:

$$P_u = t^2 F_y (10+1.25\sqrt{N/t}) \tag{2.15}$$

For reactions of interior supports or for concentrated loads located on the span:

$$P_u = t^2 F_y (15+3.25\sqrt{N/t}) \tag{2.16}$$

In the above formulas,

P_u = ultimate capacity against crippling for one solid web connecting top and bottom flanges, kips

t = web thickness, in.

N = actual length of bearing or "h", whichever is smaller, in.

h = distance between flanges, in.

R = Inside bend radius, in.

In addition, according to Addendum No. 2 of the 1968 Specification, the following interaction equation may be used to calculate the ultimate load to prevent failures caused by the combination of bending and web crippling:

$$(P/P_c) + (M/M_u) \leq 1.3 \tag{2.17}$$

where P = concentrated load or reaction, kips

P_c = ultimate web crippling load in the absence of bending moment, kips

M = applied bending moment at or immediately adjacent to the point of application of the concentrated load or reaction, kip-in.

M_u = ultimate bending moment if a bending moment only exists, kip-in.

It should be noted that there was no design expression for the interaction of bending and web crippling for I-beams in the 1968 Specification.

b. AISI 1980 and 1986 Specification for the Design of Cold-Formed Steel Structural Members:[5,6] According to Section 3.5.1 of the 1980 Specification and Section C3.4 of the 1986 Specification, the ultimate strength for web crippling of unreinforced flat webs of flexural members can be determined by the formulas given below. These formulas apply to beams when $R/t \leq 6$ and to decks when $R/t \leq 7$, $N/t \leq 210$, and $N/h \leq 3.5$.

(1) Beams Having Single Unreinforced Webs: The following design equations apply to sections with single unreinforced webs:

At locations of one concentrated load or reaction acting either on the top or bottom flange, when the clear distance between the bearing edges of this and adjacent opposite concentrated loads or reactions is greater than 1.5h, the ultimate web crippling load is determined by using Eqs. (2.18), (2.19), or (2.20).

For reactions or for concentrated loads on outer ends of cantilevers when the distance from the edge of bearing to the end of the beam is less than 1.5h (EOF):

For stiffened flanges:

$$P_c = 1.85t^2(F_y/33)(1.33-0.33(F_y/33))(1.15-0.15(R/t))$$
$$(179-0.33(h/t))(1+0.01(N/t))(0.7+0.3(\theta/90)^2) \qquad (2.18)$$

For unstiffened flanges:

$$P_c = 1.85t^2(F_y/33)(1.33-0.33(F_y/33))(1.15-0.15(R/t))$$
$$(117-0.15(h/t))(1+0.01(N/t))(0.7+0.3(\theta/90)^2) \qquad (2.19)$$

When $N/t > 60$, the factor $(1+0.01(N/t))$ in Eq. (2.19) may be increased to $(0.71+0.015(N/t))$.

For reactions of interior supports or for concentrated loads when the distance from the edge of bearing to the end of the beam is equal to or larger than 1.5h (IOF):

$$P_c = 1.85t^2(F_y/33)(1.22-0.22(F_y/33))(1.06-0.06(R/t))$$
$$(291-0.40(h/t))(1+0.007(N/t))(0.7+0.3(\theta/90)^2) \qquad (2.20)$$

When $N/t \geq 60$, the factor $(1+0.007(N/t))$ in Eq. (2.20) may be increased to $(0.75+0.011(N/t))$.

At locations of two opposite concentrated loads or of a concentrated load and an opposite reaction acting simultaneously on the top and bottom flanges, when the clear distance between their adjacent bearing edges is equal to or less than 1.5h, the ultimate web crippling load is determined by using Eq. (2.21) or (2.22).

For reactions or for concentrated loads on outer ends of cantilevers when the distance from the edge of bearing to the end of the beam is less than 1.5h (ETF):

$$P_c = 1.85t^2(F_y/33)(1.33-0.33(F_y/33))(1.15-0.15(R/t))$$
$$(132-0.31(h/t))(1+0.01(N/t))(0.7+0.3(\theta/90)^2) \qquad (2.21)$$

For reactions of interior supports or for concentrated loads when the distance from the edge of bearing to the end of the beam is equal to or larger than 1.5h (ITF):

$$P_c = 1.85t^2(F_y/33)(1.22-0.22(F_y/33))(1.06-0.06(R/t))$$
$$(471-1.22(h/t))(1+0.0013(N/t))(0.7+0.3(\theta/90)^2) \qquad (2.22)$$

(2) I-Beams: For I-beams made of two channels connected back to back or for similar sections which provide a high degree of restraint against rotation of the web, such as I-sections made by welding two angles to channels:

At locations of one concentrated load or reaction acting either on the top or bottom flange, when the clear distance between the bearing edges of this and adjacent opposite concentrated loads or reactions is greater than 1.5h, the ultimate web crippling load is determined by using Eq. (2.23) or (2.24).

For reactions or for concentrated loads on outer ends of cantilevers when the distance from the edge of bearing to the end of the beam is less than 1.5h (EOF):

$$P_c = 2.0t^2F_y(1+(h/t)/750)(5.0+0.63\sqrt{N/t}) \qquad (2.23)$$

When $h/t > 150$, a constant value of 1.20 should be used for the factor $(1+(h/t)/750)$ in Eq. (2.23).

For reactions of interior supports or for concentrated loads when the distance from the edge of bearing to the end of the beam is equal to or larger than 1.5h (IOF):

$$P_c = \frac{2.0t^2F_y(1.49-0.53(F_y/33))(0.88+0.12(t/0.075))}{(7.5+1.63\sqrt{N/t})} \quad (2.24)$$

The factor $(1.49-0.53(F_y/33))$ in Eq. (2.24) should not be less than 0.6.

At locations of two opposite concentrated loads or of a concentrated load and an opposite reaction acting simultaneously on the top and bottom flanges, when the clear distance between their adjacent bearing edges is equal to or less than 1.5h, the ultimate web crippling load is determined by using Eq. (2.25) or (2.26).

For reactions or for concentrated loads on outer ends of cantilevers when the distance from the edge of bearing to the end of the beam is less than 1.5h (ETF):

$$P_c = \frac{2.0t^2F_y((0.98-(h/t)/865)/(F_y/33))(0.64+0.31(t/0.075))}{(5.0+0.63\sqrt{N/t})} \quad (2.25)$$

For reactions of interior supports or for concentrated loads when the distance from the edge of bearing to the end of the beam is equal to or larger than 1.5h (ITF):

$$P_c = \frac{2.0t^2F_y((1.10-(h/t)/665)/(F_y/33))(0.82+0.15(t/0.075))}{(7.5+1.63\sqrt{N/t})} \quad (2.26)$$

The factor ((1.10-(h/t)/665) in Eq. (2.26) should not be greater than 1.

(3) Combined Bending and Web Crippling: Section 3.5.2 of the 1980 Specification and Section C3.5 of the 1986 Specification provide design requirements for unreinforced flat webs of shapes subjected to a combination of bending and reaction or concentrated load for allowable stress design. The following requirements should be used for ultimate strength approach:

For Shapes having single webs:[28,47]

$$1.07(P/P_c) + (M/M_u) \leq 1.42. \quad (2.27)$$

For I-beams or similar sections which provide a high degree of restraint against rotation of the web:[28,47]

$$0.82(P/P_c) + (M/M_u) \leq 1.32 \quad (2.28)$$

In the above formulas,

P = concentrated load or reaction, kips

P_c = ultimate web crippling load in the absence of bending moment, kips

M = applied bending moment at or immediately adjacent to the point of application of the concentrated load or reaction, kip-in.

M_u = ultimate bending moment if bending moment only exists, kip-in.

It should be noted that the methods for calculating bending moment of the web in the 1980 and the 1986 Specifications are different. In the 1980 Specification, the limited maximum bending stress approach is used while the effective web depth approach is used in the 1986 Specification. In addition, the definitions of "h" are different in these two editions of the AISI Specification.

2. Canada:

The present Canadian Standard, "Cold Formed Steel Structural Members" (CAN3-S136-M84),[49] is written in the form of limit states with SI units. In this review, all equations are converted to the form of ultimate capacity with U.S. customary units for the convenience of comparison.

The provisions for the design of cold-formed steel beams subjected to web crippling in this Standard are classified by three types of cross sections as follows:

1) I-beams

2) Shapes having single webs (channels and Z-sections, etc.)

3) Deck sections having multi-webs

The design equations used for the first two categories (a and b) are the same as those included in the 1980 and 1986 editions of the AISI Specification. However, for deck sections having multi-webs, the Canadian Standard uses different design criteria to determine the ultimate web crippling load.

According to Section 6.4.7 of the present Canadian Standard,[49] the ultimate web crippling loads of deck sections when $R/t \leq 10$, $N/t \leq 200$, and $N/h \leq 2$ can be determined as follows:

At locations of one concentrated load or reaction acting either on the top or bottom flange, when the clear distance between the bearing edges of this and adjacent opposite concentrated loads or reactions is greater than 1.5h

For reactions or for concentrated loads on outer ends of cantilevers when the distance from the edge of bearing to the end of the beam is less than 1.5h (EOF):

$$P_c = 10t^2F_y(\sin\theta)(1-0.1(F_y/33))(1-0.1\sqrt{R/t})(1+.005(N/t))(1-.002(h/t)) \quad (2.29)$$

For reactions of interior supports or for concentrated loads when the distance from the edge of bearing to the end of the beam is equal to or larger than 1.5h (IOF):

$$P_c = 18t^2F_y(\sin\theta)(1-0.1(F_y/33))(1-0.075\sqrt{R/t})$$
$$(1+.005(N/t))(1-.001(h/t)) \qquad (2.30)$$

At locations of two opposite concentrated loads or of a concentrated load and an opposite reaction acting simultaneously on the top and bottom flanges, when the clear distance between their adjacent bearing edges is equal to or less than 1.5h

For reactions or for concentrated loads on outer ends of cantilevers when the distance from the edge of bearing to the end of the beam is less than 1.5h (ETF):

$$P_c = 10t^2F_y(\sin\theta)(1-0.1(F_y/33))(1-0.1\sqrt{R/t})$$
$$(1+.01(N/t))(1-.002(h/t)) \qquad (2.31)$$

For reactions of interior supports or for concentrated loads when the distance from the edge of bearing to the end of the beam is equal to or larger than 1.5h (ITF):

$$P_c = 18t^2F_y(\sin\theta)(1-0.2(F_y/33))(1-0.03\sqrt{R/t})$$
$$(1+.01(N/t))(1-.0015(h/t)) \qquad (2.32)$$

For combined bending and web crippling, the Canadian Standard recommends the same equation as that of the AISI 1968 Specification (Eq. (2.17)).

3. Europe:

In the present European Recommendations (ECCS-1983),[47,50] the web crippling load is predicted by the following equation:

$$P_c = 0.15t^2\sqrt{EF_y}(1-0.1\sqrt{R/t})(0.5+\sqrt{.02(N/t)})$$
$$(2.4+(\theta/90)^2). \qquad (2.33)$$

The above equation is applicable to concentrated load or reaction located at least a distance 1.5h from the end of a member. If the distance is less than 1.5h, the design load of a single web shall be taken as one half the value computed by Eq. (2.33). The equation is limited to $R/t < 10$ and $\theta > 50$.

4. Other Countries:

The design provisions for web crippling used in the design specifications and recommendations issued in Australia,[51] India,[52] the Republic of South Africa,[53] and the United Kingdom[54] were also studied. It was found that the design procedures are based on the same equations used in the AISI 1981 Guide[3] reviewed in Article D.1.a.

III. EXPERIMENTAL INVESTIGATION

A. GENERAL

As pointed out in Section I, the current available design criteria for cold-formed steel beams subjected primarily to web crippling and a combination of web crippling and bending are intended for application with sections fabricated from materials with yield strengths up to 80 ksi. These empirical equations are based on the test results of sections cold-formed from materials having the range of yield strengths from 30 to 57 ksi. In order to verify the adequacy of these equations for sections using very high strength materials, an additional experimental study was recommended by the AISI Task Force on Structural Research of the Transportation Department.

The objective of this experimental investigation has been to determine the ultimate web crippling loads for sections formed from high strength materials in order to extend the range of material yield strengths beyond the present limitation of the AISI design criteria. In this phase of investigation, 150 hat sections and 96 I-beams fabricated from five different types of sheet steels (80DK, 80XF, 100XF, 140XF and 140SK)[55] were tested for the following four basic loading conditions:

1) Interior one-flange loading (IOF)

2) End one-flange loading (EOF)

3) Interior two-flange loading (ITF)

4) End two-flange loading (ETF)

In addition, 18 tests of hat sections were performed for the transitions between the four basic loading conditions. The results of

these tests were used to eliminate the problem of discontinuity between the basic equations to predict the ultimate web crippling loads for each type of loading conditions.

All tests were performed in the 120,000 pound Tinius Olsen universal testing machine (Fig. 3.1) located in the Engineering Research Laboratory of the University of Missouri-Rolla. The materials used in this study included hot-rolled and cold-rolled sheet steels having yield strengths ranging from 58.2 to 165.1 ksi.

The mechanical properties of the sheet steels used to form the specimens were studied in detail in Phase I of this research project.[14,56,57] The preliminary study (Phase I) of this program included a review of the literature on automotive structures, a study of the mechanical properties for a selected group of high strength sheet steels, and a critical review of various AISI Specifications for the design of cold-formed steel members. Table 3.1 gives the average values of mechanical properties (longitudinal tension) and thicknesses of all sheet steels used in this experimental investigation. The typical stress-strain curves for longitudinal tension of these materials are shown in Fig. 3.2. For other mechanical properties (longitudinal compression, transverse tension, and transverse compression) and stress-strain relationships, see Refs. 14, 56, and 57.

B. TEST SPECIMENS

Hat sections, as shown in Fig. 3.3, were used for the study of sections with single unreinforced webs while I-beams (Fig. 3.4) were used as sections that provide a high degree of restraint against rotation of the webs. Three different profiles for each type of cross sections were designed for each type of materials as presented in Tables 3.2a and 3.2b.

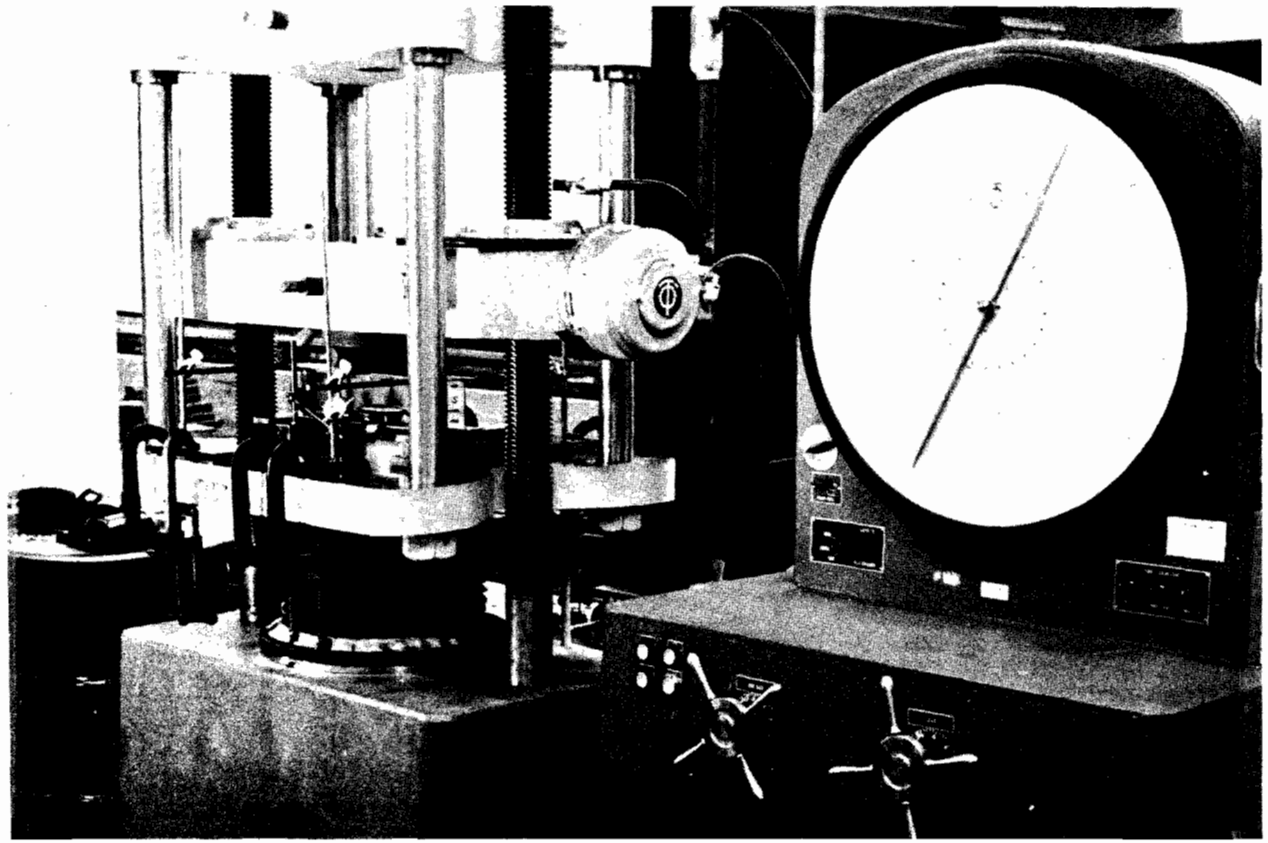

Fig. 3.1 Tinius Olsen Universal Testing Machine

Table 3.1

Material Properties* and Thicknesses of Sheet Steels Used in the Experimental Study[14,56,57]

Material	F_y (ksi)	F_u (ksi)	Elongation** (%)	t (in.)
80DK	58.2	87.6	25.7	0.048
80XF	88.3	98.7	22.8	0.082
100XF	113.1	113.1	8.1	0.062
140XF	141.2	141.2	4.4	0.047
80DK***	58.2	86.6	24.8	0.047
80XF***	77.1	89.1	20.4	0.088
100XF***	116.9	116.9	10.1	0.065
140SK***	165.1	176.2	4.3	0.046

* Material properties are based on the average longitudinal tension tests. For other material properties, see Refs. 14, 56, and 57.

** Elongation was measured over a 2-in. gage length.

*** Second set of sheet steels.

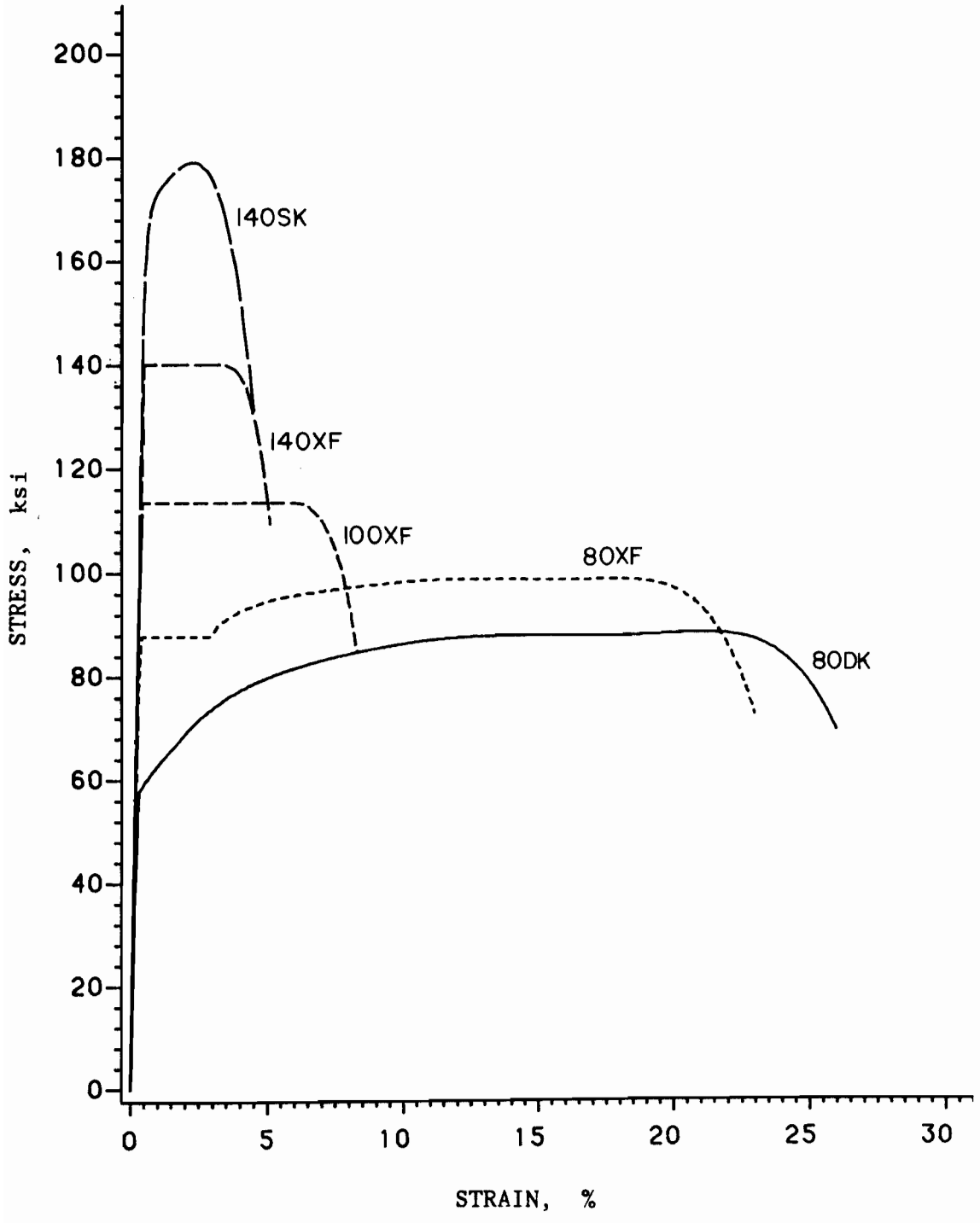

Fig. 3.2 Typical Stress-Strain Curves of Five Sheet Steels in Longitudinal Tension[14,56,57]

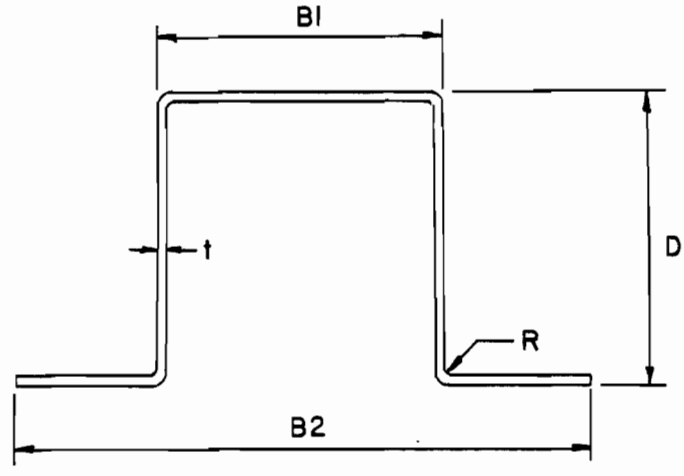

Fig. 3.3 Hat Sections Used in the Experimental Study

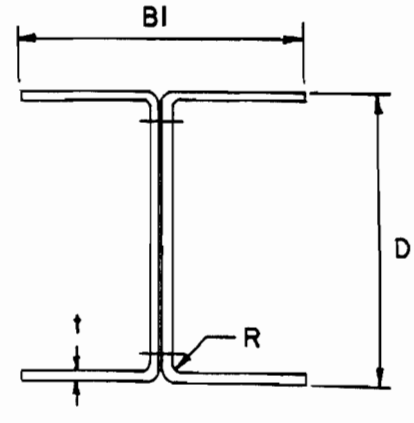

Fig. 3.4 I-Beams Used in the Experimental Study

Table 3.2a

Nominal Dimensions of Hat Sections Designed for Experimental Study

Profile No.	B1 (in.)	B2 (in.)	D1 (in.)	R (in.)
1	3.0	6.0	3.0	0.25
2	4.0	8.0	4.0	0.25
3	5.0	10.0	5.0	0.25

Note: See Fig. 3.3 for definitions of symbols.

Table 2b

Nominal Dimensions of I-Beams Designed for Experimental Study

Profile No.	B1 (in.)	D1 (in.)	R (in.)
1	3.0	3.0	0.25
2	4.0	4.0	0.25
3	5.0	5.0	0.25

Note: See Fig. 3.4 for definitions of symbols.

Because all specimens were formed by a press-braked operation, there was little or no cold working effect on mechanical properties except at the corners. Hat sections were braced by 1/8 x 3/4 in. rectangular bars at appropriate locations for each type of loading conditions to prevent the webs from spreading during the tests.

All I-beam specimens were fabricated from two identical channels connected back to back with an aid of self tapping screws (14 x 3/4 Tek screws) at a distance of 1/2 in. from top and bottom flanges. The self tapping screws were spaced along the beam length at a constant distance of 2 in. from center to center. The screws were driven from alternate sides of the webs in order to minimize the initial deformations.

The measured dimensions of test specimens and the important parameters used in calculations are presented in Appendix A.

C. TEST PROCEDURES

All specimens were loaded to failure. During the test, loads were applied slowly at an increment of approximately 15% of the expected ultimate loads and maintained constant at each load level for about 5 minutes.

Lateral deformations of the webs of hat sections at the location of expected failure were measured. The lateral movements were measured at several points with 1/2 in. spacing along the vertical center line of the bearing plate by an LVDT. Readings were taken at each load level. For I-beam specimens, there was no lateral movement of the webs until the ultimate loads were reached.

Vertical movement of the bearing plate, by which the load was applied, was recorded at each step to detect the load and time at which the bearing plate started to penetrate into the web.

Vertical strain distribution in the web under or above the bearing plate was also investigated by attaching strain gages to some of the hat sections. For each of the specimens studied, three pairs of strain gages were attached back to back vertically along a horizontal line with a distance of 1/4 in. from the center of the gages to the web-flange junction. Figures 3.5a and 3.5b show the locations of strain gages under interior bearing plate and above end bearing plate, respectively.

Details of the test arrangement for each loading condition are summarized as follows:

1. Hat Sections:

The number of specimens and the test arrangement for each case of the loading conditions are discussed as follows:

a. Interior One-Flange Loading (IOF): A total of 72 hat sections were tested as simply supported flexural members subjected to a concentrated load between end supports. The test arrangement and the test setup are shown in Figs. 3.6a and 3.7, respectively. Half of the specimens were loaded at mid-span with the clear distance between the opposite bearing plates (e_1 and e_2) of 1.5h. The remaining 36 specimens were tested under unsymmetric loading with e_1 varied from 0.75h to 1.25h and e_2 varied from 2.25h to 1.75h, accordingly.

For all tests, two 4-in. bearing plates were used at both ends and a 2-in. bearing plate was under the applied concentrated load. All specimens were braced by 1/8 x 3/4 in. rectangular bars at 1/3 points of the beam length to maintain the shape of the cross sections during the test. In order to prevent the end failure from happening before the desired interior failure to develop, wood blocks were inserted at both ends of the beams.

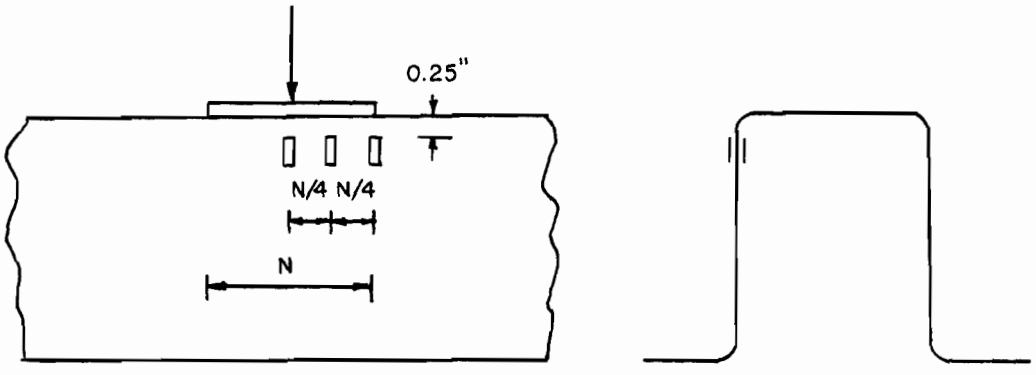

(a)

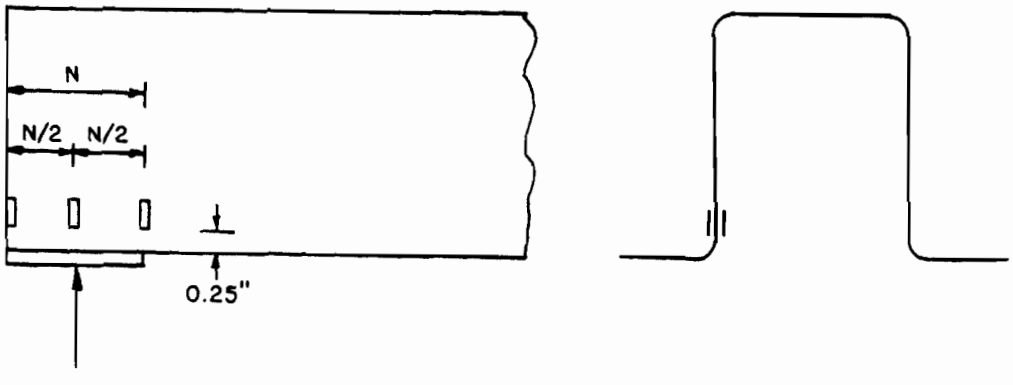

(b)

Fig. 3.5 Location of Strain Gages

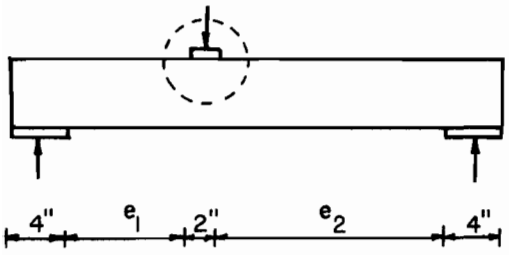

a) Interior One-Flange Loading (IOF)

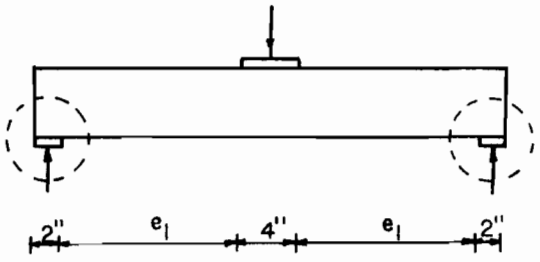

b) End One-Flange Loading (EOF)

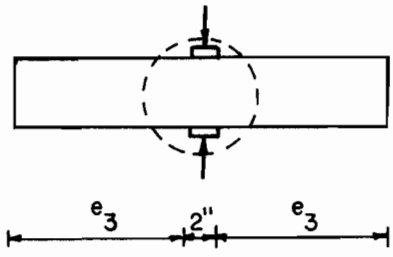

c) Interior Two-Flange Loading (ITF)

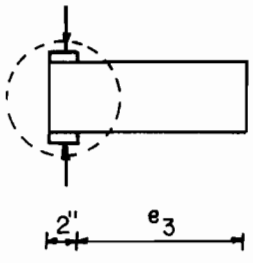

d) End Two-Flange Loading (ETF)

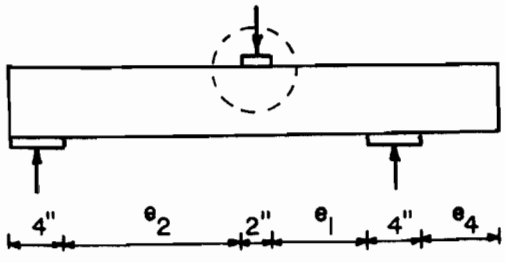

e) Transition between IOF and ITF

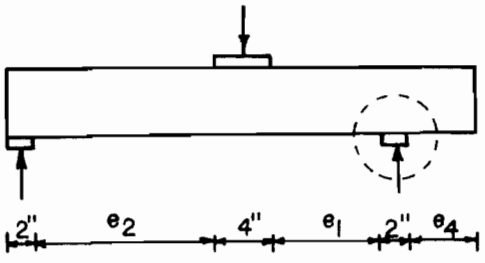

f) Transition between IOF and EOF

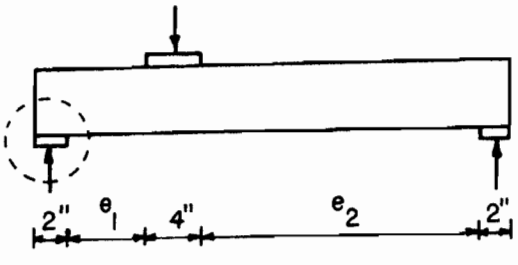

g) Transition between EOF and ETF

Note: All circles indicate regions of Failure

Fig. 3.6 Test Arrangements

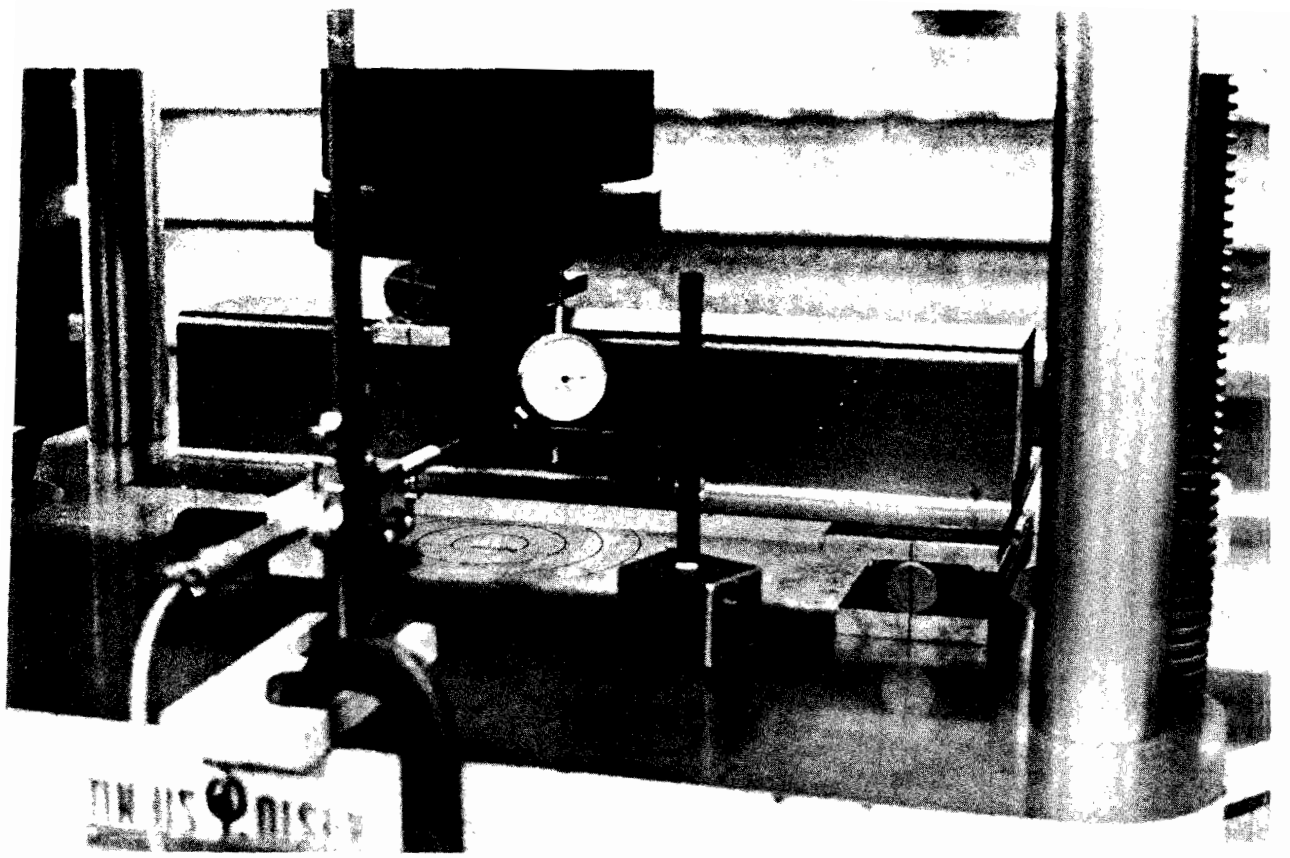

Fig. 3.7 Photograph of Test Setup for Interior One-Flange Loading of Hat Sections

b. End One-Flange Loading (EOF): All of the 30 specimens were tested as simply supported flexural members subjected to a concentrated load at mid-span (Figs. 3.6b and 3.8). As shown in Fig. 3.6b, two 2-in. bearing plates were used at both ends while a 4-in. bearing plate was under a concentrated load. The clear distances between the opposite bearing plates (e_1) were also designed to be 1.5h. Braces using rectangular bars were provided at the same location as in the previous case.

c. Interior Two-Flange Loading (ITF): A total of 24 hat sections were tested for this loading condition. Two 2-in. bearing plates were used in the middle of specimens for both top and bottom flanges. The designed clear distance between the edge of bearing plates to the end of the specimens, e_3, was 1.5h. Figures 3.6c and 3.9 show the test arrangement and the test setup, respectively. For this case, the bracing bars were attached at both ends of the specimens.

d. End Two-Flange Loading (ETF): The number of specimens and the test arrangement are the same as the ITF case except that the bearing plates were placed at one end of the beam (Fig. 3.6d) with the distance e_3 of 1.5h. At the unloaded end of the specimen, an elastic support was used to keep the specimen in a horizontal position during the test as can be seen in Fig. 3.10. One bracing bar was provided at the middle of the beam.

2. I-beams:

The pilot tests of I-beam specimens indicated that for the configurations used in this series of tests there was always a premature failure caused by the rotation of the flanges about the connection line for all loading conditions except for the case of IOF. Figure 3.11 shows

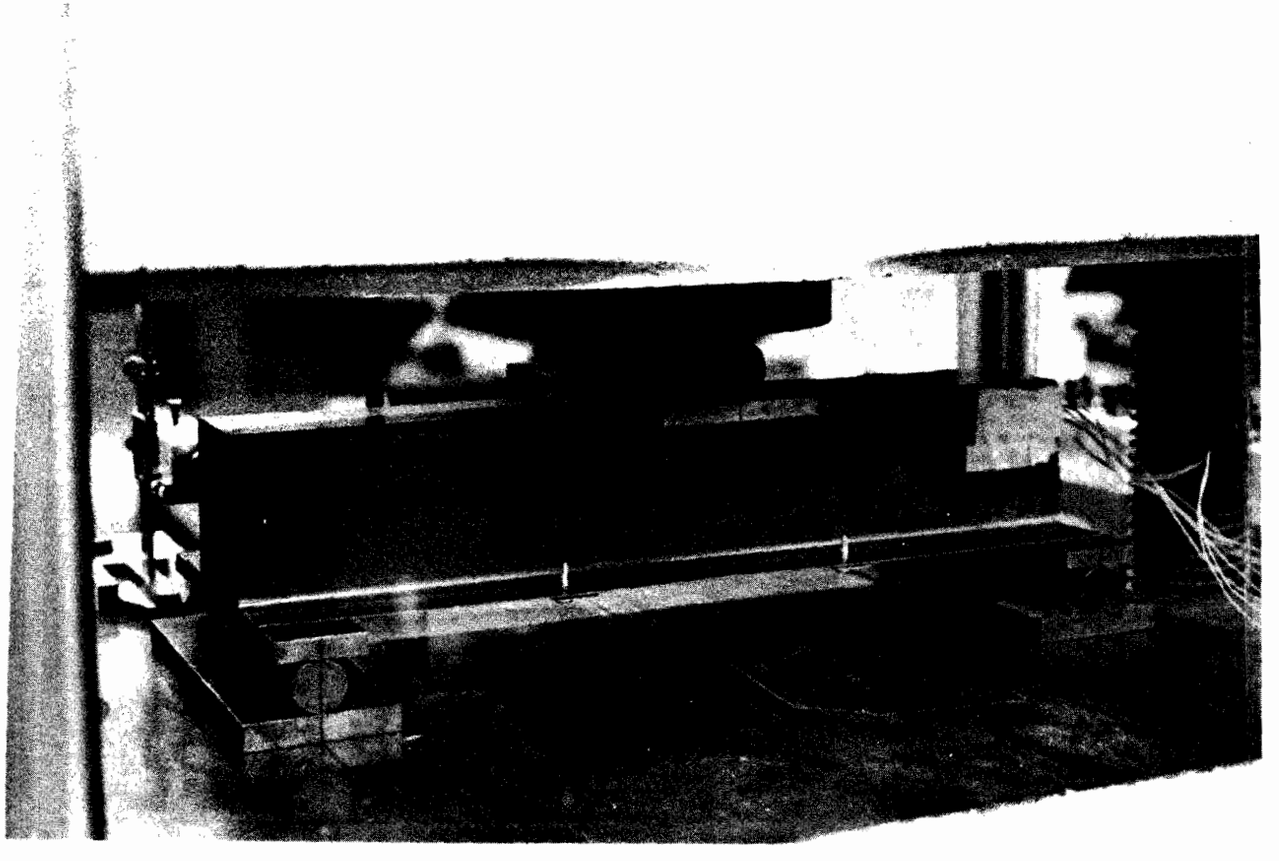

Fig. 3.8 Photograph of Test Setup for End One-Flange Loading of Hat Sections

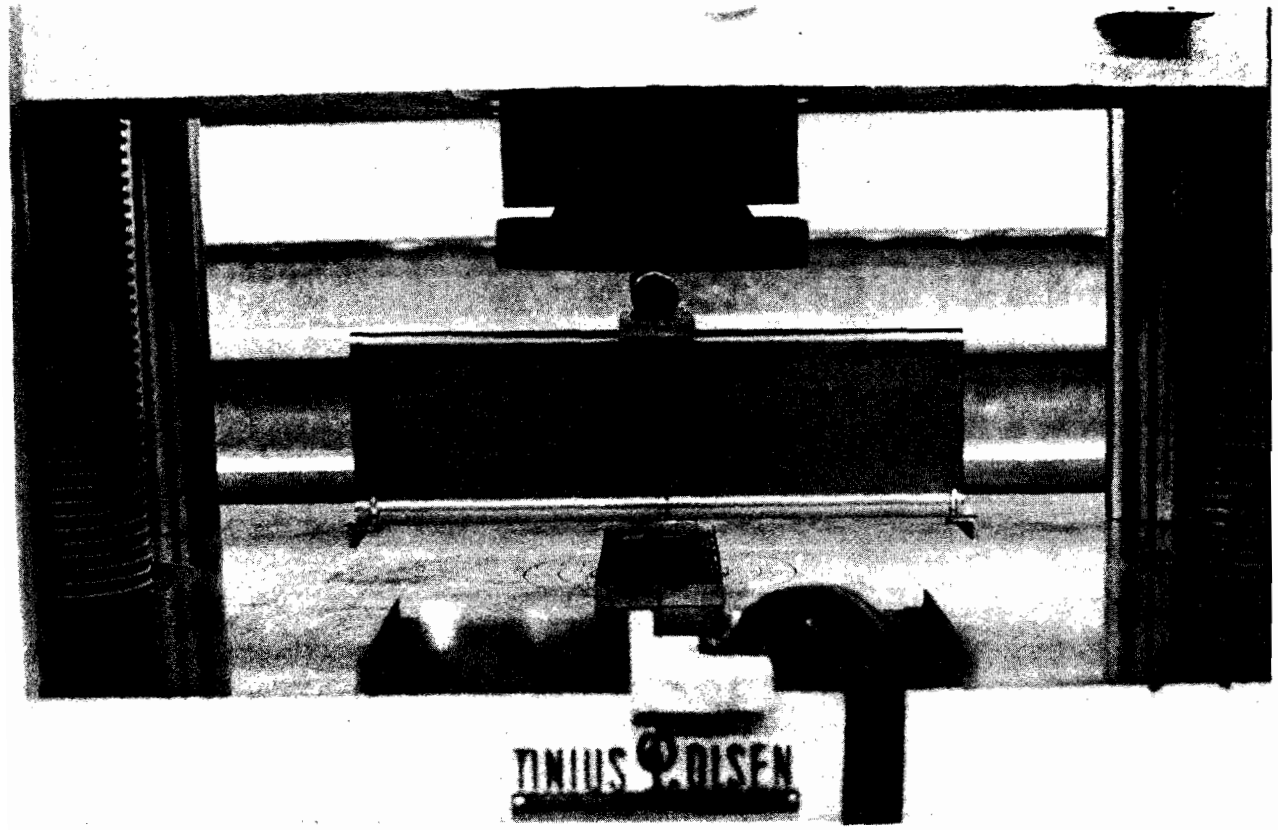

Fig. 3.9 Photograph of Test Setup for Interior Two-Flange Loading of Hat Sections

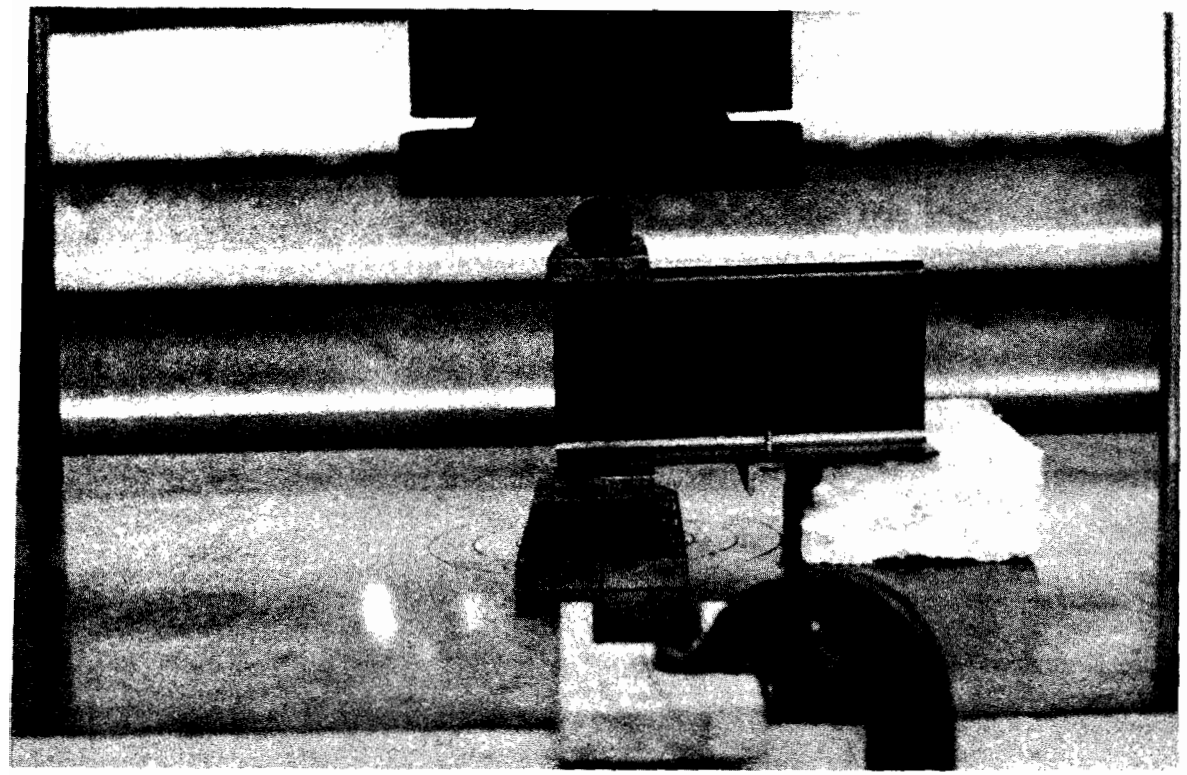

Fig. 3.10 Photograph of Test Setup for End Two-Flange Loading of Hat Sections

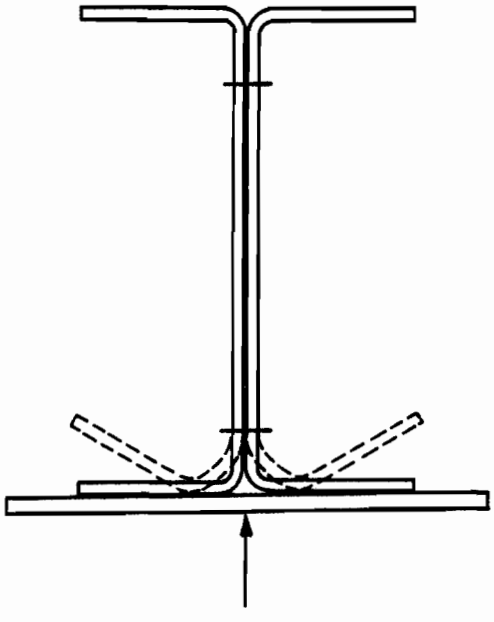

Fig. 3.11 Sketch Showing Bending Failure about Connection Line

a sketch of this type of failure. Apparently, the premature failure was caused by the thinness of material and the large bend radii, which is required for the high strength and low ductility sheet steels. This type of failure is also a function of the distance between the flange and connection line. The self tapping screws used in the fabrication of I-beam specimens were located at 1/2 in. from the flange which is the minimum clearance of the electric drill used to drive the screws. This failure mode occurred before web crippling could be developed in the webs. In order to prevent this type of premature failure, bearing plates were connected to flanges of I-beams by using machine bolts.

Because there were little, if any, lateral deformations observed in the web of I-beams prior to failure, therefore, only one stationary dial gage was set at the mid-depth of the web to determine the load under which web failure was observed. The number of specimens and the test arrangement for each type of loading conditions are discussed below:

a. Interior One-Flange Loading (IOF): A total of 24 I-beams were tested as flexural members with the same configurations as used for the case of hat sections under symmetric loading (Fig. 3.6a with $e_1 = e_2 = 1.5h$). The test setup is shown in Fig. 3.12. Wood blocks were also inserted at both ends of the beams to prevent the end failure.

b. End One-Flange Loading (EOF): Figure 3.13 shows the test setup for this case with bearing plates connected to the flanges by using machine bolts as discussed earlier. The number of specimens are the same as that of the IOF case. The test arrangement is shown in Fig. 3.6b with the distance e_1 of 1.5h.

c. Interior Two-Flange Loading (ITF): Similar as in the previous case, premature bending failure about the connection line

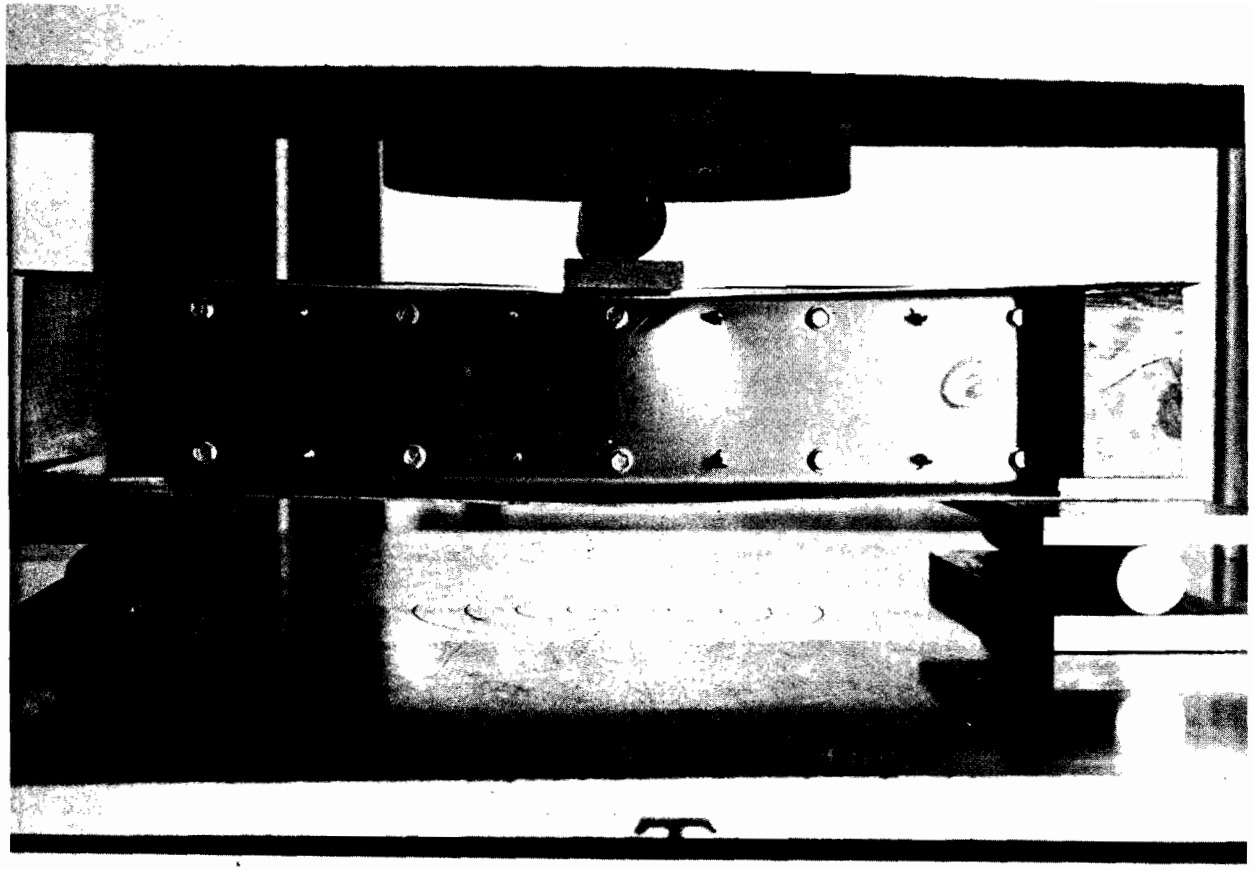

Fig. 3.12 Photograph of Test Setup for Interior One-Flange Loading of I-Beams

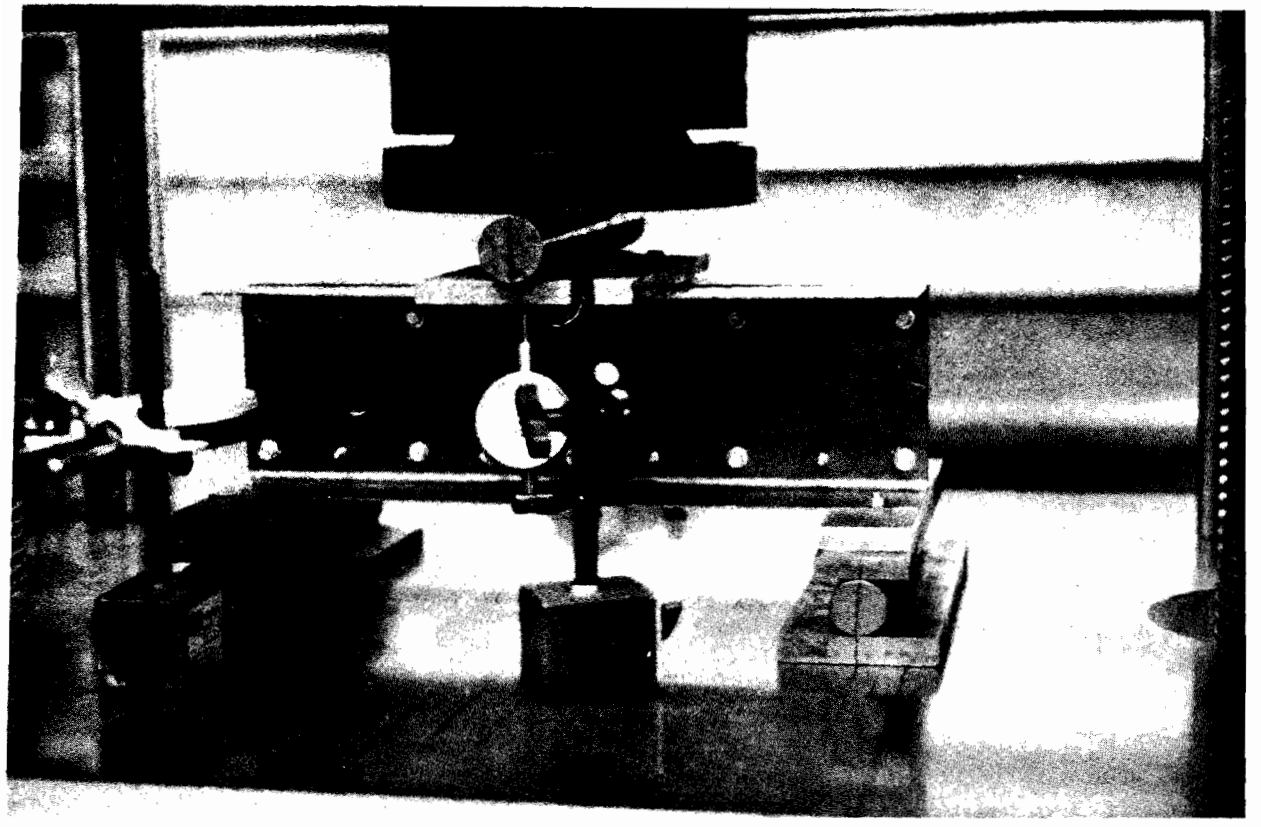

Fig. 3.13 Photograph of Test Setup for End One-Flange Loading of I-Beams

occurred before web crippling could be developed. All 24 tests were performed by using attached bearing plates (Fig. 3.14). The test arrangements are the same as that used for hat sections as shown in Fig. 3.6c (with $e_3 = 1.5h$).

d. End Two-Flange Loading (ETF): The number of specimens and the attched bearing plates are the same as that used for the ITF case. Figures 3.6d and 3.15 show the test arrangement and test setup for this case. The distance e_3 in Fig. 3.6d was also designed to be 1.5h.

3. Transition Tests:

A total of 18 hat sections were tested for the transition ranges between four basic loading conditions as follows:

a. Transition between IOF and ITF: Figure 3.6e shows the test arrangement for this case. It can be seen that the test setup is basically the same as that used for the IOF case (Fig. 3.6a) except that one end bearing plate was moved away from the end. The distance e_2 was designed to be 1.5h while e_1 varied from 0.1h to 0.75h making e_4 to vary accordingly from 1.4h to 0.75h. The expected failure was at the bearing plate under the applied concentrated load.

b. Transition between IOF and EOF: The test setup (Fig. 3.6f) was the same as that of the EOF case (Fig. 3.6b) except that the 2-in. end bearing plate was moved closer to the applied concentrated load. Failure was expected at the 2-in. bearing plate closer to the applied load due to reaction. The distance e_2 was also set at 1.5h as in the previous case but the magnitudes of the distances e_1 and e_4 were interchanged.

c. Transition between EOF and ETF: Figure 3.6g shows the test setup for this case. Similar to the previous case, the test arrangement was adapted from that used for the EOF case (Fig. 3.6b). The bearing

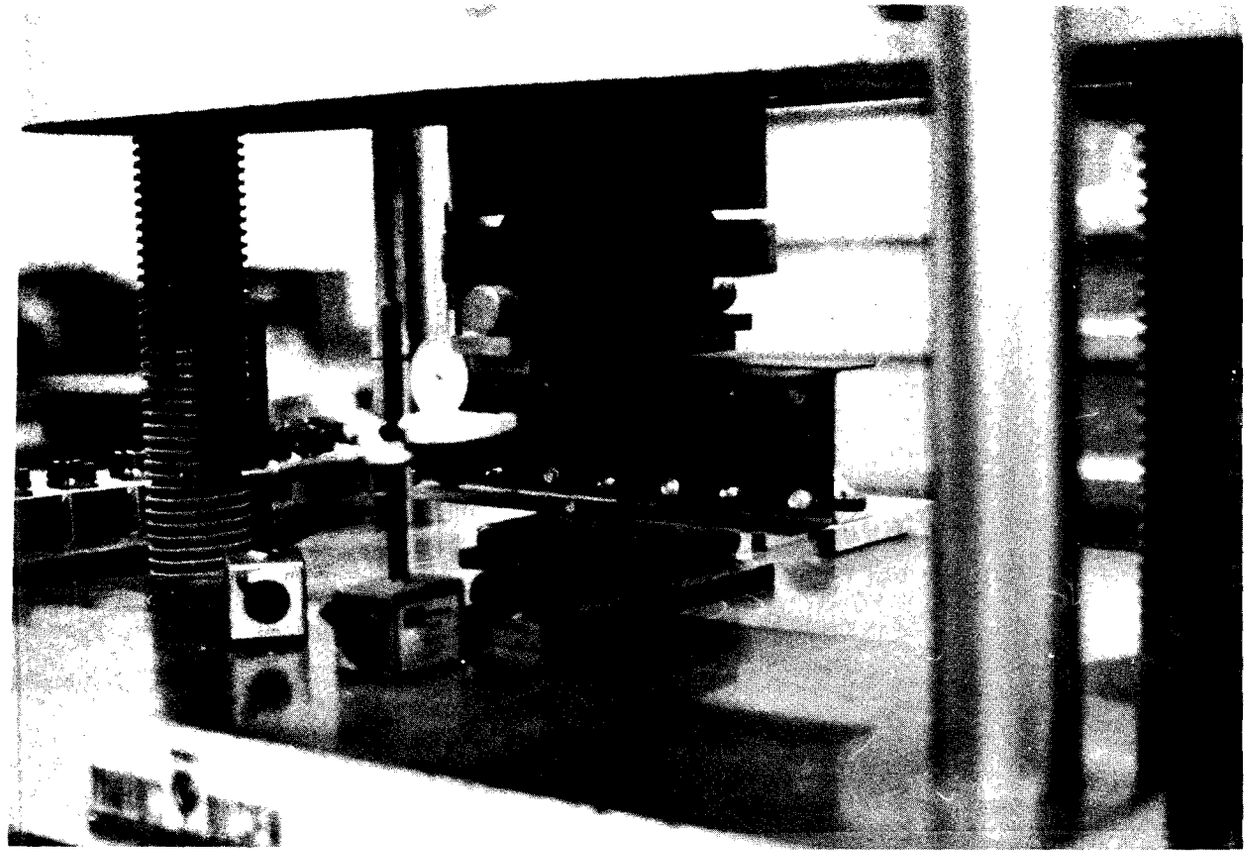

Fig. 3.14 Photograph of Test Setup for Interior Two-Flange Loading of I-Beams

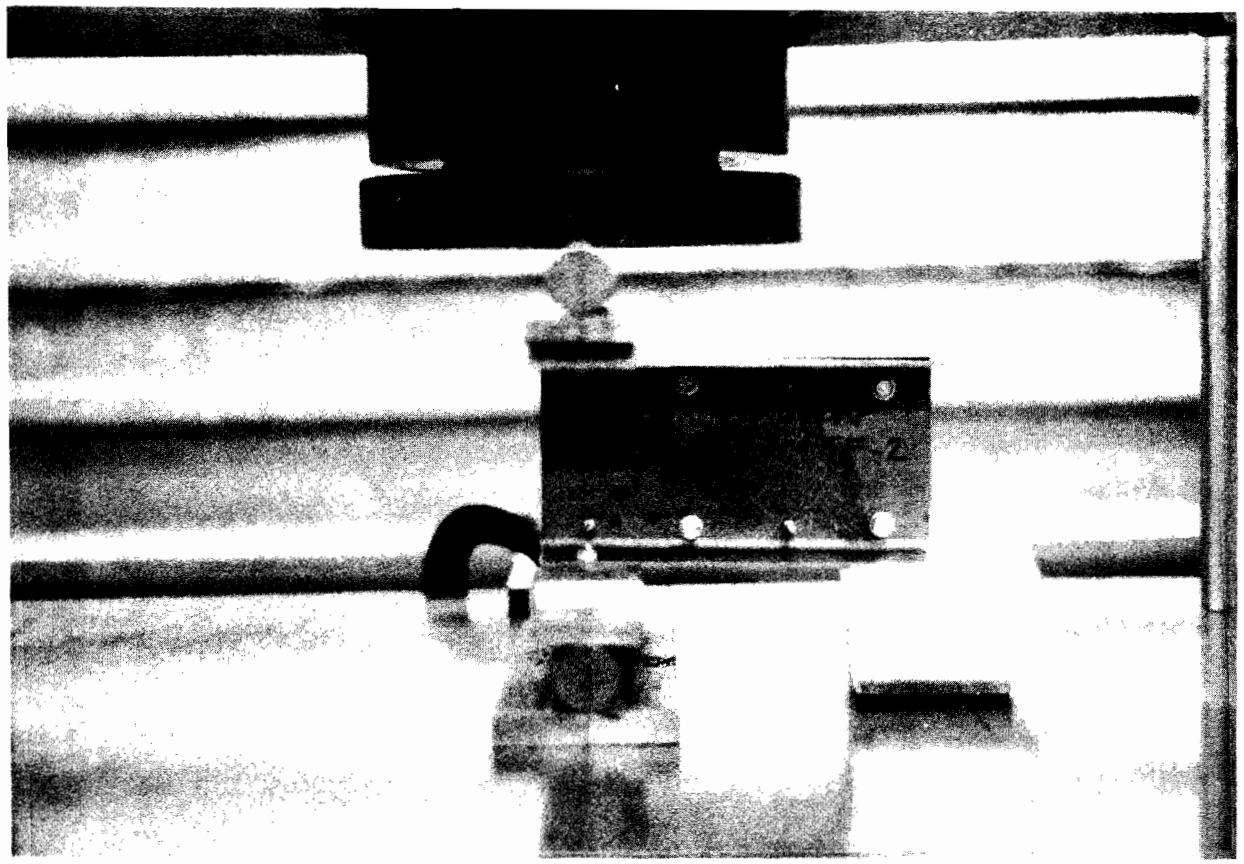

Fig. 3.15 Photograph of Test Setup for End Two-Flange Loading of I-Beams

plate under the applied concentrated load was moved closer to one end bearing plate with the distance e_1 varied from 0.1h to 0.75h and e_2 varied from 2.9h to 2.25h, accordingly. Failure was expected at the end bearing plate closer to the applied load.

D. TEST RESULTS

All lateral deformations of the web and vertical movement of the bearing plate were recorded at every loading level as discussed earlier. The ultimate loads were recorded and appeared to be very consistent for identical specimens. The recorded ultimate web crippling loads can be observed from Tables 4.3 to 4.10 in Section IV. Because all specimens were unstable at the ultimate loads, deflection and deformation measurements could not be obtained at this load level.

The nature of failure was carefully observed throughout the tests and can be summarized as follows:

1. Hat Sections under IOF:

During the test, the downward curling of the top flange of hat section under the top bearing plate was clearly visible at a load equal to approximately 40% of the ultimate load as can be seen in Fig. 3.16. This figure shows that when the load exceeds about 40% of the ultimate load, the force applied to the beam through bearing plate was transmitted directly to the end of the fillets (point A in Fig. 3.16a).

For the 80DK and 80XF specimens, web crippling failures occurred just under the bearing plates with relatively small lateral deformations in the webs. The applied load increased steadily up to the ultimate load and remained at that level for a long period of time while the bearing

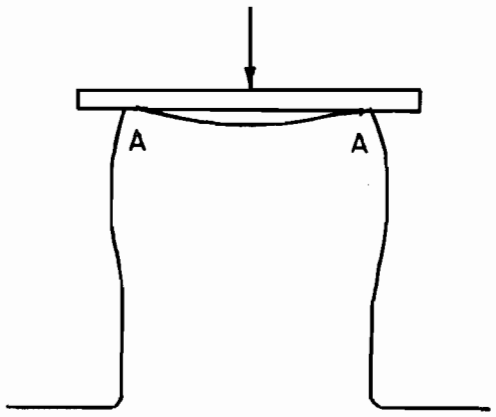

(a)

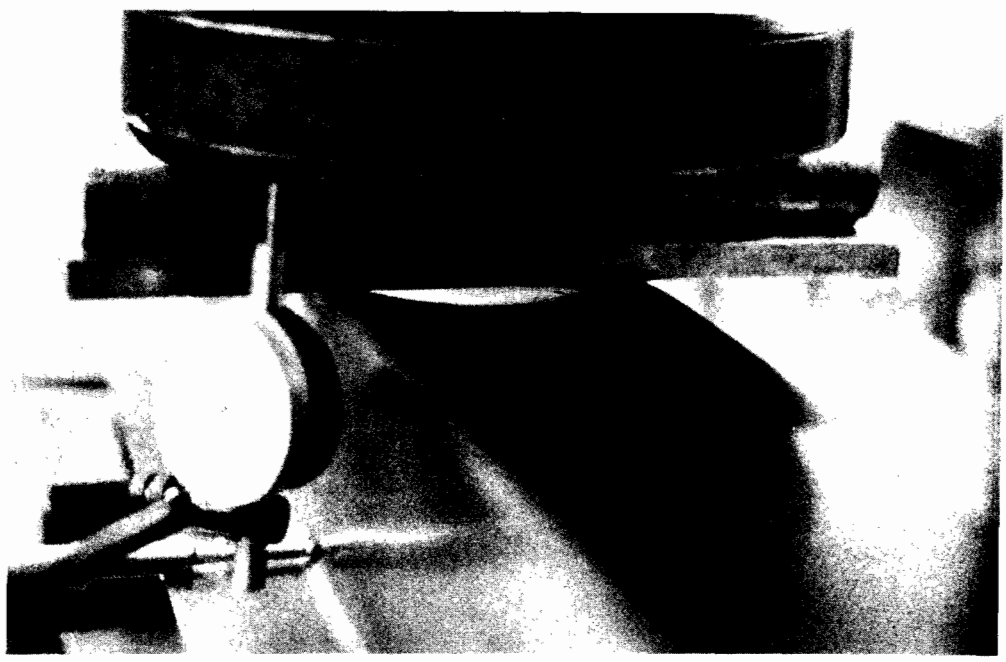

(b)

Fig. 3.16 Downward Curling of Top Flange of Hat Section

(Specimen No. 3-HIOF-A31 at 3.5 Kips Per Web)

plate gradually penetrated into the web. At this point, the vertical stress in the web underneath the bearing plate had already reached the maximum bearing capacity of the web. It was believed that overstressing underneath the bearing plate caused this type of failure. The typical failure is shown in Fig. 3.17.

Buckling in the webs was observed in the 100XF, 140XF and 140SK specimens. For this type of failure, the applied load increased steadily up to the ultimate load. Under the ultimate load, the web became unstable and the load dropped suddenly. There were relatively large lateral deformations at middle portion of the webs even before failure occurred. After the web buckled, the flange lost its support and penetrated into the deformed web as can be seen in Fig. 3.18. Paired strain gages which were attached to the webs of some specimens indicated that the strain caused by the bending of the web was much more pronounced than the strain caused by the vertical compressive stress. Figure 3.19 shows the lateral movement of the deformed web.

2. Hat Sections under EOF:

Under the applied load, all specimens used in this category sustained relatively large lateral deformations in the webs combined with large flange tip deflections at both supports. A plot of lateral deformations at each load level and a deformed cross-section are shown in Fig. 3.20 and 3.21, respectively.

For the 80DK, 80XF and 100XF specimens, the overstressing failure was observed for all tests while the sudden collapse of 140XFand 140SK specimens indicated buckling failure.

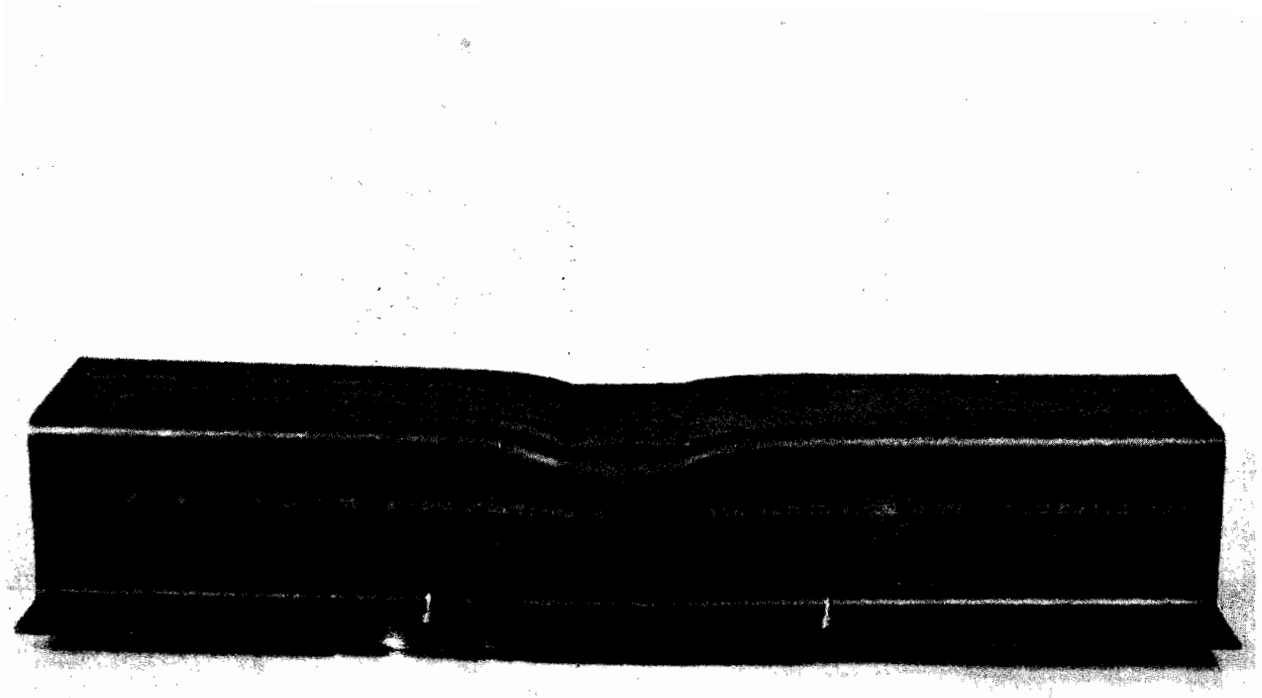

Fig. 3.17 Photograph Showing Web Crippling Failure Caused by Overstressing

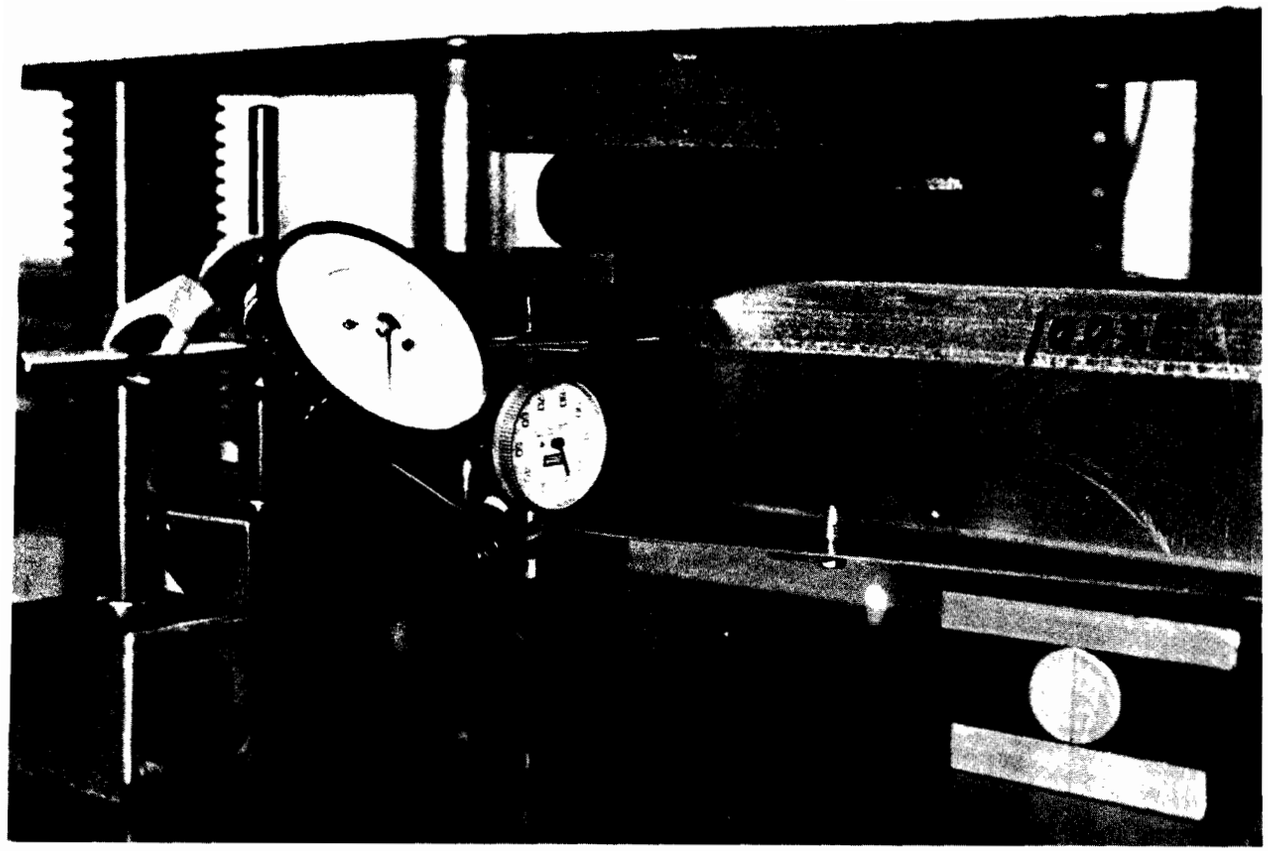

Fig. 3.18 Photograph Showing Web Crippling Failure Caused by Web Buckling

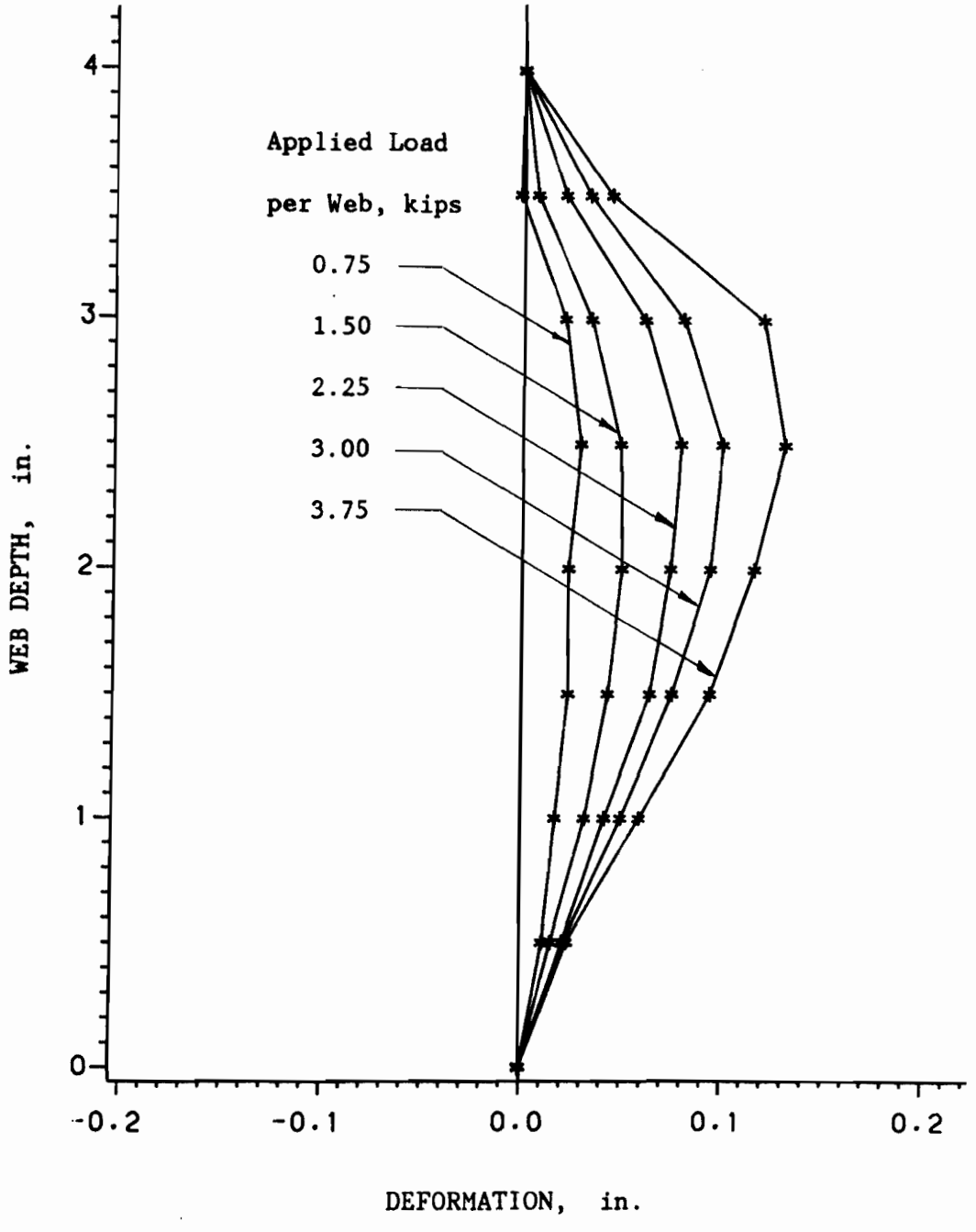

Fig. 3.19 Laterally Deformed Web of a Hat Section under Interior One-Flange Loading (Specimen No. 3-HIOF-A21)

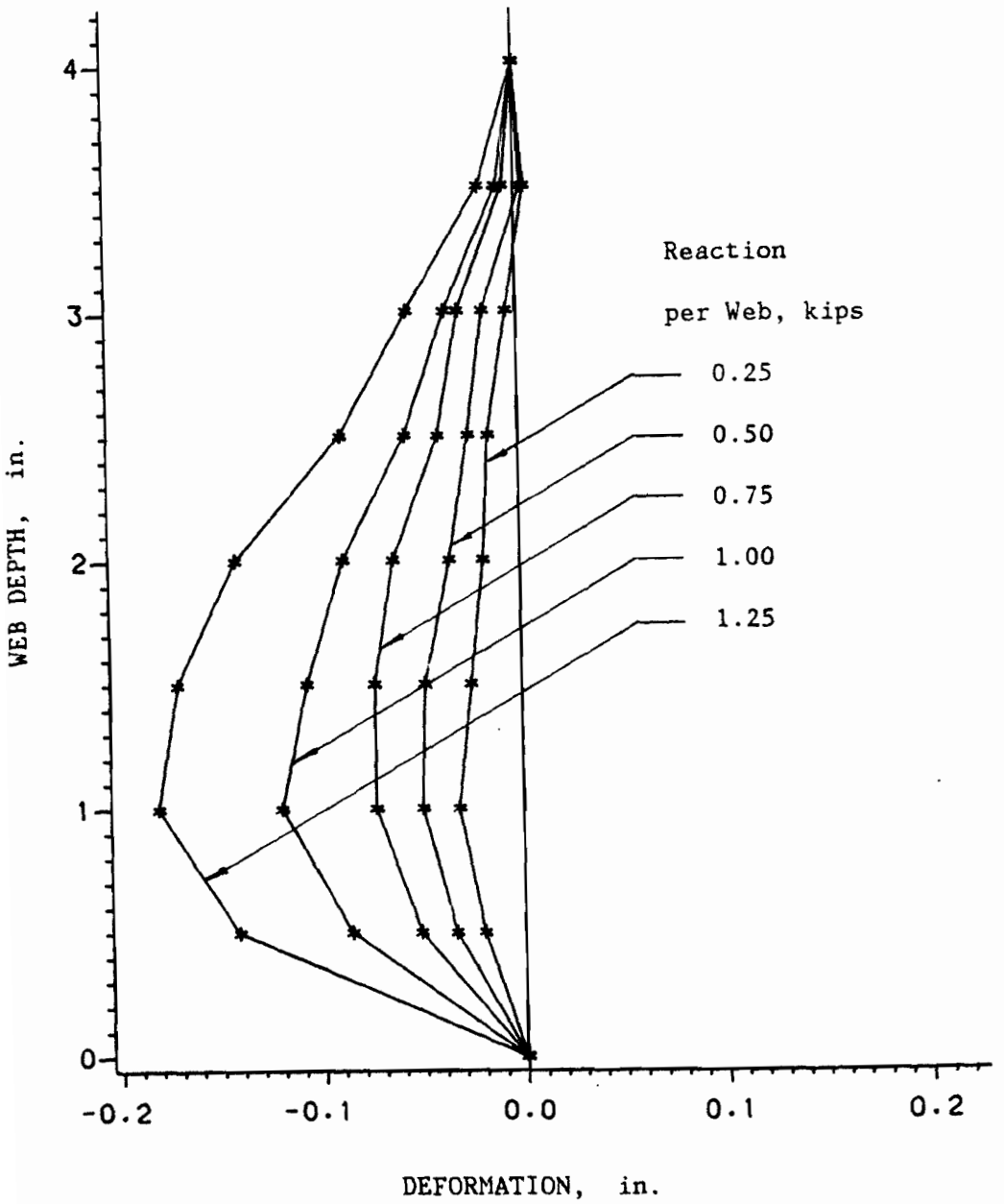

Fig. 3.20 Laterally Deformed Web of a Hat Section under End One-Flange Loading (Specimen No. 1-HEOF-A21)

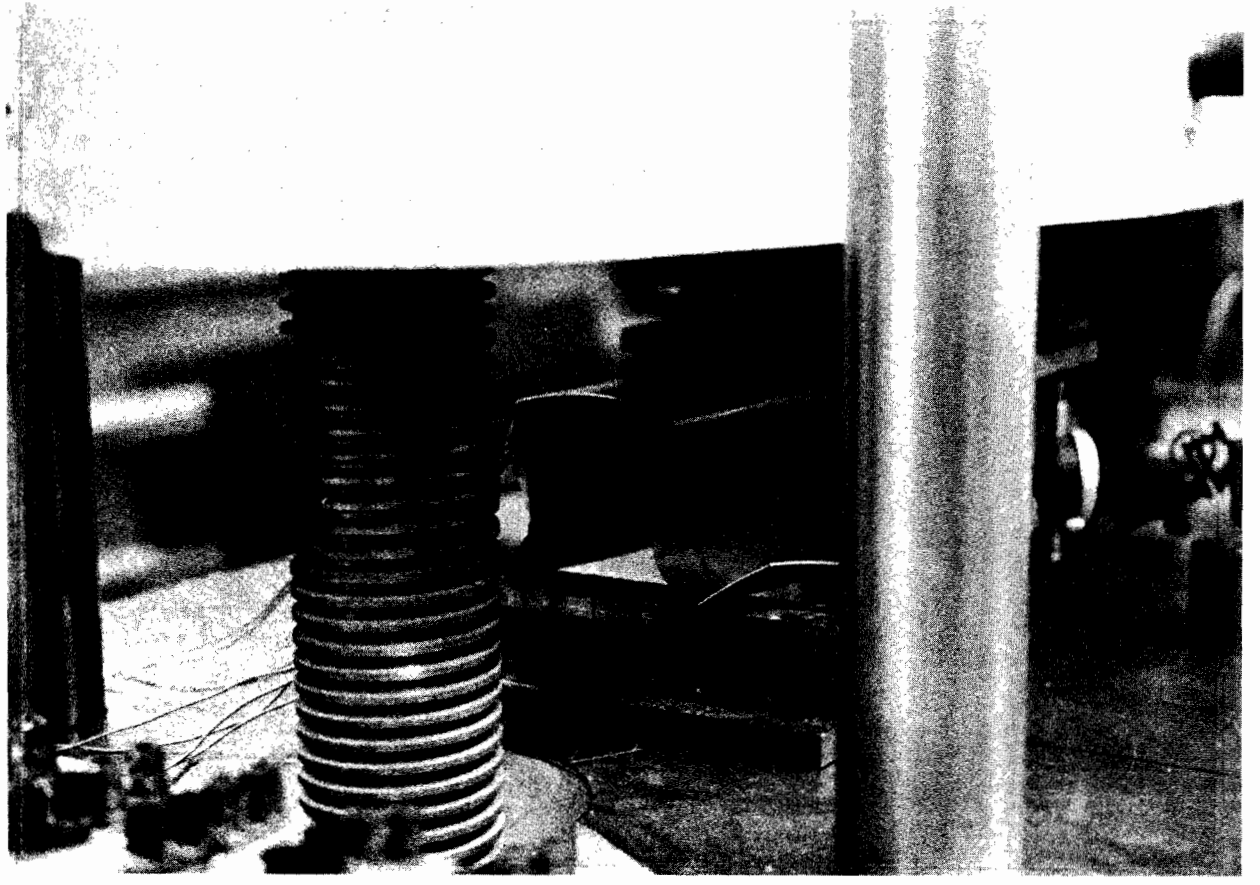

Fig. 3.21 Photograph Showing Typical Failure of Hat Section Subjected to End One-Flange Loading

3. Hat Sections under ITF:

For the 80DK and 80XF specimens, the overstressing of webs at the location of both bearing plates caused the failure. However, buckling failure in the webs was observed for the 100XF and 140SK specimens with relatively large lateral deformations. It should be noted that the webs deformed in reverse curvatures. The typical failure and laterally deformed web are shown in Figs. 3.22 and 3.23, respectively.

4. Hat Sections under ETF:

All specimens in this case failed by buckling in the webs. Similar to the previous case, the web deformed in reverse curvature. Figure 3.24 shows the typical failure mode.

5. I-Beams under IOF:

The failure mode of all specimens in this case was observed to be buckling type failure. There was virtually no lateral deflection of the web until the ultimate load was reached. The load increased steadily up to the maximum load and experienced a sudden drop when the web buckled. Figure 3.25 shows the typical failure of I-beams under IOF loading.

6. I-Beams under EOF:

As for the previous case, all specimens had a buckling type failure. The typical failure is shown in Fig. 3.26.

7. I-Beams under ITF:

The 80DK and 80XF specimens with Profile No. 1 (Table 3.2b) failed by overstressing of the webs underneath the bearing plates. For these specimens, the loads were applied steadily up to the ultimate loads and remained at that level for a long period of time before dropping. All the remaining specimens buckled as the ultimate loads were reached. Figure 3.27 shows the typical failure mode of these specimens.

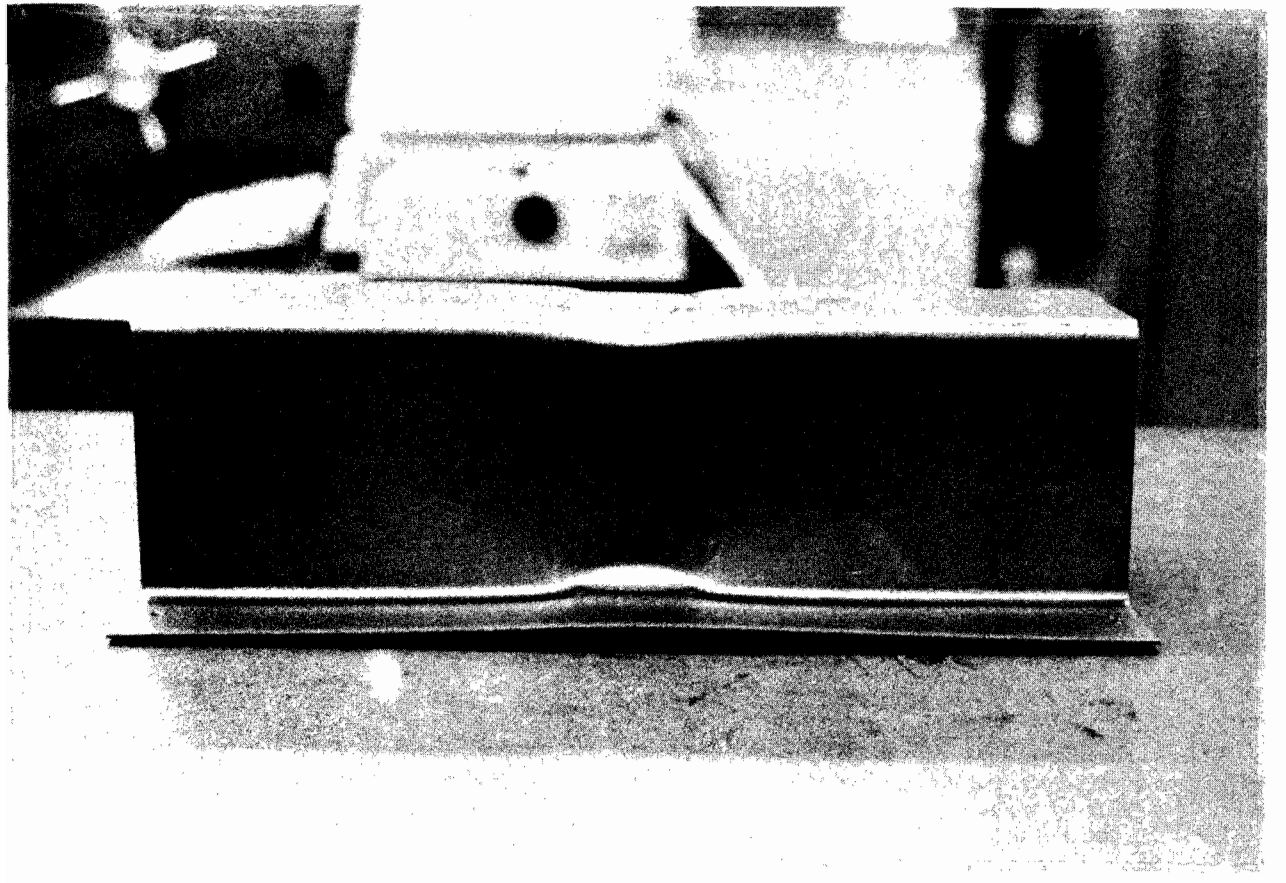

Fig. 3.22 Photograph Showing Typical Failure of Hat Section Subjected to Interior Two-Flange Loading

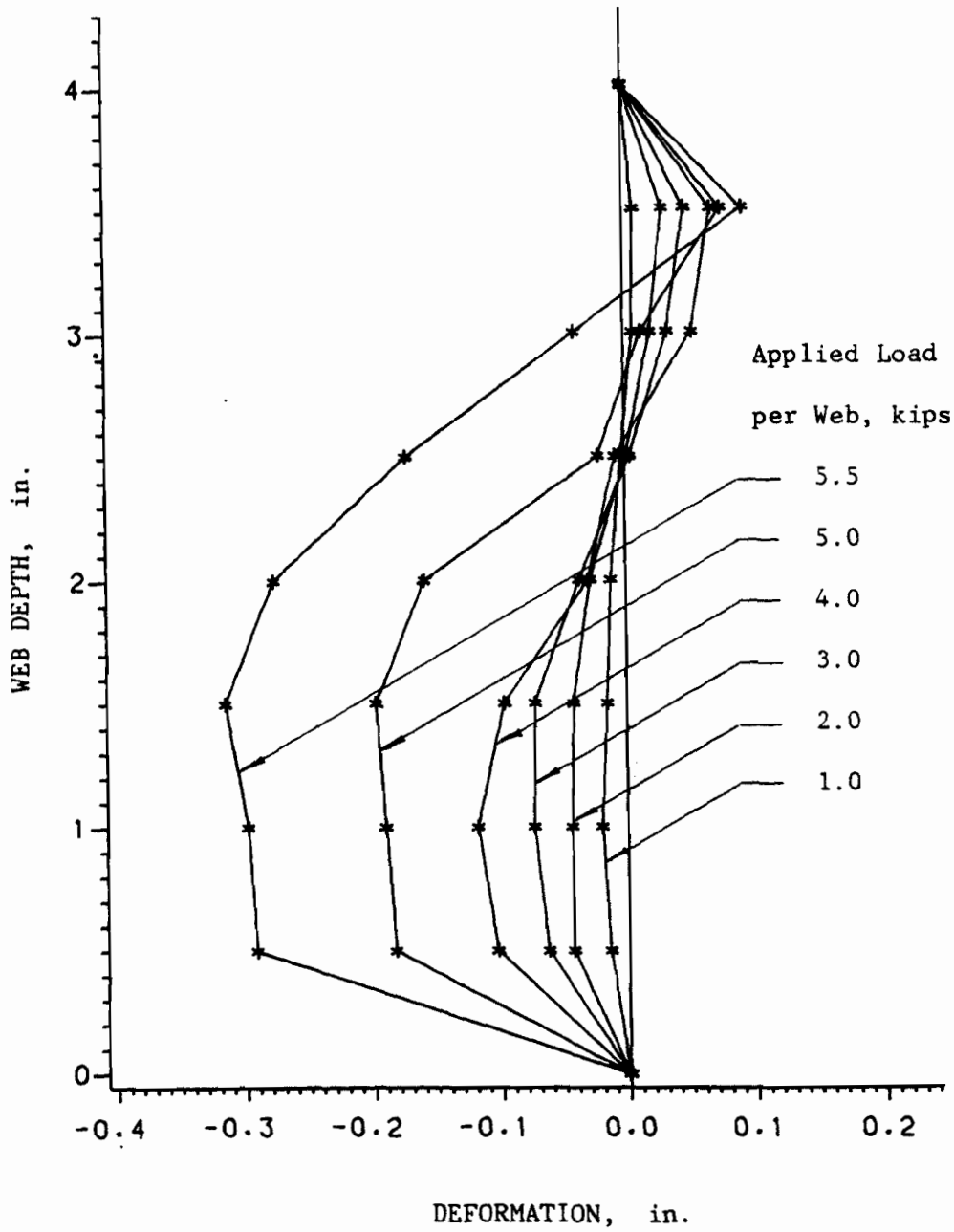

Fig. 3.23 Laterally Deformed Web of a Hat Section under Interior Two-Flange Loading (Specimen No. 5-HITF-A21)

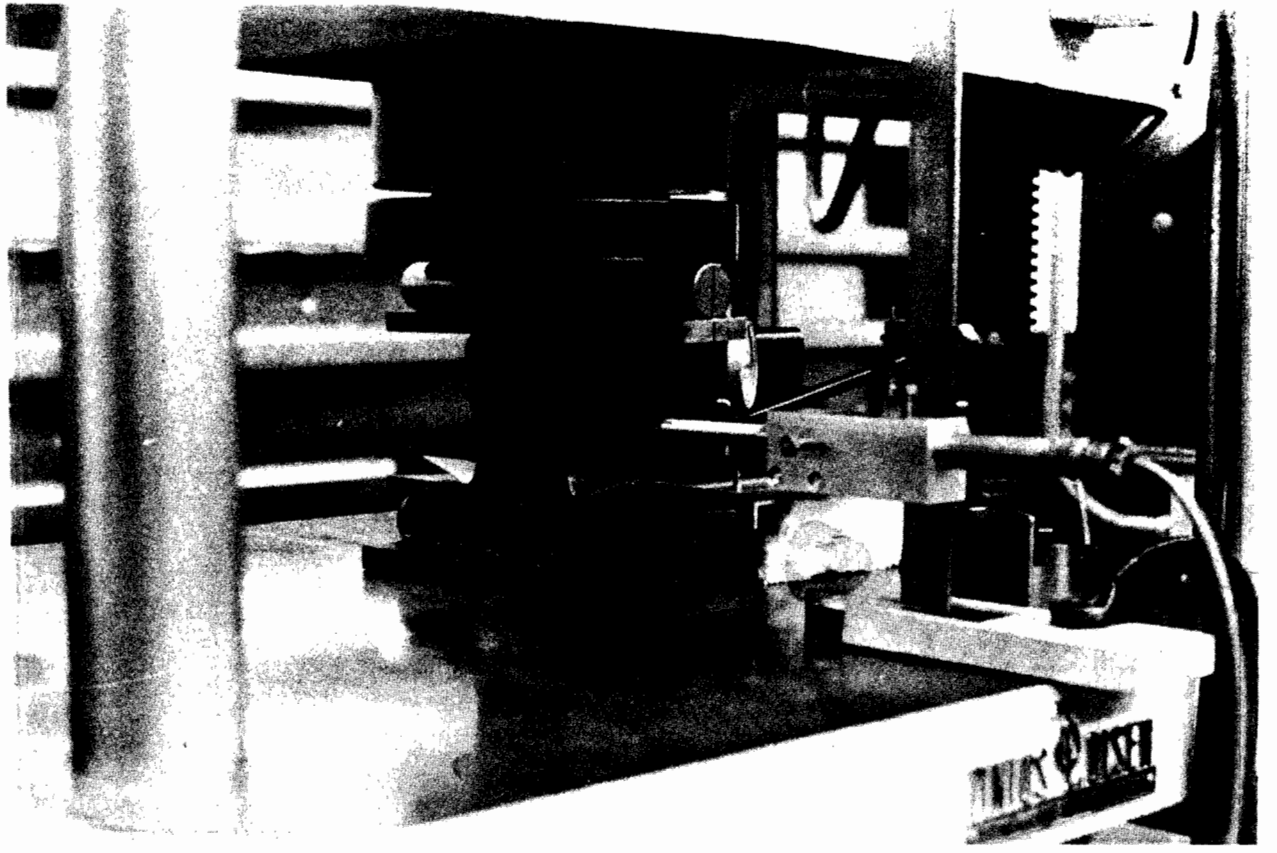

Fig. 3.24 Photograph Showing Typical Failure of Hat Section Subjected to End Two-Flange Loading

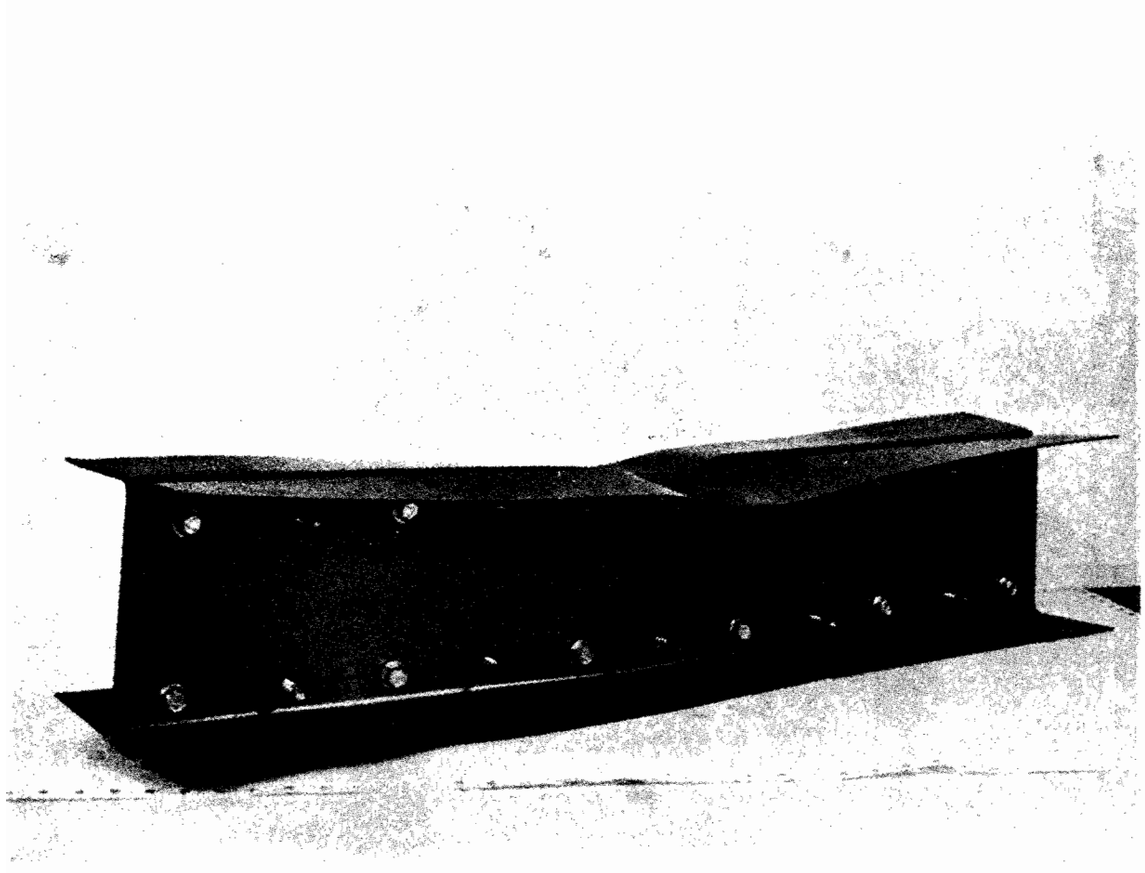

Fig. 3.25 Photograph Showing Typical Failure of I-Beam Subjected to Interior One-Flange Loading

Fig. 3.26 Photograph Showing Typical Failure of I-Beam Subjected to End One-Flange Loading

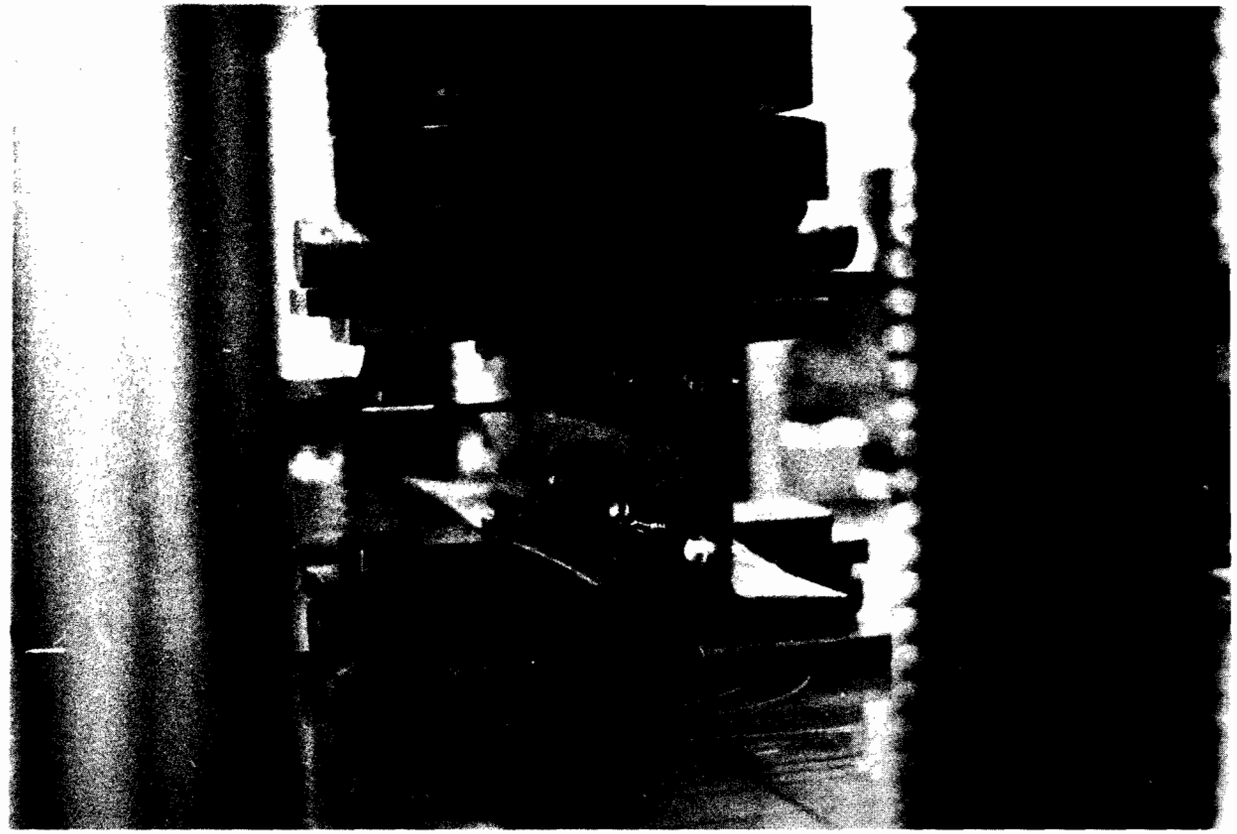

Fig. 3.27 Photograph Showing Typical Failure of I-Beam Subjected to Interior Two-Flange Loading

8. I-Beams under ETF:

All specimens experienced sudden collapse as the maximum loads were reached which indicated the buckling failure. For this case, the typical mode of failure is shown in Fig. 3.28.

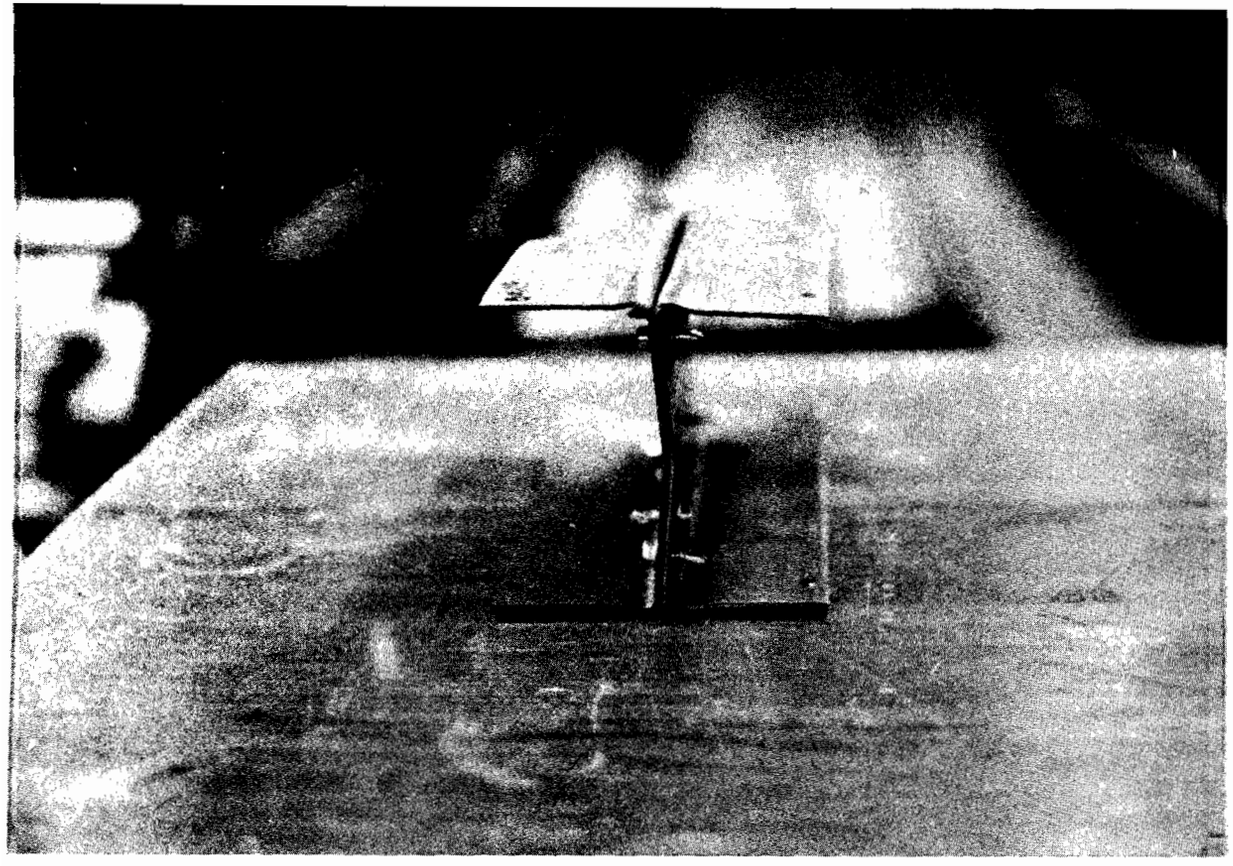

Fig. 3.28 Photograph Showing Typical Failure of I-Beam Subjected to End Two-Flange Loading

IV. EVALUATION OF EXPERIMENTAL DATA

During recent years, numerous beam tests of automotive structural components have been conducted by Inland Steel Company[10] and Ford Motor Company[11] for the purpose of studying the structural behavior and formability of bumper reinforcement beams using high strength sheet steels. The experimental data reported by Errera[9], Levy[10], and Vecchio[11] and the additional test results gathered from this phase of investigation have been reviewed and evaluated. This section presents the comparisons of the available experimental results of those sections fabricated from high strength sheet steels and the predicted failure loads based on the design criteria specified in the AISI 1981 Guide[3] and the 1980 and 1986 Editions of the Specification.[5,6]

The design provisions for web crippling and the combination of web crippling and bending moment were reviewed in Section II. Even though the existing design expressions discussed in Section II are intended for the use of materials having yield strength not greater than 80 ksi with proportional limit not less than 70% of the yield strength, nevertheless, these design expressions with some modifications on the function of yield strength have been used in this evaluation.

The effect of yield strength on the ultimate web crippling load of cold-formed steel sections with single unreinforced webs is treated in the same way in both the 1981 Guide and the 1986 Specification. Specifically, the fuctions of yield strength for interior and end loading conditions are expressed in Eqs. (4.1) and (4.2), respectively.

$$f_1(F_y) = (1.22-0.22(F_y/33))(F_y/33) \quad (4.1)$$

$$f_2(F_y) = (1.33-0.33(F_y/33))(F_y/33) \quad (4.2)$$

These functions of F_y are shown graphically in Fig. 4.1a. It can be seen that the predicted failure load for a given section increases as the yield strength, F_y, increases up to a certain value, beyond which the ultimate web crippling load decreases as the yield strength increases. The values of F_y that maximize the functions $f_1(F_y)$ and $f_2(F_y)$ are 91.5 and 66.5 ksi, respectively. In the comparisons using the 1980 and 1986 Specifications, when the actual yield strength exceeds these limits, the maximum value of the function is taken as a constant as shown in Fig. 4.1b i.e.

$$f_1(F_y) = 1.69 \quad (\text{for } F_y > 91.5 \text{ ksi}) \qquad \text{Modified (4.1)}$$

$$f_2(F_y) = 1.34 \quad (\text{for } F_y > 66.5 \text{ ksi}) \qquad \text{Modified (4.2)}$$

The comparisons of the test results and the predicted failure loads are presented in the following discussions.

A. INLAND TESTS

Hat sections (Fig. 4.2) were tested in the Research Laboratory of Inland Steel Company.[9] The test specimens were fabricated from six different types of sheet steels. The material properties and dimensions of all the Inland specimens are given in Appendix B (Tables B1 and B2). The yield strengths for specimens No. 1 through 30 (Table B1) range from 35.3 to 73 ksi. For the remaining specimens, the yield strengths of materials vary from 169 to 189 ksi. The actual yield stresses listed in

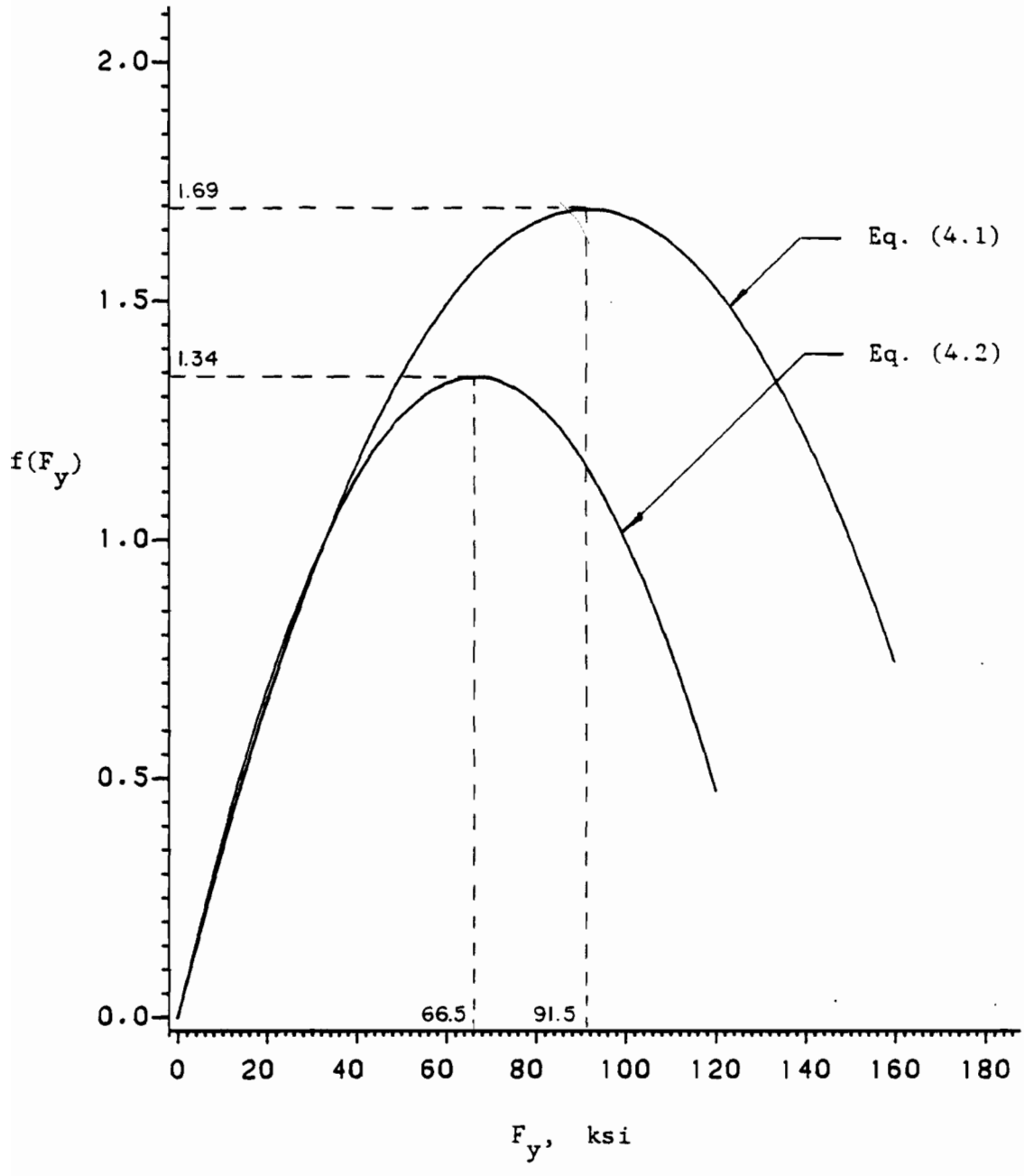

Fig. 4.1a Plot of Eqs. (4.1) and (4.2)

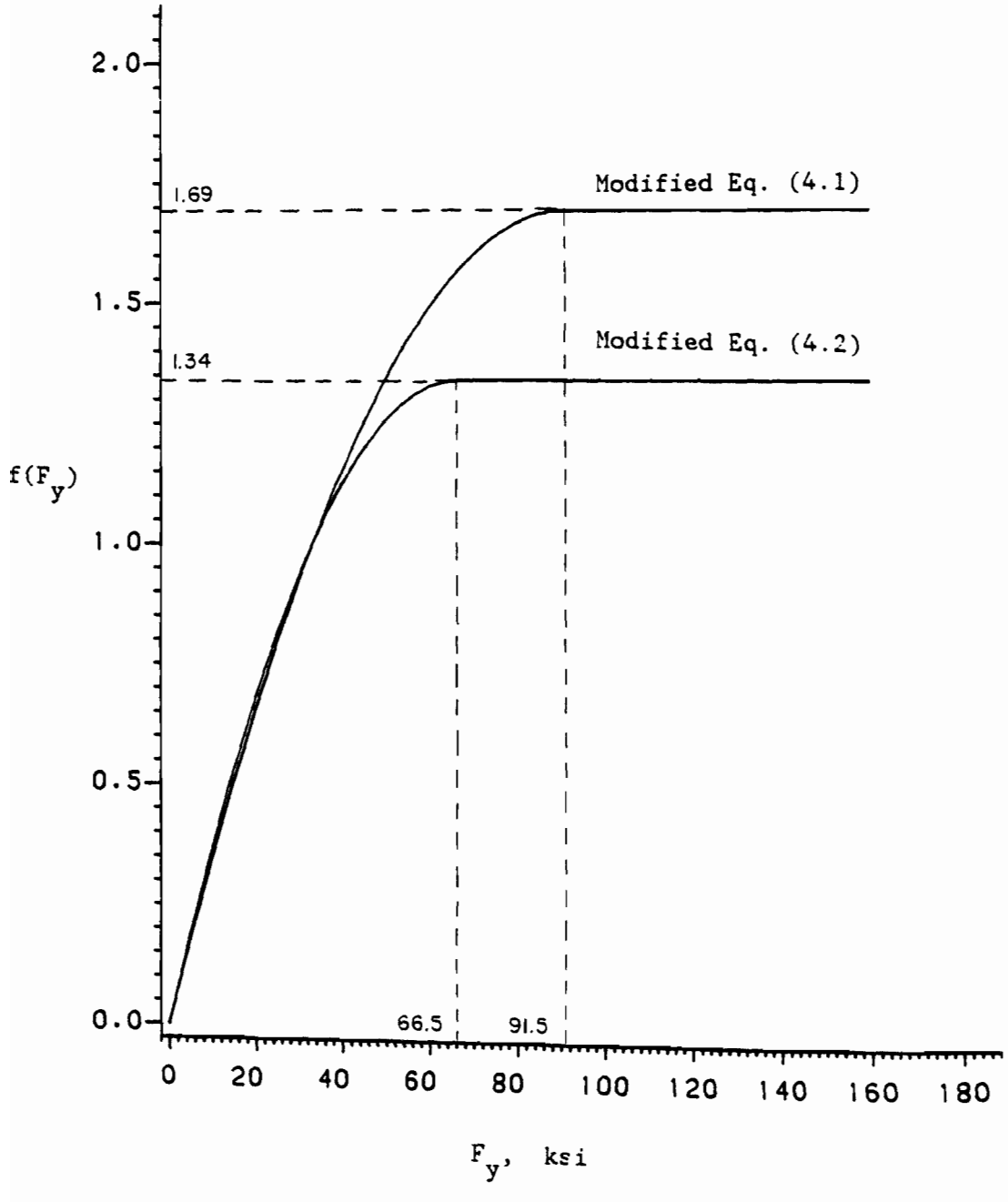

Fig. 4.1b Modified Functions of Yield Strength

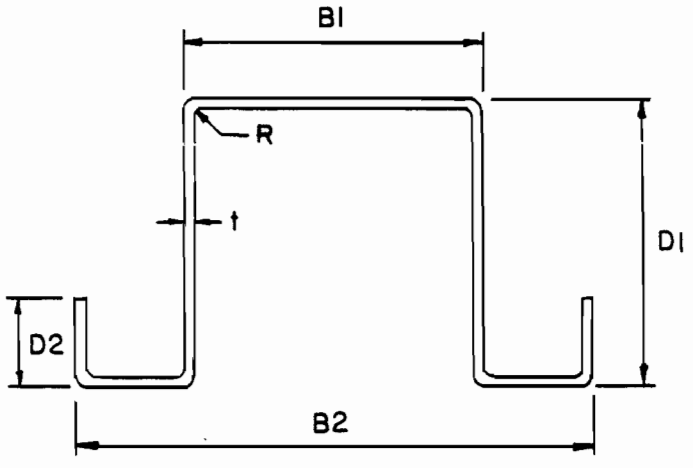

Fig. 4.2 Hat Sections Used for Inland Tests

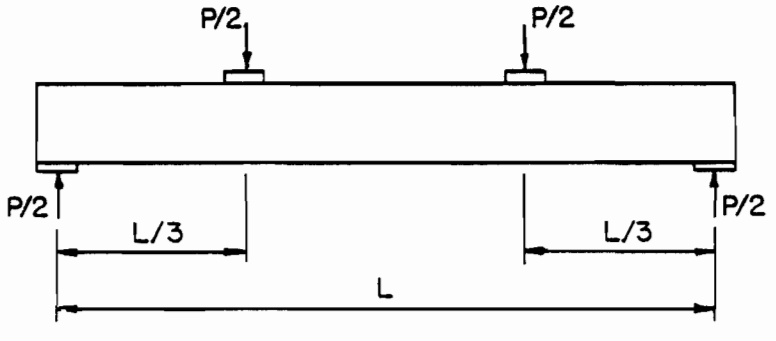

Fig. 4.3 Test Arrangement for Inland Tests

Table B1 were obtained from the tests of tensile coupons taken from flat materials. Because all the specimens were press-braked, there was little or no cold working of materials except in the corners.

All specimens were tested as simply supported flexural members under third-point loading on a 36 in. span. Figure 4.3 shows the loading arrangement used for these Inland tests.

It was reported that all specimens failed at the locations of interior bearing plates under applied concentrated loads. The tested loads listed under the column title "P_{test}" are the ultimate loads recorded just before the specimens collapsed. These values are the average of duplicate tests.

In this evaluation, failure loads were predicted by using a computer program based on the AISI requirements included in the 1981 Guide and the 1980 and 1986 Editions of the Specification with some modification in the function of yield strength as discussed earlier. The types of failure modes considered in this investigation were bending, shear, combined bending and shear, web crippling and combined bending and web crippling.

Comparisons of the test results and the predicted values for these Inland tests are presented in Tables 4.1a, 4.1b, and 4.1c. The symbols used in these tables for each type of failure loads are defined as follows:

1) P_m is the ultimate load computed for the bending moment only, kips. It was calculated from

$$P_m = 6M_u/L \qquad (4.3)$$

Table 4.1a

Comparisons of Tested and Predicted Failure Loads for Inland Tests Based on the AISI 1981 Guide

Specimen No.	P_m (kips)	P_c (kips)	P_{mc} (kips)	P_s (kips)	P_{ms} (kips)	P_{test} (kips)	Predicted Failure Mode	P_{test}/P_{comp}
1	0.163	1.520	0.163	2.153	0.172	0.216	M	1.32
2	0.415	1.599	0.415	3.294	0.426	0.414	M	1.00
3	0.707	1.654	0.644	4.080	0.714	0.618	MC	0.96
4	1.026	1.581	0.809	4.080	1.014	0.762	MC	0.94
5	1.384	1.493	0.934	4.080	1.330	0.900	MC	0.96
6	2.053	1.319	1.044	3.161	1.722	0.975	MC	0.93
7	0.219	2.396	0.219	2.911	0.232	0.306	M	1.40
8	0.560	2.515	0.560	4.472	0.580	0.594	M	1.06
9	1.000	2.608	0.940	6.034	1.017	0.876	MC	0.93
10	1.461	2.528	1.203	6.389	1.458	1.090	MC	0.91
11	1.973	2.424	1.414	6.389	1.920	1.320	MC	0.93
12	3.161	2.215	1.693	5.678	2.792	1.610	MC	0.95
13	0.260	2.703	0.260	3.467	0.277	0.384	M	1.48
14	0.667	2.837	0.667	5.326	0.690	0.726	M	1.09
15	1.160	2.941	1.082	6.972	1.180	1.100	MC	1.02
16	1.690	2.851	1.379	6.972	1.681	1.380	MC	1.00
17	2.282	2.733	1.617	6.972	2.208	1.610	MC	1.00
18	3.662	2.498	1.930	5.678	3.109	1.960	MC	1.02
19	0.311	3.008	0.311	4.139	0.330	0.498	M	1.60
20	0.796	3.158	0.796	6.360	0.824	0.905	M	1.14
21	1.349	3.273	1.242	7.619	1.368	1.360	MC	1.10
22	1.960	3.173	1.575	7.619	1.942	1.640	MC	1.04
23	2.648	3.042	1.840	7.614	2.545	1.930	MC	1.05
24	3.651	2.780	2.052	5.678	3.071	2.340	MC	1.14
25	0.471	4.814	0.471	6.341	0.507	0.678	M	1.44
26	1.218	5.036	1.218	9.795	1.273	1.260	M	1.03
27	2.118	5.220	1.959	12.582	2.167	1.840	MC	0.94
28	3.089	5.111	2.503	12.582	3.085	2.370	MC	0.95
29	4.178	4.949	2.945	12.582	4.051	2.740	MC	0.93
30	6.562	4.626	3.527	9.992	5.485	3.190	MC	0.90
31	0.786	2.063	0.740	7.893	0.820	0.705	MC	0.95
32	1.090	3.764	1.090	13.604	1.158	1.185	M	1.09
33	0.816	2.048	0.758	7.893	0.851	0.698	MC	0.92
34	1.183	3.739	1.169	12.727	1.261	1.178	MC	1.01
35	0.825	2.048	0.765	7.893	0.861	0.690	MC	0.90
36	1.206	3.739	1.186	12.727	1.286	1.140	MC	0.96
37	0.772	2.063	0.730	7.809	0.806	0.705	MC	0.97
38	0.903	3.404	0.903	12.157	0.960	1.134	M	1.26
39	1.593	2.171	1.195	6.577	1.593	1.071	MC	0.90
40	2.037	3.574	1.687	12.704	2.093	1.890	MC	1.12

Table 4.1a (Cont'd)

Comparisons of Tested and Predicted Failure Loads for Inland Tests Based on the AISI 1981 Guide

Specimen No.	P_m (kips)	P_c (kips)	P_{mc} (kips)	P_s (kips)	P_{ms} (kips)	P_{test} (kips)	Predicted Failure Mode	P_{test}/P_{comp}
41	1.580	2.239	1.204	4.890	1.504	1.470	MC	1.22
42	3.321	3.705	2.277	10.947	3.264	2.592	MC	1.14
43	1.344	2.122	1.070	3.891	1.270	1.655	MC	1.55
44	3.437	3.973	2.396	9.510	3.233	2.898	MC	1.21
45	1.244	2.072	1.011	3.755	1.181	1.584	MC	1.57
46	3.491	4.028	2.431	9.679	3.284	2.979	MC	1.23
47	1.408	2.122	1.100	3.891	1.324	1.718	MC	1.56
48	3.741	3.973	2.505	9.510	3.482	3.142	MC	1.25
49	1.366	2.072	1.070	3.755	1.284	1.635	MC	1.53
50	3.827	4.028	2.551	9.679	3.559	3.069	MC	1.20
51	1.456	2.122	1.123	3.891	1.364	1.746	MC	1.56
52	3.894	3.799	2.500	9.510	3.604	3.012	MC	1.20
53	1.493	2.072	1.128	3.755	1.387	1.599	MC	1.42
54	4.176	4.028	2.666	9.679	3.835	3.168	MC	1.19
55	1.417	2.122	1.105	3.891	1.331	1.805	MC	1.63
56	3.787	3.973	2.520	9.510	3.518	3.048	MC	1.21
57	1.323	2.072	1.050	3.755	1.248	1.536	MC	1.46
58	3.331	3.701	2.279	8.698	3.111	3.243	MC	1.42
59	1.369	1.987	1.054	3.232	1.261	2.091	MC	1.98
60	3.294	3.435	2.186	7.215	2.997	3.522	MC	1.61
61	1.182	1.717	0.910	2.413	1.061	2.302	MC	2.53
62	2.972	3.489	2.087	5.882	2.653	4.135	MC	1.98
63	1.221	1.717	0.928	2.413	1.089	2.470	MC	2.66
64	3.159	3.489	2.155	5.882	2.783	4.405	MC	2.04
65	1.225	1.717	0.930	2.413	1.093	2.475	MC	2.66
66	3.184	3.489	2.164	5.882	2.800	4.628	MC	2.14
67	1.257	1.717	0.943	2.413	1.115	2.607	MC	2.76
68	2.984	3.131	1.986	5.381	2.610	4.562	MC	2.30
Mean Value**								1.072
Standard Deviation**								0.187

** For specimens with material yield strengths up to 80 ksi.

Note: Predicted Failure Mode
M represents bending moment
MC represents combined bending and web crippling

Table 4.1b

Comparisons of Tested and Predicted Failure Loads for Inland Tests Based on the AISI 1980 Specification

Specimen No.	P_m (kips)	P_c (kips)	P_{mc} (kips)	P_s (kips)	P_{ms} (kips)	P_{test} (kips)	Predicted Failure Mode	P_{test}/P_{comp}
1	0.251*	1.823	0.251	2.153	0.196	0.216	M	1.10
2	0.415	1.776	0.415	3.294	0.473	0.414	M	1.00
3	0.707	1.729	0.698	4.435	0.765	0.618	MC	0.89
4	1.026	1.682	0.882	4.736	1.055	0.762	MC	0.86
5	1.384	1.635	1.032	4.246	1.333	0.900	MC	0.87
6	2.080	1.541	1.208	3.170	1.739	0.975	MC	0.81
7	0.350*	2.726	0.350	2.911	0.268	0.306	M	1.14
8	0.621*	2.668	0.621	4.472	0.652	0.594	M	0.96
9	1.000	2.611	1.000	6.034	1.110	0.876	M	0.88
10	1.461	2.554	1.287	7.415	1.547	1.090	MC	0.85
11	1.973	2.497	1.518	7.415	1.988	1.320	MC	0.87
12	3.085	2.382	1.836	5.692	2.712	1.610	MC	0.88
13	0.414*	3.074	0.414	3.467	0.318	0.384	M	1.21
14	0.667	3.009	0.667	5.326	0.770	0.726	M	1.09
15	1.160	2.945	1.159	7.186	1.273	1.100	MC	0.95
16	1.690	2.880	1.474	8.092	1.762	1.380	MC	0.94
17	2.282	2.816	1.736	7.634	2.243	1.610	MC	0.93
18	3.490	2.687	2.073	5.692	2.975	1.960	MC	0.95
19	0.462*	3.422	0.462	4.139	0.377	0.498	M	1.32
20	0.796	3.350	0.796	6.360	0.912	0.905	M	1.14
21	1.349	3.278	1.330	8.581	1.460	1.360	MC	1.02
22	1.960	3.206	1.683	8.843	2.008	1.640	MC	0.97
23	2.648	3.134	1.975	7.634	2.522	1.930	MC	0.98
24	3.947	2.990	2.323	5.692	3.244	2.340	MC	1.01
25	0.754*	5.344	0.754	6.341	0.582	0.678	M	1.16
26	1.218	5.252	1.218	9.795	1.417	1.260	M	1.03
27	2.118	5.160	2.090	13.249	2.332	1.840	MC	0.88
28	3.089	5.067	2.655	14.603	3.223	2.370	MC	0.89
29	4.178	4.975	3.125	13.450	4.090	2.740	MC	0.88
30	6.373	4.790	3.734	10.017	5.377	3.190	MC	0.85
31	0.786	2.552	0.786	9.161	0.851	0.705	M	0.90
32	1.090	4.274	1.090	13.604	1.257	1.185	M	1.09
33	0.816	2.561	0.816	9.161	0.893	0.698	M	0.86
34	1.183	4.285	1.183	12.727	1.380	1.178	M	1.00
35	0.825	2.561	0.825	9.161	0.903	0.690	M	0.84
36	1.206	4.285	1.206	12.727	1.408	1.140	M	0.95
37	0.772	2.552	0.772	9.063	0.838	0.705	M	0.91
38	0.903	3.881	0.903	12.157	1.043	1.134	M	1.26
39	1.557	2.480	1.323	6.594	1.516	1.071	MC	0.81
40	2.037	3.798	1.838	14.805	2.142	1.890	MC	1.03

Table 4.1b (Cont'd)

Comparisons of Tested and Predicted Failure Loads for Inland Tests Based on the AISI 1980 Specification

Specimen No.	P_m (kips)	P_c (kips)	P_{mc} (kips)	P_s (kips)	P_{ms} (kips)	P_{test} (kips)	Predicted Failure Mode	P_{test}/P_{comp}
41	2.271	2.408	1.605	4.902	2.061	1.470	MC	0.92
42	3.262	3.715	2.388	10.975	3.127	2.592	MC	1.09
43	2.771	2.335	1.734	3.901	2.259	1.655	MC	0.95
44	4.364	4.008	2.862	9.535	3.968	2.898	MC	1.01
45	2.480	2.291	1.632	3.765	2.071	1.584	MC	0.97
46	4.311	4.061	2.866	9.704	3.940	2.979	MC	1.04
47	2.902	2.335	1.769	3.901	2.328	1.718	MC	0.97
48	4.750	4.008	2.974	9.535	4.251	3.142	MC	1.06
49	2.723	2.291	1.702	3.765	2.206	1.635	MC	0.96
50	4.726	4.061	2.989	9.704	4.249	3.069	MC	1.03
51	2.956	2.335	1.783	3.901	2.356	1.746	MC	0.98
52	4.611	3.832	2.862	9.535	4.151	3.012	MC	1.05
53	2.976	2.291	1.768	3.765	2.335	1.599	MC	0.90
54	5.157	4.061	3.105	9.704	4.554	3.168	MC	1.02
55	2.921	2.335	1.774	3.901	2.338	1.805	MC	1.02
56	4.808	4.008	2.990	9.535	4.293	3.048	MC	1.02
57	2.774	2.291	1.716	3.765	2.233	1.536	MC	0.90
58	4.442	3.748	2.781	8.720	3.958	3.243	MC	1.17
59	3.557	2.263	1.884	3.240	2.395	2.091	MC	1.11
60	5.513	3.549	2.941	7.234	4.385	3.522	MC	1.20
61	4.060	2.119	1.890	2.419	2.078	2.302	MC	1.22
62	7.622	3.742	3.404	5.897	4.664	4.135	MC	1.21
63	4.194	2.119	1.910	2.419	2.096	2.470	MC	1.29
64	8.101	3.742	3.469	5.897	4.768	4.405	MC	1.27
65	4.210	2.119	1.912	2.419	2.098	2.475	MC	1.29
66	8.164	3.742	3.477	5.897	4.780	4.628	MC	1.33
67	4.293	2.119	1.924	2.419	2.108	2.607	MC	1.35
68	7.535	3.383	3.163	5.395	4.386	4.562	MC	1.44
Mean Value**								0.977
Standard Deviation**								0.124

* Inelastic reserve capacity was employed.
** For specimens with material yield strengths up to 80 ksi.
Note: Predicted Failure Mode
M represents bending moment
MC represents combined bending and web crippling

Table 4.1c

Comparisons of Tested and Predicted Failure Loads for Inland Tests Based on the AISI 1986 Specification

Specimen No.	P_m (kips)	P_c (kips)	P_{mc} (kips)	P_s (kips)	P_{ms} (kips)	P_{test} (kips)	Predicted Failure Mode	P_{test}/P_{comp}
1	0.251*	1.823	0.163	2.153	0.196	0.216	M	1.10
2	0.415	1.776	0.415	3.294	0.473	0.414	M	1.00
3	0.707	1.729	0.698	4.435	0.765	0.618	MC	0.89
4	1.026	1.682	0.882	4.736	1.055	0.762	MC	0.86
5	1.384	1.635	1.032	4.246	1.333	0.900	MC	0.87
6	2.221	1.541	1.241	3.170	1.739	0.975	MC	0.79
7	0.350*	2.726	0.219	2.911	0.268	0.306	M	1.14
8	0.621*	2.668	0.560	4.472	0.652	0.594	M	0.96
9	1.000	2.611	1.000	6.034	1.110	0.876	M	0.88
10	1.461	2.554	1.287	7.415	1.547	1.090	MC	0.85
11	1.973	2.497	1.518	7.415	1.988	1.320	MC	0.87
12	3.161	2.382	1.855	5.692	2.712	1.610	MC	0.87
13	0.414*	3.074	0.260	3.467	0.318	0.384	M	1.21
14	0.667	3.009	0.667	5.326	0.770	0.726	M	1.09
15	1.160	2.945	1.159	7.186	1.273	1.100	MC	0.95
16	1.690	2.880	1.474	8.092	1.762	1.380	MC	0.94
17	2.282	2.816	1.736	7.634	2.243	1.610	MC	0.93
18	3.662	2.687	2.115	5.692	2.975	1.960	MC	0.93
19	0.462*	3.422	0.311	4.139	0.377	0.498	M	1.32
20	0.796	3.350	0.796	6.360	0.912	0.905	M	1.14
21	1.349	3.278	1.330	8.581	1.460	1.360	MC	1.02
22	1.960	3.206	1.683	8.843	2.008	1.640	MC	0.97
23	2.648	3.134	1.975	7.634	2.522	1.930	MC	0.98
24	4.257	2.990	2.396	5.692	3.244	2.340	MC	0.98
25	0.754*	5.344	0.471	6.341	0.582	0.678	M	1.16
26	1.218	5.252	1.218	9.795	1.417	1.260	M	1.03
27	2.118	5.160	2.090	13.249	2.332	1.840	MC	0.88
28	3.089	5.067	2.655	14.603	3.223	2.370	MC	0.89
29	4.178	4.975	3.125	13.450	4.090	2.740	MC	0.88
30	6.717	4.790	3.815	10.017	5.377	3.190	MC	0.84
31	0.786	2.552	0.786	9.161	0.851	0.705	M	0.90
32	1.090	4.274	1.090	13.604	1.257	1.185	M	1.09
33	0.816	2.561	0.816	9.161	0.893	0.698	M	0.86
34	1.183	4.285	1.183	12.727	1.380	1.178	M	1.00
35	0.825	2.561	0.825	9.161	0.903	0.690	M	0.84
36	1.206	4.285	1.206	12.727	1.408	1.140	M	0.95
37	0.772	2.552	0.772	9.063	0.838	0.705	M	0.91
38	0.903	3.881	0.903	12.157	1.043	1.134	M	1.26
39	1.593	2.480	1.341	6.594	1.516	1.071	MC	0.80
40	2.037	3.798	1.838	14.805	2.142	1.890	MC	1.03

Table 4.1c (Cont'd)

Comparisons of Tested and Predicted Failure Loads for Inland Tests Based on the AISI 1986 Specification

Specimen No.	P_m (kips)	P_c (kips)	P_{mc} (kips)	P_s (kips)	P_{ms} (kips)	P_{test} (kips)	Predicted Failure Mode	P_{test}/P_{comp}
41	2.591	2.408	1.710	4.902	2.061	1.470	MC	0.86
42	3.321	3.715	2.411	10.975	3.127	2.592	MC	1.08
43	3.572	2.335	1.924	3.901	2.259	1.655	MC	0.86
44	4.826	4.008	2.995	9.535	3.968	2.898	MC	0.97
45	3.148	2.291	1.810	3.765	2.071	1.584	MC	0.88
46	4.720	4.061	2.988	9.704	3.940	2.979	MC	1.00
47	3.740	2.335	1.957	3.901	2.328	1.718	MC	0.88
48	5.250	4.008	3.104	9.535	4.251	3.142	MC	1.01
49	3.463	2.291	1.879	3.765	2.206	1.635	MC	0.87
50	5.190	4.061	3.113	9.704	4.249	3.069	MC	0.99
51	3.787	2.335	1.966	3.901	2.356	1.746	MC	0.89
52	5.017	3.832	2.968	9.535	4.151	3.012	MC	1.01
53	3.793	2.291	1.943	3.765	2.335	1.599	MC	0.82
54	5.680	4.061	3.231	9.704	4.554	3.168	MC	0.98
55	3.765	2.335	1.962	3.901	2.338	1.805	MC	0.92
56	5.314	4.008	3.120	9.535	4.293	3.048	MC	0.98
57	3.599	2.291	1.907	3.765	2.233	1.536	MC	0.81
58	4.965	3.748	2.916	8.720	3.958	3.243	MC	1.11
59	5.180	2.263	2.133	3.240	2.395	2.091	MC	0.98
60	6.586	3.549	3.132	7.234	4.385	3.522	MC	1.12
61	8.220	2.119	2.119	2.419	2.078	2.302	C	1.11
62	11.010	3.742	3.742	5.897	4.664	4.135	C	1.10
63	8.491	2.119	2.119	2.419	2.096	2.470	C	1.18
64	11.700	3.742	3.742	5.897	4.768	4.405	C	1.18
65	8.523	2.119	2.119	2.419	2.098	2.475	C	1.18
66	11.789	3.742	3.742	5.897	4.780	4.628	C	1.24
67	8.556	2.119	2.119	2.419	2.108	2.607	C	1.24
68	10.782	3.383	3.383	5.395	4.386	4.562	C	1.35
Mean Value**								0.974
Standard Deviation**								0.126

* Inelastic reserve capacity was employed.
** For specimens with material yield strengths up to 80 ksi.
Note: Predicted Failure Mode
M represents bending moment
C represents web crippling
MC represents combined bending and web crippling

where M_u = ultimate bending moment if bending moment only exist, kip-in.

L = span length of beam specimen, in.

The ultimate bending moment, M_u, was determined by using Eq. (4.4) as follows:

$$M_u = S_{eff} F_{yf} \tag{4.4}$$

where S_{eff} = effective section modulus of the cross section, $in.^3$

F_{yf} = yield strength of beam flange obtained from tensile coupon test of virgin material, ksi

The computed bending moment was also checked against the maximum bending moment capacity based on bending in the webs and the effect of shear lag. For bending in the webs, the maximum bending moment capacity was calculated on the basis of Section 3.4.4 of the 1981 Guide, Section 3.4.2 of the 1980 Specification, and the effective depth approach of the 1986 Specification where applicable. In determining the bending moment capacity based on shear lag of unusually short span, the effective widths of both tension and compression flanges were limited according to Section 3.4.8 of the 1981 Guide depending on the ratio of span length to flange width, L/w_f. The same method is being used in the 1980 and 1986 Specifications.

2) P_c is the total ultimate load for the entire beam computed only for web crippling in the absence of bending moment, kips. It was calculated according to Eqs. (2.14) and (2.20) where applicable.

3) P_{mc} is the total ultimate load computed for combined bending moment and web crippling, kips. Based on the 1981 Guide, P_{mc} can be determined by using Eq. (2.17) which can be rewritten as

$$P_{mc} = 1.3P_m P_c/(P_m+P_c). \tag{4.5}$$

According to the 1980 and 1986 Specification, P_{mc} can be calculated from

$$P_{mc} = 1.42P_m P_c/(1.07P_m+P_c). \tag{4.6}$$

Equation (4.6) is based on Eq. (2.27).

4) P_s is the ultimate load computed for shear in the webs, kips. It was calculated according to Section 3.4.5 of the 1981 Guide, Section 3.4.1 of the 1980 Specification, or Section C3.2 of the 1986 Specification.

5) P_{ms} is the ultimate load computed for combined bending moment and shear, kips. It was determined according to the interaction equations in Section 3.4.6 of the 1981 Guide, Section 3.4.3 of the 1980 Specification, and Section C3.3 of the 1986 Specification. Because P_{ms} cannot be calculated directly, an iteration procedure was used to obtain the ultimate loads which satisfy the interaction equation.

6) P_{comp} is the smallest value of P_m, P_c, P_{mc}, P_s and P_{ms} discussed above, kips.

7) P_{test} is the tested failure load for the entire beam, kips.

8) P_{test}/P_{comp} is the ratio of the tested failure load to the predicted failure load.

It should be noted that the modes of failure indicated in Table 4.1 are determined from the computed values. Figure 4.4 shows the effect of the material yield strength, F_y, on the ratio of P_{test}/P_{comp}.

From Table 4.1 and Fig. 4.4, it can be seen that both the AISI Guide and the AISI Specification can provide reasonable estimates of the failure loads for sections with yield strengths up to 80 ksi except for some shallow sections (Specimens No. 1, 7, 13, 19, and 25) for which bending moment alone is the governing mode of failure. For these beams, the 1981 Guide usually underestimate the failure loads. This underestimation may be caused by the following factors:

1) The cold-work effect of a large portion of narrow compression flange may cause a significant increase in yield strength.

2) The inelastic reserve capacity may result in a higher ultimate load for compact sections, for which the local buckling of the compression flange and the compression portion of the web is prevented.

In the calculations of bending moment capacity based on the 1980 and 1986 Specifications, the design provisions for the inelastic reserve capacity of flexural members were employed where applicable. The asterik in Tables 4.1b and 4.1c indicates the utilization of inelastic reserve capacity.

Good agreements between the tested loads and the predicted failure loads based on the Guide and the Specifications were found for Specimens No. 31 to 40 which were formed from 160SK sheet steels having yield strengths from 169 to 189 ksi. The high values of the ratio P_{mc}/P_m for this group of specimens indicate that bending moment is the dominant cause of failure. The predicted ultimate loads for bending moment only (P_m) for these specimens are computed by Eqs. (4.3) and (4.4).

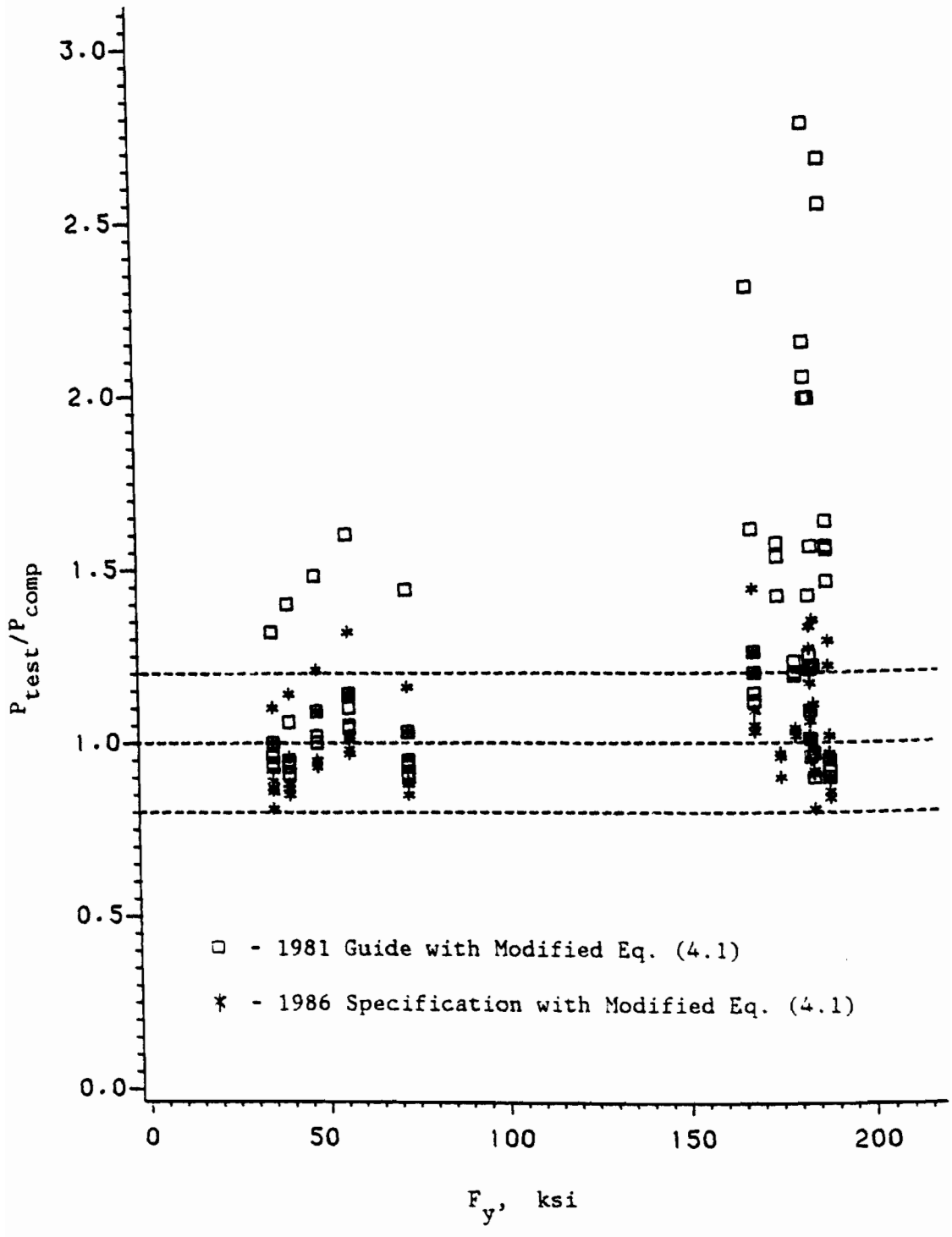

Fig. 4.4 Effect of F_y on the Ratio P_{test}/P_{comp} for Inland Tests Based on the AISI 1981 Guide and 1986 Specification

For specimens No. 41 to 68 which were also formed from 160SK sheet steels, the 1981 Guide underestimates the failure loads. The degree of underestimation increases as the web depth to thickness ratio (h/t) increases. This incident is caused by very low values of calculated bending moments governed by bending in the webs. According to Section 3.4.4 of the AISI 1981 Guide, the compressive stress in the flat web of a beam due to bending in its plane is limited by Eq. (4.7) as follows:

$$F_{bwu} = 640000/(h/t)^2 \leq F_y. \qquad (4.7)$$

It can be seen that the value F_{bwu} decreases as the parameter h/t increases. For these specimens, the calculated values of F_{bwu} are much less than the yield strengths of materials. For example, according to Eq. (4.7), the maximum bending stress in the web of Specimen No. 68 (F_y = 169 ksi and h/t = 118) is limited to 46 ksi which is much less than the actual yield strength of 169 ksi.

In the 1980 Specification, Equation (4.7) was changed to

$$F_{bwu} = (1.21-0.00034(h/t)\sqrt{F_y})F_y \leq F_y \qquad (4.8)$$

and the accuracy of predictions is improved. By using Eq. (4.8) the value of F_{bwu} for Specimen No. 68 increases to 116 ksi. However, the underestimation still exists for Specimens No. 61 to 68 where the combination of web crippling and bending moment is the expected mode of failure. The ultimate bending moment capacities for these specimens are governed by bending in the webs and Eq. (4.8) seems to still underestimate the values of P_m.

In the 1986 Specification, an effective web depth approach is used. According to Section B2.3 of the Specification, the webs of all specimens

are fully effective. As a result, the values of P_m for Specimens No. 41 to 68 in Table 4.1c are larger than those presented in Tables 4.1a and 4.1b. However, the predicted ultimate loads for Specimens No. 61 to 68 are still found to be conservative. For these specimens, web crippling alone is the expected mode of failure. The underestimations are apparently due to the use of the constant value of F_y = 91.5 ksi for these very high strength materials.

B. FORD TESTS

A total of 39 composite sections (Fig. 4.5) tested by Ford Motor Company were used in this evaluation. Each section consisted of a hat section and a 0.030 in. thick coverplate welded to the tension flange of the hat section. The yield strengths of the materials used for the hat sections range from 27.5 to 108.4 ksi. However, the yield strength of all the coverplates is 27.5 ksi.

Because the current AISI design provision for the ultimate web crippling load is intended for the application of sections having flat flange surfaces contacted to bearing plates, the test data reported by Vecchio[10] for the remaining specimens with beaded top flanges were excluded from the investigation.

All specimens were tested as simply supported flexural members under third-point loading on an 18 in. span (Fig. 4.3). The material properties and the measured dimensions of Ford test specimens are also listed in Appendix B. Each of the 13 test data used in this evaluation is the average value of the data obtained from three identical tests of each specimen. The yield strengths listed in Table B4 were obtained from the following two conditions:

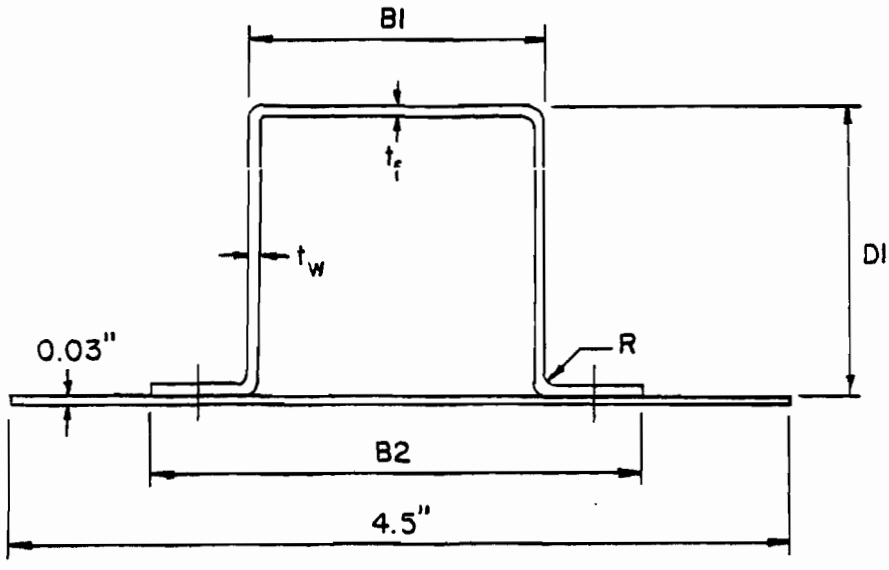

Fig. 4.5 Composite Sections Used for Ford Tests

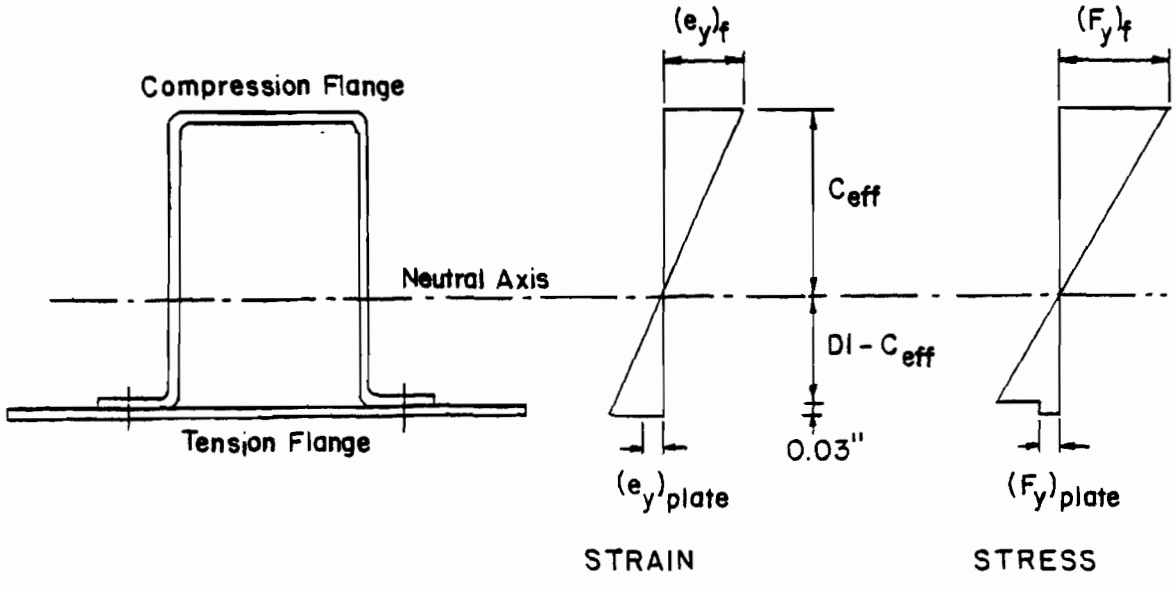

Fig. 4.6 Strain and Stress Diagrams for Composite Sections

1) As received properties for flat materials before forming.

2) As formed properties for flanges and webs of formed hat sections.

In Tables B4 and B5, the subscripts "f" and "w" represent flange and web, respectively. Other dimensions of composite sections are given in Table B5.

In Table B4, it can be seen that there is a significant increase in strengths in the webs of the formed sections. In some cases, the increase of yield strength is as high as 110% over the virgin steel. The increase in yield strength is not only caused by the die-forming process but is also due to the type of material used. The percentage increase in yield strength is higher for mild dual phase steels than high strength low alloy steels.

In the calculations, the "As Formed" data were used. The yield strengths of the flanges, F_{yf}, were used to calculate the bending moment capacities, whereas the yield strengths of the webs, F_{yw}, were used in determining shear capacities and web crippling loads.

The effect of lower yield strength in the coverplates on bending moment capacity was considered by assuming that 1) the strain varies linearly from top to bottom of the section and 2) the coverplate has a perfect elastic-plastic stress-strain curve. Figure 4.6 shows the strain and stress diagrams for a composite section with consideration being given to the effect of lower yield strength in the coverplate.

Comparisons of the test results and predicted values are presented in Tables 4.2a and 4.2b. It should be noted that the predicted failure loads based on the 1980 and 1986 Editions of the AISI Specification for this group of specimens are identical. The symbols used in these tables

Table 4.2a

Comparisons of Tested and Predicted Failure Loads for Ford Tests Based on the AISI 1981 Guide

Specimen No.	P_m (kips)	P_c (kips)	P_{mc} (kips)	P_s (kips)	P_{ms} (kips)	P_{test} (kips)	Predicted Failure Mode	P_{test}/P_{comp}
1	1.810	2.857	1.440	4.558	1.711	1.616	MC	1.12
2	2.963	4.434	2.309	6.930	2.775	2.320	MC	1.00
3	3.543	3.610	2.324	7.251	3.932	2.377	MC	1.02
4	3.289	3.353	2.158	7.163	3.041	2.453	MC	1.14
5	3.193	2.629	1.874	5.649	2.816	1.948	MC	1.04
6	3.356	2.629	1.916	5.815	2.944	2.031	MC	1.06
7	4.831	3.610	2.686	8.734	4.957	2.995	MC	1.12
8	3.964	5.886	3.079	9.904	3.375	3.602	MC	1.17
9	4.753	6.308	3.524	13.048	4.049	4.195	MC	1.19
10	3.084	10.846	3.122	8.950	3.047	4.567	M	1.48
11	4.231	10.467	3.917	14.540	5.257	4.858	MC	1.24
12	3.966	11.430	3.828	13.217	4.839	5.783	MC	1.51
13	5.159	10.993	4.565	19.720	7.042	6.065	MC	1.33
Mean Value*								1.179
Standard Deviation*								0.173

* For specimens with material yield strengths up to 80 ksi.

Table 4.2b

Comparisons of Tested and Predicted Failure Loads for Ford Tests Based on the AISI 1980 and 1986 Specifications

Specimen No.	P_m (kips)	P_c (kips)	P_{mc} (kips)	P_s (kips)	P_{ms} (kips)	P_{test} (kips)	Predicted Failure Mode	P_{test}/P_{comp}
1	1.810	2.955	1.553	7.113	3.099	1.616	MC	1.04
2	2.963	4.463	2.460	10.180	4.467	2.320	MC	0.94
3	3.543	3.734	2.496	7.831	4.934	2.377	MC	0.95
4	3.289	3.506	2.331	9.840	5.673	2.453	MC	1.05
5	3.193	2.856	2.064	5.930	3.928	1.948	MC	0.94
6	3.356	2.856	2.111	5.933	3.777	2.031	MC	0.96
7	4.831	3.734	2.877	8.757	5.244	2.995	MC	1.04
8	3.964	5.858	3.265	13.399	4.532	3.602	MC	1.10
9	4.753	6.263	3.725	17.665	5.626	4.195	MC	1.13
10	3.084	10.644	3.343	14.991	5.975	4.567	M	1.48
11	4.231	10.303	4.174	16.473	6.833	4.858	MC	1.16
12	3.966	11.232	4.087	20.967	8.588	5.783	M	1.46
13	5.159	10.812	4.850	26.980	10.621	6.065	MC	1.25
Mean Value*								1.110
Standard Deviation*								0.194

* For specimens with material yield strengths up to 80 ksi.

were defined previously in Item A for Inland Tests. The relationships between the ratio of P_{test}/P_{comp} and the material yield strength, F_y, is shown in Fig. 4.7.

It can be seen that both the 1981 Guide and the 1986 Specification provide reasonable predictions of the failure loads for Specimens No. 1 through 9 which failed in the combined bending and web crippling mode. For Specimens No. 10 through 13 where bending moments seem to be the dominant factor to cause the failure, a relatively higher degree of underestimation is realized. This underestimation may be due to the following reasons:

1) Because the ratios of tensile strength to yield strength, F_u/F_y, are large, a substantial amount of cold-work may cause the average yield stress in corners of the compression flange to be much higher than the yield stress of the middle portion of the flange, F_{yf}, and the yield stress of the virgin steel, F_y. However, the values of F_{yf} for these specimens are relatively low when comparing to F_y and F_{yw}. In some cases, the values of F_{yf} are even lower than the yield strength of virgin steels, F_y, due to the die-forming process.
2) The ultimate bending moment may be increased by the inelastic reserve capacity of the entire cross section.

C. PRESENT UMR TESTS ON HIGH STRENGTH STEEL BEAMS

Hat sections and I-beams fabricated from high strength sheet steels were tested under different types of loading conditions as discussed in Section III. Because it was intended to use the test results in the

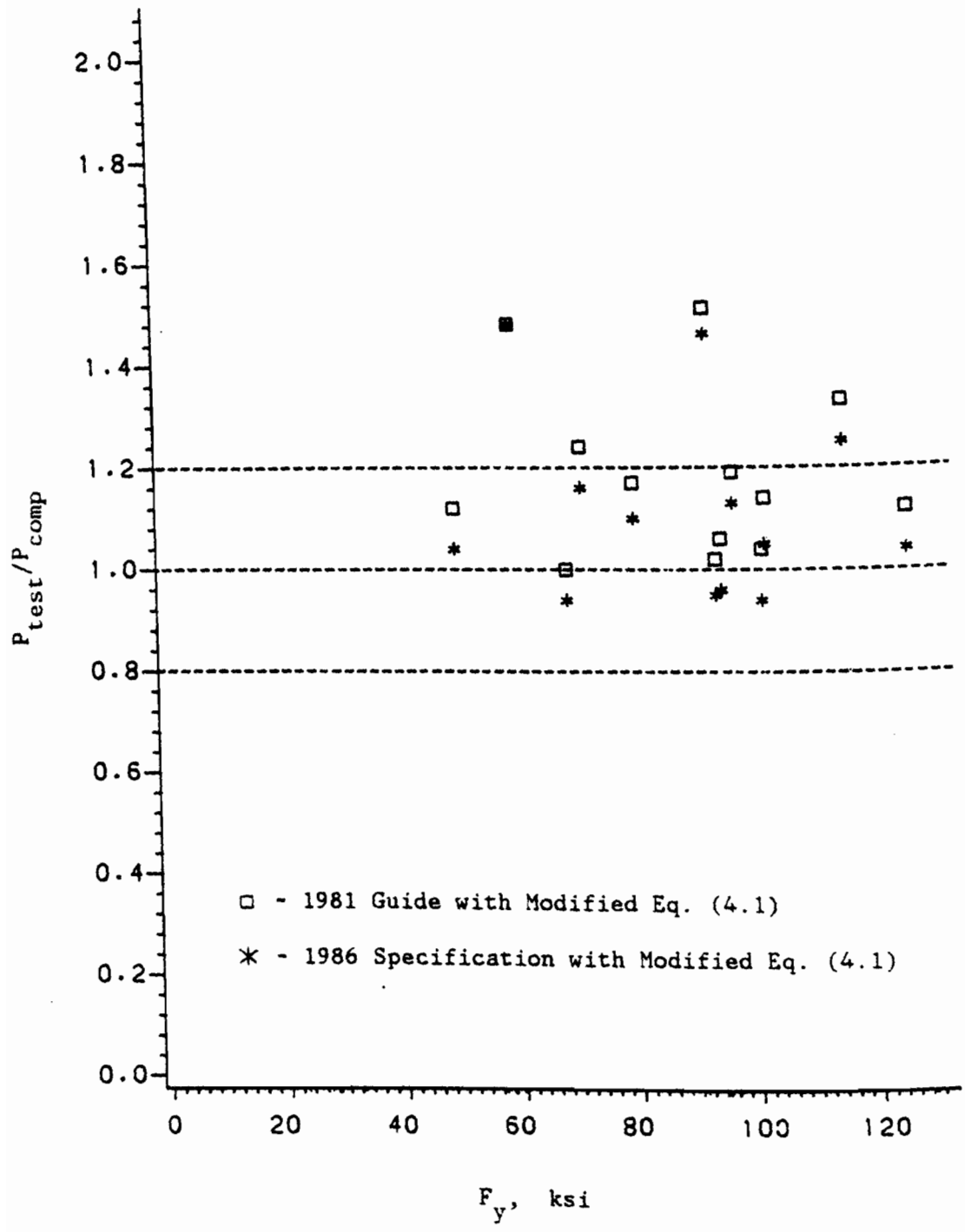

Fig. 4.7 Effect of F_y on the Ratio P_{test}/P_{comp} for Ford Tests Based on the AISI 1981 Guide and 1986 Specification

development of web crippling design criteria all specimens were designed to fail by web crippling. In the comparisons of the tested and predicted failure loads for this group of test data, only web crippling design criteria are considered.

The comparisons of the tested failure loads and the predicted loads for this group of specimens are presented in Tables 4.3 to 4.10. The symbols used in these tables are defined as follows:

1) P_{test} is the tested failure load per web, kips.
2) P_{cg} is the ultimate web crippling load per web based on the 1981 Guide, kips.
3) P_{cs} is the ultimate web crippling load per web based on the 1986 Specification with the modified Eqs. (4.1) and (4.2), kips.
4) P_{test}/P_{cg} is the ratio of the tested failure load to the predicted failure load based on the 1981 Guide.
5) P_{test}/P_{cs} is the ratio of the tested failure load to the predicted failure load based on the 1986 Specification.

The effect of the material yield strength, F_y, on the ratio of P_{test}/P_{comp} is shown for each case in Figs. 4.8 to 4.15.

According to these comparisons, the validities of the existing design criteria for various types of sections subjected to different loading conditions are discussed as follows:

1. Hat-Sections Subjected to Interior One-Flange Loading:

It can be seen from Table 4.3 and Fig. 4.8 that both the 1981 Guide and the 1986 Specification can provide good estimates of the failure loads for 80DK and 80XF specimens which have yield strengths up to 88.3 ksi. However, for the 100XF, 140XF, and 140SK specimens, underestimations were observed possibly due to the use of a constant

Table 4.3

Comparisons of Tested and Predicted Failure Loads for Hat Sections Subjected to Interior One-Flange Loading Based on the 1981 Guide and the 1986 Specification

Specimen No.	Material	P_{test} (kips)	P_{cg} (kips)	P_{cs} (kips)	P_{test}/P_{cg}	P_{test}/P_{cs}
1-HIOF-A11	80DK	1.425	1.625	1.645	0.92	0.87
1-HIOF-A12	80DK	1.400	1.622	1.646	0.90	0.85
1-HIOF-A21	80DK	1.465	1.673	1.557	0.91	0.94
1-HIOF-A22	80DK	1.465	1.673	1.496	0.91	0.98
1-HIOF-A31	80DK	1.450	1.655	1.531	0.91	0.95
1-HIOF-A32	80DK	1.500	1.655	1.510	0.94	0.99
2-HIOF-A11	80XF	5.400	5.400	6.210	1.04	0.87
2-HIOF-A12	80XF	5.365	5.365	6.090	1.04	0.88
2-HIOF-A21	80XF	5.740	5.740	5.985	1.03	0.96
2-HIOF-A22	80XF	5.700	5.738	5.984	1.03	0.95
2-HIOF-A31	80XF	6.265	6.004	5.914	1.08	1.06
2-HIOF-A32	80XF	6.375	6.007	5.913	1.10	1.08
3-HIOF-A11	100XF	4.290	3.290	3.492	1.36	1.23
3-HIOF-A12	100XF	4.300	3.361	3.612	1.33	1.19
3-HIOF-A21	100XF	4.290	3.521	3.531	1.27	1.21
3-HIOF-A22	100XF	4.265	3.544	3.560	1.25	1.20
3-HIOF-A31	100XF	4.325	3.632	3.561	1.23	1.21
3-HIOF-A32	100XF	4.350	3.525	3.419	1.28	1.27
4-HIOF-A11	140XF	2.720	2.125	2.262	1.33	1.20
4-HIOF-A12	140XF	2.600	2.157	2.308	1.26	1.13
4-HIOF-A21	140XF	2.725	2.062	2.048	1.37	1.33
4-HIOF-A22	140XF	2.740	2.080	2.069	1.37	1.32
4-HIOF-A31	140XF	2.700	2.108	2.091	1.35	1.29
4-HIOF-A32	140XF	2.630	2.093	2.069	1.33	1.27
4-HIOF-A13	140XF	2.490	1.902	1.772	1.36	1.41
4-HIOF-A14	140XF	2.475	1.902	1.772	1.35	1.40
4-HIOF-A23	140XF	2.625	1.960	1.715	1.40	1.53
4-HIOF-A24	140XF	2.665	1.961	1.715	1.42	1.55
4-HIOF-A33	140XF	2.575	1.903	1.660	1.45	1.55
4-HIOF-A34	140XF	2.610	1.903	1.660	1.47	1.57
5-HIOF-A11	140SK	2.365	1.837	1.684	1.34	1.40
5-HIOF-A12	140SK	2.325	1.839	1.685	1.32	1.38
5-HIOF-A21	140SK	2.500	1.859	1.628	1.40	1.54
5-HIOF-A22	140SK	2.535	1.859	1.629	1.42	1.56
5-HIOF-A31	140SK	2.465	1.822	1.574	1.46	1.57
5-HIOF-A32	140SK	2.435	1.820	1.573	1.45	1.55
3-HIOF-D11	100XF	4.363	3.130	3.291	1.45	1.33
3-HIOF-D12	100XF	4.275	3.133	3.291	1.42	1.30
3-HIOF-C11	100XF	4.225	3.091	3.291	1.42	1.28
3-HIOF-C12	100XF	4.250	3.085	3.291	1.43	1.29

Table 4.3 (Cont'd)

Comparisons of Tested and Predicted Failure Loads for Hat Sections
Subjected to Interior One-Flange Loading
Based on the 1981 Guide and the 1986 Specification

Specimen No.	Material	P_{test} (kips)	P_{cg} (kips)	P_{cs} (kips)	P_{test}/P_{cg}	P_{test}/P_{cs}
3-HIOF-B11	100XF	4.150	3.055	3.291	1.41	1.26
3-HIOF-B12	100XF	4.188	3.055	3.291	1.43	1.27
3-HIOF-D21	100XF	4.375	3.362	3.291	1.37	1.33
3-HIOF-D22	100XF	4.325	3.357	3.291	1.36	1.31
3-HIOF-C21	100XF	4.175	3.315	3.291	1.31	1.27
3-HIOF-C22	100XF	4.150	3.316	3.291	1.30	1.26
3-HIOF-B21	100XF	4.100	3.279	3.291	1.30	1.25
3-HIOF-B22	100XF	4.063	3.285	3.291	1.28	1.23
3-HIOF-D31	100XF	4.500	3.503	3.291	1.41	1.37
3-HIOF-D32	100XF	4.400	3.507	3.291	1.38	1.34
3-HIOF-C31	100XF	4.188	3.460	3.291	1.31	1.27
3-HIOF-C32	100XF	4.200	3.460	3.291	1.32	1.28
3-HIOF-B31	100XF	4.087	3.434	3.291	1.28	1.24
3-HIOF-B32	100XF	4.250	3.434	3.291	1.33	1.29
5-HIOF-D11	140SK	2.450	1.723	1.749	1.48	1.40
5-HIOF-D12	140SK	2.500	1.716	1.749	1.51	1.43
5-HIOF-C11	140SK	2.475	1.695	1.749	1.52	1.41
5-HIOF-C12	140SK	2.400	1.694	1.749	1.47	1.37
5-HIOF-B11	140SK	2.587	1.691	1.749	1.59	1.48
5-HIOF-B12	140SK	2.600	1.683	1.749	1.60	1.49
5-HIOF-D21	140SK	2.587	1.806	1.749	1.55	1.48
5-HIOF-D22	140SK	2.500	1.809	1.749	1.50	1.43
5-HIOF-C21	140SK	2.537	1.780	1.749	1.52	1.45
5-HIOF-C22	140SK	2.613	1.783	1.749	1.56	1.49
5-HIOF-B21	140SK	2.537	1.766	1.749	1.52	1.45
5-HIOF-B22	140SK	2.600	1.769	1.749	1.56	1.49
5-HIOF-D31	140SK	2.688	1.857	1.749	1.61	1.54
5-HIOF-D32	140SK	2.712	1.855	1.749	1.62	1.55
5-HIOF-C31	140SK	2.675	1.831	1.749	1.60	1.53
5-HIOF-C32	140SK	2.650	1.830	1.749	1.59	1.52
5-HIOF-B31	140SK	2.762	1.813	1.749	1.65	1.58
5-HIOF-B32	140SK	2.700	1.815	1.749	1.62	1.54
Mean Value*					0.915	0.930
Standard Deviation*					0.014	0.058

* For specimens with material yield strengths up to 80 ksi.

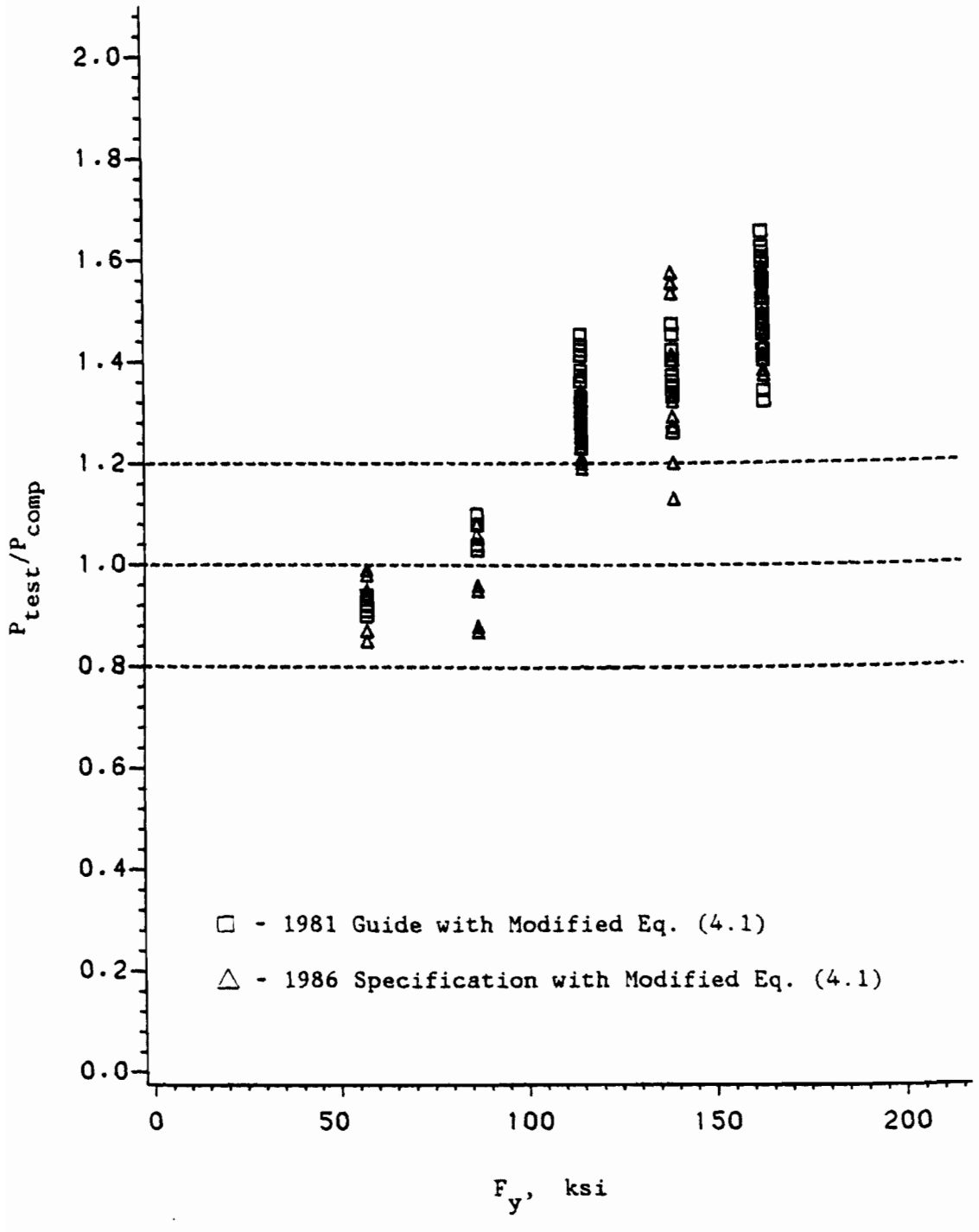

Fig. 4.8 Effect of F_y on the Ratio P_{test}/P_{comp} for Hat Sections Subjected to Interior One-Flange Loading Based on the AISI 1981 Guide and 1986 Specification

yield strength of 91.5 ksi (Modified Eq. (4.1)) in place of the actual higher value of yield strengths.

For this group of data, test results indicate that the degree of underestimation increases as the yield strength increases when the actual yield strength exceeds the present limit of 80 ksi. However, this comparison does not agree with the results of Inland tests. It seems to suggest that the function of F_y is not the only factor that causes the inaccuracy in the prediction of the ultimate web crippling load for the sections fabricated from high strength sheet steels having yield strengths exceeding 80 ksi.

2. Hat-Sections Subjected to End One-Flange Loading:

The 1986 Specification has two different equations to determine the ultimate web crippling loads for sections having stiffened and unstiffened flanges. However, the 1981 Guide has only one equation for both cases. All hat sections used in this study were tested in such a way that the unstiffened flanges were in contact with the bearing plates at both ends.

It can be seen from Table 4.4 and Fig. 4.9 that the predicted failure loads for this case are rather conservative partly because of the use of a constant F_y instead of the actual yield strength of the high strength sheet steels (Modified Eq. (4.2)). Furthermore, for some specimens, the buckling type of failure was observed. This type of failure is independent of material yield strength.

3. Hat-Sections Subjected to Interior Two-Flange Loading:

Table 4.5 indicates that for the 80DK and 80XF specimens, both the 1981 Guide and the 1986 Specification provide good predictions for the ultimate web crippling loads. For the 100XF and 140SK specimens using

Table 4.4

Comparisons of Tested and Predicted Failure Loads for Hat Sections
Subjected to End One-Flange Loading
Based on the 1981 Guide and the 1986 Specification

Specimen No.	Material	P_{test} (kips)	P_{cg} (kips)	P_{cs} (kips)	P_{test}/P_{cg}	P_{test}/P_{cs}
1-HEOF-A11	80DK	0.719	0.662	0.472	1.09	1.52
1-HEOF-A12	80DK	0.700	0.662	0.472	1.06	1.48
1-HEOF-A21	80DK	0.694	0.611	0.460	1.14	1.51
1-HEOF-A22	80DK	0.688	0.609	0.460	1.13	1.50
1-HEOF-A31	80DK	0.669	0.552	0.447	1.21	1.50
1-HEOF-A32	80DK	0.643	0.552	0.447	1.16	1.44
2-HEOF-A11	80XF	2.919	2.366	1.828	1.23	1.60
2-HEOF-A12	80XF	2.981	2.455	1.896	1.21	1.57
2-HEOF-A21	80XF	2.994	2.328	1.834	1.29	1.63
2-HEOF-A22	80XF	3.125	2.415	1.901	1.29	1.64
2-HEOF-A31	80XF	2.713	2.242	1.803	1.21	1.50
2-HEOF-A32	80XF	2.825	2.285	1.837	1.24	1.54
3-HEOF-A11	100XF	2.050	1.406	1.032	1.46	1.99
3-HEOF-A12	100XF	2.106	1.519	1.114	1.39	1.89
3-HEOF-A21	100XF	2.006	1.402	1.064	1.43	1.89
3-HEOF-A22	100XF	2.075	1.403	1.064	1.48	1.95
3-HEOF-A31	100XF	1.894	1.288	1.015	1.47	1.87
3-HEOF-A32	100XF	1.869	1.221	0.963	1.53	1.94
4-HEOF-A11	140XF	1.313	0.915	0.650	1.43	2.02
4-HEOF-A12	140XF	1.300	0.775	0.548	1.68	2.37
4-HEOF-A21	140XF	1.219	0.675	0.511	1.81	2.39
4-HEOF-A22	140XF	1.125	0.622	0.471	1.81	2.39
4-HEOF-A31	140XF	1.088	0.652	0.534	1.67	2.04
4-HEOF-A32	140XF	1.063	0.750	0.613	1.42	1.73
5-HEOF-A11	140SK	1.295	0.627	0.445	2.07	2.91
5-HEOF-A12	140SK	1.285	0.628	0.445	2.05	2.89
5-HEOF-A21	140SK	1.200	0.565	0.431	2.12	2.78
5-HEOF-A11	140SK	1.178	0.567	0.431	2.08	2.73
5-HEOF-A11	140SK	1.050	0.504	0.417	2.08	2.52
5-HEOF-A11	140SK	1.035	0.506	0.418	2.04	2.48
Mean Value*					1.132	1.492
Standard Deviation*					0.053	0.029

* For specimens with material yield strengths up to 80 ksi.

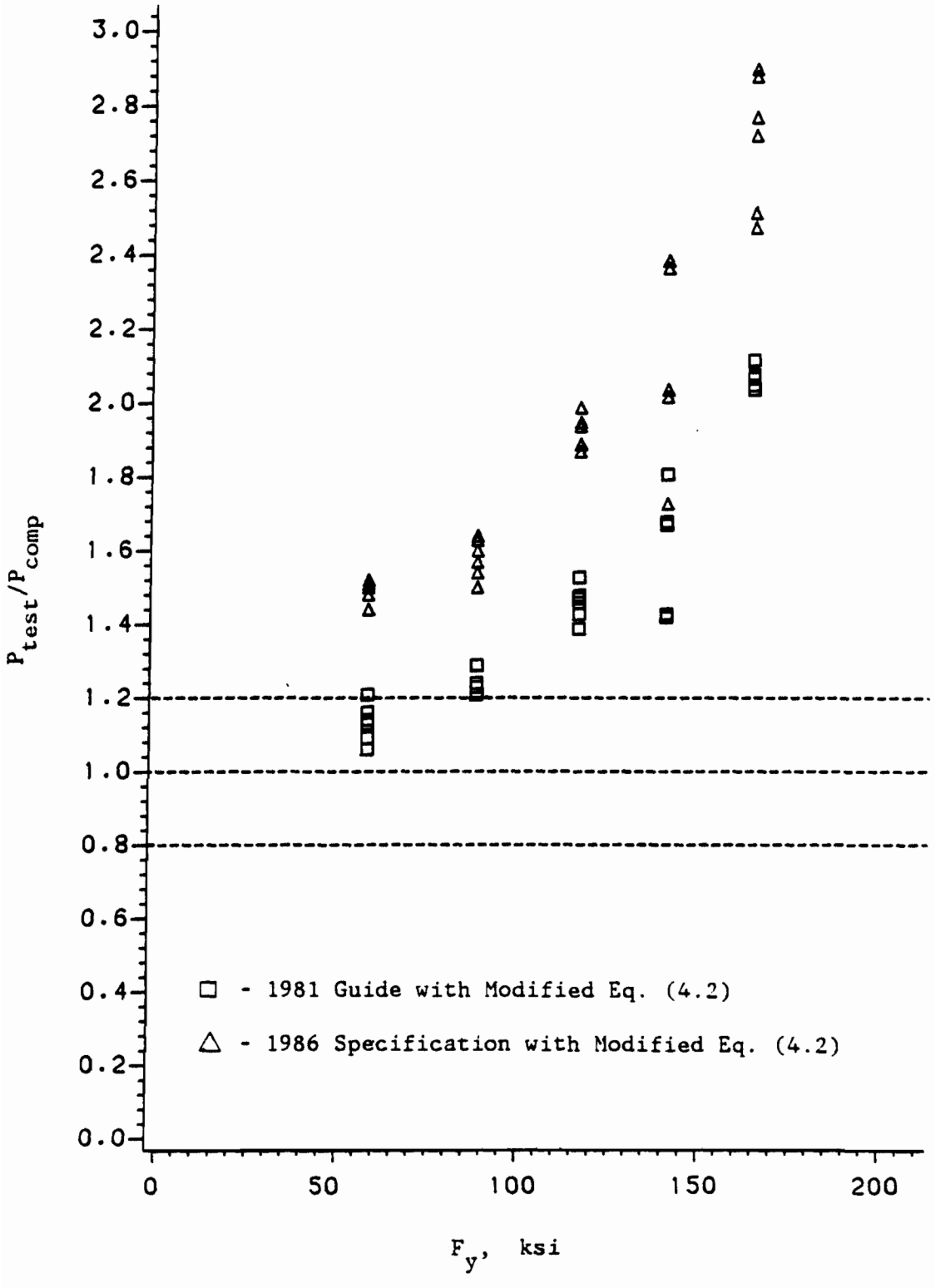

Fig. 4.9 Effect of F_y on the Ratio P_{test}/P_{comp} for Hat Sections Subjected to End One-Flange Loading Based on the AISI 1981 Guide and 1986 Specification

Table 4.5

Comparisons of Tested and Predicted Failure Loads for Hat Sections Subjected to Interior Two-Flange Loading Based on the 1981 Guide and the 1986 Specification

Specimen No.	Material	P_{test} (kips)	P_{cg} (kips)	P_{cs} (kips)	P_{test}/P_{cg}	P_{test}/P_{cs}
1-HITF-A11	80DK	1.650	1.716	1.772	0.96	0.93
1-HITF-A12	80DK	1.625	1.716	1.772	0.95	0.92
1-HITF-A21	80DK	1.650	1.623	1.638	1.02	1.01
1-HITF-A22	80DK	1.625	1.622	1.636	1.00	0.99
1-HITF-A31	80DK	1.600	1.525	1.495	1.05	1.07
1-HITF-A32	80DK	1.625	1.526	1.496	1.06	1.09
2-HITF-A11	80XF	6.875	7.043	8.177	0.98	0.84
2-HITF-A12	80XF	6.900	7.043	8.177	0.98	0.84
2-HITF-A21	80XF	6.875	6.873	7.874	1.00	0.87
2-HITF-A22	80XF	6.800	6.869	7.868	0.99	0.86
2-HITF-A31	80XF	6.875	6.696	7.559	1.03	0.91
2-HITF-A32	80XF	6.900	6.697	7.562	1.03	0.91
3-HITF-A11	100XF	5.050	3.744	4.129	1.35	1.22
3-HITF-A12	100XF	5.150	3.748	4.136	1.37	1.25
3-HITF-A21	100XF	4.850	3.619	3.926	1.34	1.24
3-HITF-A22	100XF	4.800	3.619	3.926	1.33	1.22
3-HITF-A31	100XF	4.800	3.484	3.706	1.38	1.30
3-HITF-A32	100XF	4.700	3.484	3.706	1.35	1.27
5-HITF-A11	140SK	2.950	1.891	1.942	1.56	1.52
5-HITF-A12	140SK	3.000	1.891	1.942	1.59	1.54
5-HITF-A21	140SK	2.775	1.793	1.800	1.55	1.54
5-HITF-A22	140SK	2.750	1.791	1.797	1.54	1.53
5-HITF-A31	140SK	2.625	1.678	1.635	1.56	1.61
5-HITF-A32	140SK	2.613	1.676	1.632	1.56	1.60
Mean Value*					1.007	1.001
Standard Deviation*					0.045	0.070

* For specimens with material yield strengths up to 80 ksi.

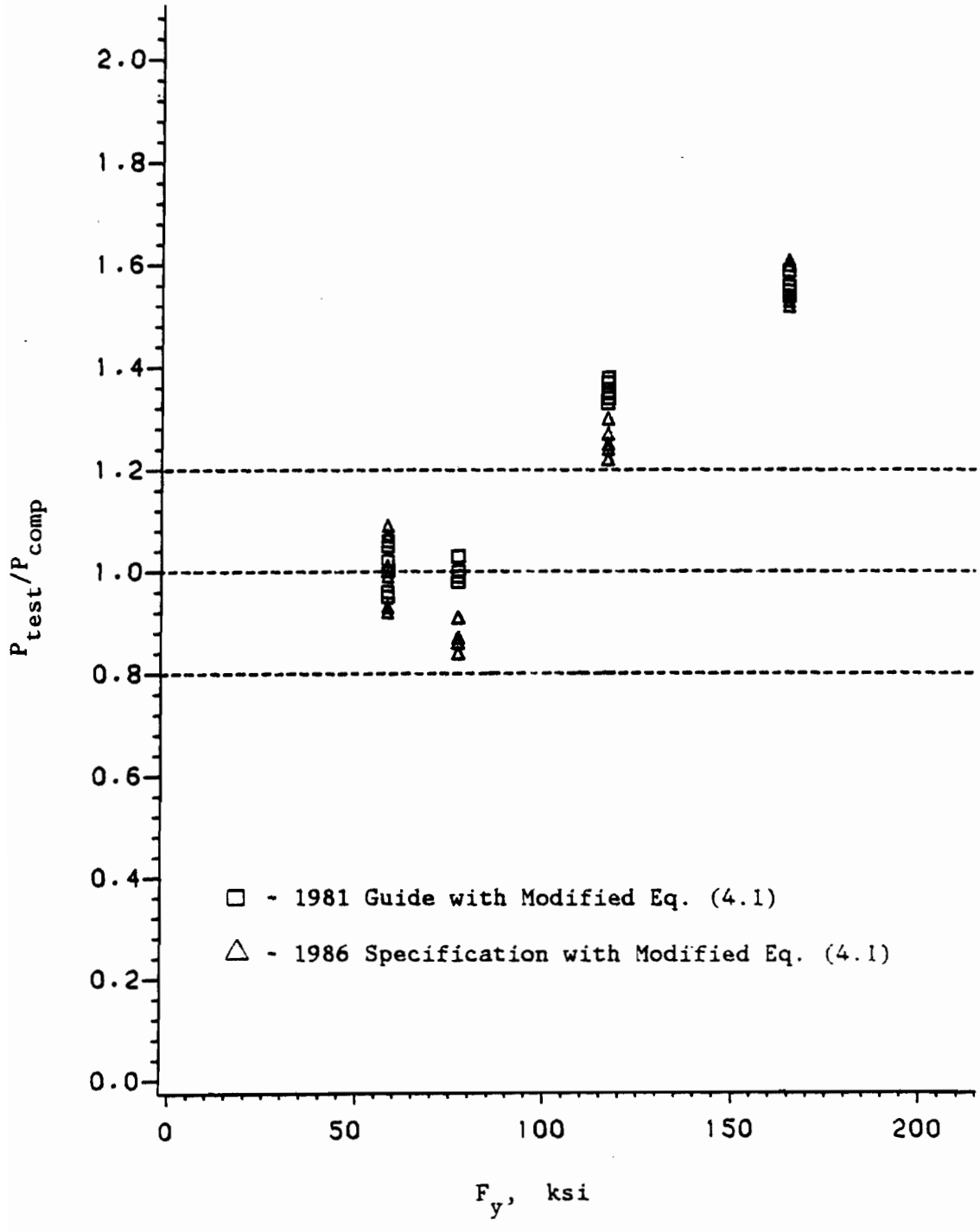

Fig. 4.10 Effect of F_y on the Ratio P_{test}/P_{comp} for Hat Sections Subjected to Interior Two-Flange Loading Based on the AISI 1981 Guide and 1986 Specification

very high yield strengths, the underestimation of web crippling loads was observed as can be seen clearly from Fig. 4.10.

It should be noted that the 1981 Guide uses the same equation for interior one-flange loading and the interior two-flange loading while the 1986 Specification has different equations for both cases.

4. Hat-Sections Subjected to End Two-Flange Loading:

As the previous case, the 1981 Guide uses the same equation for both end one-flange loading and end two-flange loading. It can be seen from Table 4.6 and Fig. 4.11 that both the 1981 Guide and 1986 Specification underestimate the ultimate web crippling loads for most of the specimens. This underestimation may be caused by using improper parameters in the prediction equations.

5. I-Beams Subjected to Interior One-Flange Loading:

Table 4.7 and Fig. 4.12 indicates that the predicted web crippling loads are higher than the tested failure loads especially for the predicted values based on the 1981 Guide which have very high degree of overestimation. The 1986 Specification gives reasonable estimates for the 80DK and 80XF specimens but overestimates the web crippling loads for the 100XF and 140SK specimens. It should be noted that all specimens used in this phase of study failed by web buckling.

6. I-Beams Subjected to End One-Flange Loading:

The comparisons of the tested and predicted failure loads are shown in Table 4.8. It can be seen that both the 1981 Guide and the Specification provide good estimations of ultimate web crippling loads for the 80DK and 80XF specimens but overestimate the web crippling capacities of the 100XF and 140SK specimens. Figure 4.13 shows the

Table 4.6

Comparisons of Tested and Predicted Failure Loads for Hat Sections Subjected to End Two-Flange Loading Based on the 1981 Guide and the 1986 Specification

Specimen No.	Material	P_{test} (kips)	P_{cg} (kips)	P_{cs} (kips)	P_{test}/P_{cg}	P_{test}/P_{cs}
1-HETF-A11	80DK	0.725	0.640	0.476	1.13	1.52
1-HETF-A12	80DK	0.713	0.639	0.476	1.12	1.50
1-HETF-A21	80DK	0.725	0.581	0.448	1.25	1.62
1-HETF-A22	80DK	0.725	0.580	0.448	1.25	1.62
1-HETF-A31	80DK	0.650	0.522	0.420	1.25	1.55
1-HETF-A32	80DK	0.662	0.522	0.420	1.27	1.57
2-HETF-A11	80XF	2.825	2.452	2.082	1.15	1.36
2-HETF-A12	80XF	2.787	2.452	2.082	1.14	1.34
2-HETF-A21	80XF	2.700	2.372	2.022	1.14	1.34
2-HETF-A22	80XF	2.650	2.372	2.022	1.12	1.31
2-HETF-A31	80XF	2.425	2.289	1.960	1.06	1.24
2-HETF-A32	80XF	2.400	2.290	1.960	1.05	1.22
3-HETF-A11	100XF	1.525	1.172	0.928	1.30	1.64
3-HETF-A12	100XF	1.600	1.172	0.928	1.37	1.72
3-HETF-A21	100XF	1.413	1.109	0.890	1.27	1.59
3-HETF-A22	100XF	1.487	1.109	0.891	1.34	1.67
3-HETF-A31	100XF	1.300	1.042	0.851	1.25	1.53
3-HETF-A32	100XF	1.312	1.044	0.852	1.26	1.54
5-HETF-A11	140SK	0.750	0.627	0.464	1.20	1.61
5-HETF-A12	140SK	0.762	0.627	0.465	1.21	1.64
5-HETF-A21	140SK	0.675	0.565	0.436	1.19	1.55
5-HETF-A22	140SK	0.700	0.565	0.436	1.24	1.61
5-HETF-A31	140SK	0.612	0.507	0.409	1.21	1.50
5-HETF-A32	140SK	0.600	0.508	0.410	1.18	1.47
Mean Value*					1.212	1.563
Standard Deviation*					0.068	0.050

* For specimens with material yield strengths up to 80 ksi.

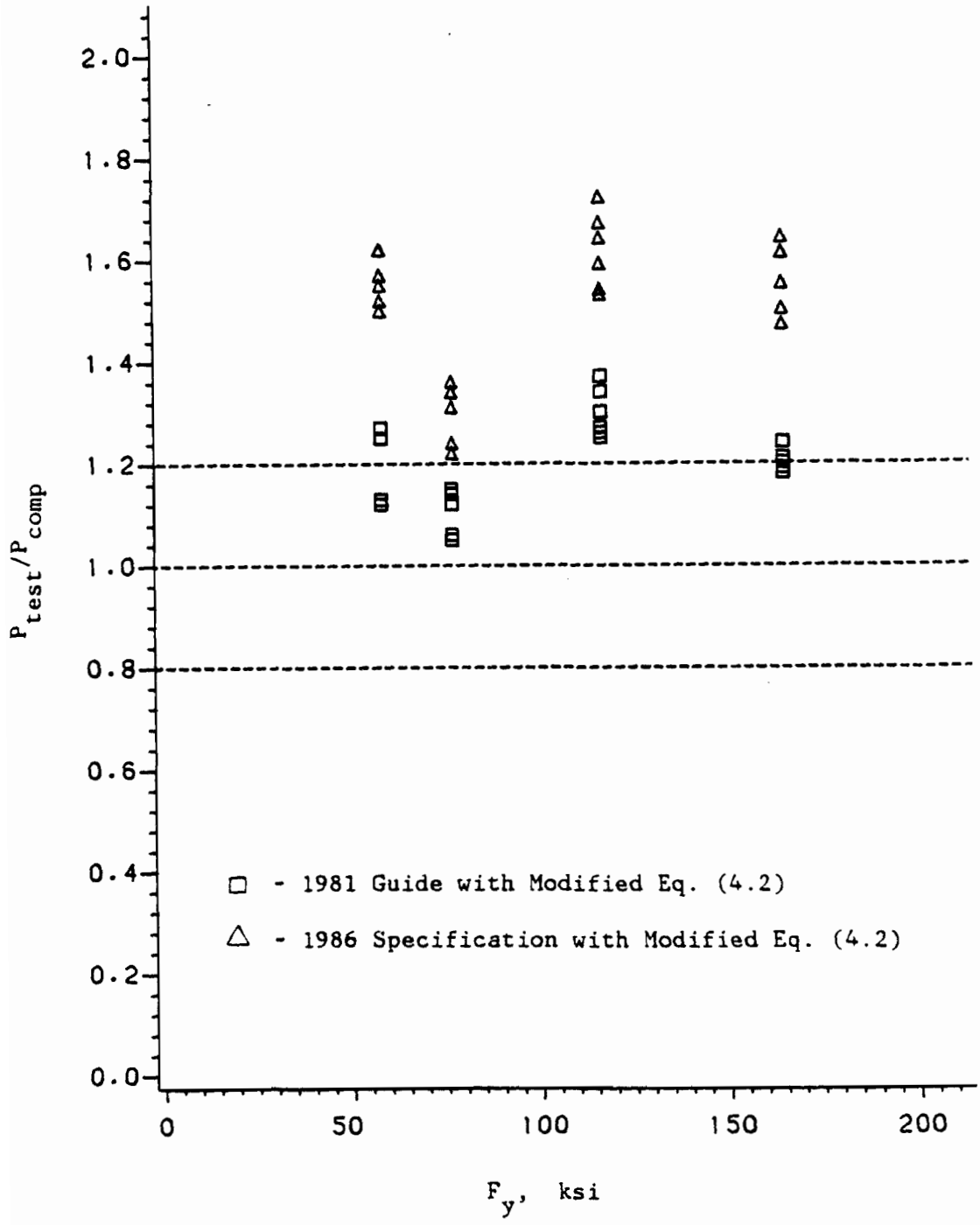

Fig. 4.11 Effect of F_y on the Ratio P_{test}/P_{comp} for Hat Sections Subjected to End Two-Flange Loading Based on the AISI 1981 Guide and 1986 Specification

Table 4.7

Comparisons of Tested and Predicted Failure Loads for I-Beams Subjected to Interior One-Flange Loading Based on the 1981 Guide and the 1986 Specification

Specimen No.	Material	P_{test} (kips)	P_{cg} (kips)	P_{cs} (kips)	P_{test}/P_{cg}	P_{test}/P_{cs}
1-IIOF-A11	80DK	2.450	4.486	2.572	0.55	0.95
1-IIOF-A12	80DK	2.400	4.486	2.572	0.53	0.93
1-IIOF-A21	80DK	2.625	4.486	2.572	0.59	1.02
1-IIOF-A22	80DK	2.450	4.486	2.572	0.55	0.95
1-IIOF-A31	80DK	2.325	4.486	2.572	0.52	0.90
1-IIOF-A32	80DK	2.350	4.486	2.572	0.52	0.91
2-IIOF-A11	80XF	8.750	18.436	11.203	0.47	0.78
2-IIOF-A12	80XF	8.775	18.436	11.203	0.48	0.78
2-IIOF-A21	80XF	9.300	18.436	11.203	0.50	0.83
2-IIOF-A22	80XF	9.463	18.436	11.203	0.51	0.84
2-IIOF-A31	80XF	9.175	18.436	11.203	0.50	0.82
2-IIOF-A32	80XF	9.500	18.436	11.203	0.52	0.85
3-IIOF-A11	100XF	6.175	16.204	9.598	0.38	0.64
3-IIOF-A12	100XF	6.325	16.204	9.598	0.39	0.66
3-IIOF-A21	100XF	6.825	16.204	9.598	0.42	0.71
3-IIOF-A22	100XF	6.563	16.204	9.598	0.41	0.68
3-IIOF-A31	100XF	5.912	16.204	9.598	0.36	0.62
3-IIOF-A32	100XF	6.250	16.204	9.598	0.39	0.65
5-IIOF-A11	140SK	3.275	12.727	7.295	0.26	0.45
5-IIOF-A12	140SK	3.117	12.727	7.295	0.24	0.43
5-IIOF-A21	140SK	3.100	12.727	7.295	0.24	0.42
5-IIOF-A22	140SK	3.175	12.727	7.295	0.25	0.44
5-IIOF-A31	140SK	3.075	12.727	7.295	0.24	0.42
5-IIOF-A32	140SK	3.200	12.727	7.295	0.25	0.44
Mean Value*					0.543	0.943
Standard Deviation*					0.027	0.043

* For specimens with material yield strengths up to 80 ksi.

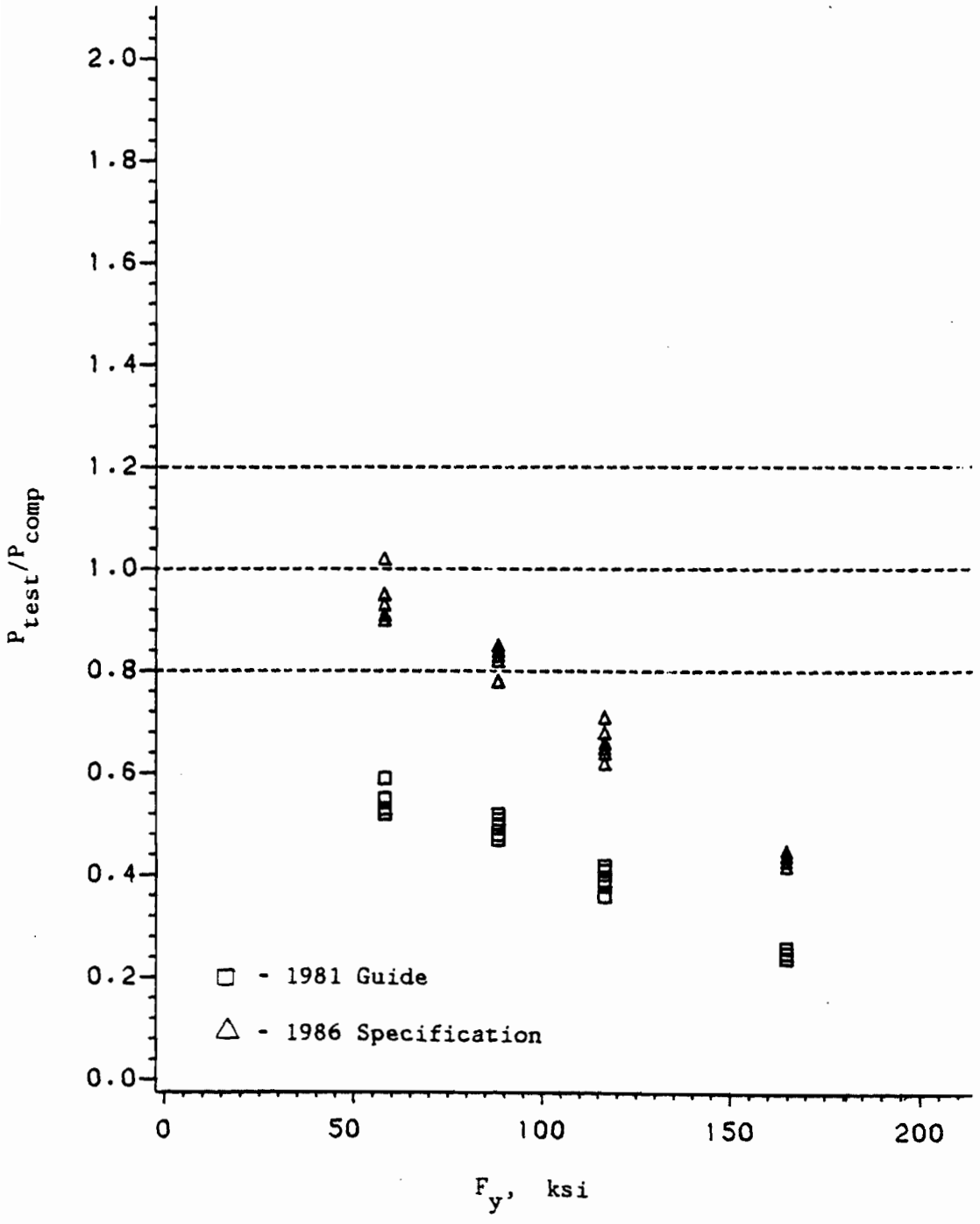

Fig. 4.12 Effect of F_y on the Ratio P_{test}/P_{comp} for I-Beams Subjected to Interior One-Flange Loading Based on the AISI 1981 Guide and 1986 Specification

Table 4.8

Comparisons of Tested and Predicted Failure Loads for I-Beams
Subjected to End One-Flange Loading
Based on the 1981 Guide and the 1986 Specification

Specimen No.	Material	P_{test} (kips)	P_{cg} (kips)	P_{cs} (kips)	P_{test}/P_{cg}	P_{test}/P_{cs}
1-IEOF-A11	80DK	2.830	2.423	2.629	1.17	1.08
1-IEOF-A12	80DK	2.750	2.423	2.632	1.14	1.04
1-IEOF-A21	80DK	2.630	2.423	2.698	1.09	0.97
1-IEOF-A22	80DK	2.675	2.423	2.697	1.10	0.99
1-IEOF-A31	80DK	2.750	2.423	2.766	1.14	0.99
1-IEOF-A32	80DK	2.695	2.423	2.768	1.11	0.97
2-IEOF-A11	80XF	8.017	9.603	10.096	0.83	0.79
2-IEOF-A12	80XF	8.100	9.603	10.100	0.84	0.80
2-IEOF-A21	80XF	7.850	9.603	10.256	0.82	0.77
2-IEOF-A22	80XF	7.600	9.603	10.253	0.79	0.74
2-IEOF-A31	80XF	7.625	9.603	10.405	0.79	0.73
2-IEOF-A32	80XF	7.775	9.603	10.405	0.81	0.75
3-IEOF-A11	100XF	4.395	7.434	7.951	0.59	0.55
3-IEOF-A12	100XF	4.370	7.434	7.936	0.59	0.55
3-IEOF-A21	100XF	4.250	7.434	8.098	0.57	0.52
3-IEOF-A22	100XF	4.125	7.434	8.092	0.55	0.51
3-IEOF-A31	100XF	4.125	7.434	8.255	0.55	0.50
3-IEOF-A32	100XF	4.000	7.434	8.256	0.54	0.48
5-IEOF-A11	140SK	2.217	6.373	6.939	0.35	0.32
5-IEOF-A12	140SK	2.175	6.373	6.935	0.34	0.31
5-IEOF-A21	140SK	2.200	6.373	7.128	0.35	0.31
5-IEOF-A22	140SK	2.075	6.373	7.122	0.33	0.29
5-IEOF-A31	140SK	2.117	6.373	7.311	0.33	0.29
5-IEOF-A32	140SK	2.015	6.373	7.317	0.32	0.28
Mean Value*					1.125	1.007
Standard Deviation*					0.030	0.044

* For specimens with material yield strengths up to 80 ksi.

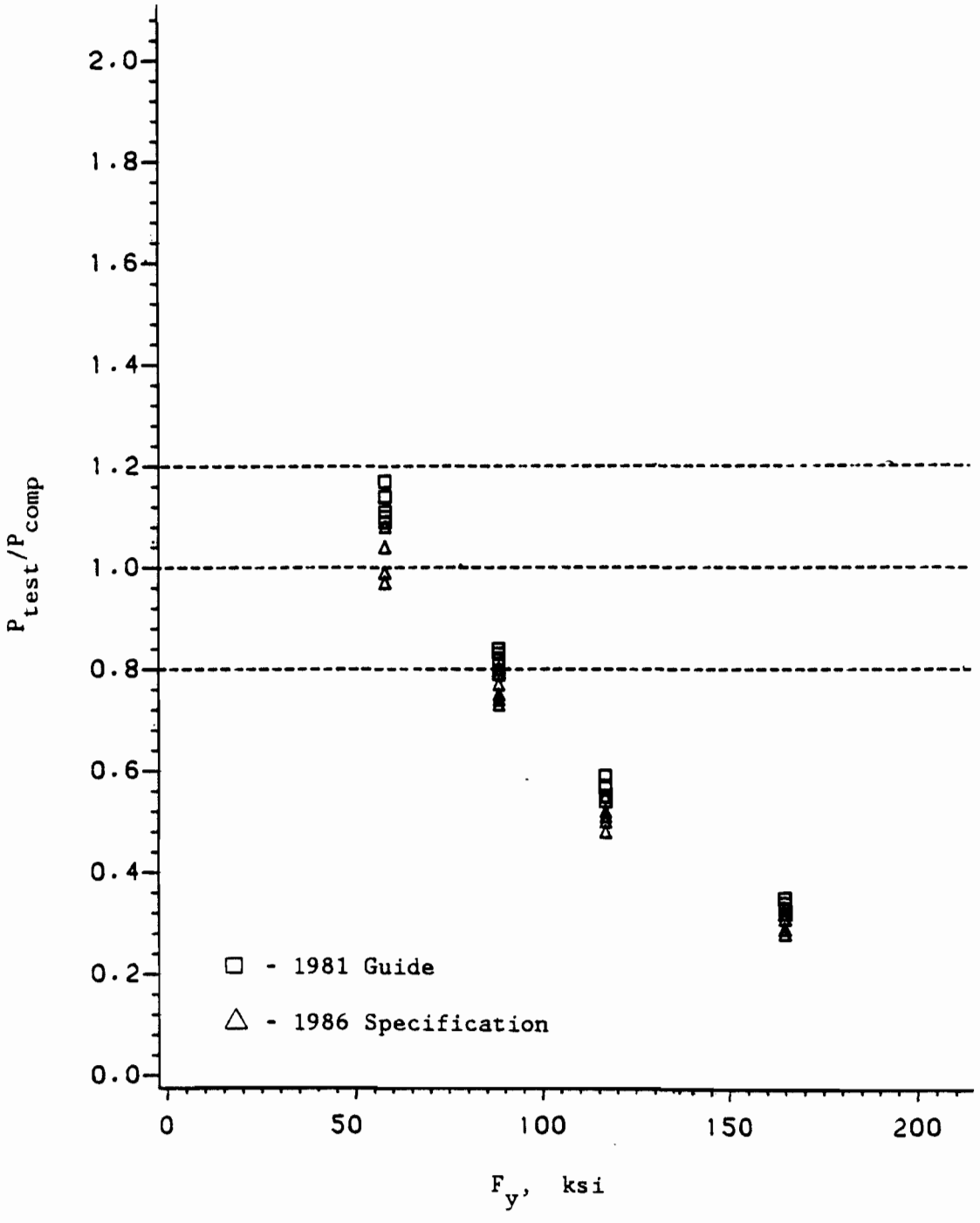

Fig. 4.13 Effect of F_y on the Ratio P_{test}/P_{comp} for I-Beams Subjected to End One-Flange Loading Based on the AISI 1981 Guide and 1986 Specification

relationships between the ratio of P_{test}/P_{comp} and F_y. The overestimation of web crippling load may be caused by the same reason as discussed for the previous case.

7. I-Beams Subjected to Interior Two-Flange Loading:

The equation used for this case to predict the ultimate web crippling on the basis of the the 1981 Guide is the same as the case for interior one-flange loading. Table 4.9 presents the comparisons of the tested and predicted failure loads. Based on the 1981 Guide, the degree of overestimation increases as the yield strength increases. The accuracy of predictions based on the 1986 Specification are inconsistent as can be seen from Fig. 4.14.

It can be seen from the equation used to predict the ultimate web crippling load for I-beams subjected to interior one-flange loading that Eq. 2.26 is independent of yield strength of material, F_y. Even though there are two terms of F_y in the equation, one in the numerator and the other in the denominator, they are simply cancelled out. The independence of F_y in this equation agrees with the test results which indicate web buckling failure for all specimens used in this case. However, the inconsistency in the accuracy of prediction may arise from using improper parameters in the equation.

8. I-Beams Subjected to End Two-Flange Loading:

Same as the hat sections, the 1981 Guide has only one equation to predict both end one-flange loading and end two-flange loading cases. Table 4.10 shows the same trend of overestimation for the 1981 Guide as the previous case. The 1986 Specification underestimates the failure loads. Figure 4.15 shows the relationships between the ratio of

Table 4.9

Comparisons of Tested and Predicted Failure Loads for I-Beams Subjected to Interior Two-Flange Loading Based on the 1981 Guide and the 1986 Specification

Specimen No.	Material	P_{test} (kips)	P_{cg} (kips)	P_{cs} (kips)	P_{test}/P_{cg}	P_{test}/P_{cs}
1-IITF-A11	80DK	4.350	4.654	2.416	0.93	1.80
1-IITF-A12	80DK	4.450	4.654	2.416	0.96	1.84
1-IITF-A21	80DK	2.775	4.654	2.354	0.60	1.18
1-IITF-A22	80DK	2.750	4.654	2.354	0.59	1.17
1-IITF-A31	80DK	2.188	4.654	2.277	0.47	0.96
1-IITF-A32	80DK	2.150	4.654	2.278	0.46	0.94
2-IITF-A11	80XF	19.875	18.207	7.774	1.09	2.56
2-IITF-A12	80XF	20.050	18.207	7.774	1.10	2.58
2-IITF-A21	80XF	17.000	18.207	7.774	0.93	2.19
2-IITF-A22	80XF	16.500	18.207	7.774	0.91	2.12
2-IITF-A31	80XF	11.850	18.207	7.774	0.65	1.52
2-IITF-A32	80XF	12.125	18.207	7.774	0.67	1.56
3-IITF-A11	100XF	14.125	16.312	4.382	0.87	3.22
3-IITF-A12	100XF	14.050	16.312	4.382	0.86	3.21
3-IITF-A21	100XF	7.188	16.312	4.382	0.44	1.64
3-IITF-A22	100XF	7.300	16.312	4.382	0.45	1.67
3-IITF-A31	100XF	5.375	16.312	4.324	0.33	1.24
3-IITF-A32	100XF	5.500	16.312	4.325	0.34	1.27
5-IITF-A11	140SK	5.025	12.727	2.324	0.39	2.16
5-IITF-A12	140SK	4.975	12.727	2.324	0.39	2.14
5-IITF-A21	140SK	3.000	12.727	2.260	0.24	1.33
5-IITF-A11	140SK	2.975	12.727	2.260	0.23	1.32
5-IITF-A11	140SK	2.025	12.727	2.183	0.16	0.93
5-IITF-A11	140SK	2.125	12.727	2.182	0.17	0.97
Mean Value*					0.668	1.315
Standard Deviation*					0.222	0.404

* For specimens with material yield strengths up to 80 ksi.

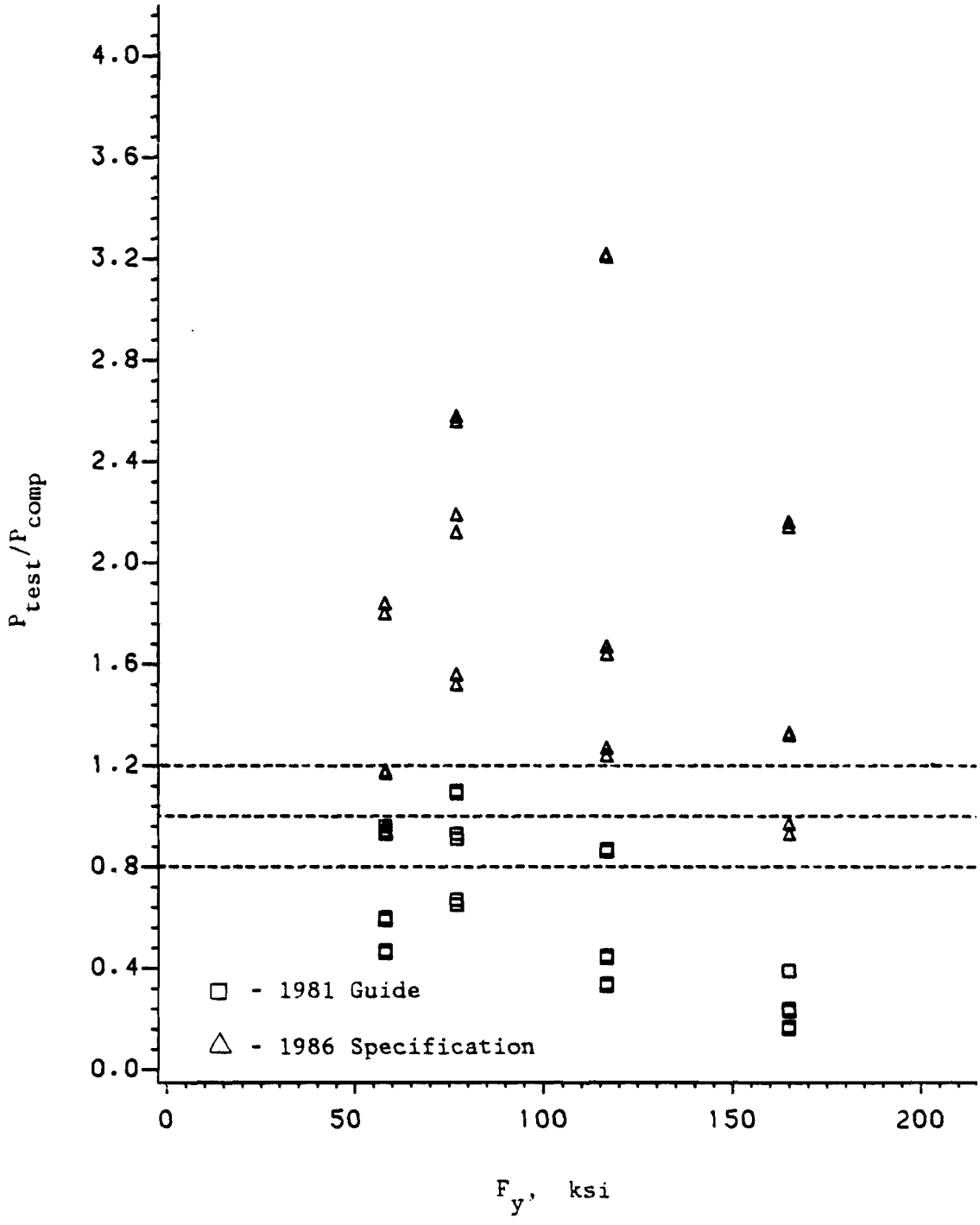

Fig. 4.14 Effect of F_y on the Ratio P_{test}/P_{comp} for I-Beams Subjected to Interior Two-Flange Loading Based on the AISI 1981 Guide and 1986 Specification

Table 4.10

Comparisons of Tested and Predicted Failure Loads for I-Beams
Subjected to End Two-Flange Loading
Based on the 1981 Guide and the 1986 Specification

Specimen No.	Material	P_{test} (kips)	P_{cg} (kips)	P_{cs} (kips)	P_{test}/P_{cg}	P_{test}/P_{cs}
1-IETF-A11	80DK	1.575	2.334	1.006	0.67	1.57
1-IETF-A12	80DK	1.562	2.334	1.006	0.67	1.55
1-IETF-A21	80DK	1.475	2.334	0.979	0.63	1.51
1-IETF-A22	80DK	1.512	2.334	0.979	0.65	1.54
1-IETF-A31	80DK	1.287	2.334	0.951	0.55	1.35
1-IETF-A32	80DK	1.225	2.334	0.951	0.52	1.29
2-IETF-A11	80XF	5.175	9.529	3.871	0.54	1.34
2-IETF-A12	80XF	5.050	9.529	3.870	0.53	1.30
2-IETF-A21	80XF	4.237	9.529	3.816	0.44	1.11
2-IETF-A22	80XF	4.350	9.529	3.817	0.46	1.14
2-IETF-A31	80XF	4.012	9.529	3.765	0.42	1.07
2-IETF-A32	80XF	3.950	9.529	3.764	0.41	1.05
3-IETF-A11	100XF	2.775	8.364	1.998	0.33	1.39
3-IETF-A12	100XF	2.700	8.364	1.998	0.32	1.35
3-IETF-A21	100XF	2.312	8.364	1.960	0.28	1.18
3-IETF-A22	100XF	2.275	8.364	1.960	0.27	1.16
3-IETF-A31	100XF	2.237	8.364	1.921	0.27	1.16
3-IETF-A32	100XF	2.300	8.364	1.922	0.28	1.20
5-IETF-A11	140SK	1.325	6.373	0.961	0.21	1.38
5-IETF-A12	140SK	1.312	6.373	0.962	0.21	1.36
5-IETF-A21	140SK	1.250	6.373	0.935	0.20	1.34
5-IETF-A11	140SK	1.175	6.373	0.935	0.18	1.26
5-IETF-A11	140SK	1.000	6.373	0.908	0.16	1.10
5-IETF-A11	140SK	0.962	6.373	0.909	0.15	1.06
Mean Value*					0.615	1.468
Standard Deviation*					0.064	0.118

* For specimens with material yield strengths up to 80 ksi.

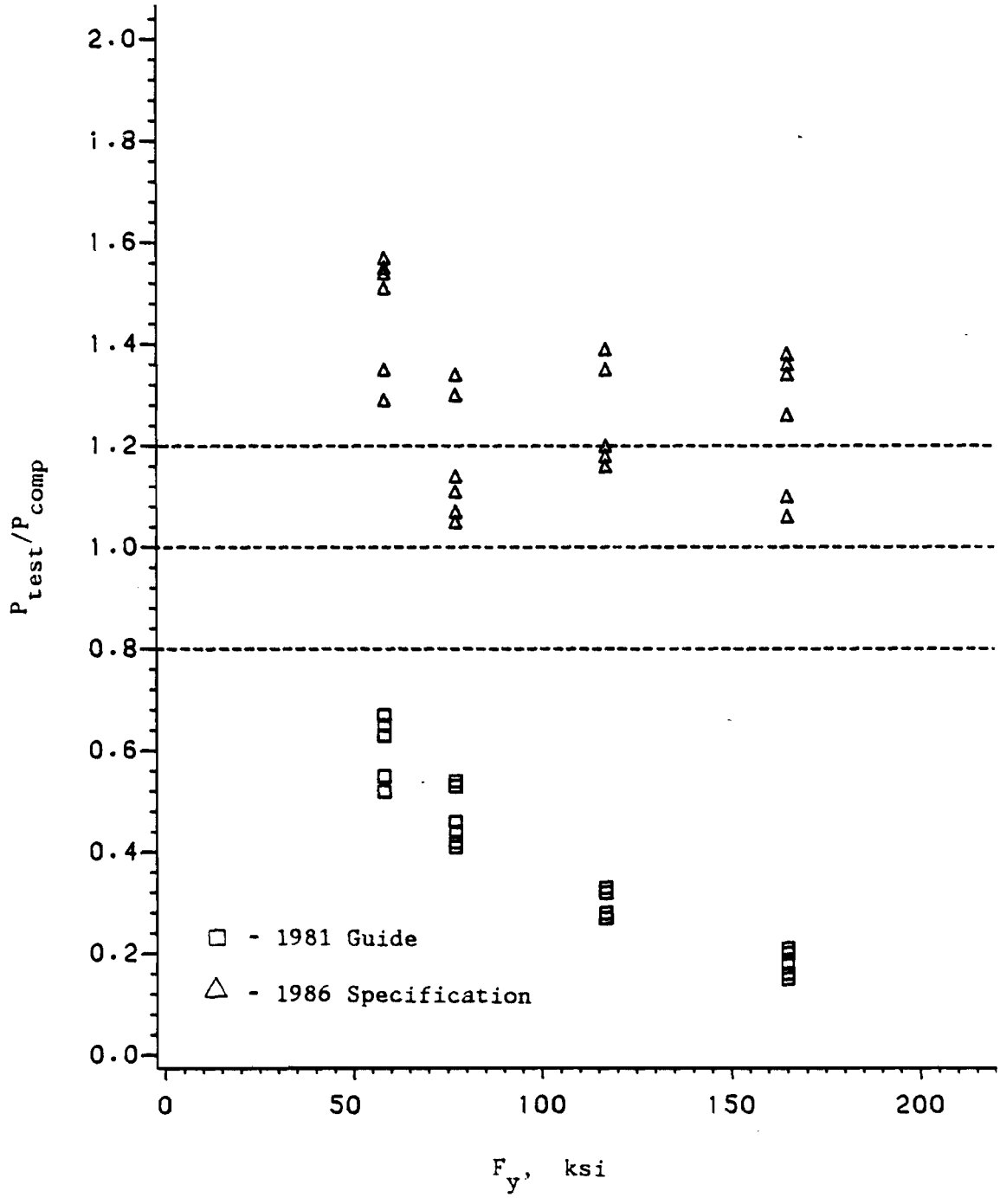

Fig. 4.15 Effect of F_y on the Ratio P_{test}/P_{comp} for I-Beams Subjected to End Two-Flange Loading Based on the AISI 1981 Guide and 1986 Specification

P_{test}/P_{comp} and the yield strength, F_y. As discussed for the previous case, the equation used in the 1986 Specification is independent of F_y but has the correction factor for thickness of material. It should be noted that all specimens used in this case experienced a buckling type of failure.

Based on the evaluations of the experimental data, it is obvious that a modification of the present design criteria for web crippling is desirable especially for the function of the yield strength, $f(F_y)$. Furthermore, it was observed during the tests that some specimens failed by buckling in the webs instead of web crippling. The equations used to predict the failure loads of this buckling type are independent of F_y.

In order to improve the accuracy of prediction, the format of web crippling equations may be changed to reflect each individual type of failure. The developments of new equations are discussed in Section VI.

V. ANALYTICAL STUDY

A. GENERAL

Web crippling is a type of failure caused by highly localized compressive stress. It may result from a concentrated load and/or reaction applied over a short length of beams. This type of loading is usually considered to be a partial edge load for the web element.

As discussed in Section II, the theoretical analysis of web crippling of thin-walled beams is very complicated because it involves:

1) nonuniform stress distribution under the applied load;
2) local yielding in the immediate region of load application;
3) elastic and inelastic stabilities of the web;
4) out of plane bending due to the nature of eccentric loading;
5) initial imperfection and large deformation at failure;
6) various edge restraints provided by beam flanges and the interaction between beam flange and web element; and
7) effect of cold work on material properties.

The mathematical difficulties that arise from the above reasons do not permit an exact or a closed-form solution for the problem of web crippling.

The numerical method such as the finite element approach may be used as alternative means of analysis for determining the approximate ultimate web crippling loads of thin-walled beams. There are a large number of publications (books, papers and reports) now available for the use of the finite element procedures. Because the development of the finite element computer program is not the major objective of this

investigation, the comprehensive finite element formulations are not reviewed in this Section.

The existing finite element program entitled "Automatic Dynamic Incremental Nonlinear Analysis" (ADINA),[58,59] which is available at UMR, was used in this study. This program has the capability of handling both geometrical and material nonlinearities so that the ultimate web crippling loads may be predicted. In this investigation, hat and channel sections with single unreinforced webs subjected to four different types of loading conditions (IOF, EOF, ITF, and ETF) were studied analytically by using the "ADINA" program.

ADINA is a computer program for the static and dynamic displacement and stress analysis of solids, structures, and fluid-structure systems. The program can be employed to perform linear and nonlinear analyses.

The program was designed to perform a linear analysis very effectively. A nonlinear analysis can be carried out following the linear analysis with only a relatively few input changes. This feature is practically useful because in many cases only a nonlinear analysis is required and it should be preceded by linear analysis.

The theory used in ADINA is summarized in Ref. 60 and additional details on the theory with further sample solutions are given in Ref. 58.

The structural systems analyzed by using ADINA can be composed of different finite elements. The presently available version of ADINA program at UMR contains the following element types:

1) Three-dimensional truss element
2) Two-dimensional plane stress and plane strain element
3) Three-dimensional plane stress element

4) Two-dimensional axisymmetric shell or solid shell element

5) Three-dimensional solid and thick shell element

6) Three-dimensional two-node beam element

7) Isoparametric beam element

8) Three-node plate/shell element

9) Isoparametric thin shell element

10) Two and three-dimensional fluid element.

The nonlinearities may be due to large displacements, large strains, and nonlinear material behavior.

Program ADINA is an out-of-core solver, i.e., the equilibrium equations are processed in blocks, so very large finite element systems can be considered. Also, all structural matrices are stored in compacted forms[61], i.e., only nonzero elements are processed, resulting in maximum system capacity and solution efficiency.

In nonlinear analysis, the finite element system response is evaluated using an incremental solution of the equations of equilibrium. The incremental solution schemes that can be used are an accelerated modified Newton - Raphson iteration or the BFGS (Broyden Fletcher Goldfarb Shanno) method. To increase the solution efficiency and to assure an accurate solution one can specify solution steps in which a new effective stiffness matrix shall be formed and steps in which equilibrium iterations are to be carried out.

In nonlinear static analysis, linear and nonlinear element groups are defined. Damping and mass effects are neglected.

Before applying the step-by-step solution, the linear stiffness matrix corresponding to the linear elements of the complete element assemblage is calculated. Degrees-of-freedom that correspond to linear

elements can be condensed out. The final linear stiffness matrix is then adapted in preselected load steps by the stiffness matrices of the nonlinear elements to form the current stiffness matrix. The interval of load steps between forming a new tangent stiffness matrix is input to the program.

Depending on the nonlinear formulations and the nonlinear material models used, and also depending on the magnitude of the load steps, the accuracy of the solution may be significantly increased by using equilibrium iteration. The program load steps at which equilibrium iteration shall be performed can be defined in the input control data.

In the analysis of large structure systems, it is important to be able to check the data read and generated by the program. For this purpose, an option is given in which the program simply reads, generates, and prints all data.

It can also be requested that the program reads the node points and element data from a tape created by a pre-processor.

B. ELEMENT TYPE

The research work presented in Refs. 35 and 62 to 64 indicated that flat rectangular elements can be used satisfactorily in determining the ultimate web crippling loads of hat sections under interior one-flange loading. In this investigation, due to the availability of the ADINA program, a 3-node flat triangular plate/shell element with an updated lagrangian formulation has been employed for very large displacements and rotations but small strain. As shown in Fig. 5.1, the element has six degrees of freedom at each node, i.e., three components of translation and three of rotation. The stiffness matrix is constructed

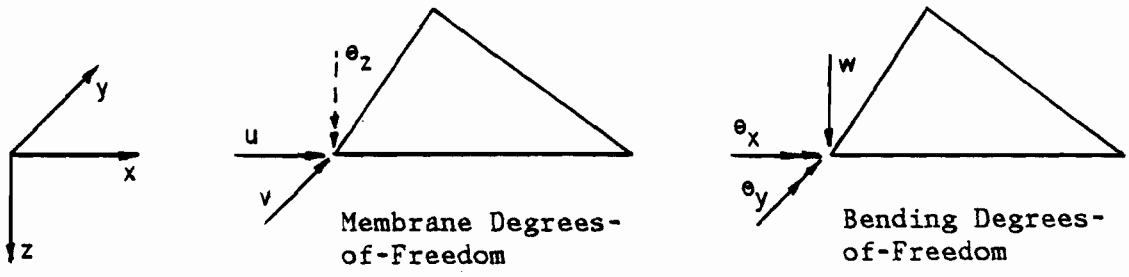

Fig. 5.1 A Flat Element Subjected to In-Plane and Bending Actions

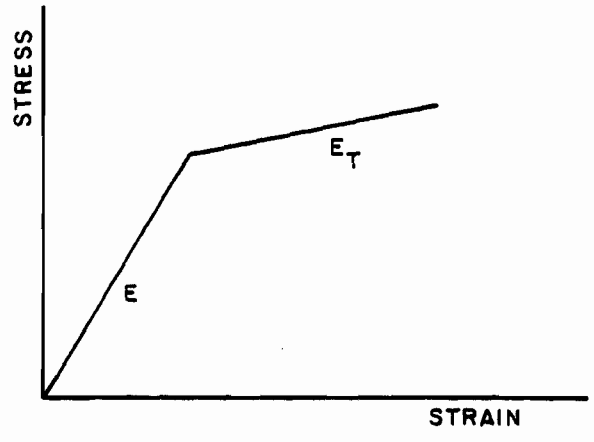

Fig. 5.2 Stress-Strain Relationships of the Elastic-Linear Strain Hardening Material

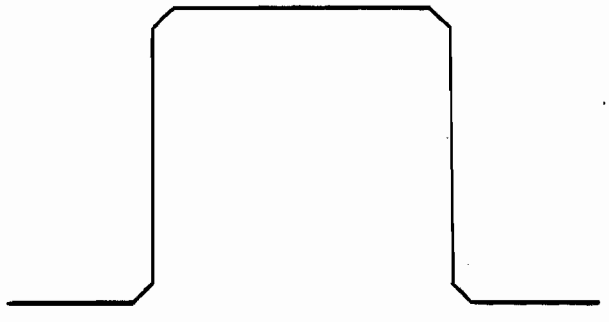

Fig. 5.3 Idealized Hat Sections

by superimposing the bending and membrane parts in the current local coordinate system. For material nonlinearity, the stress-strain relationships are treated as elastic-linear strain hardening type (Fig. 5.2). The theoretical developments of this type of element are well documented in Refs. 59 and 60.

Figure 5.3 shows the idealized hat sections used in this investigation. In order to take into account the curved bend between the web and flange, a longitudinal row of elements was introduced at the web-flange junction.

C. PREDICTION OF ULTIMATE WEB CRIPPLING LOADS

The ADINA program with 3-node triangular plate/shell element as discussed above was used in this study to predict the ultimate web crippling loads of sections with single unreinforced webs. Appropriate analytical models were selected to simulate the hat sections used in the experimental study. In this process, due considerations were given to the finite element modeling to best fit the following conditions involved in the tests:

1) Hat sections were braced by strips at the lower unstiffened flanges to prevent the webs from spreading apart during the test.

2) Wood blocks were inserted at both ends to prevent the end failure in the case of interior one-flange loading.

3) The downward curling of the top flange of hat sections (Fig. 3.16) caused the bearing plate to contact the specimen only at the tangent of the curved transition between the web and flange.

As discussed earlier, the ADINA program limits the nonlinear material model for plate/shell element only to bilinear stress-strain

relationships (Fig. 5.2). For the 80DK material which has a gradual yielding type stress-strain curve (Fig. 3.2), the value of E_T was assumed to be 0.3E. For the 80XF, 100XF, 140XF, and 140SK materials, the values of E_T were assumed to be zero.

The web crippling loads predicted by the finite element method for four types of loading conditions are discussed below. This study dealt with various hat sections using different materials and dimensions. The comparisons between the predicted ultimate web crippling loads using the finite element method and the tested failure loads of the specimens used in this phase of investigation are presented in Tables 5.1 to 5.4.

1. Interior One-Flange Loading:

As an example, a hat section fabricated from the 100XF sheet steel (Table 3.1) with profile No. 2 (Table 3.2a) is used. The beam is 19 in. long and is simply supported by two 4-in. bearing plates at both ends. It is loaded through a 2-in. bearing plate at mid-span. The 100XF material has a perfectly elastic-plastic stress-strain relationship as shown in Fig. 3.2.

Considering the symmetry in two directions, only one quarter of the beam was analyzed. Figure 5.4 shows the finite element model for this specimen with a total of 72 nodes and 112 elements. The beam was restrained vertically at Nodes 14 to 16 for the end support and restrained laterally at Nodes 9 to 16 to reflect the use of bracing strips. Nodes 24, 32, 40, 48, and 56 were restrained laterally to simulate the action of the wood block. Symmetric boundary conditions were employed at nodes along the lines of symmetry. Load was applied at Nodes 57-59.

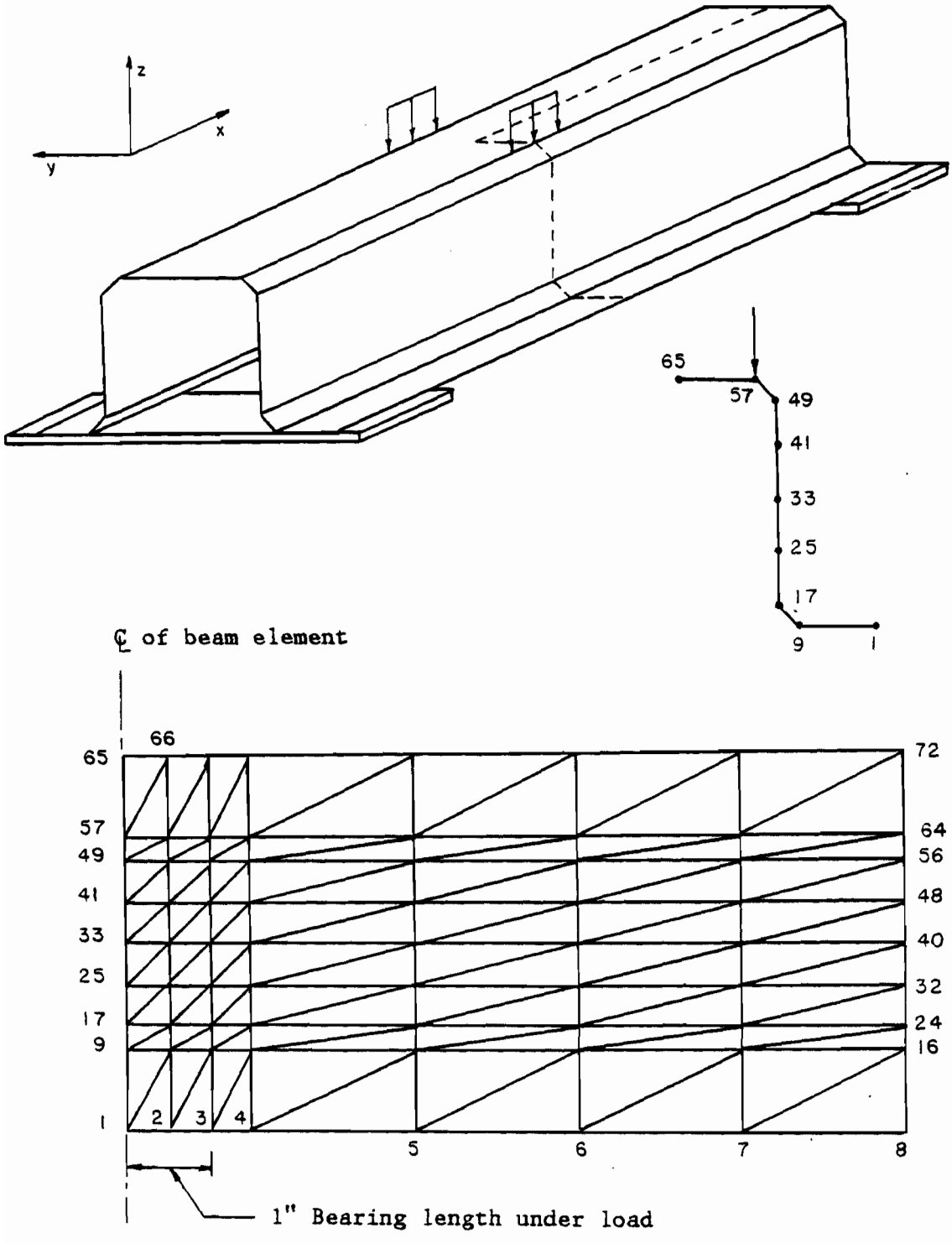

Fig. 5.4 Finite Element Model of a Hat Section Subjected to Interior One-Flange Loading

Figure 5.5a shows the computed curves of lateral deformations for nodes along the centerline of test specimen No. 3-HIOF-A21. Large lateral deformations were observed for Nodes 41 and 33.

Because the stiffness matrix was not positive definite after the applied load reached 3.7 kips per web, the program was terminated and the ultimate web crippling load was assumed. It can be seen from Fig. 5.5a that the stiffness at Nodes 41 and 33 diminished as the applied load approached 3.7 kips per web. Comparing to the tested failure load of 4.3 kips per web, this model underestimated the failure load by 16%.

A comparison of the computed and measured lateral deformations along the centerline of the interior bearing plate at several load steps for this specimen is shown in Fig. 5.5b. It can be seen that the finite element model shows a reasonable agreement for the middle portion of beam web. However, for the portion of beam web just under the bearing plate up to 1/3 of the beam depth, the measured lateral deformations are smaller than the computed values. The degree of discrepancy tends to increase as the load increases.

An attempt was made to improve the accuracy of prediction by increasing the number of elements but virtually no improvement was achieved.

The finite element method for other specimens also predicted lower ultimate web crippling loads than the actual tested loads. As compared in Table 5.1, the accuracy was found to be within 21%. The average value of the ratio of tested loads and computed loads by using the finite element method (P_{test}/P_{fin}) for these specimens is 1.144 with the standard deviation of 0.045.

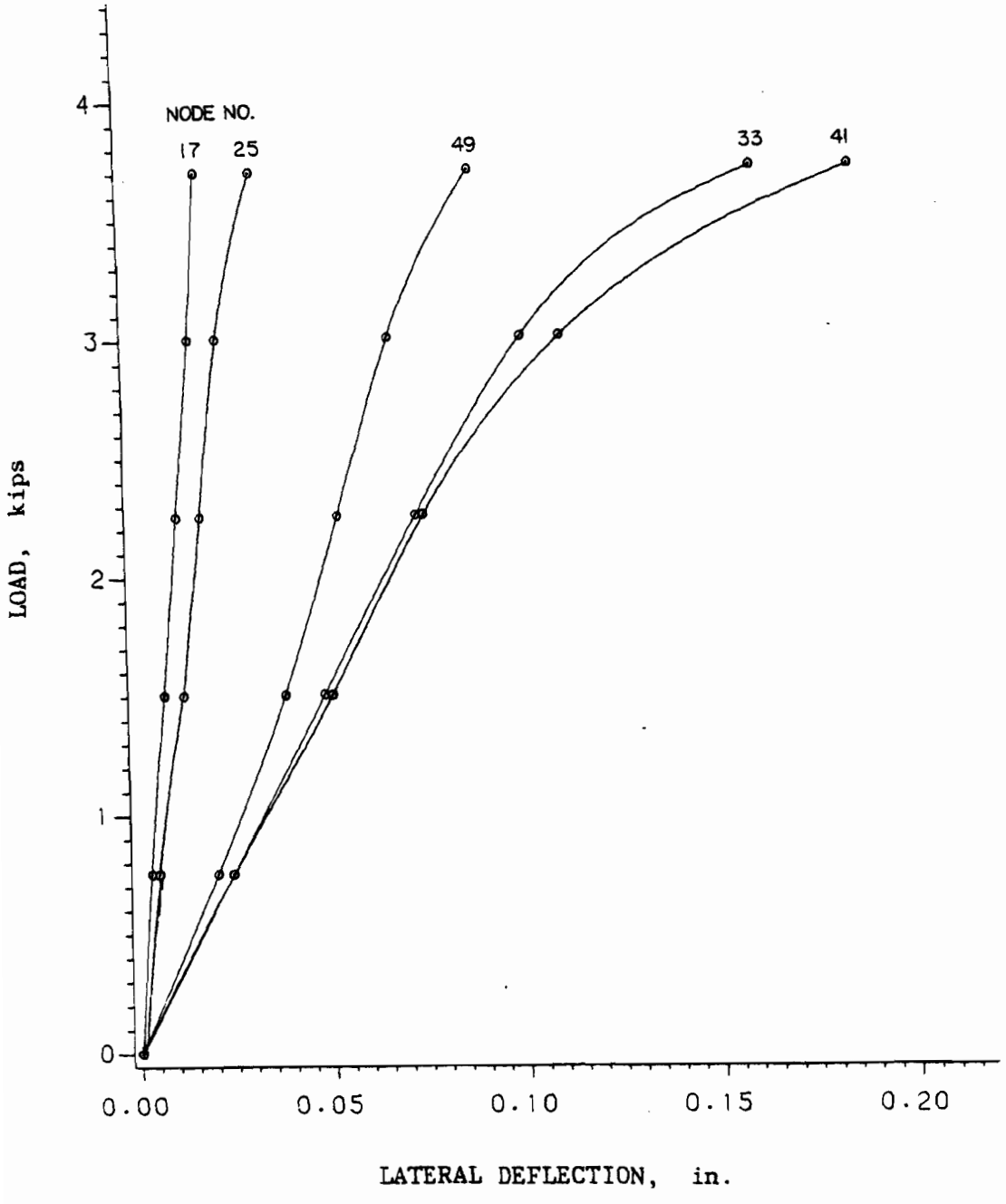

Fig. 5.5a Lateral Deformation at Mid-Span of a Hat Section Subjected to Interior One-Flange Loading (Specimen No. 3-HIOF-A21)

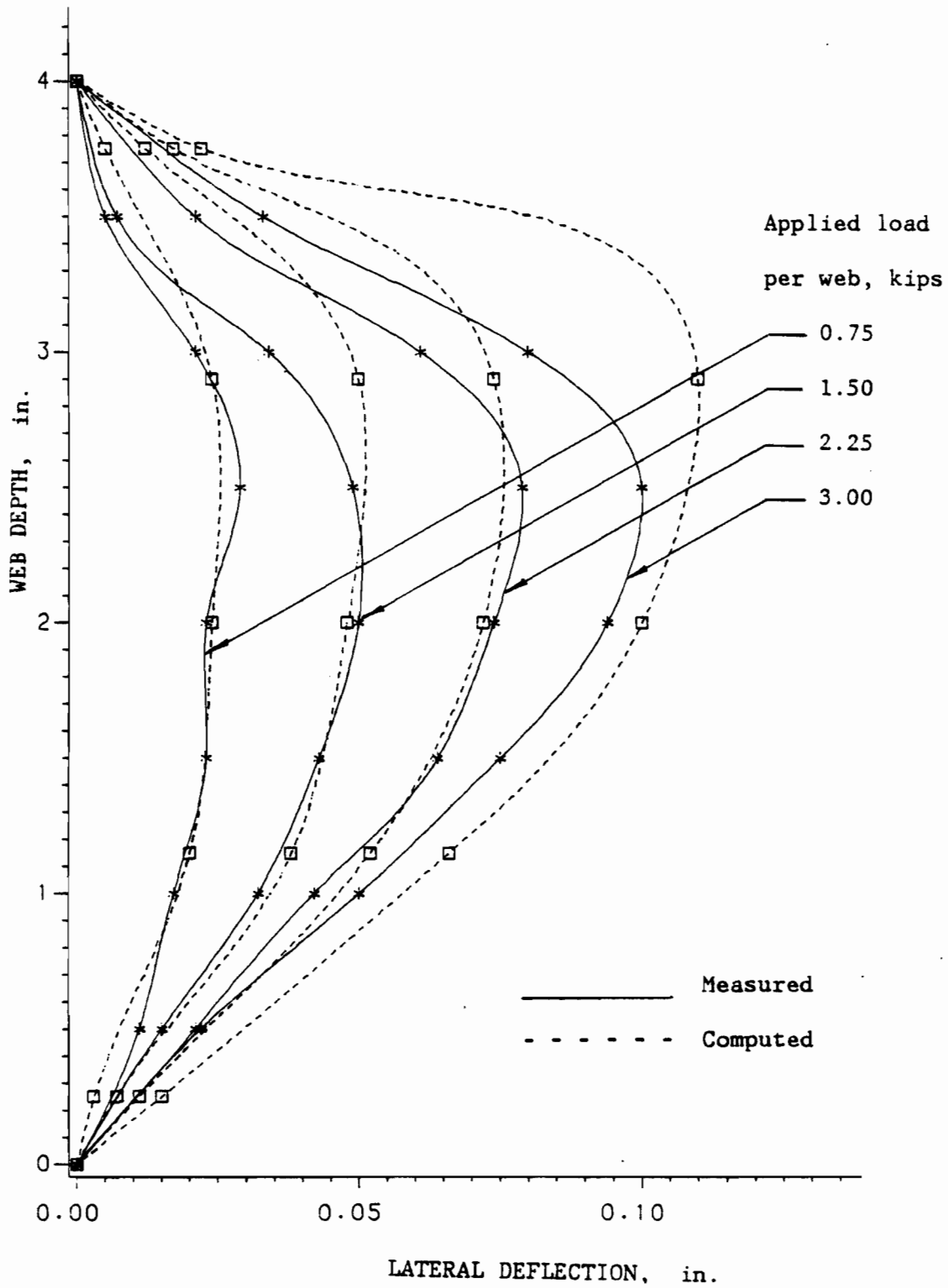

Fig. 5.5b Comparison of the Computed and Measured Lateral Deformations at Mid-Span of a Hat Section Subjected to Interior-One Flange Loading (Specimen No. 3-HIOF-A21)

Table 5.1

Comparisons of Predicted Ultimate Loads by Finite Element Method to Tested Failure Loads for Interior One-Flange Loading

Specimen No.	P_{test} (kips)	P_{fin} (kips)	P_{test}/P_{fin}
1-HIOF-A11	1.425	1.345	1.06
1-HIOF-A21	1.465	1.300	1.13
1-HIOF-A31	1.450	1.270	1.14
2-HIOF-A11	5.400	4.540	1.19
2-HIOF-A21	5.740	5.035	1.14
2-HIOF-A31	6.265	5.220	1.10
3-HIOF-A11	4.290	3.920	1.09
3-HIOF-A21	4.290	3.705	1.16
3-HIOF-A31	4.325	3.850	1.12
4-HIOF-A11	2.490	2.260	1.10
4-HIOF-A21	2.625	2.190	1.20
4-HIOF-A31	2.575	2.175	1.18
5-HIOF-A11	2.365	2.080	1.14
5-HIOF-A21	2.500	2.065	1.21
5-HIOF-A31	2.465	2.050	1.20
Mean Value			1.144
Standard Deviation			0.045

The underestimation of web crippling load may be due to the fact that during the test, the contact point between the bearing plate and the specimen moves toward the web as the load increases (Fig. 3.15). However, in the finite element model, the applied load is stationary. The shifting of the loading point is caused by the rotation of the web-flange junction. As a result, the out-of-plane bending caused by the eccentric load applied in the actual test was smaller than that used in the finite element model. It was observed that the degree of underestimation decreases with a reduction in the bend radius of the specimen.

In addition to the above reason, the cold-work effect may be another cause of underestimation. The press-brake forming results in higher yield strength at the corners or web-flange junctions of the test specimens. However, the material properties used in the finite element models are those of the virgin sheet steels.

2. End One-Flange Loading:

Same as the previous case, only one quarter of the beam specimen was analyzed. A total of 108 nodes and 175 elements were used for the finite element model as shown in Fig. 5.6 for the case of end one-flange loading. The boundary conditions for this model were the same as that for the interior one-flange loading except that wood blocks were not used at both end supports. Load was applied vertically at Nodes 85 through 89 to accomodate the 4-in bearing plate. At Nodes 20 through 24, which was the location of 2-in. end bearing plate, a restraint was provided for the vertical translation.

For all specimens used for the end one-flange loading case, the diminishing in stiffness at nodes 46 to 48 indicates failure in the webs

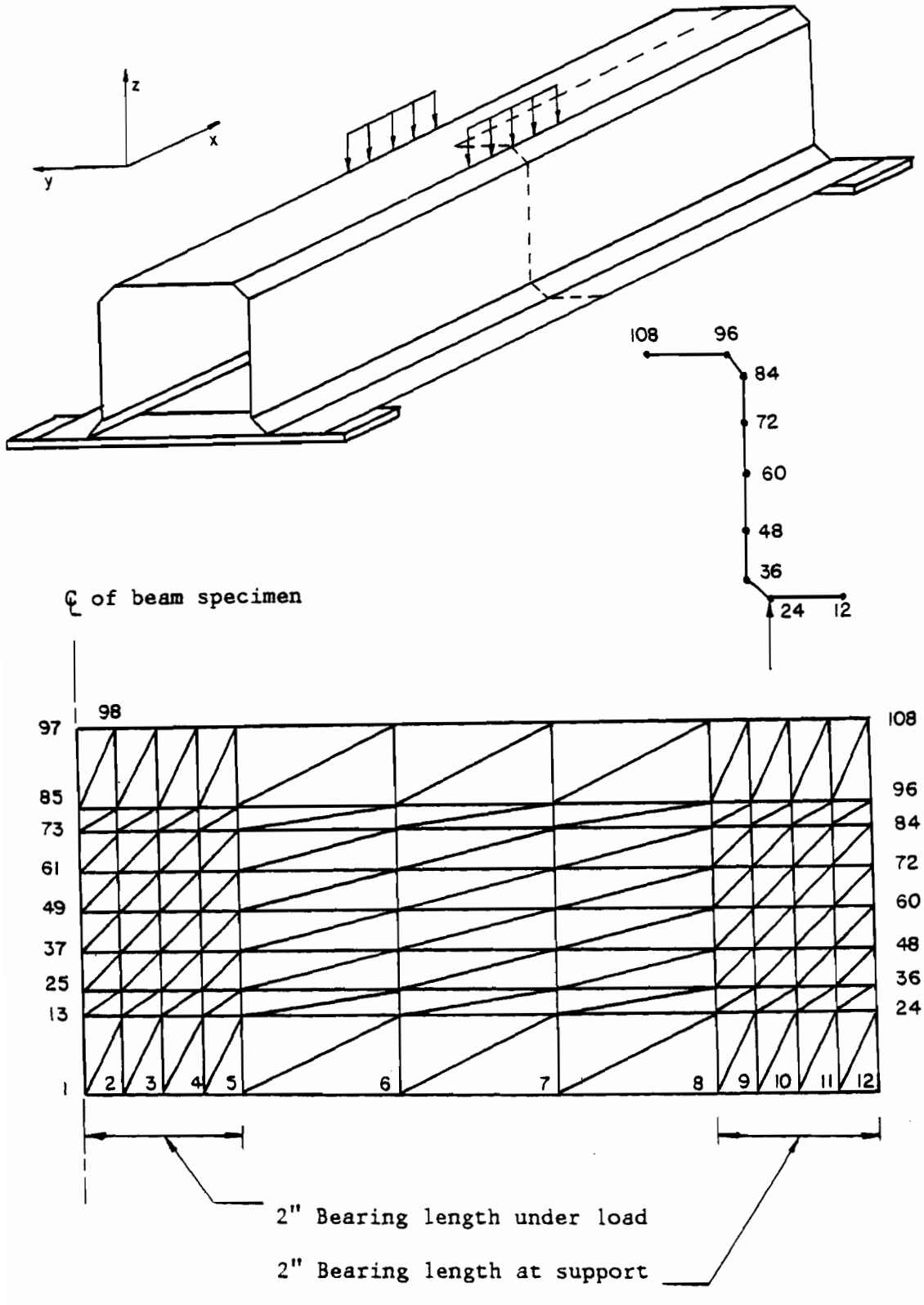

Fig. 5.6 Finite Element Model of a Hat Section Subjected to End One-Flange Loading

Table 5.2

Comparisons of Predicted Ultimate Loads by Finite Element Method to Tested Failure Loads for End One-Flange Loading

Specimen No.	P_{test} (kips)	P_{fin} (kips)	P_{test}/P_{fin}
1-HEOF-A11	0.719	0.605	1.19
1-HEOF-A21	0.694	0.600	1.16
1-HEOF-A31	0.669	0.590	1.13
2-HEOF-A11	2.919	2.555	1.14
2-HEOF-A21	2.994	2.600	1.15
2-HEOF-A31	2.713	2.450	1.11
3-HEOF-A11	2.050	1.720	1.19
3-HEOF-A21	2.006	1.645	1.22
3-HEOF-A31	1.894	1.620	1.17
4-HEOF-A11	1.313	1.205	1.09
4-HEOF-A21	1.219	1.150	1.06
4-HEOF-A31	1.088	1.035	1.05
5-HEOF-A11	1.295	1.055	1.23
5-HEOF-A21	1.200	0.995	1.21
5-HEOF-A31	1.050	0.885	1.19
Mean Value			1.153
Standard Deviation			0.056

at the locations of end supports. The program was terminated due to nonpositive definiteness of the stiffness matrix and the ultimate web crippling load was assumed as done in the case of interior one-flange loading.

A total of 15 high strength hat sections were studied in this case. The comparisons of the predicted ultimate loads by using finite element method and the tested failure loads are presented in Table 5.2. It can be seen that the finite element models slightly underestimate the ultimate web crippling loads for all specimens in this case. The accuracy of prediction was within 23% of the actual tested loads with a mean value of 1.153 and the standard deviation of 0.056.

Same as in the case of interior one-flange loading, the underestimation of ultimate web crippling loads may be due to the stationary reaction used in the finite element model and the cold-work effect at the corners of test specimens. During the test, the contact point between the end bearing plate and the specimen moves toward the web as the load increases. Under the applied load, all specimens sustain relatively large lateral deformations and flange tip deflections at both ends of the beam (Fig. 3.21). The rotation of the web-flange juction causes the shifting of the contact point. Hence, the stationary reaction used in the finite element model gives a larger out-of-plane bending due to the eccentric force as compared with actual test. This results in smaller calculated loads than the tested failure loads. Same as the previous case, a better accuracy was realized for the section with smaller bend radius.

3. Interior Two-Flange Loading:

A total of 12 high strength hat sections were investigated for the case of interior two-flange loading. Figure 5.7 shows the typical finite element model selected for this case. Due to symmetry in two directions, only one quarter of the specimen was analyzed. The model consisted of 63 nodes and 96 elements. Nodes 8 through 14 were restrained laterally to reflect the use of bracing strips. Nodes 8 through 10 were treated as a support simulating a 2-in. bearing plate which was restrained vertically. Symmetric boundary conditions were applied along all lines of symmetry. Load was applied vertically at Nodes 50 through 52.

The ultimate web crippling load was determined at the termination of the program as discussed in the previous two cases. For this case, the diminishing in stiffness at Nodes 22 and 36 was observed as the applied load approached the maximum load.

As can be seen from Table 5.3, the predicted ultimate web crippling loads for all specimens studied in this case are considerably lower than the actual tested failure loads. The inaccuracy in predictions is as high as 55% for some specimens. The average value of the ratio of P_{test}/P_{fin} is 1.405 with a standard deviation of 0.086.

The underestimation is caused by the same reason as discussed for the case of interior one-flange loading. In addition, the rotation of the web-flange junction for this case was more pronounced which resulted in a higher degree of inaccuracy in prediction.

4. End Two-Flange Loading:

Because there is only one direction of symmetry, one half of the specimen was analyzed for the end two-flange loading case. The typical finite element model used for this case is shown in Fig. 5.8. It can be

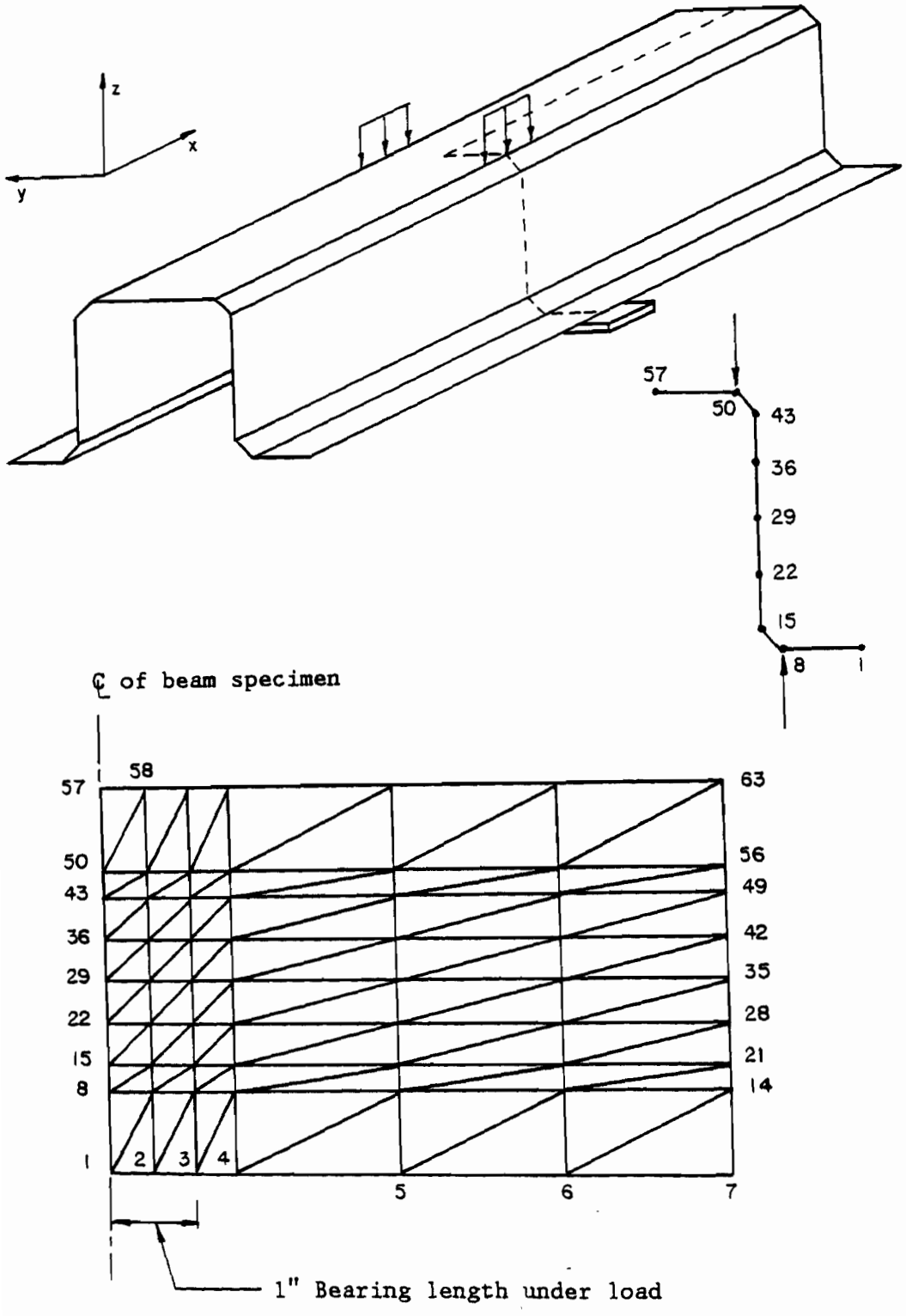

Fig. 5.7 Finite Element Model of a Hat Section Subjected to Interior Two-Flange Loading

Table 5.3

Comparisons of Predicted Ultimate Loads by Finite Element Method to Tested Failure Loads for Interior Two-Flange Loading

Specimen No.	P_{test} (kips)	P_{fin} (kips)	P_{test}/P_{fin}
1-HITF-A11	1.650	1.200	1.38
1-HITF-A21	1.650	1.175	1.40
1-HITF-A31	1.600	1.165	1.37
2-HITF-A11	6.875	5.415	1.27
2-HITF-A21	6.875	5.350	1.29
2-HITF-A31	6.875	5.220	1.32
3-HITF-A11	5.050	3.500	1.44
3-HITF-A21	4.850	3.405	1.42
3-HITF-A31	4.800	3.350	1.43
5-HITF-A11	2.950	1.900	1.55
5-HITF-A21	2.775	1.825	1.52
5-HITF-A31	2.625	1.785	1.47
Mean Value			1.405
Standard Deviation			0.086

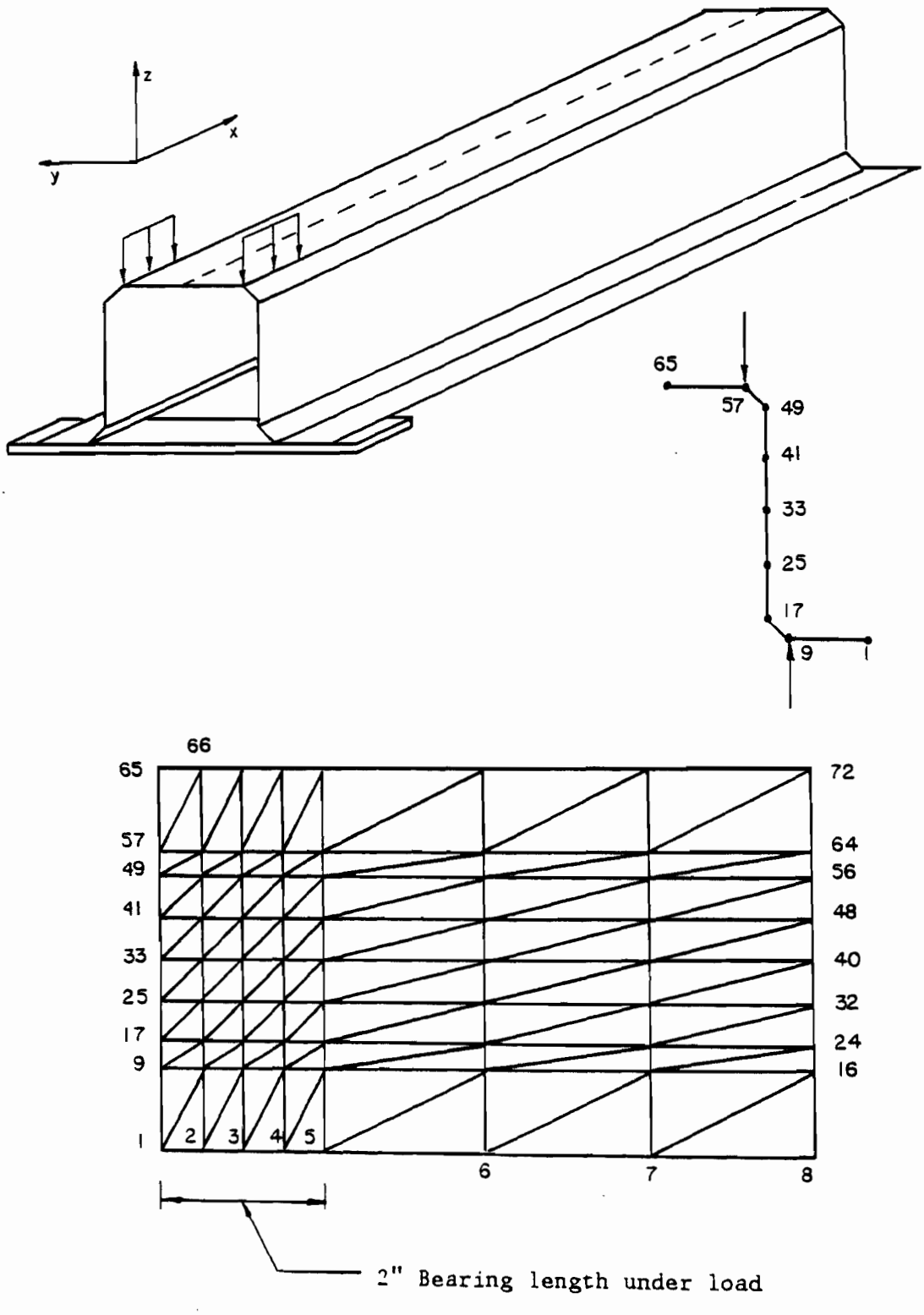

Fig. 5.8 Finite Element Model of a Hat Section Subjected to End Two-Flange Loading

seen that a total of 72 nodes and 112 elements were employed. Nodes 9 through 16 were restrained laterally to simulate the effect of the bracing strip used to prevent the webs from spreading out. Nodes 9 through 13 were treated as a support representing the 2-in. end bearing plate with vertical restraint. A vertical load was applied at nodes 57 through 61 simulating the 2-in. bearing plate under the applied concentrated load.

For all specimens used for the end two-flange loading case, the diminishing in stiffness at Nodes 25 and 41 indicates the web failure. The ultimate web crippling loads were determined as discussed earlier in the previous cases.

Same as the case of interior-two-flange loading, a total of 12 high strength hat sections were used in this study. Table 5.4 presents the comparison between tested failure loads and predicted ultimate web crippling loads calculated on the basis of the finite element method. The mean value for the ratio of P_{test}/P_{fin} was found to be 1.422 with a standard deviation of 0.095. For this case, the inaccuracy is as high as 60%. The reason for this inaccuracy is basically the same as the case of end one-flange loading. In addition, the large lateral deformation of the web and the excessive rotation of the web-flange junction result in a higher degree of underestimation.

In addition to the hat sections using high strength materials, channel sections with relatively low yield strengths tested in the previous UMR study[41] were also briefly investigated. The same trend of accuracy as for the high strength hat sections was obtained for each type of loading condition.

Table 5.4

Comparisons of Predicted Ultimate Loads by Finite Element Method to Tested Failure Loads for End Two-Flange Loading

Specimen No.	P_{test} (kips)	P_{fin} (kips)	P_{test}/P_{fin}
1-HETF-A11	0.725	0.505	1.44
1-HETF-A21	0.725	0.490	1.48
1-HETF-A31	0.650	0.480	1.35
2-HETF-A11	2.825	2.015	1.40
2-HETF-A21	2.700	1.955	1.38
2-HETF-A31	2.425	1.875	1.29
3-HETF-A11	1.525	0.955	1.60
3-HETF-A21	1.413	0.925	1.53
3-HETF-A31	1.300	0.900	1.44
5-HETF-A11	0.750	0.505	1.49
5-HETF-A21	0.675	0.490	1.38
5-HETF-A31	0.612	0.480	1.28
Mean Value			1.422
Standard Deviation			0.095

D. DISCUSSIONS

As mentioned at the beginning of this section, the exact or closed-form solution for the problem of web crippling of thin-walled beams can not be achieved due to several reasons. By using a numerical approximation method such as the finite element approach, some of these features may be taken into account. The effects of the selected finite element models on these problems are discussed as follows:

1) Nonuniform stress distribution - Theoretically, if the elements are adequately small the overall stress distribution should be fairly accurate.

2) Local yielding - Because the nonlinear material model has been employed, the problem of local yielding in the immediate region of load application has been considered. However, it should be noted that the stress-strain relationship used in the finite element model in this study is a bilinear type while some sheet steels are gradual yielding type materials.

3) Stability - Due to the method of formulation in the ADINA program, the theoretical initial buckling load (bifurcation point) is by-passed. Only the ultimate or collapse load was predicted.

4) Out-of-plane bending - This problem has been taken into account by applying the load along the line of transition between curved and flat elements of the flange (Figs. 5.4 and 5.6 to 5.8).

5) Initial imperfection and large deformation - The problem of large deformation is treated by the nonlinear geometry with updated lagrangian formulation but the actual initial imperfection of the specimen was not considered in the model.

6) Interaction between flange and web - If the elements are small enough the overall behavior along the transition line should be reasonable. It should be noted that the curved bend between the web and flange was modeled by a longitudinal row of elements (Fig. 5.2) which may cause some discrepancy.

7) Cold-work effect - In this investigation, the effect of cold-work of forming was not considered in the finite element model.

Even though the finite element method does not provide excellent agreements with the test data obtained from the experimental study of web crippling, it seems to be a reasonable analytical tool to deal with this problem. It should also be noted that because of the complicated boundary conditions at the connected lines of I-beams, the web crippling problem of such members has not been fully investigated in this analytical study.

According to the comparisons of the predicted ultimate loads and the tested failure loads, the underestimation of the finite element models was realized for all loading conditions. However, for the case of interior one-flange loading and end one flange-loading, the accuracy of prediction is fairly reasonable. For the case of interior two-flange loading and end two-flange loading, the prediction is rather conservative. Beacuse the standard deviations of the ratios of P_{test}/P_{fin} for all cases (Tables 5.1 to 5.4) are relatively low and the consistency in the prediction of the ultimate loads, the finite element method may be useful in the parametric study of this type of problem.

As mentioned in Section I, the main objective of this research project is to improve the existing design provisions and to develop new design criteria for cold-formed steel beams subjected to web crippling

and a combination of web crippling and bending moment. Because the exact or closed-form solution for the problem cannot be achieved analytically, the desired design expressions have to be developed empirically. The development of new prediction equations is discussed in the next section.

VI. DEVELOPMENT OF NEW EQUATIONS

As discussed in Section IV, the present AISI provisions on web crippling are not suitable for the sections fabricated from materials with yield strengths beyond the limit of 80 ksi. Even though attempts have been made on the modification of the function of yield strength to accommodate this situation, comparisons of the tested and predicted values indicate that further improvements of the function of F_y and the formulation of new design equations are desirable.

This section includes the development of new equations to predict the ultimate web crippling loads for sections with single unreinforced webs and I-beams under four different types of loading conditions (IOF, EOF, ITF and ETF). In the derivation of new design equations, web crippling was distinguished by buckling failure and overstressing (bearing) failure. The same approach has been used for the design of aluminum structures.[67]

For the type of web crippling caused by buckling of the webs, new equations were derived on the basis of the same nondimensional parameters used for rectangular flat plates which are subjected to partial edge loading. As reviewed in Section II, the important nondimensional parameters used for plate buckling are $P/(t^2E)$, N/h, h/t and L/h. The definitions of these terms are the same as those defined in Section II. In deriving the equations for cold-formed steel beams, the parameter L/h was replaced by e/h, where "e" is the clear distance between the opposite bearing plates or the clear distance from the bearing plate to the end of beam where applicable. By using the e/h ratio, the newly developed

equations can be applied to either symmetric or unsymmetric loading. In general, the form of web buckling equation for cold-formed steel beams may be written as

$$P_{cb} = t^2 Ef((N/h), (h/t), (e/h)) \tag{6.1a}$$

or

$$P_{cb} = At^2E(1+B(N/h)^C)(1+D(h/t)^G)(1+H(e/h)^J) \tag{6.1b}$$

where A, B, C, D, G, H, and J are constants to be determined empirically.

For the type of web crippling failure caused by overstressing, the new equations were derived from the basic nondimensional terms $P/(t^2F_y)$, N/t, and R/t. According to Baehre,[45] the h/t ratio has little or no influence on this localized failure. In the present European recommendations,[46,47] the parameter h/t was not included in the web crippling equations. The equation for web crippling caused by overstressing was determined to be

$$P_{cy} = t^2F_y f((N/t), (R/t)) \tag{6.2a}$$

or

$$P_{cy} = Kt^2F_y(1+P(N/t)^Q)(1+U(R/t)^V) \tag{6.2b}$$

where K, P, Q, U, and V are empirical constants.

A nonlinear least squares regression[68,69] was used in determining the constants for the empirical formulas (Eqs. (6.1b) and (6.2b)). As the first step, all constants were guessed and the sum of squares of error was calculated. An iteration process was then carried on until the least sum of squares of error was achieved.

New equations presented herein were developed on the basis of available data obtained from the following sources:

1) Previous Cornell and UMR tests reported in Ref. 41

2) Recent UMR tests conducted by Lin[44]

3) New tests using high strength sheet steels conducted in the present phase of study

The overall ranges of parameters used in this study are shown below.

Parameter	Range
Thickness of specimen, in.	0.046 - 0.148
Depth of section, in.	3 - 12
Yield strength, ksi	30 - 165
h/t	32 - 250
N/t	20 - 65
N/h	0.08 - 0.75
R/t	1 - 6

All test data obtained from previous research work that are used in the development of new equations are given in Appendix C. Comparisons between the tested failure loads and predicted loads for the data used to derive each individual equation are presented in Appendix C. The developments of new equations for each case are discussed as follows:

A. SINGLE UNREINFORCED WEBS

1. Interior One-Flange Loading:

a. Overstressing Failure: The equation to predict the ultimate loads for this case is intended to apply for both interior one-flange loading and interior two-flange loading. A total of 74 test data (Table D1) were used to develop this equation. All the data used for this case were selected in such a way that the ratio of actual moment to the

ultimate bending moment capacity, M/M_u, was less than 0.3. It was found from previous research work by Baehre[45] that when this moment ratio is less than 0.3 there was little or no interaction between web crippling and bending moment. The empirical equation was then determined to be

$$P_{cy} = 7.8t^2F_y(1+.217\sqrt{N/t})(1-.0814(R/t)) \qquad (6.3)$$

with $(1+.217\sqrt{N/t}) \leq 3.17$ and $(1-.0814(R/t)) \geq 0.43$.

The ranges of parameters used in the derivation of Eq. (6.3) are

Parameter	Range
Thickness of specimen, in.	0.046 - 0.088
Yield strength, ksi	36 - 77
N/t	19 - 62
R/t	1 - 6

Because all of the test specimens in this case with yield strengths beyond 77 ksi failed by web buckling, Eq. (6.3) was derived from the test data with yield strengths up to 77 ksi.

b. Buckling Failure: The equation to determine the ultimate web buckling loads under interior one-flange loading was derived from 72 test data (Table D2). The ultimate web crippling load caused by web buckling can be calculated from

$$P_{cb} = 0.028t^2E(1+2.4(N/h))(1-.0017(h/t))(1-.12(e_1/h)) \qquad (6.4)$$

with $(1+2.4(N/h)) \leq 1.96$, $(1-.0017(h/t)) \leq 0.81$ and $(1-.12(e_1/h)) \geq 0.40$.

The ranges of parameters used in the derivation of Eq. (6.4) are

Parameter	Range
Thickness of specimen, in.	0.046 - 0.065
h/t	44 - 254
N/h	0.1 - 0.7
e_1/h	0.75 - 2.50

The smaller value of P_{cy} and P_{cb} calculated from Eqs. (6.3) and (6.4), respectively, is the governing value for web crippling load.

2. End One-Flange Loading:

Same as the previous case, web crippling failure is distinguished into overstressing and web buckling.

a. Overstressing Failure: A total of 61 test data (Table D3) were used in the development of Eq. (6.5).

$$P_{cy} = 9.9t^2F_y(1+.0122(N/t))(1-.247(R/t)) \qquad (6.5)$$

with $(1+.0122(N/t) \leq 2.22$ and $(1-.247(R/t)) \geq 0.32$.

The ranges of parameters used in the derivation of Eq. (6.5) are

Parameter	Range
Thickness of specimen, in.	0.046 - 0.085
Yield strength, ksi	36 - 113
N/t	20 - 62
R/t	1 - 5

b. Buckling Failure: For the type of web crippling failure caused by buckling in the web, the empirical expression was determined from 27 test data (Table D4). This equation is

$$P_{cb} = 0.028t^2E(1-.00348(h/t))(1-.298(e_1/h)) \qquad (6.6)$$

with $(1-.00348(h/t)) > 0.32$ and $(1-.298(e_1/h)) > 0.52$. The parameter N/h was also considered in determining this equation but the influence of this ratio on the buckling load is minimal.

The ranges of parameters used in the derivation of Eq. (6.6) are

Parameter	Range
Thickness of specimen, in.	0.046 - 0.051
h/t	63 - 258
N/h	0.1 - 0.7
e_1/h	1.30 - 1.57

The smaller value of P_{cy} and P_{cb} determined from Eqs. (6.5) and (6.7), respectively, governs the design.

3. Interior Two-Flange Loading:

The ultimate web crippling load under interior two-flange loading can be determined as follows:

a. Overstressing Failure: The ultimate web crippling load under interior two-flange loading caused by overstressing can be calculated from the same equation used for the case of interior one-flange loading (Eq. (6.3)) as discussed in Section A.3.a.

b. Buckling Failure: A total of 50 test data (Table D5) were used to derive Eq. (6.7) as follows:

$$P_{cb} = 0.0041t^2E(1+.729(N/h))(1-.0000141(h/t)^2)(1+4.547(e_3/h)) \quad (6.7)$$

with $(1+0.729(N/h)) \leq 1.30$, $(1-0.0000141(h/t)^2) \geq 0.44$ and $(1+4.547(e_3/h)) \leq 7.82$.

The ranges of parameters used in the derivation of Eq. (6.7) are

Parameter	Range
Thickness of specimen, in.	0.046 - 0.065
h/t	44 - 258
N/h	0.1 - 0.7
e_3/h	0.25 - 1.55

The predicted ultimate web crippling load is the smaller value of P_{cy} and P_{cb} determined from Eqs. (6.3) and (6.7), respectively.

4. End Two-Flange Loading:

For this case, only buckling failure was observed and P_{cb} can be calculated from

$$P_{cb} = 0.011t^2E(1+.54(N/h))(1-.00245(h/t))(1+.56(e_3/h)) \qquad (6.8)$$

with $(1+.54(N/h) \leq 1.41$, $(1-.00245(h/t)) \geq 0.51$, and $(1+.56(e_3/h)) \leq 1.98$.

Equation (6.8) was developed on the basis of 74 test data (Table D6) with the ranges of parameters given below:

Parameter	Range
Thickness of specimen, in.	0.046 - 0.088
h/t	32 - 260
N/h	0.1 - 0.7
e_3/h	0.25 - 2.89.

B. I-BEAMS

As discussed in Section III, some I-beam specimens developed a premature failure caused by the rotation of the flanges about the connection line. This incident was avoided by connecting flanges to bearing plates. Because of this reason, the new equations developed to

predict the ultimate web crippling loads for I-beams may be applied only to I-beams having flanges connected to bearing plates except for interior one-flange loading.

1. Interior One-Flange Loading:

Same as the case of beams having single webs, web crippling is distinguished into overstressing and web buckling failure.

a. Overstressing Failure: For this case, it was found that Eq. (3.4.7b2) of the AISI 1981 Guide[3] can provide good agreement with the test data. Because it has the desired form of nondimensional parameters, Eq. (6.9) below was selected. This equation will also be applied for the case of interior two-flange loading.

$$P_{cy} = 15t^2F_y(1+.217\sqrt{N/t}) \qquad (6.9)$$

with $(1+.217\sqrt{N/t}) \leq 3.17$. It should be noted that this function of N/t is the same as that used for sections with single webs (Eq. (6.3)).

b. Buckling Failure: The equation to determine the ultimate web crippling load caused by buckling in the web (Eq. (6.10)) was derived from 39 test data (Table D7)

$$P_{cb} = 0.032t^2E(1+1.318(N/h))(1-.00471(h/t)) \qquad (6.10)$$

with $(1+1.318(N/h)) \leq 1.53$ and $(1-.00471(h/t)) \leq 0.95$.

The ranges of parameters used in the derivation of Eq. (6.10) are

Parameter	Range
Thickness of specimen, in.	0.046 - 0.082
h/t	44 - 252
N/h	0.1 - 0.7

The smaller value of P_{cy} and P_{cb} determined from Eqs. (6.9) and (6.10), respectively, governs the design.

2. End One-Flange Loading:

For I-beams under end one-flange loading, only web buckling failure was observed. The equation to predict the ultimate load was developed on the basis of 67 test data (Table D8). This equation was found to be

$$P_{cb} = 0.063t^2E(1-.00118(h/t))(1-.233(e_1/h)) \qquad (6.11)$$

with $(1-.00118(h/t)) \leq 0.82$ and $(1-.233(e_1/h)) \geq 0.58$. The parameter N/h was also considered in deriving this equation but the effect of this ratio on the buckling load was found to be minimal.

The ranges of parameters used in the derivation of Eq. (6.11) are

Parameter	Range
Thickness of specimen, in.	0.046 - 0.108
h/t	48 - 255
N/h	0.1 - 0.7
e_1/h	1.30 - 2.22

3. Interior Two-Flange Loading:

Same as the case of interior one-flange loading, web crippling is distinguished into overstressing failure and web buckling failure.

a. Overstressing Failure: As discussed in Section B.1.a, Eq. (6.9) which is used for the case of interior-one flange loading, can also be applied for this case. This condition is consistent with single unreinforced webs.

b. Buckling Failure: For failure caused by web buckling, the prediction equation was found to be

$$P_{cb} = 0.051t^2E(1+4(N/h)^3)(1-.0060(h/t))(1+.109(e_3/h) \qquad (6.12)$$

with $(1+4(N/h)^3) \leq 2.69$, $(1-.0060(h/t)) \geq 0.46$, and $(1+.109(e_3/h)) \leq 1.22$.

Equation (6.12) was developed based on 47 test data (Table D9) with the ranges of parameters below

Parameter	Range
Thickness of specimen, in.	0.046 - 0.088
h/t	43 - 260
N/h	0.1 - 0.7
e_3/h	0.91 - 1.57.

The predicted failure load is the smaller value of P_{cy} and P_{cb} calculated from Eqs. (6.9) and (6.12), respectively.

4. End Two-Flange Loading:

Same as the case of end one-flange loading, there is only web buckling failure. Equation (6.13) was derived on the basis of 79 test data (Table D10).

$$P_{cb} = 0.015t^2E(1-.0017(h/t))(1+1.262(N/h)^{1.5}) \qquad (6.13)$$

with $(1-.00170(h/t)) \geq 0.66$ and $(1+1.262(N/h)^{1.5} \leq 1.82$.

The ranges of parameters used in the derivation of Eq. (6.13) are

Parameter	Range
Thickness of specimen, in.	0.046 - 0.148
h/t	27 - 266
N/h	0.1 - 0.7
e_3/h	1.51 - 4.03.

C. COMBINED BENDING AND WEB CRIPPLING

When the ratio of actual moment to the ultimate bending moment capacity, M/M_u, is larger than 0.3, there is a significant interaction between web crippling load and bending moment. The design procedure recommended in the 1986 AISI Specification[6] was reviewed in Section II. The current practice uses interaction formulas between bending moment ratio, M/M_u, and web crippling load ratio, P/P_c. Interaction equations in the form of various stress ratios have been widely used in the aircraft industry.[70]

In this study, other different forms of interaction equation were considered. Because the web element under the bearing plate is subjected to the vertical bearing stress and the horizontal compressive bending stress, stress ratios were used in the derivation of interaction equations. In this regard, two forms of equations were considered in Eqs. (6.14) and (6.15):

$$(f_b/F_{bwu}) + A(f_c/F_y) \leq B \tag{6.14}$$

and

$$(f_b/F_{bwu})^C + (f_c/F_y)^D \leq 1.0 \tag{6.15}$$

where f_b = actual compressive bending stress at the junction of flange and web, ksi.

F_{bwu} = maximum compressive stress in the flat web of beam due to bending, ksi. According to the 1980 AISI Specification,[5] $F_{bwu} = (1.21-0.00034(h/t)\sqrt{F_y})F_y$.

f_c = actual average bearing stress in the web under the bearing plate, ksi.

F_y = yield strength, ksi.

A,B,C,D = constants which are determined empirically.

The actual average bearing stress in the web, f_c, can be expressed as

$$f_c = P_{mc}/(N_e t) \tag{6.16}$$

in which

P_{mc} = predicted ultimate load for combined bending and web crippling, kips.

N_e = effective bearing width, in..

The effective bearing width, N_e, is considered as the width required to develop a uniform stress equal to the yield stress such that the total applied load on this "effective width" is equal to the ultimate web crippling load under the overstressing (bearing) type failure, P_{cy}, determined from Eqs. (6.3) or (6.9) where applicable. In other words,

$$N_e = P_{cy}/(F_y t) \tag{6.17}$$

For the convenience of calculation, by substituting f_c and N_e from Eqs. (6.16) and (6.17) into Eqs. (6.14) and (6.15), the load ratio (P_{mc}/P_{cy}) may be used in place of f_c/F_y as

$$(f_b/F_{bwu}) + A(P_{mc}/P_{cy}) \leq B \tag{6.18}$$

and

$$(f_b/F_{bwu})^C + (P_{mc}/P_{cy})^D \leq 1.0 \tag{6.19}$$

As discussed earlier, the interaction equations used in the 1986 AISI Specification are expressed in terms of moment and load ratios. In this study, simpler equations were also developed as an alternative to the one using stress ratios. This equation can be written as

$$(M/M_u) + E(P_{mc}/P_{cy}) \leq F \tag{6.20}$$

in which

M = applied bending moment at or immediately adjacent to the point of application of the concentrated load or reaction, P_{mc}, kip-in.

M_u = ultimate bending moment if bending moment only exists, kip-in.

P_{mc} and P_{cy} were defined previously.

It should be noted that the predicted combined bending and web crippling load, P_{mc}, determined either from Eq. (6.18), (6.19), or (6.20) must be checked against P_{cb} of the interior one-flange loading case. The smaller value between these predicted loads governs the design.

The newly developed interaction equations for combined bending and web crippling for each type of sections are as follows:

1. Shapes Having Single Webs:

Three equations in the form of Eqs. (6.18), (6.19), and (6.20) were derived for sections with single unreinforced webs. A total of 47 test data obtained from Ref. 41 were used in the derivation. The measured dimensions and important paramaters for this group of test data are listed in Tables C3 and C8, respectively. These new equations are as follows:

$$(f_b/F_{bwu}) + 1.05(P_{mc}/P_{cy}) \leq 1.34 \tag{6.21}$$

$$(f_b/F_{bwu})^2 + (P_{mc}/P_{cy})^{1.5} \leq 1.0 \tag{6.22}$$

$$(M/M_u) + 1.10(P_{mc}/P_{cy}) \leq 1.42 \tag{6.23}$$

where P_{cy} can be calculated from Eq. (6.3). Tables D11 to D13 present

the comparisons between P_{test} and P_{mc} calculated according to Eqs. (6.21), (6.22), and (6.23), respectively. The above three equations are plotted along with the corresponding test data in Figs. 6.1 and 6.2. The value of P_{mc} determined either from Eq. (6.21), (6.22), or (6.23) should not be larger than P_{cb} which is calculated from Eq. (6.4).

It should be noted that F_{bwu} in Eqs. (6.21) and (6.22) should be determined according to the 1980 AISI Specification as discussed earlier. The ultimate bending moment, M_u, in Eq. (6.23) should be calculated based on the 1986 Specification.

2. I-Beams:

For I-beams, 71 test data (Tables C5 and C10) obtained from Ref. 41 were used in the development of interaction equations. The ultimate load for combined bending moment and web crippling, P_{mc}, can be calculated according to the following equations:

$$(f_b/F_{bwu}) + 0.92(P_{mc}/P_{cy}) \leq 1.10 \qquad (6.24)$$

$$(f_b/F_{bwu}) + (P_{mc}/P_{cy})^{1.65} \leq 1.0 \qquad (6.25)$$

$$(M/M_u) + 1.07(P_{mc}/P_{cy}) \leq 1.28 \qquad (6.26)$$

where P_{cy} is determined from Eq. (6.9). The predicted load for combined bending and web crippling, P_{mc}, which is calculated either from Eq. (6.24), (6.25), or (6.26) should be checked against P_{cb} determined by Eq. (6.10). The smaller value between these predicted loads governs the design. Tables D14 to D16 present the comparisons between P_{test} and P_{mc} determined from Eqs. (6.24), (6.25), and (6.26), respectively. Figures 6.3 and 6.4 show a plot of the above three equations along with the corresponding test data.

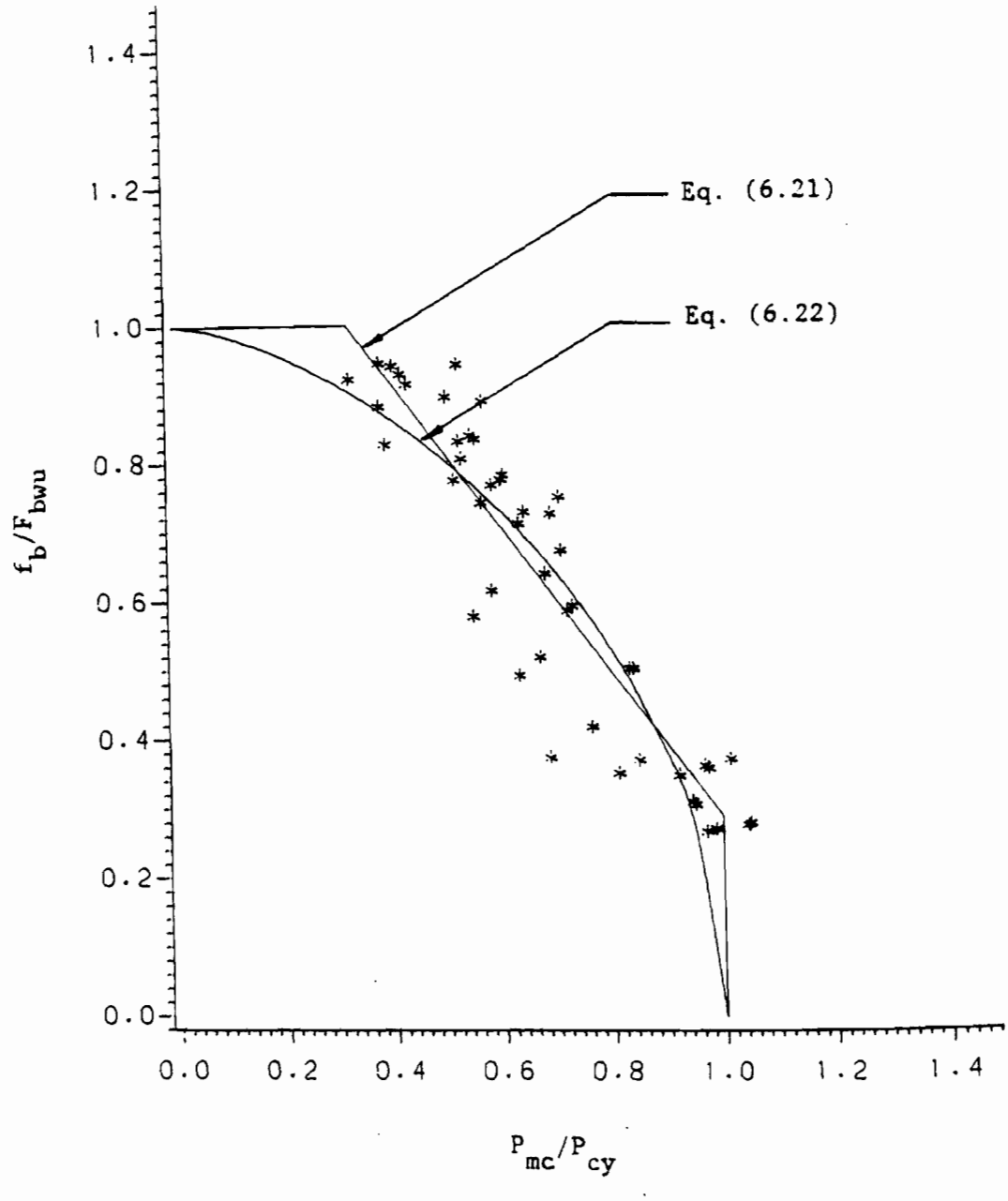

Fig. 6.1 Interaction Equations for Combined Bending and Web Crippling of Sections with Single Unreinforced Webs Using Bending Stress Ratio

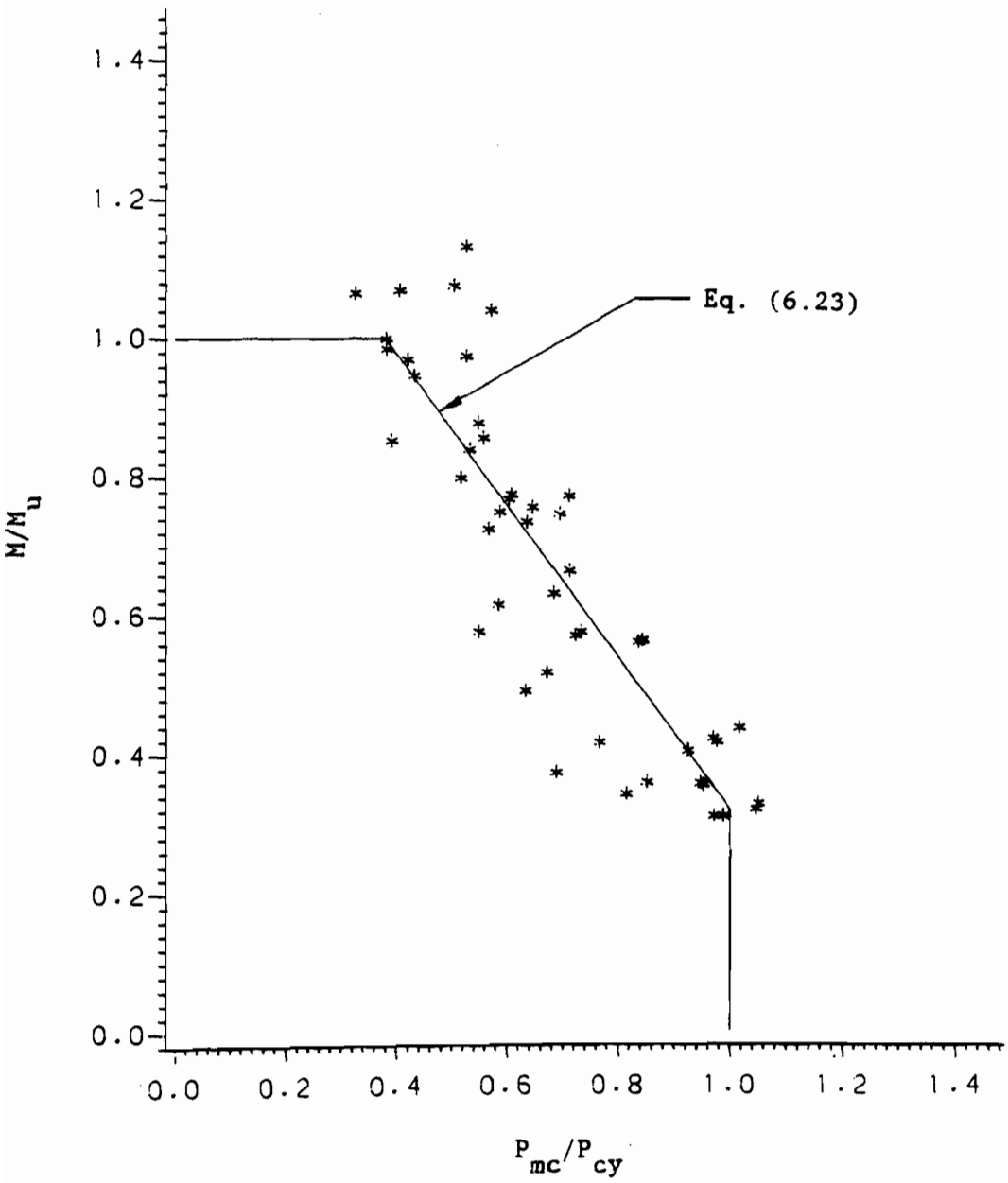

Fig. 6.2 Interaction Equations for Combined Bending and Web Crippling of Sections with Single Unreinforced Webs Using Bending Moment Ratio

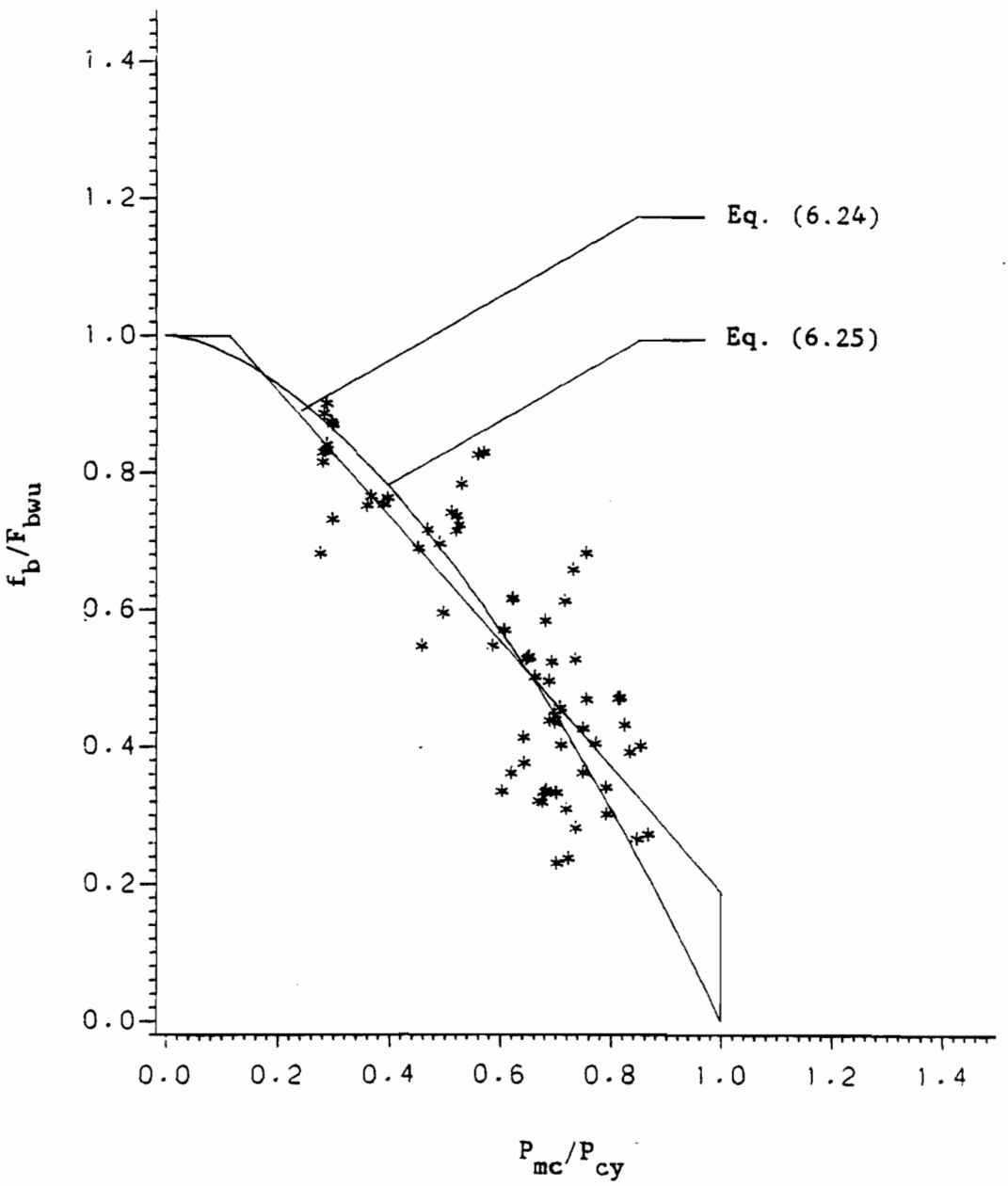

Fig. 6.3 Interaction Equations for Combined Bending and Web Crippling of I-Beams Using Bending Stress Ratio

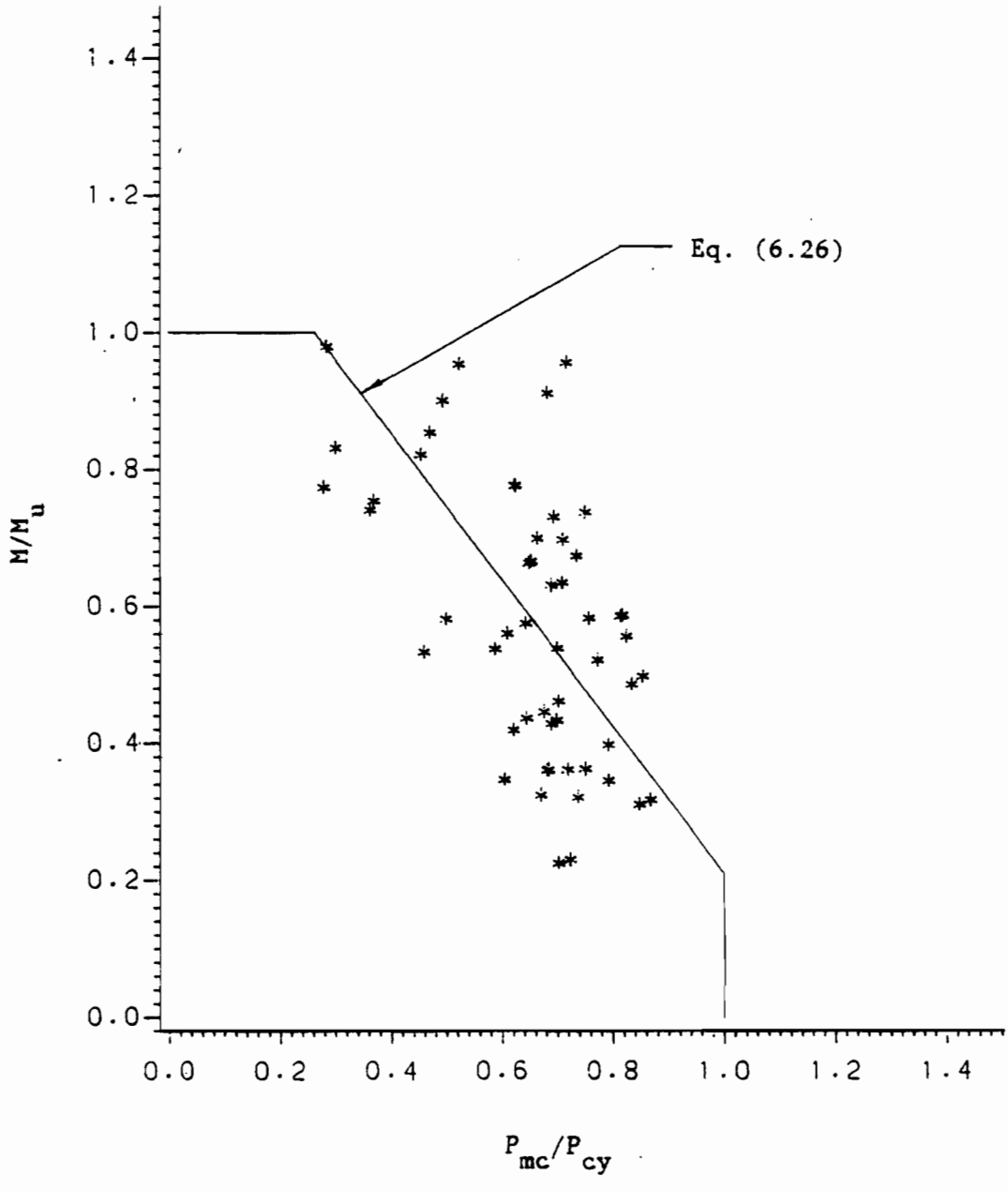

Fig. 6.4 Interaction Equations for Combined Bending and Web Crippling of I-Beams Using Bending Moment Ratio

Similar to shapes having single webs, F_{bwu} in Eqs. (6.24) and (6.25) should be determined based on the 1980 AISI Specification while M_u in Eq. (6.26) should be calculated according to the 1986 Specification.

D. PROPOSED DESIGN RECOMMENDATIONS

Based on the equations developed in Sections A, B, and C, new design formulas are proposed in this section to prevent possible failure modes concerning web crippling and a combination of web crippling and bending moment. The following design equations predict the ultimate strengths without applying any factor of safety. They provide transition equations for four different basic loading conditions (IOF, EOF, ITF, and ETF).

1. Concentrated Loads and Reactions:

The ultimate strengths of unreinforced beam webs subjected to concentrated loads or reactions can be estimated by the equations given in Table 6.1 for beams having single webs and in Table 6.2 for I-beams with flanges connected to bearing plates. The equations apply to beams when $F_y \leq 190$ ksi, $h/t \leq 200$, $N/t \leq 100$, $N/h \leq 2.5$, and $R/t \leq 10$.

The design equations for web crippling listed in Tables 6.1 and 6.2 are categorized into nine cases depending on the values of e and Z (Figs. 6.5a and 6.5b). The equations used for Cases 1, 2, 4, and 5 were derived from the test data obtained from four basic loading conditions classified as end one-flange loading, interior one-flange loading, end two-flange loading, and interior two-flange loading, respectively. Cases 3, 6, 7, 8, and 9 represent the transitions between four basic loading conditions and can be determined by using simple interpolation.

The symbols used in Tables 6.1 and 6.2 are defined as follows:

Table 6.1

Ultimate Concentrated Loads and Reactions for Shapes Having Single Unreinforced Webs

$e \geq .5h$	1) $Z = 0$: $(P_c)_1$ is the smaller of P_{cy} and P_{cb} where $P_{cy} = 9.9t^2F_yc_{11}c_{21}(\sin\theta)$ (6.27) $P_{cb} = 0.047t^2Ec_{41}c_{51}(\sin\theta)$ (6.28)
	2) $Z \geq 0.5h$: $(P_c)_2$ is the smaller of P_{cy} and P_{cb} where $P_{cy} = 7.80t^2F_yc_{12}c_{22}(\sin\theta)$ (6.29) $P_{cb} = 0.028t^2Ec_{32}c_{42}c_{52}(\sin\theta)$ (6.30)
	3) $0 < Z < .5h$: $(P_c)_3 = (P_c)_1 + ((P_c)_2-(P_c)_1)(Z/.5h)$
$e = 0$	4) $Z = 0$: $(P_c)_4 = P_{cb}$ where $P_{cb} = 0.011t^2Ec_{33}c_{43}c_{73}(\sin\theta)$ (6.31)
	5) $Z \geq .5h$: $(P_c)_5$ is the smaller of P_{cy} and P_{cb} where $P_{cy} = 7.8t^2F_yc_{12}c_{22}(\sin\theta)$ (6.32) $P_{cb} = 0.0041t^2Ec_{34}c_{44}c_{64}(\sin\theta)$ (6.33)
	6) $0 < Z < .5h$: $(P_c)_6 = (P_c)_4 + ((P_c)_5-(P_c)_4)(Z/.5h)$
$0 < e < .5h$	7) $Z = 0$: $(P_c)_7 = (P_c)_4 + ((P_c)_1-(P_c)_4)(e/.5h)$
	8) $Z \geq .5h$: $(P_c)_8 = (P_c)_5 + ((P_c)_2-(P_c)_5)(e/.5h)$
	9) $0 < Z < .5h$: $(P_c)_9 = (P_c)_6 + ((P_c)_3-(P_c)_6)(e/.5h)$

Note: Allowable load = Ultimate load/Factor of safety

Table 6.2

Ultimate Concentrated Loads and Reactions for I-Beams with Unreinforced Webs

$e \geq .5h$	1) $Z = 0$: $(P_c)_1 = P_{cb}$ where $P_{cb} = 0.063t^2Ec_{45}c_{55}$ (6.34)
	2) $Z \geq 0.5h$: $(P_c)_2$ is the smaller of P_{cy} and P_{cb} where $P_{cy} = 15t^2F_yc_{12}$ (6.35) $P_{cb} = 0.032t^2Ec_{36}c_{46}$ (6.36)
	3) $0 < Z < .5h$: $(P_c)_3 = (P_c)_1 + ((P_c)_2-(P_c)_1)(Z/.5h)$
$e = 0$	4) $Z = 0$: $(P_c)_4 = P_{cb}$ where $P_{cb} = 0.015t^2Ec_{37}c_{47}$ (6.37)
	5) $Z \geq .5h$: $(P_c)_5$ is the smaller of P_{cy} and P_{cb} where $P_{cy} = 15t^2F_yc_{12}$ (6.38) $P_{cb} = 0.051t^2Ec_{38}c_{48}c_{68}$ (6.39)
	6) $0 < Z < .5h$: $(P_c)_6 = (P_c)_4 + ((P_c)_5-(P_c)_4)(Z/.5h)$
$0 < e < .5h$	7) $Z = 0$: $(P_c)_7 = (P_c)_4 + ((P_c)_1-(P_c)_4)(e/.5h)$
	8) $Z \geq .5h$: $(P_c)_8 = (P_c)_5 + ((P_c)_2-(P_c)_5)(e/.5h)$
	9) $0 < Z < .5h$: $(P_c)_9 = (P_c)_6 + ((P_c)_3-(P_c)_6)(e/.5h)$

Note: Allowable load = Ultimate load/Factor of safety

e = clear distance between edges of the adjacent opposite bearing plates, in.. For reactions or concentrated loads on cantilevers, see Fig. 6.5a. For interior concentrated load shown in Fig. 6.5b, e is taken as the smaller value of e_1 and e_2.

F_y = yield strength of the web, ksi

h = clear distance between flanges measured along the plane of web, in.

N = actual length of bearing, in.

P_c = governing ultimate web crippling load, per web, kips

P_{cb} = web crippling load caused by buckling, per web, kips

P_{cy} = web crippling load caused by bearing, per web, kips

R = inside bend radius, in.

t = web thickness, in.

Z = distance between the edge of the bearing plate to the near end of the beam, in.. See Figs. 6.5 and 6.6.

Z_1 = distance between the edge of the bearing plate to the far end of the beam, in.. See Figs. 6.5.

θ = angle between the plane of web and the plane of bearing surface ≥ 45 but no more than 90, degrees

$c_{11} = 1+.0122(N/t) \leq 2.22$

$c_{12} = 1+.217(N/t)^{.5} \leq 3.17$

$c_{21} = 1-.247(R/t) \geq 0.32$

$c_{22} = 1-.0814(R/t) \geq 0.43$

$c_{32} = 1+2.4(N/h) \leq 1.96$

$c_{33} = 1+.54(N/h) \leq 1.41$

$c_{34} = 1+.729(N/h) \leq 1.30$

$c_{36} = 1+1.318(N/h) \leq 1.53$

$c_{37} = 1+1.262(N/h)^{1.5} \leq 1.82$

$c_{38} = 1+4(N/h)^{3} \leq 2.69$

$c_{41} = 1-.00348(h/t) \geq 0.32$

$c_{42} = 1-.00170(h/t) \leq 0.81$

$c_{43} = 1-.00245(h/t) \geq 0.51$

$c_{44} = 1-.0000141(h/t)^{2} \geq 0.44$

$c_{45} = 1-.00118(h/t) \leq 0.82$

$c_{46} = 1-.000471(h/t) \leq 0.95$

$c_{47} = 1-.0017(h/t) \geq 0.66$

$c_{48} = 1-.0060(h/t) \geq 0.46$

$c_{51} = 1-.298(e/h) \geq 0.52$

$c_{52} = 1-.120(e/h) \geq 0.40$

$c_{55} = 1-.233(e/h) \geq 0.58$

$c_{64} = 1+4.547(Z/h) \leq 7.82$

$c_{68} = 1+0.109(Z/h) \leq 1.22$

$c_{73} = 1+.56(Z_1/h) \leq 1.98$

For uniform loading, the distance "e" should be considered as follows:

1) For end reactions, e is taken as half of the clear distance between the adjacent bearing plates, see Fig. 6.6a, i.e., $e = L_n/2$.

2) For interior reactions (Fig. 6.6b), e is taken as the larger value of $L_{n1}/2$ and $L_{n2}/2$.

It should be noted that the above criteria proposed for beams supporting uniformly distributed loads are not based on test data. It

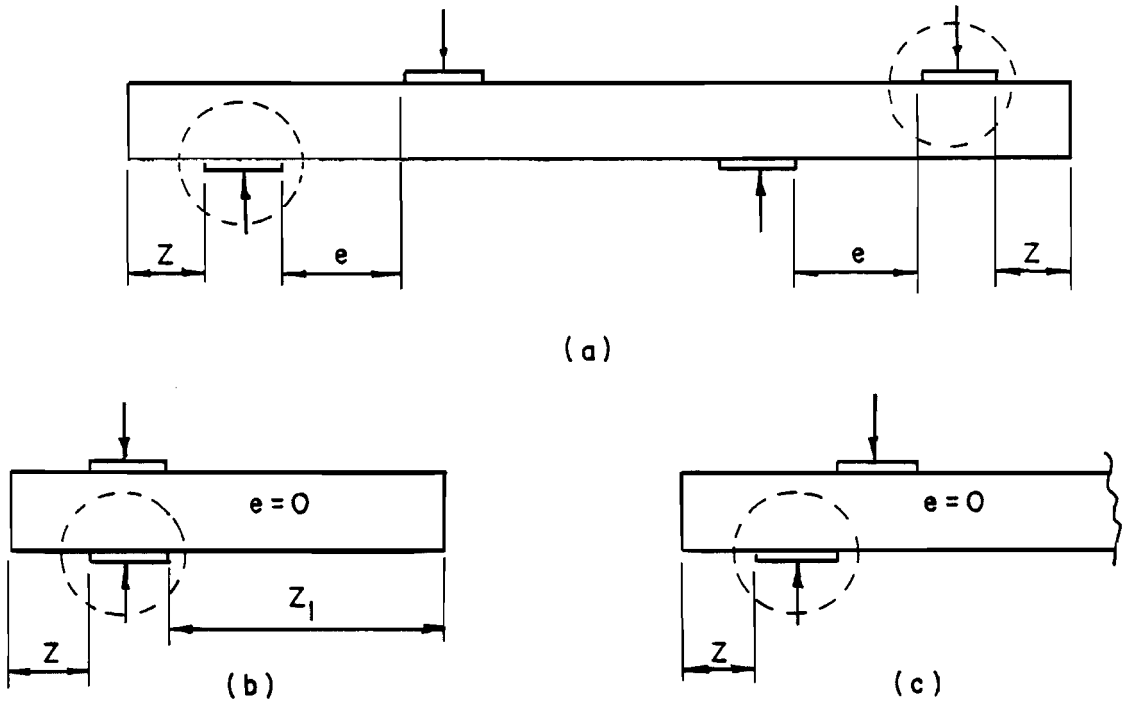

Fig. 6.5a Definitions of e and Z for Reactions and Concentrated Loads on Cantilevers

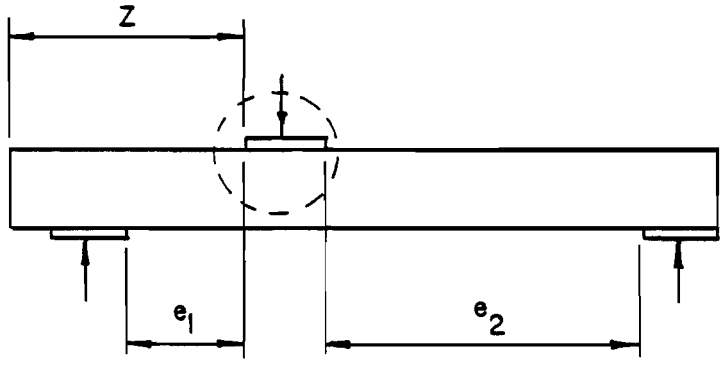

Fig. 6.5b Definitions of e and Z for Interior Concentrated Loads

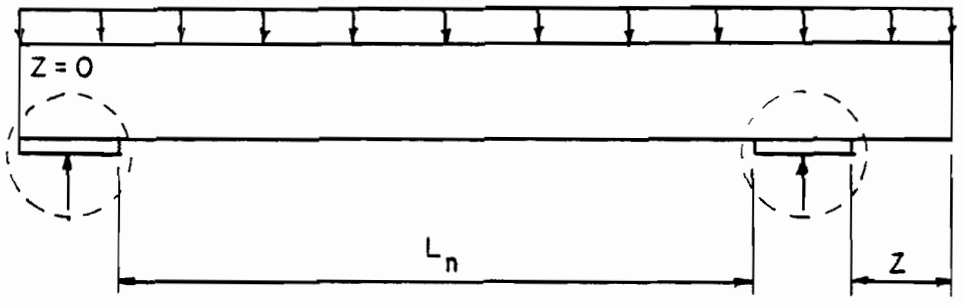

$e = L_n/2$

Fig. 6.6a Definitions of e and Z for End Reactions of Beams Supporting Uniformly Distributed Loads

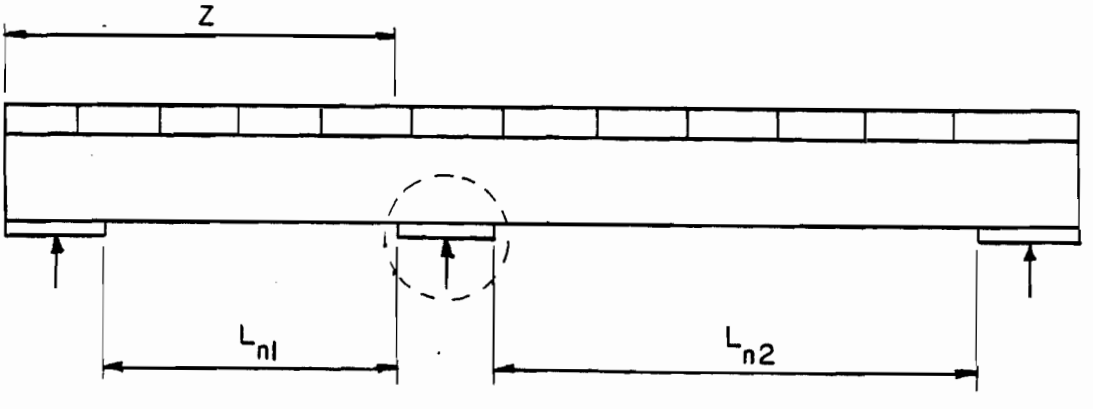

e = larger value of $L_{n1}/2$ and $L_{n2}/2$

Fig. 6.6b Definitions of e and Z for Interior Reactions of Continuous Beams Supporting Uniformly Distributed Loads

was intended to make it compatible with the case of beams supporting concentrated loads. Therefore, some modification may be needed when the test data are available.

2. Combined Bending and Web Crippling:

Unreinforced flat webs of shapes subjected to a combination of bending and reaction or concentrated load shall be designed to meet the following requirements:

a. Shapes Having Single Webs:

$$(M/M_u) + 1.10(P_{mc}/P_{cy}) \leq 1.42 \qquad (6.40)$$

where M = applied bending moment, at or immediately adjacent to the point of application of the concentrated load or reaction, P_{mc}, kip-in.

M_u = ultimate bending moment permitted if bending moment only exists, kip-in.

P_{mc} = concentrated load or reaction in the presence of bending moment, kips

P_{cy} = concentrated load or reaction in the absence of bending moment determined from Eq. (6.29), kips

The value of P_{mc} determined from Eq. (6.40) shall not be larger than P_{cb} calculated from Eq. (6.30).

Equation (6.40) has the same form of equation as used in the current AISI Specification[6] except that the proposed method uses P_{cy} instead of P_c. In addition, the calculated ultimate load for combined bending and web crippling must be checked against the calculated web buckling load (P_{cb}). It should be noted that the current Specification does not distinguish web crippling failure into overstressing and buckling.

b. I-Beams:

$$(M/M_u) + 1.07(P_{mc}/P_{cy}) \leq 1.28 \qquad (6.41)$$

where P_{cy} shall be determined from Eq. (6.35). The value of P_{mc} determined from Eq. (6.41) shall not be larger than P_{cb} calculated from Eq. (6.36). M and M_u are defined in Section 1 above.

The difference between the current method and the proposed method is the same as discussed for the case of single unreinforced webs.

E. COMPARISONS TO TEST DATA

The proposed design methods were used to predict the ultimate web crippling loads and to compare with the test results. The test data used in this comparison are the same as those evaluated in Section IV.

1. Present UMR Tests:

Tables 6.3 through 6.10 present the comparisons of tested and predicted failure loads for the specimens used in this phase of investigation. The symbols used in these Tables are defined as follows:

P_{test} = Tested failure load per web, kips.

P_{cy} = Predicted load caused by overstressing, kips.

P_{cb} = Predicted load caused by web buckling, kips.

P_{mc} = Predicted load for combined bending and web crippling, kips.

P_{comp} = Ultimate web crippling load which is the smaller of P_{cy}, P_{mc} and P_{cb}, kips.

P_{test}/P_{comp} = Ratio of tested and predicted ultimate loads.

By comparing these tables with the corresponding tables included in Section IV, it can be seen that a significant improvement was achieved in

Table 6.3

Comparisons of Tested and Predicted Failure Loads for Hat Sections Subjected to Interior One-Flange Loading Based on the Proposed Design Recommendations

Specimen No.	Material	P_{test}	P_{cy}	P_{mc}	P_{cb}	P_{comp}	P_{test}/P_{comp}
1-HIOF-A11	80DK	1.425	1.512	1.404	2.478	1.404	1.01
1-HIOF-A12	80DK	1.400	1.512	1.400	2.476	1.400	1.00
1-HIOF-A21	80DK	1.465	1.488	1.465	2.466	1.465	1.00
1-HIOF-A22	80DK	1.465	1.488	1.465	2.465	1.465	1.00
1-HIOF-A31	80DK	1.450	1.488	1.488	2.457	1.488	0.97
1-HIOF-A32	80DK	1.500	1.488	1.488	2.458	1.488	1.01
2-HIOF-A11	80XF	5.400	7.654	5.755	7.136	5.755	0.94
2-HIOF-A12	80XF	5.365	7.431	5.690	7.153	5.690	0.94
2-HIOF-A21	80XF	5.740	7.431	6.260	7.158	6.260	0.92
2-HIOF-A22	80XF	5.700	7.431	6.262	7.162	6.262	0.91
2-HIOF-A31	80XF	6.265	7.505	6.705	7.171	6.705	0.93
2-HIOF-A32	80XF	6.375	7.505	6.710	7.174	6.710	0.95
3-HIOF-A11	100XF	4.290	5.625	4.466	4.105	4.105	1.05
3-HIOF-A12	100XF	4.300	5.935	4.603	4.108	4.108	1.05
3-HIOF-A21	100XF	4.290	5.935	5.012	4.099	4.099	1.05
3-HIOF-A22	100XF	4.265	6.012	5.057	4.102	4.102	1.04
3-HIOF-A31	100XF	4.325	6.246	5.427	4.103	4.103	1.05
3-HIOF-A32	100XF	4.350	5.857	5.200	4.098	4.098	1.06
4-HIOF-A11	140XF	2.720	4.998	3.748	2.370	2.370	1.15
4-HIOF-A12	140XF	2.600	5.157	3.819	2.373	2.373	1.10
4-HIOF-A21	140XF	2.725	4.521	3.811	2.375	2.375	1.15
4-HIOF-A22	140XF	2.740	4.601	3.864	2.379	2.379	1.15
4-HIOF-A31	140XF	2.700	4.918	4.167	2.358	2.358	1.14
4-HIOF-A32	140XF	2.630	4.839	4.123	2.358	2.358	1.12
4-HIOF-A13	140XF	2.490	3.482	2.956	2.343	2.343	1.06
4-HIOF-A14	140XF	2.475	3.482	2.961	2.343	2.343	1.06
4-HIOF-A23	140XF	2.625	3.482	3.205	2.394	2.394	1.10
4-HIOF-A24	140XF	2.665	3.482	3.209	2.395	2.395	1.11
4-HIOF-A33	140XF	2.575	3.482	3.256	2.349	2.349	1.10
4-HIOF-A34	140XF	2.610	3.482	3.252	2.349	2.349	1.11
5-HIOF-A11	140SK	2.365	3.925	3.305	2.251	2.251	1.05
5-HIOF-A12	140SK	2.325	3.925	3.301	2.250	2.250	1.03
5-HIOF-A21	140SK	2.500	3.925	3.515	2.258	2.258	1.11
5-HIOF-A22	140SK	2.535	3.925	3.511	2.255	2.255	1.12
5-HIOF-A31	140SK	2.465	3.925	3.618	2.257	2.257	1.09
5-HIOF-A32	140SK	2.435	3.925	3.621	2.260	2.260	1.08
3-HIOF-D11	100XF	4.363	5.827	4.810	5.024	4.810	0.91
3-HIOF-D12	100XF	4.275	5.827	4.820	5.024	4.820	0.89
3-HIOF-C11	100XF	4.225	5.827	4.735	4.858	4.735	0.89
3-HIOF-C12	100XF	4.250	5.827	4.724	4.858	4.724	0.90

Table 6.3 (Cont'd)

Comparisons of Tested and Predicted Failure Loads for Hat Sections Subjected to Interior One-Flange Loading Based on the Proposed Design Recommendations

Specimen No.	Material	P_{test}	P_{cy}	P_{mc}	P_{cb}	P_{comp}	P_{test}/P_{comp}
3-HIOF-B11	100XF	4.150	5.827	4.662	4.693	4.662	0.89
3-HIOF-B12	100XF	4.188	5.827	4.663	4.693	4.663	0.90
3-HIOF-D21	100XF	4.375	5.827	5.298	5.024	5.024	0.87
3-HIOF-D22	100XF	4.325	5.827	5.288	5.024	5.024	0.86
3-HIOF-C21	100XF	4.175	5.827	5.186	4.858	4.858	0.86
3-HIOF-C22	100XF	4.150	5.827	5.187	4.858	4.858	0.85
3-HIOF-B21	100XF	4.100	5.827	5.111	4.693	4.693	0.87
3-HIOF-B22	100XF	4.063	5.827	5.129	4.693	4.693	0.87
3-HIOF-D31	100XF	4.500	5.827	5.579	5.024	5.024	0.90
3-HIOF-D32	100XF	4.400	5.827	5.583	5.024	5.024	0.88
3-HIOF-C31	100XF	4.188	5.827	5.477	4.858	4.858	0.86
3-HIOF-C32	100XF	4.200	5.827	5.478	4.858	4.858	0.86
3-HIOF-B31	100XF	4.087	5.827	5.419	4.693	4.693	0.87
3-HIOF-B32	100XF	4.250	5.827	5.420	4.693	4.693	0.91
5-HIOF-D11	140SK	2.450	3.925	3.436	2.516	2.516	0.97
5-HIOF-D12	140SK	2.500	3.925	3.421	2.516	2.516	0.99
5-HIOF-C11	140SK	2.475	3.925	3.364	2.433	2.433	1.02
5-HIOF-C12	140SK	2.400	3.925	3.359	2.433	2.433	0.99
5-HIOF-B11	140SK	2.587	3.925	3.350	2.350	2.350	1.10
5-HIOF-B12	140SK	2.600	3.925	3.332	2.350	2.350	1.11
5-HIOF-D21	140SK	2.587	3.925	3.642	2.516	2.516	1.03
5-HIOF-D22	140SK	2.500	3.925	3.649	2.516	2.516	0.99
5-HIOF-C21	140SK	2.537	3.925	3.570	2.433	2.433	1.04
5-HIOF-C22	140SK	2.613	3.925	3.578	2.433	2.433	1.07
5-HIOF-B21	140SK	2.537	3.925	3.528	2.350	2.350	1.08
5-HIOF-B22	140SK	2.600	3.925	3.538	2.350	2.350	1.11
5-HIOF-D31	140SK	2.688	3.925	3.761	2.516	2.516	1.07
5-HIOF-D32	140SK	2.712	3.925	3.758	2.516	2.516	1.08
5-HIOF-C31	140SK	2.675	3.925	3.685	2.433	2.433	1.10
5-HIOF-C32	140SK	2.650	3.925	3.682	2.433	2.433	1.09
5-HIOF-B31	140SK	2.762	3.925	3.636	2.350	2.350	1.18
5-HIOF-B32	140SK	2.700	3.925	3.639	2.350	2.350	1.15
Mean Value							1.01
Standard Deviation							0.093

Table 6.4

Comparisons of Tested and Predicted Failure Loads for Hat Sections Subjected to End One-Flange Loading Based on the Proposed Design Recommendations

Specimen No.	Material	P_{test}	P_{cy}	P_{cb}	P_{comp}	P_{test}/P_{comp}
1-HEOF-A11	80DK	0.719	0.766	1.374	0.766	0.94
1-HEOF-A12	80DK	0.700	0.766	1.374	0.766	0.91
1-HEOF-A21	80DK	0.694	0.766	1.230	0.766	0.91
1-HEOF-A22	80DK	0.688	0.766	1.233	0.766	0.90
1-HEOF-A31	80DK	0.669	0.766	1.114	0.766	0.87
1-HEOF-A32	80DK	0.643	0.766	1.113	0.766	0.84
2-HEOF-A11	80XF	2.919	3.109	4.494	3.109	0.94
2-HEOF-A12	80XF	2.981	3.109	4.508	3.109	0.96
2-HEOF-A21	80XF	2.994	3.109	4.388	3.109	0.96
2-HEOF-A22	80XF	3.125	3.147	4.388	3.147	0.99
2-HEOF-A31	80XF	2.713	3.109	4.262	3.109	0.87
2-HEOF-A32	80XF	2.825	3.109	4.250	3.109	0.91
3-HEOF-A11	100XF	2.050	2.489	2.571	2.489	0.82
3-HEOF-A12	100XF	2.106	2.489	2.578	2.489	0.85
3-HEOF-A21	100XF	2.006	2.489	2.460	2.460	0.82
3-HEOF-A22	100XF	2.075	2.489	2.451	2.451	0.85
3-HEOF-A31	100XF	1.894	2.489	2.321	2.321	0.82
3-HEOF-A32	100XF	1.869	2.489	2.321	2.321	0.81
4-HEOF-A11	140XF	1.313	1.802	1.320	1.320	0.99
4-HEOF-A12	140XF	1.300	1.794	1.291	1.291	1.01
4-HEOF-A21	140XF	1.219	1.794	1.180	1.180	1.03
4-HEOF-A22	140XF	1.125	1.794	1.178	1.178	0.96
4-HEOF-A31	140XF	1.088	1.794	1.064	1.064	1.02
4-HEOF-A32	140XF	1.063	1.802	1.063	1.063	1.00
5-HEOF-A11	140SK	1.295	2.025	1.239	1.239	1.05
5-HEOF-A12	140SK	1.285	2.025	1.234	1.234	1.04
5-HEOF-A21	140SK	1.200	2.025	1.126	1.126	1.07
5-HEOF-A22	140SK	1.178	2.025	1.122	1.122	1.05
5-HEOF-A31	140SK	1.050	2.025	1.007	1.007	1.04
5-HEOF-A32	140SK	1.035	2.025	1.005	1.005	1.03
Mean Value						0.94
Standard Deviation						0.083

Table 6.5

Comparisons of Tested and Predicted Failure Loads for Hat Sections Subjected to Interior Two-Flange Loading Based on the Proposed Design Recommendations

Specimen No.	Material	P_{test}	P_{cy}	P_{cb}	P_{comp}	P_{test}/P_{comp}
1-HITF-A11	80DK	1.650	1.372	2.648	1.372	1.20
1-HITF-A12	80DK	1.625	1.372	2.648	1.372	1.18
1-HITF-A21	80DK	1.650	1.372	2.509	1.372	1.20
1-HITF-A22	80DK	1.625	1.372	2.502	1.372	1.18
1-HITF-A31	80DK	1.600	1.372	2.307	1.372	1.17
1-HITF-A32	80DK	1.625	1.372	2.313	1.372	1.18
2-HITF-A11	80XF	6.875	7.279	9.916	7.279	0.94
2-HITF-A12	80XF	6.900	7.279	9.916	7.279	0.95
2-HITF-A21	80XF	6.875	7.279	9.638	7.279	0.94
2-HITF-A22	80XF	6.800	7.279	9.592	7.279	0.93
2-HITF-A31	80XF	6.875	7.279	9.318	7.279	0.94
2-HITF-A32	80XF	6.900	7.279	9.336	7.279	0.95
3-HITF-A11	100XF	5.050	5.827	5.179	5.179	0.98
3-HITF-A12	100XF	5.150	5.827	5.229	5.229	0.98
3-HITF-A21	100XF	4.850	5.827	5.091	5.091	0.95
3-HITF-A22	100XF	4.800	5.827	5.091	5.091	0.94
3-HITF-A31	100XF	4.800	5.827	4.875	4.875	0.98
3-HITF-A32	100XF	4.700	5.827	4.875	4.875	0.96
5-HITF-A11	140SK	2.950	3.691	2.486	2.486	1.19
5-HITF-A12	140SK	3.000	3.691	2.486	2.486	1.21
5-HITF-A21	140SK	2.775	3.691	2.404	2.404	1.15
5-HITF-A22	140SK	2.750	3.691	2.390	2.390	1.15
5-HITF-A31	140SK	2.625	3.691	2.185	2.185	1.20
5-HITF-A32	140SK	2.613	3.691	2.174	2.174	1.20
Mean Value						1.06
Standard Deviation						0.119

Table 6.6

Comparisons of Tested and Predicted Failure Loads for Hat Sections Subjected to End Two-Flange Loading Based on the Proposed Design Recommendations

Specimen No.	Material	P_{test}	P_{cy}	P_{cb}	P_{comp}	P_{test}/P_{comp}
1-HETF-A11	80DK	0.725	1.372	0.775	0.775	0.94
1-HETF-A12	80DK	0.713	1.372	0.770	0.770	0.93
1-HETF-A21	80DK	0.725	1.372	0.676	0.676	1.07
1-HETF-A22	80DK	0.725	1.372	0.673	0.673	1.08
1-HETF-A31	80DK	0.650	1.372	0.603	0.603	1.08
1-HETF-A32	80DK	0.662	1.372	0.603	0.603	1.10
2-HETF-A11	80XF	2.825	7.279	3.043	3.043	0.93
2-HETF-A12	80XF	2.787	7.279	3.043	3.043	0.92
2-HETF-A21	80XF	2.700	7.279	2.717	2.717	0.99
2-HETF-A22	80XF	2.650	7.279	2.717	2.717	0.98
2-HETF-A31	80XF	2.425	7.279	2.489	2.489	0.97
2-HETF-A32	80XF	2.400	7.279	2.493	2.493	0.96
3-HETF-A11	100XF	1.525	5.827	1.578	1.578	0.97
3-HETF-A12	100XF	1.600	5.827	1.573	1.573	1.02
3-HETF-A21	100XF	1.413	5.827	1.396	1.396	1.01
3-HETF-A22	100XF	1.487	5.827	1.399	1.399	1.06
3-HETF-A31	100XF	1.300	5.827	1.261	1.261	1.03
3-HETF-A32	100XF	1.312	5.827	1.266	1.266	1.04
5-HETF-A11	140SK	0.750	3.691	0.739	0.739	1.01
5-HETF-A12	140SK	0.762	3.691	0.741	0.741	1.03
5-HETF-A21	140SK	0.675	3.691	0.641	0.641	1.05
5-HETF-A22	140SK	0.700	3.691	0.641	0.641	1.09
5-HETF-A31	140SK	0.612	3.691	0.576	0.576	1.06
5-HETF-A32	140SK	0.600	3.691	0.577	0.577	1.04
Mean Value						1.01
Standard Deviation						0.055

Table 6.7

Comparisons of Tested and Predicted Failure Loads for I-Beams Subjected to Interior One-Flange Loading Based on the Proposed Design Recommendations

Specimen No.	Material	P_{test}	P_{cy}	P_{cb}	P_{comp}	P_{test}/P_{comp}
1-IIOF-A11	80DK	2.450	4.487	2.886	2.886	0.85
1-IIOF-A12	80DK	2.400	4.487	2.886	2.886	0.83
1-IIOF-A21	80DK	2.625	4.487	2.886	2.886	0.91
1-IIOF-A22	80DK	2.450	4.487	2.886	2.886	0.85
1-IIOF-A31	80DK	2.325	4.487	2.886	2.886	0.81
1-IIOF-A32	80DK	2.350	4.487	2.886	2.886	0.81
2-IIOF-A11	80XF	8.750	18.437	9.172	9.172	0.95
2-IIOF-A12	80XF	8.775	18.437	9.172	9.172	0.96
2-IIOF-A21	80XF	9.300	18.437	9.172	9.172	1.01
2-IIOF-A22	80XF	9.463	18.437	9.172	9.172	1.03
2-IIOF-A31	80XF	9.175	18.437	9.172	9.172	1.00
2-IIOF-A32	80XF	9.500	18.437	9.172	9.172	1.04
3-IIOF-A11	100XF	6.175	16.205	5.942	5.942	1.04
3-IIOF-A12	100XF	6.325	16.205	5.942	5.942	1.06
3-IIOF-A21	100XF	6.825	16.205	5.942	5.942	1.15
3-IIOF-A22	100XF	6.563	16.205	5.942	5.942	1.10
3-IIOF-A31	100XF	5.912	16.205	5.942	5.942	0.99
3-IIOF-A32	100XF	6.250	16.205	5.942	5.942	1.05
5-IIOF-A11	140SK	3.275	12.728	2.886	2.886	1.13
5-IIOF-A12	140SK	3.117	12.728	2.886	2.886	1.08
5-IIOF-A21	140SK	3.100	12.728	2.886	2.886	1.07
5-IIOF-A22	140SK	3.175	12.728	2.886	2.886	1.10
5-IIOF-A31	140SK	3.075	12.728	2.886	2.886	1.07
5-IIOF-A32	140SK	3.200	12.728	2.886	2.886	1.11
Mean Value						1.00
Standard Deviation						0.105

Table 6.8

Comparisons of Tested and Predicted Failure Loads for I-Beams Subjected to End One-Flange Loading Based on the Proposed Design Recommendations

Specimen No.	Material	P_{test}	P_{cy}	P_{cb}	P_{comp}	P_{test}/P_{comp}
1-IEOF-A11	80DK	2.830	******	2.419	2.419	1.17
1-IEOF-A12	80DK	2.750	******	2.438	2.438	1.13
1-IEOF-A21	80DK	2.630	******	2.399	2.399	1.10
1-IEOF-A22	80DK	2.675	******	2.391	2.391	1.12
1-IEOF-A31	80DK	2.750	******	2.380	2.380	1.16
1-IEOF-A32	80DK	2.695	******	2.388	2.388	1.13
2-IEOF-A11	80XF	8.017	******	7.104	7.104	1.13
2-IEOF-A12	80XF	8.100	******	7.128	7.128	1.14
2-IEOF-A21	80XF	7.850	******	7.031	7.031	1.12
2-IEOF-A22	80XF	7.600	******	7.010	7.010	1.08
2-IEOF-A31	80XF	7.625	******	6.938	6.938	1.10
2-IEOF-A32	80XF	7.775	******	6.935	6.935	1.12
3-IEOF-A11	100XF	4.395	******	4.122	4.122	1.07
3-IEOF-A12	100XF	4.370	******	4.069	4.069	1.07
3-IEOF-A21	100XF	4.250	******	4.019	4.019	1.06
3-IEOF-A22	100XF	4.125	******	4.000	4.000	1.03
3-IEOF-A31	100XF	4.125	******	3.977	3.977	1.04
3-IEOF-A32	100XF	4.000	******	3.978	3.978	1.01
5-IEOF-A11	140SK	2.217	******	2.222	2.222	1.00
5-IEOF-A12	140SK	2.175	******	2.215	2.215	0.98
5-IEOF-A21	140SK	2.200	******	2.202	2.202	1.00
5-IEOF-A22	140SK	2.075	******	2.194	2.194	0.95
5-IEOF-A31	140SK	2.117	******	2.183	2.183	0.97
5-IEOF-A32	140SK	2.015	******	2.190	2.190	0.92
Mean Value						1.06
Standard Deviation						0.092

Table 6.9

Comparisons of Tested and Predicted Failure Loads for I-Beams Subjected to Interior Two-Flange Loading Based on the Proposed Design Recommendations

Specimen No.	Material	P_{test}	P_{cy}	P_{cb}	P_{comp}	P_{test}/P_{comp}
1-IITF-A11	80DK	4.350	4.655	5.669	4.655	0.93
1-IITF-A12	80DK	4.450	4.655	5.622	4.655	0.96
1-IITF-A21	80DK	2.775	4.655	2.982	2.982	0.93
1-IITF-A22	80DK	2.750	4.655	2.982	2.982	0.92
1-IITF-A31	80DK	2.188	4.655	2.280	2.280	0.96
1-IITF-A32	80DK	2.150	4.655	2.284	2.284	0.94
2-IITF-A11	80XF	19.875	18.208	26.486	18.208	1.09
2-IITF-A12	80XF	20.050	18.208	26.685	18.208	1.10
2-IITF-A21	80XF	17.000	18.208	15.958	15.958	1.07
2-IITF-A22	80XF	16.500	18.208	15.958	15.958	1.03
2-IITF-A31	80XF	11.850	18.208	11.830	11.830	1.00
2-IITF-A32	80XF	12.125	18.208	11.830	11.830	1.02
3-IITF-A11	100XF	14.125	16.314	12.858	12.858	1.10
3-IITF-A12	100XF	14.050	16.314	12.760	12.760	1.10
3-IITF-A21	100XF	7.188	16.314	7.431	7.431	0.97
3-IITF-A22	100XF	7.300	16.314	7.431	7.431	0.98
3-IITF-A31	100XF	5.375	16.314	5.225	5.225	1.03
3-IITF-A32	100XF	5.500	16.314	5.242	5.242	1.05
5-IITF-A11	140SK	5.025	12.728	5.263	5.263	0.95
5-IITF-A12	140SK	4.975	12.728	5.220	5.220	0.95
5-IITF-A21	140SK	3.000	12.728	2.823	2.823	1.06
5-IITF-A22	140SK	2.975	12.728	2.823	2.823	1.05
5-IITF-A31	140SK	2.025	12.728	2.187	2.187	0.93
5-IITF-A32	140SK	2.125	12.728	2.183	2.183	0.97
Mean Value						1.00
Standard Deviation						0.062

Table 6.10

Comparisons of Tested and Predicted Failure Loads for I-Beams Subjected to End Two-Flange Loading Based on the Proposed Design Recommendations

Specimen No.	Material	P_{test}	P_{cy}	P_{cb}	P_{comp}	P_{test}/P_{comp}
1-IETF-A11	80DK	1.575	1.934	1.507	1.507	1.04
1-IETF-A12	80DK	1.562	1.934	1.511	1.511	1.03
1-IETF-A21	80DK	1.475	1.934	1.260	1.260	1.17
1-IETF-A22	80DK	1.512	1.934	1.264	1.264	1.20
1-IETF-A31	80DK	1.287	1.934	1.095	1.095	1.17
1-IETF-A32	80DK	1.225	1.934	1.098	1.098	1.12
2-IETF-A11	80XF	5.175	7.550	5.392	5.392	0.96
2-IETF-A12	80XF	5.050	7.550	5.368	5.368	0.94
2-IETF-A21	80XF	4.237	7.550	4.545	4.545	0.93
2-IETF-A22	80XF	4.350	7.550	4.557	4.557	0.95
2-IETF-A31	80XF	4.012	7.550	4.130	4.130	0.97
2-IETF-A32	80XF	3.950	7.550	4.127	4.127	0.96
3-IETF-A11	100XF	2.775	6.725	2.887	2.887	0.96
3-IETF-A12	100XF	2.700	6.725	2.899	2.899	0.93
3-IETF-A21	100XF	2.312	6.725	2.466	2.466	0.94
3-IETF-A22	100XF	2.275	6.725	2.466	2.466	0.92
3-IETF-A31	100XF	2.237	6.725	2.233	2.233	1.00
3-IETF-A32	100XF	2.300	6.725	2.237	2.237	1.03
5-IETF-A11	140SK	1.325	5.293	1.431	1.431	0.93
5-IETF-A12	140SK	1.312	5.293	1.440	1.440	0.91
5-IETF-A21	140SK	1.250	5.293	1.204	1.204	1.04
5-IETF-A22	140SK	1.175	5.293	1.202	1.202	0.98
5-IETF-A31	140SK	1.000	5.293	1.044	1.044	0.96
5-IETF-A32	140SK	0.962	5.293	1.048	1.048	0.92
Mean Value						1.00
Standard Deviation						0.086

the prediction of ultimate web crippling loads for high strength steel sections. The improvement is mainly due to the fact that most of test specimens failed by buckling in the webs which is recognized in the proposed design methods. It should be noted that the yield strengths of these specimens are beyond the limitation of the present AISI design recommendations.[3,6]

Figures 6.7 through 6.14 show the effect of F_y on the ratio P_{test}/P_{comp} for each type of sections and loading conditions. These plots include the test data obtained from the present investigation and the previous UMR tests on relative low strength sections. As a result of these comparisons, it can be seen that good agreement between the tested and predicted failure loads can be achieved for sections with yield strengths up to 165 ksi.

In addition, the proposed design methods were checked against the test data for the transition ranges. Table 6.11 indicates that by using a simple interpolation between the predicted failure loads for four basic loading conditions, a reasonable accuracy of prediction can be achieved.

2. Inland Tests:

The validity of these newly developed equations was also checked against the test data conducted at Inland Steel Company. The new equations involved in the calculations are those for the cases of interior one-flange loading and the combined bending and web crippling. The comparisons between the predicted and tested failure loads are presented in Table 6.12. The symbols used in this table are the same as that used in the evaluation of experimental data (Section IV). Figure 6.15 shows the relationships of the ratio P_{test}/P_{comp} and the yield strength of materials, F_y.

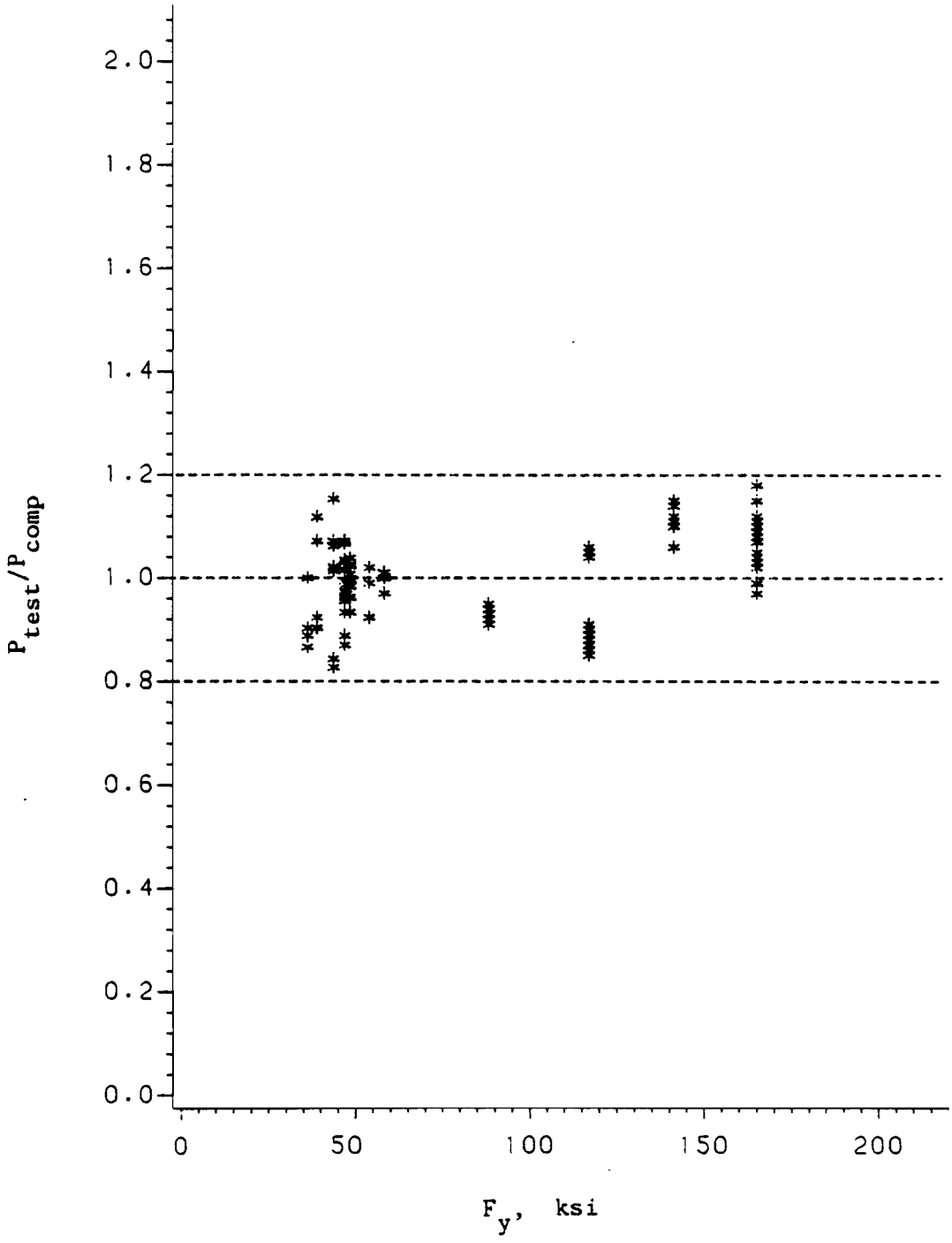

Fig. 6.7 Effect of F_y on the Ratio P_{test}/P_{comp} for Hat Sections Subjected to Interior One-Flange Loading Based on the Proposed Design Recommendations

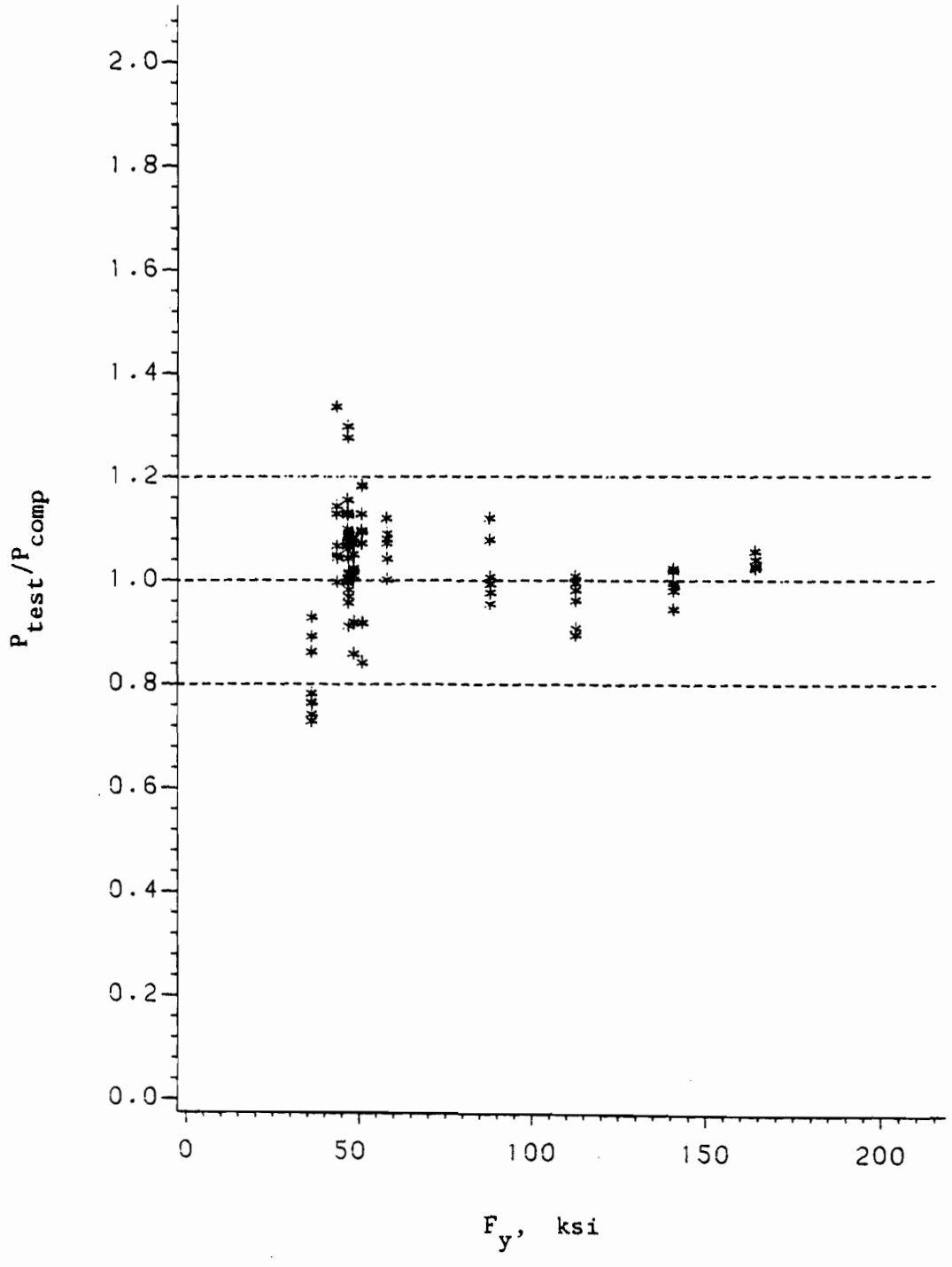

Fig. 6.8 Effect of F_y on the Ratio P_{test}/P_{comp} for Hat Sections Subjected to End One-Flange Loading Based on the Proposed Design Recommendations

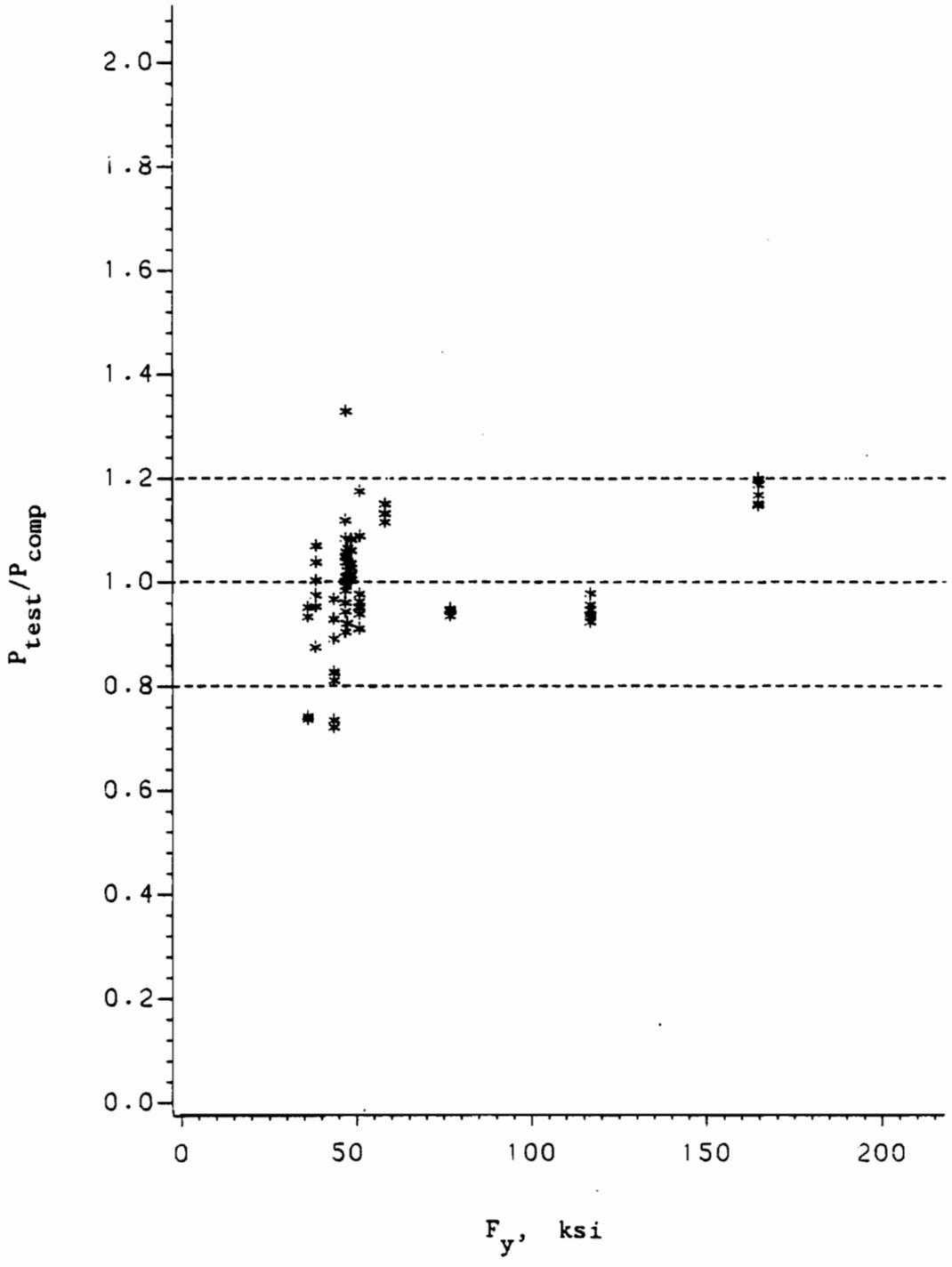

Fig. 6.9 Effect of F_y on the Ratio P_{test}/P_{comp} for Hat Sections Subjected to Interior Two-Flange Loading Based on the Proposed Design Recommendations

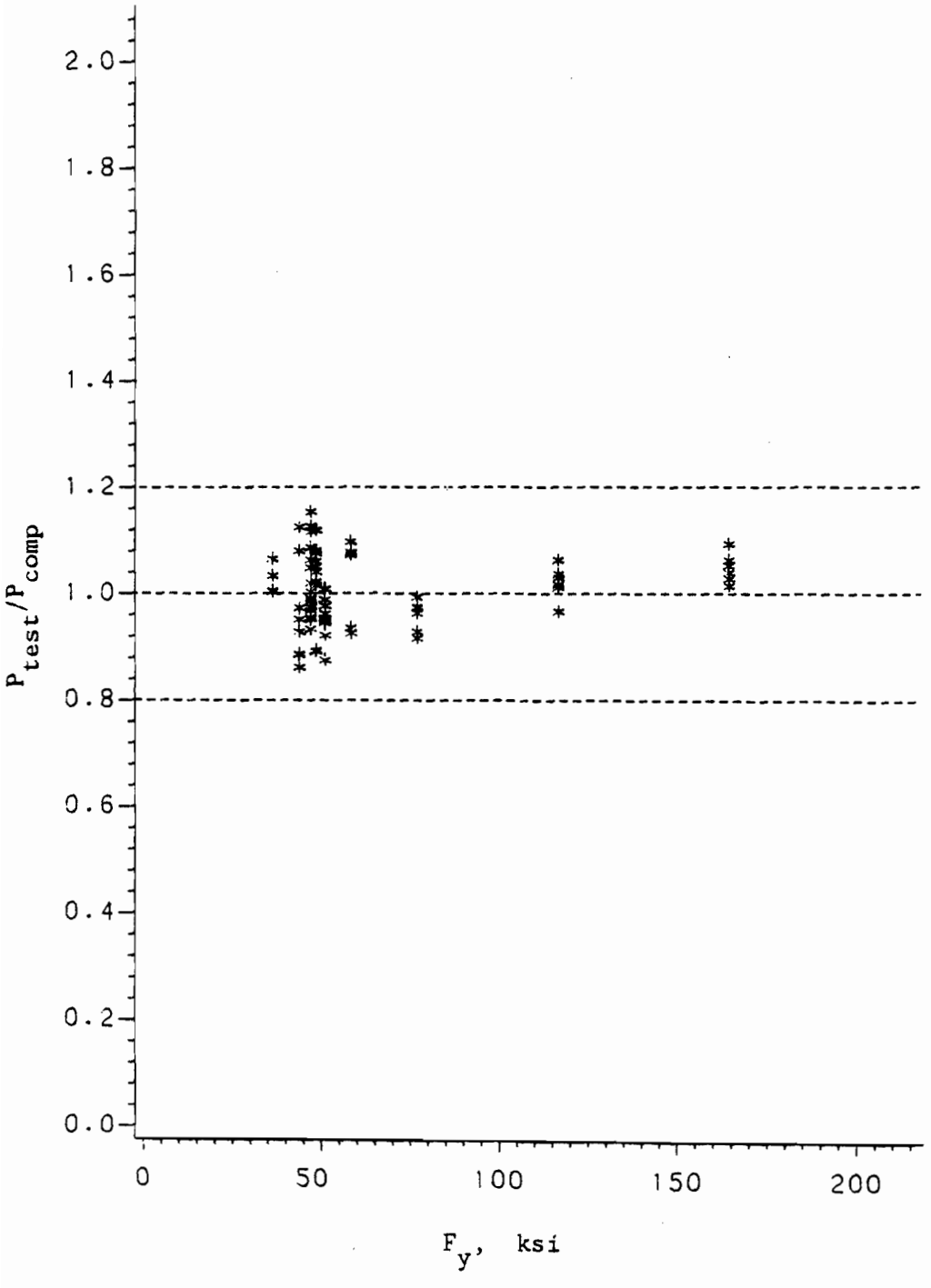

Fig. 6.10 Effect of F_y on the Ratio P_{test}/P_{comp} for Hat Sections Subjected to End Two-Flange Loading Based on the Proposed Design Recommendations

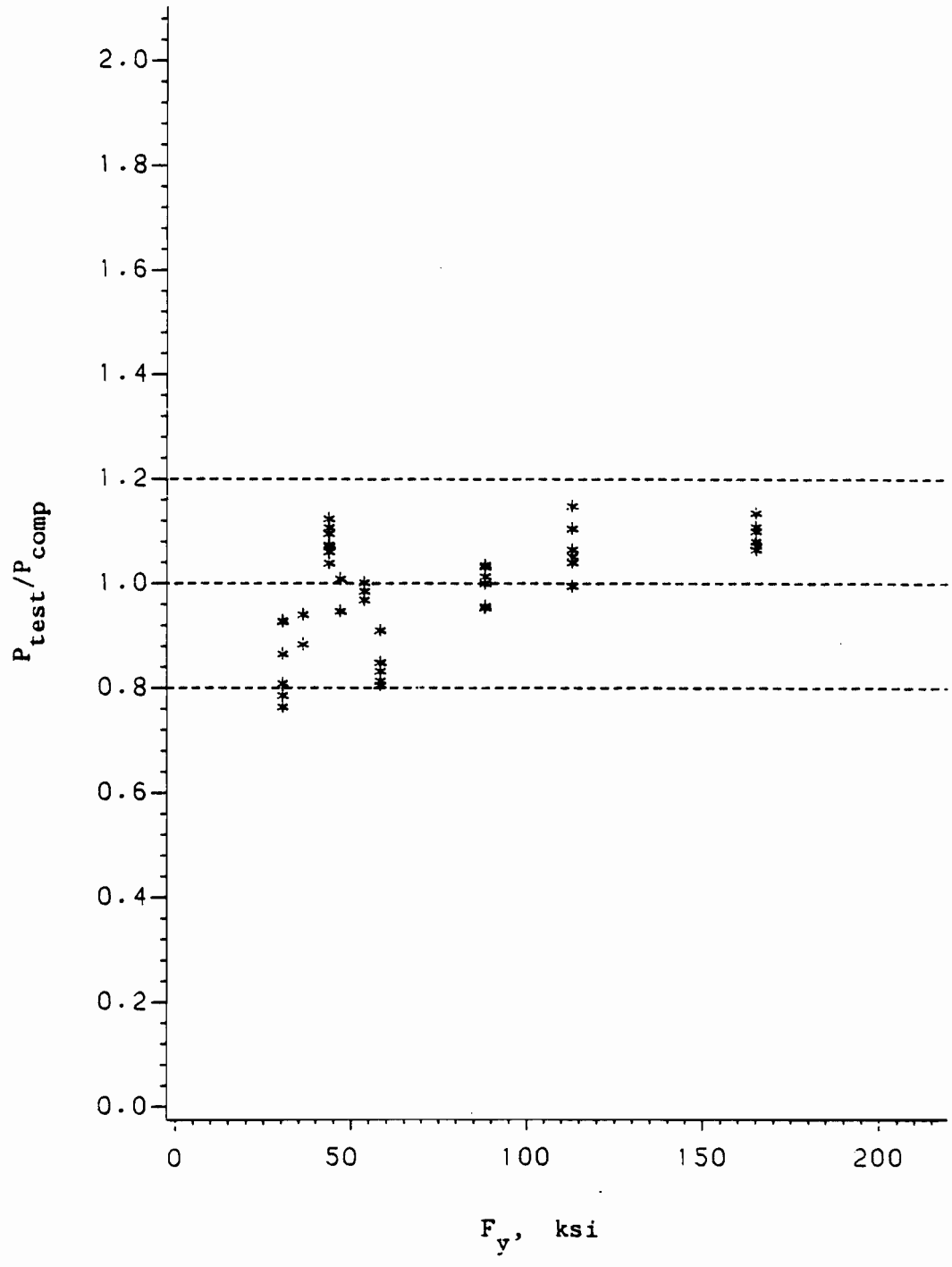

Fig. 6.11 Effect of F_y on the Ratio P_{test}/P_{comp} for I-Beams Subjected to Interior One-Flange Loading Based on the Proposed Design Recommendations

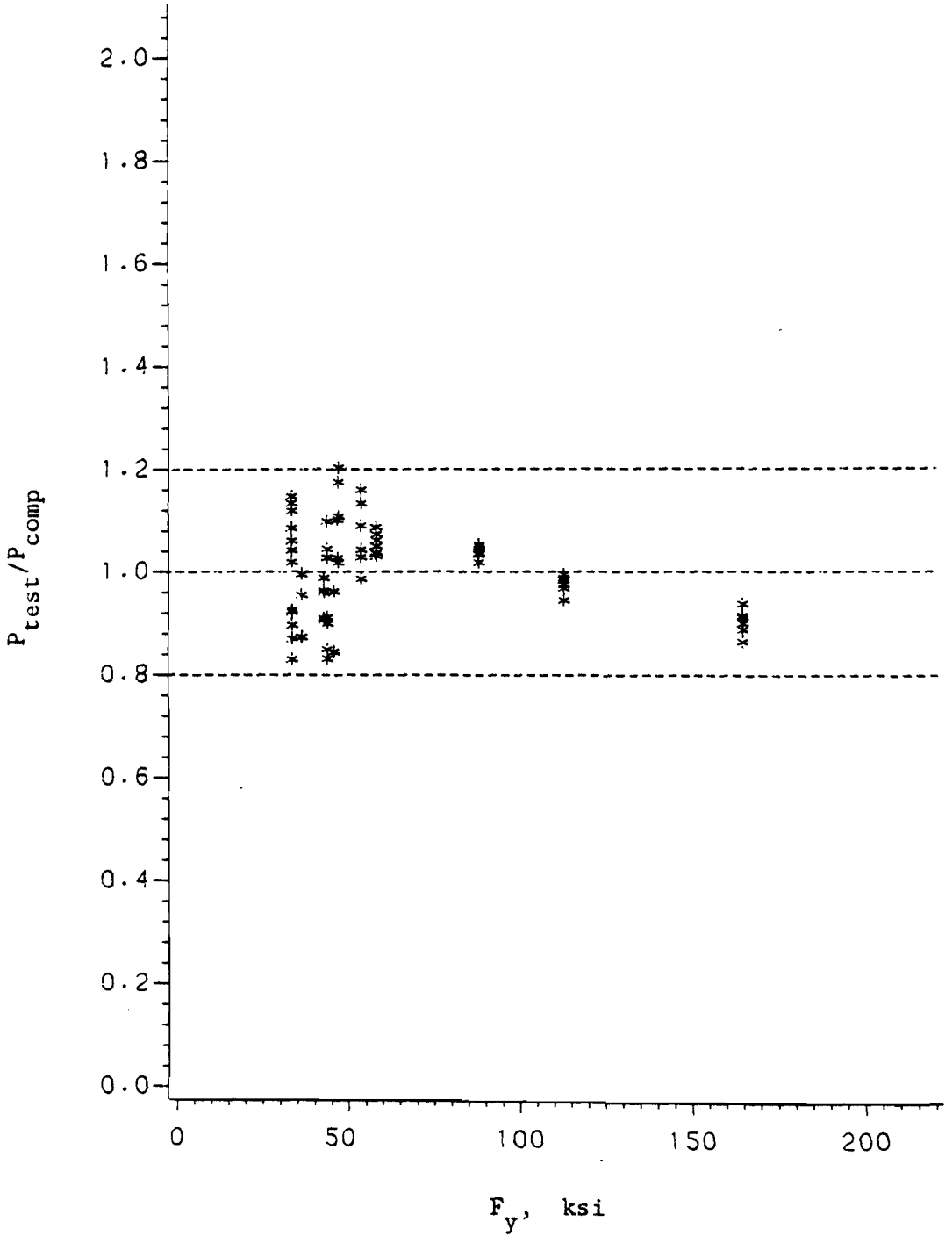

Fig. 6.12 Effect of F_y on the Ratio P_{test}/P_{comp} for I-Beams Subjected to End One-Flange Loading Based on the Proposed Design Recommendations

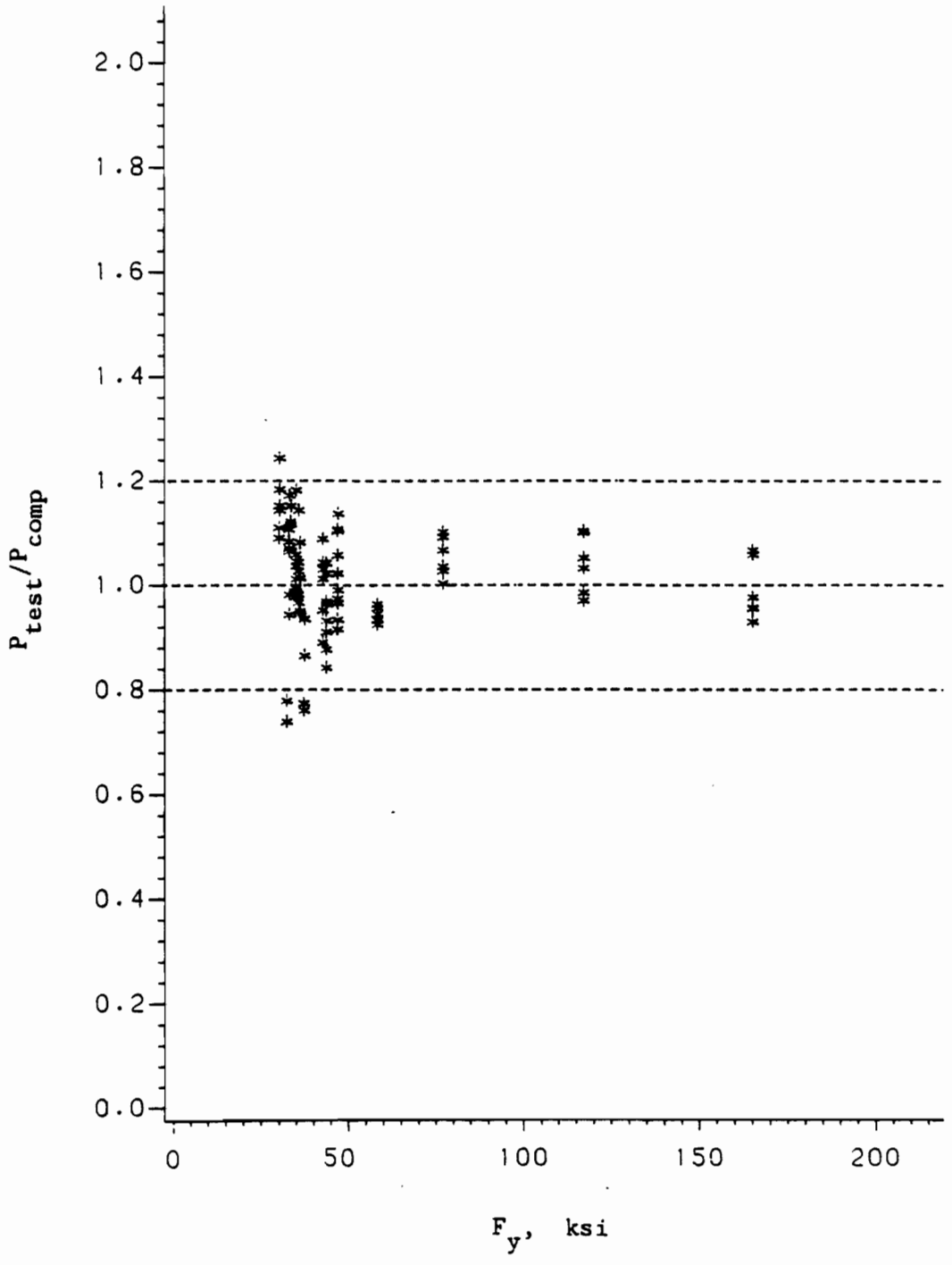

Fig. 6.13 Effect of F_y on the Ratio P_{test}/P_{comp} for I-Beams Subjected to Interior Two-Flange Loading Based on the Proposed Design Recommendations

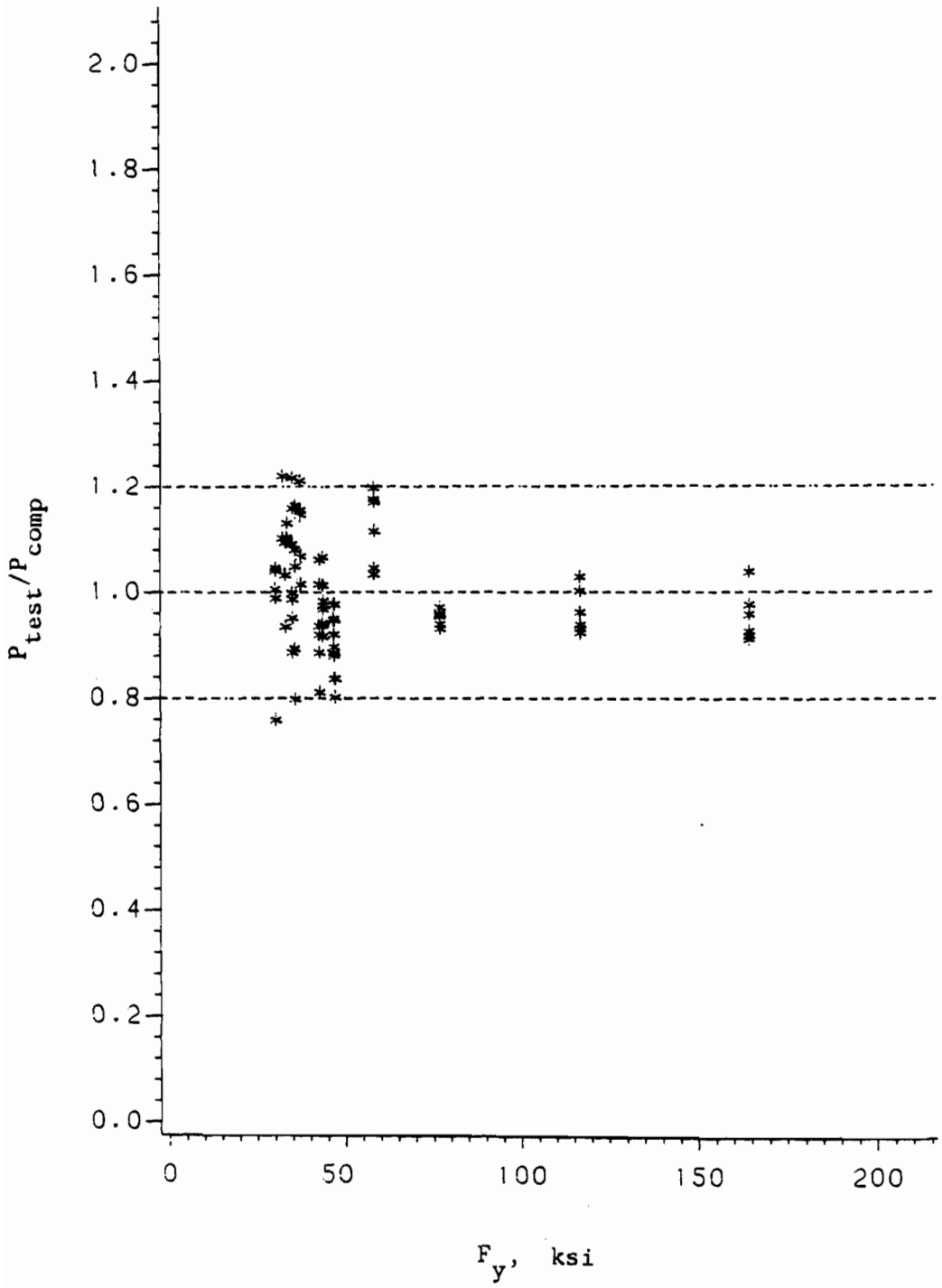

Fig. 6.14 Effect of F_y on the Ratio P_{test}/P_{comp} for I-Beams Subjected to End Two-Flange Loading Based on the Proposed Design Recommendations

Table 6.11

Comparisons of Tested and Predicted Failure Loads for the Tests of Transition Ranges Based on the Proposed Design Recommendations

Specimen No.	Material	e/h	P_{test}	P_{comp}	P_{test}/P_{comp}
T-IOF-ITF-1	100XF	0.500	4.975	5.189	0.96
T-IOF-ITF-2	140SK	0.450	2.775	2.602	1.07
T-IOF-ITF-3	100XF	0.400	5.200	5.219	1.00
T-IOF-ITF-4	140SK	0.300	2.725	2.641	1.03
T-IOF-ITF-5	100XF	0.200	5.425	5.296	1.02
T-IOF-ITF-6	140SK	0.100	2.700	2.398	1.13
T-IOF-EOF-1	100XF	0.750	4.563	5.024	0.91
T-IOF-EOF-2	140SK	0.500	2.750	2.433	1.13
T-IOF-EOF-3	100XF	0.400	4.188	4.416	0.95
T-IOF-EOF-4	140SK	0.300	1.875	2.008	0.93
T-IOF-EOF-5	100XF	0.200	3.200	3.568	0.90
T-IOF-EOF-6	140SK	0.100	1.438	1.316	1.09
T-EOF-ETF-1	100XF	0.750	4.050	3.838	1.06
T-EOF-ETF-2	140SK	0.500	1.802	1.755	1.03
T-EOF-ETF-3	100XF	0.400	3.135	3.318	0.95
T-EOF-ETF-4	140SK	0.300	1.457	1.562	0.93
T-EOF-ETF-5	100XF	0.200	2.359	2.635	0.90
T-EOF-ETF-6	140SK	0.100	0.770	0.849	0.91
Mean Value					0.994
Standard Deviation					0.079

Table 6.12

Comparisons of Tested and Predicted Failure Loads for Inland Tests[10] Based on the Proposed Design Recommendations

Specimen No.	$P_{\bar{m}}$ (kips)	P_{cy} (kips	P_{mc} (kips)	P_{cb} (kips)	P_{ms} (kips)	P_{test} (kips)	Failure Mode	P_{test}/P_{comp}
1	0.251*	1.450	0.163	1.639	0.196	0.216	M	1.10
2	0.415	1.450	0.415	1.639	0.473	0.414	M	1.00
3	0.707	1.450	0.636	1.639	0.765	0.618	MC	0.97
4	1.026	1.450	0.797	2.086	1.055	0.762	MC	0.96
5	1.384	1.450	0.931	2.427	1.333	0.900	MC	0.97
6	2.080	1.450	1.111	2.667	1.739	0.975	MC	0.88
7	0.350*	2.266	0.350	2.416	0.268	0.306	M	1.14
8	0.621*	2.266	0.621	2.416	0.652	0.594	M	0.96
9	1.000	2.266	0.934	2.416	1.110	0.876	MC	0.94
10	1.461	2.266	1.183	3.061	1.547	1.090	MC	0.92
11	1.973	2.266	1.395	3.569	1.988	1.320	MC	0.95
12	3.085	2.266	1.701	4.148	2.712	1.610	MC	0.95
13	0.414*	2.699	0.414	2.416	0.318	0.384	M	1.21
14	0.667	2.699	0.667	2.416	0.770	0.726	M	1.09
15	1.160	2.699	1.100	2.416	1.273	1.100	MC	1.00
16	1.690	2.699	1.385	3.061	1.762	1.380	MC	1.00
17	2.282	2.699	1.635	3.569	2.243	1.610	MC	0.98
18	3.490	2.699	1.981	4.148	2.975	1.960	MC	0.99
19	0.462*	3.223	0.462	2.416	0.377	0.498	M	1.32
20	0.796	3.223	0.796	2.416	0.912	0.905	M	1.14
21	1.349	3.223	1.291	2.416	1.460	1.360	MC	1.05
22	1.960	3.223	1.638	3.061	2.008	1.640	MC	1.00
23	2.648	3.223	1.927	3.569	2.522	1.930	MC	1.00
24	3.947	3.223	2.331	4.148	3.244	2.340	MC	1.00
25	0.754*	5.707	0.754	3.514	0.582	0.678	M	1.16
26	1.218	5.707	1.218	3.514	1.417	1.260	M	1.03
27	2.118	5.707	2.093	3.514	2.332	1.840	MC	0.88
28	3.089	5.707	2.684	4.426	3.223	2.370	MC	0.88
29	4.178	5.707	3.203	5.173	4.090	2.740	MC	0.86
30	6.373	5.707	3.926	6.095	5.377	3.190	MC	0.81
31	0.786	6.681	0.786	1.371	0.851	0.705	M	0.90
32	1.090	10.685	1.090	2.474	1.257	1.185	M	1.09
33	0.816	6.681	0.816	1.371	0.893	0.698	M	0.86
34	1.183	10.685	1.183	2.474	1.380	1.178	M	1.00
35	0.825	6.681	0.825	1.371	0.903	0.690	M	0.84
36	1.206	10.685	1.206	2.474	1.408	1.140	M	0.95
37	0.772	6.540	0.772	1.371	0.838	0.705	M	0.91
38	0.903	9.337	0.903	2.332	1.043	1.134	M	1.26
39	1.557	6.540	1.557	1.371	1.516	1.071	B	0.78
40	2.037	9.337	2.037	2.332	2.142	1.890	B	0.81

Table 6.12 (Cont'd)

Comparisons of Tested and Predicted Failure Loads for Inland Tests[10] Based on the Proposed Design Recommendations

Specimen No.	P_m (kips)	P_{cy} (kips)	P_{mc} (kips)	P_{cb} (kips)	P_{ms} (kips)	P_{test} (kips)	Failure Mode	P_{test}/P_{comp}
41	2.271	6.540	2.225	1.370	2.061	1.470	B	1.07
42	3.262	9.337	3.191	2.332	3.127	2.592	B	1.11
43	2.771	6.681	2.581	1.747	2.259	1.655	B	0.95
44	4.364	10.685	4.084	3.132	3.968	2.898	B	0.93
45	2.480	6.100	2.326	1.706	2.071	1.584	B	0.93
46	4.311	10.555	4.037	3.168	3.940	2.979	B	0.94
47	2.902	6.681	2.665	1.747	2.328	1.718	B	0.98
48	4.750	10.685	4.332	3.132	4.251	3.142	B	1.00
49	2.723	6.100	2.480	1.706	2.206	1.635	B	0.96
50	4.726	10.555	4.299	3.168	4.249	3.069	B	0.97
51	2.956	6.540	2.681	1.747	2.356	1.746	B	1.00
52	4.611	9.814	4.131	3.132	4.151	3.012	B	0.96
53	2.976	6.100	2.633	1.706	2.335	1.599	B	0.94
54	5.157	10.555	4.557	3.168	4.554	3.168	B	1.00
55	2.921	6.681	2.678	1.747	2.338	1.805	B	1.03
56	4.808	10.685	4.365	3.132	4.293	3.048	B	0.97
57	2.774	6.551	2.568	1.706	2.233	1.536	B	0.90
58	4.442	10.166	4.070	2.955	3.958	3.243	B	1.10
59	3.557	6.540	3.027	2.009	2.395	2.091	B	1.04
60	5.513	9.337	4.553	3.445	4.385	3.522	B	1.02
61	4.060	6.681	3.314	2.164	2.078	2.302	MS	1.11
62	7.622	10.685	5.830	4.259	4.664	4.135	B	0.97
63	4.194	6.681	3.383	2.164	2.096	2.470	MS	1.18
64	8.101	10.685	6.038	4.259	4.768	4.405	B	1.03
65	4.210	6.681	3.391	2.164	2.098	2.475	MS	1.18
66	8.164	10.685	6.061	4.259	4.780	4.628	B	1.09
67	4.293	6.540	3.400	2.164	2.108	2.607	MS	1.24
68	7.535	9.337	5.461	3.986	4.386	4.562	B	1.14
Mean Value								1.00
Standard Deviation								0.109

* Inelastic reserve capacity was employed.

Note: Predicted Failure Mode
B represents web buckling
M represents bending moment
MC represents combined bending and web crippling
MS represents combined bending and shear

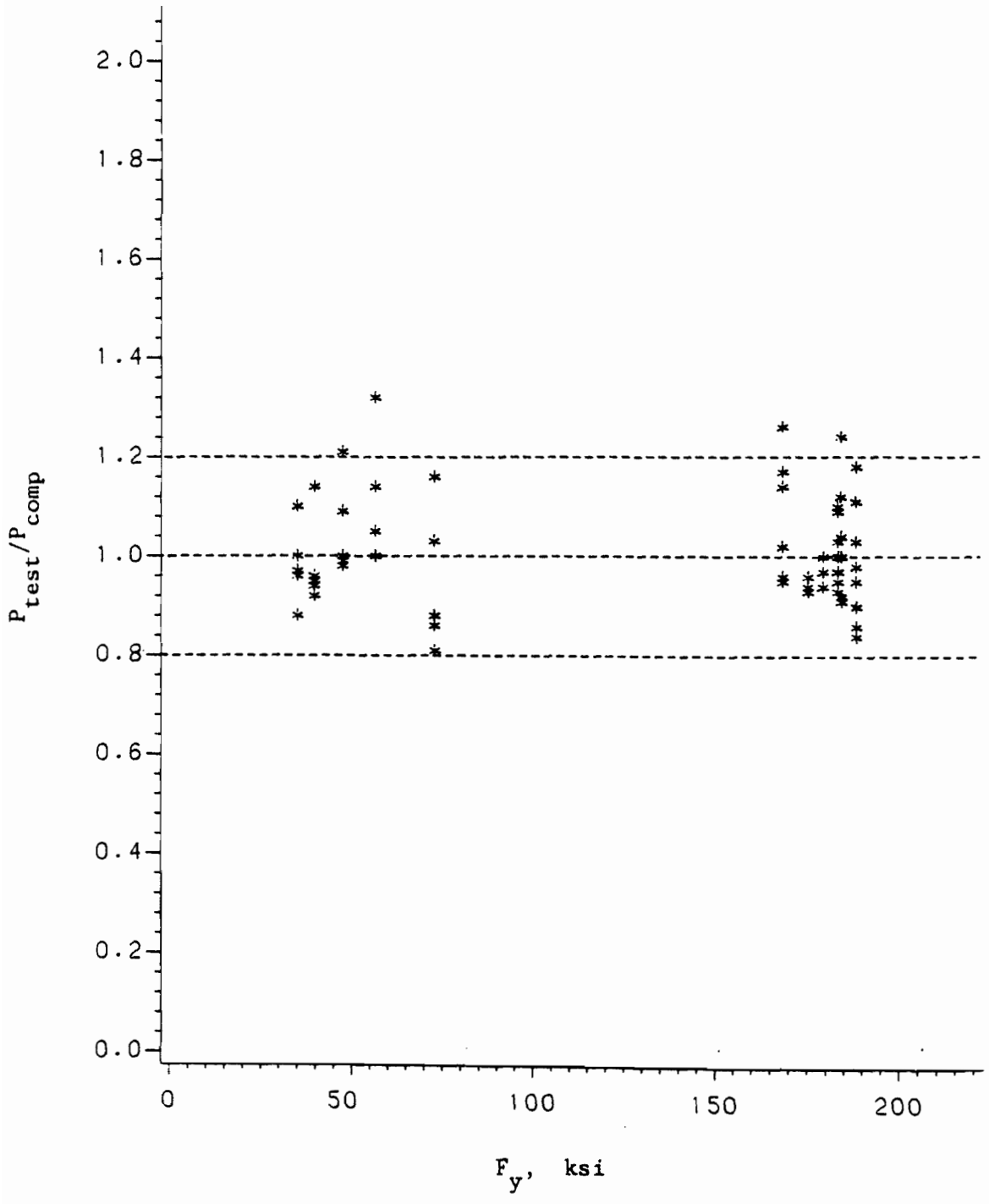

Fig. 6.15 Effect of F_y on the Ratio P_{test}/P_{comp} for Inland Tests Based on the Proposed Design Recommendations

For specimens that expected to fail by web crippling or combined web crippling and bending moment, the proposed design methods can provide resonable estimates of the failure loads with the accuracy within 20%. The Inland test specimens were formed from sheet steels with yield strengths up to 190 ksi. Underestimations were observed for Specimen Nos. 13, 16, 38, and 67 in which combined bending and shear or bending moment alone is expected to be the mode of failure. The reasons for this inaccuracy were discussed in Section IV.

3. Ford Tests:

For Ford tests, the material properties used in the calculations were obtained from flanges and webs of formed hat sections. The procedure used in calculations of these composite sections was the same as those employed in Section IV, except that the predicted ultimate loads for web crippling and a combination of web crippling and bending moment were determined according to the newly developed equations.

Table 6.13 compares the predicted and tested failure loads. The mean value and standard deviation for the ratio P_{test}/P_{comp} in this table are calculated only for Specimen Nos. 1 through 9. The failure mode of these specimens are expected to be a combination of bending moment and web crippling. Figure 6.16 shows the effect of material yield strength, F_y, on the ratio P_{test}/P_{comp} for Specimen Nos. 1 to 9. Based on the mean value of 0.892 and a standard deviation of 0.109, the newly developed equations generally overestimated the failure loads.

The overestimation may be mainly due to the fact that a die forming process was used in the fabrication of the hat sections. The as formed yield strength in the web, F_{yw}, was determined from the tension coupons taken from the middle portion of the webs. By using the die forming, the

Table 6.13

Comparisons of Tested and Predicted Failure Loads for Ford Tests[11] Based on the Proposed Design Recommendations

Specimen No.	P_m (kips)	P_{cy} (kips)	P_{mc} (kips)	P_{cb} (kips)	P_{ms} (kips)	P_{test} (kips)	Failure Mode	P_{test}/P_{comp}
1	1.810	2.819	1.506	3.724	3.099	1.616	MC	1.07
2	2.963	5.028	2.553	4.782	4.467	2.320	MC	0.91
3	3.543	5.331	2.906	3.724	4.934	2.377	MC	0.82
4	3.289	5.410	2.799	3.479	5.673	2.453	MC	0.88
5	3.193	4.278	2.490	2.798	3.928	1.948	MC	0.78
6	3.356	3.987	2.475	2.798	3.777	2.031	MC	0.82
7	4.831	7.112	3.926	3.724	5.244	2.995	B	0.80
8	3.964	7.327	3.529	5.969	4.532	3.602	MC	1.02
9	4.753	9.303	4.321	6.284	5.626	4.195	MC	0.97
10	3.084	10.722	3.327	11.224	5.975	4.567	M	1.48
11	4.231	11.519	4.279	10.002	6.833	4.858	M	1.15
12	3.966	15.490	4.394	10.416	8.588	5.783	M	1.46
13	5.159	18.533	5.608	10.021	10.621	6.065	M	1.18
Mean Value*								0.897
Standard Deviation*								0.104

* Based on Specimen Nos. 1-9 which are expected to fail by a combination of bending and web crippling or web buckling.

Note: Predicted Failure Mode
M represents bending moment
B represents web buckling
MC represents combined bending and web crippling

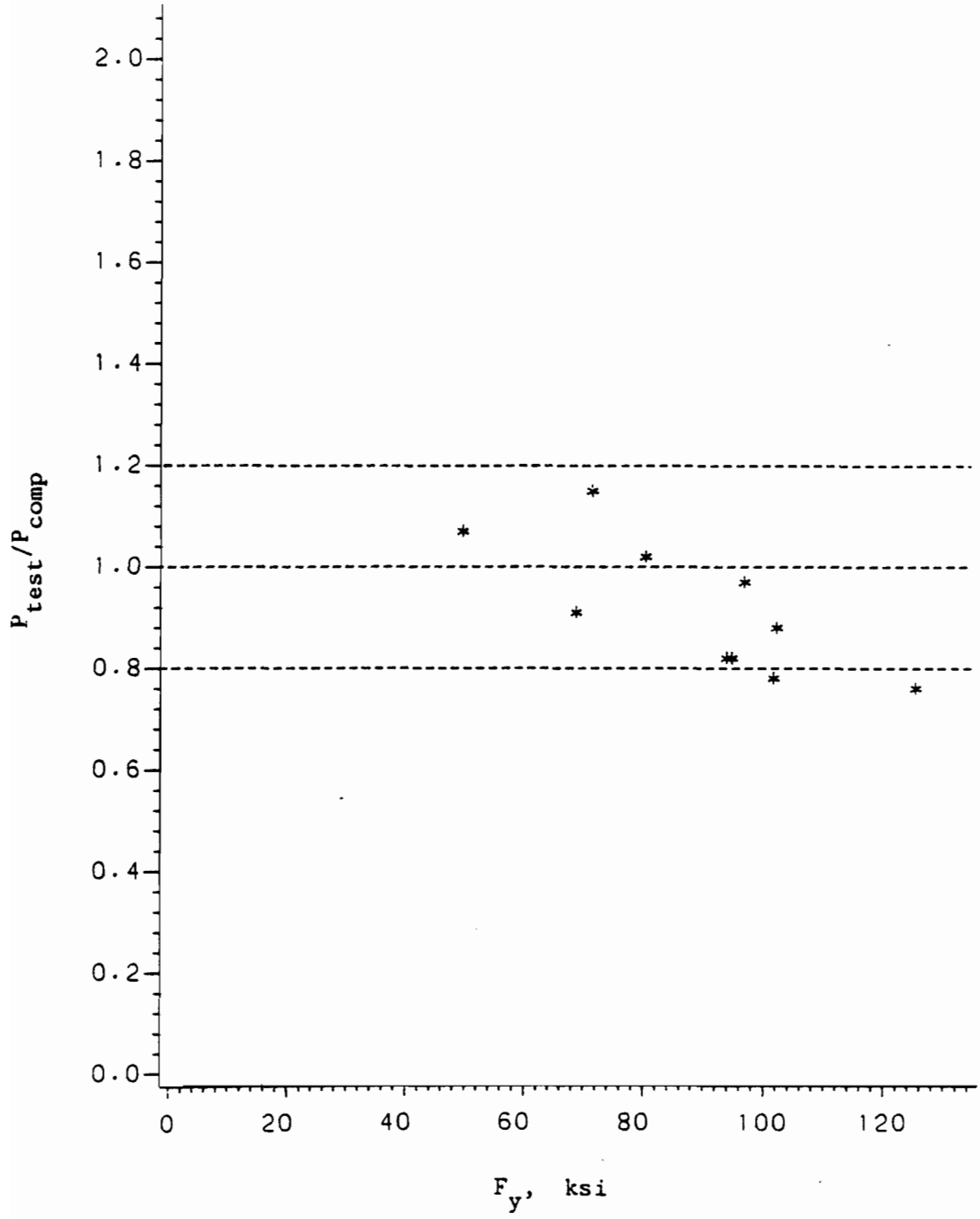

Fig. 6.16 Effect of F_y on the Ratio P_{test}/P_{comp} for Ford Tests Based on the Proposed Design Recommendations

middle portion of the web may experience appreciable extension. Therefore, F_{yw} may not represent the average yield strength of the entire web. In some cases, the values of F_{yw} are as high as 110% over the yield strengths of the as received steels.

For Specimen Nos. 10 to 13, bending moment alone is the governing mode of failure. Underestimations of the failure loads are observed. In the calculations of bending moment capacity, the as-formed yield strengths in the flanges (F_{yf}) were used as the limiting stress for the entire cross section which may not be practical. In some cases, the values of F_{yf} are even lower than the yield strengths of virgin steels. The inaccuracy in the calculations of ultimate bending moment capacity of these composite sections may be due to this reason. Furthermore, the provisions for inelastic reserve capacity included in the present AISI Specification, which may increase the predicted bending moment capacity of the sections, are not applicable to these specimens because the effect of cold-forming was considered in the calculations.

4. Discussions:

It can be seen that the proposed design recommendations can provide good estimates of failure loads for both sections with single unreinforced webs and I-beams subjected to web crippling and a combination of web crippling and bending moment. By using nondimensional parameters in the derivation and distinguishing between overstressing and buckling failure, the newly developed equations become more general. These equations are found to be applicable to sections with material yield strengths up to 190 ksi. The new design methods avoid the problem of discontinuity between the equation for each basic loading condition by using a simple interpolation.

VII. CONCLUSIONS

In recent years, various types of high strength sheet steels with yield strengths greater than 80 ksi have been successfully used by automotive engineers to reduce car weight for the purpose of achieving fuel economy and complying with federal safety standards. Because there is only a limited amount of information available for the structural design of automotive components using such high strength sheet steels, a research project has been conducted at the University of Missouri-Rolla under the sponsorship of the American Iron and Steel Institute (AISI) since 1982. The primary goals of the project were to establish the applicability of the existing design criteria[3] and to develop the necessary new criteria for a comprehensive design of high strength steel sections used in the automobile industry. This dissertation deals with the web crippling strength and a combination of web crippling and bending moment of beams which are formed from high strength sheet steels. This subject is one of the three phases of the overall project.

Following a literature review of the available publications and the current design criteria, an analytical investigation was conducted to study the web crippling strength of cold-formed steel beams. Because of the difficulties involved in the theoretical analysis of web crippling strength, an extensive experimental investigation was carried out for the purpose of obtaining background information for the formulation of design criteria. In this phase of research work, 150 hat sections and 96 I-beams were tested for four basic loading conditions (interior one-

flange loading, end one-flange loading, interior two-flange loading, and end two-flange loading). Additional 18 tests were also performed for the transition ranges between the basic loading conditions. Test specimens were fabricated from high strength sheet steels with yield strengths ranging from 58.2 to 165.1 ksi. Details of test specimens and test results are presented in Section III.

The results of tests have been evaluated in Section IV according to the AISI 1981 Guide for the preliminary design of automotive structural components and the 1986 Specification for the design of cold-formed steel structural members used for buildings with some modification of the F_y function. It was found that the available design provisions for web crippling are not suitable for those sections fabricated from very high strength materials. Also included in this evaluation were the experimental data obtained from the tests conducted by Inland Steel Company and Ford Motor Company.

In the analytical study discussed in Section V, a finite element program (ADINA) which is available at UMR has been used to predict the ultimate web crippling load of sections with single unreinforced webs. A 3-node triangular plate/shell element was used with both geometric and material nonlinearity. The analytical results reveal that predicted ultimate loads underestimate the actual web crippling strengths, even though a reasonable accuracy (within 23%) was realized for the cases of interior one-flange and end one-flange loadings.

New equations have been developed for determining the ultimate web crippling loads for cold-formed steel beams having single unreinforced webs and for I-beams under different loading conditions. These equations

are dealing with the web buckling failure and the overstressing failure. By using a simple interpolation between the predicted ultimate web crippling loads between four basic loading conditions, reasonable accuracy of prediction can be achieved for the transition ranges. Interaction equations for the combination of web crippling and bending moment were also derived in terms of stress ratios with an alternative of moment and load ratios. The comparisons between the tested failure loads and predicted failure loads indicate good agreements between the proposed design recommendations and the available test data with yield strengths from 30 to 190 ksi.

In order to generalize the design procedure for web crippling, future studies are needed in the following areas:

1) Failure caused by bending of flanges about connection lines of I-beams when the flanges are not connected to bearing plates.

2) Overstressing failure of single web sections under end one-flange loading and of I-beams under end one-flange and end two-flange loadings.

3) Web crippling failure under dynamic loading.

This report also includes the following information:

1) Plots showing the effect of important parameters (h/t, N/h, e/h, N/t, and R/t) on the accuracy of the predicted ultimate web crippling loads based on the proposed design methods. These plots are presented in Appendix E. The test data used for these plots are the same as those used in Section VI for the study of the effect of F_y on the ratio P_{test}/P_{comp}.

2) Computer programs used to predict the ultimate loads for Inland and Ford tests (Appendix F).

3) Comparisons of ultimate web crippling loads based on the AISI 1986 Specification and the proposed design methods. These comparisons are presented in Appendix G by including a computer program along with several examples.

BIBLIOGRAPHY

1. American Iron and Steel Institute, "The Material Decision," SG-834.
2. American Iron and Steel Institute, "Automotive Steels: They Still Do It Better," SG-937.
3. American Iron and Steel Institute, "Guide for Preliminary Design of Sheet Steel Automotive Structural Components," 1981 Edition.
4. American Iron and Steel Institute, "Specification for the Design of Cold-Formed Steel Structural Members," 1968 Edition.
5. American Iron and Steel Institute, "Specification for the Design of Cold-Formed Steel Structural Members," 1980 Edition.
6. American Iron and Steel Institute, "Specification for the Design of Cold-Formed Steel Structural Members," 1986 Edition.
7. American Iron and Steel Institute, "High Strength Sheet Steel Source Guide," SG-603D.
8. American Iron and Steel Institute, "Steel Meets the Automotive Engineering Challenges," Supplemental Booklet Presented at the 1983 SAE Exposition.
9. Errera, S. J., "Automotive Structural Design Using the AISI Guide," SAE Technical Paper Series 820021.
10. Levy, B. S., "Advances in Designing Ultra High Strength Steel Bumper Reinforcement Beams," SAE Technical Paper Series 830399.
11. Vecchio, M. T., "Design Analysis and Behavior of a Variety of As-Formed Mild and High Strength Sheet Materials in Large Deflection Bending," SAE Technical Paper Series 830398.

12. Levy, B. S., "Predicting Yield Strength and Tensile Strength After Forming for Automotive Integral Body Structural Rail Type Parts," SAE Technical Paper Series 840009.

13. Vecchio, M. T., "Forming Technology - A Design Parameter for the Eighties," Body Engineering Journal, Spring 1984.

14. Yu, W. W., Santaputra, C., and Parks, M. B., "Design of Automotive Structural Components Using High Strength Sheet Steels," First Progress Report, Civil Engineering Study 83-1, University of Missouri-Rolla, January 1983.

15. Santaputra, C., and Yu, W. W., "Design of Automotive Structural Components Using High Strength Sheet Steels," Third Progress Report, Civil Engineering Study 83-4, University of Missouri-Rolla, August 1983.

16. Santaputra, C., and Yu, W. W., "Design of Automotive Structural Components Using High Strength Sheet Steels," Fifth Progress Report, Civil Engineering Study 84-1, University of Missouri-Rolla, October 1984.

17. Santaputra, C., Parks, M. B., and Yu, W. W., "Web Crippling of Cold-Formed Steel Beams Using High Strength Sheet Steels," SAE Technical Paper Series 860823.

18. Timoshenko, S. P., and Gere, G. M., Theory of Elastic Stability. 2nd Edition, New York: McGraw-Hill Book Company, Inc., 1961.

19. Timoshenko, S. P., Zeitschrift fur Math. und Physik, Vol. 58, 1910.

20. Yamaki, N., "Buckling of a Rectangular Plate Under Locally Distributed Force Applied on the Two Opposite Edges," 1st and 2nd Report, the Institute of High Speed Mechanics, Tohoku University, Japan, Vol. 3, 1953.

21. Khan, M. Z., and Walker, A. C., "Buckling of Plates Subjected to Localized Edge Loading," The Structural Engineer, Vol. 50, No. 6, June 1972, pp. 225-232.

22. Walker, A. C., Design and Analysis of Cold-Formed Sections. New York: John Wiley & Sons, Inc., 1975.

23. Girkmann, K., "Stability of the Webs of Plate Girders Taking Account of Concentrated Loads," Final Report, International Association for Bridge and Structural Engineering, 1936.

24. Zetlin, L., "Elastic Instability of Flat Plates Subjected to Partial Edge Loads," Journal of the Structural Division, ASCE Proceedings, Vol. 81, September 1955.

25. White, R. N., and Cottingham, W. S., "Stability of Plates under Partial Edge Loading," Journal of Engineering Mechanics Division, ASCE Proceedings, Vol. 88, October 1962.

26. Khan, M. Z., Johns, K. C., and Hayman, B., "Buckling of Plates with Partially Loaded Edges," Journal of the Structural Division, ASCE Proceedings, Vol. 103, March 1977.

27. Alfutov, N. A., and Balabukn, L. I., "On the Possibility of Solving Plate Stability Problems without a Preliminary Determination of the Initial State of Stress," Journal of Applied Mathematics and Mechanics, Vol. 31, pp. 730-736.

28. Yu, W. W., Cold-Formed Steel Design. New York: John Wiley & Sons, Inc., 1985.

29. Bagchi, D. K., and Rockey, K. C., "A Note on the Buckling of a Plate Girder Web Due to Partial Edge Loadings," Final Report, International Association for Bridge and Structural Engineering, September 1968.

30. Rockey, K. C., and Bagchi, D. K., "Buckling of Plate Girder Webs under Partial Edge Loadings," International Journal of Mechanical Science, Vol. 12, Pergamon Press, 1970.

31. Rockey, K. C., El-gaaly, M. A., and Bagchi, D. K., "Failure of Thin Walled Members under Patch Loadings," Journal of the Structural Division, ASCE Proceedings, Vol. 98, December 1972.

32. El-gaaly, D. K., and Rockey, K. C., "Ultimate Strength of Thin Walled Members under Patch Loading and Bending: Current Research and Design Trends," Proceeding of the Second Specialty Conference on Cold-Formed Steel Structures, University of Missouri-Rolla, October 1973.

33. Graves Smith, T. R., and Sridharan, S., "A Finite Strip Method for The Buckling of Plate Structures under Arbitrary Loading," International Journal of Mechanical Science, Vol. 20, May 1978.

34. Gierlinski, J. T., and Graves Smith T. R., "The Geometric Nonlinear Analysis of Thin-Walled Structures by Finite Strips," Thin-Walled Structures, England: Elsevier Applied Science Publishers Ltd., 1984.

35. Lee, H. P., Harris, P. J., and Hsu, C. T., "A Nonlinear Finite Element Computer Program for Thin-Walled Members," Thin-Walled Structures, England: Elsevier Applied Science Publishers Ltd., 1984.

36. Lyse, I., and Godfrey, H. J., "Investigation of Web Buckling in Steel Beams," ASCE Transactions, Vol. 100, 1935.

37. Manual of Steel Construction, 8th Ed., Chicago: American Institute of Steel Construction, Inc., 1980.

38. Cornell University, 65th and 66th Progress Reports on Light Gage Steel Beams of Cold-Formed Steel, September 1952 and January 1953, respectively (unpublished).

39. Winter, G., and Pian, R. H. J., "Crushing Strength of Thin Steel Webs," Engineering Experiment Station, Bulletin No. 35, Cornell University, New York, April 1946.

40. Winter, G., "Commentary on the 1968 Edition of the Specification for the Design of Cold-Formed Steel Structural Members," American Iron and Steel Institute, 1970 ed.

41. Hetrakul, N., and Yu, W. W., "Strucural Behavior of Beam Webs Subjected to Web Crippling and a Combination of Web Crippling and Bending," Final Report, Civil Engineering Study 78-4, University of Missouri-Rolla, June 1978.

42. American Iron and Steel Institute, "Commentary on the 1980 Edition of the Specification for the Design of Cold-Formed Steel Structural Members," 1983 ed.

43. American Iron and Steel Institute, "Commentary on the 1986 Edition of the Specification for the Design of Cold-Formed Steel Structural Members," 1986 ed.

44. Lin, S. H., "Structural Behavior of Cold-Formed Steel Beam Webs Subjected to Partial Edge Loading," Master Thesis, Civil Engineering Department, University of Missouri-Rolla, December 1984.

45. Baehre, R., "Sheet Metal Panels for Use in Building Construction: Recent Research Projects in Sweden," Proceedings of the Third International Specialty Conference on Cold-Formed Steel Structures, University of Missouri-Rolla, 1975.

46. StBK-N5., "Code for the Structural Use of Steel and Aluminum Sheeting," National Swedish Committee on Regulations for Steel Structures, Stockholm, 1978.

47. ECCS-TC7. "European Recommendations for the Design of Light Gauge Steel Members," 1983.

48. Wing, Bradley A. and Schuster, R. M., "Web Crippling and the Interaction of Bending and Web Crippling of Unreinforced Multi-Web Cold Formed Steel Sections," Volumes 1 and 2, University of Waterloo, 1981.

49. Canadian Standard Association, "CSA Standard CAN3-S136-M84, Cold-Formed Steel Structural Members," Rexdale, Ontario, Canada, December 1984.

50. ECCS-TC7. "European Recommendations for the Design of Profiled Sheeting," 1983.

51. Standards Association of Australia, "SAA Cold-Formed Steel Structures Code," AS 1538-1974 (with Amendment No. 1), 1977.

52. Indian Standards Institution, "Indian Standard Code of Practice for Use of Cold-Formed Light Gauge Steel Structural Members in General Building Construction," IS 801-1975 (First Revision), 1977.

53. South African Institute of Steel Construction, " Code of Practice for the Design of Structural Steelwork," 1983.

54. British Standards Institution, "Specification for the Use of Cold-Formed Steel Sections in Building," Addendum No.1, BS 449, Part 2, April 1975.

55. American Iron and Steel Institute, "High Strength Sheet Steel Source Guide," SG-603D.

56. Parks, M. B., "Mechanical Properties of High Strength Sheet Steels," Master Thesis, Civil Engineering Department, University of Missouri-Rolla, 1983.

57. Parks, M. B., and Yu, W. W., "Design of Automotive Structural Components Using High Strength Sheet Steels," Second Progress Report, Civil Engineering Study 83-3, University of Missouri-Rolla, August 1983.

58. "ADINA System Theory and Modeling Guide," Report AE83-4, Watertown, Ma.: Adina Engineering, Inc., September 1983.

59. "ADINA Users Manual," Report AE81-1, Watertown, Ma.: Adina Engineering, Inc., September 1981.

60. Bathe, K. J., Finite Element Procedures in Engineering Analysis. Englewood Cliffs, New Jersey: Prentice-Hall, Inc., 1982.

61. Bathe, K. J., and Wilson, E. L., Numerical Methods in Finite Element Analysis. Englewood Cliffs, New Jersey: Prentice-Hall, Inc., 1976.

62. Lee, H. P., and Harris, P. J., "Post-Buckling Strength of Thin-Walled Members," Computers and Structures, Vol. 10, pp. 689-702, 1979.

63. Tang, S. C., "Computer Model of Bumper Impact Resistance," SAE Technical Paper Series 790991.

64. Tang, S. C., and Beardmore, P., "Computer Study of Material and Prestrain Effects on Bumper Damagibility," SAE Technical Paper Series 811311.

65. Bathe, K. J., and Ho, L. W., "A Simple and Effective Element for Analysis of Shell Structures," Computers and Structures, Vol. 13, pp. 673-681, 1981.

66. Bathe, K. J., Dvorkin, E., and Ho, L. W., "Our Discrete-Kirchhoff and Isoparametric Shell Elements for Nonlinear Analysis - An Assessment," Computers and Structures, Vol. 16, pp. 89-98, 1983.

67. Aluminum Association, "Specification for Aluminum Structures," 3rd. Ed., April 1976.

68. Sas Users Guide, 1985 Ed., Cary, North Carolina: Sas Institute Inc., 1985.

69. Draper, N. R., and Smith, H., Applied Regression Analysis, New York: John Wiley & Sons, Inc., 1980.

70. Peery, D. J., Aircraft Structures, New York: McGraw-Hill Book Company, Inc., 1950.

APPENDIX A.

DIMENSIONS AND IMPORTANT PARAMETERS OF HAT SECTIONS AND I-BEAMS USED IN THE EXPERIMENTAL INVESTIGATION

Table A1

Dimensions of Hat Sections Used in the Experimental Investigation

Specimen No.	t (in.)	B1 (in.)	B2 (in.)	D (in.)	R (in.)	L (in.)
1-HIOF-A11	0.048	3.180	6.384	3.150	0.234	19.0
1-HIOF-A12	0.048	3.250	6.374	3.140	0.234	19.0
1-HIOF-A21	0.048	4.330	8.494	4.080	0.250	22.0
1-HIOF-A22	0.048	4.330	8.454	4.070	0.273	22.0
1-HIOF-A31	0.048	5.380	10.564	4.990	0.242	25.0
1-HIOF-A32	0.048	5.400	10.544	5.000	0.250	25.0
2-HIOF-A11	0.082	3.540	6.596	3.040	0.203	19.0
2-HIOF-A12	0.082	3.560	6.576	3.070	0.227	19.0
2-HIOF-A21	0.082	4.590	8.706	4.050	0.227	22.0
2-HIOF-A22	0.082	4.550	8.666	4.060	0.227	22.0
2-HIOF-A31	0.082	5.470	10.586	5.060	0.219	25.0
2-HIOF-A32	0.082	5.490	10.626	5.070	0.219	25.0
3-HIOF-A11	0.062	3.480	6.556	3.080	0.195	19.0
3-HIOF-A12	0.062	3.490	6.506	3.090	0.164	19.0
3-HIOF-A21	0.062	4.410	8.506	4.040	0.164	22.0
3-HIOF-A22	0.062	4.370	8.526	4.050	0.156	22.0
3-HIOF-A31	0.062	5.360	10.496	5.040	0.133	25.0
3-HIOF-A32	0.062	5.340	10.496	5.010	0.172	25.0
4-HIOF-A11	0.047	3.250	6.296	3.110	0.086	19.0
4-HIOF-A12	0.047	3.210	6.216	3.130	0.070	19.0
4-HIOF-A21	0.047	4.100	8.186	4.160	0.133	22.0
4-HIOF-A22	0.047	4.090	8.196	4.190	0.125	22.0
4-HIOF-A31	0.047	4.950	10.096	5.160	0.094	25.0
4-HIOF-A32	0.047	5.010	10.116	5.160	0.102	25.0
4-HIOF-A13	0.047	2.960	5.846	2.960	0.250	19.0
4-HIOF-A14	0.047	2.980	5.886	2.960	0.250	19.0
4-HIOF-A23	0.047	3.950	7.836	3.960	0.250	21.0
4-HIOF-A24	0.047	3.960	7.866	3.970	0.250	21.0
4-HIOF-A33	0.047	4.940	9.746	4.930	0.250	25.0
4-HIOF-A34	0.047	4.920	9.726	4.930	0.250	25.0
5-HIOF-A11	0.046	3.020	5.908	3.000	0.250	19.0
5-HIOF-A12	0.046	3.030	5.938	2.990	0.250	19.0
5-HIOF-A21	0.046	4.000	7.888	4.020	0.250	22.0
5-HIOF-A22	0.046	4.030	7.938	4.000	0.250	22.0
5-HIOF-A31	0.046	5.040	9.928	4.990	0.250	25.0
5-HIOF-A32	0.046	5.000	9.848	5.020	0.250	25.0
3-HIOF-D11	0.065	3.010	5.900	3.000	0.250	15.0
3-HIOF-D12	0.065	3.020	5.910	3.010	0.250	15.0
3-HIOF-C11	0.065	3.010	5.920	3.020	0.250	15.0
3-HIOF-C12	0.065	3.020	5.930	3.000	0.250	15.0

Table A1 (Cont'd)

Dimensions of Hat Sections Used in the Experimental Investigation

Specimen No.	t (in.)	B1 (in.)	B2 (in.)	D (in.)	R (in.)	L (in.)
3-HIOF-B11	0.065	2.990	5.900	3.000	0.250	15.0
3-HIOF-B12	0.065	2.990	5.900	3.000	0.250	15.0
3-HIOF-D21	0.065	4.000	7.910	4.000	0.250	19.0
3-HIOF-D22	0.065	4.030	7.960	3.970	0.250	19.0
3-HIOF-C21	0.065	3.990	7.920	3.990	0.250	19.0
3-HIOF-C22	0.065	3.980	7.890	4.000	0.250	19.0
3-HIOF-B21	0.065	4.040	7.930	3.970	0.250	19.0
3-HIOF-B22	0.065	3.990	7.900	4.000	0.250	19.0
3-HIOF-D31	0.065	5.020	9.930	5.000	0.250	24.0
3-HIOF-D32	0.065	5.000	9.910	5.000	0.250	24.0
3-HIOF-C31	0.065	5.000	9.930	5.000	0.250	24.0
3-HIOF-C32	0.065	5.000	9.930	5.000	0.250	24.0
3-HIOF-B31	0.065	4.990	9.900	5.000	0.250	24.0
3-HIOF-B32	0.065	5.020	9.910	4.990	0.250	24.0
5-HIOF-D11	0.046	2.980	5.948	3.050	0.250	15.0
5-HIOF-D12	0.046	3.000	5.968	3.000	0.250	15.0
5-HIOF-C11	0.046	2.980	5.988	3.000	0.250	15.0
5-HIOF-C12	0.046	2.990	5.938	3.000	0.250	15.0
5-HIOF-B11	0.046	3.000	5.948	3.070	0.250	15.0
5-HIOF-B12	0.046	3.030	5.978	3.020	0.250	15.0
5-HIOF-D21	0.046	4.050	7.978	4.020	0.250	19.0
5-HIOF-D22	0.046	3.990	7.918	4.070	0.250	19.0
5-HIOF-C21	0.046	3.990	7.938	4.000	0.250	19.0
5-HIOF-C22	0.046	3.980	7.928	4.030	0.250	19.0
5-HIOF-B21	0.046	4.030	7.998	3.990	0.250	19.0
5-HIOF-B22	0.046	3.960	7.928	4.030	0.250	19.0
5-HIOF-D31	0.046	5.000	9.948	5.030	0.250	25.0
5-HIOF-D32	0.046	5.050	9.998	5.000	0.250	25.0
5-HIOF-C31	0.046	5.000	9.948	5.020	0.250	25.0
5-HIOF-C32	0.046	4.930	9.898	5.000	0.250	25.0
5-HIOF-B31	0.046	5.030	9.958	5.010	0.250	25.0
5-HIOF-B32	0.046	5.000	9.988	5.030	0.250	25.0
1-HEOF-A11	0.048	3.030	5.874	3.070	0.227	17.0
1-HEOF-A12	0.048	3.010	5.874	3.070	0.219	17.0
1-HEOF-A21	0.048	4.050	7.914	3.930	0.211	20.0
1-HEOF-A22	0.048	4.020	7.944	3.950	0.227	20.0
1-HEOF-A31	0.048	5.070	9.994	4.920	0.203	23.0
1-HEOF-A32	0.048	5.030	9.914	4.910	0.219	23.0
2-HEOF-A11	0.085	3.060	5.930	2.880	0.234	17.0
2-HEOF-A12	0.085	3.070	5.900	2.890	0.219	17.0

Table A1 (Cont'd)

Dimensions of Hat Sections Used in the Experimental Investigation

Specimen No.	t (in.)	B1 (in.)	B2 (in.)	D (in.)	R (in.)	L (in.)
2-HEOF-A21	0.085	4.090	7.960	3.870	0.227	20.0
2-HEOF-A22	0.085	4.120	7.950	3.870	0.211	20.0
2-HEOF-A31	0.085	5.050	9.980	4.910	0.227	23.0
2-HEOF-A32	0.085	5.080	9.990	4.890	0.219	23.0
3-HEOF-A11	0.065	3.050	5.920	2.900	0.203	17.0
3-HEOF-A12	0.065	3.020	5.930	2.910	0.180	17.0
3-HEOF-A21	0.065	4.080	7.990	3.910	0.188	20.0
3-HEOF-A22	0.065	4.110	7.960	3.890	0.188	20.0
3-HEOF-A31	0.065	5.000	9.930	4.920	0.195	23.0
3-HEOF-A32	0.065	5.040	9.910	4.920	0.211	23.0
4-HEOF-A11	0.047	2.970	5.896	3.110	0.117	17.0
4-HEOF-A12	0.047	3.010	5.876	2.990	0.156	17.0
4-HEOF-A21	0.047	3.980	7.986	4.010	0.164	20.0
4-HEOF-A22	0.047	4.020	7.986	3.990	0.180	20.0
4-HEOF-A31	0.047	4.960	9.826	5.060	0.148	23.0
4-HEOF-A32	0.047	4.990	9.896	5.050	0.117	23.0
5-HEOF-A11	0.046	2.990	5.898	3.030	0.250	17.0
5-HEOF-A12	0.046	2.990	5.938	3.010	0.250	17.0
5-HEOF-A21	0.046	3.980	7.928	4.050	0.250	20.0
5-HEOF-A22	0.046	4.000	7.888	4.020	0.250	20.0
5-HEOF-A31	0.046	4.970	9.958	5.070	0.250	23.0
5-HEOF-A32	0.046	4.980	9.988	5.030	0.250	23.0
1-HITF-A11	0.047	2.980	5.906	3.000	0.250	11.0
1-HITF-A12	0.047	3.000	5.886	3.000	0.250	11.0
1-HITF-A21	0.047	4.010	7.916	4.000	0.250	14.0
1-HITF-A22	0.047	3.970	7.896	4.010	0.250	14.0
1-HITF-A31	0.047	4.950	9.836	5.060	0.250	17.0
1-HITF-A32	0.047	4.970	9.776	5.050	0.250	17.0
2-HITF-A11	0.088	3.020	5.884	3.000	0.250	11.0
2-HITF-A12	0.088	3.030	5.854	3.000	0.250	11.0
2-HITF-A21	0.088	4.000	7.784	4.010	0.250	14.0
2-HITF-A22	0.088	3.970	7.794	4.030	0.250	14.0
2-HITF-A31	0.088	4.950	9.734	5.060	0.250	17.0
2-HITF-A32	0.088	4.980	9.744	5.050	0.250	17.0
3-HITF-A11	0.065	2.970	5.780	3.050	0.250	11.0
3-HITF-A12	0.065	3.010	5.880	3.020	0.250	11.0
3-HITF-A21	0.065	4.010	7.820	4.000	0.250	14.0
3-HITF-A22	0.065	4.030	7.900	4.000	0.250	14.0
3-HITF-A31	0.065	4.980	9.870	5.030	0.250	17.0
3-HITF-A32	0.065	4.960	9.810	5.030	0.250	17.0

Table A1 (Cont'd)

Dimensions of Hat Sections Used in the Experimental Investigation

Specimen No.	t (in.)	B1 (in.)	B2 (in.)	D (in.)	R (in.)	L (in.)
5-HITF-A11	0.046	2.940	5.828	3.050	0.250	11.0
5-HITF-A12	0.046	2.920	5.868	3.050	0.250	11.0
5-HITF-A21	0.046	4.030	7.898	3.980	0.250	14.0
5-HITF-A22	0.046	4.000	7.928	4.000	0.250	14.0
5-HITF-A31	0.046	4.920	9.808	5.070	0.250	17.0
5-HITF-A32	0.046	4.890	9.798	5.090	0.250	17.0
1-HETF-A11	0.047	2.970	5.836	3.030	0.250	6.5
1-HETF-A12	0.047	2.950	5.856	3.050	0.250	6.5
1-HETF-A21	0.047	3.960	7.826	4.030	0.250	8.0
1-HETF-A22	0.047	3.940	7.866	4.050	0.250	8.0
1-HETF-A31	0.047	4.980	9.926	5.030	0.250	9.5
1-HETF-A32	0.047	5.000	14.846	5.030	0.250	9.5
2-HETF-A11	0.088	3.030	5.854	3.000	0.250	6.5
2-HETF-A12	0.088	3.030	5.794	3.000	0.250	6.5
2-HETF-A21	0.088	4.020	7.864	4.000	0.250	8.0
2-HETF-A22	0.088	4.000	7.924	4.000	0.250	8.0
2-HETF-A31	0.088	4.970	9.794	5.030	0.250	9.5
2-HETF-A32	0.088	5.000	9.824	5.020	0.250	9.5
3-HETF-A11	0.065	2.960	5.890	3.020	0.250	6.5
3-HETF-A12	0.065	2.950	5.820	3.030	0.250	6.5
3-HETF-A21	0.065	3.920	7.830	4.030	0.250	8.0
3-HETF-A22	0.065	3.950	7.780	4.020	0.250	8.0
3-HETF-A31	0.065	3.950	7.840	5.080	0.250	9.5
3-HETF-A32	0.065	4.000	7.790	5.060	0.250	9.5
5-HETF-A11	0.046	2.970	5.878	3.030	0.250	6.5
5-HETF-A12	0.046	3.010	5.838	3.020	0.250	6.5
5-HETF-A21	0.046	3.980	7.948	4.050	0.250	8.0
5-HETF-A22	0.046	4.000	7.868	4.050	0.250	8.0
5-HETF-A31	0.046	5.010	9.978	5.010	0.250	9.5
5-HETF-A32	0.046	5.040	9.908	5.000	0.250	9.5

Note: See Fig. 3.3 for definitions of symbols.

Table A2

Parameters and Sectional Properties of Hat Sections

Specimen No.	Material	t (in.)	F_y (ksi)	h/t	N/h	e/h	N/t	R/t
1-HIOF-A11	80DK	0.048	58.2	63.6	0.655	1.473	41.7	4.883
1-HIOF-A12	80DK	0.048	58.2	63.4	0.657	1.478	41.7	4.883
1-HIOF-A21	80DK	0.048	58.2	83.0	0.502	1.506	41.7	5.208
1-HIOF-A22	80DK	0.048	58.2	82.8	0.503	1.510	41.7	5.696
1-HIOF-A31	80DK	0.048	58.2	102.0	0.409	1.532	41.7	5.046
1-HIOF-A32	80DK	0.048	58.2	102.2	0.408	1.529	41.7	5.208
2-HIOF-A11	80XF	0.082	88.3	35.1	0.695	1.565	24.4	2.477
2-HIOF-A12	80XF	0.082	88.3	35.4	0.688	1.549	24.4	2.763
2-HIOF-A21	80XF	0.082	88.3	47.4	0.515	1.544	24.4	2.763
2-HIOF-A22	80XF	0.082	88.3	47.5	0.513	1.540	24.4	2.763
2-HIOF-A31	80XF	0.082	88.3	59.7	0.408	1.532	24.4	2.668
2-HIOF-A32	80XF	0.082	88.3	59.8	0.408	1.529	24.4	2.668
3-HIOF-A11	100XF	0.062	113.1	47.7	0.677	1.522	32.3	3.150
3-HIOF-A12	100XF	0.062	113.1	47.8	0.674	1.517	32.3	2.647
3-HIOF-A21	100XF	0.062	113.1	63.2	0.511	1.532	32.3	2.647
3-HIOF-A22	100XF	0.062	113.1	63.3	0.509	1.528	32.3	2.521
3-HIOF-A31	100XF	0.062	113.1	79.3	0.407	1.526	32.3	2.142
3-HIOF-A32	100XF	0.062	113.1	78.8	0.409	1.535	32.3	2.773
4-HIOF-A11	140XF	0.047	141.2	64.2	0.663	1.492	42.6	1.828
4-HIOF-A12	140XF	0.047	141.2	64.6	0.659	1.482	42.6	1.496
4-HIOF-A21	140XF	0.047	141.2	86.5	0.492	1.476	42.6	2.826
4-HIOF-A22	140XF	0.047	141.2	87.1	0.488	1.465	42.6	2.660
4-HIOF-A31	140XF	0.047	141.2	107.8	0.395	1.480	42.6	1.996
4-HIOF-A32	140XF	0.047	141.2	107.8	0.395	1.480	42.6	2.162
4-HIOF-A13	140XF	0.047	141.2	61.0	0.698	1.570	42.6	5.319
4-HIOF-A14	140XF	0.047	141.2	61.0	0.698	1.570	42.6	5.319
4-HIOF-A23	140XF	0.047	141.2	82.3	0.517	1.423	42.6	5.319
4-HIOF-A24	140XF	0.047	141.2	82.5	0.516	1.419	42.6	5.319
4-HIOF-A33	140XF	0.047	141.2	102.9	0.414	1.551	42.6	5.319
4-HIOF-A34	140XF	0.047	141.2	102.9	0.414	1.551	42.6	5.319
5-HIOF-A11	140SK	0.046	165.1	63.2	0.688	1.547	43.5	5.435
5-HIOF-A12	140SK	0.046	165.1	63.0	0.690	1.553	43.5	5.435
5-HIOF-A21	140SK	0.046	165.1	85.4	0.509	1.527	43.5	5.435
5-HIOF-A22	140SK	0.046	165.1	85.0	0.512	1.535	43.5	5.435
5-HIOF-A31	140SK	0.046	165.1	106.5	0.408	1.531	43.5	5.435
5-HIOF-A32	140SK	0.046	165.1	107.1	0.406	1.522	43.5	5.435
3-HIOF-D11	100XF	0.065	116.9	44.2	0.697	0.750	30.8	3.846
3-HIOF-D11	100XF	0.065	116.9	44.3	0.694	0.750	30.8	3.846
3-HIOF-C11	100XF	0.065	116.9	44.5	0.692	1.000	30.8	3.846
3-HIOF-C11	100XF	0.065	116.9	44.2	0.697	1.000	30.8	3.846

Table A2 (Cont'd)

Parameters and Sectional Properties of Hat Sections

Specimen No.	Material	t (in.)	F_y (ksi)	h/t	N/h	e/h	N/t	R/t
3-HIOF-B11	100XF	0.065	116.9	44.2	0.697	1.250	30.8	3.846
3-HIOF-B11	100XF	0.065	116.9	44.2	0.697	1.250	30.8	3.846
3-HIOF-D11	100XF	0.065	116.9	59.5	0.517	0.750	30.8	3.846
3-HIOF-D11	100XF	0.065	116.9	59.1	0.521	0.750	30.8	3.846
3-HIOF-C11	100XF	0.065	116.9	59.4	0.518	1.000	30.8	3.846
3-HIOF-C11	100XF	0.065	116.9	59.5	0.517	1.000	30.8	3.846
3-HIOF-B11	100XF	0.065	116.9	59.1	0.521	1.250	30.8	3.846
3-HIOF-B11	100XF	0.065	116.9	59.5	0.517	1.250	30.8	3.846
3-HIOF-D11	100XF	0.065	116.9	74.9	0.411	0.750	30.8	3.846
3-HIOF-D11	100XF	0.065	116.9	74.9	0.411	0.750	30.8	3.846
3-HIOF-C11	100XF	0.065	116.9	74.9	0.411	1.000	30.8	3.846
3-HIOF-C11	100XF	0.065	116.9	74.9	0.411	1.000	30.8	3.846
3-HIOF-B11	100XF	0.065	116.9	74.9	0.411	1.250	30.8	3.846
3-HIOF-B11	100XF	0.065	116.9	74.8	0.412	1.250	30.8	3.846
5-HIOF-D11	140SK	0.046	165.1	64.3	0.676	0.750	43.5	5.435
5-HIOF-D11	140SK	0.046	165.1	63.2	0.688	0.750	43.5	5.435
5-HIOF-C11	140SK	0.046	165.1	63.2	0.688	1.000	43.5	5.435
5-HIOF-C11	140SK	0.046	165.1	63.2	0.688	1.000	43.5	5.435
5-HIOF-B11	140SK	0.046	165.1	64.7	0.672	1.250	43.5	5.435
5-HIOF-B11	140SK	0.046	165.1	63.7	0.683	1.250	43.5	5.435
5-HIOF-D11	140SK	0.046	165.1	85.4	0.509	0.750	43.5	5.435
5-HIOF-D11	140SK	0.046	165.1	86.5	0.503	0.750	43.5	5.435
5-HIOF-C11	140SK	0.046	165.1	85.0	0.512	1.000	43.5	5.435
5-HIOF-C11	140SK	0.046	165.1	85.6	0.508	1.000	43.5	5.435
5-HIOF-B11	140SK	0.046	165.1	84.7	0.513	1.250	43.5	5.435
5-HIOF-B11	140SK	0.046	165.1	85.6	0.508	1.250	43.5	5.435
5-HIOF-D11	140SK	0.046	165.1	107.3	0.405	0.750	43.5	5.435
5-HIOF-D11	140SK	0.046	165.1	106.7	0.407	0.750	43.5	5.435
5-HIOF-C11	140SK	0.046	165.1	107.1	0.406	1.000	43.5	5.435
5-HIOF-C11	140SK	0.046	165.1	106.7	0.407	1.000	43.5	5.435
5-HIOF-B11	140SK	0.046	165.1	106.9	0.407	1.250	43.5	5.435
5-HIOF-B11	140SK	0.046	165.1	107.3	0.405	1.250	43.5	5.435
1-HEOF-A11	80DK	0.048	58.2	62.0	0.672	1.513	41.7	4.721
1-HEOF-A12	80DK	0.048	58.2	62.0	0.672	1.513	41.7	4.558
1-HEOF-A21	80DK	0.048	58.2	79.9	0.522	1.565	41.7	4.394
1-HEOF-A22	80DK	0.048	58.2	80.3	0.519	1.557	41.7	4.721
1-HEOF-A31	80DK	0.048	58.2	100.5	0.415	1.555	41.7	4.231
1-HEOF-A32	80DK	0.048	58.2	100.3	0.415	1.558	41.7	4.558
2-HEOF-A11	80XF	0.085	88.3	31.9	0.738	1.661	23.5	2.758
2-HEOF-A12	80XF	0.085	88.3	32.0	0.735	1.654	23.5	2.574

Table A2 (Cont'd)

Parameters and Sectional Properties of Hat Sections

Specimen No.	Material	t (in.)	F_y (ksi)	h/t	N/h	e/h	N/t	R/t
2-HEOF-A21	80XF	0.085	88.3	43.5	0.541	1.622	23.5	2.666
2-HEOF-A22	80XF	0.085	88.3	43.5	0.541	1.622	23.5	2.481
2-HEOF-A31	80XF	0.085	88.3	55.8	0.422	1.582	23.5	2.666
2-HEOF-A32	80XF	0.085	88.3	55.5	0.424	1.589	23.5	2.574
3-HEOF-A11	100XF	0.065	113.1	42.6	0.722	1.625	30.8	3.125
3-HEOF-A12	100XF	0.065	113.1	42.8	0.719	1.619	30.8	2.765
3-HEOF-A21	100XF	0.065	113.1	58.2	0.529	1.587	30.8	2.885
3-HEOF-A22	100XF	0.065	113.1	57.8	0.532	1.596	30.8	2.885
3-HEOF-A31	100XF	0.065	113.1	73.7	0.418	1.566	30.8	3.005
3-HEOF-A32	100XF	0.065	113.1	73.7	0.418	1.566	30.8	3.245
4-HEOF-A11	140XF	0.047	141.2	64.2	0.663	1.492	42.6	2.494
4-HEOF-A12	140XF	0.047	141.2	61.6	0.691	1.554	42.6	3.326
4-HEOF-A21	140XF	0.047	141.2	83.3	0.511	1.532	42.6	3.491
4-HEOF-A22	140XF	0.047	141.2	82.9	0.513	1.540	42.6	3.823
4-HEOF-A31	140XF	0.047	141.2	105.7	0.403	1.510	42.6	3.157
4-HEOF-A32	140XF	0.047	141.2	105.4	0.404	1.513	42.6	2.494
5-HEOF-A11	140SK	0.046	165.1	63.9	0.681	1.532	43.5	5.435
5-HEOF-A12	140SK	0.046	165.1	63.4	0.685	1.542	43.5	5.435
5-HEOF-A21	140SK	0.046	165.1	86.0	0.505	1.516	43.5	5.435
5-HEOF-A22	140SK	0.046	165.1	85.4	0.509	1.527	43.5	5.435
5-HEOF-A31	140SK	0.046	165.1	108.2	0.402	1.507	43.5	5.435
5-HEOF-A32	140SK	0.046	165.1	107.3	0.405	1.519	43.5	5.435
1-HITF-A11	80DK	0.047	58.2	61.8	0.688	1.549	42.6	5.319
1-HITF-A12	80DK	0.047	58.2	61.8	0.688	1.549	42.6	5.319
1-HITF-A21	80DK	0.047	58.2	83.1	0.512	1.536	42.6	5.319
1-HITF-A22	80DK	0.047	58.2	83.3	0.511	1.532	42.6	5.319
1-HITF-A31	80DK	0.047	58.2	105.7	0.403	1.510	42.6	5.319
1-HITF-A32	80DK	0.047	58.2	105.4	0.404	1.513	42.6	5.319
2-HITF-A11	80XF	0.088	77.1	32.1	0.708	1.593	22.7	2.841
2-HITF-A12	80XF	0.088	77.1	32.1	0.708	1.593	22.7	2.841
2-HITF-A21	80XF	0.088	77.1	43.6	0.522	1.565	22.7	2.841
2-HITF-A22	80XF	0.088	77.1	43.8	0.519	1.557	22.7	2.841
2-HITF-A31	80XF	0.088	77.1	55.5	0.410	1.536	22.7	2.841
2-HITF-A32	80XF	0.088	77.1	55.4	0.410	1.539	22.7	2.841
3-HITF-A11	100XF	0.065	116.9	44.9	0.685	1.541	30.8	3.846
3-HITF-A12	100XF	0.065	116.9	44.5	0.692	1.557	30.8	3.846
3-HITF-A21	100XF	0.065	116.9	59.5	0.517	1.550	30.8	3.846
3-HITF-A22	100XF	0.065	116.9	59.5	0.517	1.550	30.8	3.846
3-HITF-A31	100XF	0.065	116.9	75.4	0.408	1.531	30.8	3.846
3-HITF-A32	100XF	0.065	116.9	75.4	0.408	1.531	30.8	3.846

Table A2 (Cont'd)

Parameters and Sectional Properties of Hat Sections

Specimen No.	Material	t (in.)	F_y (ksi)	h/t	N/h	e/h	N/t	R/t
5-HITF-A11	140SK	0.046	165.1	64.3	0.676	1.521	43.5	5.435
5-HITF-A12	140SK	0.046	165.1	64.3	0.676	1.521	43.5	5.435
5-HITF-A21	140SK	0.046	165.1	84.5	0.514	1.543	43.5	5.435
5-HITF-A22	140SK	0.046	165.1	85.0	0.512	1.535	43.5	5.435
5-HITF-A31	140SK	0.046	165.1	108.2	0.402	1.507	43.5	5.435
5-HITF-A32	140SK	0.046	165.1	108.7	0.400	1.501	43.5	5.435
1-HETF-A11	80DK	0.047	58.2	62.5	0.681	1.533	42.6	5.319
1-HETF-A12	80DK	0.047	58.2	62.9	0.677	1.522	42.6	5.319
1-HETF-A21	80DK	0.047	58.2	83.7	0.508	1.524	42.6	5.319
1-HETF-A22	80DK	0.047	58.2	84.2	0.506	1.517	42.6	5.319
1-HETF-A31	80DK	0.047	58.2	105.0	0.405	1.519	42.6	5.319
1-HETF-A32	80DK	0.047	58.2	105.0	0.405	1.519	42.6	5.319
2-HETF-A11	80XF	0.088	77.1	32.1	0.708	1.593	22.7	2.841
2-HETF-A12	80XF	0.088	77.1	32.1	0.708	1.593	22.7	2.841
2-HETF-A21	80XF	0.088	77.1	43.5	0.523	1.569	22.7	2.841
2-HETF-A22	80XF	0.088	77.1	43.5	0.523	1.569	22.7	2.841
2-HETF-A31	80XF	0.088	77.1	55.2	0.412	1.545	22.7	2.841
2-HETF-A32	80XF	0.088	77.1	55.0	0.413	1.548	22.7	2.841
3-HETF-A11	100XF	0.065	116.9	44.5	0.692	1.557	30.8	3.846
3-HETF-A12	100XF	0.065	116.9	44.6	0.690	1.552	30.8	3.846
3-HETF-A21	100XF	0.065	116.9	60.0	0.513	1.538	30.8	3.846
3-HETF-A22	100XF	0.065	116.9	59.8	0.514	1.542	30.8	3.846
3-HETF-A31	100XF	0.065	116.9	76.2	0.404	1.515	30.8	3.846
3-HETF-A32	100XF	0.065	116.9	75.8	0.406	1.521	30.8	3.846
5-HETF-A11	140SK	0.046	165.1	63.9	0.681	1.532	43.5	5.435
5-HETF-A12	140SK	0.046	165.1	63.7	0.683	1.537	43.5	5.435
5-HETF-A21	140SK	0.046	165.1	86.0	0.505	1.516	43.5	5.435
5-HETF-A22	140SK	0.046	165.1	86.0	0.505	1.516	43.5	5.435
5-HETF-A31	140SK	0.046	165.1	106.9	0.407	1.525	43.5	5.435
5-HETF-A32	140SK	0.046	165.1	106.7	0.407	1.528	43.5	5.435

Table A3

Dimensions of I-Beams Used in the Experimental Investigation

Specimen No.	t (in.)	B1 (in.)	D (in.)	R (in.)	L (in.)
1-IIOF-A11	0.046	3.240	3.032	0.219	19.0
1-IIOF-A12	0.046	3.221	3.082	0.219	19.0
1-IIOF-A21	0.046	4.314	4.032	0.219	22.0
1-IIOF-A22	0.046	4.248	4.052	0.219	22.0
1-IIOF-A31	0.046	5.266	5.062	0.219	25.0
1-IIOF-A32	0.046	5.252	5.082	0.219	25.0
2-IIOF-A11	0.082	3.297	3.194	0.219	19.0
2-IIOF-A12	0.082	3.298	3.144	0.219	19.0
2-IIOF-A21	0.082	4.285	4.164	0.219	22.0
2-IIOF-A22	0.082	4.290	4.144	0.219	22.0
2-IIOF-A31	0.082	5.327	5.134	0.219	25.0
2-IIOF-A32	0.082	5.296	5.084	0.219	25.0
3-IIOF-A11	0.066	3.320	3.092	0.188	19.0
3-IIOF-A12	0.066	3.240	3.122	0.188	19.0
3-IIOF-A21	0.066	4.258	4.102	0.188	22.0
3-IIOF-A22	0.066	4.261	4.102	0.188	22.0
3-IIOF-A31	0.066	5.279	5.102	0.188	25.0
3-IIOF-A32	0.066	5.266	5.112	0.188	25.0
5-IIOF-A11	0.046	3.040	3.062	0.250	19.0
5-IIOF-A12	0.046	3.070	3.042	0.250	19.0
5-IIOF-A21	0.046	4.080	4.042	0.250	22.0
5-IIOF-A22	0.046	4.050	4.062	0.250	22.0
5-IIOF-A31	0.046	5.070	5.052	0.250	25.0
5-IIOF-A32	0.046	5.030	5.072	0.250	25.0
1-IEOF-A11	0.048	3.230	3.023	0.219	17.0
1-IEOF-A12	0.048	3.227	3.071	0.219	17.0
1-IEOF-A21	0.048	4.261	4.048	0.219	20.0
1-IEOF-A22	0.048	4.266	4.022	0.219	20.0
1-IEOF-A31	0.048	5.279	5.044	0.219	23.0
1-IEOF-A32	0.048	5.237	5.080	0.219	23.0
2-IEOF-A11	0.082	3.281	3.130	0.219	17.0
2-IEOF-A12	0.082	3.283	3.152	0.219	17.0
2-IEOF-A21	0.082	4.240	4.152	0.219	20.0
2-IEOF-A22	0.082	4.304	4.128	0.219	20.0
2-IEOF-A31	0.082	5.301	5.102	0.219	23.0
2-IEOF-A32	0.082	5.347	5.098	0.219	23.0
3-IEOF-A11	0.062	3.264	3.190	0.188	17.0
3-IEOF-A12	0.062	3.267	3.102	0.188	17.0
3-IEOF-A21	0.062	4.260	4.111	0.188	20.0
3-IEOF-A22	0.062	4.355	4.072	0.188	20.0

Table A3 (Cont'd)

Dimensions of I-Beams Used in the Experimental Investigation

Specimen No.	t (in.)	B1 (in.)	D (in.)	R (in.)	L (in.)
3-IEOF-A31	0.062	5.268	5.090	0.188	23.0
3-IEOF-A32	0.062	5.249	5.093	0.188	23.0
5-IEOF-A11	0.046	3.050	3.020	0.250	17.0
5-IEOF-A11	0.046	3.080	3.000	0.250	17.0
5-IEOF-A11	0.046	4.060	4.040	0.250	20.0
5-IEOF-A11	0.046	4.100	4.010	0.250	20.0
5-IEOF-A11	0.046	5.080	5.030	0.250	23.0
5-IEOF-A11	0.046	5.040	5.060	0.250	23.0
1-IITF-A11	0.047	3.050	3.000	0.250	11.0
1-IITF-A12	0.047	3.060	3.010	0.250	11.0
1-IITF-A21	0.047	4.070	4.020	0.250	14.0
1-IITF-A22	0.047	4.040	4.020	0.250	14.0
1-IITF-A31	0.047	5.050	5.020	0.250	17.0
1-IITF-A32	0.047	5.090	5.010	0.250	17.0
2-IITF-A11	0.088	3.070	3.020	0.250	11.0
2-IITF-A12	0.088	3.090	3.010	0.250	11.0
2-IITF-A21	0.088	4.100	4.000	0.250	14.0
2-IITF-A22	0.088	4.080	4.000	0.250	14.0
2-IITF-A31	0.088	5.060	5.000	0.250	17.0
2-IITF-A32	0.088	5.110	5.000	0.250	17.0
3-IITF-A11	0.065	3.060	3.010	0.250	11.0
3-IITF-A12	0.065	3.030	3.020	0.250	11.0
3-IITF-A21	0.065	4.080	4.010	0.250	14.0
3-IITF-A22	0.065	4.050	4.010	0.250	14.0
3-IITF-A31	0.065	5.080	5.020	0.250	17.0
3-IITF-A32	0.065	5.100	5.010	0.250	17.0
5-IITF-A11	0.046	3.070	3.020	0.250	11.0
5-IITF-A12	0.046	3.050	3.030	0.250	11.0
5-IITF-A21	0.046	4.090	4.000	0.250	14.0
5-IITF-A22	0.046	4.050	4.000	0.250	14.0
5-IITF-A31	0.046	5.060	5.010	0.250	17.0
5-IITF-A32	0.046	5.110	5.020	0.250	17.0
1-IETF-A11	0.047	3.070	3.020	0.250	6.5
1-IETF-A12	0.047	3.090	3.010	0.250	6.5
1-IETF-A21	0.047	4.050	4.030	0.250	8.0
1-IETF-A22	0.047	4.090	4.010	0.250	8.0
1-IETF-A31	0.047	5.060	5.050	0.250	9.5
1-IETF-A32	0.047	5.100	5.030	0.250	9.5
2-IETF-A11	0.088	3.080	3.010	0.250	6.5
2-IETF-A12	0.088	3.080	3.030	0.250	6.5

Table A3 (Cont'd)

Dimensions of I-Beams Used in the Experimental Investigation

Specimen No.	t (in.)	B1 (in.)	D (in.)	R (in.)	L (in.)
2-IETF-A21	0.088	4.040	4.020	0.250	8.0
2-IETF-A22	0.088	4.070	4.000	0.250	8.0
2-IETF-A31	0.088	5.120	4.980	0.250	9.5
2-IETF-A32	0.088	5.090	4.990	0.250	9.5
3-IETF-A11	0.065	3.030	3.050	0.250	6.5
3-IETF-A12	0.065	3.060	3.030	0.250	6.5
3-IETF-A21	0.065	4.030	4.020	0.250	8.0
3-IETF-A22	0.065	4.060	4.020	0.250	8.0
3-IETF-A31	0.065	5.080	5.040	0.250	9.5
3-IETF-A32	0.065	5.100	5.020	0.250	9.5
5-IETF-A11	0.046	3.030	3.060	0.250	6.5
5-IETF-A12	0.046	3.070	3.030	0.250	6.5
5-IETF-A21	0.046	4.060	4.020	0.250	8.0
5-IETF-A22	0.046	4.030	4.030	0.250	8.0
5-IETF-A31	0.046	5.040	5.050	0.250	9.5
5-IETF-A32	0.046	5.090	5.020	0.250	9.5

Note: See Fig. 3.4 for definitions of symbols.

Table A4

Parameters and Sectional Properties of I-beams

Specimen No.	Material	t (in.)	F_y (ksi)	h/t	N/h	e/h	N/t	R/t
1-IIOF-A11	80DK	0.046	58.2	63.9	0.680	1.531	43.5	4.761
1-IIOF-A12	80DK	0.046	58.2	65.0	0.669	1.505	43.5	4.761
1-IIOF-A21	80DK	0.046	58.2	85.7	0.508	1.523	43.5	4.761
1-IIOF-A22	80DK	0.046	58.2	86.1	0.505	1.515	43.5	4.761
1-IIOF-A31	80DK	0.046	58.2	108.0	0.402	1.509	43.5	4.761
1-IIOF-A32	80DK	0.046	58.2	108.5	0.401	1.503	43.5	4.761
2-IIOF-A11	80XF	0.082	88.3	37.0	0.660	1.485	24.4	2.671
2-IIOF-A12	80XF	0.082	88.3	36.3	0.671	1.510	24.4	2.671
2-IIOF-A21	80XF	0.082	88.3	48.8	0.500	1.500	24.4	2.671
2-IIOF-A22	80XF	0.082	88.3	48.5	0.503	1.508	24.4	2.671
2-IIOF-A31	80XF	0.082	88.3	60.6	0.402	1.509	24.4	2.671
2-IIOF-A32	80XF	0.082	88.3	60.0	0.407	1.524	24.4	2.671
3-IIOF-A11	100XF	0.066	113.1	44.8	0.676	1.520	30.3	2.848
3-IIOF-A12	100XF	0.066	113.1	45.3	0.669	1.505	30.3	2.848
3-IIOF-A21	100XF	0.066	113.1	60.2	0.504	1.511	30.3	2.848
3-IIOF-A22	100XF	0.066	113.1	60.2	0.504	1.511	30.3	2.848
3-IIOF-A31	100XF	0.066	113.1	75.3	0.402	1.509	30.3	2.848
3-IIOF-A32	100XF	0.066	113.1	75.5	0.402	1.506	30.3	2.848
5-IIOF-A11	140SK	0.046	165.1	64.6	0.673	1.515	43.5	5.435
5-IIOF-A12	140SK	0.046	165.1	64.1	0.678	1.525	43.5	5.435
5-IIOF-A21	140SK	0.046	165.1	85.9	0.506	1.519	43.5	5.435
5-IIOF-A22	140SK	0.046	165.1	86.3	0.504	1.511	43.5	5.435
5-IIOF-A31	140SK	0.046	165.1	107.8	0.403	1.512	43.5	5.435
5-IIOF-A32	140SK	0.046	165.1	108.3	0.402	1.506	43.5	5.435
1-IEOF-A11	80DK	0.048	58.2	61.0	0.683	1.367	41.7	4.562
1-IEOF-A12	80DK	0.048	58.2	62.0	0.672	1.345	41.7	4.562
1-IEOF-A21	80DK	0.048	58.2	82.3	0.506	1.392	41.7	4.562
1-IEOF-A22	80DK	0.048	58.2	81.8	0.509	1.401	41.7	4.562
1-IEOF-A31	80DK	0.048	58.2	103.1	0.404	1.415	41.7	4.562
1-IEOF-A32	80DK	0.048	58.2	103.8	0.401	1.404	41.7	4.562
2-IEOF-A11	80XF	0.082	88.3	36.2	0.674	1.349	24.4	2.671
2-IEOF-A12	80XF	0.082	88.3	36.4	0.669	1.339	24.4	2.671
2-IEOF-A21	80XF	0.082	88.3	48.6	0.502	1.379	24.4	2.671
2-IEOF-A22	80XF	0.082	88.3	48.3	0.505	1.387	24.4	2.671
2-IEOF-A31	80XF	0.082	88.3	60.2	0.405	1.418	24.4	2.671
2-IEOF-A32	80XF	0.082	88.3	60.2	0.405	1.419	24.4	2.671
3-IEOF-A11	100XF	0.062	113.1	49.5	0.652	1.305	32.3	3.032
3-IEOF-A12	100XF	0.062	113.1	48.0	0.672	1.343	32.3	3.032
3-IEOF-A21	100XF	0.062	113.1	64.3	0.502	1.379	32.3	3.032
3-IEOF-A22	100XF	0.062	113.1	63.7	0.507	1.393	32.3	3.032

Table A4 (Cont'd)

Parameters and Sectional Properties of I-beams

Specimen No.	Material	t (in.)	F_y (ksi)	h/t	N/h	e/h	N/t	R/t
3-IEOF-A31	100XF	0.062	113.1	80.1	0.403	1.410	32.3	3.032
3-IEOF-A32	100XF	0.062	113.1	80.1	0.402	1.409	32.3	3.032
5-IEOF-A11	140SK	0.046	165.1	63.7	0.683	1.366	43.5	5.435
5-IEOF-A12	140SK	0.046	165.1	63.2	0.688	1.376	43.5	5.435
5-IEOF-A21	140SK	0.046	165.1	85.8	0.507	1.393	43.5	5.435
5-IEOF-A22	140SK	0.046	165.1	85.2	0.510	1.404	43.5	5.435
5-IEOF-A31	140SK	0.046	165.1	107.3	0.405	1.418	43.5	5.435
5-IEOF-A32	140SK	0.046	165.1	108.0	0.403	1.409	43.5	5.435
1-IITF-A11	80DK	0.047	58.2	61.8	0.688	1.549	42.6	5.319
1-IITF-A12	80DK	0.047	58.2	62.0	0.686	1.543	42.6	5.319
1-IITF-A21	80DK	0.047	58.2	83.5	0.509	1.528	42.6	5.319
1-IITF-A22	80DK	0.047	58.2	83.5	0.509	1.528	42.6	5.319
1-IITF-A31	80DK	0.047	58.2	104.8	0.406	1.523	42.6	5.319
1-IITF-A32	80DK	0.047	58.2	104.6	0.407	1.526	42.6	5.319
2-IITF-A11	80XF	0.088	77.1	32.3	0.703	1.582	22.7	2.841
2-IITF-A12	80XF	0.088	77.1	32.2	0.706	1.588	22.7	2.841
2-IITF-A21	80XF	0.088	77.1	43.5	0.523	1.569	22.7	2.841
2-IITF-A22	80XF	0.088	77.1	43.5	0.523	1.569	22.7	2.841
2-IITF-A31	80XF	0.088	77.1	54.8	0.415	1.555	22.7	2.841
2-IITF-A32	80XF	0.088	77.1	54.8	0.415	1.555	22.7	2.841
3-IITF-A11	100XF	0.065	116.9	44.3	0.694	1.562	30.8	3.846
3-IITF-A12	100XF	0.065	116.9	44.5	0.692	1.557	30.8	3.846
3-IITF-A21	100XF	0.065	116.9	59.7	0.515	1.546	30.8	3.846
3-IITF-A22	100XF	0.065	116.9	59.7	0.515	1.546	30.8	3.846
3-IITF-A31	100XF	0.065	116.9	75.2	0.409	1.534	30.8	3.846
3-IITF-A32	100XF	0.065	116.9	75.1	0.410	1.537	30.8	3.846
5-IITF-A11	140SK	0.046	165.1	63.7	0.683	1.537	43.5	5.435
5-IITF-A12	140SK	0.046	165.1	63.9	0.681	1.532	43.5	5.435
5-IITF-A21	140SK	0.046	165.1	85.0	0.512	1.535	43.5	5.435
5-IITF-A22	140SK	0.046	165.1	85.0	0.512	1.535	43.5	5.435
5-IITF-A31	140SK	0.046	165.1	106.9	0.407	1.525	43.5	5.435
5-IITF-A32	140SK	0.046	165.1	107.1	0.406	1.522	43.5	5.435
1-IETF-A11	80DK	0.047	58.2	62.3	0.684	1.538	42.6	5.319
1-IETF-A12	80DK	0.047	58.2	62.0	0.686	1.543	42.6	5.319
1-IETF-A21	80DK	0.047	58.2	83.7	0.508	1.524	42.6	5.319
1-IETF-A22	80DK	0.047	58.2	83.3	0.511	1.532	42.6	5.319
1-IETF-A31	80DK	0.047	58.2	105.4	0.404	1.513	42.6	5.319
1-IETF-A32	80DK	0.047	58.2	105.0	0.405	1.519	42.6	5.319
2-IETF-A11	80XF	0.088	77.1	32.2	0.706	1.588	22.7	2.841
2-IETF-A12	80XF	0.088	77.1	32.4	0.701	1.577	22.7	2.841

Table A4 (Cont'd)

Parameters and Sectional Properties of I-beams

Specimen No.	Material	t (in.)	F_y (ksi)	h/t	N/h	e/h	N/t	R/t
2-IETF-A21	80XF	0.088	77.1	43.7	0.520	1.561	22.7	2.841
2-IETF-A22	80XF	0.088	77.1	43.5	0.523	1.569	22.7	2.841
2-IETF-A31	80XF	0.088	77.1	54.6	0.416	1.561	22.7	2.841
2-IETF-A32	80XF	0.088	77.1	54.7	0.415	1.558	22.7	2.841
3-IETF-A11	100XF	0.065	116.9	44.9	0.685	1.541	30.8	3.846
3-IETF-A12	100XF	0.065	116.9	44.6	0.690	1.552	30.8	3.846
3-IETF-A21	100XF	0.065	116.9	59.8	0.514	1.542	30.8	3.846
3-IETF-A22	100XF	0.065	116.9	59.8	0.514	1.542	30.8	3.846
3-IETF-A31	100XF	0.065	116.9	75.5	0.407	1.527	30.8	3.846
3-IETF-A32	100XF	0.065	116.9	75.2	0.409	1.534	30.8	3.846
5-IETF-A11	140SK	0.046	165.1	64.5	0.674	1.516	43.5	5.435
5-IETF-A12	140SK	0.046	165.1	63.9	0.681	1.532	43.5	5.435
5-IETF-A21	140SK	0.046	165.1	85.4	0.509	1.527	43.5	5.435
5-IETF-A22	140SK	0.046	165.1	85.6	0.508	1.524	43.5	5.435
5-IETF-A31	140SK	0.046	165.1	107.8	0.403	1.513	43.5	5.435
5-IETF-A32	140SK	0.046	165.1	107.1	0.406	1.522	43.5	5.435

Table A5

Dimensions of Hat Sections Used for the Transition Tests

Specimen No.	t (in.)	B1 (in.)	B2 (in.)	D (in.)	R (in.)	L (in.)
T-IOF-ITF-1	0.065	2.990	6.010	3.010	0.250	15.0
T-IOF-ITF-2	0.046	4.000	7.970	4.010	0.250	19.0
T-IOF-ITF-3	0.065	4.980	10.020	5.010	0.250	24.0
T-IOF-ITF-4	0.046	3.020	6.030	3.000	0.250	15.0
T-IOF-ITF-5	0.065	4.030	7.990	4.000	0.250	19.0
T-IOF-ITF-6	0.046	4.980	10.010	5.010	0.250	25.0
T-IOF-EOF-1	0.065	2.970	6.030	3.010	0.250	15.0
T-IOF-EOF-2	0.046	4.020	8.020	4.000	0.250	19.0
T-IOF-EOF-3	0.065	5.040	9.980	4.990	0.250	24.0
T-IOF-EOF-4	0.046	3.030	6.010	2.990	0.250	15.0
T-IOF-EOF-5	0.065	3.960	8.020	4.010	0.250	19.0
T-IOF-EOF-6	0.046	4.950	10.010	5.030	0.250	25.0
T-EOF-ETF-1	0.065	2.980	6.020	3.030	0.250	15.0
T-EOF-ETF-2	0.046	3.990	8.000	4.010	0.250	19.0
T-EOF-ETF-3	0.065	4.970	10.020	5.010	0.250	24.0
T-EOF-ETF-4	0.046	2.990	6.020	3.020	0.250	15.0
T-EOF-ETF-5	0.065	3.960	8.030	4.020	0.250	19.0
T-EOF-ETF-6	0.046	4.970	10.010	5.010	0.250	25.0

Note: See Fig. 3.3 for definitions of symbols.

Table A6

Parameters and Sectional Properties of Hat Sections
Used for the Transition Tests

Specimen No.	Material	t (in.)	F_y (ksi)	h/t	N/h	e/h	N/t	R/t
T-IOF-ITF-1	100XF	0.065	116.9	44.3	0.694	0.500	30.8	3.846
T-IOF-ITF-2	140SK	0.046	165.1	85.2	0.510	0.450	43.5	5.435
T-IOF-ITF-3	100XF	0.065	116.9	75.1	0.410	0.400	30.8	3.846
T-IOF-ITF-4	140SK	0.046	165.1	63.2	0.688	0.300	43.5	5.435
T-IOF-ITF-5	100XF	0.065	116.9	59.5	0.517	0.200	30.8	3.846
T-IOF-ITF-6	140SK	0.046	165.1	106.9	0.407	0.100	43.5	5.435
T-IOF-EOF-1	100XF	0.065	116.9	44.3	0.694	0.750	30.8	3.846
T-IOF-EOF-2	140SK	0.046	165.1	85.0	0.512	0.500	43.5	5.435
T-IOF-EOF-3	100XF	0.065	116.9	74.8	0.412	0.400	30.8	3.846
T-IOF-EOF-4	140SK	0.046	165.1	63.0	0.690	0.300	43.5	5.435
T-IOF-EOF-5	100XF	0.065	116.9	59.7	0.515	0.200	30.8	3.846
T-IOF-EOF-6	140SK	0.046	165.1	107.3	0.405	0.100	43.5	5.435
T-EOF-ETF-1	100XF	0.065	116.9	44.6	0.690	0.750	30.8	3.846
T-EOF-ETF-2	140SK	0.046	165.1	85.2	0.510	0.500	43.5	5.435
T-EOF-ETF-3	100XF	0.065	116.9	75.1	0.410	0.400	30.8	3.846
T-EOF-ETF-4	140SK	0.046	165.1	63.7	0.683	0.300	43.5	5.435
T-EOF-ETF-5	100XF	0.065	116.9	59.8	0.514	0.200	30.8	3.846
T-EOF-ETF-6	140SK	0.046	165.1	106.9	0.407	0.100	43.5	5.435

APPENDIX B

TEST DATA OBTAINED FROM INLAND AND FORD TESTS

Table B1

Material Properties of Inland Specimens

Specimen No.	Material Designation	F_y (ksi)	Source Specimen No. Used in Refs. 9 & 10
1	CRLC	35.3	Ref. 9: C1
2	CRLC	35.3	C2
3	CRLC	35.3	C3
4	CRLC	35.3	C4
5	CRLC	35.3	C5
6	CRLC	35.3	C6
7	40XK	39.8	H1
8	40XK	39.8	H2
9	40XK	39.8	H3
10	40XK	39.8	H4
11	40XK	39.8	H5
12	40XK	39.8	H6
13	60DF	47.4	D1
14	60DF	47.4	D2
15	60DF	47.4	D3
16	60DF	47.4	D4
17	60DF	47.4	D5
18	60DF	47.4	D6
19	80DF	56.6	E1
20	80DF	56.6	E2
21	80DF	56.6	E3
22	80DF	56.6	E4
23	80DF	56.6	E5
24	80DF	56.6	E6
25	60XK	73.0	G1
26	60XK	73.0	G2
27	60XK	73.0	G3
28	60XK	73.0	G4
29	60XK	73.0	G5
30	60XK	73.0	G6
31	160SK	189.0	Ref. 10: 7-1
32	160SK	184.0	7-2
33	160SK	189.0	8-1
34	160SK	184.0	8-2
35	160SK	189.0	9-1
36	160SK	184.0	9-2
37	160SK	185.0	1-1
38	160SK	169.0	1-2
39	160SK	185.0	2-1
40	160SK	169.0	2-2

Table B1 (Cont'd)

Material Properties of Inland Specimens

Specimen No.	Material Designation	F_y (ksi)	Source Specimen No. Used in Refs. 9 & 10
41	160SK	185.0	3-1
42	160SK	169.0	3-2
43	160SK	189.0	10-1
44	160SK	184.0	10-2
45	160SK	176.0	18-1
46	160SK	180.0	18-2
47	160SK	189.0	11-1
48	160SK	184.0	11-2
49	160SK	176.0	16-1
50	160SK	180.0	16-2
51	160SK	185.0	4-1
52	160SK	169.0	4-2
53	160SK	176.0	19-1
54	160SK	180.0	19-2
55	160SK	189.0	12-1
56	160SK	184.0	12-2
57	160SK	189.0	20-1
58	160SK	184.0	20-2
59	160SK	185.0	5-1
60	160SK	169.0	5-2
61	160SK	189.0	13-1
62	160SK	184.0	13-2
63	160SK	189.0	14-1
64	160SK	184.0	14-2
65	160SK	189.0	15-1
66	160SK	184.0	15-2
67	160SK	185.0	6-1
68	160SK	169.0	6-2

Table B2

Dimensions of Inland Specimens

Specimen No.	t (in.)	B1 (in.)	B2 (in.)	D1 (in.)	D2 (in.)	R (in.)	L (in.)
1	0.0280	1.0	2.2	1.0	0.30	0.25	36.0
2	0.0280	1.5	3.2	1.5	0.31	0.25	36.0
3	0.0280	2.0	4.2	2.0	0.44	0.25	36.0
4	0.0280	2.5	5.2	2.5	0.38	0.25	36.0
5	0.0280	3.0	6.2	3.0	0.44	0.25	36.0
6	0.0280	4.0	8.2	4.0	0.44	0.25	36.0
7	0.0340	1.0	2.2	1.0	0.30	0.25	36.0
8	0.0340	1.5	3.2	1.5	0.31	0.25	36.0
9	0.0340	2.0	4.2	2.0	0.44	0.25	36.0
10	0.0340	2.5	5.2	2.5	0.38	0.25	36.0
11	0.0340	3.0	6.2	3.0	0.44	0.25	36.0
12	0.0340	4.0	8.2	4.0	0.44	0.25	36.0
13	0.0340	1.0	2.2	1.0	0.30	0.25	36.0
14	0.0340	1.5	3.2	1.5	0.31	0.25	36.0
15	0.0340	2.0	4.2	2.0	0.44	0.25	36.0
16	0.0340	2.5	5.2	2.5	0.38	0.25	36.0
17	0.0340	3.0	6.2	3.0	0.44	0.25	36.0
18	0.0340	4.0	8.2	4.0	0.44	0.25	36.0
19	0.0340	1.0	2.2	1.0	0.30	0.25	36.0
20	0.0340	1.5	3.2	1.5	0.31	0.25	36.0
21	0.0340	2.0	4.2	2.0	0.44	0.25	36.0
22	0.0340	2.5	5.2	2.5	0.38	0.25	36.0
23	0.0340	3.0	6.2	3.0	0.44	0.25	36.0
24	0.0340	4.0	8.2	4.0	0.44	0.25	36.0
25	0.0410	1.0	2.2	1.0	0.30	0.25	36.0
26	0.0410	1.5	3.2	1.5	0.31	0.25	36.0
27	0.0410	2.0	4.2	2.0	0.44	0.25	36.0
28	0.0410	2.5	5.2	2.5	0.38	0.25	36.0
29	0.0410	3.0	6.2	3.0	0.44	0.25	36.0
30	0.0410	4.0	8.2	4.0	0.44	0.25	36.0
31	0.0256	1.0	2.1	1.0	0.25	0.19	36.0
32	0.0344	1.0	2.2	1.0	0.41	0.19	36.0
33	0.0256	2.5	3.9	0.9	0.50	0.19	36.0
34	0.0344	2.5	3.9	0.9	0.50	0.19	36.0
35	0.0256	4.0	5.4	0.9	0.50	0.19	36.0
36	0.0344	4.0	5.4	0.9	0.50	0.19	36.0
37	0.0256	1.0	2.1	1.0	0.30	0.25	36.0
38	0.0334	1.0	2.1	1.0	0.30	0.25	36.0
39	0.0256	1.5	3.1	1.5	0.31	0.25	36.0
40	0.0334	1.5	3.1	1.5	0.31	0.25	36.0

Table B2 (Cont'd)

Dimensions of Inland Specimens

Specimen No.	t (in.)	B1 (in.)	B2 (in.)	D1 (in.)	D2 (in.)	R (in.)	L (in.)
41	0.0256	2.0	4.1	2.0	0.44	0.25	36.0
42	0.0334	2.0	4.1	2.0	0.44	0.25	36.0
43	0.0256	1.0	3.4	2.5	0.50	0.19	36.0
44	0.0344	1.0	3.4	2.5	0.50	0.19	36.0
45	0.0253	2.5	3.7	2.5	0.44	0.19	36.0
46	0.0346	2.5	3.7	2.5	0.44	0.19	36.0
47	0.0256	2.5	4.9	2.5	0.38	0.19	36.0
48	0.0344	2.5	4.9	2.5	0.50	0.19	36.0
49	0.0253	2.5	4.9	2.5	0.44	0.19	36.0
50	0.0346	2.5	4.9	2.5	0.44	0.19	36.0
51	0.0256	2.5	5.1	2.5	0.38	0.25	36.0
52	0.0344	2.5	5.1	2.5	0.38	0.25	36.0
53	0.0253	2.5	7.4	2.5	0.44	0.19	36.0
54	0.0346	2.5	7.4	2.5	0.44	0.19	36.0
55	0.0256	4.0	6.4	2.5	0.53	0.19	36.0
56	0.0344	4.0	6.4	2.5	0.53	0.19	36.0
57	0.0253	4.0	5.9	2.5	0.44	0.19	36.0
58	0.0334	4.0	5.9	2.5	0.44	0.19	36.0
59	0.0256	3.0	6.1	3.0	0.44	0.25	36.0
60	0.0334	3.0	6.1	3.0	0.44	0.25	36.0
61	0.0256	1.0	4.9	4.0	0.56	0.19	36.0
62	0.0344	1.0	4.9	4.0	0.56	0.19	36.0
63	0.0256	2.5	6.4	4.0	0.56	0.19	36.0
64	0.0344	2.5	6.4	4.0	0.56	0.19	36.0
65	0.0256	4.0	7.9	4.0	0.44	0.19	36.0
66	0.0344	4.0	7.9	4.0	0.44	0.19	36.0
67	0.0256	4.0	8.1	4.0	0.44	0.25	36.0
68	0.0334	4.0	8.1	4.0	0.44	0.25	36.0

Note: See Fig. 4.2 for definitions of symbols.

Table B3

Parameters and Sectional Properties of Inland Specimens

Specimen No.	Material	t (in.)	F_y (ksi)	h/t	N/h	e/h	N/t	R/t
1	CRLC	0.0280	35.3	33.7	2.119	10.593	71.43	8.93
2	CRLC	0.0280	35.3	51.6	1.385	6.925	71.43	8.93
3	CRLC	0.0280	35.3	69.4	1.029	5.144	71.43	8.93
4	CRLC	0.0280	35.3	87.3	0.818	4.092	71.43	8.93
5	CRLC	0.0280	35.3	105.1	0.679	3.397	71.43	8.93
6	CRLC	0.0280	35.3	140.9	0.507	2.535	71.43	8.93
7	40XK	0.0340	39.8	27.4	2.146	10.730	58.82	7.35
8	40XK	0.0340	39.8	42.1	1.397	6.983	58.82	7.35
9	40XK	0.0340	39.8	56.8	1.035	5.176	58.82	7.35
10	40XK	0.0340	39.8	71.5	0.822	4.112	58.82	7.35
11	40XK	0.0340	39.8	86.2	0.682	3.411	58.82	7.35
12	40XK	0.0340	39.8	115.6	0.509	2.543	58.82	7.35
13	60DF	0.0340	47.4	27.4	2.146	10.730	58.82	7.35
14	60DF	0.0340	47.4	42.1	1.397	6.983	58.82	7.35
15	60DF	0.0340	47.4	56.8	1.035	5.176	58.82	7.35
16	60DF	0.0340	47.4	71.5	0.822	4.112	58.82	7.35
17	60DF	0.0340	47.4	86.2	0.682	3.411	58.82	7.35
18	60DF	0.0340	47.4	115.6	0.509	2.543	58.82	7.35
19	80DF	0.0340	56.6	27.4	2.146	10.730	58.82	7.35
20	80DF	0.0340	56.6	42.1	1.397	6.983	58.82	7.35
21	80DF	0.0340	56.6	56.8	1.035	5.176	58.82	7.35
22	80DF	0.0340	56.6	71.5	0.822	4.112	58.82	7.35
23	80DF	0.0340	56.6	86.2	0.682	3.411	58.82	7.35
24	80DF	0.0340	56.6	115.6	0.509	2.543	58.82	7.35
25	60XK	0.0410	73.0	22.4	2.179	10.893	48.78	6.10
26	60XK	0.0410	73.0	34.6	1.410	7.052	48.78	6.10
27	60XK	0.0410	73.0	46.8	1.043	5.214	48.78	6.10
28	60XK	0.0410	73.0	59.0	0.827	4.136	48.78	6.10
29	60XK	0.0410	73.0	71.2	0.685	3.427	48.78	6.10
30	60XK	0.0410	73.0	95.6	0.510	2.552	48.78	6.10
31	160SK	0.0256	189.0	37.1	2.108	10.540	78.12	7.42
32	160SK	0.0344	184.0	27.1	2.148	10.739	58.14	5.52
33	160SK	0.0256	189.0	33.2	2.356	11.781	78.12	7.42
34	160SK	0.0344	184.0	24.2	2.406	12.031	58.14	5.52
35	160SK	0.0256	189.0	33.2	2.356	11.781	78.12	7.42
36	160SK	0.0344	184.0	24.2	2.406	12.031	58.14	5.52
37	160SK	0.0256	185.0	37.1	2.108	10.540	78.12	9.77
38	160SK	0.0334	169.0	27.9	2.143	10.716	59.88	7.49
39	160SK	0.0256	185.0	56.6	1.380	6.902	78.12	9.77
40	160SK	0.0334	169.0	42.9	1.395	6.977	59.88	7.49

Table B3 (Cont'd)

Parameters and Sectional Properties of Inland Specimens

Specimen No.	Material	t (in.)	F_y (ksi)	h/t	N/h	e/h	N/t	R/t
41	160SK	0.0256	185.0	76.1	1.026	5.131	78.12	9.77
42	160SK	0.0334	169.0	57.9	1.035	5.173	59.88	7.49
43	160SK	0.0256	189.0	95.7	0.817	4.084	78.12	7.42
44	160SK	0.0344	184.0	70.7	0.823	4.113	58.14	5.52
45	160SK	0.0253	176.0	96.8	0.817	4.083	79.05	7.51
46	160SK	0.0346	180.0	70.3	0.823	4.114	57.80	5.49
47	160SK	0.0256	189.0	95.7	0.817	4.084	78.12	7.42
48	160SK	0.0344	184.0	70.7	0.823	4.113	58.14	5.52
49	160SK	0.0253	176.0	96.8	0.817	4.083	79.05	7.51
50	160SK	0.0346	180.0	70.3	0.823	4.114	57.80	5.49
51	160SK	0.0256	185.0	95.7	0.817	4.084	78.12	9.77
52	160SK	0.0344	169.0	70.7	0.823	4.113	58.14	7.27
53	160SK	0.0253	176.0	96.8	0.817	4.083	79.05	7.51
54	160SK	0.0346	180.0	70.3	0.823	4.114	57.80	5.49
55	160SK	0.0256	189.0	95.7	0.817	4.084	78.12	7.42
56	160SK	0.0344	184.0	70.7	0.823	4.113	58.14	5.52
57	160SK	0.0253	189.0	96.8	0.817	4.083	79.05	7.51
58	160SK	0.0334	184.0	72.9	0.822	4.110	59.88	5.69
59	160SK	0.0256	185.0	115.2	0.678	3.391	78.12	9.77
60	160SK	0.0334	169.0	87.8	0.682	3.409	59.88	7.49
61	160SK	0.0256	189.0	154.2	0.506	2.532	78.12	7.42
62	160SK	0.0344	184.0	114.3	0.509	2.544	58.14	5.52
63	160SK	0.0256	189.0	154.2	0.506	2.532	78.12	7.42
64	160SK	0.0344	184.0	114.3	0.509	2.544	58.14	5.52
65	160SK	0.0256	189.0	154.2	0.506	2.532	78.12	7.42
66	160SK	0.0344	184.0	114.3	0.509	2.544	58.14	5.52
67	160SK	0.0256	185.0	154.2	0.506	2.532	78.12	9.77
68	160SK	0.0334	169.0	117.8	0.508	2.542	59.88	7.49

Table B4

Material Properties of Ford Tests

Specimen No.	Material Designation	As Received F_y(ksi)	As Formed F_{yf}(ksi)	As Formed F_{yw}(ksi)	Source Specimen Designation Used in Ref. 10
1	MILD	27.5	31.0	49.7	U
2	HSLA-50	41.7	44.8	68.8	A
3	DPL-85T	67.0	69.6	94.0	T
4	DPA-90T	48.3	56.1	102.3	S
5	DPLB-85-T-M	58.8	56.9	101.7	W
6	DPLB-85-T	62.3	61.1	94.8	X
7	HSLA-80	108.4	108.4	125.4	R
8	DPL-85T	61.3	62.7	80.4	P
9	HSLA-80	71.3	75.9	97.0	O
10	MILD	35.7	39.8	59.8	L
11	HSLA-50	63.2	55.3	71.6	K
12	DPA-90T	58.5	55.9	92.8	M
13	HSLA-80	84.2	84.2	115.2	N

Table B.5

Dimensions of Ford Specimens

Specimen No.	t (in.)	t_f (in.)	t_w (in.)	B1 (in.)	B2 (in.)	D1 (in.)	R (in.)	N (in.)
1	0.0315	0.0330	0.0300	1.563	3.0	2.402	0.1	2.0
2	0.0350	0.0356	0.0340	1.570	3.0	2.405	0.1	2.0
3	0.0318	0.0323	0.0300	1.564	3.0	2.402	0.1	2.0
4	0.0343	0.0346	0.0290	1.569	3.0	2.404	0.1	2.0
5	0.0290	0.0300	0.0260	1.558	3.0	2.399	0.1	2.0
6	0.0290	0.0302	0.0260	1.558	3.0	2.399	0.1	2.0
7	0.0330	0.0330	0.0300	1.566	3.0	2.403	0.1	2.0
8	0.0380	0.0400	0.0380	1.576	3.0	2.408	0.1	2.0
9	0.0420	0.0440	0.0390	1.584	3.0	2.412	0.1	2.0
10	0.0590	0.0594	0.0540	1.618	3.0	1.959	0.1	2.0
11	0.0540	0.0594	0.0510	1.608	3.0	1.954	0.1	2.0
12	0.0530	0.0543	0.0520	1.606	3.0	1.953	0.1	2.0
13	0.0550	0.0550	0.0510	1.610	3.0	1.955	0.1	2.0

Note: See Fig. 4.5 for definitions of symbols.

Table B6

Parameters and Sectional Properties of Ford Specimens

Specimen No.	Material	t (in.)	F_y (ksi)	h/t	N/h	e/h	N/t	R/t
1	MILD	0.0300	49.7	78.1	0.854	1.708	66.67	3.33
2	HSLA-50	0.0340	68.8	68.7	0.856	1.712	58.82	2.94
3	DPL-85T	0.0300	94.0	78.1	0.854	1.708	66.67	3.33
4	DPA-90T	0.0290	102.3	80.9	0.853	1.705	68.97	3.45
5	DPLB-85-T-M	0.0260	101.7	90.3	0.852	1.704	76.92	3.85
6	DPLB-85-T	0.0260	94.8	90.3	0.852	1.704	76.92	3.85
7	HSLA-80	0.0300	125.4	78.1	0.854	1.707	66.67	3.33
8	DPL-85T	0.0380	80.4	61.4	0.858	1.715	52.63	2.63
9	HSLA-80	0.0390	97.0	59.8	0.857	1.714	51.28	2.56
10	MILD	0.0540	59.8	34.3	1.080	2.161	37.04	1.85
11	HSLA-50	0.0510	71.6	36.3	1.080	2.160	39.22	1.96
12	DPA-90T	0.0520	92.8	35.6	1.082	2.163	38.46	1.92
13	HSLA-80	0.0510	115.2	36.3	1.079	2.159	39.22	1.96

APPENDIX C

TEST DATA OBTAINED FROM REFERENCES 41 AND 44

Table C1

Measured Dimensions of Single-Web Specimens from Reference 41

Specimen No.	t (in.)	B1 (in.)	B2 (in.)	D1 (in.)	D2 (in.)	D3 (in.)	R (in.)	N (in.)	L (in.)
SU-1-IOF-1	.048	1.524	1.482	9.924	0.617	0.690	.1330	1.0	42.0
SU-1-IOF-2	.047	1.486	1.497	9.504	0.597	0.671	.1250	1.0	42.0
SU-1-IOF-5	.049	1.466	1.503	9.951	0.686	0.602	.1250	3.0	42.0
SU-1-IOF-6	.048	1.503	1.495	9.944	0.661	0.679	.1250	3.0	42.0
SU-2-IOF-1	.050	1.512	1.454	12.345	0.632	0.688	.1250	1.0	48.0
SU-2-IOF-2	.048	1.457	1.498	12.310	0.683	0.682	.1250	1.0	48.0
SU-2-IOF-5	.049	1.514	1.464	12.305	0.647	0.706	.1250	3.0	48.0
SU-2-IOF-6	.049	1.483	1.487	12.345	0.662	0.668	.1250	3.0	48.0
SU-5-IOF-1	.049	2.648	2.660	6.193	0.611	0.606	.0938	1.0	30.0
SU-5-IOF-2	.050	2.651	2.662	6.177	0.606	0.600	.0938	1.0	30.0
SU-5-IOF-3	.050	2.641	2.651	6.194	0.606	0.619	.0977	2.0	30.0
SU-5-IOF-4	.051	2.650	2.655	6.180	0.622	0.607	.0938	2.0	30.0
SU-5-IOF-5	.050	2.655	2.661	6.186	0.613	0.615	.0898	3.0	30.0
SU-5-IOF-6	.050	2.647	2.648	6.192	0.609	0.616	.0938	3.0	30.0
SU-6-IOF-1	.050	3.134	3.139	7.371	0.615	0.618	.0938	1.0	30.0
SU-6-IOF-2	.050	3.134	3.113	7.410	0.616	0.597	.0859	1.0	30.0
SU-6-IOF-3	.049	3.137	3.131	7.380	0.616	0.598	.0898	2.0	30.0
SU-6-IOF-4	.050	3.104	3.118	7.438	0.597	0.610	.0938	2.0	30.0
SU-6-IOF-5	.049	3.135	3.136	7.396	0.620	0.596	.0938	3.0	30.0
SU-6-IOF-6	.050	3.133	3.137	7.379	0.612	0.604	.0898	3.0	30.0
M-SU-6-IOF-1	.050	3.124	3.134	7.397	0.615	0.607	.0938	1.0	30.0
M-SU-6-IOF-2	.050	3.128	3.120	7.389	0.625	0.609	.0938	1.0	30.0
M-SU-6-IOF-5	.051	3.148	3.121	7.386	0.616	0.613	.0938	3.0	30.0
M-SU-6-IOF-6	.050	3.136	3.139	7.363	0.619	0.614	.0938	3.0	30.0
U-SU-17-IOF-5	.049	1.396	1.417	4.908	0.0	0.0	.0470	3.0	26.0
U-SU-17-IOF-6	.049	1.390	1.385	4.901	0.0	0.0	.0470	3.0	26.0
U-SU-18-IOF-5	.049	2.175	2.188	9.540	0.0	0.0	.0470	3.0	40.0
U-SU-18-IOF-6	.049	2.184	2.163	9.609	0.0	0.0	.0470	3.0	40.0
SU-1-EOF-1	.047	1.510	1.488	9.977	0.617	0.677	.1250	1.0	42.0
SU-1-EOF-2	.048	1.472	1.507	9.961	0.696	0.610	.1250	1.0	42.0
SU-1-EOF-5	.049	1.514	1.494	9.958	0.649	0.619	.1250	3.0	42.0
SU-1-EOF-6	.050	1.533	1.490	9.961	0.604	0.667	.1406	3.0	42.0
SU-2-EOF-1	.049	1.462	1.450	12.225	0.698	0.719	.1250	1.0	48.0
SU-2-EOF-2	.048	1.461	1.459	12.220	0.714	0.729	.1250	1.0	48.0
SU-2-EOF-5	.048	1.453	1.441	12.290	0.693	0.750	.1250	3.0	48.0
SU-2-EOF-6	.047	1.465	1.484	12.245	0.727	0.691	.1250	3.0	48.0
SU-4-EOF-1	.050	2.164	2.161	4.925	0.610	0.620	.0870	1.0	30.0
SU-4-EOF-2	.050	2.157	2.148	4.931	0.613	0.625	.0781	1.0	30.0
SU-4-EOF-3	.050	2.157	2.163	4.921	0.619	0.615	.0859	2.0	30.0
SU-4-EOF-4	.049	2.157	2.163	4.945	0.620	0.600	.0876	2.0	30.0

Table C1 (Cont'd)

Measured Dimensions of Single-Web Specimens from Reference 41

Specimen No.	t (in.)	B1 (in.)	B2 (in.)	D1 (in.)	D2 (in.)	D3 (in.)	R (in.)	N (in.)	L (in.)
SU-4-EOF-5	.050	2.165	2.167	4.938	0.610	0.595	.0846	3.0	30.0
SU-4-EOF-6	.049	2.152	2.152	4.952	0.618	0.603	.0859	3.0	30.0
SU-5-EOF-1	.050	2.695	2.655	6.189	0.603	0.599	.0938	1.0	30.0
SU-5-EOF-2	.051	2.667	2.677	6.157	0.613	0.614	.0898	1.0	30.0
SU-5-EOF-3	.051	2.651	2.651	6.206	0.614	0.596	.0938	2.0	30.0
SU-5-EOF-4	.051	2.648	2.643	6.204	0.619	0.609	.1016	2.0	30.0
SU-5-EOF-5	.051	2.658	2.651	6.190	0.616	0.604	.0938	3.0	30.0
SU-5-EOF-6	.050	2.653	2.656	6.188	0.615	0.602	.0938	3.0	30.0
SU-6-EOF-1	.050	3.135	3.142	7.384	0.607	0.611	.0859	1.0	30.0
SU-6-EOF-2	.049	3.134	3.131	7.392	0.617	0.607	.0938	1.0	30.0
SU-6-EOF-3	.049	3.126	3.142	7.387	0.619	0.597	.0859	2.0	30.0
SU-6-EOF-4	.049	3.136	3.142	7.394	0.605	0.609	.0977	2.0	30.0
SU-6-EOF-5	.050	3.142	3.139	7.394	0.610	0.603	.0938	3.0	30.0
SU-6-EOF-6	.050	3.139	3.136	7.400	0.604	0.606	.0938	3.0	30.0
M-SU-4-EOF-1	.050	2.161	2.184	4.899	0.603	0.619	.0898	1.0	30.0
M-SU-4-EOF-2	.051	2.169	2.164	4.939	0.606	0.611	.0938	1.0	30.0
M-SU-4-EOF-5	.050	2.159	2.174	4.895	0.607	0.607	.0859	3.0	30.0
M-SU-4-EOF-6	.050	2.165	2.174	4.919	0.605	0.601	.0938	3.0	30.0
M-SU-6-EOF-1	.050	3.124	3.131	7.371	0.620	0.613	.0938	1.0	30.0
M-SU-6-EOF-2	.051	3.128	3.146	7.375	0.616	0.604	.0938	1.0	30.0
M-SU-6-EOF-5	.050	3.148	3.132	7.365	0.617	0.609	.0938	3.0	30.0
M-SU-6-EOF-6	.051	3.136	3.136	7.380	0.616	0.610	.0938	3.0	30.0
U-SU-17-EOF-1	.049	1.397	1.387	4.959	0.0	0.0	.0470	3.0	26.0
U-SU-17-EOF-2	.049	1.429	1.386	4.915	0.0	0.0	.0470	3.0	26.0
U-SU-17-EOF-5	.049	1.433	1.424	4.891	0.0	0.0	.0470	3.0	26.0
U-SU-17-EOF-6	.049	1.388	1.446	4.919	0.0	0.0	.0470	3.0	26.0
U-SU-18-EOF-1	.049	2.182	2.177	9.555	0.0	0.0	.0470	3.0	40.0
U-SU-18-EOF-2	.049	2.124	2.133	9.636	0.0	0.0	.0470	3.0	40.0
U-SU-18-EOF-5	.050	2.130	2.131	9.330	0.0	0.0	.0470	3.0	40.0
U-SU-18-EOF-6	.049	2.133	2.136	9.332	0.0	0.0	.0470	3.0	40.0
SU-1-ITF-1	.048	1.465	1.503	9.955	0.676	0.611	.1250	1.0	21.0
SU-1-ITF-2	.048	1.485	1.484	9.943	0.663	0.613	.1250	1.0	21.0
SU-1-ITF-5	.048	1.462	1.488	9.955	0.630	0.663	.1250	3.0	21.0
SU-1-ITF-6	.047	1.493	1.482	9.959	0.643	0.638	.1250	3.0	21.0
SU-2-ITF-1	.048	1.483	1.518	12.340	0.646	0.616	.1250	1.0	24.0
SU-2-ITF-2	.048	1.473	1.536	12.305	0.652	0.595	.1250	1.0	24.0
SU-2-ITF-5	.048	1.457	1.464	12.255	0.688	0.711	.1250	3.0	24.0
SU-2-ITF-6	.047	1.457	1.470	12.215	0.689	0.737	.1250	3.0	24.0
SU-4-ITF-1	.052	2.166	2.156	4.944	0.587	0.614	.0938	1.0	15.0
SU-4-ITF-2	.052	2.150	2.154	4.960	0.588	0.615	.0938	1.0	15.0

Table C1 (Cont'd)

Measured Dimensions of Single-Web Specimens from Reference 41

Specimen No.	t (in.)	B1 (in.)	B2 (in.)	D1 (in.)	D2 (in.)	D3 (in.)	R (in.)	N (in.)	L (in.)
SU-4-ITF-3	.050	2.169	2.170	4.941	0.594	0.605	.0938	2.0	15.0
SU-4-ITF-4	.051	2.164	2.166	4.957	0.612	0.594	.0940	2.0	15.0
SU-4-ITF-5	.052	2.137	2.162	4.947	0.620	0.597	.1054	3.0	15.0
SU-4-ITF-6	.051	2.170	2.147	4.928	0.620	0.628	.1015	3.0	15.0
SU-5-ITF-1	.050	2.668	2.670	6.179	0.612	0.619	.0938	1.0	15.0
SU-5-ITF-2	.050	2.682	2.657	6.171	0.623	0.610	.0938	1.0	15.0
SU-5-ITF-3	.051	2.654	2.654	6.192	0.615	0.618	.0938	2.0	15.0
SU-5-ITF-4	.050	2.645	2.646	6.174	0.620	0.612	.0938	2.0	15.0
SU-5-ITF-5	.050	2.664	2.665	6.159	0.615	0.615	.0938	3.0	15.0
SU-5-ITF-6	.050	2.664	2.649	6.175	0.615	0.612	.0938	3.0	15.0
SU-6-ITF-1	.050	3.169	3.124	7.354	0.615	0.610	.0938	1.0	15.0
SU-6-ITF-2	.050	3.155	3.126	7.375	0.605	0.619	.0859	1.0	15.0
SU-6-ITF-3	.050	3.145	3.136	7.360	0.608	0.616	.0859	2.0	15.0
SU-6-ITF-4	.050	3.151	3.130	7.380	0.600	0.613	.0938	2.0	15.0
SU-6-ITF-5	.050	3.125	3.131	7.376	0.622	0.614	.0938	3.0	15.0
SU-6-ITF-6	.049	3.160	3.125	7.378	0.626	0.597	.0938	3.0	15.0
U-SU-17-ITF-5	.050	1.421	1.425	4.858	0.0	0.0	.0470	3.0	13.0
U-SU-17-ITF-6	.049	1.450	1.467	4.811	0.0	0.0	.0470	3.0	13.0
U-SU-19-ITF-5	.049	0.599	0.600	9.628	0.0	0.0	.0470	3.0	20.0
U-SU-19-ITF-6	.049	0.592	0.604	9.691	0.0	0.0	.0470	3.0	20.0
SU-1-ETF-1	.046	1.478	1.480	9.917	0.650	0.643	.1250	1.0	21.0
SU-1-ETF-2	.047	1.474	1.481	9.938	0.663	0.641	.1250	1.0	21.0
SU-1-ETF-5	.048	1.464	1.482	9.942	0.648	0.658	.1250	3.0	21.0
SU-1-ETF-6	.048	1.453	1.479	9.949	0.649	0.653	.1250	3.0	21.0
SU-2-ETF-1	.047	1.508	1.455	12.305	0.630	0.711	.1250	1.0	24.0
SU-2-ETF-2	.049	1.527	1.455	12.310	0.614	0.710	.1250	1.0	24.0
SU-2-ETF-5	.047	1.513	1.445	12.330	0.628	0.685	.1250	3.0	24.0
SU-2-ETF-6	.049	1.508	1.446	12.320	0.638	0.692	.1250	3.0	24.0
SU-4-ETF-1	.050	2.149	2.120	4.964	0.593	0.620	.0938	1.0	15.0
SU-4-ETF-2	.052	2.162	2.159	4.940	0.617	0.608	.1015	1.0	15.0
SU-4-ETF-3	.051	2.151	2.160	4.951	0.601	0.590	.0938	2.0	15.0
SU-4-ETF-4	.051	2.171	2.167	4.928	0.609	0.600	.0938	2.0	15.0
SU-4-ETF-5	.050	2.165	2.152	4.941	0.589	0.605	.0938	3.0	15.0
SU-4-ETF-6	.050	2.166	2.172	4.935	0.611	0.598	.0938	3.0	15.0
SU-5-ETF-1	.051	2.668	2.666	6.165	0.606	0.613	.0898	1.0	15.0
SU-5-ETF-2	.051	2.655	2.650	6.197	0.617	0.605	.0898	1.0	15.0
SU-5-ETF-3	.051	2.659	2.667	6.204	0.593	0.606	.0938	2.0	15.0
SU-5-ETF-4	.050	2.663	2.663	6.186	0.603	0.619	.1016	2.0	15.0
SU-5-ETF-5	.051	2.657	2.653	6.176	0.612	0.614	.0938	3.0	15.0
SU-5-ETF-6	.050	2.655	2.656	6.187	0.618	0.612	.0938	3.0	15.0

Table C1 (Cont'd)

Measured Dimensions of Single-Web Specimens from Reference 41

Specimen No.	t (in.)	B1 (in.)	B2 (in.)	D1 (in.)	D2 (in.)	D3 (in.)	R (in.)	N (in.)	L (in.)
SU-6-ETF-1	.049	3.153	3.122	7.377	0.609	0.614	.0938	1.0	15.0
SU-6-ETF-2	.050	3.152	3.148	7.372	0.613	0.602	.0938	1.0	15.0
SU-6-ETF-3	.049	3.129	3.126	7.380	0.623	0.616	.0977	2.0	15.0
SU-6-ETF-4	.050	3.133	3.158	7.379	0.603	0.607	.0938	2.0	15.0
SU-6-ETF-5	.050	3.123	3.126	7.409	0.607	0.607	.0938	3.0	15.0
SU-6-ETF-6	.050	3.157	3.117	7.387	0.599	0.614	.0938	3.0	15.0
U-SU-17-ETF-5	.049	1.379	1.394	4.949	0.0	0.0	.0470	3.0	13.0
U-SU-17-ETF-6	.049	1.441	1.341	4.930	0.0	0.0	.0470	3.0	13.0
U-SU-19-ETF-5	.049	0.584	0.594	9.643	0.0	0.0	.0470	3.0	20.0
U-SU-19-ETF-6	.049	0.611	0.610	9.627	0.0	0.0	.0470	3.0	20.0

Note: See definitions of symbols in Fig. C1.

Table C2

Measured Dimensions of Single-Web Specimens from Reference 44

Specimen No.	t (in.)	B1 (in.)	B2 (in.)	D1 (in.)	D2 (in.)	D3 (in.)	R (in.)	N (in.)	L (in.)
A-3	.050	2.519	2.500	4.950	0.600	0.620	.0781	2.0	4.4
A-4	.050	2.501	2.519	4.946	0.620	0.600	.0781	2.0	4.4
A-5	.050	2.516	2.512	4.964	0.610	0.609	.0781	2.0	9.2
A-6	.050	2.512	2.525	4.933	0.607	0.611	.0781	2.0	9.2
A-7	.050	2.512	2.508	4.961	0.605	0.604	.0781	2.0	14.0
A-8	.050	2.500	2.512	4.962	0.605	0.602	.0781	2.0	14.0
A-9	.051	2.509	2.513	4.952	0.600	0.620	.0781	2.0	3.2
A-10	.051	2.507	2.512	4.958	0.600	0.620	.0781	2.0	3.2
A-11	.051	2.519	2.518	4.938	0.610	0.605	.0781	2.0	4.4
A-12	.051	2.518	2.516	4.954	0.600	0.617	.0781	2.0	4.4
A-13	.051	2.518	2.523	4.946	0.605	0.610	.0781	2.0	5.6
A-14	.051	2.518	2.506	4.933	0.609	0.605	.0781	2.0	5.6
A-15	.050	2.507	2.519	4.922	0.618	0.603	.0781	2.0	6.8
A-16	.050	2.510	2.520	4.913	0.618	0.609	.0781	2.0	6.8
A-17	.050	2.510	2.507	4.944	0.605	0.619	.0781	2.0	8.0
A-18	.050	2.500	2.519	4.939	0.630	0.602	.0781	2.0	8.0
A-21	.052	2.561	2.565	5.948	0.600	0.620	.0781	2.0	4.9
A-22	.051	2.561	2.569	5.941	0.630	0.590	.0781	2.0	4.9
A-23	.052	2.572	2.577	5.911	0.612	0.605	.0781	2.0	10.7
A-24	.051	2.555	2.579	5.914	0.618	0.611	.0781	2.0	10.7
A-25	.052	2.573	2.554	5.940	0.575	0.620	.0781	2.0	16.5
A-26	.052	2.549	2.554	5.939	0.586	0.620	.0781	2.0	16.5
A-27	.052	2.561	2.554	5.953	0.630	0.628	.0781	2.0	3.5
A-28	.051	2.541	2.567	5.954	0.626	0.630	.0781	2.0	3.5
A-29	.052	2.550	2.571	5.928	0.612	0.607	.0781	2.0	4.9
A-30	.052	2.547	2.572	5.930	0.594	0.604	.0781	2.0	4.9
A-31	.052	2.544	2.559	5.943	0.620	0.595	.0781	2.0	6.4
A-32	.052	2.540	2.558	5.944	0.610	0.600	.0781	2.0	6.4
A-33	.052	2.534	2.561	5.940	0.625	0.590	.0781	2.0	7.8
A-34	.052	2.540	2.557	5.938	0.650	0.570	.0781	2.0	7.8
A-35	.051	2.535	2.545	5.938	0.630	0.575	.0781	2.0	9.3
A-36	.051	2.524	2.556	5.938	0.635	0.630	.0781	2.0	9.3
C1-3	.051	2.531	2.535	4.881	0.617	0.623	.0781	2.0	7.0
C1-4	.051	2.537	2.536	4.892	0.624	0.628	.0781	2.0	7.0
C1-5	.050	2.528	2.534	4.946	0.621	0.620	.0781	2.0	11.9
C1-6	.050	2.535	2.535	4.945	0.617	0.624	.0781	2.0	11.9
C1-7	.051	2.516	2.520	4.948	0.606	0.604	.0781	2.0	16.8
C1-8	.050	2.502	2.502	5.020	0.595	0.628	.0781	2.0	16.8
C1-9	.050	2.490	2.499	4.971	0.616	0.596	.0781	2.0	21.7
C1-10	.051	2.528	2.523	5.933	0.613	0.620	.0781	2.0	21.7
C1-13	.046	2.573	2.505	5.817	0.779	0.446	.0703	2.0	7.9
C1-14	.046	2.568	2.479	5.830	0.830	0.410	.0703	2.0	7.9

Table C2 (Cont'd)

Measured Dimensions of Single-Web Specimens from Reference 44

Specimen No.	t (in.)	B1 (in.)	B2 (in.)	D1 (in.)	D2 (in.)	D3 (in.)	R (in.)	N (in.)	L (in.)
C1-15	.046	2.536	2.459	5.854	0.860	0.368	.0703	2.0	13.8
C1-16	.046	2.562	2.534	5.813	0.630	0.568	.0703	2.0	13.8
C1-17	.046	2.523	2.503	5.890	0.632	0.600	.0703	2.0	19.7
C1-18	.046	2.544	2.508	5.882	0.635	0.570	.0703	2.0	19.7
C1-19	.052	2.540	2.553	5.959	0.590	0.550	.0703	2.0	25.6
C1-20	.052	2.557	2.565	5.974	0.615	0.608	.0703	2.0	25.6
C2-3	.050	2.507	2.506	4.943	0.611	0.619	.0781	1.0	11.9
C2-4	.050	2.521	2.505	4.938	0.611	0.607	.0781	1.0	11.9
C2-5	.050	2.516	2.521	4.912	0.612	0.612	.0781	1.0	16.9
C2-6	.050	2.513	2.501	4.940	0.621	0.595	.0781	1.0	16.9
C2-7	.050	2.503	2.502	4.960	0.618	0.611	.0781	1.0	21.8
C2-8	.050	2.517	2.521	4.932	0.614	0.612	.0781	1.0	21.8
C2-9	.050	2.519	2.530	4.950	0.604	0.612	.0781	1.0	26.7
C2-10	.050	2.530	2.505	4.949	0.612	0.600	.0781	1.0	26.7
C2-13	.052	2.545	2.550	5.991	0.532	0.568	.0703	1.0	12.9
C2-14	.052	2.549	2.560	5.994	0.620	0.532	.0703	1.0	12.9
C2-15	.052	2.552	2.559	5.973	0.554	0.600	.0703	1.0	18.8
C2-16	.052	2.539	2.545	5.973	0.620	0.604	.0703	1.0	18.8
C2-17	.052	2.541	2.539	5.978	0.589	0.607	.0703	1.0	24.7
C2-18	.052	2.551	2.567	5.950	0.608	0.587	.0703	1.0	24.7
C2-19	.052	2.544	2.565	5.927	0.612	0.608	.0703	1.0	30.6
C2-20	.052	2.559	2.533	5.956	0.592	0.609	.0703	1.0	30.6
C3-1	.050	2.521	2.517	4.920	0.606	0.618	.0781	1.0	11.0
C3-2	.050	2.514	2.523	4.946	0.600	0.604	.0781	1.0	11.9
C3-3	.051	2.513	2.507	4.962	0.616	0.614	.0781	1.0	15.9
C3-4	.051	2.512	2.506	4.963	0.621	0.615	.0781	1.0	15.9
C3-5	.051	2.523	2.521	4.950	0.602	0.604	.0781	1.0	20.8
C3-6	.050	2.501	2.518	4.958	0.610	0.590	.0781	1.0	20.8
C3-7	.050	2.519	2.526	4.939	0.617	0.606	.0781	1.0	25.7
C3-8	.051	2.525	2.502	4.956	0.611	0.610	.0781	1.0	25.7
C3-9	.049	2.512	2.526	4.945	0.630	0.580	.0781	1.0	30.6
C3-10	.050	2.514	2.509	4.948	0.600	0.630	.0781	1.0	30.6
C3-11	.045	2.521	2.496	5.892	0.603	0.700	.0859	1.0	11.0
C3-12	.045	2.507	2.493	5.903	0.594	0.714	.0859	1.0	11.0
C3-13	.045	2.496	2.499	5.926	0.543	0.692	.0859	1.0	16.9
C3-14	.045	2.514	2.497	5.946	0.566	0.716	.0859	1.0	16.9
C3-15	.049	2.641	2.646	6.156	0.625	0.621	.0703	1.0	22.8
C3-16	.049	2.633	2.667	6.143	0.622	0.640	.0703	1.0	22.8
C3-17	.052	3.016	3.015	5.845	0.751	0.737	.0703	1.0	28.7
C3-18	.052	3.045	3.032	5.828	0.656	0.607	.0703	1.0	28.7
C3-19	.052	3.036	3.036	5.914	0.555	0.576	.0703	1.0	34.6
C3-20	.052	3.030	3.044	5.909	0.602	0.560	.0703	1.0	34.6

Note: See definitions of symbols in Fig. C1.

Table C3

Measured Dimensions of Single-Web Specimens from Reference 41
Used for Combined Bending and Web Crippling

Specimen No.	t (in.)	B1 (in.)	B2 (in.)	D1 (in.)	D2 (in.)	D3 (in.)	R (in.)	N (in.)	L (in.)
SU-BC-1-1	.046	1.959	1.908	4.774	0.607	0.585	.0625	3.0	40.0
SU-BC-1-2	.046	1.930	1.913	4.781	0.582	0.590	.0625	3.0	40.0
SU-BC-1-3	.046	1.935	1.936	4.727	0.613	0.601	.0625	3.0	74.0
SU-BC-1-4	.047	1.926	1.954	4.689	0.632	0.639	.0625	3.0	74.0
SU-BC-1-5	.047	1.930	1.932	4.723	0.633	0.637	.0625	3.0	138.0
SU-BC-1-6	.046	1.889	1.929	4.699	0.629	0.640	.0625	3.0	138.0
SU-BC-3-1	.049	1.642	1.649	9.808	0.639	0.617	.0470	3.0	66.0
SU-BC-3-2	.049	1.638	1.639	9.781	0.641	0.617	.0470	3.0	66.0
SU-BC-3-3	.049	1.644	1.643	9.778	0.635	0.620	.0470	3.0	94.0
SU-BC-3-4	.049	1.638	1.635	9.812	0.639	0.632	.0470	3.0	94.0
SU-BC-3-5	.048	1.636	1.633	9.780	0.625	0.638	.0470	3.0	128.0
SU-BC-3-6	.049	1.645	1.639	9.807	0.628	0.632	.0470	3.0	128.0
SU-BC-15-1	.050	3.141	3.160	7.428	0.620	0.584	.0781	3.0	46.0
SU-BC-15-2	.051	3.130	3.166	7.443	0.603	0.625	.0781	3.0	46.0
SU-BC-15-3	.051	3.154	3.145	7.423	0.605	0.615	.0781	3.0	86.0
SU-BC-15-4	.050	3.124	3.155	7.431	0.581	0.620	.0781	3.0	86.0
SU-BC-15-5	.051	3.155	3.156	7.406	0.615	0.612	.0781	3.0	138.0
SU-BC-15-6	.052	3.153	3.154	7.412	0.611	0.613	.0781	3.0	138.0
SU-4-IOF-1	.049	2.158	2.156	4.960	0.596	0.585	.0781	1.0	25.0
SU-4-IOF-2	.050	2.155	2.153	4.935	0.593	0.610	.0781	1.0	25.0
SU-4-IOF-3	.050	2.169	2.173	4.941	0.587	0.610	.0938	2.0	25.0
SU-4-IOF-4	.050	2.169	2.165	4.931	0.624	0.588	.0859	2.0	25.0
SU-4-IOF-5	.050	2.179	2.138	4.935	0.604	0.608	.0781	3.0	25.0
SU-4-IOF-6	.050	2.173	2.149	4.909	0.600	0.609	.0781	3.0	25.0
M-SU-4-IOF-1	.050	2.156	2.162	4.974	0.591	0.619	.0938	1.0	25.0
M-SU-4-IOF-2	.051	2.174	2.152	4.908	0.607	0.623	.0977	1.0	25.0
M-SU-4-IOF-5	.051	2.167	2.137	4.931	0.603	0.608	.0938	3.0	25.0
M-SU-4-IOF-6	.050	2.165	2.162	4.936	0.615	0.600	.0898	3.0	25.0
SU-BC-6-1	.050	1.633	1.627	2.561	0.637	0.628	.0781	3.0	50.5
SU-BC-6-2	.050	1.638	1.631	2.571	0.643	0.611	.0781	3.0	50.5
SU-BC-6-3	.051	1.635	1.631	2.560	0.645	0.609	.0781	3.0	78.5
SU-BC-16-1	.051	1.502	1.501	4.016	0.603	0.616	.0625	3.0	64.5
SU-BC-16-2	.050	1.488	1.487	4.033	0.601	0.613	.0625	3.0	64.5
SU-BC-16-3	.051	1.483	1.491	4.056	0.598	0.619	.0625	3.0	104.5
SU-BC-16-4	.051	1.808	1.803	4.047	0.608	0.607	.0625	3.0	104.5
SU-BC-7-1	.047	2.498	2.486	4.786	0.598	0.581	.0625	3.0	76.5
SU-BC-7-2	.046	2.487	2.503	4.787	0.615	0.589	.0625	3.0	76.5
SU-BC-7-3	.046	2.497	2.510	4.733	0.614	0.598	.0625	3.0	108.5
SU-BC-7-4	.046	2.498	2.508	4.753	0.623	0.590	.0625	3.0	108.5
SU-BC-8-1	.050	3.042	3.000	6.150	0.606	0.607	.0781	3.0	86.5

Table C3 (Cont'd)

Measured Dimensions of Single-Web Specimens from Reference 41 Used for Combined Bending and Web Crippling

Specimen No.	t (in.)	B1 (in.)	B2 (in.)	D1 (in.)	D2 (in.)	D3 (in.)	R (in.)	N (in.)	L (in.)
SU-BC-8-2	.050	2.983	2.981	6.195	0.602	0.626	.0781	3.0	86.5
SU-BC-8-3	.050	2.995	3.005	6.190	0.616	0.602	.0781	3.0	118.5
SU-BC-8-4	.050	2.996	2.992	6.192	0.618	0.611	.0781	3.0	118.5
SU-BC-8'-1	.076	2.259	2.262	4.021	0.729	0.732	.0938	3.0	70.5
SU-BC-8'-2	.076	2.250	2.242	4.075	0.713	0.722	.0938	3.0	70.5
SU-BC-8'-3	.076	2.259	2.263	4.132	0.716	0.691	.0938	3.0	106.5
SU-BC-8'-4	.076	2.261	2.264	4.120	0.709	0.727	.0938	3.0	106.5

Note: See definitions of symbols in Fig. C1.

Table C4

Measured Dimensions of I-Beams from Reference 41

Specimen No.	t (in.)	B1 (in.)	B2 (in.)	D1 (in.)	D2 (in.)	D3 (in.)	R (in.)	N (in.)	L (in.)
I-1-IOF-1	0.048	1.500	1.490	9.980	0.609	0.649	.1250	1.0	42.0
I-1-IOF-2	0.048	1.450	1.472	10.047	0.646	0.652	.1250	1.0	42.0
I-1-IOF-5	0.048	1.450	1.453	9.975	0.659	0.625	.1250	3.0	42.0
I-1-IOF-6	0.048	1.398	1.485	9.953	0.705	0.653	.1250	3.0	42.0
I-2-IOF-1	0.049	1.460	1.435	12.338	0.703	0.673	.1250	1.0	48.0
I-2-IOF-2	0.050	1.465	1.506	12.360	0.658	0.680	.1250	1.0	48.0
I-2-IOF-5	0.049	1.448	1.513	12.327	0.654	0.682	.1250	3.0	48.0
I-2-IOF-6	0.050	1.483	1.507	12.360	0.647	0.631	.1250	3.0	48.0
I-3-IOF-1	0.049	1.981	1.992	7.380	0.608	0.605	.0938	1.0	34.0
I-3-IOF-2	0.050	1.972	1.975	7.389	0.601	0.609	.0938	1.0	34.0
I-6"-IOF-1	0.046	2.997	3.027	7.090	0.640	0.600	.0938	1.0	32.0
I-6"-IOF-2	0.046	2.941	2.995	6.950	0.670	0.680	.0938	1.0	32.0
I-9-IOF-1	0.046	3.467	3.480	6.988	0.602	0.467	.0938	1.0	32.0
I-9-IOF-2	0.045	3.447	3.478	7.004	0.507	0.518	.0938	1.0	32.0
I-9-IOF-5	0.045	3.461	3.475	6.965	0.596	0.476	.0938	3.0	32.0
I-9-IOF-6	0.044	3.464	3.494	6.947	0.575	0.488	.0938	3.0	32.0
I-12-IOF-1	0.051	1.482	1.517	7.433	0.593	0.580	.0938	1.0	34.0
I-12-IOF-2	0.052	1.500	1.521	7.449	0.604	0.608	.0938	1.0	34.0
I-12-IOF-5	0.051	1.485	1.461	7.468	0.591	0.599	.0938	3.0	34.0
I-U-18-IOF-5	0.049	2.114	2.125	9.655	-	-	.0470	3.0	40.0
I-U-18-IOF-6	0.049	2.136	2.159	9.636	-	-	.0470	3.0	40.0
I-1-EOF-1	0.047	1.487	1.481	9.935	0.605	0.688	.1250	1.0	42.0
I-1-EOF-2	0.047	1.379	1.475	9.894	0.735	0.681	.1250	1.0	42.0
I-1-EOF-5	0.047	1.459	1.510	9.945	0.678	0.628	.1250	3.0	42.0
I-1-EOF-6	0.046	1.434	1.453	9.936	0.710	0.626	.1250	3.0	42.0
I-2-EOF-1	0.049	1.497	1.522	12.340	0.662	0.673	.1250	1.0	48.0
I-2-EOF-2	0.048	1.481	1.488	12.340	0.700	0.680	.1250	1.0	48.0
I-2-EOF-5	0.049	1.513	1.491	12.340	0.648	0.682	.1250	3.0	48.0
I-2-EOF-6	0.050	1.454	1.469	12.340	0.722	0.631	.1250	3.0	48.0
I-3-EOF-1	0.049	2.008	2.013	7.361	0.620	0.607	.0938	1.0	34.0
I-3-EOF-2	0.050	2.003	2.007	7.337	0.605	0.599	.0938	1.0	34.0
I-3-EOF-5	0.049	2.000	2.005	7.362	0.606	0.603	.0938	3.0	34.0
I-3-EOF-6	0.049	1.997	2.001	7.367	0.612	0.610	.0938	3.0	34.0
I-3'-EOF-1	0.046	1.962	1.915	7.114	0.596	0.628	.0983	1.0	32.0
I-3'-EOF-2	0.046	1.949	1.903	7.017	0.635	0.590	.0983	1.0	32.0
I-3'-EOF-5	0.046	1.942	1.956	7.095	0.642	0.639	.0983	3.0	32.0
I-3'-EOF-6	0.046	1.950	1.934	7.031	0.630	0.608	.0983	3.0	32.0
I-5'-EOF-5	0.060	1.739	1.744	7.300	0.532	0.523	.0938	3.0	34.0
I-5'-EOF-6	0.060	1.740	1.742	7.297	0.534	0.516	.0938	3.0	34.0
I-6-EOF-1	0.075	1.750	1.751	7.405	0.509	0.544	.1016	1.0	34.0

Table C4 (Cont'd)

Measured Dimensions of I-Beams from Reference 41

Specimen No.	t (in.)	B1 (in.)	B2 (in.)	D1 (in.)	D2 (in.)	D3 (in.)	R (in.)	N (in.)	L (in.)
I-6-EOF-2	0.075	1.750	1.750	7.397	0.509	0.522	.0938	1.0	34.0
I-6-EOF-5	0.075	1.789	1.783	7.411	0.493	0.529	.0938	3.0	34.0
I-6-EOF-6	0.075	1.768	1.772	7.386	0.496	0.517	.0938	3.0	34.0
I-6-EOF-7	0.077	1.768	1.762	7.323	0.497	0.521	.0859	3.0	34.0
I-6-EOF-8	0.076	1.767	1.770	7.378	0.502	0.515	.0938	3.0	34.0
I-6"-EOF-1	0.046	3.002	2.998	7.121	0.600	0.630	.0938	1.0	32.0
I-6"-EOF-2	0.047	2.972	3.033	6.924	0.642	0.681	.0938	1.0	32.0
I-6"-EOF-5	0.046	2.988	2.976	6.975	0.679	0.664	.0938	3.0	32.0
I-6"-EOF-6	0.046	3.016	3.020	7.105	0.657	0.580	.0938	3.0	32.0
I-9-EOF-1	0.046	3.500	3.457	6.919	0.476	0.612	.0938	1.0	32.0
I-9-EOF-2	0.046	3.469	3.447	6.991	0.476	0.590	.0938	1.0	32.0
I-9-EOF-5	0.046	3.478	3.487	7.002	0.483	0.551	.0938	3.0	32.0
I-9-EOF-6	0.046	3.461	3.469	6.936	0.456	0.648	.0938	3.0	32.0
I-12-EOF-1	0.051	1.506	1.520	7.445	0.601	0.614	.0938	1.0	34.0
I-12-EOF-2	0.050	1.519	1.513	7.445	0.612	0.617	.0938	1.0	34.0
I-12-EOF-5	0.051	1.512	1.513	7.435	0.607	0.612	.0938	3.0	34.0
I-12-EOF-6	0.051	1.509	1.498	7.409	0.597	0.629	.0938	3.0	34.0
I-12'-EOF-5	0.108	3.953	3.937	5.503	1.048	1.038	.1094	3.0	28.0
I-12'-EOF-6	0.108	3.939	3.977	5.528	1.038	1.040	.1094	3.0	28.0
I-16-EOF-1	0.053	2.516	2.524	3.979	0.565	0.582	.0938	1.0	24.0
I-16-EOF-2	0.051	2.519	2.516	3.994	0.617	0.556	.0938	1.0	24.0
I-16-EOF-5	0.051	2.493	2.513	3.023	0.611	0.556	.0938	3.0	24.0
I-16-EOF-6	0.051	2.524	2.502	3.977	0.616	0.600	.0938	3.0	24.0
I-U-17-EOF-5	0.049	1.400	1.375	4.950	-	-	.0470	3.0	26.0
I-U-17-EOF-6	0.049	1.376	1.450	4.881	-	-	.0470	3.0	26.0
I-U-18-EOF-5	0.049	2.118	2.100	9.641	-	-	.0470	3.0	40.0
I-U-18-EOF-6	0.049	2.120	2.150	9.641	-	-	.0470	3.0	40.0
I-1-ITF-1	0.047	1.509	1.497	9.946	0.633	0.699	.1250	1.0	21.0
I-1-ITF-2	0.048	1.462	1.463	9.982	0.656	0.646	.1250	1.0	21.0
I-1-ITF-5	0.046	1.498	1.468	9.942	0.678	0.638	.1250	3.0	21.0
I-1-ITF-6	0.047	1.490	1.521	9.939	0.671	0.632	.1250	3.0	21.0
I-2-ITF-1	0.048	1.478	1.470	12.290	0.698	0.632	.1250	1.0	24.0
I-2-ITF-2	0.047	1.500	1.500	12.280	0.606	0.645	.1250	1.0	24.0
I-2-ITF-5	0.047	1.500	1.497	12.320	0.629	0.637	.1250	3.0	24.0
I-2-ITF-6	0.048	1.497	1.473	12.320	0.640	0.660	.1250	3.0	24.0
I-3-ITF-1	0.050	1.984	1.995	7.371	0.607	0.608	.0898	1.0	17.0
I-3-ITF-2	0.050	1.979	1.981	7.384	0.601	0.618	.0938	1.0	17.0
I-3-ITF-5	0.050	1.990	1.990	7.374	0.609	0.620	.0898	3.0	17.0
I-3-ITF-6*	0.049	1.999	2.002	7.381	0.611	0.608	.0938	3.0	17.0
I-3-ITF-1*	0.049	1.986	1.983	7.373	0.611	0.613	.0938	1.0	17.0

Table C4 (Cont'd)

Measured Dimensions of I-Beams from Reference 41

Specimen No.	t (in.)	B1 (in.)	B2 (in.)	D1 (in.)	D2 (in.)	D3 (in.)	R (in.)	N (in.)	L (in.)
I-3-ITF-2*	0.050	1.987	1.992	7.393	0.627	0.596	.0938	1.0	17.0
I-3-ITF-5*	0.049	1.987	2.004	7.387	0.617	0.612	.0938	3.0	17.0
I-3-ITF-6*	0.049	1.977	1.984	7.387	0.612	0.605	.0938	3.0	17.0
I-5'-ITF-5	0.061	1.739	1.744	7.309	0.532	0.523	.0938	3.0	17.0
I-5'-ITF-6	0.062	1.740	1.742	7.314	0.534	0.516	.0938	3.0	17.0
I-6-ITF-1	0.075	1.787	1.766	7.405	0.493	0.521	.0938	1.0	17.0
I-6-ITF-2	0.075	1.766	1.767	7.405	0.495	0.515	.0938	1.0	17.0
I-6-ITF-5	0.075	1.781	1.772	7.360	0.495	0.520	.0938	3.0	17.0
I-6-ITF-6	0.075	1.784	1.771	7.362	0.496	0.505	.0938	3.0	17.0
I-6-ITF-7	0.076	1.746	1.753	7.391	0.512	0.530	.0938	3.0	17.0
I-6-ITF-8	0.076	1.762	1.768	7.414	0.504	0.515	.0938	3.0	17.0
I-6"-ITF-1	0.046	3.035	2.998	7.088	0.631	0.637	.0938	1.0	16.0
I-6"-ITF-2	0.047	2.987	2.996	7.079	0.626	0.621	.0938	1.0	16.0
I-6"-ITF-5	0.046	3.023	3.016	7.092	0.631	0.607	.0938	3.0	16.0
I-6"-ITF-6	0.046	3.007	3.002	7.093	0.675	0.568	.0938	3.0	16.0
I-12'-ITF-5	0.108	3.977	3.981	5.512	1.054	1.035	.1094	3.0	14.0
I-12'-ITF-6	0.108	3.971	3.964	5.500	1.054	1.048	.1094	3.0	14.0
I-1-ETF-1	0.048	1.515	1.502	9.938	0.629	0.648	.1250	1.0	21.0
I-1-ETF-2	0.049	1.487	1.484	9.969	0.625	0.647	.1250	1.0	21.0
I-1-ETF-5	0.049	1.500	1.443	9.913	0.673	0.644	.1250	3.0	21.0
I-1-ETF-6	0.049	1.542	1.449	9.967	0.655	0.619	.1250	3.0	21.0
I-2-ETF-1	0.047	1.538	1.443	12.340	0.628	0.680	.1250	1.0	24.0
I-2-ETF-2	0.046	1.509	1.491	12.330	0.679	0.678	.1250	1.0	24.0
I-2-ETF-5	0.047	1.472	1.515	12.370	0.600	0.672	.1250	3.0	24.0
I-2-ETF-6	0.046	1.482	1.494	12.290	0.686	0.672	.1250	3.0	24.0
I-3-ETF-1	0.050	1.984	1.995	7.356	0.607	0.608	.0898	1.0	17.0
I-3-ETF-2	0.049	1.979	1.981	7.352	0.601	0.618	.0938	1.0	17.0
I-3-ETF-5	0.050	1.990	1.990	7.376	0.609	0.620	.0898	3.0	17.0
I-3-ETF-6	0.049	1.999	2.002	7.376	0.611	0.608	.0938	3.0	17.0
I-3-ETF-1*	0.050	1.986	1.983	7.359	0.611	0.613	.0938	1.0	17.0
I-3-ETF-2*	0.050	1.987	1.992	7.370	0.627	0.596	.0938	1.0	17.0
I-3-ETF-5*	0.049	1.987	2.004	7.374	0.617	0.612	.0938	3.0	17.0
I-3-ETF-6*	0.050	1.977	1.984	7.366	0.612	0.605	.0938	3.0	17.0
I-5'-ETF-5	0.060	1.738	1.742	7.297	0.541	0.525	.0938	3.0	17.0
I-5'-ETF-6	0.060	1.741	1.748	7.316	0.545	0.529	.1094	3.0	17.0
I-6-ETF-1	0.075	1.775	1.775	7.365	0.496	0.514	.0938	1.0	17.0
I-6-ETF-2	0.075	1.766	1.769	7.355	0.500	0.522	.0938	1.0	17.0
I-6-ETF-5	0.075	1.772	1.757	7.365	0.500	0.527	.0938	3.0	17.0
I-6-ETF-6	0.075	1.765	1.768	7.396	0.496	0.527	.0938	3.0	17.0
I-6-ETF-7	0.075	1.762	1.776	7.373	0.508	0.503	.0938	3.0	17.0

Table C4 (Cont'd)

Measured Dimensions of I-Beams from Reference 41

Specimen No.	t (in.)	B1 (in.)	B2 (in.)	D1 (in.)	D2 (in.)	D3 (in.)	R (in.)	N (in.)	L (in.)
I-6-ETF-8	0.076	1.763	1.769	7.390	0.502	0.518	.0938	3.0	17.0
I-6"-ETF-1	0.047	2.991	3.007	7.017	0.662	0.601	.0938	1.0	16.0
I-6"-ETF-1	0.046	2.992	2.992	7.065	0.689	0.609	.0938	1.0	16.0
I-6"-ETF-1	0.046	2.988	3.030	7.111	0.591	0.591	.0938	3.0	16.0
I-6"-ETF-1	0.046	2.994	3.017	7.096	0.600	0.612	.0938	3.0	16.0
I-12'-ETF-5	0.108	3.984	3.971	5.509	1.037	1.052	.1094	3.0	14.0
I-12'-ETF-5	0.108	3.990	3.981	5.510	1.064	1.036	.1094	3.0	14.0
2b-6-ETF	0.060	2.555	2.545	3.980	0.740	0.780	-	1.5	10.0
3-4-ETF	0.060	1.975	1.965	3.970	0.560	0.530	-	2.5	10.0
4a-6-ETF	0.061	2.980	2.995	6.100	0.790	0.800	-	1.0	16.0
4a-7-ETF	0.061	2.980	2.995	6.100	0.790	0.800	-	1.5	16.0
4b-4-ETF	0.061	2.980	2.995	6.100	0.790	0.800	-	2.5	16.0
6a-5-ETF	0.065	3.020	3.020	7.980	0.800	0.800	-	1.0	16.0
6a-6-ETF	0.065	3.020	3.020	7.980	0.800	0.800	-	1.5	16.0
6b-5-ETF	0.065	3.020	3.020	7.980	0.800	0.800	-	2.5	16.0
9a-3-ETF	0.107	2.485	2.485	3.940	0.750	0.740	-	1.0	10.0
9b-5-ETF	0.107	2.485	2.485	3.940	0.750	0.740	-	1.0	10.0
9b-6-ETF	0.107	2.485	2.485	3.940	0.750	0.740	-	1.5	10.0
9b-7-ETF	0.107	2.485	2.485	3.940	0.750	0.740	-	2.5	10.0
10a-6-ETF	0.108	3.015	3.000	5.920	0.800	0.770	-	1.0	16.0
10a-7-ETF	0.108	3.015	3.000	5.920	0.800	0.770	-	1.5	16.0
10b-5-ETF	0.108	3.015	3.000	5.920	0.800	0.770	-	2.5	16.0
13a-5-ETF	0.134	2.445	2.460	3.960	0.720	0.710	-	1.0	16.0
13a-6-ETF	0.134	2.445	2.460	3.960	0.720	0.710	-	1.5	16.0
13b-4-ETF	0.134	2.445	2.460	3.960	0.720	0.710	-	2.5	16.0
14a-6-ETF	0.148	3.005	3.000	5.950	0.680	0.680	-	1.0	16.0
14a-7-ETF	0.148	3.005	3.000	5.950	0.680	0.680	-	1.5	16.0
14b-5-ETF	0.148	3.005	3.000	5.950	0.680	0.680	-	2.5	16.0
16d-3-ETF	0.046	1.200	1.510	8.020	0.640	1.020	-	1.0	16.0
16d-4-ETF	0.046	1.200	1.510	8.020	0.640	1.020	-	2.5	16.0
17d-3-ETF	0.076	1.450	1.990	7.980	0.840	1.000	-	1.0	36.0
17d-4-ETF	0.076	1.450	1.990	7.980	0.840	1.000	-	2.5	36.0
18a-3-ETF	0.123	2.510	3.500	8.100	1.020	1.020	-	1.0	16.0
18a-4-ETF	0.123	2.510	3.500	8.100	1.020	1.020	-	2.5	16.0

Note: See definition of symbols in Fig. C2

Table C5

Measured Dimensions of I-Beams from Reference 41
Used for Combined Bending and Web Crippling

Specimen No.	t (in.)	B1 (in.)	B2 (in.)	D1 (in.)	D2 (in.)	D3 (in.)	R (in.)	N (in.)	L (in.)
I-BC-4-1	.046	2.060	2.060	4.690	4.690	0.600	.0938	3.0	35.0
I-BC-4-2	.046	2.060	2.060	4.690	4.690	0.600	.0938	3.0	35.0
I-BC-4-3	.046	2.060	2.060	4.690	4.690	0.600	.0938	3.0	60.0
I-BC-4-4	.046	2.060	2.060	4.690	4.690	0.600	.0938	3.0	60.0
I-BC-4-5	.046	2.060	2.060	4.690	4.690	0.600	.0938	3.0	118.0
I-BC-4-6	.046	2.060	2.060	4.690	4.690	0.600	.0938	3.0	118.0
I-BC-5-1	.049	4.500	4.500	9.750	9.750	0.700	.0938	3.0	40.0
I-BC-5-2	.049	4.500	4.500	9.750	9.750	0.700	.0938	3.0	40.0
I-BC-5-3	.049	4.500	4.500	9.750	9.750	0.700	.0938	3.0	72.0
I-BC-5-4	.049	4.500	4.500	9.750	9.750	0.700	.0938	3.0	72.0
I-BC-5-5	.049	4.500	4.500	9.750	9.750	0.700	.0938	3.0	130.0
I-BC-5-6	.049	4.500	4.500	9.750	9.750	0.700	.0938	3.0	130.0
I-BC-6-1	.049	1.625	1.625	2.500	2.500	0.600	.0938	3.0	26.0
I-BC-6-2	.049	1.625	1.625	2.500	2.500	0.600	.0938	3.0	26.0
I-BC-6-3	.049	1.625	1.625	2.500	2.500	0.600	.0938	3.0	34.0
I-BC-6-4	.049	1.625	1.625	2.500	2.500	0.600	.0938	3.0	34.0
I-BC-6-5	.049	1.625	1.625	2.500	2.500	0.600	.0938	3.0	48.0
I-BC-6-6	.049	1.625	1.625	2.500	2.500	0.600	.0938	3.0	48.0
I-BC-8-1	.076	2.250	2.250	4.000	4.000	0.700	.1250	3.0	28.0
I-BC-8-2	.076	2.250	2.250	4.000	4.000	0.700	.1250	3.0	28.0
I-BC-8-3	.076	2.250	2.250	4.000	4.000	0.700	.1250	3.0	42.0
I-BC-8-4	.076	2.250	2.250	4.000	4.000	0.700	.1250	3.0	42.0
I-BC-8-5	.076	2.250	2.250	4.000	4.000	0.700	.1250	3.0	82.0
I-BC-8-6	.076	2.250	2.250	4.000	4.000	0.700	.1250	3.0	82.0
I-BC-9-1	.076	2.250	2.250	7.680	7.680	0.700	.1250	3.0	52.0
I-BC-9-2	.076	2.250	2.250	7.680	7.680	0.700	.1250	3.0	52.0
I-BC-9-3	.076	2.250	2.250	7.680	7.680	0.700	.1250	3.0	92.0
I-BC-9-4	.076	2.250	2.250	7.680	7.680	0.700	.1250	3.0	92.0
I-BC-9-5	.076	2.250	2.250	7.680	7.680	0.700	.1250	3.0	144.0
I-BC-9-6	.076	2.250	2.250	7.680	7.680	0.700	.1250	3.0	144.0
I-BC-9'-1	.048	3.500	3.500	7.300	7.300	0.600	.0781	3.0	38.0
I-BC-9'-2	.048	3.500	3.500	7.300	7.300	0.600	.0781	3.0	38.0
I-BC-9'-3	.048	3.500	3.500	7.300	7.300	0.600	.0781	3.0	68.0
I-BC-9'-4	.048	3.500	3.500	7.300	7.300	0.600	.0781	3.0	68.0
I-BC-9'-5	.048	3.500	3.500	7.300	7.300	0.600	.0781	3.0	144.0
I-BC-9'-6	.048	3.500	3.500	7.300	7.300	0.600	.0781	3.0	144.0
I-BC-10-1	.107	2.375	2.375	5.438	5.438	0.800	.1094	3.0	32.0
I-BC-10-2	.107	2.375	2.375	5.438	5.438	0.800	.1094	3.0	32.0
I-BC-10-3	.107	2.375	2.375	5.438	5.438	0.800	.1094	3.0	50.0
I-BC-10-4	.107	2.375	2.375	5.438	5.438	0.800	.1094	3.0	50.0

Table C5 (Cont'd)

Measured Dimensions of I-Beams from Reference 41
Used for Combined Bending and Web Crippling

Specimen No.	t (in.)	B1 (in.)	B2 (in.)	D1 (in.)	D2 (in.)	D3 (in.)	R (in.)	N (in.)	L (in.)
I-BC-10-5	.107	2.375	2.375	5.438	5.438	0.800	.1094	3.0	94.0
I-BC-10-6	.107	2.375	2.375	5.438	5.438	0.800	.1094	3.0	94.0
I-BC-13-1	.107	5.000	5.000	10.690	10.690	1.000	.1250	3.0	60.0
I-BC-13-2	.107	5.000	5.000	10.690	10.690	1.000	.1250	3.0	60.0
I-BC-13-3	.107	5.000	5.000	10.690	10.690	1.000	.1250	3.0	80.0
I-BC-13-4	.107	5.000	5.000	10.690	10.690	1.000	.1250	3.0	80.0
I-BC-13-5	.107	5.000	5.000	10.690	10.690	1.000	.1250	3.0	108.0
I-BC-13-6	.107	5.000	5.000	10.690	10.690	1.000	.1250	3.0	108.0
I-3-IOF-5	.048	2.000	2.000	7.300	7.300	0.600	.0938	3.0	34.0
I-3-IOF-6	.048	2.000	2.000	7.300	7.300	0.600	.0938	3.0	34.0
I-3'-IOF-1	.046	1.940	1.940	6.990	6.990	0.600	.0938	1.0	32.0
I-3'-IOF-2	.046	1.940	1.940	6.990	6.990	0.600	.0938	1.0	32.0
I-3'-IOF-5	.046	1.940	1.940	6.990	6.990	0.600	.0938	3.0	32.0
I-3'-IOF-6	.046	1.940	1.940	6.990	6.990	0.600	.0938	3.0	32.0
I-5'-IOF-5	.060	1.750	1.750	7.250	7.250	0.550	.0938	3.0	34.0
I-5'-IOF-6	.060	1.750	1.750	7.250	7.250	0.550	.0938	3.0	34.0
I-6-IOF-1	.075	1.750	1.750	7.250	7.250	0.550	.0938	1.0	34.0
I-6-IOF-2	.075	1.750	1.750	7.250	7.250	0.550	.0938	1.0	34.0
I-6-IOF-5	.075	1.750	1.750	7.250	7.250	0.550	.0938	3.0	34.0
I-6-IOF-6	.075	1.750	1.750	7.250	7.250	0.550	.0938	3.0	34.0
I-6-IOF-7	.075	1.750	1.750	7.250	7.250	0.550	.0938	3.0	34.0
I-6-IOF-8	.075	1.750	1.750	7.250	7.250	0.550	.0938	3.0	34.0
I-6"-IOF-5	.046	3.010	3.010	6.990	6.990	0.600	.0938	3.0	32.0
I-6"-IOF-6	.046	3.010	3.010	6.990	6.990	0.600	.0938	3.0	32.0
I-12-IOF-6	.051	1.500	1.500	7.450	7.450	0.600	.0938	3.0	34.0
I-12'-IOF-5	.108	4.000	4.000	5.438	5.438	1.000	.1094	3.0	28.0
I-12'-IOF-6	.108	4.000	4.000	5.438	5.438	1.000	.1094	3.0	28.0
I-16-IOF-1	.051	2.500	2.500	4.000	4.000	0.600	.0938	1.0	24.0
I-16-IOF-2	.051	2.500	2.500	4.000	4.000	0.600	.0938	1.0	24.0
I-16-IOF-5	.051	2.500	2.500	4.000	4.000	0.600	.0938	3.0	24.0
I-16-IOF-6	.051	2.500	2.500	4.000	4.000	0.600	.0938	3.0	24.0

Note: See definition of symbols in Fig. C2

Table C6

Parameters and Test Data of Single-Web Specimens from Reference 41

Specimen No.	t (in.)	h/t	R/t	N/t	N/h	F_y (ksi)	P_{test} (kips)
SU-1-IOF-1	0.048	204.7	2.77	20.83	0.10	43.8	1.260
SU-1-IOF-2	0.047	200.2	2.66	21.28	0.11	43.8	1.175
SU-1-IOF-5	0.049	201.1	2.55	61.22	0.30	43.8	1.450
SU-1-IOF-6	0.048	205.2	2.60	62.50	0.30	43.8	1.385
SU-2-IOF-1	0.050	244.9	2.50	20.00	0.08	43.8	1.145
SU-2-IOF-2	0.048	254.5	2.60	20.83	0.08	43.8	1.305
SU-2-IOF-5	0.049	249.1	2.55	61.22	0.25	43.8	1.385
SU-2-IOF-6	0.049	249.9	2.55	61.22	0.24	43.8	1.455
SU-5-IOF-1	0.049	124.4	1.91	20.41	0.16	47.1	1.403
SU-5-IOF-2	0.050	121.5	1.88	20.00	0.16	47.1	1.480
SU-5-IOF-3	0.050	121.9	1.95	40.00	0.33	47.1	1.750
SU-5-IOF-4	0.051	119.2	1.84	39.22	0.33	47.1	1.830
SU-5-IOF-5	0.050	121.7	1.80	60.00	0.49	47.1	2.080
SU-5-IOF-6	0.050	121.8	1.88	60.00	0.49	47.1	1.835
SU-6-IOF-1	0.050	145.4	1.88	20.00	0.14	47.1	1.480
SU-6-IOF-2	0.050	146.2	1.72	20.00	0.14	47.1	1.580
SU-6-IOF-3	0.049	148.6	1.83	40.82	0.27	47.1	1.890
SU-6-IOF-4	0.050	146.8	1.88	40.00	0.27	47.1	1.815
SU-6-IOF-5	0.049	148.9	1.91	61.22	0.41	47.1	2.085
SU-6-IOF-6	0.050	145.6	1.80	60.00	0.41	47.1	1.890
M-SU-6-IOF-1	0.050	145.9	1.88	20.00	0.14	47.1	1.650
M-SU-6-IOF-2	0.050	145.8	1.88	20.00	0.14	47.1	1.643
M-SU-6-IOF-5	0.051	142.8	1.84	58.82	0.41	47.1	2.045
M-SU-6-IOF-6	0.050	145.3	1.88	60.00	0.41	47.1	2.140
U-SU-17-IOF-5	0.049	98.2	0.96	61.22	0.62	36.3	1.500
U-SU-17-IOF-6	0.049	98.0	0.96	61.22	0.62	36.3	1.525
U-SU-18-IOF-5	0.049	192.7	0.96	61.22	0.32	36.3	1.690
U-SU-18-IOF-6	0.049	194.1	0.96	61.22	0.32	36.3	1.465
SU-1-EOF-1	0.047	210.3	2.66	21.28	0.10	43.8	0.575
SU-1-EOF-2	0.048	205.5	2.60	20.83	0.10	43.8	0.505
SU-1-EOF-5	0.049	201.2	2.55	61.22	0.30	43.8	0.650
SU-1-EOF-6	0.050	197.2	2.81	60.00	0.30	43.8	0.620
SU-2-EOF-1	0.049	247.5	2.55	20.41	0.08	43.8	0.495
SU-2-EOF-2	0.048	252.6	2.60	20.83	0.08	43.8	0.505
SU-2-EOF-5	0.048	254.0	2.60	62.50	0.25	43.8	0.560
SU-2-EOF-6	0.047	258.5	2.66	63.83	0.25	43.8	0.560
SU-4-EOF-1	0.050	96.5	1.74	20.00	0.21	47.1	0.898
SU-4-EOF-2	0.050	96.6	1.56	20.00	0.21	47.1	0.905
SU-4-EOF-3	0.050	96.4	1.72	40.00	0.41	47.1	1.038
SU-4-EOF-4	0.049	98.9	1.79	40.82	0.41	47.1	1.000

Table C6 (Cont'd)

Parameters and Test Data of Single-Web Specimens from Reference 41

Specimen No.	t (in.)	h/t	R/t	N/t	N/h	F_y (ksi)	P_{test} (kips)
SU-4-EOF-5	0.050	96.8	1.69	60.00	0.62	47.1	1.125
SU-4-EOF-6	0.049	99.1	1.75	61.22	0.62	47.1	1.105
SU-5-EOF-1	0.050	121.8	1.88	20.00	0.16	47.1	0.880
SU-5-EOF-2	0.051	118.7	1.76	19.61	0.17	47.1	0.838
SU-5-EOF-3	0.051	119.7	1.84	39.22	0.33	47.1	0.990
SU-5-EOF-4	0.051	119.6	1.99	39.22	0.33	47.1	0.970
SU-5-EOF-5	0.051	119.4	1.84	58.82	0.49	47.1	1.006
SU-5-EOF-6	0.050	121.8	1.88	60.00	0.49	47.1	1.068
SU-6-EOF-1	0.050	145.7	1.72	20.00	0.14	47.1	0.888
SU-6-EOF-2	0.049	148.9	1.91	20.41	0.14	47.1	0.875
SU-6-EOF-3	0.049	148.8	1.75	40.82	0.27	47.1	0.903
SU-6-EOF-4	0.049	148.9	1.99	40.82	0.27	47.1	0.935
SU-6-EOF-5	0.050	145.9	1.88	60.00	0.41	47.1	1.045
SU-6-EOF-6	0.050	146.0	1.88	60.00	0.41	47.1	1.119
M-SU-4-EOF-1	0.050	96.0	1.80	20.00	0.21	47.1	0.875
M-SU-4-EOF-2	0.051	94.8	1.84	19.61	0.21	47.1	0.873
M-SU-4-EOF-5	0.050	95.9	1.72	60.00	0.63	47.1	1.483
M-SU-4-EOF-6	0.050	96.4	1.88	60.00	0.62	47.1	1.406
M-SU-6-EOF-1	0.050	145.4	1.88	20.00	0.14	47.1	0.850
M-SU-6-EOF-2	0.051	142.6	1.84	19.61	0.14	47.1	0.869
M-SU-6-EOF-5	0.050	145.3	1.88	60.00	0.41	47.1	1.175
M-SU-6-EOF-6	0.051	142.7	1.84	58.82	0.41	47.1	1.180
U-SU-17-EOF-1	0.049	99.2	0.96	61.22	0.62	36.3	0.628
U-SU-17-EOF-2	0.049	98.3	0.96	61.22	0.62	36.3	0.598
U-SU-17-EOF-5	0.049	97.8	0.96	61.22	0.63	36.3	0.898
U-SU-17-EOF-6	0.049	98.4	0.96	61.22	0.62	36.3	0.835
U-SU-18-EOF-1	0.049	193.0	0.96	61.22	0.32	36.3	0.472
U-SU-18-EOF-2	0.049	194.7	0.96	61.22	0.31	36.3	0.428
U-SU-18-EOF-5	0.050	184.6	0.94	60.00	0.33	36.3	0.568
U-SU-18-EOF-6	0.049	188.4	0.96	61.22	0.32	36.3	0.545
SU-1-ITF-1	0.048	205.4	2.60	20.83	0.10	43.8	0.770
SU-1-ITF-2	0.048	205.1	2.60	20.83	0.10	43.8	0.785
SU-1-ITF-5	0.048	205.4	2.60	62.50	0.30	43.8	0.795
SU-1-ITF-6	0.047	209.9	2.66	63.83	0.30	43.8	0.820
SU-2-ITF-1	0.048	255.1	2.60	20.83	0.08	43.8	0.610
SU-2-ITF-2	0.048	254.4	2.60	20.83	0.08	43.8	0.610
SU-2-ITF-5	0.048	253.3	2.60	62.50	0.25	43.8	0.630
SU-2-ITF-6	0.047	257.9	2.66	63.83	0.25	43.8	0.595
SU-4-ITF-1	0.052	93.1	1.80	19.23	0.21	47.1	1.715
SU-4-ITF-2	0.052	93.4	1.80	19.23	0.21	47.1	1.725

Table C6 (Cont'd)

Parameters and Test Data of Single-Web Specimens from Reference 41

Specimen No.	t (in.)	h/t	R/t	N/t	N/h	F_y (ksi)	P_{test} (kips)
SU-4-ITF-3	0.050	96.8	1.88	40.00	0.41	47.1	1.915
SU-4-ITF-4	0.051	95.2	1.84	39.22	0.41	47.1	1.980
SU-4-ITF-5	0.052	93.1	2.03	57.69	0.62	47.1	2.210
SU-4-ITF-6	0.051	94.6	1.99	58.82	0.62	47.1	2.310
SU-5-ITF-1	0.050	121.6	1.88	20.00	0.16	47.1	1.508
SU-5-ITF-2	0.050	121.4	1.88	20.00	0.16	47.1	1.530
SU-5-ITF-3	0.051	119.4	1.84	39.22	0.33	47.1	1.550
SU-5-ITF-4	0.050	121.5	1.88	40.00	0.33	47.1	1.710
SU-5-ITF-5	0.050	121.2	1.88	60.00	0.50	47.1	1.620
SU-5-ITF-6	0.050	121.5	1.88	60.00	0.49	47.1	1.610
SU-6-ITF-1	0.050	145.1	1.88	20.00	0.14	47.1	1.465
SU-6-ITF-2	0.050	145.5	1.72	20.00	0.14	47.1	1.233
SU-6-ITF-3	0.050	145.2	1.72	40.00	0.28	47.1	1.225
SU-6-ITF-4	0.050	145.6	1.88	40.00	0.27	47.1	1.280
SU-6-ITF-5	0.050	145.5	1.88	60.00	0.41	47.1	1.330
SU-6-ITF-6	0.049	148.6	1.91	61.22	0.41	47.1	1.250
U-SU-17-ITF-5	0.050	95.2	0.94	60.00	0.63	36.3	1.605
U-SU-17-ITF-6	0.049	96.2	0.96	61.22	0.64	36.3	1.605
U-SU-19-ITF-5	0.049	194.5	0.96	61.22	0.31	36.3	0.750
U-SU-19-ITF-6	0.049	195.8	0.96	61.22	0.31	36.3	0.745
SU-1-ETF-1	0.046	213.6	2.72	21.74	0.10	48.3	0.320
SU-1-ETF-2	0.047	209.4	2.66	21.28	0.10	48.3	0.310
SU-1-ETF-5	0.048	205.1	2.60	62.50	0.30	48.3	0.380
SU-1-ETF-6	0.048	205.3	2.60	62.50	0.30	48.3	0.355
SU-2-ETF-1	0.047	259.8	2.66	21.28	0.08	48.3	0.280
SU-2-ETF-2	0.049	249.2	2.55	20.41	0.08	48.3	0.280
SU-2-ETF-5	0.047	260.3	2.66	63.83	0.25	48.3	0.315
SU-2-ETF-6	0.049	249.4	2.55	61.22	0.25	48.3	0.290
SU-4-ETF-1	0.050	97.3	1.88	20.00	0.21	47.1	0.685
SU-4-ETF-2	0.052	93.0	1.95	19.23	0.21	47.1	0.668
SU-4-ETF-3	0.051	95.1	1.84	39.22	0.41	47.1	0.745
SU-4-ETF-4	0.051	94.6	1.84	39.22	0.41	47.1	0.750
SU-4-ETF-5	0.050	96.8	1.88	60.00	0.62	47.1	0.765
SU-4-ETF-6	0.050	96.7	1.88	60.00	0.62	47.1	0.775
SU-5-ETF-1	0.051	118.9	1.76	19.61	0.16	47.1	0.600
SU-5-ETF-2	0.051	119.5	1.76	19.61	0.16	47.1	0.615
SU-5-ETF-3	0.051	119.6	1.84	39.22	0.33	47.1	0.615
SU-5-ETF-4	0.050	121.7	2.03	40.00	0.33	47.1	0.625
SU-5-ETF-5	0.051	119.1	1.84	58.82	0.49	47.1	0.685
SU-5-ETF-6	0.050	121.7	1.88	60.00	0.49	47.1	0.675

Table C6 (Cont'd)

Parameters and Test Data of Single-Web Specimens from Reference 41

Specimen No.	t (in.)	h/t	R/t	N/t	N/h	F_y (ksi)	P_{test} (kips)
SU-6-ETF-1	0.049	148.6	1.91	20.41	0.14	47.1	0.585
SU-6-ETF-2	0.050	145.4	1.88	20.00	0.14	47.1	0.545
SU-6-ETF-3	0.049	148.6	1.99	40.82	0.27	47.1	0.608
SU-6-ETF-4	0.050	145.6	1.88	40.00	0.27	47.1	0.595
SU-6-ETF-5	0.050	146.2	1.88	60.00	0.41	47.1	0.665
SU-6-ETF-6	0.050	145.7	1.88	60.00	0.41	47.1	0.660
U-SU-17-ETF-5	0.049	99.0	0.96	61.22	0.62	36.3	0.780
U-SU-17-ETF-6	0.049	98.6	0.96	61.22	0.62	36.3	0.755
U-SU-19-ETF-5	0.049	194.8	0.96	61.22	0.31	36.3	0.455
U-SU-19-ETF-6	0.049	194.5	0.96	61.22	0.31	36.3	0.470

Table C7

Parameters and Test Data of Single-Web Specimens from Reference 44

Specimen No.	t (in.)	h/t	R/t	N/t	N/h	F_y (ksi)	P_{test} (kips)
A-3	0.051	95.9	1.55	39.60	0.41	48.5	0.870
A-4	0.051	96.8	1.55	39.60	0.41	48.5	0.860
A-5	0.050	96.7	1.56	40.00	0.41	48.5	1.535
A-6	0.050	96.4	1.56	40.00	0.41	48.5	1.510
A-7	0.050	114.8	1.56	39.20	0.34	48.5	2.115
A-8	0.050	112.5	1.56	38.50	0.34	48.5	2.130
A-9	0.051	95.3	1.54	39.37	0.41	48.5	0.485
A-10	0.051	95.5	1.54	39.45	0.41	48.5	0.500
A-11	0.051	94.6	1.53	39.22	0.41	48.5	0.540
A-12	0.051	94.8	1.53	39.22	0.41	48.5	0.520
A-13	0.051	94.6	1.53	39.22	0.41	48.5	0.505
A-14	0.051	94.4	1.53	39.22	0.41	48.5	0.505
A-15	0.050	96.0	1.56	40.00	0.41	48.5	0.640
A-16	0.050	96.0	1.56	40.00	0.41	48.5	0.625
A-17	0.050	96.7	1.56	40.00	0.41	48.5	0.670
A-18	0.050	96.6	1.56	40.00	0.41	48.5	0.655
A-21	0.052	113.3	1.52	38.83	0.34	51.0	0.775
A-22	0.051	114.4	1.53	39.21	0.34	51.0	0.750
A-23	0.052	112.6	1.51	38.68	0.34	51.0	1.490
A-24	0.051	113.5	1.53	39.22	0.34	51.0	1.570
A-25	0.052	112.1	1.50	38.46	0.34	51.0	1.990
A-26	0.052	113.2	1.52	38.84	0.34	51.0	2.005
A-27	0.052	113.4	1.52	38.84	0.34	51.0	0.425
A-28	0.051	114.5	1.52	38.83	0.34	51.0	0.415
A-29	0.051	112.6	1.52	38.84	0.34	51.0	0.470
A-30	0.052	112.9	1.52	38.84	0.34	51.0	0.450
A-31	0.052	112.1	1.50	38.46	0.34	51.0	0.525
A-32	0.052	113.3	1.52	38.84	0.34	51.0	0.500
A-33	0.052	113.2	1.52	38.84	0.34	51.0	0.505
A-34	0.052	113.1	1.52	38.84	0.34	51.0	0.555
A-35	0.051	114.4	1.53	39.22	0.34	51.0	0.565
A-36	0.051	114.3	1.53	39.22	0.34	51.0	0.580
C1-3	0.051	95.5	1.53	39.22	0.41	47.5	1.300
C1-4	0.051	95.6	1.53	39.22	0.41	47.5	1.150
C1-5	0.050	98.7	1.58	40.40	0.41	47.5	1.670
C1-6	0.050	98.6	1.58	40.40	0.41	47.5	1.860
C1-7	0.051	94.8	1.56	39.20	0.41	47.5	2.000
C1-8	0.050	96.9	1.56	40.00	0.41	47.5	1.990
C1-9	0.050	97.2	1.56	40.00	0.41	47.5	1.975
C1-10	0.051	93.9	1.56	39.20	0.42	47.5	2.005
C1-13	0.046	125.7	1.55	43.96	0.35	38.6	0.710
C1-14	0.046	126.0	1.55	43.96	0.35	38.6	0.745

Table C7 (Cont'd)

Parameters and Test Data of Single-Web Specimens from Reference 44

Specimen No.	t (in.)	h/t	R/t	N/t	N/h	F_y (ksi)	P_{test} (kips)
C1-15	0.046	124.7	1.53	43.48	0.35	38.6	1.320
C1-16	0.046	124.8	1.53	43.67	0.35	38.6	1.175
C1-17	0.046	127.9	1.53	43.48	0.34	38.6	1.450
C1-18	0.046	125.6	1.53	43.67	0.35	38.6	1.395
C1-19	0.051	114.8	1.38	39.22	0.34	51.0	2.115
C1-20	0.052	112.5	1.35	38.46	0.34	51.0	2.130
C2-3	0.050	96.9	1.56	20.00	0.21	48.6	0.845
C2-4	0.050	96.8	1.56	20.00	0.21	48.6	0.803
C2-5	0.050	96.2	1.56	20.00	0.21	48.6	0.945
C2-6	0.050	96.8	1.56	20.00	0.21	48.6	0.925
C2-7	0.050	97.2	1.56	20.00	0.21	48.6	0.983
C2-8	0.050	96.6	1.56	20.00	0.21	48.6	1.013
C2-9	0.050	97.0	1.56	20.00	0.21	48.6	0.940
C2-10	0.050	97.0	1.56	20.00	0.21	48.6	0.935
C2-13	0.052	113.2	1.35	19.23	0.17	51.1	0.833
C2-14	0.052	113.3	1.35	19.23	0.17	51.1	0.908
C2-15	0.052	112.9	1.35	19.23	0.17	51.1	1.085
C2-16	0.052	112.9	1.35	19.23	0.17	51.1	1.035
C2-17	0.052	113.0	1.35	19.23	0.17	51.1	1.143
C2-18	0.052	112.4	1.35	19.23	0.17	51.1	1.140
C2-19	0.052	112.0	1.35	19.23	0.17	51.1	1.063
C2-20	0.052	112.5	1.35	19.23	0.17	51.1	1.055
C3-1	0.050	96.4	1.56	20.00	0.21	48.6	1.640
C3-2	0.050	96.9	1.56	20.00	0.21	48.6	1.665
C3-3	0.051	95.3	1.53	19.61	0.21	48.6	1.690
C3-4	0.051	95.3	1.53	19.61	0.21	48.6	1.600
C3-5	0.051	95.1	1.53	19.61	0.21	48.6	1.685
C3-6	0.050	97.2	1.56	20.00	0.21	48.6	1.670
C3-7	0.050	96.8	1.56	20.00	0.21	48.6	1.600
C3-8	0.051	95.2	1.53	19.61	0.21	48.6	1.620
C3-9	0.049	98.9	1.59	20.41	0.21	48.6	1.535
C3-10	0.050	97.0	1.56	20.00	0.21	48.6	1.520
C3-11	0.045	128.9	1.91	22.22	0.17	38.9	0.970
C3-12	0.045	129.2	1.91	22.22	0.17	38.9	0.950
C3-13	0.045	129.7	1.91	22.22	0.17	38.9	1.200
C3-14	0.045	130.1	1.91	22.22	0.17	38.9	1.150
C3-15	0.049	123.6	1.43	20.41	0.17	47.4	1.565
C3-16	0.049	123.4	1.43	20.41	0.17	47.4	1.505
C3-17	0.052	110.4	1.35	19.23	0.17	54.0	1.835
C3-18	0.052	110.1	1.35	19.23	0.17	54.0	1.800
C3-19	0.052	111.7	1.35	19.23	0.17	54.0	1.825
C3-20	0.052	111.6	1.35	19.23	0.17	54.0	1.770

Table C8

Parameters and Test Data of Single-Web Specimens from Reference 41 Used for Combined Bending and Web Crippling

Specimen No.	t (in.)	h/t	R/t	N/t	N/h	F_y (ksi)	P_{test} (kips)
SU-BC-1-1	0.046	101.8	1.36	65.22	0.64	33.46	2.280
SU-BC-1-2	0.046	101.9	1.36	65.22	0.64	33.46	2.260
SU-BC-1-3	0.046	100.8	1.36	65.22	0.65	33.46	1.720
SU-BC-1-4	0.047	98.8	1.34	64.52	0.65	33.46	1.780
SU-BC-1-5	0.047	98.5	1.33	63.83	0.65	33.46	1.220
SU-BC-1-6	0.046	100.2	1.36	65.22	0.65	33.46	1.060
SU-BC-3-1	0.049	196.5	0.95	60.73	0.31	36.88	2.400
SU-BC-3-2	0.049	196.0	0.95	60.73	0.31	36.88	2.670
SU-BC-3-3	0.049	195.9	0.95	60.73	0.31	36.88	2.210
SU-BC-3-4	0.049	196.6	0.95	60.73	0.31	36.88	2.340
SU-BC-3-5	0.048	200.1	0.97	61.98	0.31	36.88	1.850
SU-BC-3-6	0.049	196.5	0.95	60.73	0.31	36.88	2.040
SU-BC-15-1	0.050	146.6	1.56	60.00	0.41	53.79	4.180
SU-BC-15-2	0.051	143.9	1.53	58.82	0.41	53.79	4.150
SU-BC-15-3	0.051	143.5	1.53	58.82	0.41	53.79	3.680
SU-BC-15-4	0.050	146.6	1.56	60.00	0.41	53.79	3.600
SU-BC-15-5	0.051	143.2	1.53	58.82	0.41	53.79	3.000
SU-BC-15-6	0.052	140.5	1.50	57.69	0.41	53.79	3.000
SU-4-IOF-1	0.049	98.4	1.58	20.24	0.21	47.12	3.052
SU-4-IOF-2	0.050	97.1	1.57	20.08	0.21	47.12	3.050
SU-4-IOF-3	0.050	96.4	1.87	39.84	0.41	47.12	3.540
SU-4-IOF-4	0.050	96.6	1.72	40.00	0.41	47.12	3.550
SU-4-IOF-5	0.050	96.7	1.56	60.00	0.62	47.12	4.170
SU-4-IOF-6	0.050	96.2	1.56	60.00	0.62	47.12	3.970
M-SU-4-IOF-1	0.050	97.5	1.88	20.00	0.21	47.12	3.210
M-SU-4-IOF-2	0.051	95.2	1.93	19.80	0.21	47.12	3.260
M-SU-4-IOF-3	0.051	94.7	1.84	58.82	0.62	47.12	4.400
M-SU-4-IOF-4	0.050	96.1	1.79	59.64	0.62	47.12	4.150
SU-BC-6-1	0.050	49.5	1.57	60.36	1.22	36.88	1.760
SU-BC-6-2	0.050	49.7	1.57	60.36	1.21	36.88	1.680
SU-BC-6-3	0.051	48.5	1.54	59.17	1.22	36.88	1.130
SU-BC-16-1	0.051	76.7	1.23	58.82	0.77	53.79	2.880
SU-BC-16-2	0.050	78.7	1.25	60.00	0.76	53.79	2.700
SU-BC-16-3	0.051	77.5	1.23	58.82	0.76	53.79	2.010
SU-BC-16-4	0.051	77.4	1.23	58.82	0.76	53.79	2.210
SU-BC-7-1	0.047	99.8	1.33	63.83	0.64	33.46	2.000
SU-BC-7-2	0.046	102.1	1.36	65.22	0.64	33.46	1.880
SU-BC-7-3	0.046	100.9	1.36	65.22	0.65	33.46	1.400
SU-BC-7-4	0.046	101.3	1.36	65.22	0.64	33.46	1.510
SU-BC-8-1	0.050	121.0	1.56	60.00	0.50	47.12	3.070

Table C8 (Cont'd)

Parameters and Test Data of Single-Web Specimens from Reference 41 Used for Combined Bending and Web Crippling

Specimen No.	t (in.)	h/t	R/t	N/t	N/h	F_y (ksi)	P_{test} (kips)
SU-BC-8-2	0.050	121.9	1.56	60.00	0.49	47.12	2.940
SU-BC-8-3	0.050	121.8	1.56	60.00	0.49	47.12	2.620
SU-BC-8-4	0.050	121.8	1.56	60.00	0.49	47.12	2.600
SU-BC-8'-1	0.076	50.9	1.23	39.47	0.78	43.60	4.410
SU-BC-8'-2	0.076	52.0	1.24	39.74	0.76	43.60	4.730
SU-BC-8'-3	0.076	52.4	1.23	39.47	0.75	43.60	3.180
SU-BC-8'-4	0.076	52.2	1.23	39.47	0.76	43.60	3.400

Table C9

Parameter and Test Data for I-Beams Obtained from Reference 41

Specimen No.	t (in.)	h/t	R/t	N/t/	F_y (ksi)	P_{test} (kips)
I-1-IOF-1	0.048	205.9	20.83	0.10	43.82	2.385
I-1-IOF-2	0.048	207.3	20.83	0.10	43.82	2.490
I-1-IOF-5	0.048	205.8	62.50	0.30	43.82	2.910
I-1-IOF-6	0.048	205.4	62.50	0.30	43.82	2.850
I-2-IOF-1	0.049	249.8	20.41	0.08	43.82	2.420
I-2-IOF-2	0.050	245.2	20.00	0.08	43.82	2.470
I-2-IOF-5	0.049	252.2	61.86	0.25	43.82	2.860
I-2-IOF-6	0.050	245.2	60.00	0.24	43.82	2.950
I-3-IOF-1	0.049	148.6	20.41	0.14	47.12	2.505
I-3-IOF-2	0.050	145.8	20.00	0.14	47.12	2.450
I-6"-IOF-1	0.046	152.1	21.74	0.14	30.46	1.800
I-6"-IOF-2	0.046	149.1	21.74	0.15	30.46	1.805
I-9-IOF-1	0.046	149.9	21.74	0.15	30.46	1.680
I-9-IOF-2	0.045	151.9	21.98	0.14	30.46	1.540
I-9-IOF-5	0.045	154.5	67.42	0.44	30.46	1.975
I-9-IOF-6	0.044	155.9	68.18	0.44	30.46	1.885
I-12-IOF-1	0.051	145.2	19.80	0.14	53.79	2.645
I-12-IOF-2	0.052	142.6	19.42	0.14	53.79	2.660
I-12-IOF-5	0.051	145.9	59.41	0.41	53.79	3.365
I-U-18-IOF-5	0.049	195.0	61.22	0.31	36.26	2.730
I-U-18-IOF-6	0.049	194.7	61.22	0.31	36.26	2.565
I-1-EOF-1	0.047	207.2	21.05	0.10	43.82	1.840
I-1-EOF-2	0.047	208.5	21.28	0.10	43.82	1.770
I-1-EOF-5	0.047	209.6	63.83	0.30	43.82	2.175
I-1-EOF-6	0.046	214.0	65.22	0.30	43.82	2.210
I-2-EOF-1	0.049	252.4	20.62	0.08	43.82	1.730
I-2-EOF-2	0.048	255.1	20.83	0.08	43.82	1.650
I-2-EOF-5	0.049	249.8	61.22	0.25	43.82	2.305
I-2-EOF-6	0.050	244.8	60.00	0.25	43.82	2.375
I-3-EOF-1	0.049	148.2	20.41	0.14	47.12	2.355
I-3-EOF-2	0.050	144.7	20.00	0.14	47.12	2.470
I-3-EOF-5	0.049	146.7	60.61	0.41	47.12	2.990
I-3-EOF-6	0.049	148.3	61.22	0.41	47.12	2.750
I-3'-EOF-1	0.046	152.7	21.74	0.14	33.46	1.890
I-3'-EOF-2	0.046	150.5	21.74	0.14	33.46	1.690
I-3'-EOF-5	0.046	152.2	65.22	0.43	33.46	2.390
I-3'-EOF-6	0.046	150.8	65.22	0.43	33.46	2.440
I-5'-EOF-5	0.060	119.7	50.00	0.42	47.13	4.120
I-5'-EOF-6	0.060	119.6	50.00	0.42	47.13	4.470
I-6-EOF-1	0.075	96.7	13.33	0.14	42.86	5.200

Table C9 (Cont'd)

Parameter and Test Data for I-Beams Obtained *from* Reference 41

Specimen No.	t (in.)	h/t	R/t	N/t	F_y (ksi)	P_{test} (kips)
I-6-EOF-2	0.075	96.4	13.30	0.14	42.86	5.385
I-6-EOF-5	0.075	96.8	40.00	0.41	42.86	5.630
I-6-EOF-6	0.075	96.2	39.89	0.41	42.86	5.315
I-6-EOF-7	0.077	92.5	38.71	0.42	42.86	5.635
I-6-EOF-8	0.076	95.1	39.47	0.42	42.86	6.750
I-6"-EOF-1	0.046	152.8	21.74	0.14	33.46	1.780
I-6"-EOF-2	0.047	146.9	21.51	0.15	33.46	1.920
I-6"-EOF-5	0.046	149.6	65.22	0.44	33.46	2.540
I-6"-EOF-6	0.046	152.5	65.22	0.43	33.46	2.350
I-9-EOF-1	0.046	148.4	21.74	0.15	33.46	2.075
I-9-EOF-2	0.046	150.0	21.74	0.14	33.46	1.825
I-9-EOF-5	0.046	150.2	65.22	0.43	33.46	2.510
I-9-EOF-6	0.046	148.8	65.22	0.44	33.46	2.565
I-12-EOF-1	0.051	144.0	19.61	0.14	53.79	2.470
I-12-EOF-2	0.050	146.0	19.88	0.14	53.79	2.505
I-12-EOF-5	0.051	143.8	58.82	0.41	53.79	2.960
I-12-EOF-6	0.051	143.3	58.82	0.41	53.79	2.830
I-12'-EOF-5	0.108	49.0	27.78	0.57	45.68	10.250
I-12'-EOF-6	0.108	49.4	27.91	0.56	45.68	11.580
I-16-EOF-1	0.053	73.1	18.87	0.26	53.79	2.560
I-16-EOF-2	0.051	77.1	19.80	0.26	53.79	3.575
I-16-EOF-5	0.051	57.3	58.82	1.03	53.79	3.050
I-16-EOF-6	0.051	76.0	58.82	0.77	53.79	3.150
I-U-17-EOF-5	0.049	99.0	61.22	0.62	36.26	2.555
I-U-17-EOF-6	0.049	97.6	61.22	0.63	36.26	2.230
I-U-18-EOF-5	0.049	196.8	61.86	0.31	36.26	2.040
I-U-18-EOF-6	0.049	194.8	61.22	0.31	36.26	2.285
I-1-ITF-1	0.047	211.9	21.51	0.10	43.82	1.625
I-1-ITF-2	0.048	206.0	20.83	0.10	43.82	1.665
I-1-ITF-5	0.046	214.1	65.22	0.30	43.82	1.875
I-1-ITF-6	0.047	209.5	63.83	0.30	43.82	1.920
I-2-ITF-1	0.048	254.0	20.83	0.08	43.82	1.490
I-2-ITF-2	0.047	256.5	21.05	0.08	43.82	1.520
I-2-ITF-5	0.047	260.1	63.83	0.25	43.82	1.715
I-2-ITF-6	0.048	254.7	62.50	0.25	43.82	1.690
I-3-ITF-1	0.050	145.4	20.00	0.14	47.12	1.915
I-3-ITF-2	0.050	145.7	20.00	0.14	47.12	2.080
I-3-ITF-5	0.050	145.5	60.00	0.41	47.12	2.375
I-3-ITF-6	0.049	148.6	61.22	0.41	47.12	2.205
I-3-ITF-1*	0.049	148.5	20.41	0.14	47.12	2.090

Table C9 (Cont'd)

Parameter and Test Data for I-Beams Obtained from Reference 41

Specimen No	t (in.)	h/t	R/t	N/t	F_y (ksi)	P_{test} (kips)
I-3-ITF-2*	0.050	145.9	20.00	0.14	47.12	2.170
I-3-ITF-5*	0.049	147.2	60.61	0.41	47.12	2.205
I-3-ITF-6*	0.049	148.8	61.22	0.41	47.12	2.335
I-5'-ITF-5	0.061	117.8	49.18	0.42	47.12	3.775
I-5'-ITF-6	0.062	116.9	48.78	0.42	47.12	4.270
I-6-ITF-1	0.075	96.7	13.33	0.14	42.86	4.480
I-6-ITF-2	0.075	96.6	13.32	0.14	42.86	4.570
I-6-ITF-5	0.075	96.0	39.95	0.42	42.86	4.975
I-6-ITF-6	0.075	96.2	40.00	0.42	42.86	5.300
I-6-ITF-7	0.076	95.3	39.47	0.41	42.86	5.956
I-6-ITF-8	0.076	95.6	39.47	0.41	42.86	6.195
I-6"-ITF-1	0.046	152.1	21.74	0.14	33.46	2.138
I-6"-ITF-2	0.047	150.2	21.51	0.14	33.46	1.958
I-6"-ITF-5	0.046	152.2	65.22	0.43	33.46	2.380
I-6"-ITF-6	0.046	152.2	65.22	0.43	33.46	2.390
I-12'-ITF-5	0.108	49.0	27.78	0.57	45.68	10.370
I-12'-ITF-6	0.108	48.9	27.78	0.57	45.68	11.390
I-1-ETF-1	0.048	205.0	20.83	0.10	43.82	0.705
I-1-ETF-2	0.049	201.4	20.41	0.10	43.82	0.690
I-1-ETF-5	0.049	200.3	61.22	0.31	43.82	0.850
I-1-ETF-6	0.049	201.4	61.22	0.30	43.82	0.935
I-2-ETF-1	0.047	260.6	21.28	0.08	43.82	0.645
I-2-ETF-2	0.046	266.0	21.74	0.08	43.82	0.665
I-2-ETF-5	0.047	258.4	63.16	0.24	43.82	0.770
I-2-ETF-6	0.046	265.2	65.22	0.25	43.82	0.690
I-3-ETF-1	0.050	145.1	20.00	0.14	47.12	0.805
I-3-ETF-2	0.049	146.5	20.20	0.14	47.12	0.850
I-3-ETF-5	0.050	145.5	60.00	0.41	47.12	1.120
I-3-ETF-6	0.049	148.5	61.22	0.41	47.12	1.035
I-3-ETF-1*	0.050	145.2	20.00	0.14	47.12	0.820
I-3-ETF-2*	0.050	145.4	20.00	0.14	47.12	0.810
I-3-ETF-5*	0.049	148.5	61.22	0.41	47.12	1.005
I-3-ETF-6*	0.050	145.3	60.00	0.41	47.12	0.960
I-5'-ETF-5	0.060	119.6	50.00	0.42	47.13	1.470
I-5'-ETF-6	0.060	119.9	50.00	0.42	47.13	1.405
I-6-ETF-1	0.075	96.1	13.32	0.14	42.86	2.035
I-6-ETF-2	0.075	96.1	13.33	0.14	42.86	2.105
I-6-ETF-5	0.075	95.9	39.89	0.42	42.86	2.935
I-6-ETF-6	0.075	96.4	39.89	0.41	42.86	3.060
I-6-ETF-7	0.075	96.3	40.00	0.42	42.86	2.690

Table C9 (Cont'd)

Parameter and Test Data for I-Beams Obtained from Reference 41

Specimen No.	t (in.)	h/t	R/t	N/t	F_y (ksi)	P_{test} (kips)
I-6-ETF-8	0.076	95.2	39.47	0.41	42.86	2.400
I-6"-ETF-1	0.047	147.3	21.28	0.14	33.46	0.885
I-6"-ETF-2	0.046	151.6	21.74	0.14	33.46	0.845
I-6"-ETF-5	0.046	152.6	65.22	0.43	33.46	1.065
I-6"-ETF-6	0.046	152.3	65.22	0.43	33.46	1.095
I-12'-ETF-5	0.108	49.0	27.78	0.57	45.68	4.650
I-12'-ETF-6	0.108	49.0	27.78	0.57	45.68	5.245
2b-6-ETF	0.060	64.0	24.88	0.39	30.20	1.870
3-4-ETF	0.060	64.3	41.74	0.65	30.20	1.800
4a-6-ETF	0.061	98.2	16.42	0.17	30.20	1.600
4a-7-ETF	0.061	98.2	24.63	0.25	30.20	1.700
4b-4-ETF	0.061	98.2	41.05	0.42	30.20	1.900
6a-5-ETF	0.065	121.3	15.46	0.13	37.30	1.850
6a-6-ETF	0.065	121.3	23.18	0.19	37.30	1.920
6b-5-ETF	0.065	121.3	38.64	0.32	37.30	2.250
9a-3-ETF	0.107	34.8	9.35	0.27	35.10	5.100
9b-5-ETF	0.107	34.8	9.35	0.27	35.10	5.350
9b-6-ETF	0.107	34.8	14.02	0.40	35.10	5.950
9b-7-ETF	0.107	34.8	23.36	0.67	35.10	6.850
10a-6-ETF	0.108	52.7	9.24	0.18	35.10	5.900
10a-7-ETF	0.108	52.7	18.86	0.26	35.10	5.950
10b-5-ETF	0.108	52.7	23.11	0.44	35.10	7.750
13a-5-ETF	0.134	27.5	7.45	0.27	35.70	6.750
13a-6-ETF	0.134	27.5	11.18	0.41	35.70	8.500
13b-4-ETF	0.134	27.5	18.63	0.68	35.70	12.800
14a-6-ETF	0.148	38.2	6.77	0.18	33.10	8.900
14a-7-ETF	0.148	38.2	10.15	0.27	33.10	11.150
14b-5-ETF	0.148	38.2	16.91	0.44	33.10	12.300
16d-3-ETF	0.046	172.3	21.74	0.13	32.20	0.880
16d-4-ETF	0.046	172.3	54.35	0.32	32.20	0.920
17d-3-ETF	0.076	103.7	13.25	0.13	35.80	2.450
17d-4-ETF	0.076	103.7	33.11	0.32	35.80	3.060
18a-3-ETF	0.123	63.9	8.13	0.13	37.60	6.800
18a-4-ETF	0.123	63.9	20.33	0.32	37.60	7.500

Table C10

Parameters and Test Data of I-Beams from Reference 41
Used for Combined Bending and Web Crippling

Specimen No.	t (in.)	h/t	R/t	N/t	N/h	F_y (ksi)	P_{test} (kips)
I-BC-4-1	0.046	100.0	2.04	65.22	0.65	33.46	2.025
I-BC-4-2	0.046	100.0	2.04	65.22	0.65	33.46	1.940
I-BC-4-3	0.046	100.0	2.04	65.22	0.65	33.46	1.530
I-BC-4-4	0.046	100.0	2.04	65.22	0.65	33.46	1.445
I-BC-4-5	0.046	100.0	2.04	65.22	0.65	33.46	0.830
I-BC-4-6	0.046	100.0	2.04	65.22	0.65	33.46	0.875
I-BC-5-1	0.049	197.0	1.91	61.22	0.31	36.88	2.590
I-BC-5-2	0.049	197.0	1.91	61.22	0.31	36.88	2.515
I-BC-5-3	0.049	197.0	1.91	61.22	0.31	36.88	2.505
I-BC-5-4	0.049	197.0	1.91	61.22	0.31	36.88	2.470
I-BC-5-5	0.049	197.0	1.91	61.22	0.31	36.88	1.785
I-BC-5-6	0.049	197.0	1.91	61.22	0.31	36.88	1.640
I-BC-6-1	0.049	49.0	1.91	61.22	1.25	36.88	1.890
I-BC-6-2	0.049	49.0	1.91	61.22	1.25	36.88	1.870
I-BC-6-3	0.049	49.0	1.91	61.22	1.25	36.88	1.405
I-BC-6-4	0.049	49.0	1.91	61.22	1.25	36.88	1.425
I-BC-6-5	0.049	49.0	1.91	61.22	1.25	36.88	1.015
I-BC-6-6	0.049	49.0	1.91	61.22	1.25	36.88	1.035
I-BC-8-1	0.076	50.6	1.64	39.47	0.78	43.60	6.755
I-BC-8-2	0.076	50.6	1.64	39.47	0.78	43.60	6.525
I-BC-8-3	0.076	50.6	1.64	39.47	0.78	43.60	5.005
I-BC-8-4	0.076	50.6	1.64	39.47	0.78	43.60	4.750
I-BC-8-5	0.076	50.6	1.64	39.47	0.78	43.60	2.545
I-BC-8-6	0.076	50.6	1.64	39.47	0.78	43.60	2.585
I-BC-9-1	0.076	99.1	1.64	39.47	0.40	43.60	5.810
I-BC-9-2	0.076	99.1	1.64	39.47	0.40	43.60	5.785
I-BC-9-3	0.076	99.1	1.64	39.47	0.40	43.60	4.040
I-BC-9-4	0.076	99.1	1.64	39.47	0.40	43.60	4.200
I-BC-9-5	0.076	99.1	1.64	39.47	0.40	43.60	2.675
I-BC-9-6	0.076	99.1	1.64	39.47	0.40	43.60	2.490
I-BC-9'-1	0.048	150.1	1.63	62.50	0.42	47.12	3.315
I-BC-9'-2	0.048	150.1	1.63	62.50	0.42	47.12	2.955
I-BC-9'-3	0.048	150.1	1.63	62.50	0.42	47.12	2.590
I-BC-9'-4	0.048	150.1	1.63	62.50	0.42	47.12	2.695
I-BC-9'-5	0.048	150.1	1.63	62.50	0.42	47.12	1.630
I-BC-9'-6	0.048	150.1	1.63	62.50	0.42	47.12	1.600
I-BC-10-1	0.107	48.8	1.02	28.04	0.57	45.68	11.500
I-BC-10-2	0.107	48.8	1.02	28.04	0.57	45.68	12.070
I-BC-10-3	0.107	48.8	1.02	28.04	0.57	45.68	9.645
I-BC-10-4	0.107	48.8	1.02	28.04	0.57	45.68	8.645

Table C10 (Cont'd)

Parameters and Test Data of I-Beams from Reference 41
Used for Combined Bending and Web Crippling

Specimen No.	t (in.)	h/t	R/t	N/t	N/h	F_y (ksi)	P_{test} (kips)
I-BC-10-5	0.107	48.8	1.02	28.04	0.57	45.68	5.065
I-BC-10-6	0.107	48.8	1.02	28.04	0.57	45.68	4.895
I-BC-13-1	0.107	97.9	1.17	28.04	0.29	45.68	13.870
I-BC-13-2	0.107	97.9	1.17	28.04	0.29	45.68	13.010
I-BC-13-3	0.107	97.9	1.17	28.04	0.29	45.68	12.390
I-BC-13-4	0.107	97.9	1.17	28.04	0.29	45.68	11.620
I-BC-13-5	0.107	97.9	1.17	28.04	0.29	45.68	10.490
I-BC-13-6	0.107	97.9	1.17	28.04	0.29	45.68	10.500
I-3-IOF-5	0.048	150.1	1.95	62.50	0.42	47.12	3.025
I-3-IOF-6	0.048	150.1	1.95	62.50	0.42	47.12	3.005
I-3'-IOF-1	0.046	150.0	2.04	21.74	0.14	33.46	1.810
I-3'-IOF-2	0.046	150.0	2.04	21.74	0.14	33.46	1.850
I-3'-IOF-5	0.046	150.0	2.04	65.22	0.43	33.46	2.100
I-3'-IOF-6	0.046	150.0	2.04	65.22	0.43	33.46	2.315
I-5'-IOF-5	0.060	118.8	1.56	50.00	0.42	47.13	4.155
I-5'-IOF-6	0.060	118.8	1.56	50.00	0.42	47.13	4.000
I-6-IOF-1	0.075	94.7	1.25	13.33	0.14	42.86	5.535
I-6-IOF-2	0.075	94.7	1.25	13.33	0.14	42.86	5.400
I-6-IOF-5	0.075	94.7	1.25	40.00	0.42	42.86	6.000
I-6-IOF-6	0.075	94.7	1.25	40.00	0.42	42.86	6.485
I-6-IOF-7	0.075	94.7	1.25	40.00	0.42	42.86	7.000
I-6-IOF-8	0.075	94.7	1.25	40.00	0.42	42.86	6.975
I-6"-IOF-5	0.046	150.0	2.04	65.22	0.43	33.46	2.155
I-6"-IOF-6	0.046	150.0	2.04	65.22	0.43	33.46	2.315
I-12-IOF-6	0.051	144.1	1.84	58.82	0.41	53.79	3.370
I-12'-IOF-5	0.108	48.6	1.02	27.91	0.57	45.68	12.070
I-12'-IOF-6	0.108	48.6	1.02	27.91	0.57	45.68	12.750
I-16-IOF-1	0.051	77.2	1.86	19.80	0.26	53.79	2.730
I-16-IOF-2	0.051	77.2	1.86	19.80	0.26	53.79	2.838
I-16-IOF-5	0.051	77.2	1.86	59.41	0.77	53.79	3.530
I-16-IOF-6	0.051	77.2	1.86	59.41	0.77	53.79	3.900

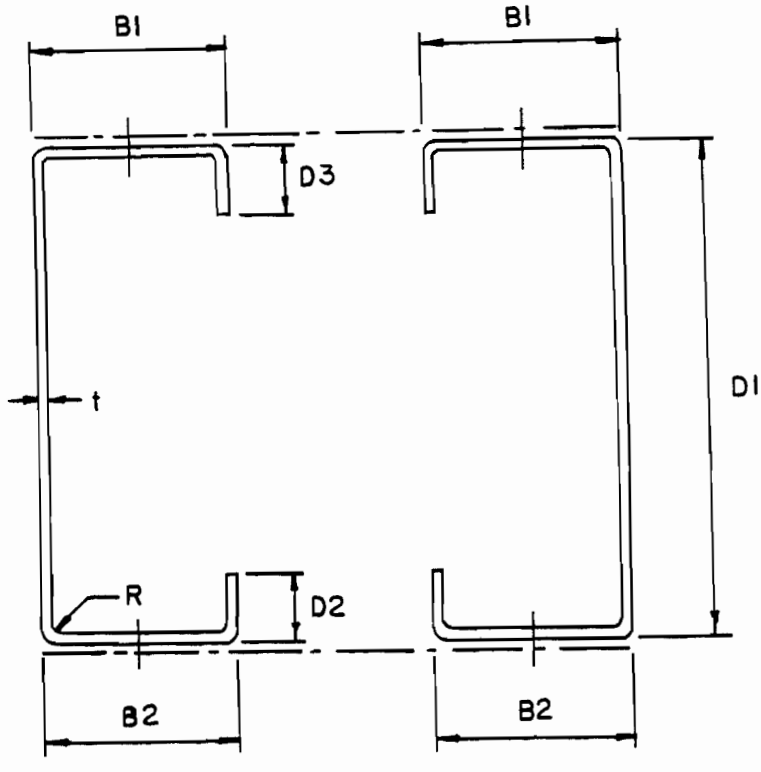

Fig. C1 Cross Section of Single Web Specimens Used in References 41 and 44

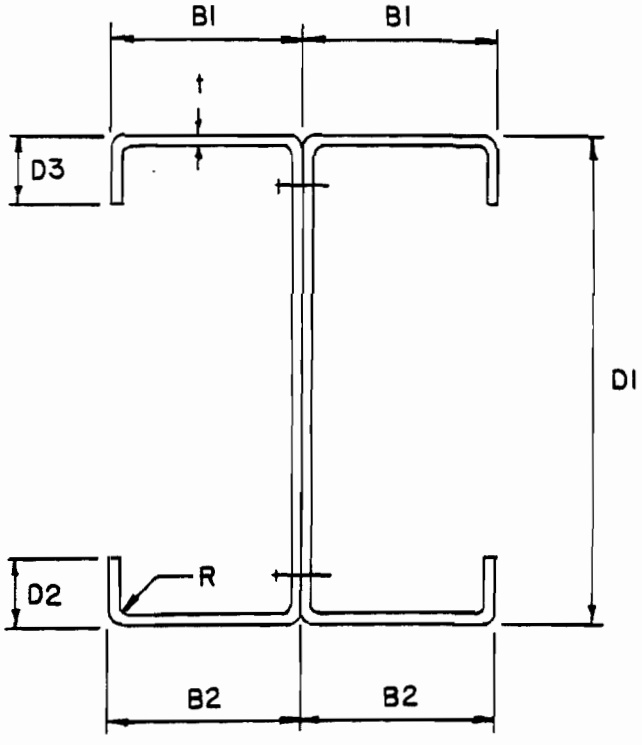

Fig. C2 Cross Section of I-Beams Used in Reference 41

APPENDIX D

COMPARISONS OF TESTED FAILURE LOADS AND PREDICTED ULTIMATE LOADS FOR THE TEST DATA USED IN THE DEVELOPMENT OF NEW EQUATIONS

Table D1

Comparisons of Tested Failure Loads and Predicted Ultimate Loads for the Test Data Used in the Development of Eq. (6.3)

Specimen No.	Type of Section	Reference	P_{test} (kips)	P_{cy} (kips)	P_{test}/P_{cy}
SU-5-IOF-1	CHANNEL	41	1.403	1.505	0.93
SU-5-IOF-2	CHANNEL	41	1.480	1.546	0.96
SU-5-IOF-3	CHANNEL	41	1.750	1.833	0.95
SU-5-IOF-4	CHANNEL	41	1.830	1.882	0.97
SU-5-IOF-5	CHANNEL	41	2.080	2.135	0.97
SU-5-IOF-6	CHANNEL	41	1.835	2.111	0.87
SU-6-IOF-1	CHANNEL	41	1.480	1.534	0.96
SU-6-IOF-2	CHANNEL	41	1.580	1.557	1.01
SU-6-IOF-3	CHANNEL	41	1.890	1.826	1.03
SU-6-IOF-4	CHANNEL	41	1.815	1.826	0.99
SU-6-IOF-5	CHANNEL	41	2.085	2.025	1.03
SU-6-IOF-6	CHANNEL	41	1.890	2.127	0.89
M-SU-6-IOF-1	CHANNEL	41	1.650	1.546	1.07
M-SU-6-IOF-2	CHANNEL	41	1.643	1.534	1.07
M-SU-6-IOF-5	CHANNEL	41	2.045	2.126	0.96
M-SU-6-IOF-6	CHANNEL	41	2.140	2.072	1.03
U-SU-17-IOF-5	CHANNEL	41	1.500	1.689	0.89
U-SU-17-IOF-6	CHANNEL	41	1.525	1.689	0.90
U-SU-18-IOF-5	CHANNEL	41	1.690	1.689	1.00
U-SU-18-IOF-6	CHANNEL	41	1.465	1.689	0.87
C3-1	CHANNEL	44	1.640	1.628	1.01
C3-2	CHANNEL	44	1.665	1.628	1.02
C3-3	CHANNEL	44	1.690	1.628	1.04
C3-4	CHANNEL	44	1.600	1.628	0.98
C3-5	CHANNEL	44	1.685	1.691	1.00
C3-6	CHANNEL	44	1.670	1.628	1.03
C3-7	CHANNEL	44	1.600	1.628	0.98
C3-8	CHANNEL	44	1.620	1.628	0.99
C3-9	CHANNEL	44	1.535	1.597	0.96
C3-10	CHANNEL	44	1.520	1.628	0.93
C3-11	CHANNEL	44	0.970	1.051	0.92
C3-12	CHANNEL	44	0.950	1.051	0.90
C3-13	CHANNEL	44	1.200	1.074	1.12
C3-14	CHANNEL	44	1.150	1.074	1.07
C3-15	CHANNEL	44	1.565	1.583	0.99
C3-16	CHANNEL	44	1.505	1.553	0.97
1-HIOF-A11	HAT	--	1.425	1.512	0.94
1-HIOF-A12	HAT	--	1.400	1.512	0.93
1-HIOF-A21	HAT	--	1.465	1.488	0.98
1-HIOF-A22	HAT	--	1.465	1.488	0.98

Table D1 (Cont'd)

Comparisons of Tested Failure Loads and Predicted Ultimate Loads for the Test Data Used in the Development of Eq. (6.3)

Specimen No.	Type of Section	Reference	P_{test} (kips)	P_{cy} (kips)	P_{test}/P_{cy}
1-HIOF-A31	HAT	--	1.450	1.488	0.97
1-HIOF-A32	HAT	--	1.500	1.488	1.01
SU-4-ITF-1	CHANNEL	41	1.715	1.635	1.05
SU-4-ITF-2	CHANNEL	41	1.725	1.648	1.05
SU-4-ITF-3	CHANNEL	41	1.915	1.846	1.04
SU-4-ITF-4	CHANNEL	41	1.980	1.887	1.05
SU-4-ITF-5	CHANNEL	41	2.210	2.212	1.00
SU-4-ITF-6	CHANNEL	41	2.310	2.133	1.08
U-SU-17-ITF-5	CHANNEL	41	1.605	1.718	0.93
U-SU-17-ITF-6	CHANNEL	41	1.605	1.688	0.95
A-7	CHANNEL	44	2.010	1.957	1.03
A-8	CHANNEL	44	2.025	1.957	1.03
C1-7	CHANNEL	44	2.000	1.988	1.01
C1-8	CHANNEL	44	1.990	1.917	1.04
C1-9	CHANNEL	44	1.975	1.917	1.03
C1-10	CHANNEL	44	2.005	1.988	1.01
C1-15	CHANNEL	44	1.320	1.355	0.97
C1-16	CHANNEL	44	1.175	1.344	0.87
C1-17	CHANNEL	44	1.450	1.355	1.07
C1-18	CHANNEL	44	1.395	1.344	1.04
C1-19	CHANNEL	44	2.115	2.165	0.98
C1-20	CHANNEL	44	2.130	2.244	0.95
1-HITF-A11	HAT	--	1.650	1.435	1.15
1-HITF-A12	HAT	--	1.625	1.435	1.13
1-HITF-A21	HAT	--	1.650	1.435	1.15
1-HITF-A22	HAT	--	1.625	1.435	1.13
1-HITF-A31	HAT	--	1.600	1.435	1.11
1-HITF-A32	HAT	--	1.625	1.435	1.13
2-HITF-A11	HAT	--	6.875	7.279	0.94
2-HITF-A12	HAT	--	6.900	7.279	0.95
2-HITF-A21	HAT	--	6.875	7.279	0.94
2-HITF-A22	HAT	--	6.800	7.279	0.93
2-HITF-A31	HAT	--	6.875	7.279	0.94
2-HITF-A32	HAT	--	6.900	7.279	0.95
Mean Value					0.997
Standard Deviation					0.067

Table D2

Comparisons of Tested Failure Loads and Predicted Ultimate Loads for the Test Data Used in the Development of Eq. (6.4)

Specimen No.	Type of Section	Reference	P_{test} (kips)	P_{cb} (kips)	P_{test}/P_{cb}
SU-1-IOF-1	CHANNEL	41	1.260	1.186	1.06
SU-1-IOF-2	CHANNEL	41	1.175	1.151	1.02
SU-1-IOF-5	CHANNEL	41	1.450	1.719	0.84
SU-1-IOF-6	CHANNEL	41	1.385	1.676	0.83
SU-2-IOF-1	CHANNEL	41	1.145	1.069	1.07
SU-2-IOF-2	CHANNEL	41	1.305	1.131	1.15
SU-2-IOF-5	CHANNEL	41	1.385	1.361	1.02
SU-2-IOF-6	CHANNEL	41	1.455	1.436	1.01
C3-17	CHANNEL	44	1.835	1.987	0.92
C3-18	CHANNEL	44	1.800	1.949	0.92
C3-19	CHANNEL	44	1.825	1.789	1.02
C3-20	CHANNEL	44	1.770	1.789	0.99
3-HIOF-A11	HAT	--	4.290	4.105	1.04
3-HIOF-A12	HAT	--	4.300	4.108	1.05
3-HIOF-A21	HAT	--	4.290	4.099	1.05
3-HIOF-A22	HAT	--	4.265	4.102	1.04
3-HIOF-A31	HAT	--	4.325	4.103	1.05
3-HIOF-A32	HAT	--	4.350	4.098	1.06
4-HIOF-A11	HAT	--	2.720	2.370	1.15
4-HIOF-A12	HAT	--	2.600	2.373	1.10
4-HIOF-A21	HAT	--	2.725	2.375	1.15
4-HIOF-A22	HAT	--	2.740	2.379	1.15
4-HIOF-A31	HAT	--	2.700	2.359	1.14
4-HIOF-A32	HAT	--	2.630	2.359	1.12
4-HIOF-A13	HAT	--	2.490	2.343	1.06
4-HIOF-A14	HAT	--	2.475	2.343	1.06
4-HIOF-A23	HAT	--	2.625	2.394	1.10
4-HIOF-A24	HAT	--	2.665	2.395	1.11
4-HIOF-A33	HAT	--	2.575	2.349	1.10
4-HIOF-A34	HAT	--	2.610	2.349	1.11
5-HIOF-A11	HAT	--	2.365	2.251	1.05
5-HIOF-A12	HAT	--	2.325	2.250	1.03
5-HIOF-A21	HAT	--	2.500	2.258	1.11
5-HIOF-A22	HAT	--	2.535	2.255	1.12
5-HIOF-A31	HAT	--	2.465	2.257	1.09
5-HIOF-A32	HAT	--	2.435	2.260	1.08
3-HIOF-D11	HAT	--	4.363	5.024	0.87
3-HIOF-D12	HAT	--	4.275	5.024	0.85
3-HIOF-C11	HAT	--	4.225	4.858	0.87
3-HIOF-C12	HAT	--	4.250	4.858	0.87

Table D2 (Cont'd)

Comparisons of Tested Failure Loads and Predicted Ultimate Loads for the Test Data Used in the Development of Eq. (6.4)

Specimen No.	Type of Section	Reference	P_{test} (kips)	P_{cb} (kips)	P_{test}/P_{cb}
3-HIOF-B11	HAT	--	4.150	4.693	0.88
3-HIOF-B12	HAT	--	4.188	4.693	0.89
3-HIOF-D21	HAT	--	4.375	5.024	0.87
3-HIOF-D22	HAT	--	4.325	5.024	0.86
3-HIOF-C21	HAT	--	4.175	4.858	0.86
3-HIOF-C22	HAT	--	4.150	4.858	0.85
3-HIOF-B21	HAT	--	4.100	4.693	0.87
3-HIOF-B22	HAT	--	4.063	4.693	0.87
3-HIOF-D31	HAT	--	4.500	5.024	0.90
3-HIOF-D32	HAT	--	4.400	5.024	0.88
3-HIOF-C31	HAT	--	4.188	4.858	0.86
3-HIOF-C32	HAT	--	4.200	4.858	0.86
3-HIOF-B31	HAT	--	4.087	4.693	0.87
3-HIOF-B32	HAT	--	4.250	4.693	0.91
5-HIOF-D11	HAT	--	2.450	2.516	0.97
5-HIOF-D12	HAT	--	2.500	2.516	0.99
5-HIOF-C11	HAT	--	2.475	2.433	1.02
5-HIOF-C12	HAT	--	2.400	2.433	0.99
5-HIOF-B11	HAT	--	2.587	2.350	1.10
5-HIOF-B12	HAT	--	2.600	2.350	1.11
5-HIOF-D21	HAT	--	2.587	2.516	1.03
5-HIOF-D22	HAT	--	2.500	2.516	0.99
5-HIOF-C21	HAT	--	2.537	2.433	1.04
5-HIOF-C22	HAT	--	2.613	2.433	1.07
5-HIOF-B21	HAT	--	2.537	2.350	1.08
5-HIOF-B22	HAT	--	2.600	2.350	1.11
5-HIOF-D31	HAT	--	2.688	2.516	1.07
5-HIOF-D32	HAT	--	2.712	2.516	1.08
5-HIOF-C31	HAT	--	2.675	2.433	1.10
5-HIOF-C32	HAT	--	2.650	2.433	1.09
5-HIOF-B31	HAT	--	2.762	2.350	1.18
5-HIOF-B32	HAT	--	2.700	2.350	1.15
Mean Value					1.011
Standard Deviation					0.102

Table D3

Comparisons of Tested Failure Loads and Predicted Ultimate Loads for the Test Data Used in the Development of Eq. (6.5)

Specimen No.	Type of Section	Reference	P_{test} (kips)	P_{cy} (kips)	P_{test}/P_{cy}
SU-1-EOF-1	CHANNEL	41	0.575	0.431	1.34
SU-1-EOF-2	CHANNEL	41	0.505	0.447	1.13
SU-2-EOF-1	CHANNEL	41	0.495	0.464	1.07
SU-2-EOF-2	CHANNEL	41	0.505	0.447	1.13
SU-4-EOF-1	CHANNEL	41	0.898	0.827	1.09
SU-4-EOF-2	CHANNEL	41	0.905	0.891	1.02
SU-4-EOF-3	CHANNEL	41	1.038	0.980	1.06
SU-4-EOF-4	CHANNEL	41	1.000	0.961	1.04
SU-4-EOF-5	CHANNEL	41	1.125	1.176	0.96
SU-4-EOF-6	CHANNEL	41	1.105	1.109	1.00
SU-5-EOF-1	CHANNEL	41	0.880	0.779	1.13
SU-5-EOF-2	CHANNEL	41	0.838	0.854	0.98
SU-5-EOF-3	CHANNEL	41	0.990	0.979	1.01
SU-5-EOF-4	CHANNEL	41	0.970	0.888	1.09
SU-6-EOF-1	CHANNEL	41	0.888	0.827	1.07
SU-6-EOF-2	CHANNEL	41	0.875	0.758	1.15
SU-6-EOF-4	CHANNEL	41	0.935	0.851	1.10
M-SU-4-EOF-1	CHANNEL	41	0.875	0.807	1.08
M-SU-4-EOF-2	CHANNEL	41	0.873	0.808	1.08
M-SU-4-EOF-5	CHANNEL	41	1.483	1.163	1.28
M-SU-4-EOF-6	CHANNEL	41	1.406	1.084	1.30
M-SU-6-EOF-1	CHANNEL	41	0.850	0.783	1.09
M-SU-6-EOF-2	CHANNEL	41	0.869	0.799	1.09
U-SU-17-EOF-1	CHANNEL	41	0.628	0.821	0.76
U-SU-17-EOF-2	CHANNEL	41	0.598	0.821	0.73
U-SU-17-EOF-5	CHANNEL	41	0.898	1.149	0.78
U-SU-17-EOF-6	CHANNEL	41	0.835	1.127	0.74
C2-3	CHANNEL	44	0.845	0.918	0.92
C2-4	CHANNEL	44	0.803	0.936	0.86
C2-5	CHANNEL	44	0.945	0.900	1.05
C2-6	CHANNEL	44	0.925	0.918	1.01
C2-7	CHANNEL	44	0.983	0.918	1.07
C2-8	CHANNEL	44	1.013	0.936	1.08
C2-9	CHANNEL	44	0.940	0.918	1.02
C2-10	CHANNEL	44	0.935	0.918	1.02
C2-13	CHANNEL	44	0.833	0.989	0.84
C2-14	CHANNEL	44	0.908	0.989	0.92
C2-15	CHANNEL	44	1.085	0.989	1.10
C2-16	CHANNEL	44	1.035	0.965	1.07
C2-17	CHANNEL	44	1.143	0.965	1.18

Table D3 (Cont'd)

Comparisons of Tested Failure Loads and Predicted Ultimate Loads for the Test Data Used in the Development of Eq. (6.5)

Specimen No.	Type of Section	Reference	P_{test} (kips)	P_{cy} (kips)	P_{test}/P_{cy}
C2-18	CHANNEL	44	1.140	0.965	1.18
C2-19	CHANNEL	44	1.063	0.942	1.13
C2-20	CHANNEL	44	1.055	0.965	1.09
1-HEOF-A11	HAT	--	0.719	0.642	1.12
1-HEOF-A12	HAT	--	0.700	0.642	1.09
1-HEOF-A21	HAT	--	0.694	0.642	1.08
1-HEOF-A22	HAT	--	0.688	0.642	1.07
1-HEOF-A31	HAT	--	0.669	0.642	1.04
1-HEOF-A32	HAT	--	0.643	0.642	1.00
2-HEOF-A11	HAT	--	2.919	2.607	1.12
2-HEOF-A12	HAT	--	2.981	2.960	1.01
2-HEOF-A21	HAT	--	2.994	2.776	1.08
2-HEOF-A22	HAT	--	3.125	3.147	0.99
2-HEOF-A31	HAT	--	2.713	2.776	0.98
2-HEOF-A32	HAT	--	2.825	2.960	0.95
3-HEOF-A11	HAT	--	2.050	2.087	0.98
3-HEOF-A12	HAT	--	2.106	2.087	1.01
3-HEOF-A21	HAT	--	2.006	2.087	0.96
3-HEOF-A22	HAT	--	2.075	2.087	0.99
3-HEOF-A31	HAT	--	1.894	2.087	0.91
3-HEOF-A32	HAT	--	1.869	2.087	0.90
Mean Value					1.034
Standard Deviation					0.119

Table D4

Comparisons of Tested Failure Loads and Predicted Ultimate Loads for the Test Data Used in the Development of Eq. (6.6)

Specimen No.	Type of Section	Reference	P_{test} (kips)	P_{cb} (kips)	P_{test}/P_{cb}
SU-1-EOF-5	CHANNEL	41	0.650	0.568	1.14
SU-1-EOF-6	CHANNEL	41	0.620	0.592	1.05
SU-2-EOF-5	CHANNEL	41	0.560	0.562	1.00
SU-2-EOF-6	CHANNEL	41	0.560	0.537	1.04
SU-5-EOF-5	CHANNEL	41	1.006	1.103	0.91
SU-5-EOF-6	CHANNEL	41	1.068	1.073	1.00
SU-6-EOF-3	CHANNEL	41	0.903	0.933	0.97
SU-6-EOF-5	CHANNEL	41	1.045	1.043	1.00
SU-6-EOF-6	CHANNEL	41	1.119	1.043	1.07
M-SU-6-EOF-5	CHANNEL	41	1.175	1.045	1.12
M-SU-6-EOF-6	CHANNEL	41	1.180	1.108	1.06
U-SU-18-EOF-1	CHANNEL	41	0.472	0.548	0.86
U-SU-18-EOF-2	CHANNEL	41	0.428	0.561	0.76
U-SU-18-EOF-5	CHANNEL	41	0.568	0.637	0.89
U-SU-18-EOF-6	CHANNEL	41	0.545	0.587	0.93
4-HEOF-A11	HAT	--	1.313	1.340	0.98
4-HEOF-A12	HAT	--	1.300	1.314	0.99
4-HEOF-A21	HAT	--	1.219	1.192	1.02
4-HEOF-A22	HAT	--	1.125	1.190	0.95
4-HEOF-A31	HAT	--	1.088	1.068	1.02
4-HEOF-A32	HAT	--	1.063	1.068	1.00
5-HEOF-A11	HAT	--	1.295	1.259	1.03
5-HEOF-A12	HAT	--	1.285	1.255	1.02
5-HEOF-A21	HAT	--	1.200	1.135	1.06
5-HEOF-A22	HAT	--	1.178	1.132	1.04
5-HEOF-A31	HAT	--	1.050	1.010	1.04
5-HEOF-A32	HAT	--	1.035	1.009	1.03
Mean Value					0.999
Standard Deviation					0.079

Table D5

Comparisons of Tested Failure Loads and Predicted Ultimate Loads for the Test Data Used in the Development of Eq. (6.7)

Specimen No.	Type of Section	Reference	P_{test} (kips)	P_{cb} (kips)	P_{test}/P_{cb}
SU-1-ITF-1	CHANNEL	41	0.770	0.829	0.93
SU-1-ITF-2	CHANNEL	41	0.785	0.813	0.97
SU-1-ITF-5	CHANNEL	41	0.795	0.962	0.83
SU-1-ITF-6	CHANNEL	41	0.820	0.922	0.89
SU-2-ITF-1	CHANNEL	41	0.610	0.753	0.81
SU-2-ITF-2	CHANNEL	41	0.610	0.739	0.83
SU-2-ITF-5	CHANNEL	41	0.630	0.860	0.73
SU-2-ITF-6	CHANNEL	41	0.595	0.827	0.72
SU-5-ITF-1	CHANNEL	41	1.508	1.492	1.01
SU-5-ITF-2	CHANNEL	41	1.530	1.517	1.01
SU-5-ITF-3	CHANNEL	41	1.550	1.717	0.90
SU-5-ITF-4	CHANNEL	41	1.710	1.692	1.01
SU-5-ITF-5	CHANNEL	41	1.620	1.687	0.96
SU-5-ITF-6	CHANNEL	41	1.610	1.706	0.94
SU-6-ITF-1	CHANNEL	41	1.465	1.102	1.33
SU-6-ITF-2	CHANNEL	41	1.233	1.103	1.12
SU-6-ITF-3	CHANNEL	41	1.225	1.246	0.98
SU-6-ITF-4	CHANNEL	41	1.280	1.209	1.06
SU-6-ITF-5	CHANNEL	41	1.330	1.342	0.99
SU-6-ITF-6	CHANNEL	41	1.250	1.249	1.00
U-SU-19-ITF-5	CHANNEL	41	0.750	1.018	0.74
U-SU-19-ITF-6	CHANNEL	41	0.745	1.004	0.74
A-3	CHANNEL	44	0.870	0.868	1.00
A-4	CHANNEL	44	0.860	0.848	1.01
A-5	CHANNEL	44	1.535	1.420	1.08
A-6	CHANNEL	44	1.510	1.424	1.06
A-21	CHANNEL	44	0.775	0.806	0.96
A-22	CHANNEL	44	0.750	0.788	0.95
A-23	CHANNEL	44	1.490	1.369	1.09
A-24	CHANNEL	44	1.570	1.336	1.18
A-25	CHANNEL	44	1.990	2.186	0.91
A-26	CHANNEL	44	2.005	2.135	0.94
C1-3	CHANNEL	44	1.300	1.082	0.92
C1-4	CHANNEL	44	1.150	1.081	1.06
C1-5	CHANNEL	44	1.670	1.816	0.92
C1-6	CHANNEL	44	1.860	1.819	1.02
C1-13	CHANNEL	44	0.710	0.745	0.95
C1-14	CHANNEL	44	0.745	0.743	1.00
3-HITF-A11	HAT	--	5.050	5.381	0.94
3-HITF-A12	HAT	--	5.150	5.440	0.95

Table D5 (Cont'd)

Comparisons of Tested Failure Loads and Predicted Ultimate Loads for the Test Data Used in the Development of Eq. (6.7)

Specimen No.	Type of Section	Reference	P_{test} (kips)	P_{cb} (kips)	P_{test}/P_{cb}
3-HITF-A21	HAT	--	4.850	5.199	0.93
3-HITF-A22	HAT	--	4.800	5.199	0.92
3-HITF-A31	HAT	--	4.800	4.909	0.98
3-HITF-A32	HAT	--	4.700	4.909	0.96
5-HITF-A11	HAT	--	2.950	2.524	1.17
5-HITF-A12	HAT	--	3.000	2.524	1.19
5-HITF-A21	HAT	--	2.775	2.411	1.15
5-HITF-A22	HAT	--	2.750	2.396	1.15
5-HITF-A31	HAT	--	2.625	2.189	1.20
5-HITF-A32	HAT	--	2.613	2.178	1.20
Mean Value					0.986
Standard Deviation					0.130

Table D6

Comparisons of Tested Failure Loads and Predicted Ultimate Loads for the Test Data Used in the Development of Eq. (6.8)

Specimen No.	Type of Section	Reference	P_{test} (kips)	P_{cb} (kips)	P_{test}/P_{cb}
SU-1-ETF-1	CHANNEL	41	0.320	0.329	0.97
SU-1-ETF-2	CHANNEL	41	0.310	0.351	0.88
SU-1-ETF-5	CHANNEL	41	0.380	0.400	0.95
SU-1-ETF-6	CHANNEL	41	0.355	0.412	0.86
SU-2-ETF-1	CHANNEL	41	0.280	0.259	1.08
SU-2-ETF-2	CHANNEL	41	0.280	0.302	0.93
SU-2-ETF-5	CHANNEL	41	0.315	0.280	1.13
SU-2-ETF-6	CHANNEL	41	0.290	0.327	0.89
SU-4-ETF-1	CHANNEL	41	0.685	0.654	1.05
SU-4-ETF-2	CHANNEL	41	0.668	0.702	0.95
SU-4-ETF-3	CHANNEL	41	0.745	0.754	0.99
SU-4-ETF-4	CHANNEL	41	0.750	0.756	0.99
SU-4-ETF-5	CHANNEL	41	0.765	0.787	0.97
SU-4-ETF-6	CHANNEL	41	0.775	0.787	0.98
SU-5-ETF-1	CHANNEL	41	0.600	0.606	0.99
SU-5-ETF-2	CHANNEL	41	0.615	0.613	1.00
SU-5-ETF-3	CHANNEL	41	0.615	0.659	0.93
SU-5-ETF-4	CHANNEL	41	0.625	0.642	0.97
SU-5-ETF-5	CHANNEL	41	0.685	0.718	0.95
SU-5-ETF-6	CHANNEL	41	0.675	0.697	0.97
SU-6-ETF-1	CHANNEL	41	0.585	0.507	1.15
SU-6-ETF-2	CHANNEL	41	0.545	0.534	1.02
SU-6-ETF-3	CHANNEL	41	0.608	0.545	1.12
SU-6-ETF-4	CHANNEL	41	0.595	0.559	1.06
SU-6-ETF-5	CHANNEL	41	0.665	0.590	1.13
SU-6-ETF-6	CHANNEL	41	0.660	0.607	1.09
U-SU-17-ETF-5	CHANNEL	41	0.780	0.732	1.07
U-SU-17-ETF-6	CHANNEL	41	0.755	0.751	1.00
U-SU-19-ETF-5	CHANNEL	41	0.455	0.454	1.00
U-SU-19-ETF-6	CHANNEL	41	0.470	0.455	1.03
A-9	CHANNEL	44	0.485	0.449	1.08
A-10	CHANNEL	44	0.500	0.447	1.12
A-11	CHANNEL	44	0.540	0.510	1.06
A-12	CHANNEL	44	0.520	0.509	1.02
A-13	CHANNEL	44	0.505	0.565	0.89
A-14	CHANNEL	44	0.505	0.566	0.89
A-15	CHANNEL	44	0.640	0.596	1.07
A-16	CHANNEL	44	0.625	0.596	1.05
A-17	CHANNEL	44	0.670	0.645	1.04
A-18	CHANNEL	44	0.655	0.646	1.01

Table D6 (Cont'd)

Comparisons of Tested Failure Loads and Predicted Ultimate Loads for the Test Data Used in the Development of Eq. (6.8)

Specimen No.	Type of Section	Reference	P_{test} (kips)	P_{cb} (kips)	P_{test}/P_{cb}
A-27	CHANNEL	44	0.425	0.421	1.01
A-28	CHANNEL	44	0.415	0.412	1.01
A-29	CHANNEL	44	0.470	0.475	0.99
A-30	CHANNEL	44	0.450	0.474	0.95
A-31	CHANNEL	44	0.525	0.537	0.98
A-32	CHANNEL	44	0.500	0.525	0.95
A-33	CHANNEL	44	0.505	0.577	0.88
A-34	CHANNEL	44	0.555	0.577	0.96
A-35	CHANNEL	44	0.565	0.613	0.92
A-36	CHANNEL	44	0.580	0.614	0.95
1-HETF-A11	HAT	--	0.725	0.775	0.94
1-HETF-A12	HAT	--	0.713	0.770	0.93
1-HETF-A21	HAT	--	0.725	0.676	1.07
1-HETF-A22	HAT	--	0.725	0.673	1.08
1-HETF-A31	HAT	--	0.650	0.603	1.08
1-HETF-A32	HAT	--	0.662	0.603	1.10
2-HETF-A11	HAT	--	2.825	3.043	0.93
2-HETF-A12	HAT	--	2.787	3.043	0.92
2-HETF-A21	HAT	--	2.700	2.717	0.99
2-HETF-A22	HAT	--	2.650	2.717	0.98
2-HETF-A31	HAT	--	2.425	2.489	0.97
2-HETF-A32	HAT	--	2.400	2.493	0.96
3-HETF-A11	HAT	--	1.525	1.578	0.97
3-HETF-A12	HAT	--	1.600	1.573	1.02
3-HETF-A21	HAT	--	1.413	1.396	1.01
3-HETF-A22	HAT	--	1.487	1.399	1.06
3-HETF-A31	HAT	--	1.300	1.261	1.03
3-HETF-A32	HAT	--	1.312	1.266	1.04
5-HETF-A11	HAT	--	0.750	0.739	1.01
5-HETF-A12	HAT	--	0.762	0.741	1.03
5-HETF-A21	HAT	--	0.675	0.641	1.05
5-HETF-A22	HAT	--	0.700	0.641	1.09
5-HETF-A31	HAT	--	0.612	0.576	1.06
5-HETF-A32	HAT	--	0.600	0.577	1.04
Mean Value					1.004
Standard Deviation					0.067

Table D7

Comparisons of Tested Failure Loads and Predicted Ultimate Loads for the Test Data Used in the Development of Eq. (6.10)

Specimen No.	Type of Section	Reference	P_{test} (kips)	P_{cb} (kips)	P_{test}/P_{cb}
I-1-IOF-1	I-BEAM	41	2.385	2.221	1.07
I-1-IOF-2	I-BEAM	41	2.490	2.218	1.12
I-1-IOF-5	I-BEAM	41	2.910	2.744	1.06
I-1-IOF-6	I-BEAM	41	2.850	2.747	1.04
I-2-IOF-1	I-BEAM	41	2.420	2.211	1.09
I-2-IOF-2	I-BEAM	41	2.470	2.307	1.07
I-2-IOF-5	I-BEAM	41	2.860	2.584	1.11
I-2-IOF-6	I-BEAM	41	2.950	2.755	1.07
I-3-IOF-1	I-BEAM	41	2.505	2.484	1.01
I-3-IOF-2	I-BEAM	41	2.450	2.590	0.95
I-12-IOF-1	I-BEAM	41	2.645	2.640	1.00
I-12-IOF-2	I-BEAM	41	2.660	2.749	0.97
I-12-IOF-5	I-BEAM	41	3.365	3.417	0.98
I-U-18-IOF-5	I-BEAM	41	2.730	2.904	0.94
I-U-18-IOF-6	I-BEAM	41	2.565	2.906	0.88
1-IIOF-A11	I-BEAM	--	2.450	2.886	0.85
1-IIOF-A12	I-BEAM	--	2.400	2.886	0.83
1-IIOF-A21	I-BEAM	--	2.625	2.886	0.91
1-IIOF-A22	I-BEAM	--	2.450	2.886	0.85
1-IIOF-A31	I-BEAM	--	2.325	2.886	0.81
1-IIOF-A32	I-BEAM	--	2.350	2.886	0.81
2-IIOF-A11	I-BEAM	--	8.750	9.172	0.95
2-IIOF-A12	I-BEAM	--	8.775	9.172	0.96
2-IIOF-A21	I-BEAM	--	9.300	9.172	1.01
2-IIOF-A22	I-BEAM	--	9.463	9.172	1.03
2-IIOF-A31	I-BEAM	--	9.175	9.172	1.00
2-IIOF-A32	I-BEAM	--	9.500	9.172	1.04
3-IIOF-A11	I-BEAM	--	6.175	5.942	1.04
3-IIOF-A12	I-BEAM	--	6.325	5.942	1.06
3-IIOF-A21	I-BEAM	--	6.825	5.942	1.15
3-IIOF-A22	I-BEAM	--	6.563	5.942	1.10
3-IIOF-A31	I-BEAM	--	5.912	5.942	0.99
3-IIOF-A32	I-BEAM	--	6.250	5.942	1.05
5-IIOF-A11	I-BEAM	--	3.275	2.886	1.13
5-IIOF-A12	I-BEAM	--	3.117	2.886	1.08
5-IIOF-A21	I-BEAM	--	3.100	2.886	1.07
5-IIOF-A22	I-BEAM	--	3.175	2.886	1.10
5-IIOF-A31	I-BEAM	--	3.075	2.886	1.07
5-IIOF-A32	I-BEAM	--	3.200	2.886	1.11
Mean Value					1.010
Standard Deviation					0.093

Table D8

Comparisons of Tested Failure Loads and Predicted Ultimate Loads for the Test Data Used in the Development of Eq. (6.11)

Specimen No.	Type of Section	Reference	P_{test} (kips)	P_{cb} (kips)	P_{test}/P_{cb}
I-1-EOF-1	I-BEAM	41	1.840	2.017	0.91
I-1-EOF-2	I-BEAM	41	1.770	1.966	0.90
I-1-EOF-5	I-BEAM	41	2.175	2.115	1.03
I-1-EOF-6	I-BEAM	41	2.210	2.011	1.10
I-2-EOF-1	I-BEAM	41	1.730	2.035	0.85
I-2-EOF-2	I-BEAM	41	1.650	1.985	0.83
I-2-EOF-5	I-BEAM	41	2.305	2.205	1.05
I-2-EOF-6	I-BEAM	41	2.375	2.315	1.03
I-3-EOF-1	I-BEAM	41	2.355	2.311	1.02
I-3-EOF-2	I-BEAM	41	2.470	2.407	1.03
I-3-EOF-5	I-BEAM	41	2.990	2.546	1.17
I-3-EOF-6	I-BEAM	41	2.750	2.496	1.10
I-3'-EOF-1	I-BEAM	41	1.890	2.044	0.92
I-3'-EOF-2	I-BEAM	41	1.690	2.036	0.83
I-3'-EOF-5	I-BEAM	41	2.390	2.255	1.06
I-3'-EOF-6	I-BEAM	41	2.440	2.249	1.09
I-5'-EOF-5	I-BEAM	41	4.120	3.718	1.11
I-5'-EOF-6	I-BEAM	41	4.470	3.717	1.20
I-6-EOF-1	I-BEAM	41	5.200	5.415	0.96
I-6-EOF-2	I-BEAM	41	5.385	5.444	0.99
I-6-EOF-5	I-BEAM	41	5.630	5.845	0.96
I-6-EOF-6	I-BEAM	41	5.315	5.865	0.91
I-6-EOF-7	I-BEAM	41	5.635	6.197	0.91
I-6"-EOF-1	I-BEAM	41	1.780	2.045	0.87
I-6"-EOF-2	I-BEAM	41	1.920	2.082	0.92
I-6"-EOF-5	I-BEAM	41	2.540	2.242	1.13
I-6"-EOF-6	I-BEAM	41	2.350	2.256	1.04
I-9-EOF-1	I-BEAM	41	2.075	2.037	1.02
I-9-EOF-2	I-BEAM	41	1.825	2.037	0.90
I-9-EOF-5	I-BEAM	41	2.510	2.246	1.12
I-9-EOF-6	I-BEAM	41	2.565	2.236	1.15
I-12-EOF-1	I-BEAM	41	2.470	2.504	0.99
I-12-EOF-2	I-BEAM	41	2.505	2.436	1.03
I-12-EOF-5	I-BEAM	41	2.960	2.717	1.09
I-12-EOF-6	I-BEAM	41	2.830	2.712	1.04
I-12'-EOF-5	I-BEAM	41	10.250	12.135	0.84
I-12'-EOF-6	I-BEAM	41	11.580	12.051	0.96
I-16-EOF-5	I-BEAM	41	3.050	2.689	1.13
I-16-EOF-6	I-BEAM	41	3.150	2.717	1.16
I-U-17-EOF-5	I-BEAM	41	2.555	2.569	0.99

Table D8 (Cont'd)

Comparisons of Tested Failure Loads and Predicted Ultimate Loads for the Test Data Used in the Development of Eq. (6.11)

Specimen No.	Type of Section	Reference	P_{test} (kips)	P_{cb} (kips)	P_{test}/P_{cb}
I-U-17-EOF-6	I-BEAM	41	2.230	2.553	0.87
I-U-18-EOF-5	I-BEAM	41	2.040	2.337	0.87
I-U-18-EOF-6	I-BEAM	41	2.285	2.392	0.96
1-IEOF-A11	I-BEAM	--	2.830	2.637	1.07
1-IEOF-A12	I-BEAM	--	2.750	2.651	1.04
1-IEOF-A21	I-BEAM	--	2.630	2.553	1.03
1-IEOF-A22	I-BEAM	--	2.675	2.546	1.05
1-IEOF-A31	I-BEAM	--	2.750	2.532	1.09
1-IEOF-A32	I-BEAM	--	2.695	2.540	1.06
2-IEOF-A11	I-BEAM	--	8.017	7.730	1.04
2-IEOF-A12	I-BEAM	--	8.100	7.749	1.05
2-IEOF-A21	I-BEAM	--	7.850	7.474	1.05
2-IEOF-A22	I-BEAM	--	7.600	7.458	1.02
2-IEOF-A31	I-BEAM	--	7.625	7.382	1.03
2-IEOF-A32	I-BEAM	--	7.775	7.379	1.05
3-IEOF-A11	I-BEAM	--	4.395	4.467	0.98
3-IEOF-A12	I-BEAM	--	4.370	4.425	0.99
3-IEOF-A21	I-BEAM	--	4.250	4.273	0.99
3-IEOF-A22	I-BEAM	--	4.125	4.257	0.97
3-IEOF-A31	I-BEAM	--	4.125	4.231	0.98
3-IEOF-A32	I-BEAM	--	4.000	4.232	0.95
5-IEOF-A11	I-BEAM	--	2.217	2.422	0.92
5-IEOF-A12	I-BEAM	--	2.175	2.416	0.90
5-IEOF-A21	I-BEAM	--	2.200	2.343	0.94
5-IEOF-A22	I-BEAM	--	2.075	2.337	0.89
5-IEOF-A31	I-BEAM	--	2.117	2.323	0.91
5-IEOF-A32	I-BEAM	--	2.015	2.329	0.87
Mean Value					0.998
Standard Deviation					0.090

Table D9

Comparisons of Tested Failure Loads and Predicted Ultimate Loads for the Test Data Used in the Development of Eq. (6.12)

Specimen No.	Type of Section	Reference	P_{test} (kips)	P_{cb} (kips)	P_{test}/P_{cb}
I-1-ITF-1	I-BEAM	41	1.625	1.677	0.97
I-1-ITF-2	I-BEAM	41	1.665	1.787	0.93
I-1-ITF-5	I-BEAM	41	1.875	1.801	1.04
I-1-ITF-6	I-BEAM	41	1.920	1.881	1.02
I-2-ITF-1	I-BEAM	41	1.490	1.771	0.84
I-2-ITF-2	I-BEAM	41	1.520	1.735	0.88
I-2-ITF-5	I-BEAM	41	1.715	1.780	0.96
I-2-ITF-6	I-BEAM	41	1.690	1.856	0.91
I-3-ITF-1	I-BEAM	41	1.915	1.968	0.97
I-3-ITF-2	I-BEAM	41	2.080	1.967	1.06
I-3-ITF-5	I-BEAM	41	2.375	2.460	0.97
I-3-ITF-6	I-BEAM	41	2.205	2.361	0.93
I-3-ITF-1*	I-BEAM	41	2.090	1.890	1.11
I-3-ITF-2*	I-BEAM	41	2.170	1.967	1.10
I-3-ITF-5*	I-BEAM	41	2.205	2.408	0.92
I-3-ITF-6*	I-BEAM	41	2.335	2.359	0.99
I-5'-ITF-5	I-BEAM	41	3.775	3.696	1.02
I-5'-ITF-6	I-BEAM	41	4.270	3.755	1.14
I-6-ITF-1	I-BEAM	41	4.480	4.428	1.01
I-6-ITF-2	I-BEAM	41	4.570	4.440	1.03
I-6-ITF-5	I-BEAM	41	4.975	5.588	0.89
I-6-ITF-6	I-BEAM	41	5.300	5.572	0.95
I-6-ITF-7	I-BEAM	41	5.956	5.705	1.04
I-6-ITF-8	I-BEAM	41	6.195	5.691	1.09
I-6"-ITF-2	I-BEAM	41	1.958	1.700	1.15
I-6"-ITF-5	I-BEAM	41	2.380	2.131	1.12
I-6"-ITF-6	I-BEAM	41	2.390	2.131	1.12
1-IITF-A21	I-BEAM	--	2.775	2.971	0.93
1-IITF-A22	I-BEAM	--	2.750	2.971	0.93
1-IITF-A31	I-BEAM	--	2.188	2.271	0.96
1-IITF-A32	I-BEAM	--	2.150	2.274	0.95
2-IITF-A21	I-BEAM	--	17.000	15.937	1.07
2-IITF-A22	I-BEAM	--	16.500	15.937	1.04
2-IITF-A31	I-BEAM	--	11.850	11.809	1.00
2-IITF-A32	I-BEAM	--	12.125	11.809	1.03
3-IITF-A11	I-BEAM	--	14.125	12.841	1.10
3-IITF-A12	I-BEAM	--	14.050	12.743	1.10
3-IITF-A21	I-BEAM	--	7.188	7.416	0.97
3-IITF-A22	I-BEAM	--	7.300	7.416	0.98
3-IITF-A31	I-BEAM	--	5.375	5.210	1.03

Table D9 (Cont'd)

Comparisons of Tested Failure Loads and Predicted Ultimate Loads for the Test Data Used in the Development of Eq. (6.12)

Specimen No.	Type of Section	Reference	P_{test} (kips)	P_{cb} (kips)	P_{test}/P_{cb}
3-IITF-A32	I-BEAM	--	5.500	5.227	1.05
5-IITF-A11	I-BEAM	--	5.025	5.252	0.96
5-IITF-A12	I-BEAM	--	4.975	5.208	0.96
5-IITF-A21	I-BEAM	--	3.000	2.813	1.07
5-IITF-A22	I-BEAM	--	2.975	2.813	1.06
5-IITF-A31	I-BEAM	--	2.025	2.178	0.93
5-IITF-A32	I-BEAM	--	2.125	2.175	0.98
Mean Value					1.005
Standard Deviation					0.074

Table D10

Comparisons of Tested Failure Loads and Predicted Ultimate Loads for the Test Data Used in the Development of Eq. (6.13)

Specimen No.	Type of Section	Reference	P_{test} (kips)	P_{cb} (kips)	P_{test}/P_{cb}
I-1-ETF-1	I-BEAM	41	0.705	0.723	0.98
I-1-ETF-2	I-BEAM	41	0.690	0.753	0.92
I-1-ETF-5	I-BEAM	41	0.850	0.878	0.97
I-1-ETF-6	I-BEAM	41	0.935	0.876	1.07
I-2-ETF-1	I-BEAM	41	0.645	0.685	0.94
I-2-ETF-2	I-BEAM	41	0.665	0.656	1.01
I-2-ETF-5	I-BEAM	41	0.770	0.783	0.98
I-2-ETF-6	I-BEAM	41	0.690	0.736	0.94
I-3-ETF-1	I-BEAM	41	0.805	0.915	0.88
I-3-ETF-2	I-BEAM	41	0.850	0.894	0.95
I-3-ETF-5	I-BEAM	41	1.120	1.146	0.98
I-3-ETF-6	I-BEAM	41	1.035	1.093	0.95
I-3-ETF-1*	I-BEAM	41	0.820	0.915	0.90
I-3-ETF-2*	I-BEAM	41	0.810	0.914	0.89
I-3-ETF-5*	I-BEAM	41	1.005	1.093	0.92
I-3-ETF-6*	I-BEAM	41	0.960	1.147	0.84
I-5'-ETF-5	I-BEAM	41	1.470	1.756	0.84
I-5'-ETF-6	I-BEAM	41	1.405	1.753	0.80
I-6-ETF-1	I-BEAM	41	2.035	2.294	0.89
I-6-ETF-2	I-BEAM	41	2.105	2.289	0.92
I-6-ETF-5	I-BEAM	41	2.935	2.892	1.02
I-6-ETF-6	I-BEAM	41	3.060	2.884	1.06
I-6-ETF-7	I-BEAM	41	2.690	2.873	0.94
I-6-ETF-8	I-BEAM	41	2.400	2.954	0.81
I-6"-ETF-1	I-BEAM	41	0.885	0.808	1.09
I-6"-ETF-2	I-BEAM	41	0.845	0.766	1.10
I-6"-ETF-5	I-BEAM	41	1.065	0.968	1.10
I-6"-ETF-6	I-BEAM	41	1.095	0.969	1.13
2b-6-ETF	I-BEAM	41	1.870	1.891	0.99
3-4-ETF	I-BEAM	41	1.800	2.373	0.76
4a-6-ETF	I-BEAM	41	1.600	1.532	1.04
4a-7-ETF	I-BEAM	41	1.700	1.634	1.04
4b-4-ETF	I-BEAM	41	1.900	1.892	1.00
6a-5-ETF	I-BEAM	41	1.850	1.604	1.15
6a-6-ETF	I-BEAM	41	1.920	1.677	1.15
6b-5-ETF	I-BEAM	41	2.250	1.861	1.21
9a-3-ETF	I-BEAM	41	5.100	5.360	0.95
9b-5-ETF	I-BEAM	41	5.350	5.360	1.00
9b-6-ETF	I-BEAM	41	5.950	6.030	0.99
9b-7-ETF	I-BEAM	41	6.850	7.723	0.89
10a-6-ETF	I-BEAM	41	5.900	5.095	1.16
10a-7-ETF	I-BEAM	41	5.950	5.457	1.09
10b-5-ETF	I-BEAM	41	7.750	6.371	1.22

Table D10 (Cont'd)

Comparisons of Tested Failure Loads and Predicted Ultimate Loads for the Test Data Used in the Development of Eq. (6.13)

Specimen No.	Type of Section	Reference	P_{test} (kips)	P_{cb} (kips)	P_{test}/P_{cb}
13a-5-ETF	I-BEAM	41	6.750	8.450	0.80
13a-6-ETF	I-BEAM	41	8.500	9.518	0.89
13b-4-ETF	I-BEAM	41	12.800	12.218	1.05
14a-6-ETF	I-BEAM	41	8.900	9.517	0.94
14a-7-ETF	I-BEAM	41	11.150	10.201	1.09
14b-5-ETF	I-BEAM	41	12.300	11.929	1.03
16d-3-ETF	I-BEAM	41	0.880	0.721	1.22
16d-4-ETF	I-BEAM	41	0.920	0.836	1.10
17d-3-ETF	I-BEAM	41	2.450	2.267	1.08
17d-4-ETF	I-BEAM	41	3.060	2.632	1.16
18a-3-ETF	I-BEAM	41	6.800	6.371	1.07
18a-4-ETF	I-BEAM	41	7.500	7.392	1.01
1-IETF-A11	I-BEAM	--	1.575	1.507	1.04
1-IETF-A12	I-BEAM	--	1.562	1.510	1.03
1-IETF-A21	I-BEAM	--	1.475	1.260	1.17
1-IETF-A22	I-BEAM	--	1.512	1.264	1.20
1-IETF-A31	I-BEAM	--	1.287	1.095	1.17
1-IETF-A32	I-BEAM	--	1.225	1.098	1.12
2-IETF-A11	I-BEAM	--	5.175	5.392	0.96
2-IETF-A12	I-BEAM	--	5.050	5.368	0.94
2-IETF-A21	I-BEAM	--	4.237	4.545	0.93
2-IETF-A22	I-BEAM	--	4.350	4.557	0.95
2-IETF-A31	I-BEAM	--	4.012	4.130	0.97
2-IETF-A32	I-BEAM	--	3.950	4.127	0.96
3-IETF-A11	I-BEAM	--	2.775	2.887	0.96
3-IETF-A12	I-BEAM	--	2.700	2.899	0.93
3-IETF-A21	I-BEAM	--	2.312	2.466	0.94
3-IETF-A22	I-BEAM	--	2.275	2.466	0.92
3-IETF-A31	I-BEAM	--	2.237	2.233	1.00
3-IETF-A32	I-BEAM	--	2.300	2.237	1.03
5-IETF-A11	I-BEAM	--	1.325	1.431	0.93
5-IETF-A12	I-BEAM	--	1.312	1.440	0.91
5-IETF-A21	I-BEAM	--	1.250	1.204	1.04
5-IETF-A22	I-BEAM	--	1.175	1.202	0.98
5-IETF-A31	I-BEAM	--	1.000	1.044	0.96
5-IETF-A32	I-BEAM	--	0.962	1.048	0.92
Mean Value					0.998
Standard Deviation					0.104

Table D11

Comparisons of Tested Failure Loads and Predicted Ultimate Loads for the Test Data Used in the Development of Eq. (6.21)

Specimen No.	Type of Section	Reference	P_{test} (kips)	P_{mc} (kips)	P_{test}/P_{mc}
SU-BC-1-1	CHANNEL	41	2.280	2.181	1.05
SU-BC-1-2	CHANNEL	41	2.260	2.180	1.04
SU-BC-1-3	CHANNEL	41	1.720	1.653	1.04
SU-BC-1-4	CHANNEL	41	1.780	1.671	1.06
SU-BC-1-5	CHANNEL	41	1.220	1.172	1.04
SU-BC-1-6	CHANNEL	41	1.060	1.117	0.95
SU-BC-3-1	CHANNEL	41	2.400	2.919	0.82
SU-BC-3-2	CHANNEL	41	2.670	2.915	0.92
SU-BC-3-3	CHANNEL	41	2.210	2.548	0.87
SU-BC-3-4	CHANNEL	41	2.340	2.551	0.92
SU-BC-3-5	CHANNEL	41	1.850	2.137	0.87
SU-BC-3-6	CHANNEL	41	2.040	2.213	0.92
SU-BC-15-1	CHANNEL	41	4.180	4.446	0.94
SU-BC-15-2	CHANNEL	41	4.150	4.618	0.90
SU-BC-15-3	CHANNEL	41	3.680	3.692	1.00
SU-BC-15-4	CHANNEL	41	3.600	3.595	1.00
SU-BC-15-5	CHANNEL	41	3.000	2.951	1.02
SU-BC-15-6	CHANNEL	41	3.000	3.028	0.99
SU-4-IOF-1	CHANNEL	41	3.052	3.116	0.98
SU-4-IOF-2	CHANNEL	41	3.050	3.159	0.97
SU-4-IOF-3	CHANNEL	41	3.540	3.623	0.98
SU-4-IOF-4	CHANNEL	41	3.550	3.633	0.98
SU-4-IOF-5	CHANNEL	41	4.170	4.065	1.03
SU-4-IOF-6	CHANNEL	41	3.970	4.026	0.99
M-SU-4-IOF-1	CHANNEL	41	3.210	3.141	1.02
M-SU-4-IOF-2	CHANNEL	41	3.260	3.175	1.03
M-SU-4-IOF-5	CHANNEL	41	4.400	4.115	1.07
M-SU-4-IOF-6	CHANNEL	41	4.150	4.042	1.03
SU-BC-6-1	CHANNEL	41	1.760	1.444	1.22
SU-BC-6-2	CHANNEL	41	1.680	1.449	1.16
SU-BC-6-3	CHANNEL	41	1.130	1.061	1.06
SU-BC-16-1	CHANNEL	41	2.880	2.662	1.08
SU-BC-16-2	CHANNEL	41	2.700	2.595	1.04
SU-BC-16-3	CHANNEL	41	2.010	1.946	1.03
SU-BC-16-4	CHANNEL	41	2.210	2.106	1.05
SU-BC-7-1	CHANNEL	41	2.000	1.768	1.13
SU-BC-7-2	CHANNEL	41	1.880	1.712	1.10
SU-BC-7-3	CHANNEL	41	1.400	1.400	1.00
SU-BC-7-4	CHANNEL	41	1.510	1.407	1.07
SU-BC-8-1	CHANNEL	41	3.070	2.920	1.05

Table D11 (Cont'd)

Comparisons of Tested Failure Loads and Predicted Ultimate Loads for the Test Data Used in the Development of Eq. (6.21)

Specimen No.	Type of Section	Reference	P_{test} (kips)	P_{mc} (kips)	P_{test}/P_{mc}
SU-BC-8-2	CHANNEL	41	2.940	2.930	1.00
SU-BC-8-3	CHANNEL	41	2.620	2.493	1.05
SU-BC-8-4	CHANNEL	41	2.600	2.497	1.04
SU-BC-8'-1	CHANNEL	41	4.410	3.957	1.11
SU-BC-8'-2	CHANNEL	41	4.730	3.945	1.20
SU-BC-8'-3	CHANNEL	41	3.180	3.059	1.04
SU-BC-8'-4	CHANNEL	41	3.400	3.058	1.11
Mean Value					1.020
Standard Deviation					0.081

Table D12

Comparisons of Tested Failure Loads and Predicted Ultimate Loads for the Test Data Used in the Development of Eq. (6.22)

Specimen No.	Type of Section	Reference	P_{test} (kips)	P_{mc} (kips)	P_{test}/P_{mc}
SU-BC-1-1	CHANNEL	41	2.280	2.224	1.02
SU-BC-1-2	CHANNEL	41	2.260	2.222	1.02
SU-BC-1-3	CHANNEL	41	1.720	1.682	1.02
SU-BC-1-4	CHANNEL	41	1.780	1.701	1.05
SU-BC-1-5	CHANNEL	41	1.220	1.119	1.09
SU-BC-1-6	CHANNEL	41	1.060	1.072	0.99
SU-BC-3-1	CHANNEL	41	2.400	2.960	0.81
SU-BC-3-2	CHANNEL	41	2.670	2.956	0.90
SU-BC-3-3	CHANNEL	41	2.210	2.626	0.84
SU-BC-3-4	CHANNEL	41	2.340	2.629	0.89
SU-BC-3-5	CHANNEL	41	1.850	2.192	0.84
SU-BC-3-6	CHANNEL	41	2.040	2.271	0.90
SU-BC-15-1	CHANNEL	41	4.180	4.409	0.95
SU-BC-15-2	CHANNEL	41	4.150	4.574	0.91
SU-BC-15-3	CHANNEL	41	3.680	3.804	0.97
SU-BC-15-4	CHANNEL	41	3.600	3.675	0.98
SU-BC-15-5	CHANNEL	41	3.000	2.984	1.01
SU-BC-15-6	CHANNEL	41	3.000	3.071	0.98
SU-4-IOF-1	CHANNEL	41	3.052	2.956	1.03
SU-4-IOF-2	CHANNEL	41	3.050	3.001	1.02
SU-4-IOF-3	CHANNEL	41	3.540	3.504	1.01
SU-4-IOF-4	CHANNEL	41	3.550	3.522	1.01
SU-4-IOF-5	CHANNEL	41	4.170	3.965	1.05
SU-4-IOF-6	CHANNEL	41	3.970	3.962	1.00
M-SU-4-IOF-1	CHANNEL	41	3.210	2.945	1.09
M-SU-4-IOF-2	CHANNEL	41	3.260	2.978	1.10
M-SU-4-IOF-5	CHANNEL	41	4.400	4.007	1.10
M-SU-4-IOF-6	CHANNEL	41	4.150	3.934	1.06
SU-BC-6-1	CHANNEL	41	1.760	1.391	1.27
SU-BC-6-2	CHANNEL	41	1.680	1.396	1.20
SU-BC-6-3	CHANNEL	41	1.130	0.980	1.15
SU-BC-16-1	CHANNEL	41	2.880	2.637	1.09
SU-BC-16-2	CHANNEL	41	2.700	2.574	1.05
SU-BC-16-3	CHANNEL	41	2.010	1.822	1.10
SU-BC-16-4	CHANNEL	41	2.210	2.000	1.10
SU-BC-7-1	CHANNEL	41	2.000	1.806	1.11
SU-BC-7-2	CHANNEL	41	1.880	1.750	1.07
SU-BC-7-3	CHANNEL	41	1.400	1.396	1.00
SU-BC-7-4	CHANNEL	41	1.510	1.399	1.08
SU-BC-8-1	CHANNEL	41	3.070	2.998	1.02

Table D12 (Cont'd)

Comparisons of Tested Failure Loads and Predicted Ultimate Loads for the Test Data Used in the Development of Eq. (6.22)

Specimen No.	Type of Section	Reference	P_{test} (kips)	P_{mc} (kips)	P_{test}/P_{mc}
SU-BC-8-2	CHANNEL	41	2.940	2.993	0.98
SU-BC-8-3	CHANNEL	41	2.620	2.521	1.04
SU-BC-8-4	CHANNEL	41	2.600	2.523	1.03
SU-BC-8'-1	CHANNEL	41	4.410	3.870	1.14
SU-BC-8'-2	CHANNEL	41	4.730	3.868	1.22
SU-BC-8'-3	CHANNEL	41	3.180	2.853	1.11
SU-BC-8'-4	CHANNEL	41	3.400	2.854	1.19
Mean Value					1.034
Standard Deviation					0.097

Table D13

Comparisons of Tested Failure Loads and Predicted Ultimate Loads for the Test Data Used in the Development of Eq. (6.23)

Specimen No.	Type of Section	Reference	P_{test} (kips)	P_{mc} (kips)	P_{test}/P_{mc}
SU-BC-1-1	CHANNEL	41	2.280	2.235	1.02
SU-BC-1-2	CHANNEL	41	2.260	2.233	1.01
SU-BC-1-3	CHANNEL	41	1.720	1.705	1.01
SU-BC-1-4	CHANNEL	41	1.780	1.725	1.03
SU-BC-1-5	CHANNEL	41	1.220	1.217	1.00
SU-BC-1-6	CHANNEL	41	1.060	1.171	0.90
SU-BC-3-1	CHANNEL	41	2.400	3.212	0.75
SU-BC-3-2	CHANNEL	41	2.670	3.207	0.83
SU-BC-3-3	CHANNEL	41	2.210	2.860	0.77
SU-BC-3-4	CHANNEL	41	2.340	2.865	0.82
SU-BC-3-5	CHANNEL	41	1.850	2.453	0.75
SU-BC-3-6	CHANNEL	41	2.040	2.532	0.81
SU-BC-15-1	CHANNEL	41	4.180	4.739	0.88
SU-BC-15-2	CHANNEL	41	4.150	4.912	0.85
SU-BC-15-3	CHANNEL	41	3.680	4.020	0.92
SU-BC-15-4	CHANNEL	41	3.600	3.895	0.92
SU-BC-15-5	CHANNEL	41	3.000	3.251	0.92
SU-BC-15-6	CHANNEL	41	3.000	3.352	0.89
SU-4-IOF-1	CHANNEL	41	3.052	3.195	0.95
SU-4-IOF-2	CHANNEL	41	3.050	3.239	0.94
SU-4-IOF-3	CHANNEL	41	3.540	3.717	0.95
SU-4-IOF-4	CHANNEL	41	3.550	3.729	0.95
SU-4-IOF-5	CHANNEL	41	4.170	4.140	1.01
SU-4-IOF-6	CHANNEL	41	3.970	4.132	0.96
M-SU-4-IOF-1	CHANNEL	41	3.210	3.193	1.01
M-SU-4-IOF-2	CHANNEL	41	3.260	3.222	1.01
M-SU-4-IOF-5	CHANNEL	41	4.400	4.187	1.05
M-SU-4-IOF-6	CHANNEL	41	4.150	4.113	1.01
SU-BC-6-1	CHANNEL	41	1.760	1.500	1.17
SU-BC-6-2	CHANNEL	41	1.680	1.505	1.12
SU-BC-6-3	CHANNEL	41	1.130	1.126	1.00
SU-BC-16-1	CHANNEL	41	2.880	2.756	1.05
SU-BC-16-2	CHANNEL	41	2.700	2.686	1.01
SU-BC-16-3	CHANNEL	41	2.010	2.027	0.99
SU-BC-16-4	CHANNEL	41	2.210	2.190	1.01
SU-BC-7-1	CHANNEL	41	2.000	1.824	1.10
SU-BC-7-2	CHANNEL	41	1.880	1.766	1.06
SU-BC-7-3	CHANNEL	41	1.400	1.453	0.96
SU-BC-7-4	CHANNEL	41	1.510	1.456	1.04
SU-BC-8-1	CHANNEL	41	3.070	3.074	1.00

Table D13 (Cont'd)

Comparisons of Tested Failure Loads and Predicted Ultimate Loads for the Test Data Used in the Development of Eq. (6.23)

Specimen No.	Type of Section	Reference	P_{test} (kips)	P_{mc} (kips)	P_{test}/P_{mc}
SU-BC-8-2	CHANNEL	41	2.940	3.087	0.95
SU-BC-8-3	CHANNEL	41	2.620	2.647	0.99
SU-BC-8-4	CHANNEL	41	2.600	2.649	0.98
SU-BC-8'-1	CHANNEL	41	4.410	4.102	1.07
SU-BC-8'-2	CHANNEL	41	4.730	4.093	1.16
SU-BC-8'-3	CHANNEL	41	3.180	3.183	1.00
SU-BC-8'-4	CHANNEL	41	3.400	3.183	1.07
Mean Value					0.971
Standard Deviation					0.097

Table D14

Comparisons of Tested Failure Loads and Predicted Ultimate Loads for the Test Data Used in the Development of Eq. (6.24)

Specimen No.	Type of Section	Reference	P_{test} (kips)	P_{mc} (kips)	P_{test}/P_{mc}
I-BC-4-1	I-BEAM	41	4.050	3.664	1.10
I-BC-4-2	I-BEAM	41	3.880	3.664	1.06
I-BC-4-3	I-BEAM	41	3.060	2.593	1.18
I-BC-4-4	I-BEAM	41	2.890	2.592	1.11
I-BC-4-5	I-BEAM	41	1.660	1.546	1.07
I-BC-4-6	I-BEAM	41	1.750	1.546	1.13
I-BC-5-1	I-BEAM	41	5.180	6.329	0.82
I-BC-5-2	I-BEAM	41	5.030	6.331	0.79
I-BC-5-3	I-BEAM	41	5.010	5.091	0.98
I-BC-5-4	I-BEAM	41	4.940	5.090	0.97
I-BC-5-5	I-BEAM	41	3.570	3.758	0.95
I-BC-5-6	I-BEAM	41	3.280	3.758	0.87
I-BC-6-1	I-BEAM	41	3.780	2.946	1.28
I-BC-6-2	I-BEAM	41	3.740	2.949	1.27
I-BC-6-3	I-BEAM	41	2.810	2.333	1.20
I-BC-6-4	I-BEAM	41	2.850	2.333	1.22
I-BC-6-5	I-BEAM	41	2.030	1.711	1.19
I-BC-6-6	I-BEAM	41	2.070	1.710	1.21
I-BC-8-1	I-BEAM	41	13.510	9.648	1.40
I-BC-8-2	I-BEAM	41	13.050	9.644	1.35
I-BC-8-3	I-BEAM	41	10.010	7.145	1.40
I-BC-8-4	I-BEAM	41	9.500	7.141	1.33
I-BC-8-5	I-BEAM	41	5.090	4.102	1.24
I-BC-8-6	I-BEAM	41	5.170	4.103	1.26
I-BC-9-1	I-BEAM	41	11.620	11.371	1.02
I-BC-9-2	I-BEAM	41	11.570	11.375	1.02
I-BC-9-3	I-BEAM	41	8.080	8.071	1.00
I-BC-9-4	I-BEAM	41	8.400	8.074	1.04
I-BC-9-5	I-BEAM	41	5.350	5.809	0.92
I-BC-9-6	I-BEAM	41	4.980	5.812	0.86
I-BC-9'-1	I-BEAM	41	6.630	6.946	0.95
I-BC-9'-2	I-BEAM	41	5.910	6.945	0.85
I-BC-9'-3	I-BEAM	41	5.180	5.264	0.98
I-BC-9'-4	I-BEAM	41	5.390	5.312	1.02
I-BC-9'-5	I-BEAM	41	3.260	3.264	1.00
I-BC-9'-6	I-BEAM	41	3.200	3.265	0.98
I-BC-10-1	I-BEAM	41	23.000	18.740	1.23
I-BC-10-2	I-BEAM	41	24.140	18.734	1.29
I-BC-10-3	I-BEAM	41	19.290	13.655	1.41
I-BC-10-4	I-BEAM	41	17.290	13.667	1.27

Table D14 (Cont'd)

Comparisons of Tested Failure Loads and Predicted Ultimate Loads for the Test Data Used in the Development of Eq. (6.24)

Specimen No.	Type of Section	Reference	P_{test} (kips)	P_{mc} (kips)	P_{test}/P_{mc}
I-BC-10-5	I-BEAM	41	10.130	8.217	1.23
I-BC-10-6	I-BEAM	41	9.790	8.221	1.19
I-BC-13-1	I-BEAM	41	27.740	25.783	1.08
I-BC-13-2	I-BEAM	41	26.020	25.762	1.01
I-BC-13-3	I-BEAM	41	24.780	22.713	1.09
I-BC-13-4	I-BEAM	41	23.240	22.722	1.02
I-BC-13-5	I-BEAM	41	20.980	19.487	1.08
I-BC-13-6	I-BEAM	41	21.000	19.488	1.08
I-3-IOF-5	I-BEAM	41	6.050	6.877	0.88
I-3-IOF-6	I-BEAM	41	6.010	6.875	0.87
I-3'-IOF-1	I-BEAM	41	3.620	3.791	0.95
I-3'-IOF-2	I-BEAM	41	3.700	3.793	0.98
I-3'-IOF-5	I-BEAM	41	4.200	4.743	0.88
I-3'-IOF-6	I-BEAM	41	4.630	4.745	0.98
I-5'-IOF-5	I-BEAM	41	8.310	9.395	0.88
I-5'-IOF-6	I-BEAM	41	8.000	9.393	0.85
I-6-IOF-1	I-BEAM	41	11.070	10.317	1.07
I-6-IOF-2	I-BEAM	41	10.800	10.311	1.05
I-6-IOF-5	I-BEAM	41	12.000	12.196	0.98
I-6-IOF-6	I-BEAM	41	12.970	12.311	1.05
I-6-IOF-7	I-BEAM	41	14.000	12.667	1.10
I-6-IOF-8	I-BEAM	41	13.950	12.665	1.10
I-6"-IOF-5	I-BEAM	41	4.310	4.930	0.87
I-6"-IOF-6	I-BEAM	41	4.630	4.930	0.94
I-12-IOF-6	I-BEAM	41	6.740	8.290	0.81
I-12'-IOF-5	I-BEAM	41	24.140	23.072	1.05
I-12'-IOF-6	I-BEAM	41	25.500	23.093	1.10
I-16-IOF-1	I-BEAM	41	5.460	6.246	0.87
I-16-IOF-2	I-BEAM	41	5.676	6.249	0.91
I-16-IOF-5	I-BEAM	41	7.060	7.540	0.94
I-16-IOF-6	I-BEAM	41	7.800	7.606	1.03
Mean Value					1.059
Standard Deviation					0.155

Table D15

Comparisons of Tested Failure Loads and Predicted Ultimate Loads for the Test Data Used in the Development of Eq. (6.25)

Specimen No.	Type of Section	Reference	P_{test} (kips)	P_{mc} (kips)	P_{test}/P_{mc}
I-BC-4-1	I-BEAM	41	4.050	3.701	1.09
I-BC-4-2	I-BEAM	41	3.880	3.701	1.05
I-BC-4-3	I-BEAM	41	3.060	2.699	1.13
I-BC-4-4	I-BEAM	41	2.890	2.699	1.07
I-BC-4-5	I-BEAM	41	1.660	1.593	1.04
I-BC-4-6	I-BEAM	41	1.750	1.592	1.10
I-BC-5-1	I-BEAM	41	5.180	5.927	0.87
I-BC-5-2	I-BEAM	41	5.030	5.926	0.85
I-BC-5-3	I-BEAM	41	5.010	5.035	1.00
I-BC-5-4	I-BEAM	41	4.940	5.036	0.98
I-BC-5-5	I-BEAM	41	3.570	3.880	0.92
I-BC-5-6	I-BEAM	41	3.280	3.880	0.85
I-BC-6-1	I-BEAM	41	3.780	3.073	1.23
I-BC-6-2	I-BEAM	41	3.740	3.074	1.22
I-BC-6-3	I-BEAM	41	2.810	2.426	1.16
I-BC-6-4	I-BEAM	41	2.850	2.426	1.18
I-BC-6-5	I-BEAM	41	2.030	1.752	1.16
I-BC-6-6	I-BEAM	41	2.070	1.752	1.18
I-BC-8-1	I-BEAM	41	13.510	9.922	1.36
I-BC-8-2	I-BEAM	41	13.050	9.919	1.32
I-BC-8-3	I-BEAM	41	10.010	7.449	1.34
I-BC-8-4	I-BEAM	41	9.500	7.448	1.28
I-BC-8-5	I-BEAM	41	5.090	4.192	1.21
I-BC-8-6	I-BEAM	41	5.170	4.193	1.23
I-BC-9-1	I-BEAM	41	11.620	11.464	1.01
I-BC-9-2	I-BEAM	41	11.570	11.464	1.01
I-BC-9-3	I-BEAM	41	8.080	8.330	0.97
I-BC-9-4	I-BEAM	41	8.400	8.396	1.00
I-BC-9-5	I-BEAM	41	5.350	6.046	0.88
I-BC-9-6	I-BEAM	41	4.980	6.046	0.82
I-BC-9'-1	I-BEAM	41	6.630	6.718	0.99
I-BC-9'-2	I-BEAM	41	5.910	6.717	0.88
I-BC-9'-3	I-BEAM	41	5.180	5.361	0.97
I-BC-9'-4	I-BEAM	41	5.390	5.390	1.00
I-BC-9'-5	I-BEAM	41	3.260	3.407	0.96
I-BC-9'-6	I-BEAM	41	3.200	3.406	0.94
I-BC-10-1	I-BEAM	41	23.000	19.227	1.20
I-BC-10-2	I-BEAM	41	24.140	19.231	1.26
I-BC-10-3	I-BEAM	41	19.290	14.248	1.35
I-BC-10-4	I-BEAM	41	17.290	14.249	1.21

Table D15 (Cont'd)

Comparisons of Tested Failure Loads and Predicted Ultimate Loads for the Test Data Used in the Development of Eq. (6.25)

Specimen No.	Type of Section	Reference	P_{test} (kips)	P_{mc} (kips)	P_{test}/P_{mc}
I-BC-10-5	I-BEAM	41	10.130	8.429	1.20
I-BC-10-6	I-BEAM	41	9.790	8.426	1.16
I-BC-13-1	I-BEAM	41	27.740	25.086	1.11
I-BC-13-2	I-BEAM	41	26.020	25.087	1.04
I-BC-13-3	I-BEAM	41	24.780	22.692	1.09
I-BC-13-4	I-BEAM	41	23.240	22.692	1.02
I-BC-13-5	I-BEAM	41	20.980	19.898	1.05
I-BC-13-6	I-BEAM	41	21.000	19.899	1.06
I-3-IOF-5	I-BEAM	41	6.050	6.666	0.91
I-3-IOF-6	I-BEAM	41	6.010	6.668	0.90
I-3'-IOF-1	I-BEAM	41	3.620	3.567	1.02
I-3'-IOF-2	I-BEAM	41	3.700	3.566	1.04
I-3'-IOF-5	I-BEAM	41	4.200	4.547	0.92
I-3'-IOF-6	I-BEAM	41	4.630	4.577	1.01
I-5'-IOF-5	I-BEAM	41	8.310	9.243	0.90
I-5'-IOF-6	I-BEAM	41	8.000	9.241	0.87
I-6-IOF-1	I-BEAM	41	11.070	9.943	1.11
I-6-IOF-2	I-BEAM	41	10.800	9.941	1.09
I-6-IOF-5	I-BEAM	41	12.000	12.068	0.99
I-6-IOF-6	I-BEAM	41	12.970	12.148	1.07
I-6-IOF-7	I-BEAM	41	14.000	12.418	1.13
I-6-IOF-8	I-BEAM	41	13.950	12.423	1.12
I-6"-IOF-5	I-BEAM	41	4.310	4.678	0.92
I-6"-IOF-6	I-BEAM	41	4.630	4.678	0.99
I-12-IOF-6	I-BEAM	41	6.740	8.126	0.83
I-12'-IOF-5	I-BEAM	41	24.140	23.027	1.05
I-12'-IOF-6	I-BEAM	41	25.500	23.024	1.11
I-16-IOF-1	I-BEAM	41	5.460	6.067	0.90
I-16-IOF-2	I-BEAM	41	5.676	6.068	0.94
I-16-IOF-5	I-BEAM	41	7.060	7.513	0.94
I-16-IOF-6	I-BEAM	41	7.800	7.562	1.03
Mean Value					1.053
Standard Deviation					0.134

Table D16

Comparisons of Tested Failure Loads and Predicted Ultimate Loads for the Test Data Used in the Development of Eq. (6.26)

Specimen No.	Type of Section	Reference	P_{test} (kips)	P_{mc} (kips)	P_{test}/P_{mc}
I-BC-4-1	I-BEAM	41	4.050	4.271	0.95
I-BC-4-2	I-BEAM	41	3.880	4.271	0.91
I-BC-4-3	I-BEAM	41	3.060	3.108	0.99
I-BC-4-4	I-BEAM	41	2.890	3.108	0.93
I-BC-4-5	I-BEAM	41	1.660	1.905	0.87
I-BC-4-6	I-BEAM	41	1.750	1.905	0.92
I-BC-5-1	I-BEAM	41	5.180	7.452	0.69
I-BC-5-2	I-BEAM	41	5.030	7.452	0.68
I-BC-5-3	I-BEAM	41	5.010	6.298	0.80
I-BC-5-4	I-BEAM	41	4.940	6.298	0.78
I-BC-5-5	I-BEAM	41	3.570	4.918	0.73
I-BC-5-6	I-BEAM	41	3.280	4.918	0.67
I-BC-6-1	I-BEAM	41	3.780	3.550	1.06
I-BC-6-2	I-BEAM	41	3.740	3.550	1.05
I-BC-6-3	I-BEAM	41	2.810	2.848	0.99
I-BC-6-4	I-BEAM	41	2.850	2.848	1.00
I-BC-6-5	I-BEAM	41	2.030	2.116	0.96
I-BC-6-6	I-BEAM	41	2.070	2.116	0.98
I-BC-8-1	I-BEAM	41	13.510	11.391	1.19
I-BC-8-2	I-BEAM	41	13.050	11.391	1.15
I-BC-8-3	I-BEAM	41	10.010	8.617	1.16
I-BC-8-4	I-BEAM	41	9.500	8.617	1.10
I-BC-8-5	I-BEAM	41	5.090	5.082	1.00
I-BC-8-6	I-BEAM	41	5.170	5.082	1.02
I-BC-9-1	I-BEAM	41	11.620	12.837	0.90
I-BC-9-2	I-BEAM	41	11.570	12.837	0.90
I-BC-9-3	I-BEAM	41	8.080	9.266	0.87
I-BC-9-4	I-BEAM	41	8.400	9.266	0.91
I-BC-9-5	I-BEAM	41	5.350	6.806	0.79
I-BC-9-6	I-BEAM	41	4.980	6.806	0.73
I-BC-9'-1	I-BEAM	41	6.630	8.264	0.80
I-BC-9'-2	I-BEAM	41	5.910	8.264	0.71
I-BC-9'-3	I-BEAM	41	5.180	6.564	0.79
I-BC-9'-4	I-BEAM	41	5.390	6.564	0.82
I-BC-9'-5	I-BEAM	41	3.260	4.316	0.75
I-BC-9'-6	I-BEAM	41	3.200	4.316	0.74
I-BC-10-1	I-BEAM	41	23.000	22.088	1.04
I-BC-10-2	I-BEAM	41	24.140	22.088	1.09
I-BC-10-3	I-BEAM	41	19.290	16.471	1.17
I-BC-10-4	I-BEAM	41	17.290	16.471	1.05

Table D16 (Cont'd)

Comparisons of Tested Failure Loads and Predicted Ultimate Loads for the Test Data Used in the Development of Eq. (6.26)

Specimen No.	Type of Section	Reference	P_{test} (kips)	P_{mc} (kips)	P_{test}/P_{mc}
I-BC-10-5	I-BEAM	41	10.130	10.158	1.00
I-BC-10-6	I-BEAM	41	9.790	10.158	0.96
I-BC-13-1	I-BEAM	41	27.740	29.268	0.95
I-BC-13-2	I-BEAM	41	26.020	29.268	0.89
I-BC-13-3	I-BEAM	41	24.780	26.101	0.95
I-BC-13-4	I-BEAM	41	23.240	26.101	0.89
I-BC-13-5	I-BEAM	41	20.980	22.668	0.93
I-BC-13-6	I-BEAM	41	21.000	22.668	0.93
I-3-IOF-5	I-BEAM	41	6.050	8.101	0.75
I-3-IOF-6	I-BEAM	41	6.010	8.101	0.74
I-3'-IOF-1	I-BEAM	41	3.620	4.305	0.84
I-3'-IOF-2	I-BEAM	41	3.700	4.305	0.86
I-3'-IOF-5	I-BEAM	41	4.200	5.449	0.77
I-3'-IOF-6	I-BEAM	41	4.630	5.449	0.85
I-5'-IOF-5	I-BEAM	41	8.310	10.867	0.76
I-5'-IOF-6	I-BEAM	41	8.000	10.867	0.74
I-6-IOF-1	I-BEAM	41	11.070	11.464	0.97
I-6-IOF-2	I-BEAM	41	10.800	11.464	0.94
I-6-IOF-5	I-BEAM	41	12.000	13.770	0.87
I-6-IOF-6	I-BEAM	41	12.970	13.770	0.94
I-6-IOF-7	I-BEAM	41	14.000	14.139	0.99
I-6-IOF-8	I-BEAM	41	13.950	14.139	0.99
I-6"-IOF-5	I-BEAM	41	4.310	5.711	0.75
I-6"-IOF-6	I-BEAM	41	4.630	5.711	0.81
I-12-IOF-6	I-BEAM	41	6.740	9.861	0.68
I-12'-IOF-5	I-BEAM	41	24.140	26.711	0.90
I-12'-IOF-6	I-BEAM	41	25.500	26.711	0.95
I-16-IOF-1	I-BEAM	41	5.460	7.189	0.76
I-16-IOF-2	I-BEAM	41	5.676	7.189	0.79
I-16-IOF-5	I-BEAM	41	7.060	8.789	0.80
I-16-IOF-6	I-BEAM	41	7.800	8.789	0.89
Mean Value					0.894
Standard Deviation					0.128

APPENDIX E

EFFECTS OF IMPORTANT PARAMETERS ON THE ACCURACY OF THE PREDICTED ULTIMATE WEB CRIPPLING LOADS BASED ON THE PROPOSED DESIGN RECOMMENDATIONS

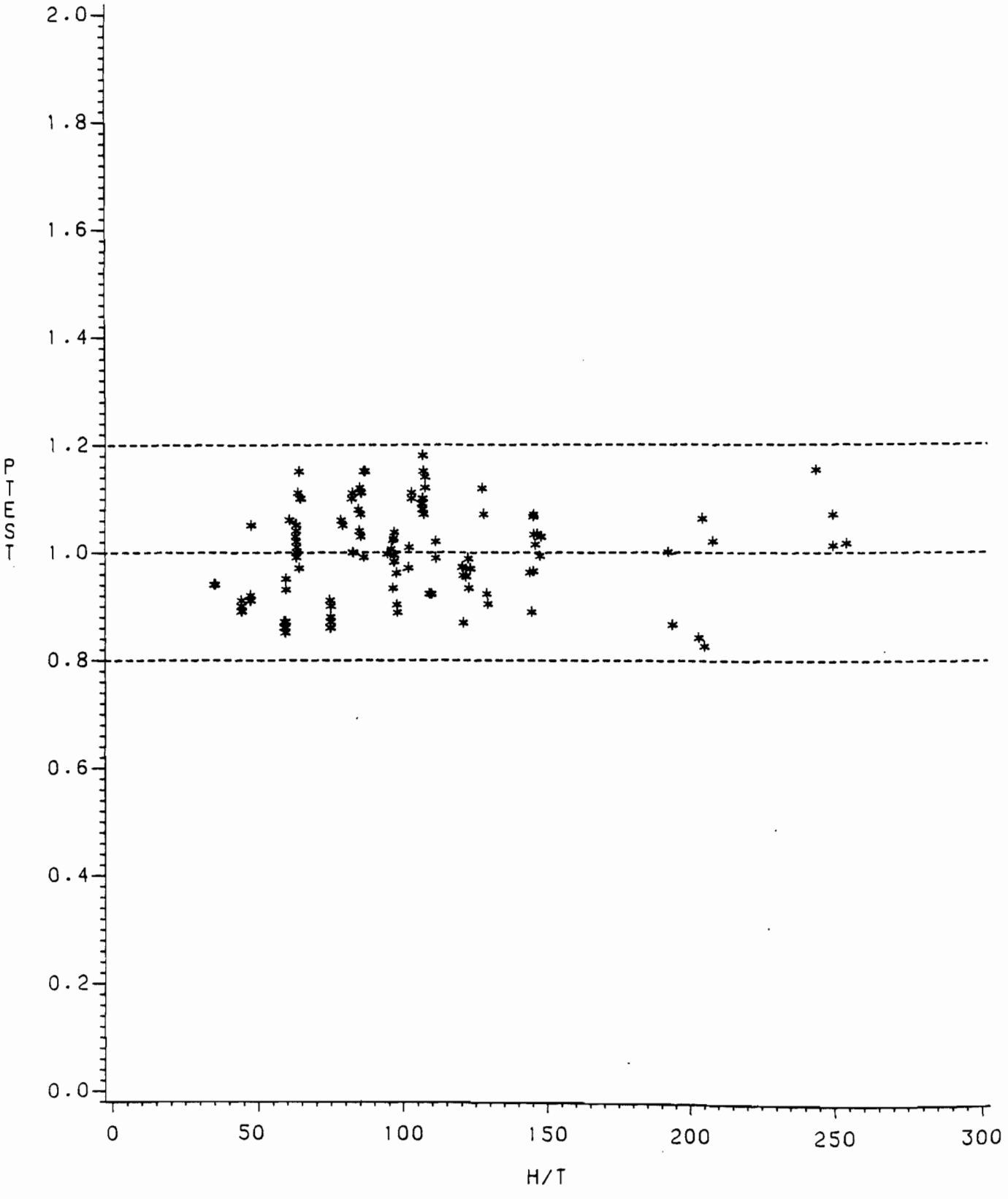

FIG. E1.1
EFFECT OF H/T ON THE RATIO PTEST/PCOMP FOR HAT SECTIONS SUBJECTED TO INTERIOR ONE-FLANGE LOADING BASED ON THE PROPOSED DESIGN RECOMMENDATIONS

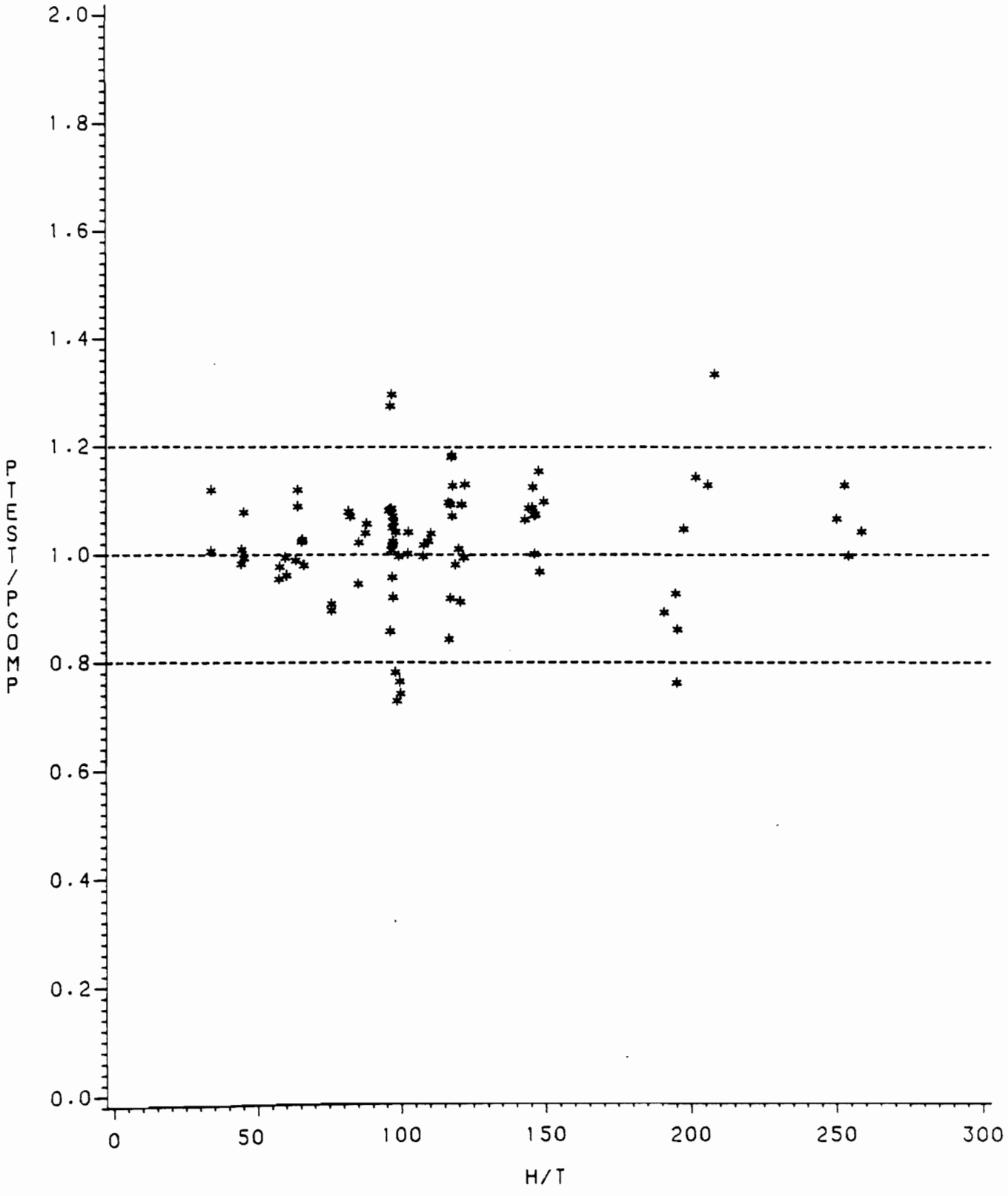

FIG. E2.1
EFFECT OF H/T ON THE RATIO PTEST/PCOMP FOR HAT SECTIONS
SUBJECTED TO END ONE-FLANGE LOADING BASED ON
THE PROPOSED DESIGN RECOMMENDATIONS

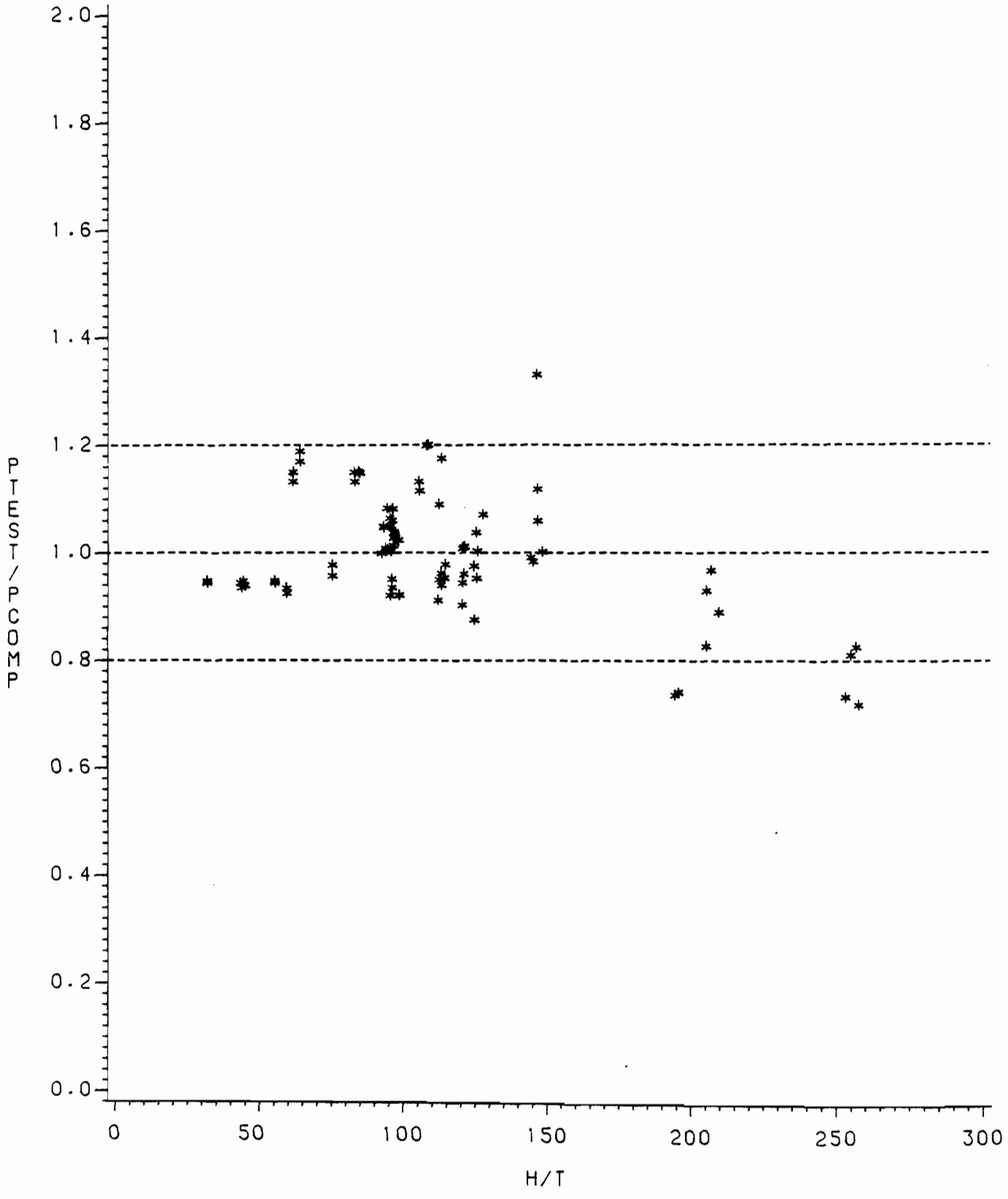

FIG. E3.1
EFFECT OF H/T ON THE RATIO PTEST/PCOMP FOR HAT SECTIONS SUBJECTED TO INTERIOR TWO-FLANGE LOADING BASED ON THE PROPOSED DESIGN RECOMMENDATIONS

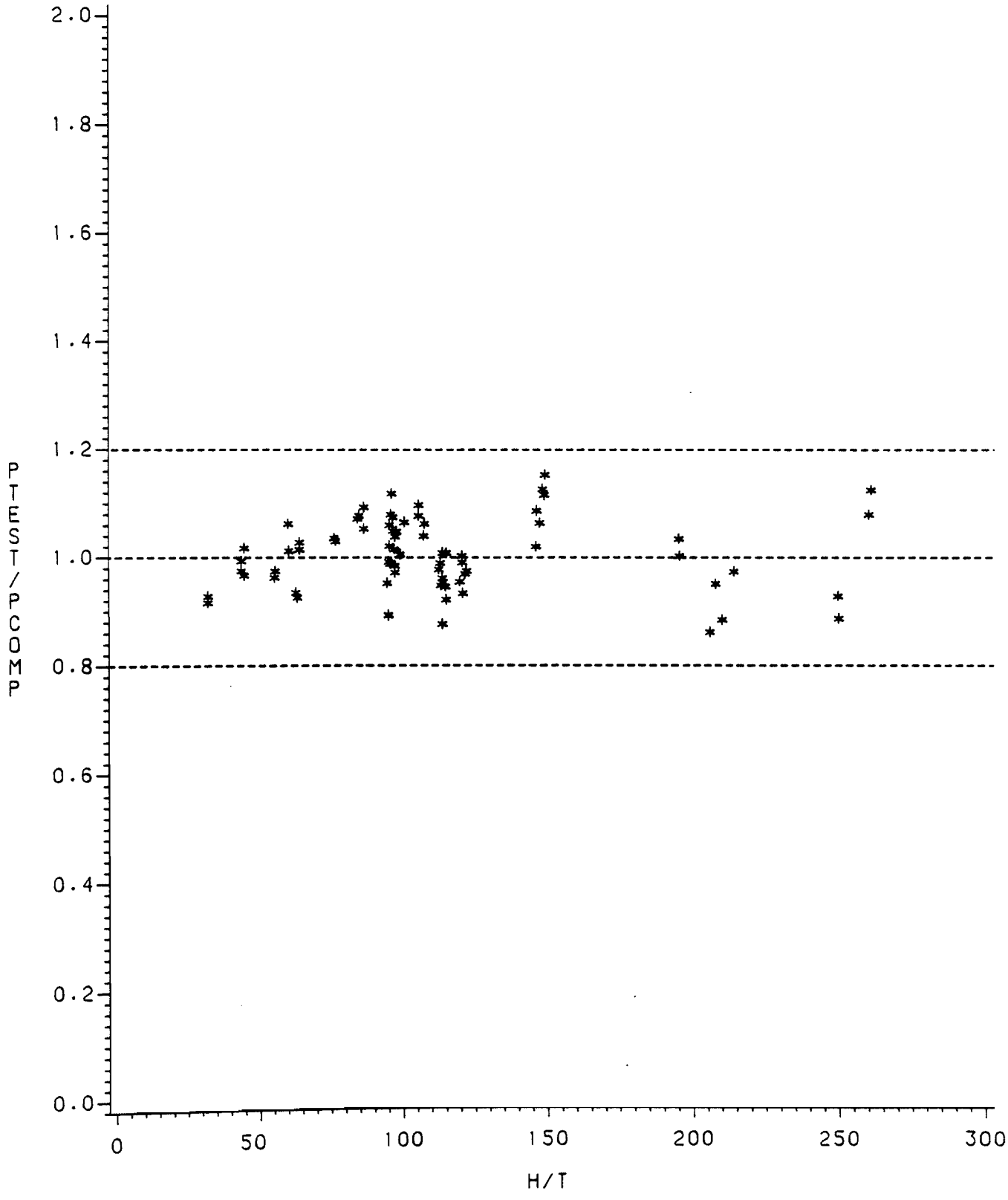

FIG. E4.1
EFFECT OF H/T ON THE RATIO PTEST/PCOMP FOR HAT SECTIONS SUBJECTED TO END TWO-FLANGE LOADING BASED ON THE PROPOSED DESIGN RECOMMENDATIONS

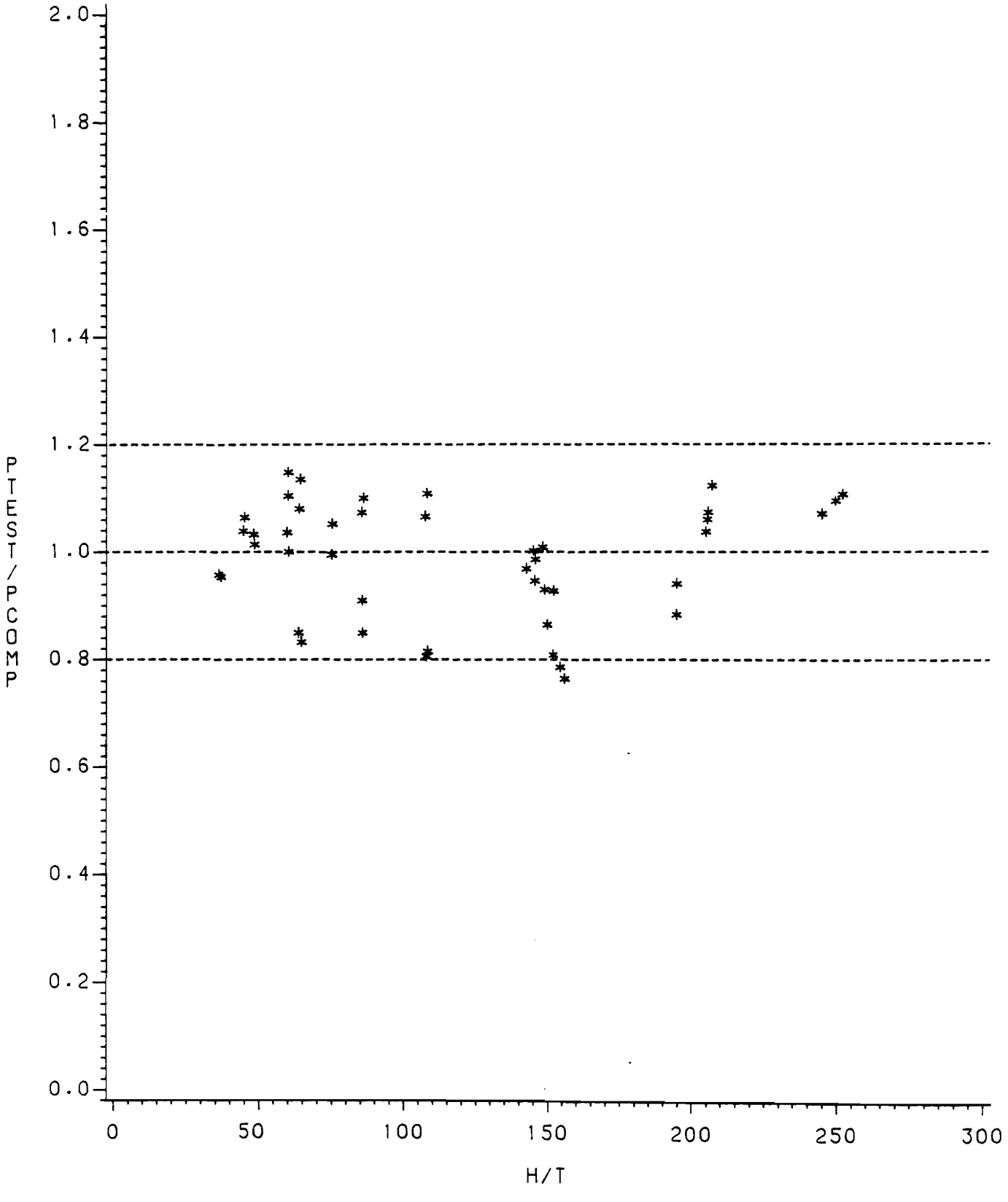

FIG. E5.1
EFFECT OF H/T ON THE RATIO PTEST/PCOMP FOR I-BEAMS SUBJECTED TO INTERIOR ONE-FLANGE LOADING BASED ON THE PROPOSED DESIGN RECOMMENDATIONS

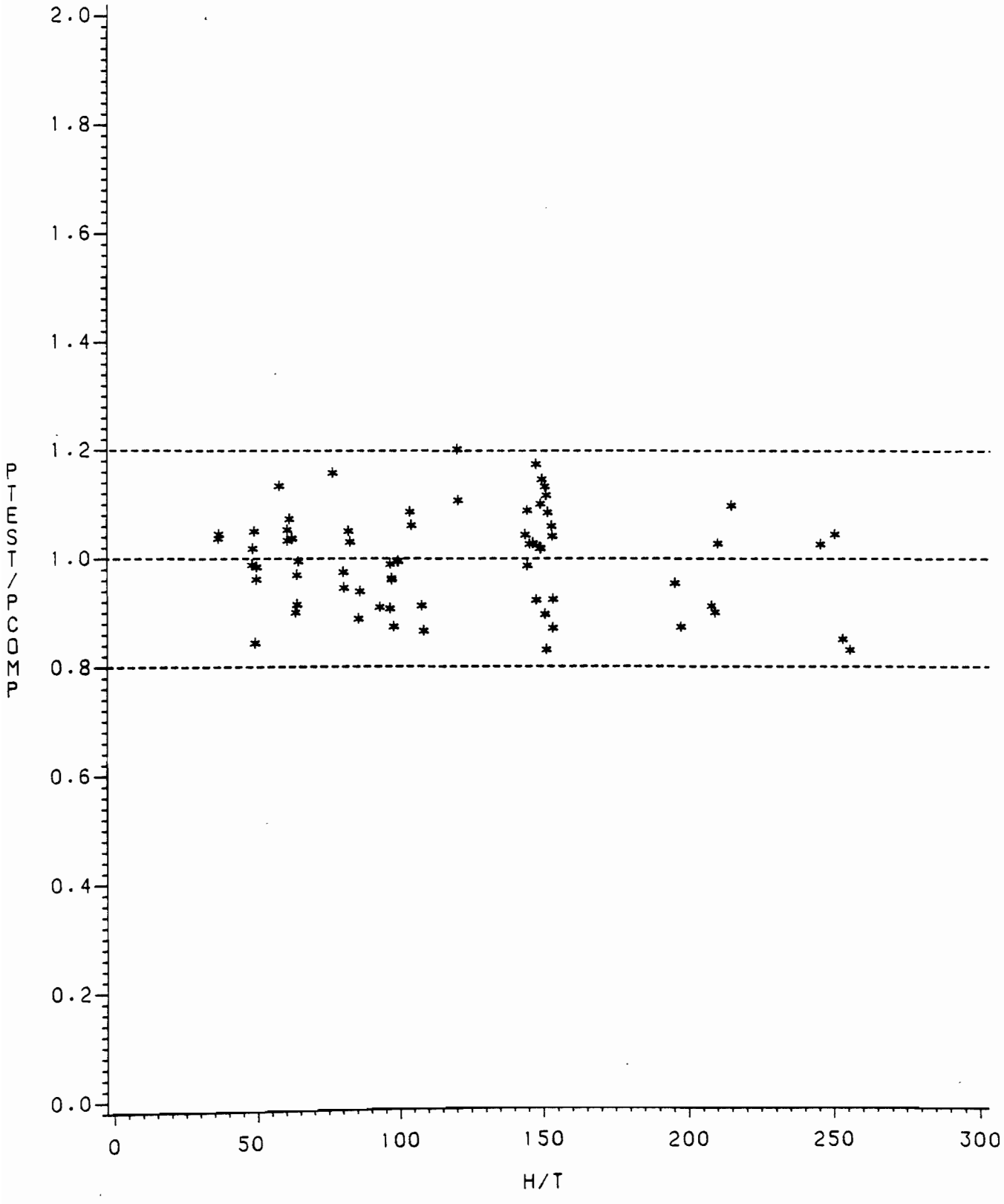

FIG. E6.1
EFFECT OF H/T ON THE RATIO PTEST/PCOMP FOR I-BEAMS
SUBJECTED TO END ONE-FLANGE LOADING BASED ON
THE PROPOSED DESIGN RECOMMENDATIONS

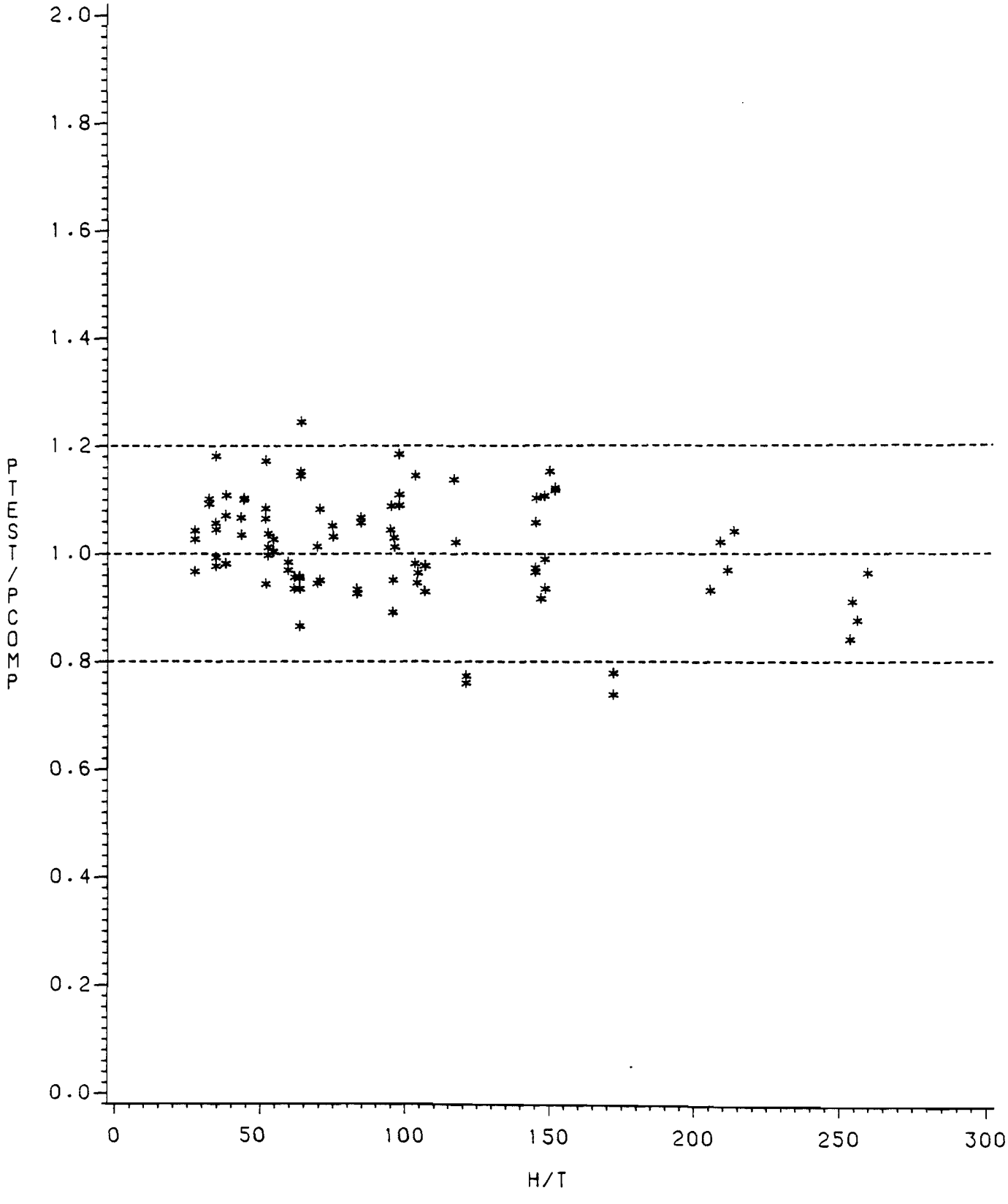

FIG. E7.1
EFFECT OF H/T ON THE RATIO PTEST/PCOMP FOR I-BEAMS SUBJECTED TO INTERIOR TWO-FLANGE LOADING BASED ON THE PROPOSED DESIGN RECOMMENDATIONS

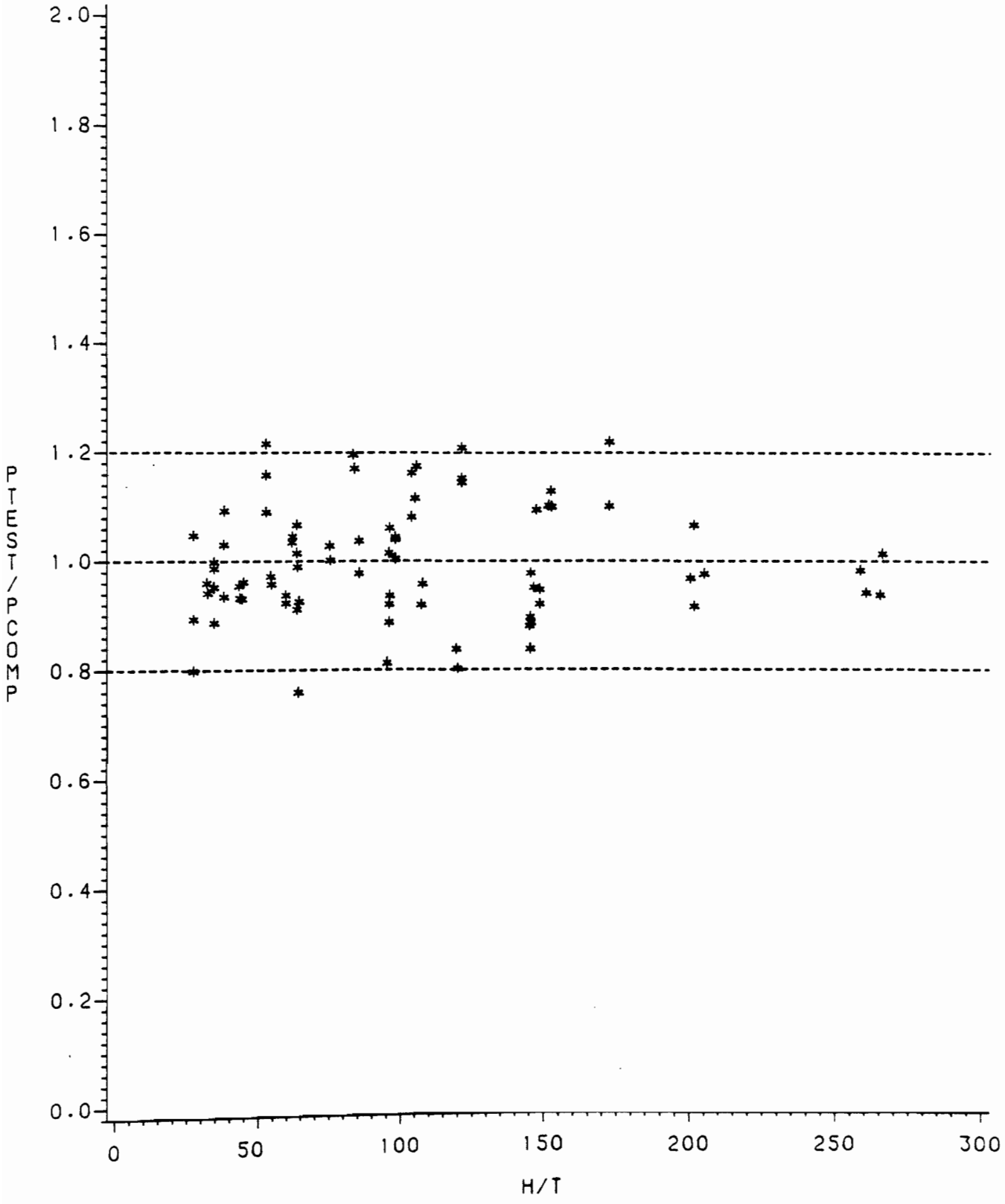

FIG. E8.1
EFFECT OF H/T ON THE RATIO PTEST/PCOMP FOR I-BEAMS
SUBJECTED TO END TWO-FLANGE LOADING BASED ON
THE PROPOSED DESIGN RECOMMENDATIONS

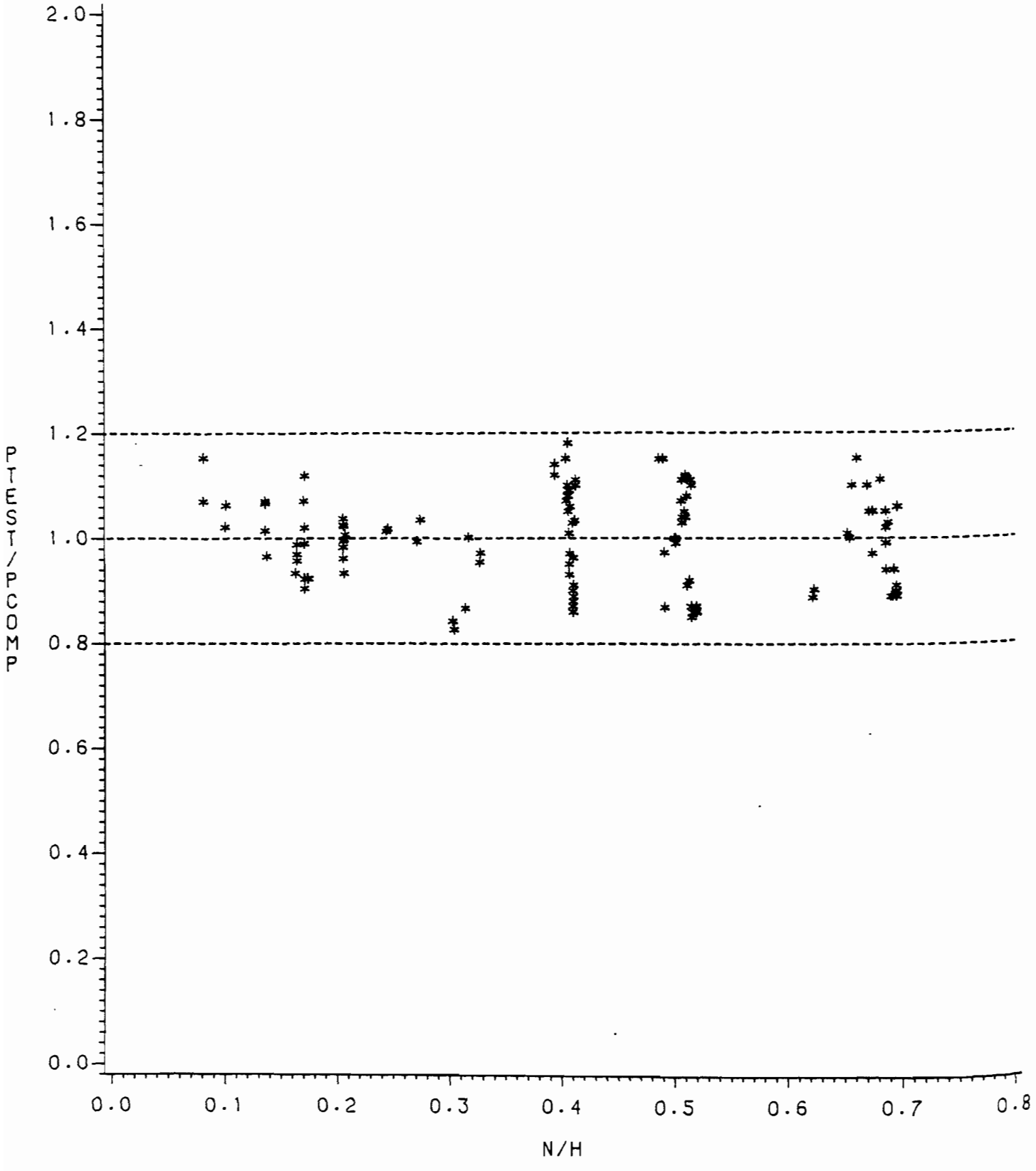

FIG. E1.2
EFFECT OF N/H ON THE RATIO PTEST/PCOMP FOR HAT SECTIONS SUBJECTED TO INTERIOR ONE-FLANGE LOADING BASED ON THE PROPOSED DESIGN RECOMMENDATIONS

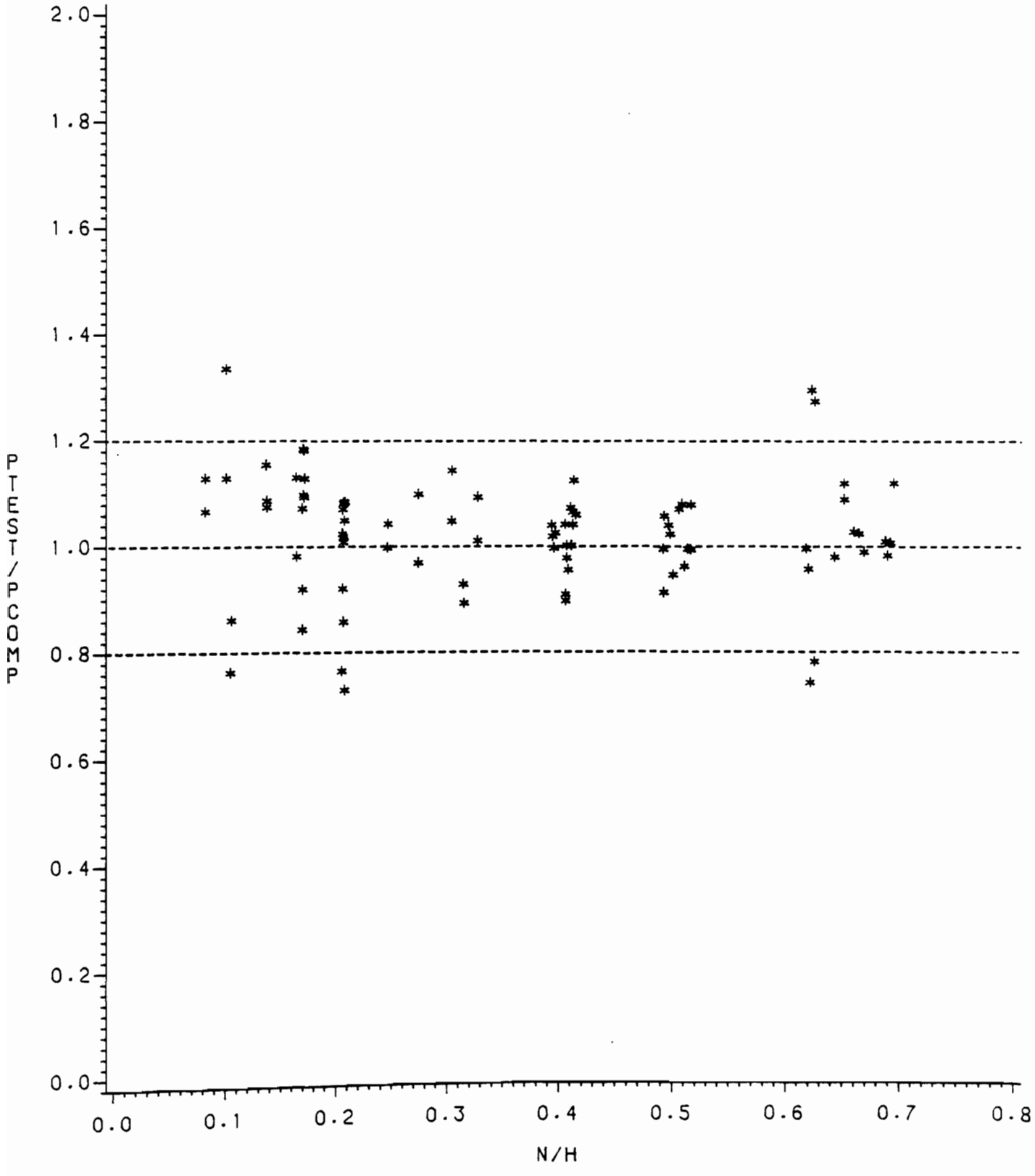

FIG. E2.2
EFFECT OF N/H ON THE RATIO PTEST/PCOMP FOR HAT SECTIONS SUBJECTED TO END ONE-FLANGE LOADING BASED ON THE PROPOSED DESIGN RECOMMENDATIONS

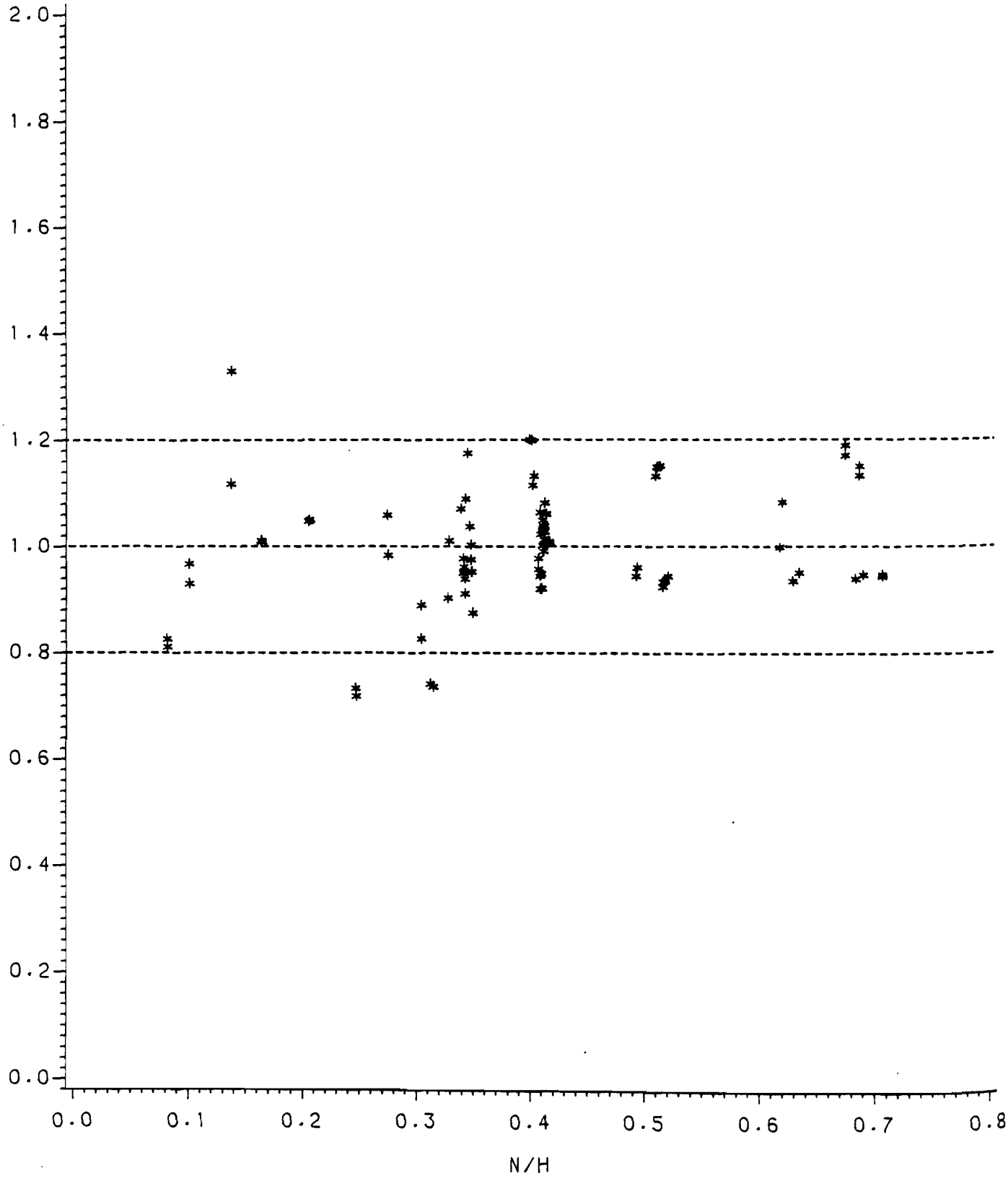

FIG. E3.2
EFFECT OF N/H ON THE RATIO PTEST/PCOMP FOR HAT SECTIONS SUBJECTED TO INTERIOR TWO-FLANGE LOADING BASED ON THE PROPOSED DESIGN RECOMMENDATIONS

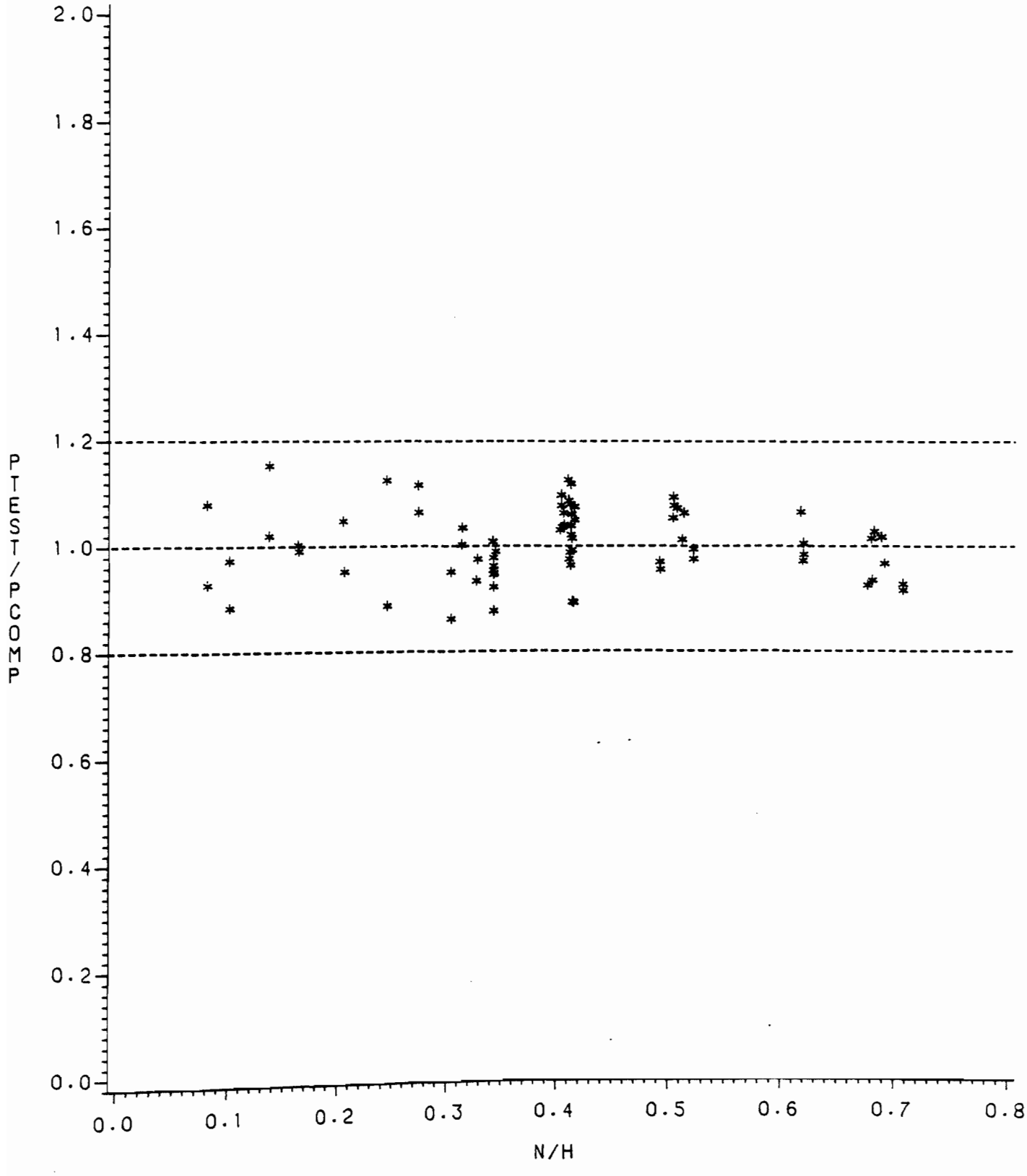

FIG. E4.2
EFFECT OF N/H ON THE RATIO PTEST/PCOMP FOR HAT SECTIONS SUBJECTED TO END TWO-FLANGE LOADING BASED ON THE PROPOSED DESIGN RECOMMENDATIONS

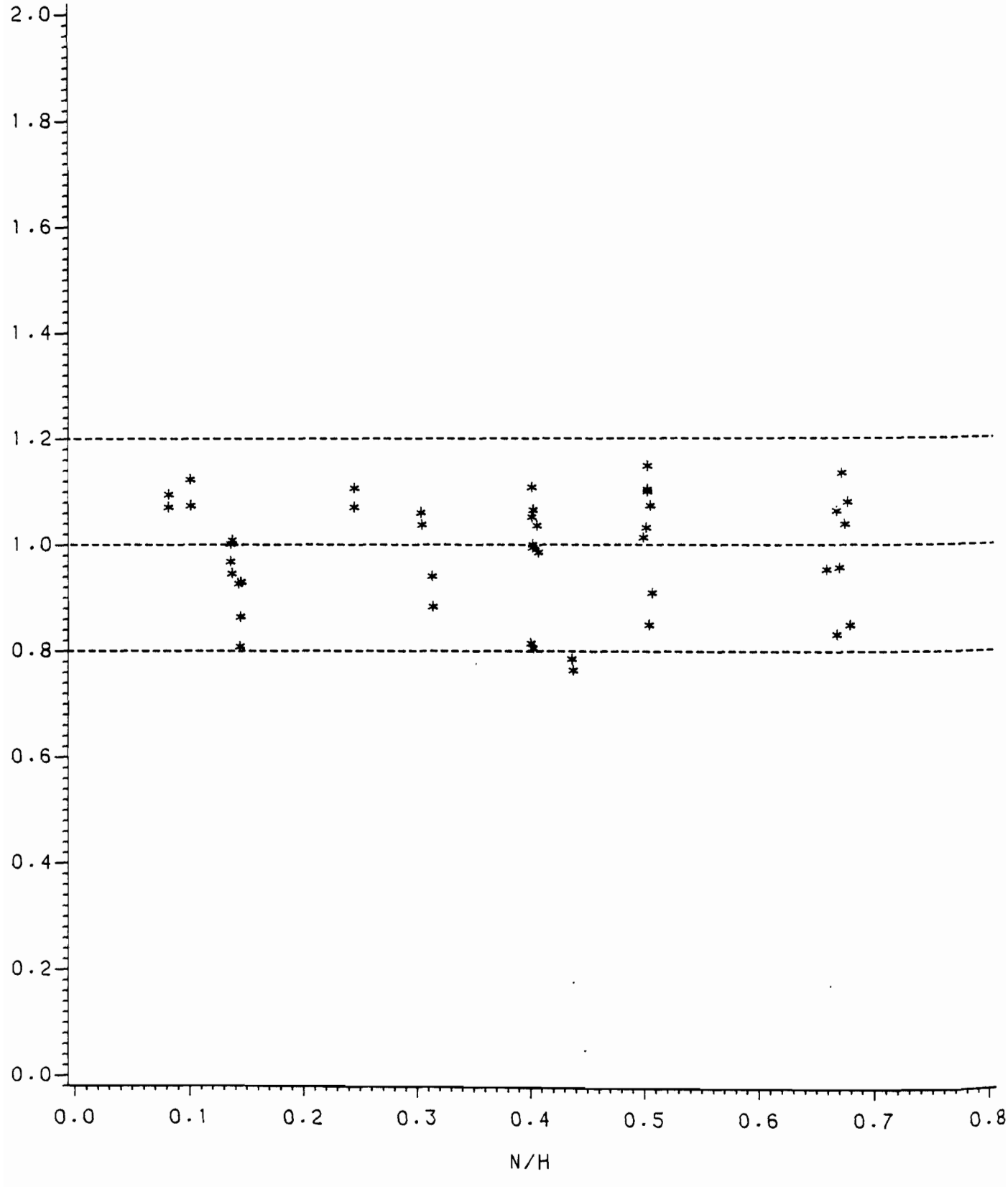

FIG. E5.2
EFFECT OF N/H ON THE RATIO PTEST/PCOMP FOR I-BEAMS SUBJECTED TO INTERIOR ONE-FLANGE LOADING BASED ON THE PROPOSED DESIGN RECOMMENDATIONS

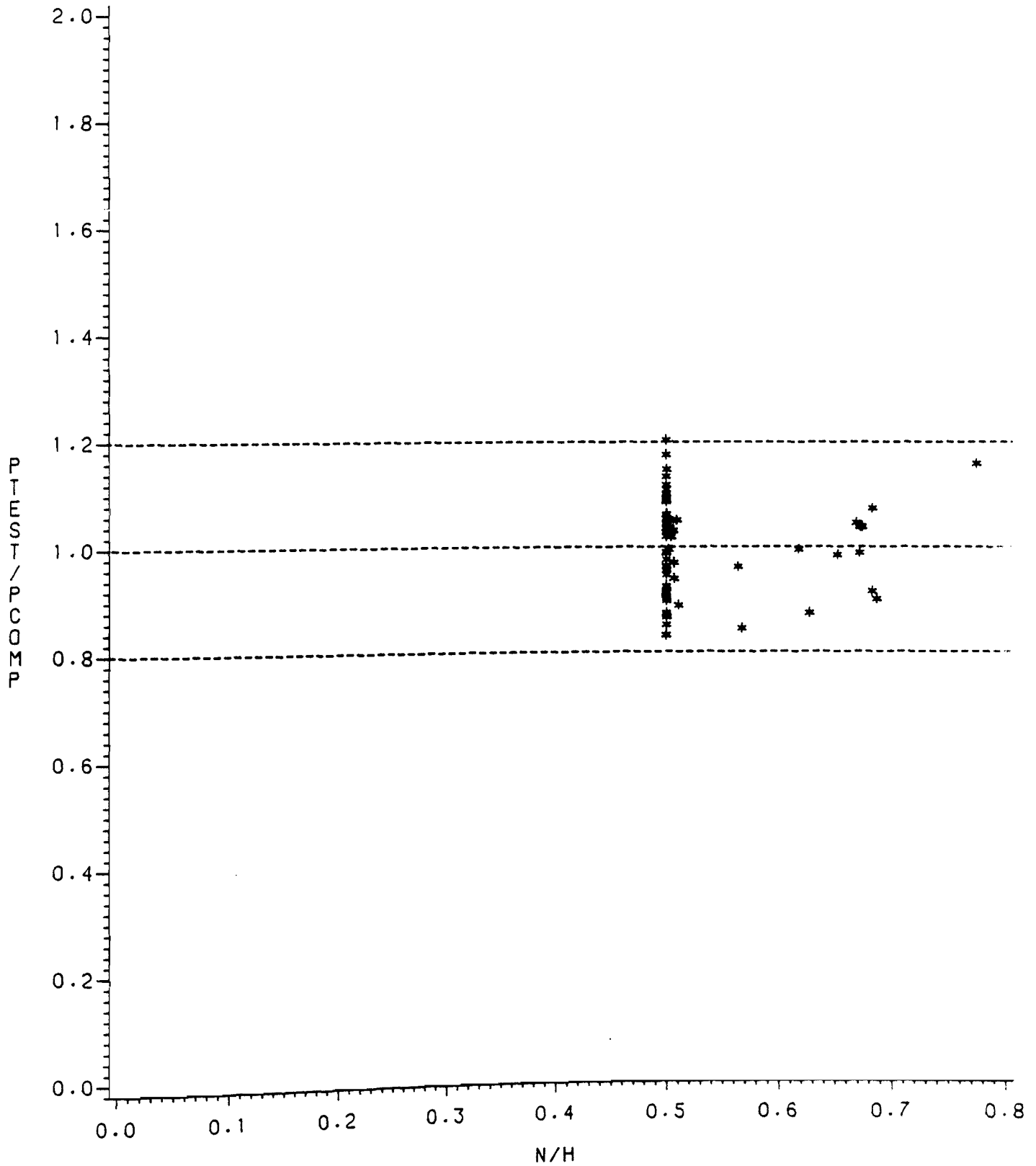

FIG. E6.2
EFFECT OF N/H ON THE RATIO PTEST/PCOMP FOR I-BEAMS SUBJECTED TO END ONE-FLANGE LOADING BASED ON THE PROPOSED DESIGN RECOMMENDATIONS

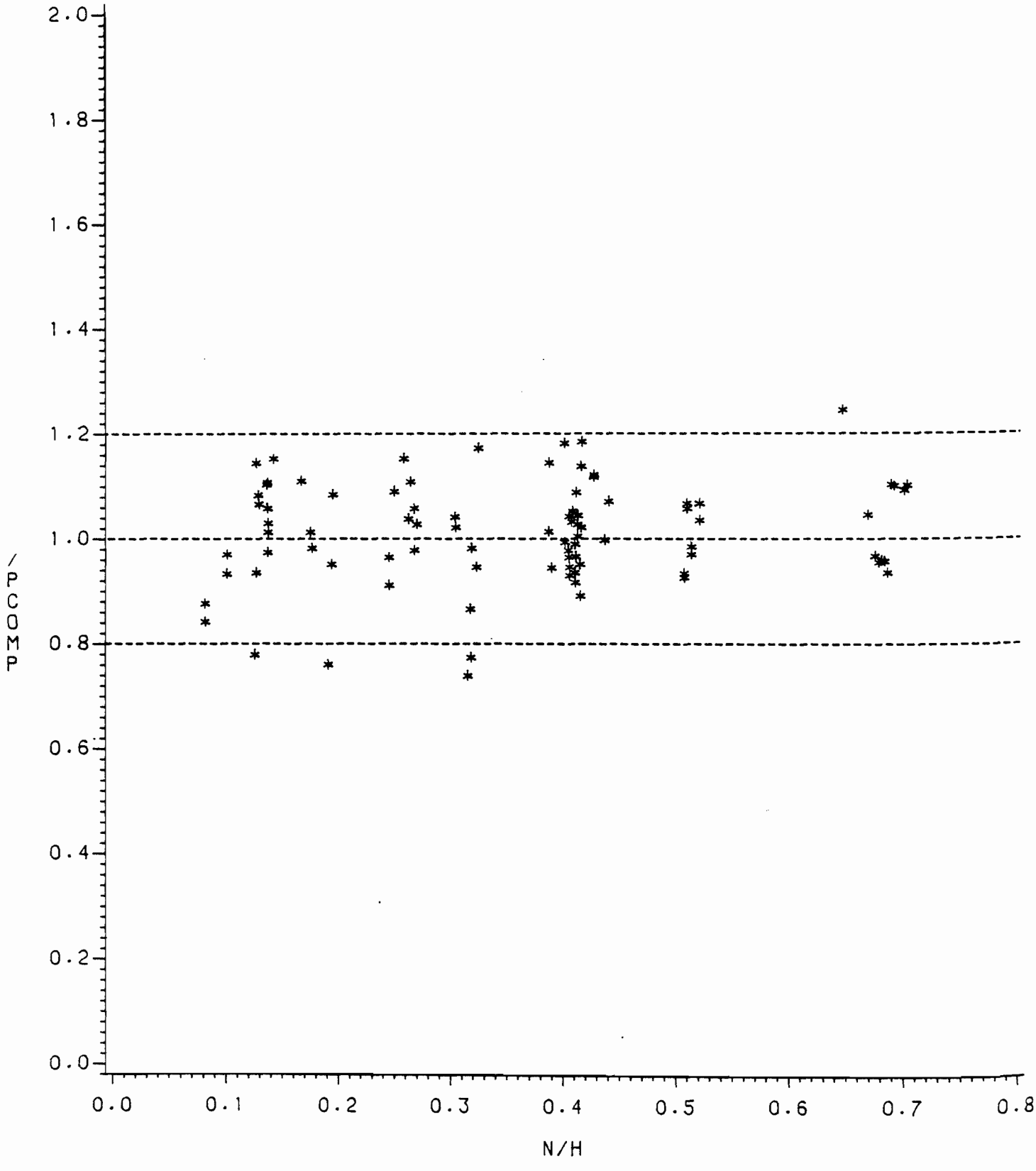

FIG. E7.2
EFFECT OF N/H ON THE RATIO PTEST/PCOMP FOR I-BEAMS SUBJECTED TO INTERIOR TWO-FLANGE LOADING BASED ON THE PROPOSED DESIGN RECOMMENDATIONS

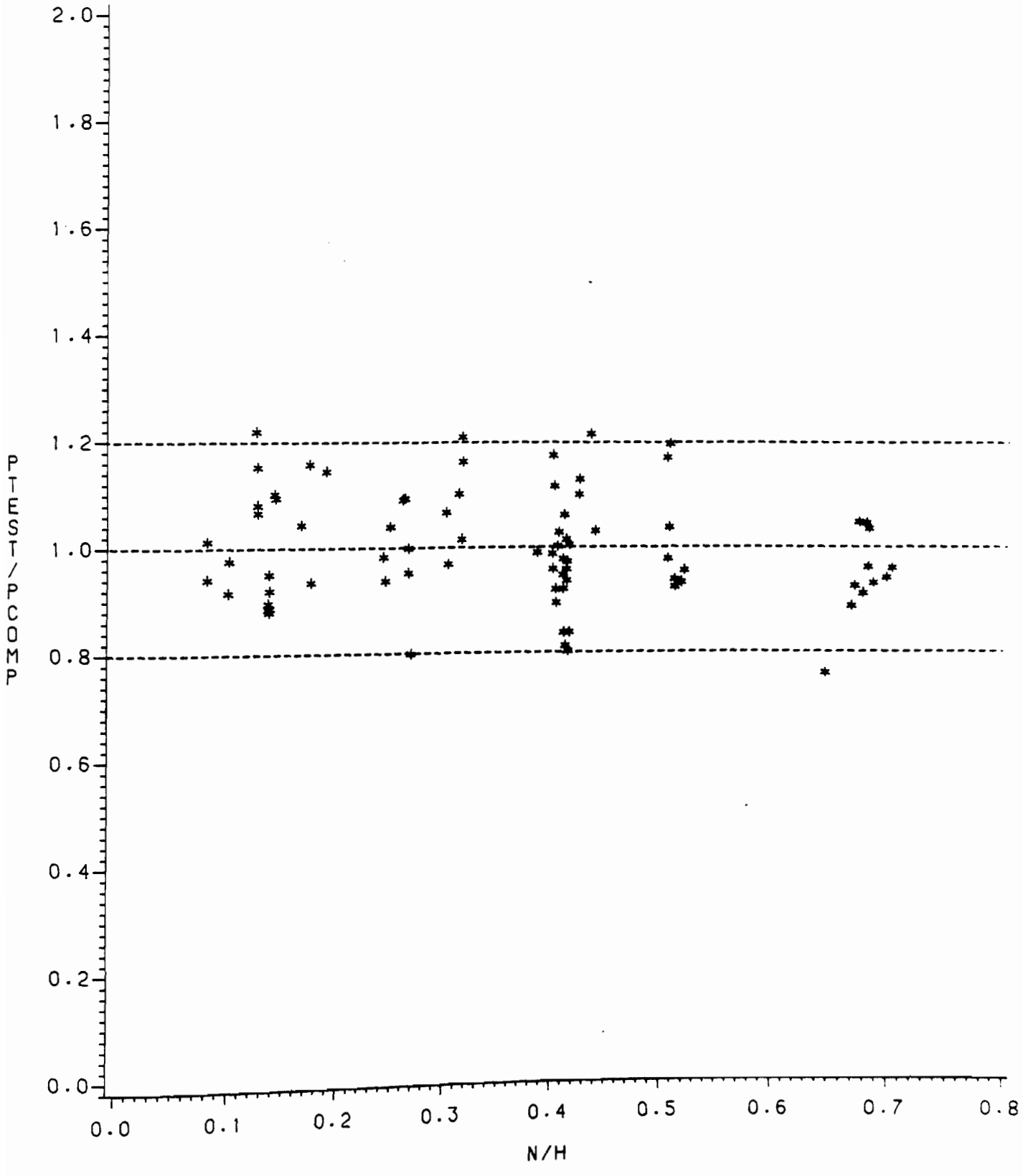

FIG. E8.2
EFFECT OF N/H ON THE RATIO PTEST/PCOMP FOR I-BEAMS SUBJECTED TO END TWO-FLANGE LOADING BASED ON THE PROPOSED DESIGN RECOMMENDATIONS

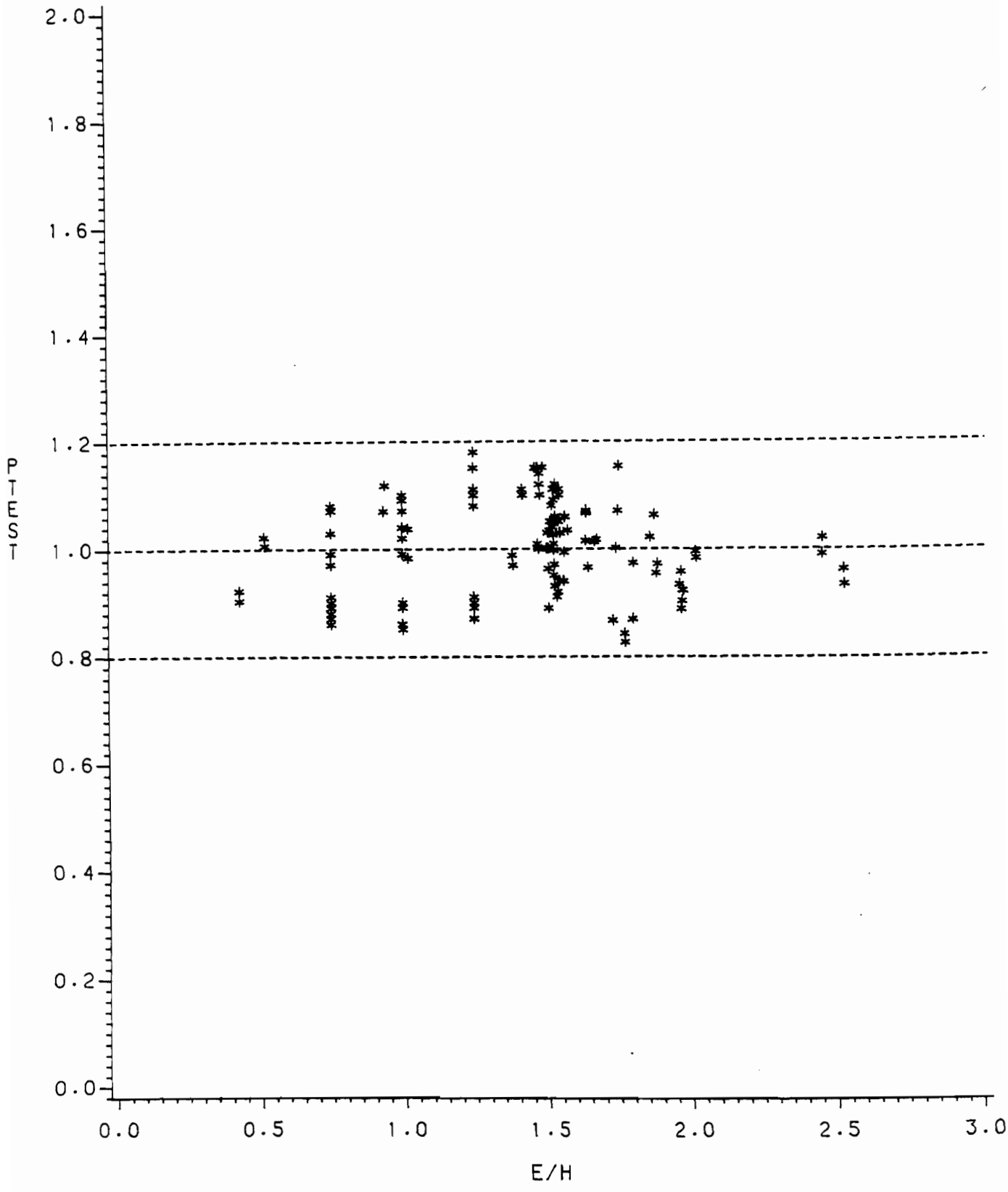

FIG. E1.3
EFFECT OF E/H ON THE RATIO PTEST/PCOMP FOR HAT SECTIONS SUBJECTED TO INTERIOR ONE-FLANGE LOADING BASED ON THE PROPOSED DESIGN RECOMMENDATIONS

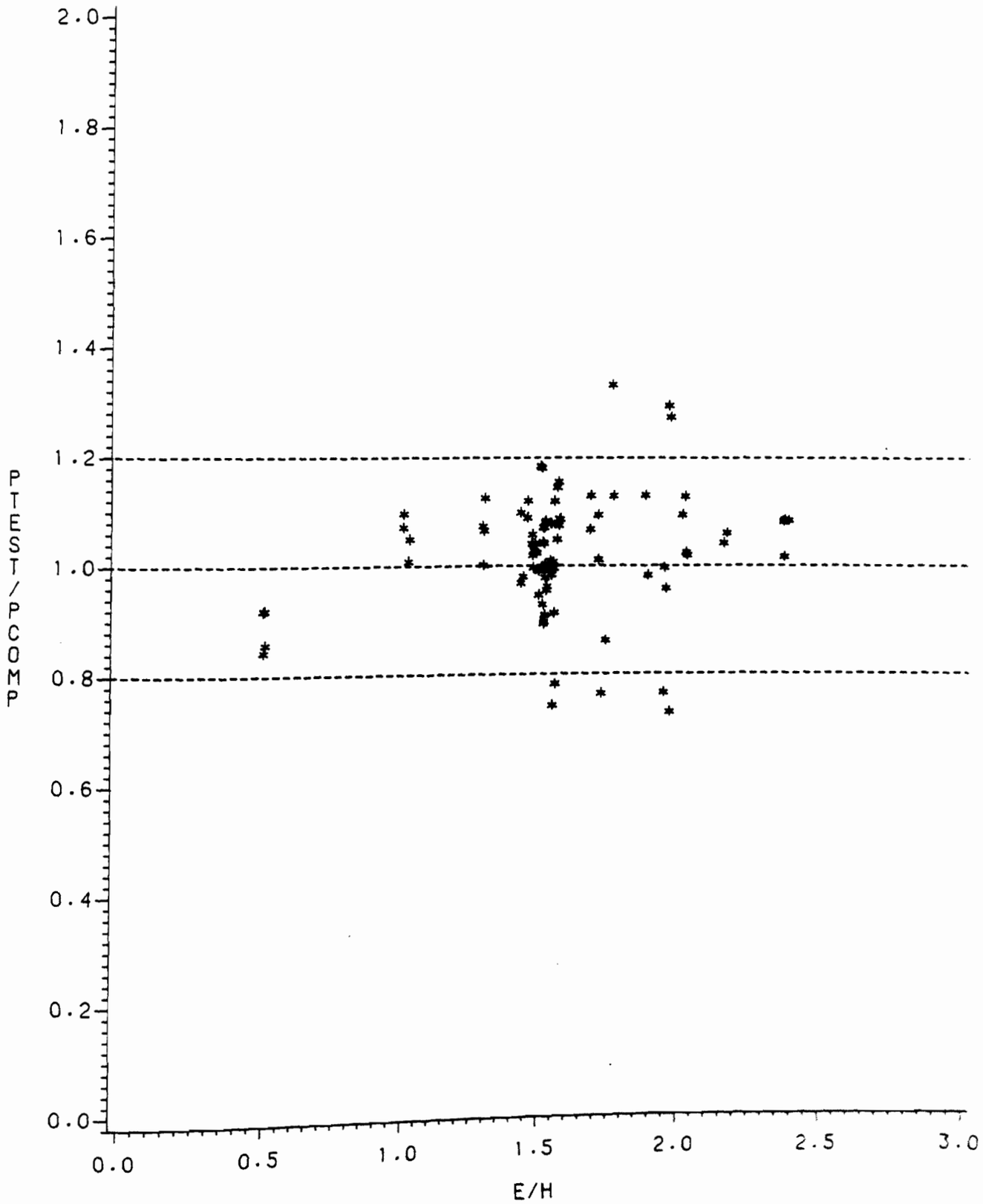

FIG. E2.3
EFFECT OF E/H ON THE RATIO PTEST/PCOMP FOR HAT SECTIONS SUBJECTED TO END ONE-FLANGE LOADING BASED ON THE PROPOSED DESIGN RECOMMENDATIONS

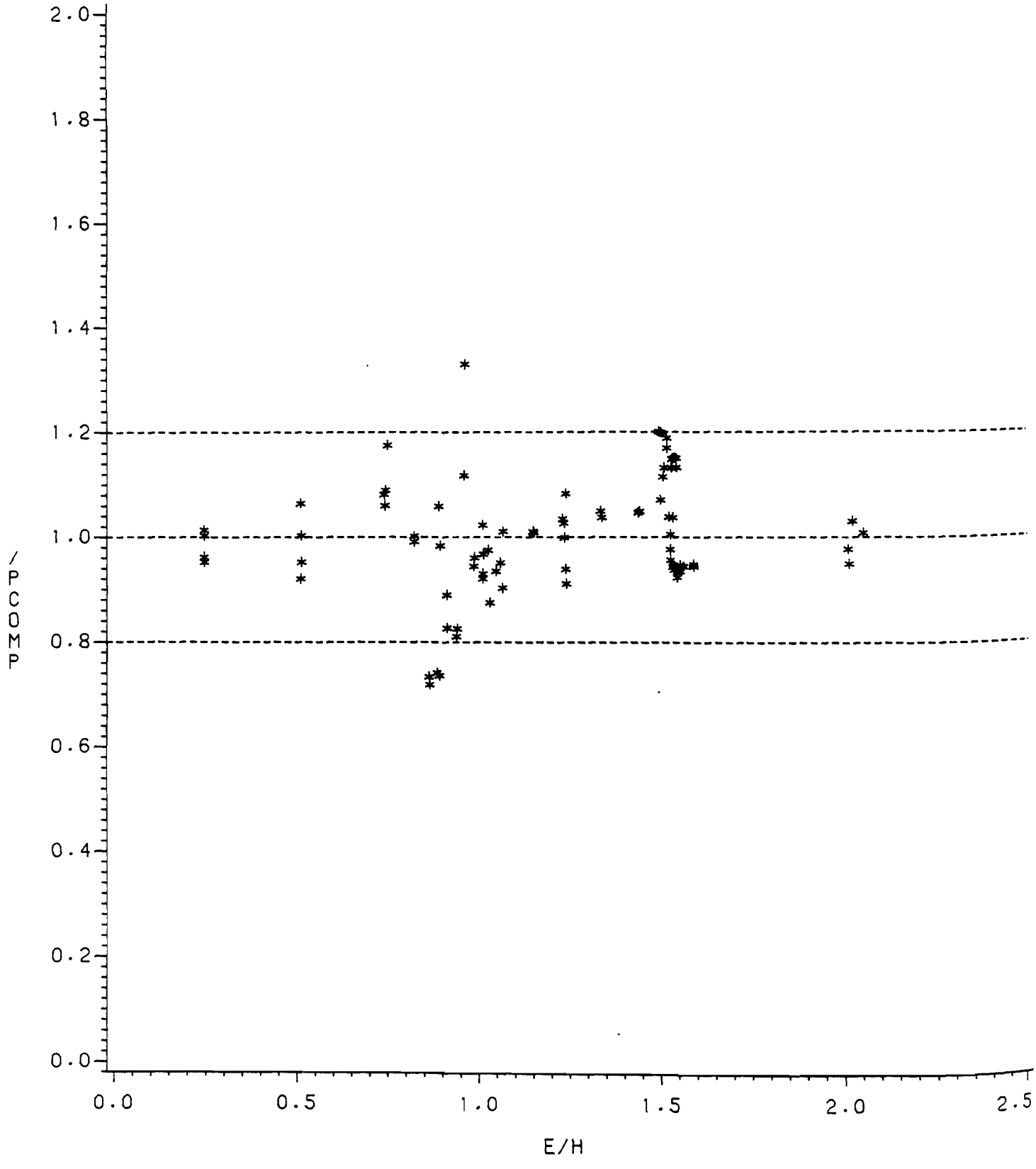

FIG. E3.3
EFFECT OF E/H ON THE RATIO PTEST/PCOMP FOR HAT SECTIONS SUBJECTED TO INTERIOR TWO-FLANGE LOADING BASED ON THE PROPOSED DESIGN RECOMMENDATIONS

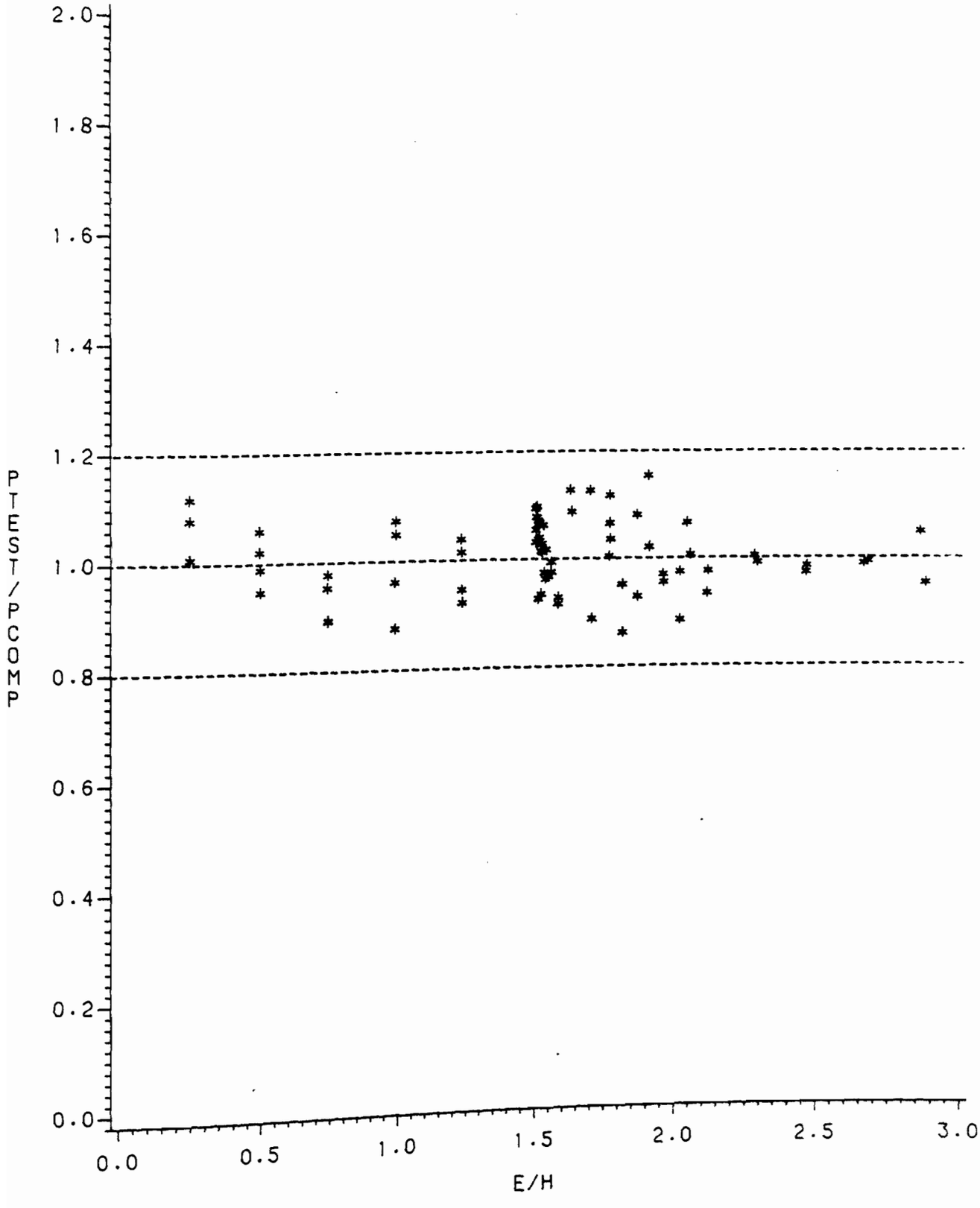

FIG. E4.3
EFFECT OF E/H ON THE RATIO PTEST/PCOMP FOR HAT SECTIONS SUBJECTED TO END TWO-FLANGE LOADING BASED ON THE PROPOSED DESIGN RECOMMENDATIONS

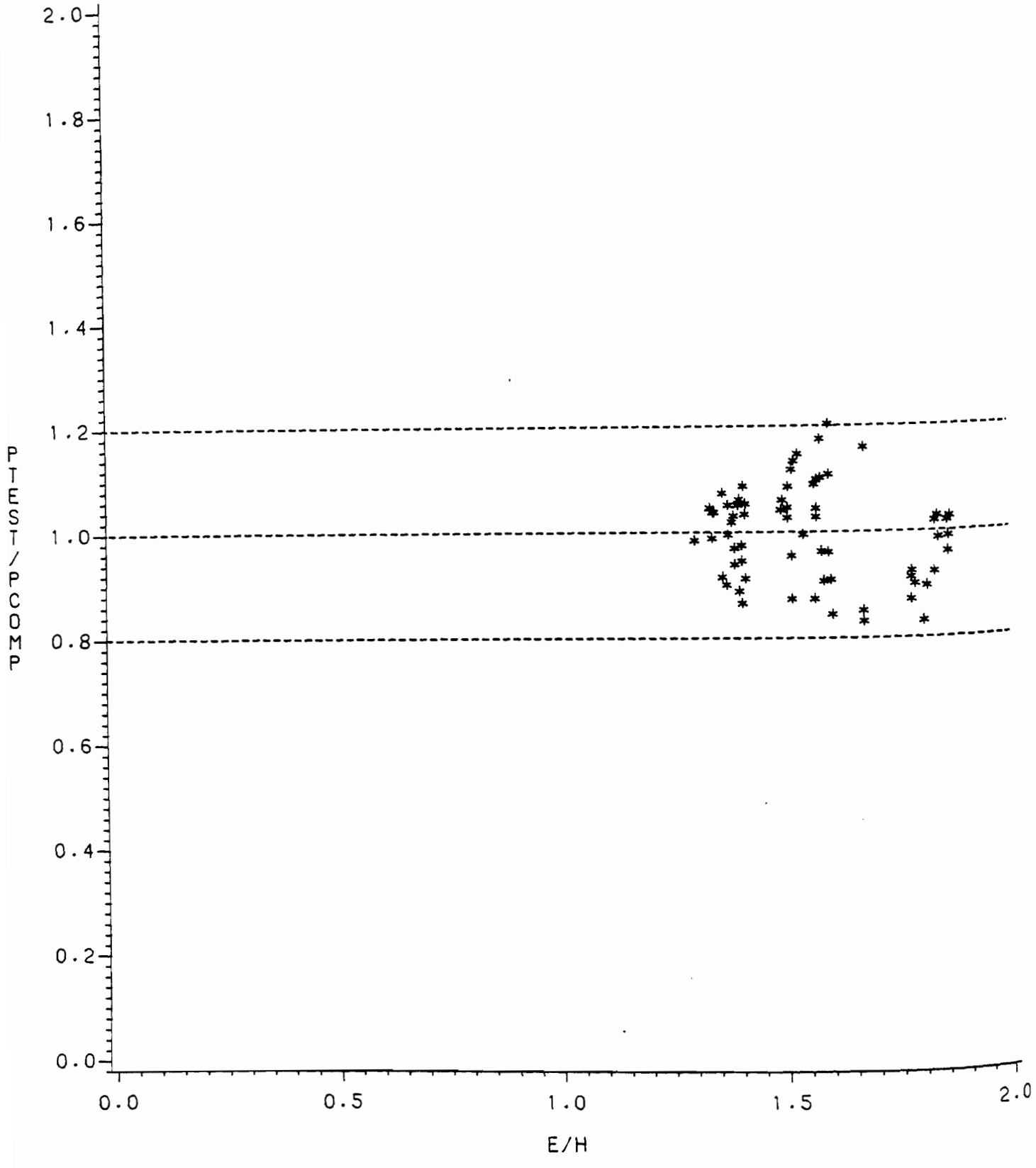

FIG. E6.3
EFFECT OF E/H ON THE RATIO PTEST/PCOMP FOR I-BEAMS
SUBJECTED TO END ONE-FLANGE LOADING BASED ON
THE PROPOSED DESIGN RECOMMENDATIONS

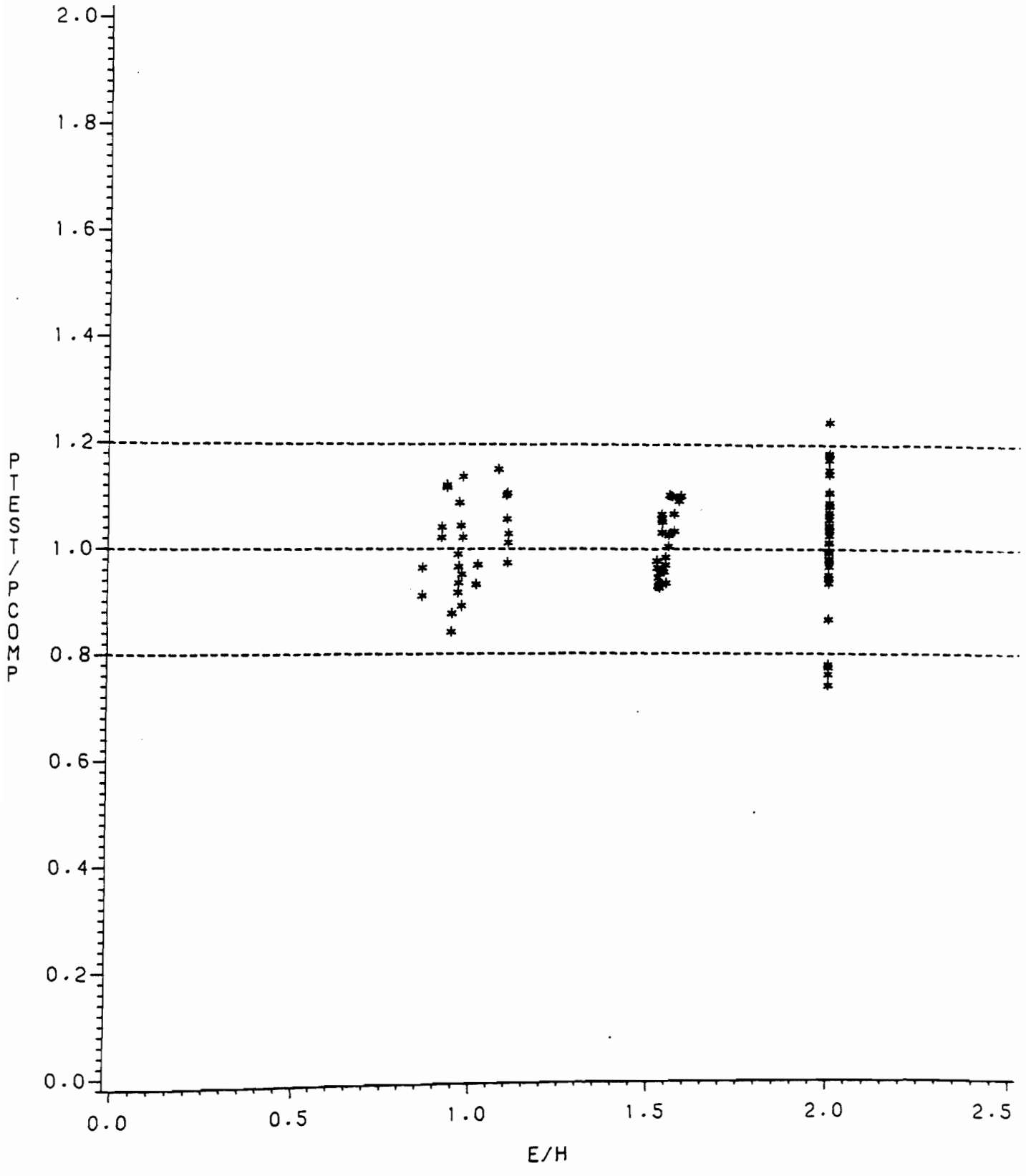

FIG. E7.3
EFFECT OF E/H ON THE RATIO PTEST/PCOMP FOR I-BEAMS SUBJECTED TO INTERIOR TWO-FLANGE LOADING BASED ON THE PROPOSED DESIGN RECOMMENDATIONS

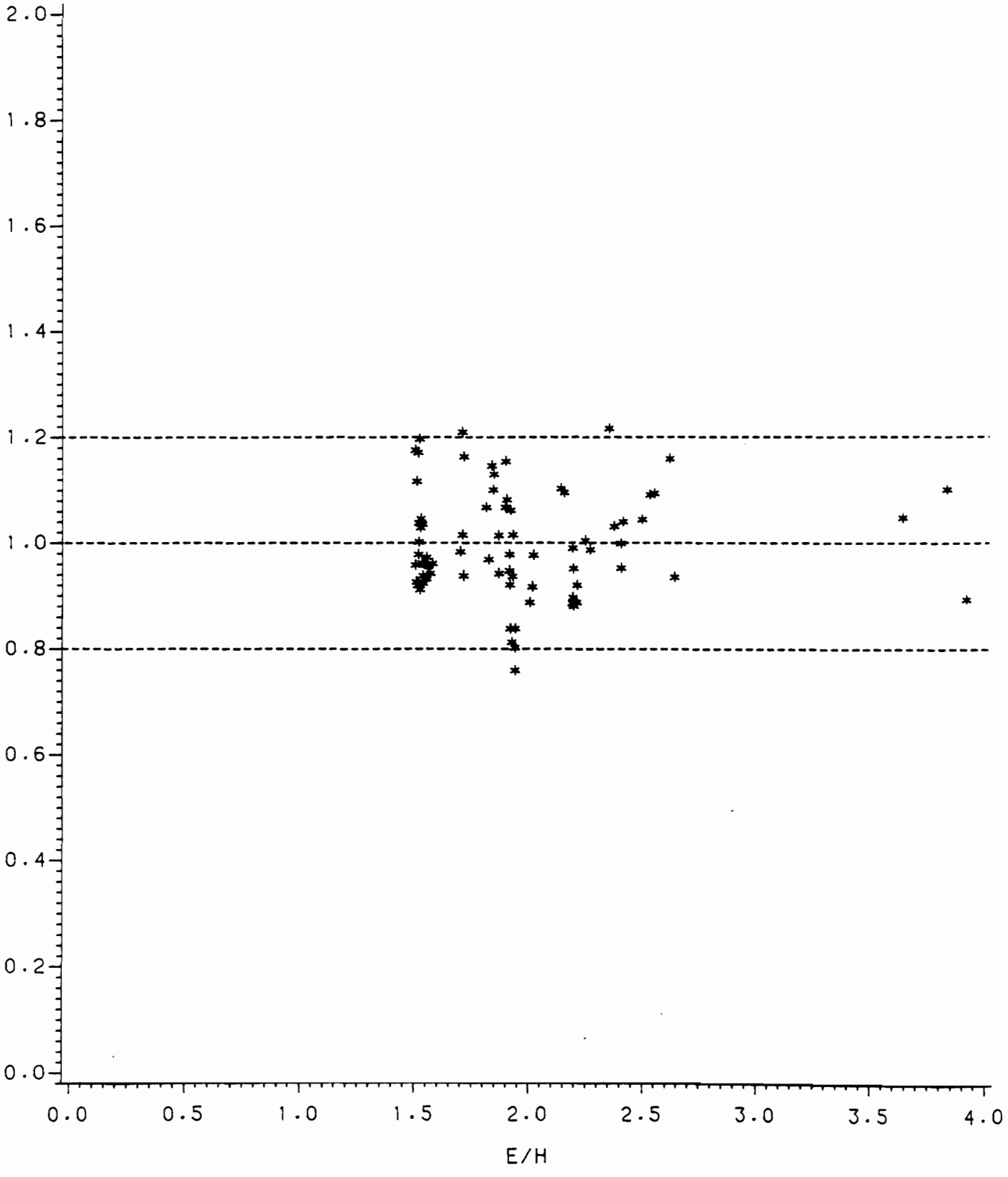

FIG. E8.3
EFFECT OF E/H ON THE RATIO PTEST/PCOMP FOR I-BEAMS
SUBJECTED TO END TWO-FLANGE LOADING BASED ON
THE PROPOSED DESIGN RECOMMENDATIONS

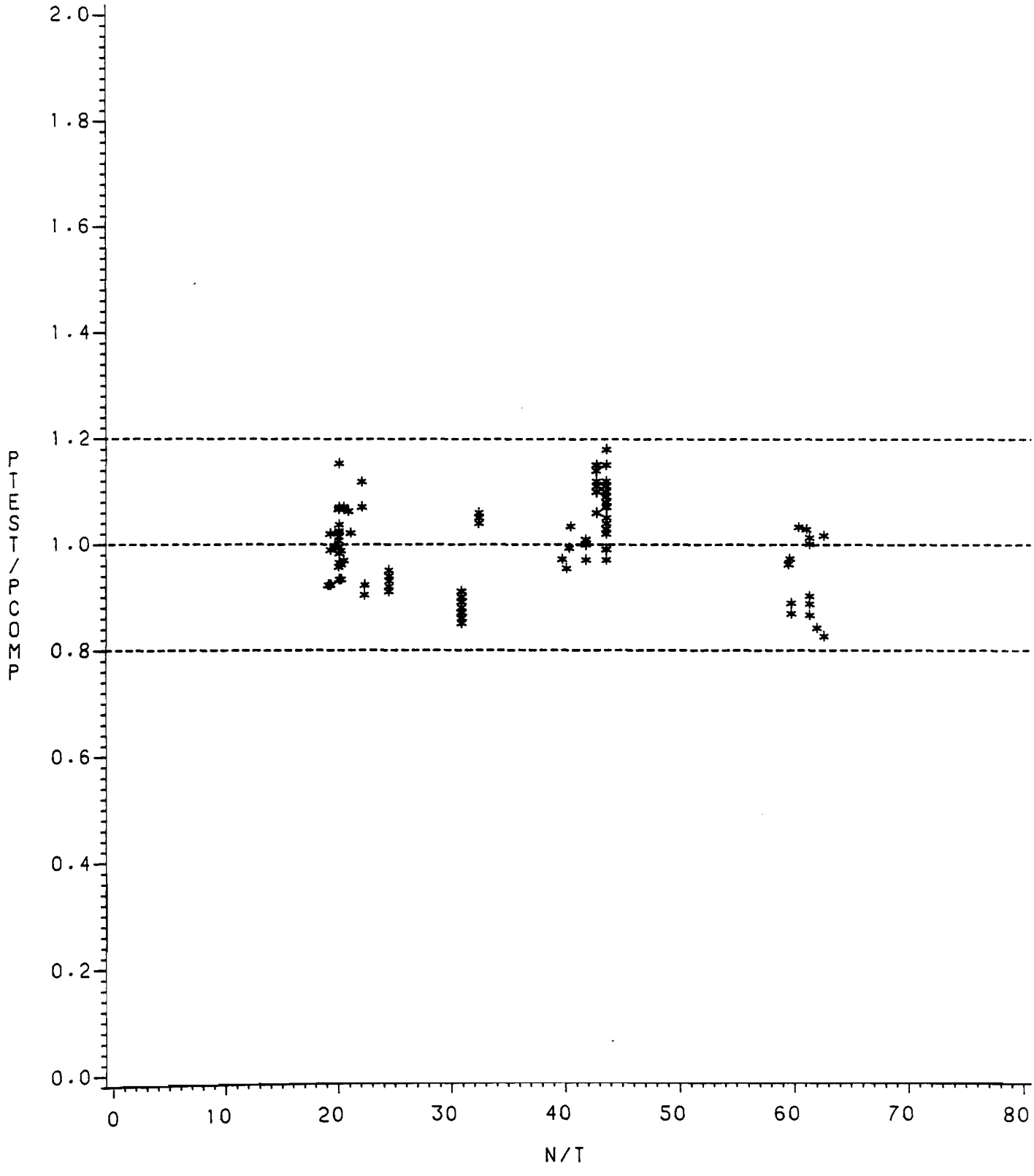

FIG. E1.4
EFFECT OF N/T ON THE RATIO PTEST/PCOMP FOR HAT SECTIONS
SUBJECTED TO INTERIOR ONE-FLANGE LOADING BASED ON
THE PROPOSED DESIGN RECOMMENDATIONS

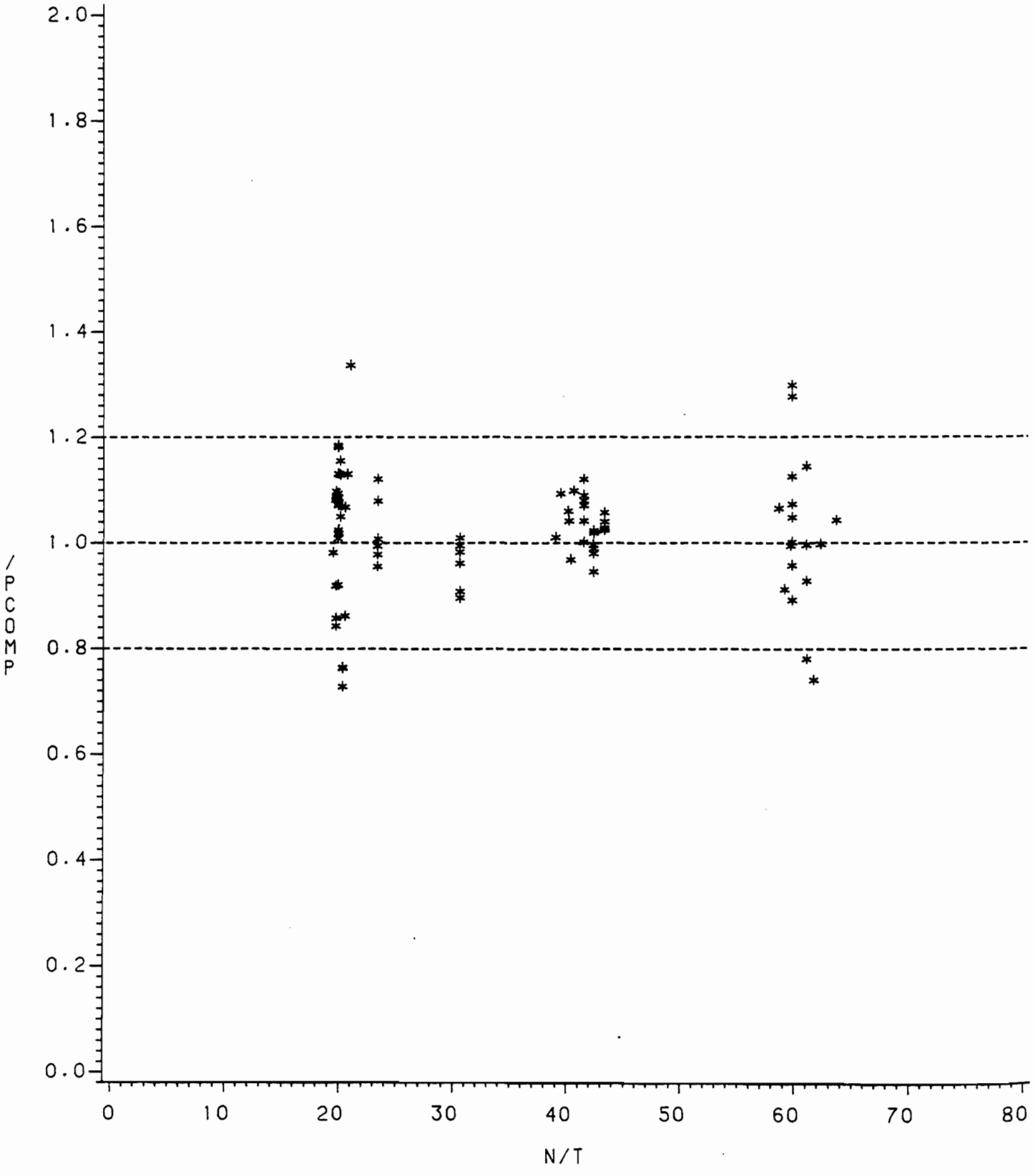

FIG. E2.4
EFFECT OF N/T ON THE RATIO PTEST/PCOMP FOR HAT SECTIONS
SUBJECTED TO END ONE-FLANGE LOADING BASED ON
THE PROPOSED DESIGN RECOMMENDATIONS

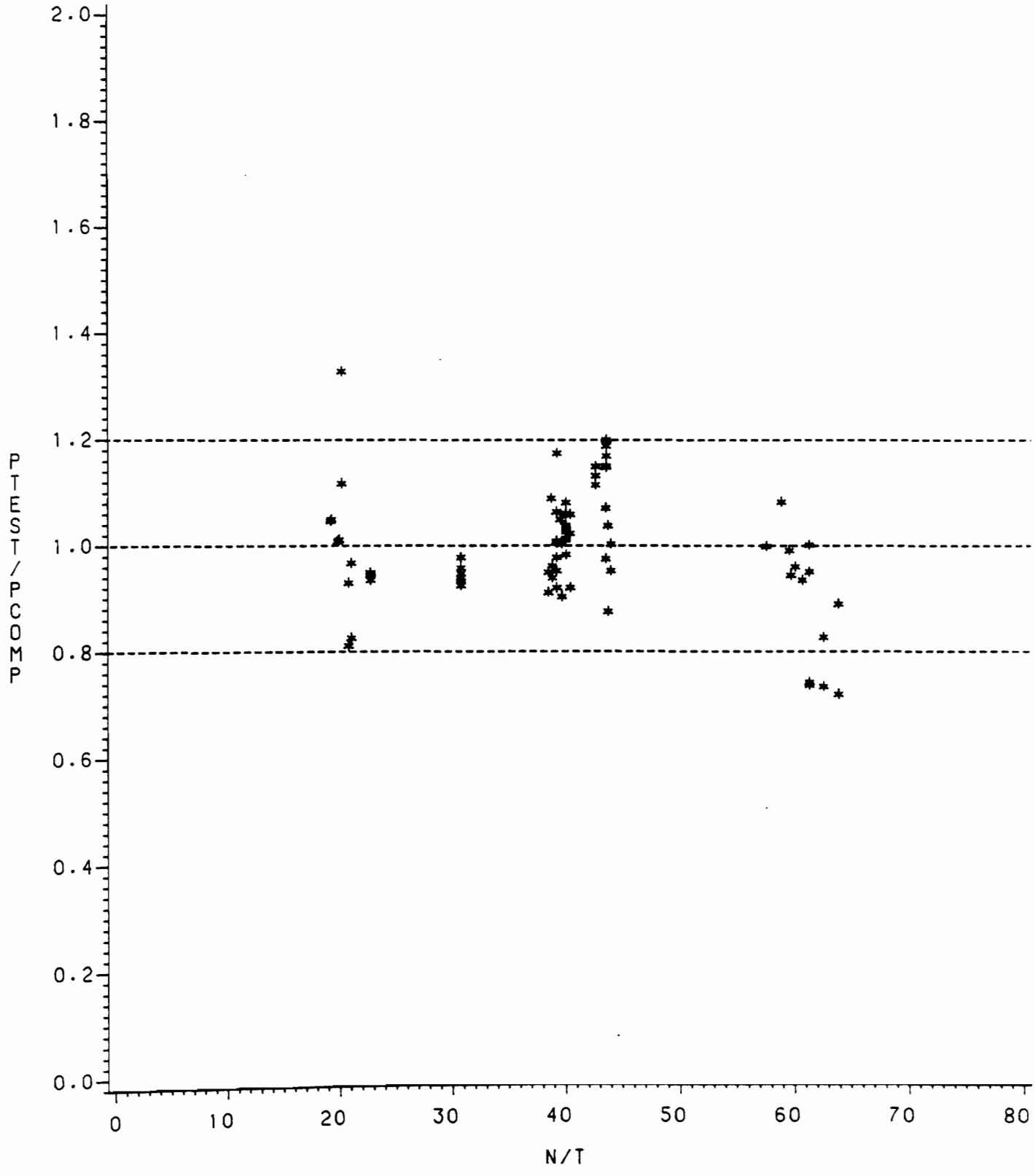

FIG. E3.4
EFFECT OF N/T ON THE RATIO PTEST/PCOMP FOR HAT SECTIONS SUBJECTED TO INTERIOR TWO-FLANGE LOADING BASED ON THE PROPOSED DESIGN RECOMMENDATIONS

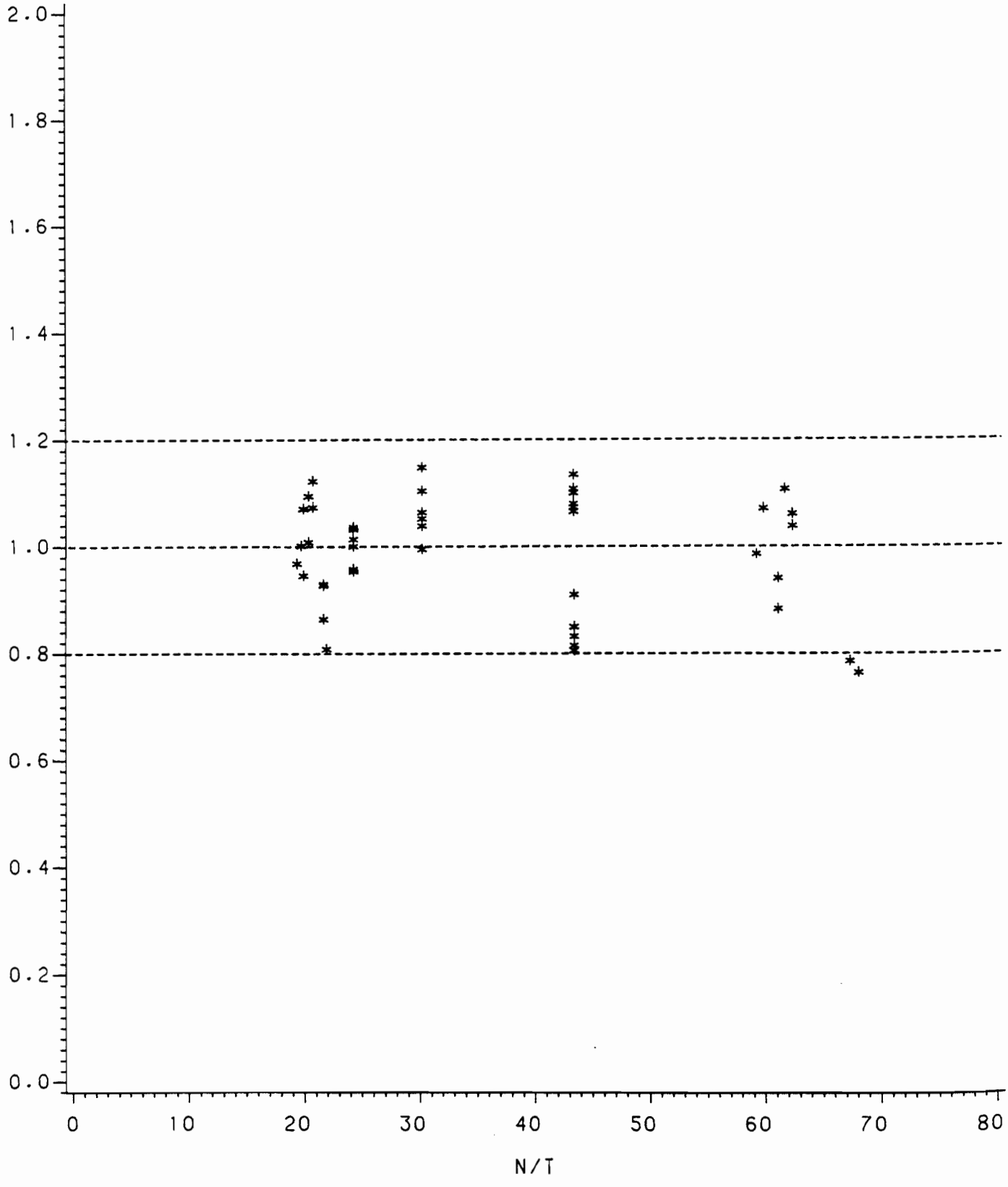

FIG. E5.4
EFFECT OF N/T ON THE RATIO PTEST/PCOMP FOR I-BEAMS SUBJECTED TO INTERIOR ONE-FLANGE LOADING BASED ON THE PROPOSED DESIGN RECOMMENDATIONS

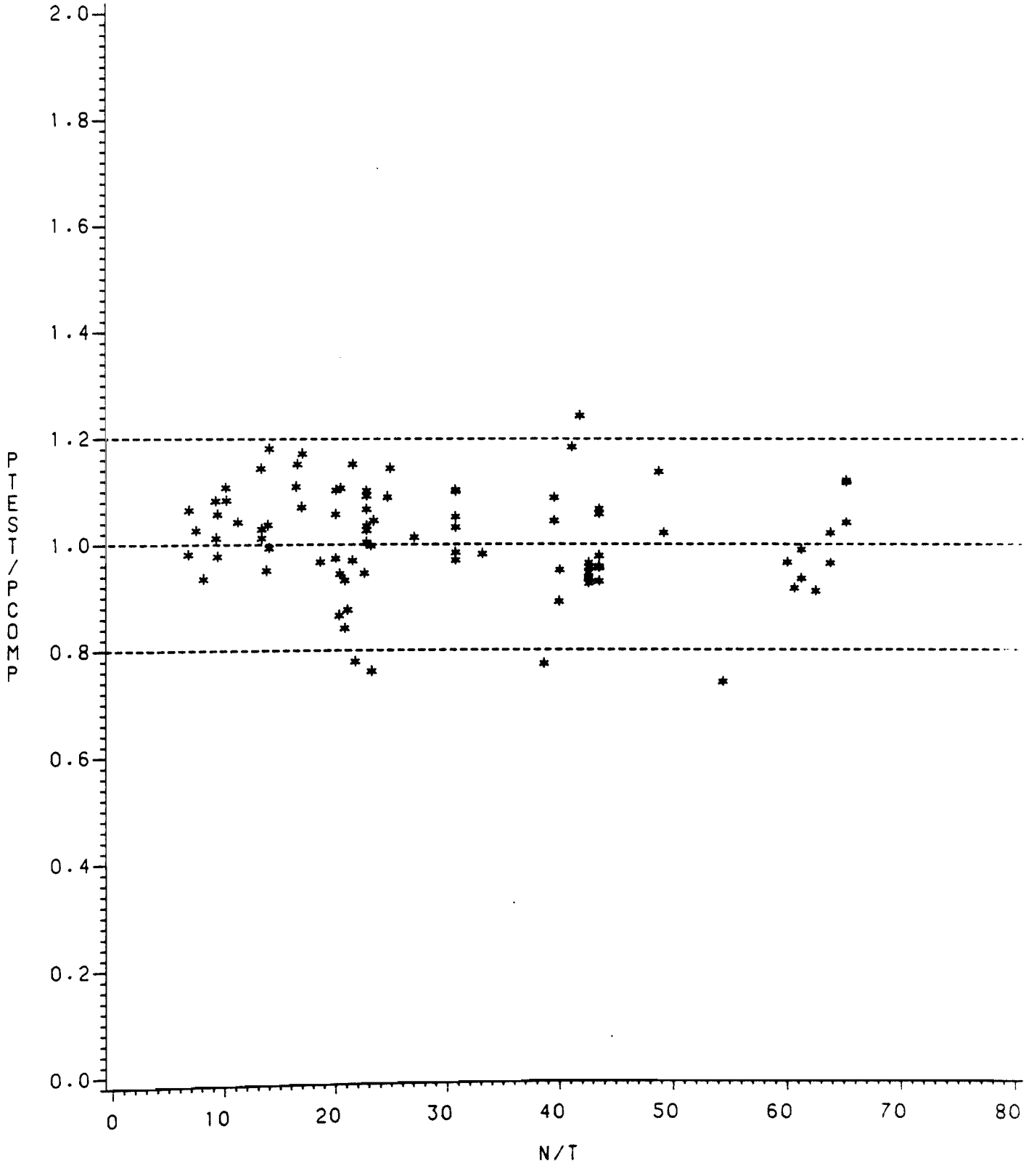

FIG. E7.4
EFFECT OF N/T ON THE RATIO PTEST/PCOMP FOR I-BEAMS SUBJECTED TO INTERIOR TWO-FLANGE LOADING BASED ON THE PROPOSED DESIGN RECOMMENDATIONS

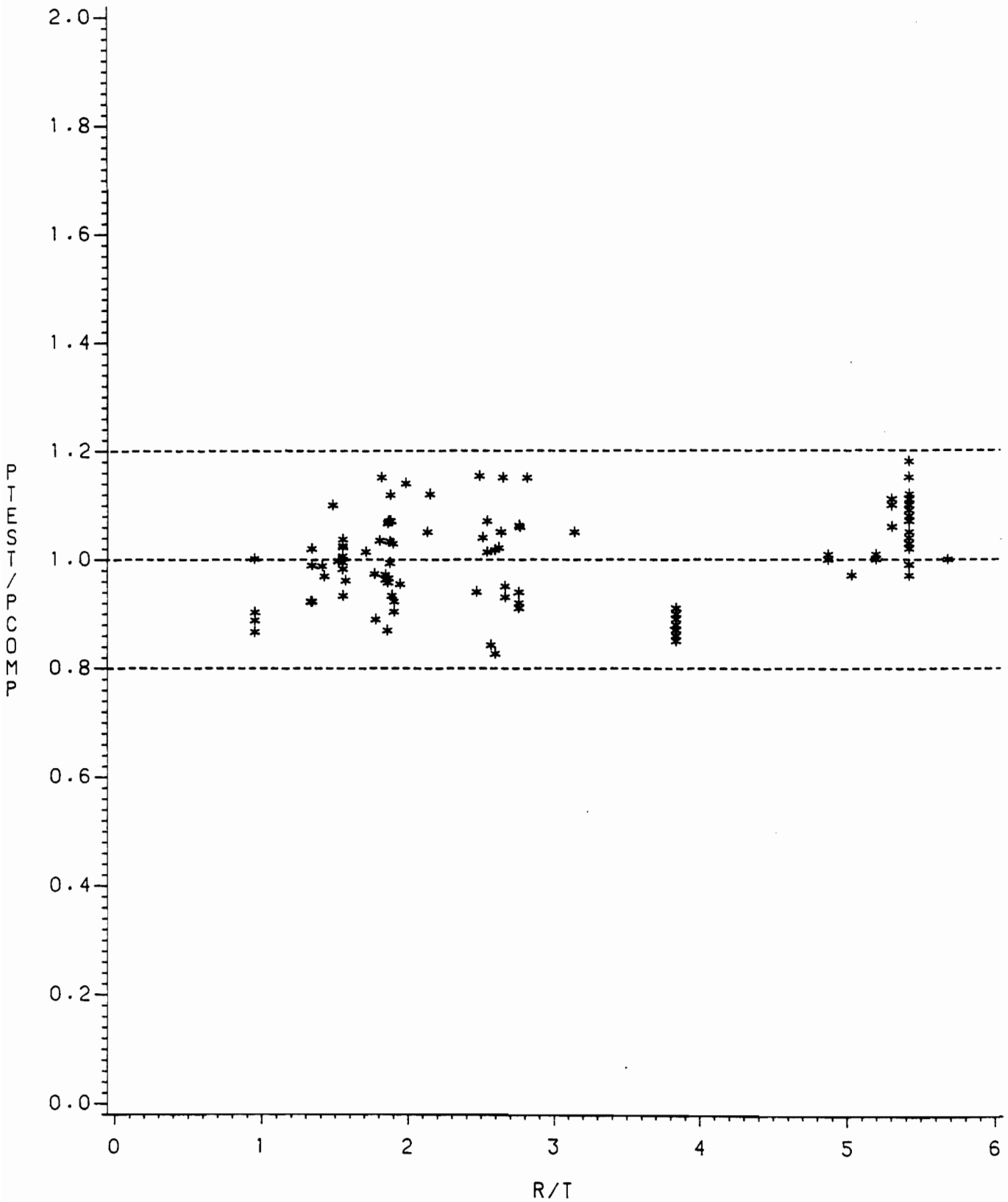

FIG. E1.5
EFFECT OF R/T ON THE RATIO PTEST/PCOMP FOR HAT SECTIONS
SUBJECTED TO INTERIOR ONE-FLANGE LOADING BASED ON
THE PROPOSED DESIGN RECOMMENDATIONS

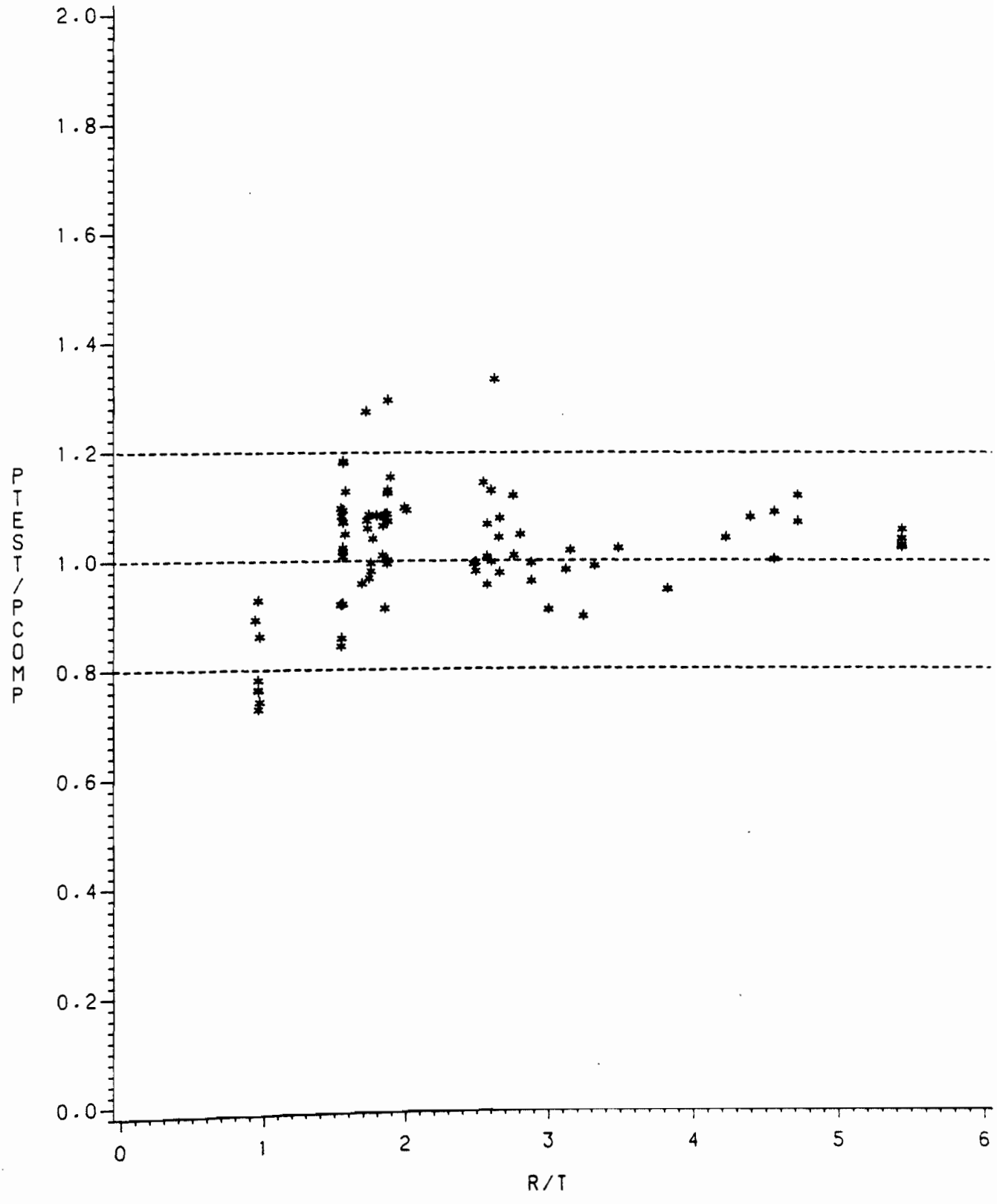

FIG. E2.5
EFFECT OF R/T ON THE RATIO PTEST/PCOMP FOR HAT SECTIONS SUBJECTED TO END ONE-FLANGE LOADING BASED ON THE PROPOSED DESIGN RECOMMENDATIONS

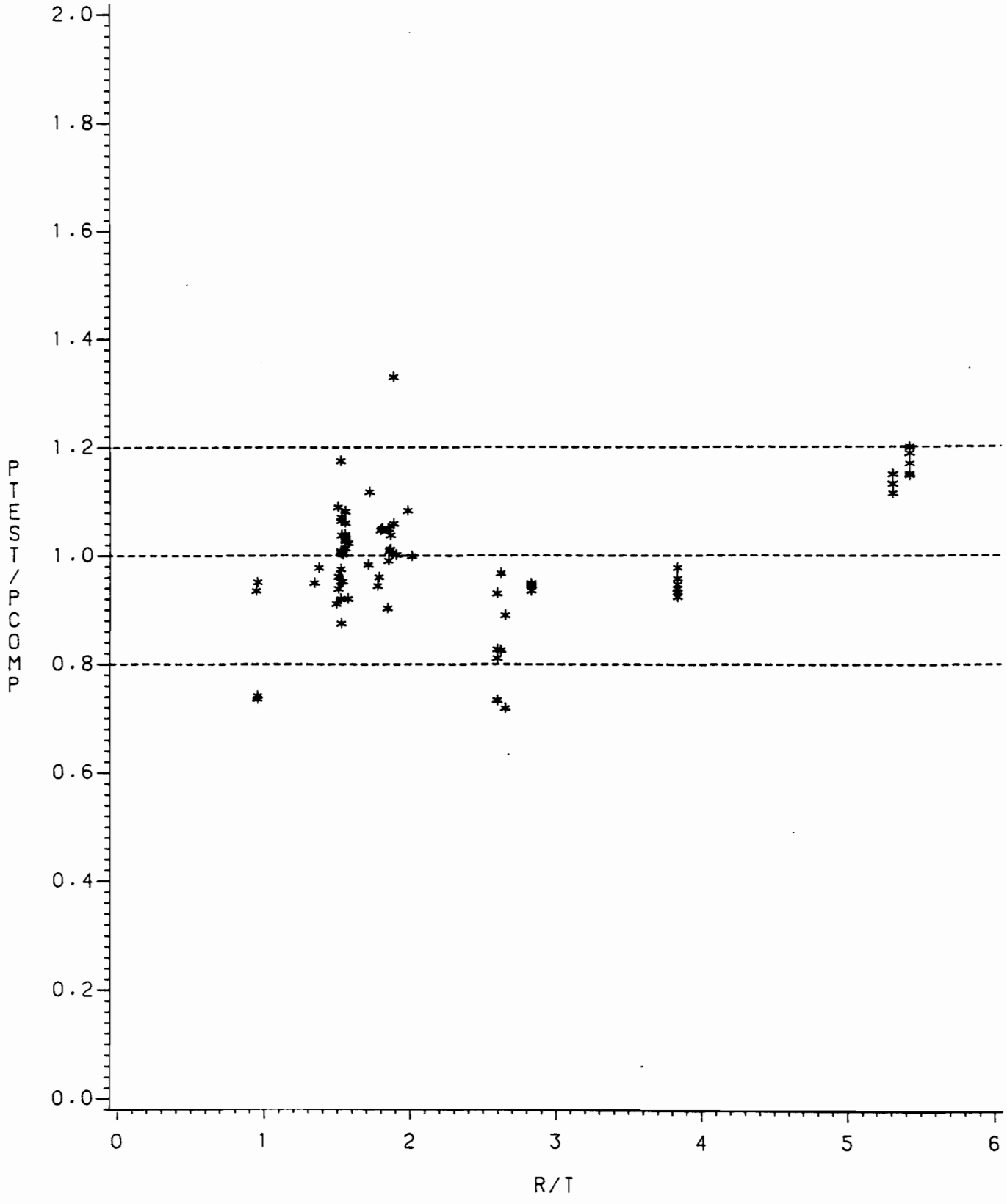

FIG. E3.5
EFFECT OF R/T ON THE RATIO PTEST/PCOMP FOR HAT SECTIONS SUBJECTED TO INTERIOR TWO-FLANGE LOADING BASED ON THE PROPOSED DESIGN RECOMMENDATIONS

APPENDIX F

COMPUTER PROGRAMS USED IN THE PREDICTIONS OF FAILURE LOADS BASED ON THE PROPOSED DESIGN RECOMMENDATIONS

```
c*************************************************************************************
c     THIS PROGRAM PREDICTS THE ULTIMATE LOADS FOR INLAND TEST DATA    *
c              BASED ON THE PROPOSED DESIGN RECOMMENDATIONS             *
c*************************************************************************************
      COMMON/DIMEN/B1,B2,D1,D2,R,T,FY,FU
      DIMENSION PC(100),PM(100),PMC(100),PTEST(100),RATIO(100),PMS(100),
     /PS(100),PBW(100),PCB(100),PMM(100)
C NN = TOTAL NUMBER OF TEST DATA
      READ(5,*)NN
      DO 60 I=1,NN
      READ(5,*)B1,B2,D1,D2,R,T,BRG,FY,FU,SPAN,PTEST(I)
      H=D1-2.*T
      TH=H/T
      IF(TH.LT.110.)TH=110.
      EH=10./H
      IF(EH.GT.5.0)EH=5.0
      TR=R/T
      TN=BRG/T
      HN=BRG/H
      IF(HN.GT.0.4)HN=0.4
C CALCULATE FLEXURAL YIELD MOMENT
      CALL MY1
C CALCULATE MOMENT,SHEAR,COMBINE MOMENT&SHEAR IN WEB
      CALL WEB(SPAN,SMP,SMP1,SP,SP1,BWP,BWP1)
      PS(I)=SP
      PBW(I)=BWP
      PMS(I)=SMP
      PC(I)=4.*7.80*T**2.*FY*(1.+.217*TN**.5)*(1.-.0814*TR)
      PCB(I)=4.*820.0*T**2.*(1.+2.4*HN)*(1-.0017*TH)*(1-.12*EH)
C FOR RAM LOAD - MOMENT=1/6*(P*L)
      PM(I)=6.*XM/SPAN
C COMPARE FLEXURAL MOMENT TO MOMENT IN WEB
      IF (PM(I).GT.PBW(I)) PM(I)=PBW(I)
C COMBINED MOMENT AND WEB CRIPPLING
      PMC(I)=1.42*PM(I)*PC(I)/(PC(I)+1.10*PM(I))
c     ASSUMP=PTEST(I)
C3000 AA=(ASSUMP/PBW(I))**2.073+(ASSUMP/PC(I))**1.504
C     AAA=ABS(1.-AA)
C     IF(AAA.LT..005) GO TO 4000
C     ASSUMP=ASSUMP+0.1*ASSUMP*(1.-AA)
C     GO TO 3000
C4000 PMC(I)=ASSUMP
c3000 AA=(ASSUMP/PBW(I))+1.045*(ASSUMP/PC(I)).
c     AAA=ABS(1.-1.341/AA)
c     IF(AAA.LT..005) GO TO 4000
c     ASSUMP=ASSUMP+0.2*ASSUMP*(1.341-AA)
c     GO TO 3000
c4000 PMC(I)=ASSUMP
      if (pMC(I)/PC(I).LT.0.38) PMC(I)=PBW(I)
      IF (PMC(I)/PBW(I).LT.0.32) PMC(I)=PC(I)
      IF (PMC(I).GT.PM(I)) PMC(I)=PM(I)
      IF (PMC(I).GT.PC(I)) PMC(I)=PC(I)
      PMM(I)=PMC(I)
```

```
      IF (PMC(I).GT.PCB(I)) PMC(I)=PCB(I)
      AA=PS(I)
      BB=PMC(I)
      CC=PMS(I)
C SELECT SMALLEST FAILURE LOAD
      CALL SELECT(AA,BB,CC,NF)
      GO TO (101,102,103),NF
  101 RATIO(I)=PS(I)/PTEST(I)
      GO TO 105
  102 RATIO(I)=PMC(I)/PTEST(I)
      GO TO 105
  103 RATIO(I)=PMS(I)/PTEST(I)
  105 RATIO(I)=1./RATIO(I)
   60 CONTINUE
      DO 70 I=1,NN
   70 WRITE(6,1004)I,PM(I),PC(I),PMM(I),PCB(I),PMS(I),PTEST(I),RATIO(I)
 1004 FORMAT(3X,I2,6(F8.3),'    MC',F11.2)
      STOP
      END
C
C
C
      SUBROUTINE MY1
      COMMON/DIMEN/B1,B2,D1,D2,R,T,FY,FU
      COMMON/VALUE/XM,XI,XS,ASSUMF,YCG,UM,LIMIT
      W=B1-2.*(R+T)
      W1=(B2-B1)/2.-T-2.*R
      D3=D1-2.*(R+T)
      D4=D2-(R+T)
      R1=R+T/2.
      U1=1.57*R1
      C1=0.637*R1
      WT=W/T
      H1=2.*D4
      H2=4.*U1
      H3=2.*W1
      H4=2.*D3
      H5=2.*U1
      HL=H1+H2+H3+H4+H5
      Y1=D1-R-T-D4/2.
      Y2=D1-R-T+C1
      Y3=D1-T/2.
      Y4=D1/2.
      Y5=R+T-C1
      HY1=H1*Y1
      HY2=H2*Y2
      HY3=H3*Y3
      HY4=H4*Y4
      HY5=H5*Y5
      HYL=HY1+HY2+HY3+HY4+HY5
      HYY1=HY1*Y1
      HYY2=HY2*Y2
      HYY3=HY3*Y3
```

```
      HYY4=HY4*Y4
      HYY5=HY5*Y5
      HYYL=HYY1+HYY2+HYY3+HYY4+HYY5
      XI0=2.*(D3**3.+D4**3.)/12.+6.*.149*R1**3.
      CALL TRIAL(W,D1,T,FY,WT,HL,HYL,HYYL,XI0,XI,XM,XS,ASSUMF,YCG)
      RETURN
      END
C
C
C
      SUBROUTINE TRIAL(W,D1,T,FY,WT,HL,HYL,HYYL,XI0,XI,XM,XS,ASSUMF,YCG)
      ASSUMF=FY
  100 SF=SQRT(ASSUMF)
      WTLIM=221./SF
      IF(WT.GT.WTLIM)GO TO 110
      BE=W
      GO TO 120
  110 BE=326./SF*(1.-71.3/WT/SF)*T
  120 HT=HL+BE
      HYT=HYL+BE*T/2.
      HYYT=HYYL+BE*T/2.*T/2.
      YCG=HYT/HT
      IF(YCG.GE.D1/2.)GO TO 200
      F=FY*YCG/(D1-YCG)
      TOL=1.-F/ASSUMF
      ATOL=ABS(TOL)
      IF(ATOL.LE.0.005)GO TO 300
      ASSUMF=F
      GO TO 100
  200 XI=(HYYT+XI0-HT*YCG**2.)*T
      XS=XI/YCG
      GO TO 400
  300 XI=(HYYT+XI0-HT*YCG**2.)*T
      XS=XI/(D1-YCG)
  400 XM=FY*XS
      RETURN
      END
C
C
C
      SUBROUTINE WEB(SPAN,PMS,PMS1,PS,PS1,PBW,PBW1)
      COMMON/DIMEN/B1,B2,D1,D2,R,T,FY,FU
      COMMON/VALUE/XM,XI,XS,ASSUMF,YCG,UM,LIMIT
      H=D1-2.*T
      HT=H/T
      SF=SQRT(FY)
C BENDING IN WEB
      FBWU1=640000./(HT)**2.
      IF (FBWU1.GT.FY) FBWU1=FY
      FBWU=(1.21-.00034*HT*SF)*FY
      CFBWU=FBWU
      IF (FBWU.GT.FY) FBWU=FY
C SHEAR IN WEB
```

```
      SFY=.577*FY
      HTLIM=237.*SQRT(5.34/FY)
      IF (HT.GT.HTLIM) GO TO 10
      FVU=110.*SQRT(5.34*FY)/HT
      CFVU=FVU
      IF (FVU.GT.SFY) FVU=SFY
      GO TO 20
   10 FVU=26660.*5.34/HT**2.
      CFVU=FVU
   20 HTLIM1=648./SF
      IF (HT.GT.HTLIM1) GO TO 30
      FVU1=219.*SF/HT
      IF (FVU1.GT.SFY) FVU1=SFY
      GO TO 40
   30 FVU1=142000/HT**2.
C SHEAR IN WEB
   40 PS=4.*H*T*FVU
      PS1=4.*H*T*FVU1
C BENDING IN WEB
      PBW=FBWU*XI*6./(YCG-T)/SPAN
      PBW1=FBWU1*XI*6./(YCG-T)/SPAN
C COMBINE BENDING AND SHEAR
      BWEB=(SPAN*(YCG-T)/6./XI/CFBWU)**2.
      BWEB1=(SPAN*(YCG-T)/6./XI/FBWU1)**2.
      SWEB=(.25/H/T/CFVU)**2.
      SWEB1=(.25/H/T/FVU1)**2.
      PMS=SQRT(1./(BWEB+SWEB))
      PMS1=SQRT(1./(BWEB1+SWEB1))
      RETURN
      END
C
C
C
      SUBROUTINE SELECT(A,B,C,NF)
      IF (A-B) 10,10,40
   10 IF (A-C) 20,20,30
   20 NF=1
      GO TO 100
   30 NF=3
      GO TO 100
   40 IF (B-C) 50,50,30
   50 NF=2
  100 RETURN
      END
```

```
c*************************************************************************************
c       THIS PROGRAM PREDICTS THE ULTIMATE LOADS FOR FORD TEST DATA      *
c              BASED ON THE PROPOSED DESIGN RECOMMENDATIONS               *
c*************************************************************************************
      COMMON/DIMEN/B1,B2,D1,R,T,FYF,FYW
      DIMENSION PC(100),PM(100),PMC(100),PTEST(100),RATIO(100),PMS(100),
     /PS(100),PBW(100),PCB(100),PMM(100)
C NN = TOTAL NUMBER OF TEST DATA
      READ(5,*)NN
      DO 60 I=1,NN
      READ(5,*)B1,B2,D1,R,T,BRG,FYF,FYW,SPAN,PTEST(I)
      H=D1-2.*T
      TH=H/T
      IF(TH.LT.110.)TH=110.
      EH=4./H
      IF(EH.GT.5.0)EH=5.0
      TR=R/T
      TN=BRG/T
      HN=BRG/H
      IF(HN.GT.0.4)HN=0.4
C CALCULATE FLEXURAL YIELD MOMENT
      CALL MY1 (UM)
C CALCULATE MOMENT,SHEAR,COMBINE MOMENT&SHEAR IN WEB
      CALL WEB(UM,SPAN,SMP,SMP1)
      PMS(I)=SMP
      PC(I)=4.*7.80*T**2.*FY*(1.+.217*TN**.5)*(1.-.0814*TR)
      PCB(I)=4.*820.0*T**2.*(1.+2.4*HN)*(1-.0017*TH)*(1-.12*EH)
C FOR RAM LOAD - MOMENT=1/6*(P*L)
      PM(I)=6.*XM/SPAN
C COMBINED MOMENT AND WEB CRIPPLING
      PMC(I)=1.42*PM(I)*PC(I)/(PC(I)+1.10*PM(I))
c     ASSUMP=PTEST(I)
C3000 AA=(ASSUMP/PBW(I))**2.073+(ASSUMP/PC(I))**1.504
C     AAA=ABS(1.-AA)
C     IF(AAA.LT..005) GO TO 4000
C     ASSUMP=ASSUMP+0.1*ASSUMP*(1.-AA)
C     GO TO 3000
C4000 PMC(I)=ASSUMP
c3000 AA=(ASSUMP/PBW(I))+1.045*(ASSUMP/PC(I))
c     AAA=ABS(1.-1.341/AA)
c     IF(AAA.LT..005) GO TO 4000
c     ASSUMP=ASSUMP+0.2*ASSUMP*(1.341-AA)
c     GO TO 3000
c4000 PMC(I)=ASSUMP
      if (pMC(I)/PC(I).LT.0.38) PMC(I)=PBW(I)
      IF (PMC(I)/PBW(I).LT.0.32) PMC(I)=PC(I)
      IF (PMC(I).GT.PM(I)) PMC(I)=PM(I)
      IF (PMC(I).GT.PC(I)) PMC(I)=PC(I)
      PMM(I)=PMC(I)
      IF (PMC(I).GT.PCB(I)) PMC(I)=PCB(I)
      AA=PM(I)
      BB=PMC(I)
      CC=PMS(I)
C SELECT SMALLEST FAILURE LOAD
```

```
      CALL SELECT(AA,BB,CC,NF)
      GO TO (101,102,103),NF
  101 RATIO(I)=PS(I)/PTEST(I)
      GO TO 105
  102 RATIO(I)=PMC(I)/PTEST(I)
      GO TO 105
  103 RATIO(I)=PMS(I)/PTEST(I)
  105 RATIO(I)=1./RATIO(I)
   60 CONTINUE
      DO 70 I=1,NN
   70 WRITE(6,1004)I,PM(I),PC(I),PMM(I),PCB(I),PMS(I),PTEST(I),RATIO(I)
 1004 FORMAT(3X,I2,6(F8.3),'    MC',F11.2)
      STOP
      END
C
C
C
      SUBROUTINE MY1 (UM)
      COMMON/DIMEN/B1,B2,D1,R,T,FYW,FYF
      W=B1-T
      W1=(B2-W)/2.
      D=D1-T
      SF=SQRT(FYF)
      WTLIM=221./SF
      WT=W/t
      IF(WT.GT.WTLIM) GO TO 100
      BE=W
      GO TO 200
  100 BE=326./SF*(1.-71.3/WT/SF)*T
  200 YC=D**2./(BE+2.*D-123.75*FYF)
      YT=D-YC
      UM=BE*FYF*YC + 2./3.*FYF*YC**2. + 2./3.*FYF*YT**3./YC + 123.75*(t+
     /0.03)/2.
C
C
C
      SUBROUTINE WEB(UM,SPAN,PMS,PMS1)
      COMMON/DIMEN/B1,B2,D1,R,T,FYF,FYW
      H=D1-2.*T
      HT=H/T
      SF=SQRT(FYW)
C BENDING IN WEB
      FBWU1=640000./(HT)**2.
      IF (FBWU1.GT.FYW) FBWU1=FYW
      FBWU=(1.21-.00034*HT*SF)*FYW
      CFBWU=FBWU
      IF (FBWU.GT.FY) FBWU=FYW
C SHEAR IN WEB
      SFY=.577*FYW
      HTLIM=237.*SQRT(5.34/FYW)
      IF (HT.GT.HTLIM) GO TO 10
      FVU=110.*SQRT(5.34*FYW)/HT
      CFVU=FVU
```

```
      IF (FVU.GT.SFY) FVU=SFY
      GO TO 20
   10 FVU=26660.*5.34/HT**2.
      CFVU=FVU
   20 HTLIM1=648./SF
      IF (HT.GT.HTLIM1) GO TO 30
      FVU1=219.*SF/HT
      IF (FVU1.GT.SFY) FVU1=SFY
      GO TO 40
   30 FVU1=142000/HT**2.
C SHEAR IN WEB
   40 PS=4.*H*T*FVU
      PS1=4.*H*T*FVU1
C COMBINE BENDING AND SHEAR
      PMU=6.*UM/SPAN
      PMS=SQRT((PMU*PS)**2./(PMU**2.+PS**2.))
      PMS1=SQRT((PMU*PS1)**2./(PMU**2.+PS1**2.))
      RETURN
      END
C
C
C
      SUBROUTINE SELECT(A,B,C,NF)
      IF (A-B) 10,10,40
   10 IF (A-C) 20,20,30
   20 NF=1
      GO TO 100
   30 NF=3
      GO TO 100
   40 IF (B-C) 50,50,30
   50 NF=2
  100 RETURN
      END
```

APPENDIX G

COMPARISONS OF THE PREDICTED ULTIMATE WEB CRIPPLING LOADS BASED ON THE AISI 1986 SPECIFICATION AND THE PROPOSED DESIGN RECOMMENDATIONS

```
C*************************************************************************
C   THIS PROGRAM COMPARES THE ULTIMATE WEB CRIPPLING LOAD BASED ON     *
C    THE PROPOSED METHOD AND THE MODIFIED AISI 1986 SPECIFICATION      *
C*************************************************************************
C  NOTE: THE MODIFIED AISI 1986 SPECIFICATION IS BASED ON THE MODIFIED
C        FUCTIONS OF YIELD STRENGTH (SEE FIG. 4.1B)
C*************************************************************************
      COMMON/IN/F,T,H,H1,R,BR,E,Z
      COMMON/PARA/TH,TH1,TN,TR,HN,HE,HZ,NTYPE
C*************************************************************************
C  NTYPE : 1 = STIFFENED FLANGE - SINGLE WEBS
C          2 = UNSTIFFENED FLANGE - SINGLE WEBS
C          3 = I-BEAMS
C   F = YIELD STRENGTH, KSI
C   T = THICKNESS, IN.
C   R = INSIDE BEND RADIUS, IN.
C  BR = BEARING LENGTH OF THE CONSIDERED LOAD OR REACTION, IN.
C   E = CLOSER CLEAR DISTANCE BETWEEN THE ADJACENT OPPOSITE BEARING
C       PLATES (E = 0.0 FOR OVERLAPPING BEARING PLATES)
C   Z = DISTANCE BETWEEN THE END OF BEARING PLATE TO THE NEAR END OF
C       THE BEAM
C*************************************************************************
C
C*************************************************************************
C INPUT  1) NTYPE (1, 2, OR 3)   2) FY      3) THICKNESS
C        4) H (D-2*T)    5) R    6) BR (BEARING LENGTH)
C*************************************************************************
      READ(5,*) NTYPE,F,T,H,R,BR
      H1 = H-2.*R
      TH = H/T
      TH1 = H1/T
      TR = R/T
      TN = BR/T
      HN = BR/H
      IF (NTYPE.EQ.3) GO TO 20
      IF (NTYPE.EQ.2) GO TO 10
      WRITE (6,1001)
 1001 FORMAT(' SINGLE WEBS WITH STIFFENED FLANGES',/)
      GO TO 30
   10 WRITE (6,1002)
 1002 FORMAT(' SINGLE WEBS WITH UNSTIFFENED FLANGES',/)
      GO TO 30
   20 WRITE (6,1003)
 1003 FORMAT(' I-BEAMS',/)
   30 WRITE (6,1004)F,T,TH,TR,TN,HN
 1004 FORMAT(' FY = ',F5.1,'  KSI',/' T = ',F4.3,'  IN.',/' H/T = ',F5.1
     /,/' R/T = ',F3.1,/' N/T = ',F4.1,/' N/H = ',F5.1,/)
C*************************************************************************
C INPUT  1) E/H     2) Z/H
C*************************************************************************
   50 READ(5,*) HE, HZ
      WRITE(6,1011)HE,HZ
 1011 FORMAT(' FOR  E/H = ',F4.1,'  AND  Z/H = ',F4.1,/)
```

```
      IF(HE.EQ.0.0.AND.HZ.EQ.0.0) GO TO 110
      IF(HE.EQ.0.0.AND.HZ.LT.0.5) GO TO 120
      IF(HE.EQ.0.0.AND.HZ.GE.0.5) GO TO 130
      IF(HE.LT.0.5.AND.HZ.EQ.0.0) GO TO 140
      IF(HE.LT.0.5.AND.HZ.LT.0.5) GO TO 150
      IF(HE.LT.0.5.AND.HZ.GE.0.5) GO TO 160
      IF(HE.GE.0.5.AND.HZ.EQ.0.0) GO TO 170
      IF(HE.GE.0.5.AND.HZ.LT.0.5) GO TO 180
      IF(HE.GE.0.5.AND.HZ.GE.0.5) CALL CASE2 (PP)
      NCASE = 2
      WRITE(6,4001) NCASE
 4001 FORMAT(/' CASE NO. = ',I2,/)
      GO TO 200
  110 CALL CASE4(PP)
      NCASE = 4
      WRITE(6,4001) NCASE
      GO TO 200
  120 CALL CASE6(PP)
      NCASE = 6
      WRITE(6,4001) NCASE
      GO TO 200
  130 CALL CASE5(PP)
      NCASE = 5
      WRITE(6,4001) NCASE
      GO TO 200
  140 CALL CASE7(PP)
      NCASE = 7
      WRITE(6,4001) NCASE
      GO TO 200
  150 CALL CASE9(PP)
      NCASE = 9
      WRITE(6,4001) NCASE
      GO TO 200
  160 CALL CASE8(PP)
      NCASE = 8
      WRITE(6,4001) NCASE
      GO TO 200
  170 CALL CASE1(PP)
      NCASE = 1
      WRITE(6,4001) NCASE
      GO TO 200
  180 CALL CASE3(PP)
      NCASE = 3
      WRITE(6,4001) NCASE
  200 IF(HE.GE.1.5.AND.HZ.LT.1.5) GO TO 210
      IF(HE.GE.1.5.AND.HZ.GE.1.5) GO TO 220
      IF(HE.LT.1.5.AND.HZ.LT.1.5) GO TO 230
      IF(HE.LT.1.5.AND.HZ.GE.1.5) CALL SPEC4 (PS)
      GO TO 300
  210 CALL SPEC1 (PS)
      GO TO 300
  220 CALL SPEC2 (PS)
      GO TO 300
```

```
  230 CALL SPEC3 (PS)
  300 RATIO = PS/PP
      WRITE(6,1012)PS,PP,RATIO
 1012 FORMAT(' PSPEC = ',F7.3,' KIPS',//,' PPROPOSE = ',F7.3,' KIPS',//
     /' PSPEC/PPROPOSE = ',F5.3)
      STOP
      END
C
      SUBROUTINE CASE1 (P1)
      COMMON/PARA/TH,TH1,TN,TR,HN,HE,HZ,NTYPE
      IF (NTYPE.EQ.3) GO TO 100
      CALL EQ1 (PE1)
      CALL EQ2 (PE2)
      WRITE(6,2001)PE1,PE2
 2001 FORMAT(/,'   PCY1 = ',F7.3,' KIPS      PCB1 = ',F7.3,' KIPS')
      P1 = PE1
      IF(P1.GT.PE2) P1 = PE2
      WRITE(6,2002)P1
 2002 FORMAT(/,'   PC1 = ',F7.3,' KIPS')
      GO TO 200
  100 CALL EQ8 (PE8)
      P1 = PE8
      WRITE(6,2003)PE8
 2003 FORMAT(/,'   PCY1 = DOES NOT APPLY      PCB1 = ',F7.3,' KIPS')
      WRITE(6,2004)P1
 2004 FORMAT(/,'   PC1 = ',F7.3,' KIPS')
  200 RETURN
      END
C
      SUBROUTINE CASE2 (P2)
      COMMON/PARA/TH,TH1,TN,TR,HN,HE,HZ,NTYPE
      IF (NTYPE.EQ.3) GO TO 100
      CALL EQ3 (PE3)
      CALL EQ4 (PE4)
      WRITE(6,2005)PE3,PE4
 2005 FORMAT(/,'   PCY2 = ',F7.3,' KIPS      PCB2 = ',F7.3,' KIPS')
      P2 = PE3
      IF(P2.GT.PE4) P2 = PE4
      WRITE(6,2006)P2
 2006 FORMAT(/,'   PC2 = ',F7.3,' KIPS')
      GO TO 200
  100 CALL EQ9 (PE9)
      CALL EQ10 (PE10)
      WRITE(6,2007)PE9,PE10
 2007 FORMAT(/,'   PCY2 = ',F7.3,' KIPS      PCB2 = ',F7.3,' KIPS')
      P2 = PE9
      IF(P2.GT.PE10) P2 = PE10
      WRITE(6,2008)P2
 2008 FORMAT(/,'   PC2 = ',F7.3,' KIPS')
  200 RETURN
      END
C
      SUBROUTINE CASE3 (P3)
```

```
      COMMON/PARA/TH,TH1,TN,TR,HN,HE,HZ,NTYPE
      CALL CASE1 (P1)
      CALL CASE2 (P2)
      P3 = (HZ/0.5)*P2 + ((0.5-HZ)/0.5)*P1
      WRITE(6,2009)P3
 2009 FORMAT(/,'   PC3 = ',F7.3,' KIPS')
      RETURN
      END
C
      SUBROUTINE CASE4 (P4)
      COMMON/PARA/TH,TH1,TN,TR,HN,HE,HZ,NTYPE
      IF (NTYPE.EQ.3) GO TO 100
      CALL EQ5 (PE5)
      P4 = PE5
      WRITE(6,2010)PE5
 2010 FORMAT(/,'   PCY4 = DOES NOT APPLY      PCB4 = ',F7.3,' KIPS')
      WRITE(6,2011)P4
 2011 FORMAT(/,'   PC4 = ',F7.3,' KIPS')
      GO TO 200
  100 CALL EQ11 (PE11)
      P4 = PE11
      WRITE(6,2012)PE11
 2012 FORMAT(/,'   PCY4 = DOES NOT APPLY      PCB4 = ',F7.3,' KIPS')
      WRITE(6,2013)P4
 2013 FORMAT(/,'   PC4 = ',F7.3,' KIPS')
  200 RETURN
      END
C
      SUBROUTINE CASE5 (P5)
      COMMON/PARA/TH,TH1,TN,TR,HN,HE,HZ,NTYPE
      IF (NTYPE.EQ.3) GO TO 100
      CALL EQ6 (PE6)
      CALL EQ7 (PE7)
      WRITE(6,2014)PE6,PE7
 2014 FORMAT(/,'   PCY5 = ',F7.3,' KIPS      PCB5 = ',F7.3,' KIPS')
      P5 = PE6
      IF(P5.GT.PE7) P5 = PE7
      WRITE(6,2015)P5
 2015 FORMAT(/,'   PC5 = ',F7.3,' KIPS')
      GO TO 200
  100 CALL EQ12 (PE12)
      CALL EQ13 (PE13)
      WRITE(6,2016)PE12,PE13
 2016 FORMAT(/,'   PCY5 = ',F7.3,' KIPS      PCB5 = ',F7.3,' KIPS')
      P5 = PE12
      IF(P5.GT.PE13) P5 = PE13
      WRITE(6,2017)P5
 2017 FORMAT(/,'   PC5 = ',F7.3,' KIPS')
  200 RETURN
      END
C
      SUBROUTINE CASE6 (P6)
      COMMON/PARA/TH,TH1,TN,TR,HN,HE,HZ,NTYPE
```

```
      CALL CASE4 (P4)
      CALL CASE5 (P5)
      P6 = (HZ/0.5)*P5 + ((0.5-HZ)/0.5)*P4
      WRITE(6,2018)P6
 2018 FORMAT(/,'   PC6 = ',F7.3,' KIPS')
      RETURN
      END
C
      SUBROUTINE CASE7 (P7)
      COMMON/PARA/TH,TH1,TN,TR,HN,HE,HZ,NTYPE
      CALL CASE1 (P1)
      CALL CASE4 (P4)
      P7 = (HE/0.5)*P1 + ((0.5-HE)/0.5)*P4
      WRITE(6,2019)P7
 2019 FORMAT(/,'   PC7 = ',F7.3,' KIPS')
      RETURN
      END
C
      SUBROUTINE CASE8 (P8)
      COMMON/PARA/TH,TH1,TN,TR,HN,HE,HZ,NTYPE
      CALL CASE2 (P2)
      CALL CASE5 (P5)
      P8 = (HE/0.5)*P2 + ((0.5-HE)/0.5)*P5
      WRITE(6,2020)P8
 2020 FORMAT(/,'   PC8 = ',F7.3,' KIPS')
      RETURN
      END
C
      SUBROUTINE CASE9 (P9)
      COMMON/PARA/TH,TH1,TN,TR,HN,HE,HZ,NTYPE
      CALL CASE3 (P3)
      CALL CASE6 (P6)
      P9 = (HE/0.5)*P3 + ((0.5-HE)/0.5)*P6
      WRITE(6,2021)P9
 2021 FORMAT(/,'   PC9 = ',F7.3,' KIPS')
      RETURN
      END
C
      SUBROUTINE EQ1 (PE1)
      COMMON/IN/F,T,H,H1,R,BR,E,S
      COMMON/PARA/TH,TH1,TN,TR,HN,HE,HZ,NTYPE
      FTN = 1.+.0122*TN
      FTR = 1.-.247*TR
      IF (FTR.LT.0.32) FTR = 0.32
      PE1 = 9.90*T**2*FTN*FTR*F
      RETURN
      END
C
      SUBROUTINE EQ2 (PE2)
      COMMON/IN/F,T,H,H1,R,BR,E,S
      COMMON/PARA/TH,TH1,TN,TR,HN,HE,HZ,NTYPE
      FTH = 1.-.00348*TH
      IF (FTH.LT.0.32) FTH = 0.32
```

```
      FHE = 1.-.298*HE
      IF (FHE.LT.0.52) FHE = 0.52
      PE2 = 1385.*T**2*FTH*FHE
      RETURN
      END
C
      SUBROUTINE EQ3 (PE3)
      COMMON/IN/F,T,H,H1,R,BR,E,S
      COMMON/PARA/TH,TH1,TN,TR,HN,HE,HZ,NTYPE
      FTN = 1.+.217*TN**.5
      FTR = 1.-.0814*TR
      PE3 = 7.80*T**2*FTN*FTR*F
      RETURN
      END
C
      SUBROUTINE EQ4 (PE4)
      COMMON/IN/F,T,H,H1,R,BR,E,S
      COMMON/PARA/TH,TH1,TN,TR,HN,HE,HZ,NTYPE
      FTH = 1.-.00170*TH
      IF (FTH.GT.0.81) FTH = 0.81
      FHE = 1.-.120*HE
      IF (FHE.LT.0.40) FHE = 0.40
      FHN = 1.+2.40*HN
      IF (FHN.GT.1.96) FHN = 1.96
      PE4 = 820.0*T**2*FTH*FHE*FHN
      RETURN
      END
C
      SUBROUTINE EQ5 (PE5)
      COMMON/IN/F,T,H,H1,R,BR,E,S
      COMMON/PARA/TH,TH1,TN,TR,HN,HE,HZ,NTYPE
      FHN = 1.+.54*HN
      FTH = 1.-.00245*TH
      PE5 = 163.0*T**2*FHN*FTH*1.98
      RETURN
      END
C
      SUBROUTINE EQ6 (PE6)
      COMMON/IN/F,T,H,H1,R,BR,E,S
      COMMON/PARA/TH,TH1,TN,TR,HN,HE,HZ,NTYPE
      FTN = 1.+.217*TN**.5
      FTR = 1.-.0814*TR
      PE6 = 7.80*T**2*FTN*FTR*F
      RETURN
      END
C
      SUBROUTINE EQ7 (PE7)
      COMMON/IN/F,T,H,H1,R,BR,E,S
      COMMON/PARA/TH,TH1,TN,TR,HN,HE,HZ,NTYPE
      FTH = 1.-.0000141*TH**2.
      IF (FTH.LT.0.44) FTH = 0.44
      FHZ = 1.+4.547*HZ
      IF (FHZ.GT.9.10) FHZ = 9.10
```

```
      FHN = 1.+.729*HN
      IF (FHN.GT.1.30) FHN = 1.30
      PE7 = 122.0*T**2*FTH*FHZ*FHN
      RETURN
      END
C
      SUBROUTINE EQ8 (PE8)
      COMMON/IN/F,T,H,H1,R,BR,E,S
      COMMON/PARA/TH,TH1,TN,TR,HN,HE,HZ,NTYPE
      FTH = 1.-.00118*TH
      IF (FTH.GT.0.82) FTH = 0.82
      FHE = 1.-.233*HE
      IF (FHE.LT.0.58) FHE = 0.58
      PE8 = 1872.*T**2.*FTH*FHE
      RETURN
      END
C
      SUBROUTINE EQ9 (PE9)
      COMMON/IN/F,T,H,H1,R,BR,E,S
      COMMON/PARA/TH,TH1,TN,TR,HN,HE,HZ,NTYPE
      FTN = 1.+.217*TN**.5
      PE9 = 15.0*T**2.*F*FTN
      RETURN
      END
C
      SUBROUTINE EQ10 (PE10)
      COMMON/IN/F,T,H,H1,R,BR,E,S
      COMMON/PARA/TH,TH1,TN,TR,HN,HE,HZ,NTYPE
      FTH = 1.-.000471*TH
      IF (FTH.GT.0.948) FTH = 0.948
      FHN = 1.+1.318*HN
      IF (FHN.GT.1.53) FHN = 1.53
      PE10 = 942.*T**2.*FTH*FHN
      RETURN
      END
C
      SUBROUTINE EQ11 (PE11)
      COMMON/IN/F,T,H,H1,R,BR,E,S
      COMMON/PARA/TH,TH1,TN,TR,HN,HE,HZ,NTYPE
      FTH = 1.-.0017*TH
      IF (FTH.LT.0.66) FTH = 0.66
      FHN = 1.+1.262*HN**1.5
      PE11 = 456.5*T**2.*FTH*FHN
      RETURN
      END
C
      SUBROUTINE EQ12 (PE12)
      COMMON/IN/F,T,H,H1,R,BR,E,S
      COMMON/PARA/TH,TH1,TN,TR,HN,HE,HZ,NTYPE
      FTN = 1.+.217*TN**.5
      PE12 = 15.0*T**2.*F*FTN
      RETURN
      END
C
```

```
      SUBROUTINE EQ13 (PE13)
      COMMON/IN/F,T,H,H1,R,BR,E,S
      COMMON/PARA/TH,TH1,TN,TR,HN,HE,HZ,NTYPE
      FTH = 1.-.0060*TH
      IF (FTH.LT.0.46) FTH = 0.46
      FHN = 1.+4.0*HN**3.
      FHZ = 1.+.109*HZ
      IF (FHZ.GT.1.218) FHZ = 1.218
      PE13 = 1512.*T**2.*FTH*FHN*FHZ
      RETURN
      END
C
      SUBROUTINE SPEC1 (PS1)
      COMMON/IN/F,T,H,H1,R,BR,E,S
      COMMON/PARA/TH,TH1,TN,TR,HN,HE,HZ,NTYPE
      IF (NTYPE.EQ.3) GO TO 200
      FTN = 1.+ .01*TN
      FFY = (1.33-.33*F/33.)*(F/33.)
      IF (F.GT.66.5) FFY = 1.340
      FTR = 1.15-.15*TR
      IF (FTR.LT.0.5) FTR = 0.5
      IF (NTYPE.EQ.2) GO TO 100
      FTH = 179.-0.33*TH1
      PS1 = 1.85*T**2.*FFY*FTR*FTH*FTN
      GO TO 300
  100 FTH = 117.-.15*TH1
      IF (TN.GT.60.) FTN = 0.71+.015*TN
      PS1 = 1.85*T**2.*FFY*FTR*FTH*FTN
      GO TO 300
  200 FTN = 5.0+0.63*TN**.5
      FTH = 1.+TH1/750.
      IF (FTH.GT.1.20) FTH = 1.20
      PS1 = 2.0*T**2.*F*FTH*FTN
  300 RETURN
      END
C
      SUBROUTINE SPEC2 (PS2)
      COMMON/IN/F,T,H,H1,R,BR,E,S
      COMMON/PARA/TH,TH1,TN,TR,HN,HE,HZ,NTYPE
      IF (NTYPE.EQ.3) GO TO 100
      FTH = 291.-.40*TH1
      FTN = 1.+ .007*TN
      IF (TN.GT.60.) FTN = 0.75+.011*TN
      FFY = (1.22-.22*F/33.)*(F/33.)
      IF (F.GT.91.5) FFY = 1.69136
      FTR = 1.06-.06*TR
      IF (FTR.LT.0.5) FTR = 0.5
      PS2 = 1.85*T**2.*FFY*FTR*FTH*FTN
      GO TO 200
  100 FFY = 1.49-0.53*F/33.
      IF (FFY.LT.0.6) FFY = 0.6
      FTT = 0.88+0.12*T/.075
      FTN = 7.50+1.63*TN**.5
```

```
      PS2 = 2.0*T**2.*F*FFY*FTT*FTN
  200 RETURN
      END
C
      SUBROUTINE SPEC3 (PS3)
      COMMON/IN/F,T,H,H1,R,BR,E,S
      COMMON/PARA/TH,TH1,TN,TR,HN,HE,HZ,NTYPE
      IF (NTYPE.EQ.3) GO TO 100
      FTH = 132.-.31*TH1
      FTN = 1.+ .01*TN
      FFY = (1.33-.33*F/33.)*(F/33.)
      IF (F.GT.66.5) FFY = 1.340
      FTR = 1.15-.15*TR
      IF (FTR.LT.0.5) FTR = 0.5
      PS3 = 1.85*T**2.*FFY*FTR*FTH*FTN
      GO TO 200
  100 FFY = (0.98-TH/865.)/(F/33.)
      FTT = 0.64+0.31*T/.075
      FTN = 5.0+0.63*TN**.5
      PS3 = 2.*T**2.*F*FFY*FTT*FTN
  200 RETURN
      END
C
      SUBROUTINE SPEC4 (PS4)
      COMMON/IN/F,T,H,H1,R,BR,E,S
      COMMON/PARA/TH,TH1,TN,TR,HN,HE,HZ,NTYPE
      IF (NTYPE.EQ.3) GO TO 100
      FTH = 417.-1.22*TH1
      FTN = 1.+ .0013*TN
      FFY = (1.22-.22*F/33.)*(F/33.)
      IF (F.GT.91.5) FFY = 1.69136
      FTR = 1.06-.06*TR
      IF (FTR.LT.0.5) FTR = 0.5
      PS4 = 1.85*T**2.*FFY*FTR*FTH*FTN
      GO TO 200
  100 FTH = 33./F
      IF (TH1.GT.150) FTH = (1.1-TH1/665.)*33./F
      FTT = 0.82+0.15*T/.075
      FTN = 7.5+1.63*TN**.5
      PS4 = 2.0*T**2.*F*FTH*FTT*FTN
  200 RETURN
      END
```

EXAMPLE 1

INPUT DATA

```
1  50.0  0.05  6.0  0.075  2.0
1.50  0.00
```

OUTPUT DATA

SINGLE WEBS WITH STIFFENED FLANGES

FY = 50.0 KSI
T = .050 IN.
H/T = 120.0
R/T = 1.5
N/T = 40.0
N/H = 0.3

FOR E/H = 1.5 AND Z/H = 0.0 (See Fig. G1a)

PCY1 = 1.159 KIPS PCB1 = 1.115 KIPS

PC1 = 1.115 KIPS

CASE NO. = 1

PSPEC = 1.057 KIPS

PPROPOSE = 1.115 KIPS

PSPEC/PPROPOSE = 0.948

EXAMPLE 2

INPUT DATA

```
1  80.0  0.05  6.0  0.075  2.0
1.50  0.00
```

OUTPUT DATA

```
SINGLE WEBS WITH STIFFENED FLANGES

FY =  80.0  KSI
T = .050  IN.
H/T = 120.0
R/T = 1.5
N/T = 40.0
N/H =   0.3

FOR  E/H =  1.5  AND  Z/H =  0.0  (See Fig. G1a)


  PCY1 =   1.855 KIPS      PCB1 =   1.115 KIPS

  PC1 =   1.115 KIPS

CASE NO. =  1

PSPEC =   1.127 KIPS

PPROPOSE =   1.115 KIPS

PSPEC/PPROPOSE = 1.010
```

EXAMPLE 3

INPUT DATA

```
3  50.0  0.05  6.0  0.075  2.0
1.50  0.00
```

OUTPUT DATA

```
I-BEAMS

FY =  50.0  KSI
T = .050  IN.
H/T = 120.0
R/T = 1.5
N/T = 40.0
N/H =   0.3

FOR  E/H =  1.5  AND  Z/H =  0.0   (See Fig. G1a)


  PCY1 = DOES NOT APPLY      PCB1 =   2.496 KIPS

  PC1 =   2.496 KIPS

CASE NO. =  1

PSPEC =   2.597 KIPS

PPROPOSE =   2.496 KIPS

PSPEC/PPROPOSE = 1.040
```

EXAMPLE 4

INPUT DATA

```
3  80.0  0.05  6.0  0.075  2.0
1.50  0.00
```

OUTPUT DATA

I-BEAMS

```
FY =  80.0  KSI
T = .050  IN.
H/T = 120.0
R/T = 1.5
N/T = 40.0
N/H =   0.3

FOR  E/H =  1.5  AND  Z/H =  0.0  (See Fig. G1a)


  PCY1 = DOES NOT APPLY      PCB1 =   2.496 KIPS

  PC1 =   2.496 KIPS

CASE NO. =  1

PSPEC =   4.154 KIPS

PPROPOSE =   2.496 KIPS

PSPEC/PPROPOSE = 1.664
```

NOTE: The large difference between these two methods is due to web buckling failure which is not specifically covered by the 1986 AISI Specification.

EXAMPLE 5

INPUT DATA

```
1  50.0  0.05  6.0  0.075  2.0
1.50  1.50
```

OUTPUT DATA

```
SINGLE WEBS WITH STIFFENED FLANGES

FY =  50.0  KSI
T = .050  IN.
H/T = 120.0
R/T = 1.5
N/T = 40.0
N/H =   0.3

FOR  E/H =  1.5  AND  Z/H >  1.5  (See Fig. G1b)

  PCY2 =   2.031 KIPS      PCB2 =   2.409 KIPS

  PC2 =   2.031 KIPS

CASE NO. =  2

PSPEC =   1.884 KIPS

PPROPOSE =   2.031 KIPS

PSPEC/PPROPOSE = 0.928
```

EXAMPLE 6

INPUT DATA

```
1  80.0  0.05  6.0  0.075  2.0
1.50  1.50
```

OUTPUT DATA

```
SINGLE WEBS WITH STIFFENED FLANGES

FY =  80.0  KSI
T = .050  IN.
H/T = 120.0
R/T = 1.5
N/T = 40.0
N/H =   0.3

FOR  E/H =  1.5  AND  Z/H >  1.5  (See Fig. G1b)


  PCY2 =   3.249 KIPS      PCB2 =   2.409 KIPS

  PC2 =   2.409 KIPS

CASE NO. =  2

PSPEC =   2.334 KIPS

PPROPOSE =   2.409 KIPS

PSPEC/PPROPOSE = 0.969
```

EXAMPLE 7

INPUT DATA

```
3  50.0  0.05  6.0  0.075  2.0
1.50  1.50
```

OUTPUT DATA

```
I-BEAMS

FY =  50.0  KSI
T = .050  IN.
H/T = 120.0
R/T = 1.5
N/T = 40.0
N/H =   0.3

FOR  E/H =  1.5  AND  Z/H >  1.5  (See Fig. G1b)

  PCY2 =   4.448 KIPS      PCB2 =   3.198 KIPS

  PC2 =   3.198 KIPS

CASE NO. =  2

PSPEC =   2.936 KIPS

PPROPOSE =   3.198 KIPS

PSPEC/PPROPOSE = 0.918
```

EXAMPLE 8

INPUT DATA

3 80.0 0.05 6.0 0.075 2.0
1.50 1.50

OUTPUT DATA

I-BEAMS

FY = 80.0 KSI
T = .050 IN.
H/T = 120.0
R/T = 1.5
N/T = 40.0
N/H = 0.3

FOR E/H = 1.5 AND Z/H > 1.5 (See Fig. G1b)

PCY2 = 7.117 KIPS PCB2 = 3.198 KIPS

PC2 = 3.198 KIPS

CASE NO. = 2

PSPEC = 4.103 KIPS

PPROPOSE = 3.198 KIPS.

PSPEC/PPROPOSE = 1.283

NOTE: The reason for the large difference between both metods is the same as that discussed for Example 4.

EXAMPLE 9

INPUT DATA

```
1  50.0  0.075  5.85  0.101  3.0
1.50  0.00
```

OUTPUT DATA

SINGLE WEBS WITH STIFFENED FLANGES

```
FY =  50.0  KSI
T = .075  IN.
H/T =  78.0
R/T = 1.3
N/T = 40.0
N/H =  0.5
```

FOR E/H = 1.5 AND Z/H = 0.0 (See Fig. G1a)

PCY1 = 2.765 KIPS PCB1 = 3.139 KIPS

PC1 = 2.765 KIPS

CASE NO. = 1

PSPEC = 2.677 KIPS

PPROPOSE = 2.765 KIPS

PSPEC/PPROPOSE = 0.968

NOTE: This example is selected from the 1983 Edition of the AISI Cold-Formed Steel Design Manual. See Example No. 7, p. IV-25.

EXAMPLE 10

INPUT DATA

```
1  50.0  0.075  5.85  0.101  3.0
1.50  1.50
```

OUTPUT DATA

```
SINGLE WEBS WITH STIFFENED FLANGES

FY =  50.0  KSI
T = .075  IN.
H/T =  78.0
R/T = 1.3
N/T = 40.0
N/H =  0.5

FOR  E/H =  1.5  AND  Z/H >  1.5  (See Fig. G1b)


  PCY2 =   4.634 KIPS      PCB2 =   6.005 KIPS

  PC2 =   4.634 KIPS

CASE NO. =  2

PSPEC =   4.571 KIPS

PPROPOSE =   4.634 KIPS

PSPEC/PPROPOSE = 0.986
```

NOTE: This example is selected from the 1983 Edition of the AISI Cold-Formed Steel Design Manual. See Example No. 7, p. IV-25.

EXAMPLE 11

INPUT DATA

```
1  50.0  0.075  3.85  0.09375  2.0
12.3  0.00
```

OUTPUT DATA

SINGLE WEBS WITH STIFFENED FLANGES

```
FY =  50.0  KSI
T = .075  IN.
H/T =  51.3
R/T = 1.3
N/T = 26.7
N/H =   0.5
```

FOR E/H = 12.3 AND Z/H = 0.0 (See Fig. G1c)

PCY1 = 2.551 KIPS PCB1 = 3.327 KIPS

PC1 = 2.551 KIPS

CASE NO. = 1

PSPEC = 2.599 KIPS

PPROPOSE = 2.551 KIPS

PSPEC/PPROPOSE = 1.019

NOTE: This example is selected from the 1983 Edition of the AISI Cold-Formed Steel Design Manual. See Example No. 15, p. IV-39.

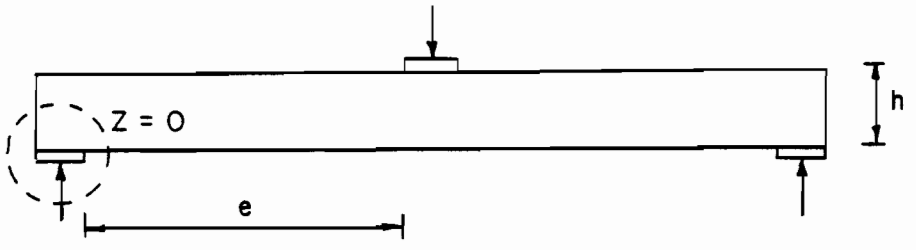

(a)

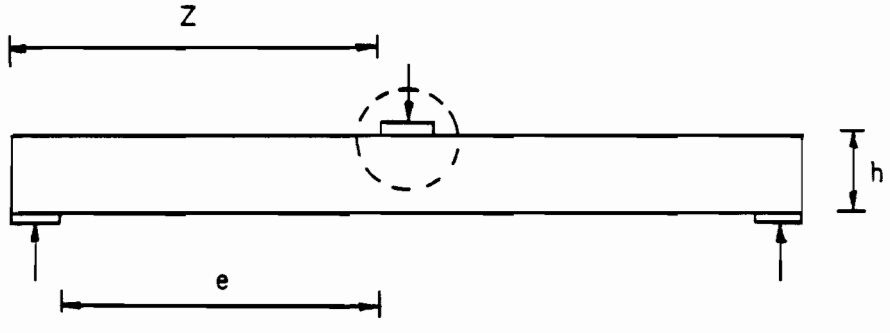

(b)

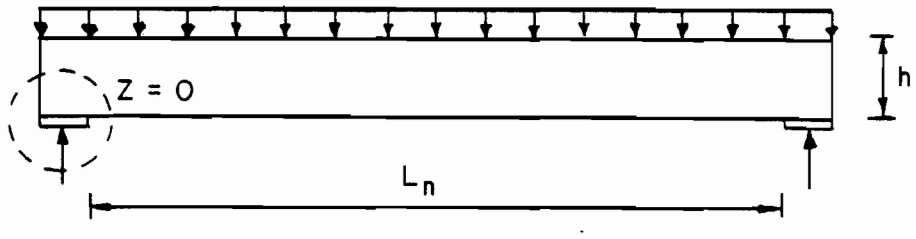

$e = L_n/2$

(c)

Fig. G1 Loading Conditions Used in the Examples

APPENDIX H - NOTATION

Symbol	Definition
D	Flexural rigidity of plate, $Et^3/12(1-\mu^2)$
e	Clear distance between edges of the adjacent opposite bearing plates, in.
E	Modulus of elasticity of steel = 29,500 ksi
f_b	Actual compression stress at junction of flange and web, ksi
f_c	Actual bearing stress in the web under the bearing plate, ksi
F_{bwu}	Maximum compression stress in the flat web of a beam due to bending, ksi
F_y	Yield strength, ksi
h	Clear distance between flanges measured along the plane of the web, in.
k	Buckling coefficient
L	Span length, in.
M	Applied bending moment, at or immediately adjacent to the point of application of the concentrated load or reaction, kip-in.
M_u	Ultimate bending moment if bending stress only exists,kip-in.
N	Actual length of bearing, in.
P	Concentrated load or reaction, kips
P_c	Governing ultimate web crippling load, kips
P_{cb}	Ultimate web crippling load due to web buckling, kips

P_{comp} Predicted ultimate load, kips

P_{cr} Elastic critical buckling load, kips

P_{cy} Ultimate web crippling load due to overstressing under the bearing plate, kips

P_{m} Computed ultimate load for moment only, kips

P_{mc} Computed load for combined bending moment and web crippling, kips

P_{ms} Computed load for combined bending moment and shear, kips

P_{s} Computed ultimate load for shear in the web, kips

P_{test} Tested failure load, kips

P_{cg} Computed ultimate web crippling load based on the AISI 1981 Guide, kips

P_{cs} Computed ultimate web crippling load based on the AISI 1980 Specification, kips

R Inside bend radius, in.

S_{eff} Effective section modulus computed on the basis of the effective design width of the compression flange, $in.^3$

t Base steel thickness, in.

Z Distance between the edge of the bearing plate to the near end of the beam, in.

Z1 Distance between the edge of the bearing plate to the far end of the beam, in.

μ Poisson's ratio

θ Angle between the plane of web and the plane of bearing surface, degrees.